UNCLASSIFIED

AD NUMBER

AD826318

NEW LIMITATION CHANGE

TO

Approved for public release, distribution unlimited

FROM

Distribution authorized to U.S. Gov't. agencies only; Administrative/Operational Use; MAY 1967. Other requests shall be referred to Air Force Flight Dynamics Lab., Wright-Patterson AFB, OH 45433.

AUTHORITY

AFSC/DOOS ltr, 30 Jul 1991

THIS PAGE IS UNCLASSIFIED

THIS REPORT HAS BEEN DELIMITED
AND CLEARED FOR PUBLIC RELEASE
UNDER DOD DIRECTIVE 5200.20 AND
NO RESTRICTIONS ARE IMPOSED UPON
ITS USE AND DISCLOSURE.

DISTRIBUTION STATEMENT A

APPROVED FOR PUBLIC RELEASE;
DISTRIBUTION UNLIMITED.

COPY 47

67-050161

WAD: R1005-F

AFFDL-TR-66-195 -Volume II

FOR OFFICIAL USE ONLY

AD826318

THE X-19 V/STOL TECHNOLOGY - A CRITICAL REVIEW

Wright Aeronautical Division
Curtiss-Wright Corporation
Wood-Ridge, New Jersey 07075

TECHNICAL REPORT AFFDL-TR-66-195

May 1967

Force Flight Dynamics Laboratory
Research and Technology Division
Air Force Systems Command
Wright-Patterson Air Force Base, Ohio

Each transmittal of this document outside the agencies of the U.S. Government must have prior approval of the Air Force Flight Dynamics Laboratory, V/STOL Technology Division (FDV), Wright-Patterson Air Force Base, Ohio 45433.

348

When Government drawings, specifications, or other data are used for any purpose other than in connection with a definitely related Government procurement operation, the United States Government thereby incurs no responsibility nor any obligation whatsoever; and the fact that the Government may have formulated, furnished, or in any way supplied said drawings, specifications, or other data, is not to be regarded by implication or otherwise as in any manner licensing the holder or any other person or corporation, or conveying any rights or permission to manufacture, use, or sell any patented invention that may in any way be related thereto.

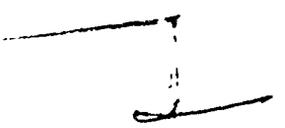

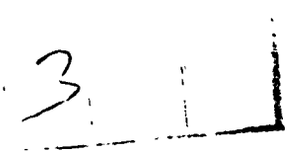

Copies of this report should not be returned to the Research and Technology Division unless return is required by security considerations, contractural obligations or notice on a specific document.

AFFDL-TR-66-195 -Volume II

Copy 58 of 100

THE X-19 V/STOL TECHNOLOGY - A CRITICAL REVIEW

Harold Fluk
"et al"

Each transmittal of this document outside the agencies of the U.S. Government must have prior approval of the Air Force Flight Dynamics Laboratory, V/STOL Technology Division (FDV), Wright-Patterson Air Force Base, Ohio 45433.

FOREWORD

The purpose of this report is to present a critical review and summary of the V/STOL technology involved in the development, component testing, ground testing, and flight testing of the X-19 aircraft. It is the final report of work accomplished by Curtiss-Wright Corporation, VTOL Systems Division, located at Caldwell, New Jersey, under Contract Number AF 33(615)-3940. The contract was administered under the direction of Captain R. M. Berg and Mr. B. Lindenbaum, FDV, Air Force Flight Dynamics Laboratory, (RTD), Wright-Patterson AFB, Ohio.

The following Curtiss-Wright Corporation personnel made the principal contributions to this report:

H. V. Borst, Chief Engineer - Technical Services
W. F. Meyer, Chief of Structures
W. Amatt, Mechanical Systems Group Leader - Structures
H. Fluk, Flight Loads Group Leader - Aerodynamics
J. H. Barker, Stability and Control Group Leader - Aerodynamics
E. L. Hassell, X-19 Performance Group Leader - Aerodynamics
E. J. Tursich, Project Engineer, P.D. - Aerodynamics

Because of the breadth of material required to be treated by the contract statement of work, each of the thirteen sections has been treated as an entity. Thus, each section has its own nomenclature, text, figures, and references. In some instances, nomenclature has been written into the text for convenience. Otherwise, it appears on the reverse side of the section divider page. The separation of nomenclature by section is intended to prevent confusion over the duplicity of meanings attached to given symbols by the different disciplines treated in the report.

It is to be noted that some of the material contained in this report is proprietary to Curtiss-Wright and is so stamped. The report is releasable only to agencies of the United States Government. Release of the report to any other organizations or individuals must have the approval of Curtiss-Wright.

Infomation in this report is embargoed under the Department of State International Traffic In Arms Regulations. This report, or information extracted from it, may be released to foreign governments by departments or agencies of the U. S. Government subject to approval of The Air Force Flight Dynamics Laboratory, or higher authority within the Department of the Air Force. Private individuals or firms require a Department of State export license.

Publication of this report does not constitute Air Force approval of the reports findings or conclusions. It is published only for the exchange and stimulation of ideas.

WILLIAM E. LAMAR
Deputy Director
Air Force Flight Dynamics Laboratory

ABSTRACT

This report contains a condensed description of the X-19 V/STOL Technology. The broad categories discussed, include in Section I, a review of the developments leading up to the X-19 program. Sections II through VI are devoted entirely to the propellers, and the considerations involved in design. The Radial Force principle is postulated in Section II. Interference effects on the wings due to the propellers are discussed in Section III. The propeller aerodynamic design in hover and cruise is presented in Section IV. Section V is devoted to the structure and control mechanisms of the propeller. Section VI relates to the use of propellers as an airplane control device. The tandem wing principle is discussed in Section VII covering stability, control, and drag. Section VIII is devoted solely to Ground Effects. The sizable wind tunnel research activity leading up to the X-19 is presented in Section IX. The structural loads in hover, transition and cruise are discussed in Section X. Section XI presents information pertinent to landing procedures in hover or cruise in the event of power failure. A summary of the flight test program is given in Section XII, including aircraft and hardware performance characteristics. Finally, Section XIII is devoted to a general discussion and assessment of the aircraft's unorthodox features.

TABLE OF CONTENTS

SECTION		PAGE
I	REVIEW OF DEVELOPMENTS LEADING TO THE X-19 PROGRAM	1
	1. REPORT OBJECTIVE	1
	2. BACKGROUND HISTORY	1
	3. X-100 AIRPLANE	2
	4. M-200 OPERATIONAL AIRCRAFT	6
	a. Initial Design Objectives	6
	(1) Tandem Wing Design Considerations	6
	(2) Turbo-Prop System	8
	(3) Selection of Hover Disk Loading	8
	(4) Selection of Fixed Wing System	9
	(5) Selection of Tandem Wing Four Propeller Configuration	9
	5. TRI-SERVICE X-19 (CW MODEL 200 DIMENSIONS AND GENERAL DATA)	10
	REFERENCES	17
II	RADIAL FORCE PRINCIPLE	19
	1. INTRODUCTION	19
	2. THEORY AND METHOD FOR COMPUTING PROPELLER FORCES	19
	a. General	19
	b. Theory of Normal Force and Yawing Moment	25
	3. APPLICATION OF PROPELLER RADIAL LIFT TO V/STOL AIRCRAFT	35
	a. General	35
	b. Application in Cruise	37
	c. Application in Transition	38
	d. Summary	43
	4. CORRELATION OF CALCULATED AND TEST RESULTS	43
	REFERENCES	51
III	WING-PROPELLER INTERFERENCE EFFECTS	53
	1. INTRODUCTION	53
	2. LIFT LOSS IN HOVER	53
	a. Theory	53
	b. Download Test Data	54
	c. Predicted Download	73
	3. PERIODIC FORCES ON WINGS AND PROPELLERS IN HOVER	73
	4. SUMMARY OF FORCES ON WINGS AND PROPELLERS	74
	a. Wings and Propellers out of Ground Effect	74
	b. Wings and Propellers in Ground Effect	97
	c. Net Forces in and out of Ground Effect	116
	5. FLAP DEFLECTION INTERFERENCE EFFECTS IN TRANSITION	120
	REFERENCES	121

TABLE OF CONTENTS (CONT'D)

SECTION		PAGE
IV	PROPELLER AERODYNAMIC DESIGN	123
	1. BLADE GEOMETRIC CHARACTERISTICS	123
	2. AERODYNAMIC DESIGN	130
	3. HOVER PERFORMANCE AS MEASURED AND CALCULATED	131
	4. CRUISE PERFORMANCE MAPS	138
	5. EFFECTS OF TIP SPEED AND BLADE TWIST IN HOVER AND CRUISE	138
	6. HOVER POWER HISTOGRAMS	149
	REFERENCES	15[illegible]
V	PROPELLER STRUCTURE AND CONTROL MECHANISM	157
	1. MECHANICAL DESIGN INCLUDING PHILOSOPHY, RELIABILITY, WEIGHT AND MAINTENANCE	157
	a. General Description	157
	b. Component Descriptions	157
	c. Blade Maintenance	162
	d. Reliability	167
	e. Propeller Weight	168
	2 BLADE STRUCTURAL DESIGN	168
	a. General	168
	b. Blade Design	171
	c. Design Details - 13166A10P3	190
	d. Design Details - 13166A12P3 Design	199
	e. Structural Analysis	199
	f. Full Scale Blade Testing	210
	3. PROPELLER DESIGN LOADING THEORY AND TEST	228
	a. General	228
	b. Theoretical Propeller Loading	228
	c. Propeller Test Loads	233
	4. WEIGHT COMPARISON OF X-19 FIBERGLASS PROPELLER	238
	a. Blade Weight Studies	238
	b. Hub Weight Studies	238
	5. PROPELLER STRUCTURAL PROBLEMS	242
	a. Blades	242
	b. Blade Shank	243
	c. Hubs	245
	d. Blade Pitch Control	245
	e. Propeller Housing	246
	6. PROPELLER INDUCED LOADS	247
	a. Theoretical Loads	247
	b. Airframe Test Results	248
	7. PROPELLER TESTING	254
	a. Propeller Hub Static Test	254
	b. Laboratory Whirl Test	257
	c. Electric Motor Whirl Test of X-19 Propeller	265
	d. 1 X P Gyroscopic Endurance	272
	e. Half Systems Rig Testing	276
	REFERENCES	282

TABLE OF CONTENTS (CONT'D)

SECTION		PAGE
VI	AIRCRAFT CONTROL BY PROPELLER THRUST MODULATION	283
	1. INTRODUCTION	283
	2. CONTROL POWERS	300
	3. TIME CONSTANT FOR PROPELLER FORCES	296
	4. PROPELLER POWER INCREMENTS DUE TO CONTROL APPLICATION	299
	5. CONTROL COUPLING AND RESPONSE	299
	6. PROPELLER CONTRIBUTION TO CENTER OF GRAVITY MOMENTS - TRANSITION	301
	7. CONTROL DEFICIENCIES AND ACTIONS	310
	8. PROPELLER POWER PENALTIES DUE TO CONTROL INPUT DEVIATIONS	313
	REFERENCES	318
VII	TANDEM WING AIRPLANE	319
	1. FLIGHT CONTROL OF TANDEM WING AIRCRAFT	319
	a. Transition Flight Regime	319
	(1) Introduction	319
	(2) Assumptions	319
	(3) Stability	319
	(4) Control and Control Systems	321
	b. Cruise Flight Regime	335
	(1) Introduction	335
	(2) Assumptions	335
	(3) Stability	335
	(4) Controls and Control Systems	349
	(5) Maneuvering Flight	351
	2. AERODYNAMIC CHARACTERISTICS (DRAG) OF TANDEM-WING SYSTEM	360
	a. Basic Data	360
	b. Drag Estimate	361
	c. Propellers off - Incompressible Profile Drag	361
	d. Effects of Lift, Power, and Compressibility	361
	e. Lift/Drag Ratio	366
	3. TEST AND THEORY COMPARISON OF AERODYNAMIC AND FLIGHT CONTROL CHARACTERISTICS	366
	a. Aerodynamic	365
	b. Flight Control	370
	4. AIRCRAFT BEHAVIOR IN GROUND EFFECT	370
	5. FLIGHT CONTROL DEFICIENCIES	370
	a. Transition Flight Regime	370
	(1) Introduction	370
	(2) Stability	371
	(3) Control	372
	b. Cruise Flight Regime	372
	(1) Introduction	372

TABLE OF CONTENTS (CONT'D)

SECTION		PAGE
	(2) Stability	373
	(3) Control	375
	6. AVAILABLE C.G. RANGE	376
	7. TILT, FLAP AND BLADE ANGLE PHASING	378
	a. Nacelle Tilt Phasing	378
	b. Flap and Collective Aileron Phasing	379
	c. Propeller Blade Angle Phasing	381
	(1) Auto Trim Schedule	381
	(2) Pitch Gain Schedule	381
	(3) Roll Gain Schedule	386
	(4) Yaw Cain Schedule	386
	8. CONTROL MIXING	386
	REFERENCES	389
VIII	GROUND EFFECTS	391
	1. INTRODUCTION	391
	2. GROUND EFFECTS UPON STABILITY AND CONTROL	391
	3. FLOW FIELD RECIRCULATION - ENGINE INLET	393
	4. HOVER POWER REQUIREMENT WITH GROUND HEIGHT	394
	REFERENCES	398
IX	WIND TUNNEL TESTS	399
	1. INTRODUCTION	399
	2. TESTS IN SUPPORT OF X-19 AND X-100 AIRCRAFT	399
	a. General	399
	b. Test Models	400
	c. Test Uses of Models	400
	d. Model Variations	401
	e. Wind Tunnel Test Facilities Used	402
	f. Other Applicable Test Programs	427
	3. TESTS IN SUPPORT OF ADVANCED TANDEM WING CONCEPTS	431
	4. TRANSITION WIND TUNNEL WALL CORRECTIONS	432
	5. CORRECTIONS OF MODEL PROPELLERS TO FULL SCALE RESULTS	433
	REFERENCES	444
X	STRUCTURAL LOADS	447
	1. INTRODUCTION	447
	2. CRUISE LOADS	447
	a. General	447
	b. Propeller-off Distributions	447
	c. Effects of Power	448
	d. Effects of Mach Number	448
	e. Effects of Reynolds Number	463
	f. Effects of Aeroelastic Twist	463
	g. Drag Distribution	464
	h. Flight-Envelope	465

TABLE OF CONTENTS (CONT'D)

SECTION		PAGE
	i. Symmetrical Gust Envelopes	465
	j. Balance Equations	467
	k. Load Breakdowns	471
	l. Spanwise Lift Distribution	471
	3. HOVER LOADS	481
	a. General	481
	b. Symmetrical Trimmed Thrusts	481
	c. Trim Button	483
	d. Throttle and Control Excursions	488
	e. Design Criteria	488
	4. TRANSITION LOADS	489
	a. General	489
	b. Airplane Characteristics	489
	c. Design Control Loads Criteria	495
	d. Design Maneuvers and Flight Envelopes	505
	e. Design Gust Loads Criteria	505
	5. DESIGN GROUND LOADS CRITERIA	514
	REFERENCES	515
XI	POWER-OFF CONSIDERATIONS	517
	1. SAFE OPERATING ENVELOPE	517
	2. ENGINE FAILURE CONSIDERATIONS	517
	3. POWER-OFF CHARACTERISTICS VS SPEED AND ALTITUDE (WIND MILLING)	519
	4. AUTOROTATIVE CHARACTERISTICS	529
XII	FLIGHT TEST SUMMARY	535
	1. INTRODUCTION	535
	2. HISTORY OF X-19 TEST FLIGHTS	536
	a. Historical Progression	536
	b. Simplified Flight Test Schedule at Curtiss Wright	536
	c. Flight Test Schedule at NAFEC	545
	d. Aircraft used in Flight Tests	548
	3. AIRCRAFT CONFIGURATION VS TIME	564
	a. Aircraft at Beginning of Flight No. 8	564
	b. Configuration Changes During Test Program	565
	c. Configuration at Flight No. 50	571
	d. Flight Test Instrumentation Thru Flight No. 37	571
	e. Flight Test Instrumentation at NAFEC	571
	4. AIRCRAFT PERFORMANCE RESULTS USING STEADY STATE DATA	575
	a. Overall Airplane Performance From Flight Tests	575
	b. Hovering Performance	575
	c. Conversion/Reconversion Flight Maneuvers	575
	d. Power Required	575

TABLE OF CONTENTS (CONT'D)

SECTION		PAGE
	e. Thrust-Power Download	582
	f. Ground Effect	583
	g. System Thrust Response to Power Excursions	587
	h. Fuel Consumption	587
	5. AIRCRAFT STABILITY AND CONTROL	592
	a. Initial Hover Stability and Control Results	592
	b. Pilot Operation Rating	592
	c. Flight Tests With S.A.S. Inoperative	592
	d. STOL Operations	602
	REFERENCES	603
XIII	ASSESSMENT OF RESULTS AND CONCLUSIONS	605
	1. INTRODUCTION	605
	2. OVERALL X-19 CONCEPT AND ITS DERIVATION	605
	a. Radial Lift Propellers	605
	b. Tilt Propeller, Fixed Wing Configuration	606
	c. Tandem Wing Configuration	608
	d. Control Power	612
	e. Transmission Design Philosophy	613
	f. Gust Sensitivity	615
	g. Propeller Control Problems	615
	3. OPERATIONAL FLIGHT CONSIDERATIONS	617
	a. Engine-out Safety	617
	b. Cruise Stall Characteristics	617

LIST OF ILLUSTRATIONS

FIGURE NO.		PAGE
	SECTION I	1
1	X-100 in the hover and cruise nacelle position.	4
2	X-100 three view drawing.	5
3	X-19 three view drawing.	15
	SECTION II	19
4	Comparison of normal force produced by wings and propellers.	20
5	Propeller inflow velocity components.	22
6	Approximate blade lift variation with rotational position.	23
7	Incremental force variation due to propeller angle of attack, A angle.	24
8	Propeller blade velocity components.	27
9	Three dimensional distribution of velocity components.	30
10	Curtiss-Wright X-100 distribution of propeller and airplane component lift distributions through equilibrium transition; G.W. 3500 lbs., 1240 RPM, $\alpha_{fus} = 5°$.	39
11	X-19, distribution of propeller and airplane component lift distributions through equilibrium transition; G.W. 12300 lbs.	40
12	Propeller lift and accelerating thrust variation with "A" angle; wind axis coordinates.	42
13	Normal force coefficient as a function of advance ratio perpendicular to the propeller disk 3(X100188) blade, Dia. = 10 ft, AF = 188, $IC_{L_i} = 0.068$;A = 15°	45
14	Normal force coefficient as a function of advance ratio perpendicular to the propeller disk 3(X100188) blade, Dia. = 10 ft, AF = 188, $IC_{L_i} = 0.068$; A = 30°	46
15	Normal force coefficient as a function of advance ratio perpendicular to the propeller disk 3(X100188) blade, Dia. = 10 ft, AF = 188, $IC_{L_i} = 0.068$; A = 45°	47
16	Normal force coefficient as a function of advance ratio perpendicular to the propeller disk 3(X100188) blade, Dia. = 10 ft, AF = 188, $IC_{L_i} = 0.068$; A = 60°	48
17	Normal force coefficient as a function of advance ratio perpendicular to the propeller disk 3(X100188) blade, Dia. = 10 ft, AF = 188, $IC_{L_i} = 0.068$; A = 75°	49

LIST OF ILLUSTRATIONS (CONT'D)

FIGURE NO.		PAGE
18	Normal force coefficient as a function of advance ratio perpendicular to the propeller disk 3(X100188) blade, Dia. = 10 ft, AF = 188, IC_{L_i} = 0.068; A = 85°.	50
	SECTION III	53
19	X-19, rear wing nomenclature.	55
20	X-19, download variation with disk loading.	57
21	X-19, rear wing download test; locations of spanwise pressure stations.	58
22	X-19, rear wing download test; locations of chordwise pressure stations.	59
23	X-19, ground clearances on the tie-down rig.	60
24	X-19, effect of disk loading on the rear wing - station 4.	63
25	X-19, effect of nacelle tilt angle on the spanwise loading; rear wing, static propeller.	64
26	X-19, rear wing pressure in the propeller wake, static propeller.	65
27	X-19, download on the rear wing.	66
28	X-19, effects on disk loading and collective aileron angle on the rear wing download.	68
29	X-19, effects of disk loading and collective aileron angle on the rear wing download, $\phi = 90^{o}$.	69
30	X-19, effects of nacelle tilt angle and collective aileron angle on the rear wing download.	70
31	X-19, effect of rear wing interference on the rear propeller thrust.	71
32	X-19, effect of slats and aileron nose piece on measured download.	72
33	X-19, lift coefficient of front propellers and front wing plus propellers as a function of thrust coefficient.	75
34	X-19, lift coefficient of rear propellers and rear wing plus rear propellers as a function of thrust coefficient.	76
35	X-19, drag coefficient of front propellers and front wing plus propellers as a function of thrust coefficient.	77
36	X-19, drag coefficient of rear propellers and rear wing plus propellers as a function of thrust coefficient.	78
37	X-19, front propeller thrust coefficient as a function of power parameter, C_p/J^3.	80
38	X-19, rear propeller thrust coefficient as a function of power parameter, C_p/J^3.	81

LIST OF ILLUSTRATIONS (CONT'D)

FIGURE NO.		PAGE
39	X-19, thrust coefficient as a function of thrust axis angle of attack.	82
40	Propeller 156109, thrust coefficient as a function of power parameter.	84
41	Propeller 156109, thrust coefficient as a function of power parameter.	85
42	X-19, variation of front propeller lift and thrust coefficient with thrust axis angle of attack.	86
43	X-19, variation of rear propeller lift and thrust coefficient with thrust axis angle of attack.	87
44	X-19, variation of front wing lift coefficient with nacelle tilt angle.	89
45	X-19, variation of rear wing lift coefficient with nacelle tilt angle.	90
46	X-19, variation of front wing drag coefficient with nacelle tilt angle.	91
47	X-19, variation of rear wing drag coefficient with nacelle tilt angle.	92
48	X-19, incremental front wing lift coefficient, due to front propeller wash, with variation in thrust axis angle of attack.	93
49	X-19, incremental rear wing lift coefficient, due to all wash, with variation in rear thrust axis angle of attack.	94
50	X-19, incremental front wing thrust coefficient, due to front propeller wash, with variation in thrust axis angle of attack.	95
51	X-19, incremental rear wing thrust coefficient, due to all wash, with variation in rear thrust axis angle of attack.	96
52	X-19, installed rear wing lift curve.	98
53	X-19, installed rear wing spanwise lift distribution, propellers off.	99
54	X-19, installed rear wing spanwise lift distribution.	100
55	X-19, installed rear wing spanwise lift distribution.	101
56	X-19, installed rear wing spanwise lift distribution.	102
57	X-19, installed rear wing lift curve.	103
58	X-19, installed rear wing spanwise lift distribution, propellers off.	104
59	X-19, installed rear wing spanwise lift distribution.	105
60	X-19, installed rear wing spanwise lift distribution.	106

LIST OF ILLUSTRATIONS (CONT'D)

FIGURE NO.		PAGE
61	X-19, installed rear wing spanwise lift distribution.	107
62	X-19, installed rear wing lift curve.	108
63	X-19, installed rear wing spanwise lift distribution.	109
64	X-19, installed rear wing lift curve.	110
65	X-19, installed rear wing spanwise lift distribution.	111
66	X-19, front propeller thrust coefficient.	112
67	X-19, rear propeller thrust coefficient.	113
68	X-19, front propeller power coefficient.	114
69	X-19, rear propeller power coefficient	115
70	X-19, airplane lift characteristics, ground effects.	117
71	X-19, airplane drag characteristics, ground effects.	118
72	X-19, airplane moment characteristics, ground effects; c.g. @ 42.8% lift chord and W.L. 123.8 inches.	119
	SECTION IV	123
73	Blade characteristics of the Curtiss-Wright X-100 propeller 3(X100188) blade; Dia. = 10 ft., AF = 188, IC_{L_i} = 0.068.	124
74	Blade characteristics of the X-19 propeller 3(130168) blade; Dia. = 13 ft., AF = 168, IC_{L_i} = 0.057.	125
75	Power loading as a function of disk loading on a static isolated propeller; density ratio σ = 1.0.	126
76	Typical drag polar as a function of design C_L.	128
77	Blade angle and thrust coefficient as a function of power coefficient, static performance, 3(X100188) blade, 500 to 800 πnD.	132
78	Thrust coefficient as a function of power coefficient, static whirl test dated 7/19/60, WPAFB whirl rig No. 2; Model 138592/10188A2F, Dia. = 10 ft., AF = 188, IC_{L_i} = 0.068; 1000 horsepower, NACA 64 section series.	133
79	Blade angle as a function of power coefficient, static whirl test dated 7/9/60, WPAFB whirl rig No. 2; Model 138542/10188A2F, Dia. = 10 ft., AF = 188, IC_{L_i} = 0.068; 1000 horsepower.	134
80	X-19 thrust coefficient as a function of power coefficient, static, Wright Field whirl rig No. 2; 3(1368A10P3), Dia. = 13 ft., AF = 168, IC_{L_i} = 0.057, NACA 64 Series sections, 1000 horsepower.	135

LIST OF ILLUSTRATIONS (CONT'D)

FIGURE NO.		PAGE
81	X-19, propeller blade angle as a function of power coefficient, static, Wright Field Whirl Rig. No. 2; 3(13168A10P3), Dia. = 13 ft. AF = 168, IC_{L_i} = 0.057. NACA 64 Series sections, 1000 horsepower.	133
82	X-19, Figure of Merit as a function of power coefficient, static, Wright Field Whirl Rig. No. 2; 3 (13168A10P3), Dia. = 13 ft., AF = 168, IC_{L_i} = 0.057, NACA 64 series sections, 1000 horsepower.	137
83	X-19, thrust coefficient versus power coefficient, static; 3(13168A10P3) blade, Curtiss Wright Whirl Test Rig.	139
84	X-19, propeller blade angle versus power coefficient, static; 3(13168A10P3) blade, Curtiss Wright Whirl Test Rig.	140
85	Propeller cruise efficiency map, Curtiss-Wright X-100 propeller, 3(X100188); AF = 188 Dia. = 10 ft., IC_{L_i} = 0.057, forward Mach No. 0.3 or less.	141
86	X-19, propeller cruise efficiency map, 3(13168A10P3) blade; AF = 168, Dia. = 13 ft., IC_{L_i} = 0.057, forward Mach No. = 0.3 or less.	142
87	X-19, propeller cruise efficiency map, 3(13168A10P3) blade; AF = 168, Dia. = 13 ft., IC_{L_i} = 0.057, forward Mach No. = 0.4.	143
88	X-19, propeller cruise efficiency map, 3(13168A10P3) blade; AF = 168, Dia. = 13 ft., IC_{L_i} = 0,057, forward Mach No. = 0.5.	144
89	X-19, propeller cruise efficiency map, 3(13168A10P3) blade; AF = 168, Dia. = 13 ft., IC_{L_i} = 0.057, forward Mach No. = 0.6.	145
90	X-19, propeller cruise efficiency map, 3(13168A10P3) blade; AF = 168, Dia. = 13 ft., IC_{L_i} = 0.057, forward Mach No. = 0.7.	146
91	X-19, propeller cruise efficiency map, 3(13168A10P3) blade; AF = 168, Dia. = 13 ft., IC_{L_i} = 0.057, forward Mach No. 0 8.	147
92	Blade characteristics of the Curtiss-Wright 109652 propeller blade; Dia. = 15 ft., AF = 115, IC_{L_i} = 0.5, NACA 65 section series.	148
93	Figure of merit of the Curtiss-Wright 109652 propeller blade as a function of power coefficient measured on Curtiss-Wright Test Rig.	150
94	Effect of blade retwist on the Figure of Merit; 3(109652) blade, 900 πnD, three blades.	151
95	X-19, histogram of transverse shaft loading flight No. 31, 12/23/64.	152

LIST OF ILLUSTRATIONS (CONT'D)

FIGURE NO.		PAGE
96	X-19 histogram of transverse shaft loading, flight No. 35, 1/7/65.	153
	SECTION V	157
97	X-19, schematic assembly of the blade pitch change mechanism.	158
98	Blade schematic illustrating the typical construction of the lightweight fiberglass blade.	163
99	Fiberglass blade repair chart illustrating the type of repair that can be performed in the field.	165
100	X-19, experimental program as scheduled for the airplane, subsystems and components.	169
101	Strength to weight comparison between fiberglass and other common structural materials.	172
102	Fiberglass propeller blades which have been built and tested. From left to right: 10'-10" diameter used on X-100 aircraft, 13'-0" diameter used on X-19 aircraft, 13'-6" diameter used in static thrust testing, 13'-6" designed/for T-64 engine tested to 4000 HP, 15'-6" designed for T-64 tested to 4400 HP.	173
103	Sectioned fiberglass propeller blade showing the steel shank, fiberglass shell, and foam filler.	174
104	Epoxy fiberglass, ultimate tensile stress and tensile modulus, variation with temperature, 1 layer Stanpreg VET 181 per CPS 5037, 3 layers Stanpreg VET 43 per CPS 5038, 17 ply thickness: ASTM: D638-60T.	175
105	Epoxy fiberglass, ultimate flexural stress and modulus variation with temperature, 1 layer Stanpreg VET 181 per CPS 5037, 3 layers Stanpreg VET 43 per CPS 5038, 17 ply thickness: ASTM: D790-59T.	176
106	Epoxy fiberglass, typical tensile stress strain curve longitudinal direction, 1 layer Stanpreg VET 181 per CPS 5037, 3 layers Stanpreg VET 43 per CPS 5038, 17 ply thickness: ASTM: D638-60T.	177
107	Epoxy fiberglass, tensile stress rupture, standard room temperature, standard humidity and 100% humidity, 1 layer Stanpreg VET 181 per CPS 5037, 3 layers Stanpreg VET 43 per CPS 5038, 17 ply thickness: ASTM: D674-56.	178
108	Epoxy fiberglass, creep rupture curve longitudinal tension, tensile stress = 75000 psi. 1 layer Stanpreg VET 181 per CPS 5037, 3 layers Stanpreg VET 43 per CPS 5038, 17 ply thickness: ASTM: 674-56.	179

LIST OF ILLUSTRATIONS (CONT'D)

FIGURE NO.		PAGE
109	Epoxy figerblass, interlaminar shear variation with temperature, 1 layer Stanpreg VET 181 per CPS 5037, 3 layers Stanpreg VET 43 per CPS 5038, 17 ply thickness: Fed. Test Method Std. 406.	180
110	Epoxy fiberglass, flexural fatigue S-N curves for smooth and notched longitudinal specimens and smooth transverse specimens at room temperature, 1 layer Stanpreg VET 181 per CPS 5037, 3 layers Stanpreg VET 43 per CPS 5038, 17 ply thickness: ASTM: D671-517.	181
111	Epoxy fiberglass, modified Goodman diagram with longitudinal and transverse directions, 1 layer Stanpreg VET 181 per CPS 5037, 3 layers Stanpreg VET 43 per CPS 5038, 17 ply thickness : ASTM: D671-51T.	182
112	Epoxy fiberglass, design modified Goodman diagram as established for propeller blades, 1 layer Stanpreg VET 181 per CPS 5037, 3 layers Stanpreg VET 43 per CPS 5038.	183
113	Comparative erosion resistance of various coating materials on fiberglass.	184
114	The effect of immersion in various solvents for 7 days on the ultimate tensile strength of epoxy fiberglass with and without urethane coating.	185
115	The strength characteristics of the various adhesives selected for use in the manufacture of fiberglass reinforced plastic blades.	186
116	Typical properties of foam plastic filler as used in the fiberglass foam plastic blade. Polyether base - freon blown, A = 7.0 lbs per ft^3, B = 5.0 lb per ft^3.	188
117	Steel shank as designed for the 13166A10P3 blade. AMS 6415 vacuum melt steel, RC 42-46.	189
118	Typical shank end cracks which occurred during fabrication and which were attributed to hydrogen embrittlement.	191
119	The 13166A10P3 blade steady stress distribution for a pitching maneuver during transition flight; 927HP, 1065 rpm, 80 knots.	203
120	The 13166A10P3 blade vibratory stress distribution for a pitching maneuver during transition flight; 927HP, 1065 rpm, V = 80 knots.	204
121	Comparison of the calculated and measured steady stress distribution around the 11 in. station in the 13166A10P3 blade. Centrifugal load = 46,000 lb, bending moment = 24000 in. lb.	207

LIST OF ILLUSTRATIONS (CONT'D)

FIGURE NO.		PAGE
122	Comparison of the calculated and measured vibratory stress distribution around the 11 in. station on the 13166A10P3 blade. Bending moment = ± 66,000 in.-lbs.	208
123	Calculated fixed root resonant frequencies of the 13166A10P3 fiberglass propeller blade.	209
124	Laboratory test set up for endurance testing propeller blades in the free-free mode.	211
125	Typical blade failure obtained in free-free endurance testing. This blade completed 10 X 10^6 cycles at each of ± 8000, ± 9000, ± 10,000, and ± 11,000 psi. Failure occurred at 1.2 X 10^6 cycles at the ± 12,000 psi level.	214
126	Laboratory test set up for fixed root endurance testing of propeller blades.	216
127	Typical blade fatigue failure obtained during fixed root endurance testing of the X-19 propeller blade.	217
128	Laboratory test set up for free-free torsion endurance testing of propeller blades.	218
129	Fatigue failure on blade P42-6 after 1.0 X 10^6 cycles of torsional endurance testing on blade P42-6.	220
130	Laboratory test set up for static tension test of the X-19 propeller unbonded blade shank.	222
131	X-19, propeller unbonded blade shank failure. Ultimate load was 128,000 lbs.	223
132	Blade retention, laboratory fatigue test set up. This facility simultaneously applies centrifugal force, steady bending moment, and vibratory bending moment.	224
133	Typical fatigue failure of the X-19 blade shank.	227
134	Basic velocity components at the disk of a tilted propeller disk.	229
135	Comparison of the propeller yawing and pitching moment coefficients at flow angularities close to 90°, and at low advance ratios, $\beta_{.75R} = 15°$.	235
136	Comparison of propeller normal and side force coefficients at flow angularities close to 90° at low advance ratios, $\beta_{.75R} = 15°$.	236
137	Comparison of calculated and measured blade vibratory shank stress for equilibrium transition flight of the X-19 aircraft.	237

LIST OF ILLUSTRATIONS (CONT'D)

FIGURE NO.		PAGE
138	Relative blade weight comparison considering various materials for the design of a hypothetical VTOL/STOL propeller; 15'-0" diameter, 120 A.F., 1000 HP @ 1146 rpm.	239
139	Relative blade weight comparison considering various materials for the design of a typical turboprop installation; 13'-6" diameter, 150 A.F., 4000 HP @ 1160 rpm.	240
140	Variation of blade weight with 1 X P excitation factor, Aq, for hollow steel and fiberglass blades on a typical turboprop installation; 13'-6" diameter, 165 A.F., 4500 HP 1020 rpm.	241
141	The 2 X P component of blade stress as measured during flight test on the X-19 aircraft showing a resonant trend with rpm.	250
142	Variation of the 2 X P blade stress component with rpm as measured during a ground vibration survey on the X-19 aircraft.	251
143	Variation of the 2 X P blade stress as measured during flight test of the X-19 aircraf as a function of the theoretical 2 X P parameter, $(V \sin\phi)^2 \sin\beta$.	253
144	Laboratory test facility for the static testing of propeller hubs under simulated flight steady and vibratory loading.	255
145	Stress coat patterns appearing on the X-19 propeller hub under a simulated design steady/ vibratory load condition.	256
146	Location of wire strain gages around outer circumference of barrels of X-19 propeller hub 162595 during static testing in hub tension machine.	258
147	Location of wire strain gages around inner and outer periphery of ring of X-19 propeller hub 162595 during static testing in hub tension machine.	259
148	Location of wire strain gages on inner and outer surfaces of rear extension of X-19 propeller hub 162595 during static testing in hub tension machine.	260
149	X-19, propeller hub showing typical location of strain gages during static test.	261
150	Laboratory whirl test facility for qualifying the propeller nacelle assembly under simulated loading.	263
151	Maximum composite blade stress taken during propeller thrust calibration on WPAFB Electric Whirl Rig.	269

LIST OF ILLUSTRATIONS (CONT'D)

FIGURE NO.		PAGE
152	Blade stress monitoring curve taken during propeller endurance test on WPAFB electric whirl rig.	270
153	Curtiss gyroscopic test facility for qualifying full scale propellers under simulated steady and vibratory loading.	273
154	X-19 blade modified Goodman diagram showing design and gyroscopic test points.	275
155	X-19 blade vibratory stresses as monitored during the gyroscopic endurance testing.	278
156	Curtiss half systems test rig for qualifying the propulsion system of the X-19.	279
	SECTION VI	283
157	X-19, block diagram of the propeller thrust modulation system.	284
158	X-19, coordinator output stroke as a function of pitch control deflection or SAS motion.	285
159	X-19, coordinator output stroke as a function of pilot pitch trim actuator displacement.	286
160	X-19, coordinator output stroke as a function of roll control deflection or SAS motion.	287
161	X-19, coordinator output stroke as a function of yaw control (pedal) deflection.	288
162	X-19, coordinator output stroke as a function of tilt angle (auto-trim schedule).	289
163	X-19, propeller pitch control gain as a function of tilt angle (pitch-gain schedule).	291
164	X-19, propeller roll control gain as a function of tilt angle (roll-gain schedule).	292
165	X-19, propeller yaw control gain as a function of tilt angle (yaw-gain schedule).	293
166	X-19, coordinator output stroke as a function of governor collective shaft displacement.	294
167	X-19, nacelle input arm position as a function of coordinator output stroke.	295
168	X-19, propeller blade angle as a function of nacelle input arm position.	297
169	X-19, hover control moment response due to a pilot commanded step input of pitch, roll or yaw control.	298
170	X-19, propeller blade angle relationships due to control column application.	300
171	X-19, roll coupling generated by a yaw control input.	302
172	X-19, pitch coupling generated by roll or yaw control input; V = 0 fps.	303

LIST OF ILLUSTRATIONS (CONT'D)

FIGURE NO.		PAGE
173	X-19, distribution of forces due to a roll control input (maximum aileron).	304
174	X-19, distribution of forces due to a yaw control input (maximum rudder).	305
175	X-19, aircraft pitching moment characteristics at $\emptyset_F$ = 20°, including airframe and propeller contributions; c.g. = 42.8% lift chord.	306
176	X-19, aircraft pitching moment characteristics at $\emptyset_F$ = 40°, including airframe and propeller contributions; c.g. = 42.8% lift chord.	307
177	X-19, aircraft pitching moment characteristics at $\emptyset_F$ = 60°, including airframe and propeller contributions; c.g. = 42.8% lift chord.	308
178	X-19, aircraft pitching moment characteristics at $\emptyset_F$ = 82.5%, including airframe and propeller contributions; c.g. = 42.8% lift chord.	309
179	X-19, time history of hover thrust response to a step power lever input, original and modified system.	314
	SECTION VII	319
180	X-19, damping characteristics of the longitudinal short period mode through transition with SAS off; W = 12,300 lb., Height = Sea Level.	330
181	X-19, damping characteristics of the Dutch Roll mode through transition with SAS off; W = 12,300 lb., Height = Sea Level.	331
182	X-19, migration of the longitudinal short period mode roots through transition with SAS off; W = 12,300 lb., Height = Sea Level, Start cruise/end transition c.g. = 42% lift chord.	332
183	X-19, migration of the longitudinal phugoid mode roots through transition with SAS off; W = 12,300 lb., Height = Sea Level. Start cruise/end transition c.g. = 42% lift chord.	333
184	X-19, migration of the roots of the lateral directional modes through transition with SAS off; W = 12,300 lb., Height = Sea Level. Start cruise/end transition c.g. = 42% lift chord.	334
185	X-19, variation of available pitch control power and required trim moments through transition.	336
186	X-19, variation of available roll control power through transition.	337
187	X-19, variation of available yaw control power through transition.	338

LIST OF ILLUSTRATIONS (CONT'D)

FIGURE NO.		PAGE
188	X-19, power-on lift and pitching moment characteristics in cruise configuration based on wind tunnel data; c.g. = 42.9% lift chord.	340
189	X-19, power-on sideforce characteristics in cruise configuration based on wind tunnel data; $\alpha_{fus} = 0°$.	341
190	X-19, power-on yawing moment characteristics in cruise configuration based on wind tunnel data; c.g. = 42.9% lift chord, $\alpha_{fus} = 0°$.	342
191	X-19, power-on rolling moment characteristics in cruise configuration based on wind tunnel data; c.g. = 42.9% lift chord, $\alpha_{fus} = 0°$.	343
192	X-19, damping characteristics of the longitudinal short period mode in cruise; W = 12,300 lb., Height = Sea Level.	344
193	X-19, damping characteristics of the longitudinal short period mode in cruise; W = 12,300 lb., Height = 15,000 ft.	345
194	X-19, damping characteristics of the Dutch Roll mode in cruise; W = 12,300 lb., Height = Sea Level.	346
195	X-19, damping characteristics of the Dutch Roll mode in cruise; W = 12,300 lb., Height = 15,000 ft.	347
196	X-19, damping characteristics of the Dutch Roll mode in cruise; W = 12,300 lb., Height = 25,000 ft.	348
197	X-19, elevator hinge moment characteristics in cruise.	350
198	X-19, aileron hinge moment characteristics in cruise; $\alpha_{fus} = 0°$.	352
199	X-19, rudder hinge moment characteristics in cruise; $\alpha_{fus} = 0°$.	353
200	X-19, cruise elevator trim settings in level flight at 15,000 ft; W = 12,300 lb. and 13,500 lb., c.g. = 39%, 42% lift chord.	354
201	X-19, cruise elevator angle per 'g' at 15,000 ft; W = 12,300 lb., 13,500 lb., c.g. = 39% and 42% lift chord.	356
202	X-19, roll performance in cruise; steady roll rate and wing tip helix angle with a stick force of 25 lb.	357
203	X-19, roll performance in cruise; bank angle attained one second after an instantaneous aileron deflection with a stick force of 25 lb.	358
204	X-19, roll performance in cruise; roll time constant.	359

LIST OF ILLUSTRATIONS (CONT'D)

FIGURE NO.		PAGE
205	X-19, effect of power and trim on the induced drag factor ($\partial C_D / \partial C_L^2$) in cruise.	364
206	X-19, effect of Mach Number and altitude on minimum cruise drag coefficient.	365
207	X-19, components of total cruise drag coefficient.	367
208	X-19, effect of speed and altitude on cruise lift-drag ratio; W = 13,660 lb.	368
209	X-19, effect of weight and altitude on cruise lift-drag ratio; V = 300 knots TAS.	369
210	Horizontal c.g. envelope for the basic 13,660 lb. design gross weight aircraft.	377
211	X-19, recommended tilt velocity schedule.	380
212	X-19, flap deflection schedule, forward lift strut.	382
213	X-19, collective aileron schedule, rear lift strut.	383
214	X-19, coordinator auto-trim schedule.	384
215	X-19, coordinator pitch-gain schedule.	385
216	X-19, coordinator roll-gain schedule.	387
217	X-19, coordinator yaw-gain schedule.	388
	SECTION VIII	391
218	Estimated hover ground effect pressure distribution for the X-200 configuration.	395
219	Comparison of ground effect augmentation of hover lift of two different types of VTOL testbed aircraft.	397
	SECTION IX	399
220	0.12 scale model of the Curtiss-Wright X-19 configuration mounted in the NACAL wind tunnel.	403
221	Longitudinal aerodynamic characteristics of the 0.12 scale model of the Curtiss-Wright X-19, power on and power off, MIT-1019 runs 28 and 100.	408

LIST OF ILLUSTRATIONS (CONT'D)

FIGURE NO.		PAGE
222	Drag characteristics of the 0.12 scale model of the Curtiss-Wright X-19.	409
223	Directional and lateral stability characteristics of the 0.12 scale model X-19 in MIT-1019 cruise simulation.	410
224	NACAL low speed tunnel X-19 type model installation for NACAL-93 wind tunnel tests.	415
225	NACAL-93 test data to demonstrate the effect of propeller and propeller speed in pitch, X-19 cruise configuration.	417
226	NACAL-93 test data to demonstrate the effect of propeller and propeller speed in pitch, X-19 transition configuration.	418
227	NACAL-93 test data to demonstrate the effect of propeller and propeller speed in yaw, X-19 cruise configuration.	419
228	NACAL-93 test data to demonstrate the effect of propeller and propeller speed in yaw, X-19 transition configuration.	420
229	NACAL low speed tunnel X-19 model installation for NACAL-120 wind tunnel tests.	421
230	NACAL-120 test data to demonstrate the effect of ground plane presence on longitudinal characteristics in hover of the X-19 model.	423
231	NACAL-120 test data to demonstrate the effect of nacelle angle on lateral-directional characteristics in hover of the X-19 model.	424
232	Curtiss-Wright test facility for the investigation of over-water aspects of high disk loading VTOL airplanes.	428
233	Installation of the X-100 research aircraft on the NASA 40 x 80 wind tunnel mounts at Ames Research Center.	430
234	Comparison of similar test configurations of the 0.12 scale X-19 model in three different wind tunnels-C_L vs α_{fus}, power off.	434
235	Comparison of similar test configurations of the 0.12 scale X-19 model in three different wind tunnels - C_D vs α_{fus}, power off.	435
236	Comparison of similar test configurations of the 0.12 scale X-19 model in three different wind tunnels - C_M vs α_{fus}, power off.	436
237	Comparison of similar test configurations of the 0.12 scale X-19 model in three different wind tunnels - C_l vs ψ, power off.	437
238	Comparison of similar test configurations of the 0.12 scale X-19 model in three different wind tunnels - C_n vs ψ, power off.	438

LIST OF ILLUSTRATIONS (CONT'D)

FIGURE NO.		PAGE
239	Comparison of similar test configurations of the 0.12 scale X-19 model in three different wind tunnels - C_y vs ψ , power off.	439
240	Comparison of calculated and test data of X-100 propeller blade angle and thrust coefficient versus power coefficient at static condition.	441
241	Comparison of X-100 full scale and model propeller data in terms of C_T and C_p.	442
242	X-100 maximum values of propeller figure of merit at various reynolds numbers based on full-scale and model test data.	443
	SECTION X	447
243	X-19, fuselage lift coefficient characteristics; S_{ref} = 154.6 sq. ft.	449
244	X-19, exposed front wing lift coefficient; S_{ref} = 154.6 sq. ft.	450
245	X-19, exposed rear wing lift coefficient; S_{ref} = 154.6 sq. ft., (external to BL 16.7 inches).	451
246	X-19, nacelle lift coefficients; S_{ref} = 154.6 sq. ft.	452
247	X-19, lift coefficient of complete airplane-propellers off; S_{ref} = 154.6 sq. ft.	453
248	X-19, pitching moment coefficient of fuselage alone about the 42.9 percent c.g.; S_{ref} = 154.6 sq. ft., $\bar{c}$ = 2.875 ft.	454
249	X-19, exposed front and rear wing pitching moments about respective quarter chords; S_{ref} = 154.6 sq. ft., $\bar{c}$ = 2.875 ft.	455
250	X-19, nacelle pitching moments about respective wing quarter chords; S_{ref} = 154.6 sq. ft., $\bar{c}$ = 2 875 ft.	456
251	X-19, pitching moment of complete airplane about the 42.9 percent c.g., propellers off; S_{ref} = 154.6 sq. ft., $\bar{c}$ = 2.875 ft.	457
252	X-19, propeller lift coefficients, front and rear; S_{ref} = 154.6 sq. ft.	458
253	X-19, propeller pitching moment coefficients front and rear; S_{ref} = 154.6 sq. ft., $\bar{c}$ = 2.875 ft.	459
254	X-19, propeller side force and yawing moment coefficient, S_{ref} = 154.6 sq. ft., $\bar{c}$ = 2.875 ft.	460
255	Propeller sign convention.	461
256	X-19, aeroelastic wing and propeller twist derivatives	462

LIST OF ILLUSTRATIONS (CONT'D)

FIGURE NO.		PAGE
257	X-19, V-n diagram, W = 13,660 pounds.	466
258	X-19, gust envelope; W = 13,660 pounds.	468
259	Diagrammatic representation of aerodynamic cruise loads.	469
260	X-19, rear wing lift coefficients based on S = 85.74 sq. ft. (exposed) area; NACA 643-418 airfoil modified.	472
261	X-19, rear wing spanwise lift distribution - propellers off.	473
262	Effects of fuselage upon the wing $\partial C_L/\partial \alpha$; wing located along fuselage x/L; various body width ratios; based on clear through wing area; z/h = 0.907.	476
263	Effects of fuselage upon wing angle of zero lift; parameters: x/L, b/W, z/h = 0.907.	477
264	X-19, fuselage and nacelle wash effects upon the rear wing at 77 percent chord position.	478
265	X-19, rear wing chordwise pressure distribution- propellers off; ϕ_F = -3 degrees.	479
266	X-19, rear wing chordwise pressure distributions- propellers off; ϕ_F = -3 degrees, α_{fus} = +2 degrees.	480
267	X-19, fuselage induced wash derivative on rear wing due to sideslip, at 77 percent chord position.	482
268	X-19, center of gravity envelope, based on empty weight.	484
269	X-19, hover transmission limit - allowable forward center of gravity position at thrust to weight = 1.0.	485
270	X-19, propeller horsepower histogram (hover).	486
271	X-19, tee-box horsepower histogram (hover).	487
272	X-19, transition lift coefficient characteristics; ϕ_F = 82.5°, V = 49 knots, 819 πnD, neutral stick.	490
273	X-19, transition lift coefficient characteristics; ϕ_F = 82.5°, V = 49 knots, 725 πnD, neutral stick.	491
274	X-19, transition lift coefficient characteristics; ϕ_F = 60°, V = 85 knots, 725 πnD , neutral stick.	492
275	X-19, transition lift coefficient characteristics; ϕ_F = 40°, V = 102 knots, 725 πnD , neutral stick.	493
276	X-19, transition lift coefficient characteristics; ϕ_F = 20°, V = 120 knots, 725 πnD , neutral stick.	494
277	X-19, transition drag coefficient characteristics; ϕ_F = 82.5°, V = 49 knots, 819 πnD , neutral stick.	496
278	X-19, transition drag coefficient characteristics; ϕ_F = 82.5°, V = 49 knots, 725 πnD , neutral stick.	497
279	X-19, transition drag coefficient characteristics; ϕ_F = 60°, V = 85 knots, 725 πnD , neutral stick.	498

LIST OF ILLUSTRATIONS (CONT'D)

FIGURE NO.		PAGE
280	X-19, transition drag coefficient characteristics; ϕ_F = 40°, V = 102 knots, 725 πnD , neutral stick.	499
281	X-19, transition drag coefficient characteristics; ϕ_F = 20°, V = 120 knots, 725 πnD , neutral stick.	500
282	X-19, transition pitching moment coefficient characteristics; ϕ_F = 82.5°, V = 49 knots, c.g. = 42.8%, neutral stick, 725 and 819 πnD.	501
283	X-19, transition pitching moment coefficient characteristics; ϕ_F = 60°, V = 85 knots, c.g. = 42.8%, neutral stick, 725 πnD.	502
284	X-19, transition pitching moment coefficient characteristics; ϕ_F = 40°, V = 102 knots, c.g. = 42.8%, neutral stick, 725 πnD.	503
285	X-19, transition pitching moment coefficient characteristics; ϕ_F = 20°, V = 120 knots, c.g. = 42.8%, neutral stick, 725 πnD.	504
286	X-19, transition front and rear propeller trim powers; ϕ_F = 82.5°, V = 49 knots, 725 πnD , c.g. = 42.8%.	506
287	X-19, transition front and rear propeller trim powers; ϕ_F = 60°, V = 85 knots, 725 πnD , c.g. = 42.8%.	507
288	X-19, transition front and rear propeller trim powers; ϕ_F = 40°, V = 102 knots, 725 πnD , c.g. = 42.8%.	508
289	X-19, transition front and rear propeller trim powers; ϕ_F = 20°, V = 120 knots, 725 πnD , c.g. = 42.8%.	509
290	X-19, effects of c.g. location on stick position; ϕ_F = 60°, πnD = 725, V = 85 knots, W = 13,660 pounds.	510
291	X-19, effects of πnD variation upon trim; ϕ_F = 60°, V = 85 knots, W = 13,660 pounds, c.g. = 41%.	511
292	X-19. effects of πnD variation upon trim; ϕ_F = 40°, W = 12,300 pounds, V = 102 knots, c.g. = 42.8%.	512
293	X-19, effects of c.g. location upon trim; ϕ_F = 40°, πnD = 725, V = 102 knots.	513

FIGURE NO.	SECTION XI	PAGE
294	X-19, hover operating envelope, single engine failure.	518
295	X-19, cruise windmilling descent, trim characteristics; W = 12,300 pounds, c.g. = 42.9 percent; ϕ_F = 16.3°, $\beta_{.75R}$ = 51 degrees.	521
296	X-19, cruise windmilling descent angle; W = 12,300 pounds, c.g. = 42.9 percent, ϕ_F = 16.3°, $\beta_{.75R}$ = 51 degrees.	522
297	X-19, cruise windmilling rate of descent flares; W = 12,300 pounds, c.g. = 42.9 percent, ϕ_F = 16.3 degrees, $\beta_{.75R}$ = 51 degrees.	523
298	X-19, cruise windmilling flared flight paths; W = 12,300 pounds, c.g. = 42.9 percent, ϕ_F = 16.3°, $\beta_{.75R}$ = 51°, α_{fus} = 14.4°.	525
299	X-19, windmilling lift coefficient characteristics at ϕ_F = 16.25°, S_{ref} = 154.6 sq. ft., δ_F = 23.2°, $\delta_{a_{coll}}$ = 21.5°.	526
300	X-19, windmilling drag coefficient characteristics at ϕ_F = 16.25°, S_{ref} = 154.6 sq. ft., δ_F = 23.2°, $\delta_{a_{coll}}$ = 21.5°.	527
301	X-19, windmilling moment coefficient characteristics at ϕ_F = 16.25°; S_{ref} = 154.6 sq. ft., c.g. = 42.9%, δ_F = 23.2°, $\delta_{a_{coll}}$ = 21.5°.	528
302	Thrust coefficient characteristics at tilt angle of 140°, CWC blade 3(156109), AF 115, IC_{L_i} = 0.482.	531
303	Thrust coefficient characteristics at tilt angle of 160°, CWC blade 3(156109), AF 115, IC_{L_i} = 0.482.	532
304	Thrust coefficient characteristics at tilt angle of 180°, CWC blade 3(156109), AF 115, IC_{L_i} = 0.482.	533
305	Blade characteristics of CWC 3(156109); AF 109, IC_{L_i} = 0.482.	534
	SECTION XII	535
306	Flight test schedule, X-19 S/N 62-12197.	543
307	X-19 flight No. 50, track velocity history (theodolite digital data).	549
308	X-19 flight No. 50, altitude time history (theodolite digital data).	551
309	X-19 flight No. 50, climb velocity vs. time (theodolite digital data).	553
310	X-19 flight No. 50, resultant velocity vs. time (theodolite digical data).	554

LIST OF ILLUSTRATIONS (CONT'D)

FIGURE NO.		PAGE
311	X-19 flight No. 50, in-flight acceleration vs. time (theodolite digital data).	555
312	X-19 flight No. 50, vertical acceleration vs. time (theodolite digital data).	556
313	X-19 flight No. 50, bank angle (theodolite film data).	557
314	X-19 flight No. 50, pitch angle and component of yaw angle (theodolite film data).	558
315	X-19 flight No. 50, roll and pitch rate (theodolite film data).	559
316	X-19 flight No. 50, front and rear nacelle angles (theodolite film data).	560
317	X-19 flight No. 50, excess thrust horsepower absorbed (average theodolite trace and digital data).	561
318	X-19 S/N 62-12197 in conversion flight at 90 kts.	562
319	X-19 S/N 62-12197 in hover flight.	563
320	X-19, flight speed range tested for steady level flight, test velocity vs. schedule velocity.	577
321	X-19, test power required for steady level flight, PIW_N vs. VIW.	579
322	X-19, test front nacelle power required for steady level flight, PIW_{N_F} vs. VIW.	580
323	X-19, test rear nacelle power required for steady level flight, PIW_{N_R} vs. VIW.	581
324	X-19, ground run No. 96, thrust coefficient and blade angle vs. power coefficient.	584
325	X-19, flights Nos. 8 thru 22, thrust coefficient vs. power coefficient for steady hover and translational flight.	585
326	X-19, test installation for ground effect tuft study.	586
327	X-19, ground run No. 97, thrust transient following throttle chop.	588
328	Estimated descent velocity vs. time following a single engine failure in hover (based on X-19 ground run No. 97).	589
329	Estimated altitude lost vs. time following a single engine failure in hover (based on X-19 ground run No. 97).	590
330	Estimated descent velocity vs. altitude lost following a single engine failure in hover (based on X-19 ground run No. 97).	591
331	X-19, category I flight test program. Scope of configuration testing thru January 1965.	594

LIST OF ILLUSTRATIONS (CONT'D)

FIGURE NO.		PAGE
332	X-19, low speed longitudinal handling qualities, with S.A.S. "off" in both axes (pilot: J. V. Ryan).	595
333	X-19, low-speed lateral handling qualities, with S.A.S. "off" in both axes (pilot: J. V. Ryan).	596
334	X-19, pilot opinion rating as a function of airspeed; pitch axis. Electronic pitch S.A.S. "on."	598
335	X-19, pilot opinion rating as a function of airspeed; roll axis. Electronic roll S.A.S. "on."	599
336	X-19, pilot opinion rating as a function of airspeed; yaw axis. No stability augmentation.	600
337	X-19, pilot opinion rating as a function of airspeed; height control. Height control system "on."	601

LIST OF TABLES

TABLE		PAGE
I	X-100 VTOL airplane characteristics.	33
II	Comparison between calculated and test values of radial force, R.	44
III	X-19, rear wing download test conditions.	61
IV	Blade design 13166A10P3; general design data and summary.	192
V	Blade design 13166A10P3; blade section characteristics data.	193
VI	Blade design 13166A10P3; summary of blade structural and mass section properties (equivalent to fiberglass).	195
VII	Blade design 13166A12P3; summary of blade structural and mass section properties (equivalent to fiberglass).	200
VIII	Design propeller shaft loads 13166A10P3 blade, X-19 aircraft.	201
IX	Summary, structural analysis; 13166A10P3 blade design, design loads for 12,300 lb. airplane G.W.	205
X	Tabulation of endurance history; 13166A10P3 blades.	212
XI	Maximum composite stresses in X-19 propeller hub 162595.	262
XII	Gage layout.	268
XIII	Vibratory and steady stress summary, X-19 blades.	277
XIV	X-19 PFVT, 13,660 lb. gross weight flight cycle.	281
XV	Stick - fixed equations of motion.	320
XVI	Formulae for the X-19 stability derivitives.	322
XVII	Incompressible power-off profile drag breakdown.	362
XVIII	Historical breakdown X-19 S/N 62-12197.	537
XIX	Typical multiplexed temperature record schedule.	572
XX	Typical test instrumentation oscillograph schedule.	573
XXI	Typical X-19 S/N 62-12197 photo panel parameter schedule.	574
XXII	Cooper Rating Scale	597

SECTION VII NOMENCLATURE

For consistency and convenience the terminology used throughout is generally that of (45), which is as follows:

Symbols

a	lift curve slope,	per rad
A_F, A_R	inflow angle of the front and rear propellers respectively,	radians
A,B,C	moment of inertia about (x,y,z) axes,	slug-ft^2
b_f,b_r	span of front and rear wings, respectively,	ft
$\bar{c}$	mean aerodynamic chord,	ft
C_D	drag coefficient, (= Drag/1/2 ρV^2 S)	
C_L	lift coefficient, (= Lift/1/2 ρV^2 S)	
C_R	radial force coefficient, (= radial force/1/2 ρV^2 S_p)	
C_1,C_2	constants obtained from NACA TR 1098 in connection with wing contribution to C_{n_p} and C_{l_r}, respectively.	
E	product of inertia, $\int xz\, dm$,	slug-ft^2
H	hinge moment, positive when tending to rotate control surface to a more positive deflection,	ft-lb
h_{P_F},h_{P_R}	vertical distance from airplane mass center to hub centers of front and rear propellers, respectively,	ft
K_1	fraction of rear propeller disk influenced by front wing downwash	
K_2	constant obtained from NACA TR 1098 in connection with wing contribution to C_{n_r}	
l	characteristic length,	ft
l_v	distance along airplane horizontal reference line between airplane mass center and aerodynamic center of vertical tail,	ft

System of Nondimensionalizing

(1) Dimensional Quantity	(2) Divisor	(3) Non-Dimensional Quantity = (1)/(2)
X Y Z	$\frac{1}{2}\rho v^2 S$	C_x C_y C_z
L M N	$\rho v^2 Sl$	C_l C_m C_n
H_a H_e H_r	$\frac{1}{2}\rho v^2 S_f C_f$	C_{h_a} C_{h_e} C_{h_r}
u v w	u_o	$\hat{u}$ β α
p q r	1/t*	$\hat{p}$ $\hat{q}$ $\hat{r}$
$\dot{\beta}$ $\dot{\alpha}$	1/t*	D_β D_α
A B C E	Sl^3	i_A i_B i_C i_D

$D = \frac{d}{dt} = t^* \frac{d}{dt}$

For longitudinal case: $l = \frac{\bar{c}}{2}$

For lateral case: $l = \frac{b_f}{2}$

Symbols

L,M,N	external moments about the airplane's mass center, positive for moments tending to cause a right roll, pitch up, nose to the right,	ft-lb
L_v	rate of change of rolling moment with lateral velocity,	ft-lb/ft/sec
M	airplane flight Mach number	
M_u	rate of change of pitching moment with forward velocity	
N	number of propellers	
$N_{\frac{1}{10}}$	cycles to damp to one tenth amplitude	
N_ψ	rate of change of yawing moment with yaw rate,	ft-lb/rad/sec
P,Q,R	aircraft angular velocity about the (x,y,z) axis; positive for right roll, pitch up, right yaw,	rad/sec
p,q,r	perturbation of (P,Q,R),	rad/sec
p_{cb}	steady roll rate,	deg/sec
r	when used with a subscript, refers to the distance between the propeller plane and its tilt axis, measured along the propeller axis,	ft
S	total wing planform area, (= S_{W_F} + S_{W_R}),	ft^2
S_p	disk area of one propeller (= $\frac{\pi}{4}$ dia.^{2}),	ft^2
S_v	vertical tail exposed planform area,	ft^2
S_{W_F}	planform area of front wing,	ft^2
S_{W_R}	planform area of rear wing,	ft^2
$t_{1/2}$	time to half or double amplitude,	sec
T	period of oscillation,	sec
T_F,T_R	thrust of one front or one rear propeller, respectively,	lb

Subscripts

F	refers to front
O	refers to reference, i.e. initial, conditions
P	refers to propeller
R	refers to rear or to propeller in-lane (radial) force
T	refers to propeller thrust
TS	refers to propeller thrust-shift moment
v	refers to vertical tail
W	refers to wing
f	refers to fuselage when used as a subscript for α or refers to flap in general in all other usages
e	refers to elevator
a	refers to aileron
r	refers to rudder

Superscripts

$\bar{(\ )}$	refers to a station or waterline coordinate when used on x or z respectively,	inch

Symbols

V_{N_F},V_{N_R}	velocity normal to front and rear propeller disks, respectively,	ft/sec
v_e	equivalent side velocity (= $V_e\beta$) used in conjunction with rolling parameter $\left\|\frac{\phi}{v_e}\right\|$ of Ref. 47*	ft/sec
W	airplane gross weight,	lb
u,v,w	perturbations of (U,V,W),	ft/sec
x_{a_F},x_{a_R}	distance along airplane horizontal reference line from the airplane's mass center to the aerodynamic centers of the front and rear wings, respectively,	ft
x_{P_F},x_{P_R}	distance along airplane horizontal reference line from the airplane's mass center to the hub centers of the front and rear propellers, respectively,	ft
X,Y,Z	components of the resultant aerodynamic force acting on the aircraft,	lb
$\bar{x}_R$, $\bar{z}_R$	reference station and waterline coordinates, respectively,	inch
z_v	vertical distance between the airplane's mass center and the center of pressure of the vertical tail,	ft
z'_v	vertical distance between the airplane's mass center and the tip of the vertical tail,	ft
X_u	rate of change of longitudinal force with forward velocity,	lb/ft/sec
Y_v	rate of change of side force with lateral velocity,	lb/ft/sec
α	angle of attack of fuselage horizontal reference line	
β	angle of sideslip, positive for nose to the left,	radians
δ_a	aileron deflection angle, = 1/2 ($\delta_{a_{up}}$ + $\delta_{a_{down}}$) positive for trailing edge down on right aileron,	radians
δ_e	elevator deflection angle, positive for trailing edge down,	radians
δ_r	rudder deflection angle, positive for trailing edge to the left,	radians
ξ	downwash angle,	radians
η_v	vertical tail efficiency factor	
ϕ_F, ϕ_R	front and rear nacelle tilt angles, respectively measured from the fuselage horizontal reference line,	radians - unless noted as degrees
ξ,η,ζ	perturbations of (δ_a, δ_e, δ_r),	radians
ρ	local mass density of air,	slug/ft^3
σ	sidewash angle, positive when it corresponds to a flow in the positive y-direction,	radians

SECTION VII

TANDEM WING AIRPLANE

1. FLIGHT CONTROL OF TANDEM WING AIRCRAFT

a. Transition Flight Regime

(1) Introduction

The transition regime is defined as the flight region between propellers fully tilted up (hover) and propellers fully tilted down (cruise). This normally corresponds to a speed range from zero to 160 knots.

Throughout transition, the relationship between front and rear nacelle angle of $\emptyset_F = 1.184\ \emptyset_R$ is maintained.

(2) Assumptions

The stick fixed equations of motion contain the following assumptions:

(a) The airplane is a rigid body.

(b) The xz plane through the airplane's center of gravity is a plane of mirror symmetry.

(c) The axes of any number of rigid spinning rotors are fixed in direction relative to the body axes and these rotors have constant angular speed relative to the body axes.

(d) No rotor gyroscopic effects.

(3) Stability

(a) General Procedure

The linearized equations of motion of (45) were used to determine the stick fixed characteristic modes of motion. The equations are written in Table XV for reference.

Solution of these equations, (together with the determination of the stick fixed stability derivatives) was accomplished with the aid of digital computer techniques.

These data were determined for transition (SAS off) at sea level for W = 12,300 lb and the allowable c.g. range.

Table XV. Stick-fixed equations of motion.

Longitudinal:

$$(2\mu D - 2C_{L_0}\tan\Theta_0 - C_{x_u})\hat{u} - C_{x_\alpha}\alpha + C_{L_0}\theta = 0$$

$$(2C_{L_0} - C_{z_u})\hat{u} + (2\mu D - C_{z_{\dot{\alpha}}}D - C_{z_\alpha})\alpha - \left[(2\mu + C_{z_q})D - C_{L_0}\tan\Theta_0\right]\theta = 0$$

$$-C_{M_u}\hat{u} - (C_{M_{\dot{\alpha}}}D + C_{M_\alpha})\alpha + (i_B D^2 - C_{M_q}D)\theta = 0$$

$$\mu = m/\rho S\ell \qquad t^* = \ell/u_0 \qquad \ell = \bar{c}/2$$

Lateral:

$$(2\mu D - C_{y_\beta})\beta - C_{y_p}\hat{p} + (2\mu - C_{y_r})\hat{r} - C_{L_0}\phi = 0$$

$$-C_{\ell_\beta}\beta + (i_A D - C_{\ell_p})\hat{p} - (i_E D + C_{\ell_r})\hat{r} + 0 = 0$$

$$-C_{n_\beta}\beta - (i_E D + C_{n_p})\hat{p} + (i_C D - C_{n_r})\hat{r} + 0 = 0$$

$$\mu = m/\rho S\ell \qquad t^* = \ell/u_0 \qquad \ell = b_F/2$$

Table XVI gives the formulas for the stability derivatives in cruise and transition. These formulas have been used for the computation of all the rate and acceleration derivatives in transition. C_{x_α}, C_{z_u} and the reference values of C_{L_α}, C_{m_α}, C_{β}, C_{n_β} and C_{ℓ_β} were determined from the wind tunnel data of (46).

(b) Normal Modes (SAS off)

The degree of compliance with (47) requirements on longitudinal short period mode damping and Dutch Roll damping is shown in Figures 180 and 181 respectively. These data are for two c.g. positions, SAS off, W = 12,300 lb and a speed range from 49 knots to 160 knots (corresponding to a nominal front propeller tilt angle range of 82.5° to -3.0°).

Migration of the longitudinal short period roots and the Phugoid roots from 0 to 160 knots are shown in Figures 182 and 183 respectively; and for the lateral directional roots (Dutch-Roll and Spiral Roll) in Figure 184 for the same speed range. The longitudinal short period and Phugoid data are shown in separate figures for clarity. These data are all with SAS-off at W = 12,300 lb, S.L., end transition c.g. = 42% lift chord.

From these figures it is seen that the longitudinal short period mode is divergent for all speeds below approximately 70 knots, the Phugoid is divergent below approximately 50 knots and the Dutch Roll is divergent for all speeds below approximately 85 knots. These are all estimated data and unfortunately no quantitative dynamic stability and control flight testing was performed with SAS off, at other than hover tilt angle, so that no transition data checks were possible.

(4) Controls and Control Systems

(a) General

In transition, control power is supplied through both propeller blade angle change and conventional surfaces.

The conventional surfaces (elevators, rudder, ailerons) and their systems are discussed in detail in Section VII, paragraph 1.b.(4).

There is no coupling of propeller forces in roll and yaw, e.g., rudder pedal deflection gives a pure yawing

Table XVI. Formulae for Curtiss X-19 stability derivatives.

Longitudinal:

$$C_{x_\alpha} = C_{L_0}\left(1 - 2C_{L_\alpha}\frac{\partial C_D}{\partial C_L{}^2}\right)$$

$$C_{z_\alpha} = -\left(C_{L_\alpha} + C_{D_0}\right)$$

$$C_{m_\alpha} = C_{m_{\alpha_{\bar{x}_R}}} + \frac{\Delta C_{m_\alpha}}{\Delta \bar{x}}\left(\bar{x} - \bar{x}_R\right)$$

$$C_{x_u} = -3\left(C_{D_0} + C_{L_0}\tan\theta_0\right) - M\frac{\partial C_D}{\partial M}$$

$$C_{z_u} = \frac{-M^2\left(C_{L_{0_{WF}}} S_{WF} + C_{L_{0_{WR}}} S_{WR}\right)}{S\left(1 - M^2\right)}$$

$$C_{m_u} = u_0\left(\frac{\partial C_m}{\partial u}\right)_0$$

$$C_{z_q} = \left(C_{z_q}\right)_W + \left(C_{z_q}\right)_R + \left(C_{z_q}\right)_T$$

Where:

$$\left(C_{z_q}\right)_W = \frac{-2}{S\bar{c}}\left(a_{WR}\, X_{a_R}\, S_{WR} - a_{WF}\, X_{a_F}\, S_{WF}\right)$$

$$\left(C_{z_q}\right)_R = \frac{-NS_p}{S\bar{c}}\left[\left(\frac{\partial C_{R_R}}{\partial A_R}\right) x'_{PR}\cos\left(\phi_R + \alpha_{f_o}\right) - \left(\frac{\partial C_{R_F}}{\partial A_F}\right) x'_{PR}\cos\left(\phi_F + \alpha_{f_o}\right)\right]$$

$$\left(C_{z_q}\right)_T = \frac{-Nu_0}{\frac{\rho}{2} u_0{}^2 S\bar{c}}\left[\left(\frac{\partial T_R}{\partial V_{N_R}}\right)_0 X_{P_R}\sin\left(\gamma_R - \phi_R\right)\sin\left(\phi_R + \alpha_{f_o}\right)\right.$$

$$\left. - \left(\frac{\partial T_F}{\partial V_{N_F}}\right)_0 x_{P_F}\sin\left(\gamma_F - \phi_F\right)\sin\left(\phi_F + \alpha_{f_o}\right)\right]$$

FURNISHED UNDER UNITED STATES GOVERNMENT CONTRACT No. AF33(615)-3940. SHALL NOT BE EITHER RELEASED OUTSIDE THE GOVERNMENT, OR BE DUPLICATED, OR DISCLOSED IN WHOLE OR IN PART FOR MANUFACTURE OR PROCUREMENT, WITHOUT THE WRITTEN PERMISSION OF CURTISS-WRIGHT CORPORATION, EXCEPT FOR (i) EMERGENCY REPAIR OR OVERHAUL WORK BY OR FOR THE GOVERNMENT, WHERE THE ITEM OR PROCESS IS NOT OTHERWISE REASONABLY AVAILABLE TO ENABLE TIMELY PERFORMANCE OF THE WORK, OR (ii) RELEASE TO A FOREIGN GOVERNMENT, AS THE INTERESTS OF THE UNITED STATES MAY REQUIRE, PROVIDED THAT IN EITHER CASE THE RELEASE, USE, DUPLICATION OR DISCLOSURE HEREOF SHALL BE SUBJECT TO THE FOREGOING LIMITATIONS. THIS LEGEND SHALL BE MARKED ON ANY REPRODUCTION HEREOF IN WHOLE OR IN PART.

Table XVI. Continued.

$$C_{m_q} = (C_{m_q})_W + (C_{m_q})_R + (C_{m_q})_T + (C_{m_q})_{TS}$$

Where:

$$(C_{m_q})_W = \frac{-2}{S\bar{c}^2}\left[a_{WF}\, S_{WF}\, X_{a_F}\, X'_{a_F} + a_{WR}\, S_{WR}\, X_{a_R}\, X'_{a_R}\right]$$

$$(C_{m_q})_R = \frac{NS_P}{S\bar{c}^2}\left[\left(\frac{\partial C_{R_R}}{\partial A_R}\right) X'_{P_R}\left\{h'_{P_R}\sin(\phi_R + \alpha_{f_o}) - X'_{P_R}\cos(\phi_R + \alpha_{f_o})\right\}\right.$$

$$\left. - \left(\frac{\partial C_{R_F}}{\partial A_F}\right) X'_{P_F}\left\{h'_{P_F}\sin(\phi_F + \alpha_{f_o}) + Y'_{P_F}\cos(\phi_F + \alpha_{f_o})\right\}\right]$$

$$(C_{m_q})_T = \frac{Nu_0}{\frac{\rho}{2}u_0^2 S\bar{c}^2}\left[\left(\frac{\partial T_F}{\partial V_{N_F}}\right)_0 X_{P_F}\sin(\gamma_F - \phi_F)\left\{X'_{P_F}\sin(\phi_F + \alpha_{f_o}) - h'_{P_F}\cos(\phi_F + \alpha_{f_o})\right\}\right.$$

$$\left. + \left(\frac{\partial T_R}{\partial V_{N_R}}\right)_0 X_{P_R}\sin(\gamma_R - \phi_R)\left\{X'_{P_R}\sin(\phi_R + \alpha_{f_o}) + h'_{P_R}\cos(\phi_R + \alpha_{f_o})\right\}\right]$$

$$(C_{m_q})_{TS} = \frac{2u_0}{\bar{c}}\left(\frac{\partial C_m}{\partial u}\right)_0\left[X_{P_R}\cos(\pi/2 - \phi_R + \alpha_{f_o}) - X_{P_F}\cos(\pi/2 - \phi_F - \alpha_{f_o})\right]$$

"FURNISHED UNDER UNITED STATES GOVERNMENT CONTRACT No. AF33(615)-3940. SHALL NOT BE EITHER RELEASED OUTSIDE THE GOVERNMENT, OR USED, DUPLICATED, OR DISCLOSED IN WHOLE OR IN PART FOR MANUFACTURE OR PROCUREMENT, WITHOUT THE WRITTEN PERMISSION OF CURTISS-WRIGHT CORPORATION, EXCEPT FOR (i) EMERGENCY REPAIR OR OVERHAUL WORK BY OR FOR THE GOVERNMENT, WHERE THE ITEM OR PROCESS IS NOT OTHERWISE REASONABLY AVAILABLE TO ENABLE TIMELY PERFORMANCE OF THE WORK, OR (ii) RELEASE TO A FOREIGN GOVERNMENT, AS THE INTERESTS OF THE UNITED STATES MAY REQUIRE. PROVIDED THAT IN EITHER CASE THE RELEASE, USE, DUPLICATION OR DISCLOSURE HEREOF SHALL BE SUBJECT TO THE FOREGOING LIMITATIONS. THIS LEGEND SHALL BE MARKED ON ANY REPRODUCTION HEREOF IN WHOLE OR IN PART."

Table XVI. Continued.

$$C_{z_{\dot{\alpha}}} = (C_{z_{\dot{\alpha}}})_{WR} + (C_{z_{\dot{\alpha}}})_P$$

Where:

$$(C_{z_{\dot{\alpha}}})_{WR} = \frac{-2a_{WR}\, S_{WR}}{S\bar{c}}\left[\frac{\partial \epsilon_{WF}}{\partial \alpha_{WF}}\frac{\partial \alpha_{WF}}{\partial \alpha_f}\,(X_{a_F} + X_{a_R}) + \frac{\partial \epsilon_{P_F}}{\partial A_F}\frac{\partial A_F}{\partial \alpha_f}(X_{P_F} + X_{a_R})\right]$$

$$(C_{z_{\dot{\alpha}}})_P = \frac{-NS_P}{S\bar{c}}\left(\frac{\partial C_{R_R}}{\partial A_R}\right)_0 \cos(\phi_R + \alpha_{f_o})\left[\frac{\partial \epsilon_{P_F}}{\partial A_F}\frac{\partial A_F}{\partial \alpha_f}\,(X_{P_F} + X_{P_R}) + K_1\frac{\partial \epsilon_{WF}}{\partial \alpha_{WF}}\frac{\partial \alpha_{WF}}{\partial \alpha_f}\,(X_{a_F} + X_{P_R})\right]$$

$$C_{m_{\dot{\alpha}}} = (C_{m_{\dot{\alpha}}})_{WR} + (C_{m_{\dot{\alpha}}})_P$$

Where:

$$(C_{m_{\dot{\alpha}}})_{WR} = \frac{-2S_{WR}\, X_{a_R}\, a_{WR}\cos\alpha_{f_o}}{S\bar{c}^2}\left[\frac{\partial \epsilon_{WF}}{\partial \alpha_{WF}}\frac{\partial \alpha_{WF}}{\partial \alpha_f}\,(X_{a_F} + X_{a_R}) + \frac{\partial \epsilon_{P_F}}{\partial A_F}\frac{\partial A_F}{\partial \alpha_f}\,(X_{P_F} + X_{a_R})\right]$$

$$(C_{m_{\dot{\alpha}}})_P = \frac{-NS_P}{S\bar{c}^2}\left(\frac{\partial C_{R_R}}{\partial A_R}\right)_0 X_{P_R}\cos(\phi_R + \alpha_{f_o})\left[\frac{\partial \epsilon_{P_F}}{\partial A_F}\frac{\partial A_F}{\partial \alpha_f}\,(X_{P_F} + X_{P_R}) + K_1\frac{\partial \epsilon_{WF}}{\partial \alpha_{WF}}\frac{\partial \alpha_{WF}}{\partial \alpha_f}\,(X_{a_F} + X_{P_R})\right]$$

FURNISHED UNDER UNITED STATES GOVERNMENT CONTRACT No. AF33(615)-3940. SHALL NOT BE EITHER RELEASED OUTSIDE THE GOVERNMENT, OR SHOWN, DUPLICATED, OR DISCLOSED IN WHOLE OR IN PART FOR MANUFACTURE OR PROCUREMENT, WITHOUT THE WRITTEN PERMISSION OF CURTISS-WRIGHT CORPORATION, EXCEPT FOR (i) EMERGENCY REPAIR OR OVERHAUL WORK BY OR FOR THE GOVERNMENT, WHERE THE ITEM OR PROCESS IS NOT OTHERWISE REASONABLY AVAILABLE TO ENABLE TIMELY PERFORMANCE OF THE WORK, OR (ii) RELEASE TO A FOREIGN GOVERNMENT, AS THE INTERESTS OF THE UNITED STATES MAY REQUIRE. PROVIDED THAT IN EITHER CASE THE RELEASE, USE, DUPLICATION OR DISCLOSURE HEREOF SHALL BE SUBJECT TO THE FOREGOING LIMITATIONS. THIS LEGEND SHALL BE MARKED ON ANY REPRODUCTION HEREOF IN WHOLE OR IN PART.

Table XVI. Continued.

Lateral:

$$C_{y_\beta} = (C_{y_\beta})_v + (C_{y_\beta})_P$$

Where:

$$(C_{y_\beta})_v = -a_v \eta_v \frac{S_v}{S} \left(1 - \frac{\partial \sigma_P}{\partial \beta}\right)$$

$$(C_{y_\beta})_P = \frac{-NS_P}{2S} \left[\left(\frac{\partial C_{R_F}}{\partial A_F}\right)_0 + \left(\frac{\partial C_{R_R}}{\partial A_R}\right)_0 \left(1 - \frac{\partial \sigma_P}{\partial \beta}\right) \right]$$

$$C_{\ell_\beta} = C_{\ell_{\beta_{\bar{z}_R}}} + \frac{\Delta C_{\ell_\beta}}{\Delta \bar{z}} \Delta z'$$

$$C_{n_\beta} = C_{n_{\beta_{\bar{x}_R}}} + \frac{\Delta C_{n_\beta}}{\Delta \bar{x}} \Delta x'$$

$$C_{y_p} = \frac{-a_v S_v}{S} \left[\frac{2z'_v}{b_F} - \left(\frac{\partial \sigma}{\partial \hat{p}}\right) \right]$$

$$C_{\ell_p} = (C_{\ell_p})_W + (C_{\ell_p})_v + (C_{\ell_p})_R$$

Where:

$$(C_{\ell_p})_v = \frac{a_v S_v}{S} \frac{z'_v}{b_F} \left[\frac{-2z'_v}{b_F} + \left(\frac{\partial \sigma}{\partial \hat{p}}\right) \right]$$

$$(C_{\ell_p})_R = \frac{-NS_P}{4S} \left[\left(\frac{\partial C_{R_F}}{\partial A_F}\right)_0 \cos(\phi_F + \alpha_{f0}) + \left(\frac{b_R}{b_F}\right)^2 \left(\frac{\partial C_{R_R}}{\partial A_R}\right)_0 \cos(\phi_R + \alpha_{f_o}) \right]$$

"FURNISHED UNDER UNITED STATES GOVERNMENT CONTRACT No. AF33(615)-3940 SHALL NOT BE EITHER RELEASED OUTSIDE THE GOVERNMENT, OR USED, DUPLICATED, OR DISCLOSED IN WHOLE OR IN PART FOR MANUFACTURE OR PROCUREMENT, WITHOUT THE WRITTEN PERMISSION OF CURTISS-WRIGHT CORPORATION, EXCEPT FOR (i) EMERGENCY REPAIR OR OVERHAUL WORK BY OR FOR THE GOVERNMENT, WHERE THE ITEM OR PROCESS IS NOT OTHERWISE REASONABLY AVAILABLE TO ENABLE TIMELY PERFORMANCE OF THE WORK, OR (ii) RELEASE TO A FOREIGN GOVERNMENT, AS THE INTERESTS OF THE UNITED STATES MAY REQUIRE, PROVIDED THAT IN EITHER CASE THE RELEASE, USE, DUPLICATION OR DISCLOSURE HEREOF SHALL BE SUBJECT TO THE FOREGOING LIMITATIONS. THIS LEGEND SHALL BE MARKED ON ANY REPRODUCTION HEREOF IN WHOLE OR IN PART."

Table XVI. Continued.

$$C_{n_P} = (C_{n_P})_W + (C_{n_P})_v + (C_{n_P})_P$$

Where:

$$(C_{n_P})_W = \frac{-C_1}{S} \left(C_{L_{0_{WF}}} S_{WF} + C_{L_{0_{WR}}} S_{WR}\right)$$

$$(C_{n_P})_v = \frac{a_v S_v}{S} \frac{\ell_v'}{b_F} \left(\frac{2z_v'}{b_F} - \frac{\partial \sigma}{\partial \hat{p}}\right)$$

$$(C_{n_P})_P = \frac{N}{2S} \left[\left(\frac{\partial C_{R_F}}{\partial A_F}\right)_0 \frac{S_P}{2} \sin(\phi_F + \alpha_{f_o}) + \left(\frac{b_R}{b_F}\right)^2 \left(\frac{\partial C_{R_R}}{\partial A_R}\right)_0 \frac{S_P}{2} \sin(\phi_R + \alpha_{f_o}) \right.$$

$$- \left(\frac{\partial T_F}{\partial V_{N_F}}\right)_0 \sin(\phi_F + \alpha_{f_o}) \cos(\phi_F + \alpha_{f_o})$$

$$\left. - \left(\frac{\partial T_R}{\partial V_{N_R}}\right)_0 \left(\frac{b_R}{b_F}\right)^2 \sin(\phi_R + \alpha_{f_o}) \cos(\phi_R + \alpha_{f_o}) \right]$$

$$C_{y_r} = \frac{2a_v S_v}{b_F S} \left[\ell_v' + \frac{\partial \sigma_P}{\partial \beta} X_{P_F}\right]$$

$$C_{\ell_r} = (C_{\ell_r})_W + (C_{\ell_r})_v + (C_{\ell_r})_P$$

Where:

$$(C_{\ell_r})_W = \frac{C_2}{S} \left(C_{L_{0_{WF}}} S_{WF} + C_{L_{0_{WR}}} S_{WR}\right)$$

$$(C_{\ell_r})_v = 2a_v S_v Z_v' \left(\ell_v' + \frac{\partial \sigma_P}{\partial \beta} X_{P_F}\right)$$

FURNISHED UNDER UNITED STATES GOVERNMENT CONTRACT No. AF33(615)-3940. SHALL NOT BE EITHER RELEASED OUTSIDE THE GOVERNMENT, OR USED, DUPLICATED, OR DISCLOSED IN WHOLE OR IN PART FOR MANUFACTURE OR PROCUREMENT, WITHOUT THE WRITTEN PERMISSION OF CURTISS-WRIGHT CORPORATION, EXCEPT FOR (i) EMERGENCY REPAIR OR OVERHAUL WORK BY OR FOR THE GOVERNMENT, WHERE THE ITEM OR PROCESS IS NOT OTHERWISE REASONABLY AVAILABLE TO ENABLE TIMELY PERFORMANCE OF THE WORK, OR (ii) RELEASE TO A FOREIGN GOVERNMENT, AS THE INTERESTS OF THE UNITED STATES MAY REQUIRE. PROVIDED THAT IN EITHER CASE THE RELEASE, USE, DUPLICATION OR DISCLOSURE HEREOF SHALL BE SUBJECT TO THE FOREGOING LIMITATIONS. THIS LEGEND SHALL BE MARKED ON ANY REPRODUCTION HEREOF IN WHOLE OR IN PART.

Table XVI. Continued.

$$(C_{\ell_r})_P = \frac{N}{2\rho u_0 S}\left[\left(\frac{\partial T_F}{\partial V_{N_F}}\right)_0 \sin(\phi_F + \alpha_{f_o})\,\mathrm{Cos}(\phi_F + \alpha_{f_o})\right.$$

$$\left. + \left(\frac{\partial T_R}{\partial V_{N_R}}\right)_0 \left(\frac{b_R}{b_F}\right)^2 \sin(\phi_R + \alpha_{f_o})\cos(\phi_R + \alpha_{f_o})\right]$$

$$- \frac{NS_P}{b_F S}\left[\left(\frac{\partial C_{R_F}}{\partial A_F}\right)_0 \frac{h'_{P_F} X_{P_F}}{b_F} - \left(\frac{\partial C_{R_R}}{\partial A_R}\right)_0 \frac{h'_{P_R} X_{P_R}}{b_R}\right]$$

$$C_{n_r} = (C_{n_r})_W + (C_{n_r})_V + (C_{n_r})_P$$

Where:

$$(C_{n_r})_W = \frac{-K_2}{S}\left(C_{D_{WF}} S_{WF} + C_{D_{WR}} S_{WR}\right)$$

$$(C_{n_r})_V = \frac{-2a_V S_V \ell'_V}{2b_F^2}\left(\ell'_V + \frac{\partial \sigma_P}{\partial \beta} X_{P_F}\right)$$

$$(C_{n_r})_P = \frac{N}{2\rho u_0 S}\left[\left(\frac{\partial T_F}{\partial V_{N_F}}\right)_0 \cos^2(\phi_F + \alpha_{f_o}) + \left(\frac{\partial T_R}{\partial V_{N_R}}\right)_0 \left(\frac{b_R}{b_F}\right)^2 \cos^2(\phi_R + \alpha_{f_o})\right]$$

$$- \frac{NS_P}{b_F S}\left[\left(\frac{\partial C_{R_F}}{\partial A_F}\right)_0 \frac{X_{P_F} X'_{P_F}}{b_F} + \left(\frac{\partial C_{R_R}}{\partial A_R}\right)_0 \frac{X_{P_R} X'_{P_R}}{b_R}\right]$$

"FURNISHED UNDER UNITED STATES GOVERNMENT CONTRACT No. AF33(6.5)-3940 SHALL NOT BE EITHER RELEASED OUTSIDE THE GOVERNMENT, OR USED, DUPLICATED, OR DISCLOSED IN WHOLE OR IN PART FOR MANUFACTURE OR PROCUREMENT, WITHOUT THE WRITTEN PERMISSION OF CURTISS-WRIGHT CORPORATION, EXCEPT FOR (i) EMERGENCY REPAIR OR OVERHAUL WORK BY OR FOR THE GOVERNMENT, WHERE THE ITEM OR PROCESS IS NOT OTHERWISE REASONABLY AVAILABLE TO ENABLE TIMELY PERFORMANCE OF THE WORK, OR (ii) RELEASE TO A FOREIGN GOVERNMENT, AS THE INTERESTS OF THE UNITED STATES MAY REQUIRE PROVIDED THAT IN EITHER CASE THE RELEASE, USE, DUPLICATION OR DISCLOSURE HEREOF SHALL BE SUBJECT TO THE FOREGOING LIMITATIONS THIS LEGEND SHALL BE MARKED ON ANY REPRODUCTION HEREOF IN WHOLE OR IN PART."

Table XVI. Continued.

Definition of Symbols Used in Preceding Formulae:

$$x'_{P_R} = x_{P_R} \cos \alpha_{f_o} + h_{P_R} \sin \alpha_{f_o}$$

$$x'_{P_F} = x_{P_F} \cos \alpha_{f_o} - h_{P_F} \sin \alpha_{f_o}$$

$$x'_{a_R} = x_{a_R} \cos \alpha_{f_o} + (\bar{z}_{T_R} - \bar{z}_R) \sin \alpha_{f_o}$$

$$x'_{a_F} = x_{a_F} \cos \alpha_{f_o} - (\bar{z}_{T_F} - \bar{z}_R) \sin \alpha_{f_o}$$

$$h'_{P_R} = h_{P_R} \cos \alpha_{f_o} - x_{P_R} \sin \alpha_{f_o}$$

$$h'_{P_F} = h_{P_F} \cos \alpha_{f_o} + x_{P_F} \sin \alpha_{f_o}$$

$$\Delta \bar{z}' = (\bar{z} - \bar{z}_R) \cos \alpha_{f_o} - (\bar{x} - \bar{x}_R) \sin \alpha_{f_o}$$

$$\Delta \bar{x}' = (\bar{x} - \bar{x}_R) \cos \alpha_{f_o} + (\bar{z} - \bar{z}_R) \sin \alpha_{f_o}$$

$$z'_v = z_v \cos \alpha_{f_o} - \ell_v \sin \alpha_{f_o}$$

$$\ell'_v = \ell_v \cos \alpha_{f_o} + z_v \sin \alpha_{f_o}$$

FURNISHED UNDER UNITED STATES GOVERNMENT CONTRACT No. AF33(615)-3940. SHALL NOT BE EITHER RELEASED OUTSIDE THE GOVERNMENT, OR USED, DUPLICATED, OR DISCLOSED IN WHOLE OR IN PART FOR MANUFACTURE OR PROCUREMENT, WITHOUT THE WRITTEN PERMISSION OF CURTISS-WRIGHT CORPORATION, EXCEPT FOR (i) EMERGENCY REPAIR OR OVERHAUL WORK BY OR FOR THE GOVERNMENT, WHERE THE ITEM OR PROCESS IS NOT OTHERWISE REASONABLY AVAILABLE TO ENABLE TIMELY PERFORMANCE OF THE WORK, OR (ii) RELEASE TO A FOREIGN GOVERNMENT, AS THE INTERESTS OF THE UNITED STATES MAY REQUIRE, PROVIDED THAT IN EITHER CASE THE RELEASE, USE, DUPLICATION OR DISCLOSURE HEREOF SHALL BE SUBJECT TO THE FOREGOING LIMITATIONS. THIS LEGEND SHALL BE MARKED ON ANY REPRODUCTION HEREOF IN WHOLE OR IN PART.

Table XVI. Concluded.

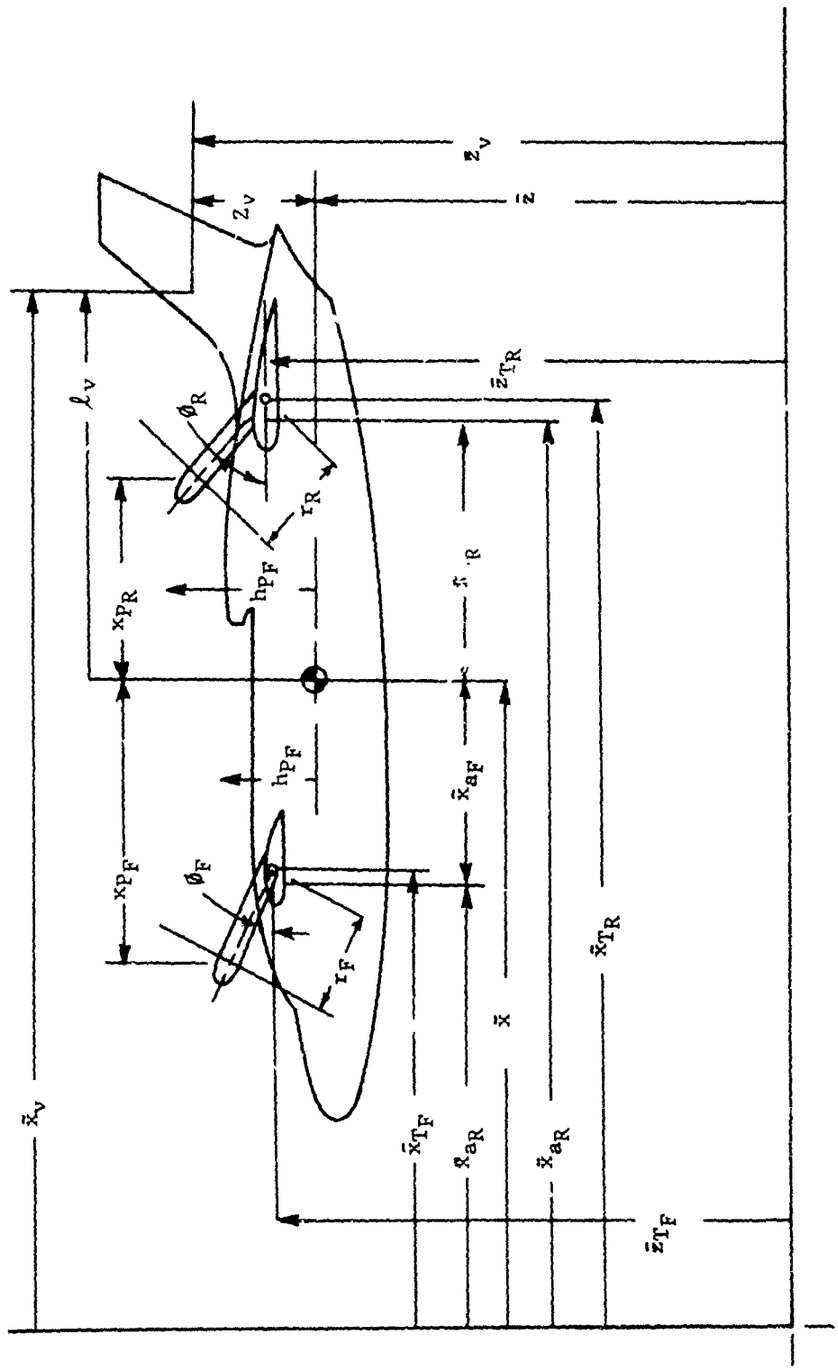

"FURNISHED UNDER UNITED STATES GOVERNMENT CONTRACT No. AF33(615)-3940 SHALL NOT BE EITHER RELEASED OUTSIDE THE GOVERNMENT, OR USED, DUPLICATED, OR DISCLOSED IN WHOLE OR IN PART FOR MANUFACTURE OR PROCUREMENT, WITHOUT THE WRITTEN PERMISSION OF CURTISS-WRIGHT CORPORATION, EXCEPT FOR (i) EMERGENCY REPAIR OR OVERHAUL WORK BY OR FOR THE GOVERNMENT, WHERE THE ITEM OR PROCESS IS NOT OTHERWISE REASONABLY AVAILABLE TO ENABLE TIMELY PERFORMANCE OF THE WORK, OR (ii) RELEASE TO A FOREIGN GOVERNMENT, AS THE INTERESTS OF THE UNITED STATES MAY REQUIRE, PROVIDED THAT IN EITHER CASE THE RELEASE, USE, PUBLICATION OR DISCLOSURE HEREOF SHALL BE SUBJECT TO THE FOREGOING LIMITATIONS. THIS LEGEND SHALL BE MARKED ON ANY REPRODUCTION HEREOF IN WHOLE OR IN PART."

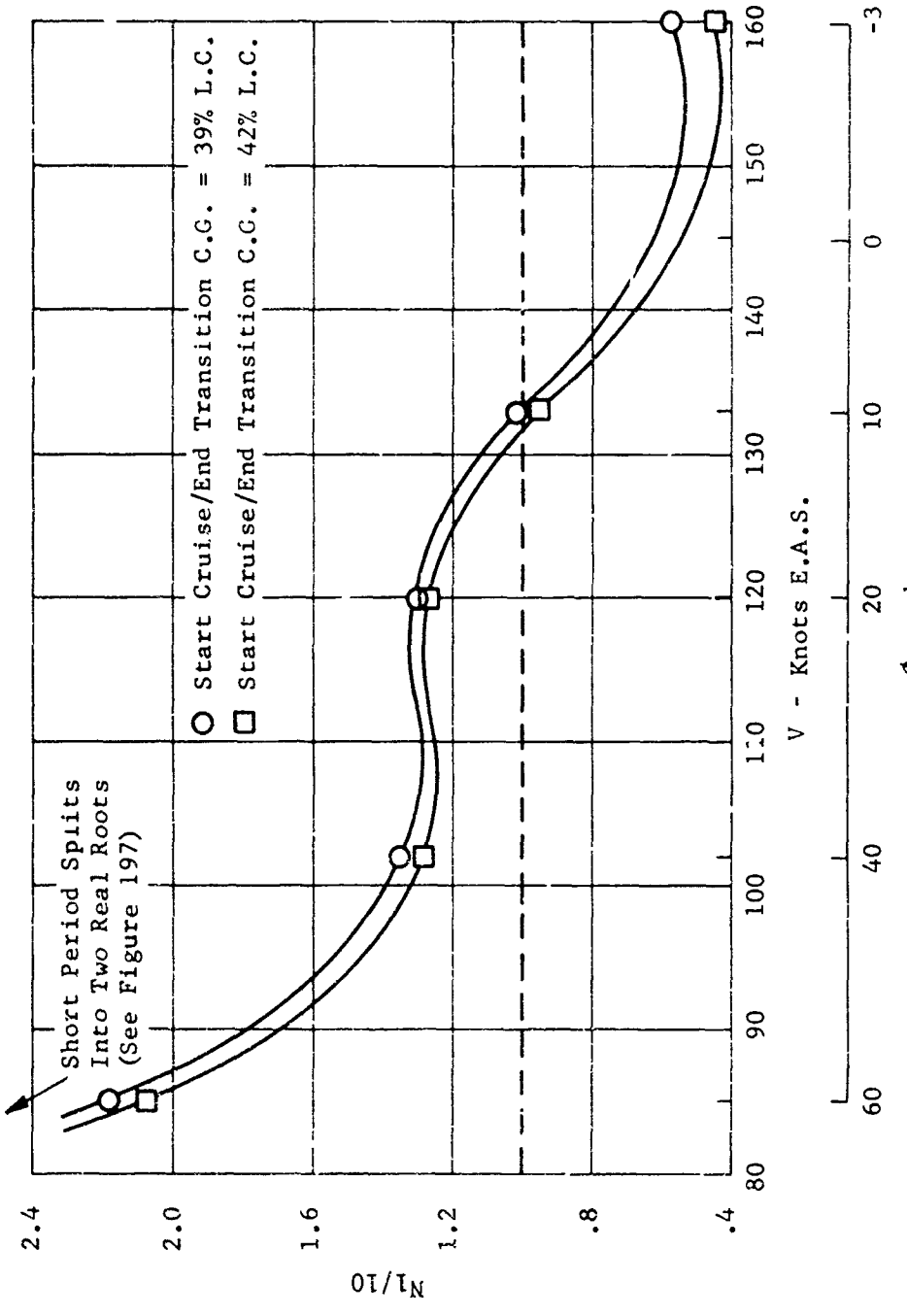

Figure 180. X-19, damping characteristics of the longitudinal short period mode through transition with S.A.S. off; W = 12,300 pounds, height = sea level.

FURNISHED UNDER UNITED STATES GOVERNMENT CONTRACT No. AF33(616)-1940. SHALL NOT BE EITHER RELEASED OUTSIDE THE GOVERNMENT, OR BE DUPLICATED, OR DISCLOSED IN WHOLE OR IN PART FOR MANUFACTURE OR PROCUREMENT, WITHOUT THE WRITTEN PERMISSION OF CURTISS-WRIGHT CORPORATION, EXCEPT FOR (i) EMERGENCY REPAIR OR OVERHAUL WORK BY OR FOR THE GOVERNMENT, WHERE THE ITEM OR PROCESS IS NOT OTHERWISE REASONABLY AVAILABLE TO ENABLE TIMELY PERFORMANCE OF THE WORK, OR (ii) RELEASE TO A FOREIGN GOVERNMENT AS IT IS IN THE INTERESTS OF THE UNITED STATES MAY REQUIRE. PROVIDED THAT IN EITHER CASE THE RELEASE, USE, DUPLICATION OR DISCLOSURE HEREUNDER SHALL BE SUBJECT TO THE FOREGOING LIMITATIONS. THIS LEGEND SHALL BE MARKED ON ANY REPRODUCTION HEREOF IN WHOLE OR IN PART.

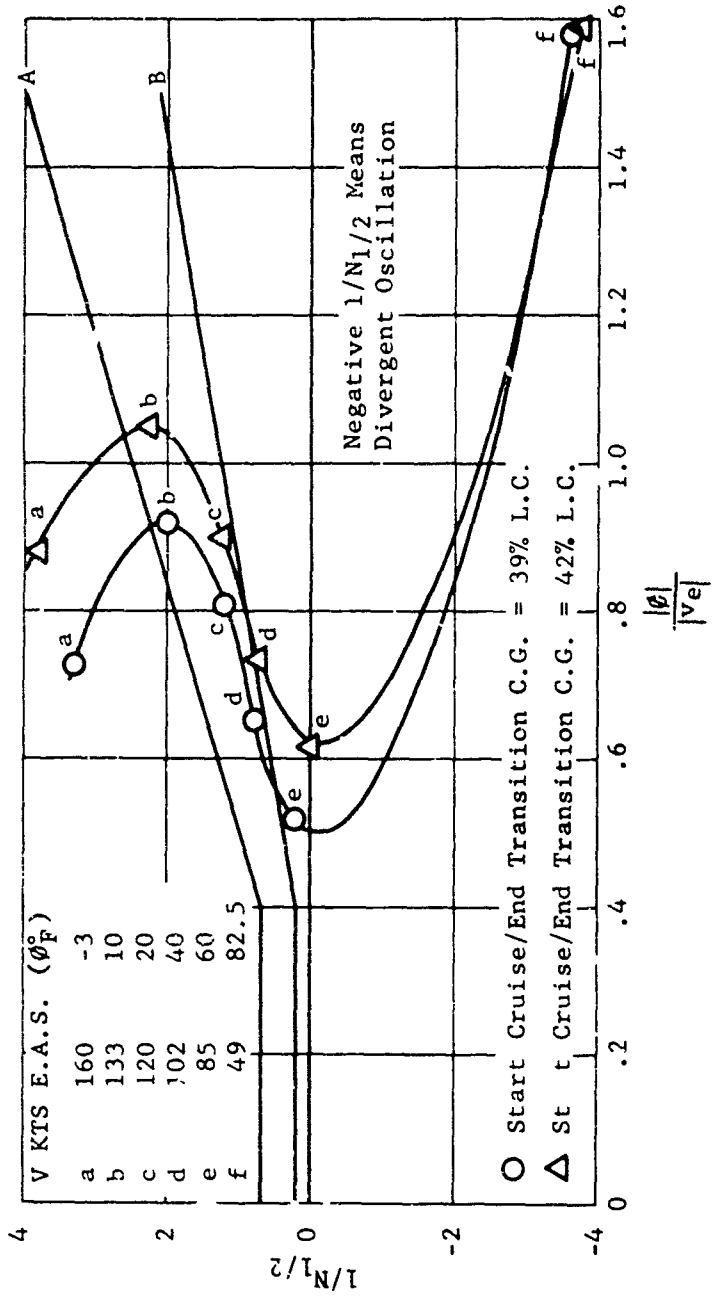

Figure 181. X-19, damping characteristics of the Dutch Roll mode through transition with S.A.S. off: W = 12,300 pounds, height = sea level.

FURNISHED UNDER UNITED STATES GOVERNMENT CONTRACT No. AF33(615)-3940 SHALL NOT BE EITHER RELEASED OUTSIDE THE GOVERNMENT, OR USED, DUPLICATED, OR DISCLOSED IN WHOLE OR IN PART FOR MANUFACTURE OR PROCUREMENT, WITHOUT THE WRITTEN PERMISSION OF CURTISS-WRIGHT CORPORATION, EXCEPT FOR (i) EMERGENCY REPAIR OR OVERHAUL WORK BY OR FOR THE GOVERNMENT WHERE THE ITEM OR PROCESS IS NOT OTHERWISE REASONABLY AVAILABLE TO ENABLE TIMELY PERFORMANCE OF THE WORK, OR (ii) RELEASE TO A FOREIGN GOVERNMENT, AS THE INTERESTS OF THE UNITED STATES MAY REQUIRE PROVIDED THAT IN EITHER CASE THE RELEASE, USE, DUPLICATION OR DISCLOSURE HEREOF SHALL BE SUBJECT TO THE FOREGOING LIMITATIONS THIS LEGEND SHALL BE MARKED ON ANY REPRODUCTION HEREOF IN WHOLE OR IN PART."

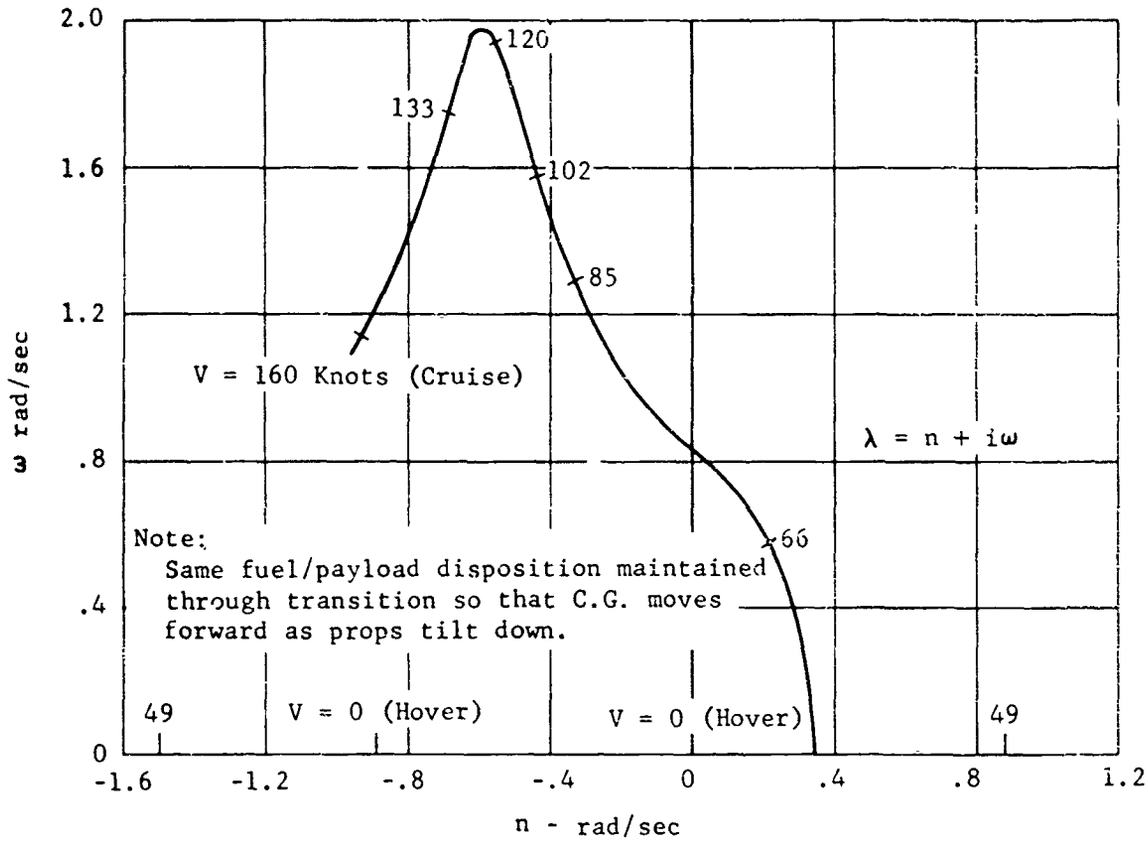

Figure 182. X-19, migration of the longitudinal short period mode roots through transition with S.A.S. off; W = 12,300 pounds, height = sea level, start cruise/end transition c.g. = 42% lift chord.

FURNISHED UNDER UNITED STATES GOVERNMENT CONTRACT No. AF33(615)-3940 SHALL NOT BE EITHER RELEASED OUTSIDE THE GOVERNMENT, OR USED DUPLICATED, OR DISCLOSED IN WHOLE OR IN PART FOR MANUFACTURE OR PROCUREMENT, WITHOUT THE WRITTEN PERMISSION OF CURTISS-WRIGHT CORPORATION, EXCEPT FOR (i) EMERGENCY REPAIR OR OVERHAUL WORK BY OR FOR THE GOVERNMENT WHERE THE ITEM OR PROCESS IS NOT OTHERWISE REASONABLY AVAILABLE TO ENABLE TIMELY PERFORMANCE OF THE WORK, OR (ii) RELEASE TO A FOREIGN GOVERNMENT, AS THE INTERESTS OF THE UNITED STATES MAY REQUIRE PROVIDED THAT IN EITHER CASE THE RELEASE, USE, DUPLICATION OR DISCLOSURE THEREOF SHALL BE SUBJECT TO THE FOREGOING LIMITATIONS. THIS LEGEND SHALL BE MARKED ON ANY REPRODUCTION HEREOF IN WHOLE OR IN PART

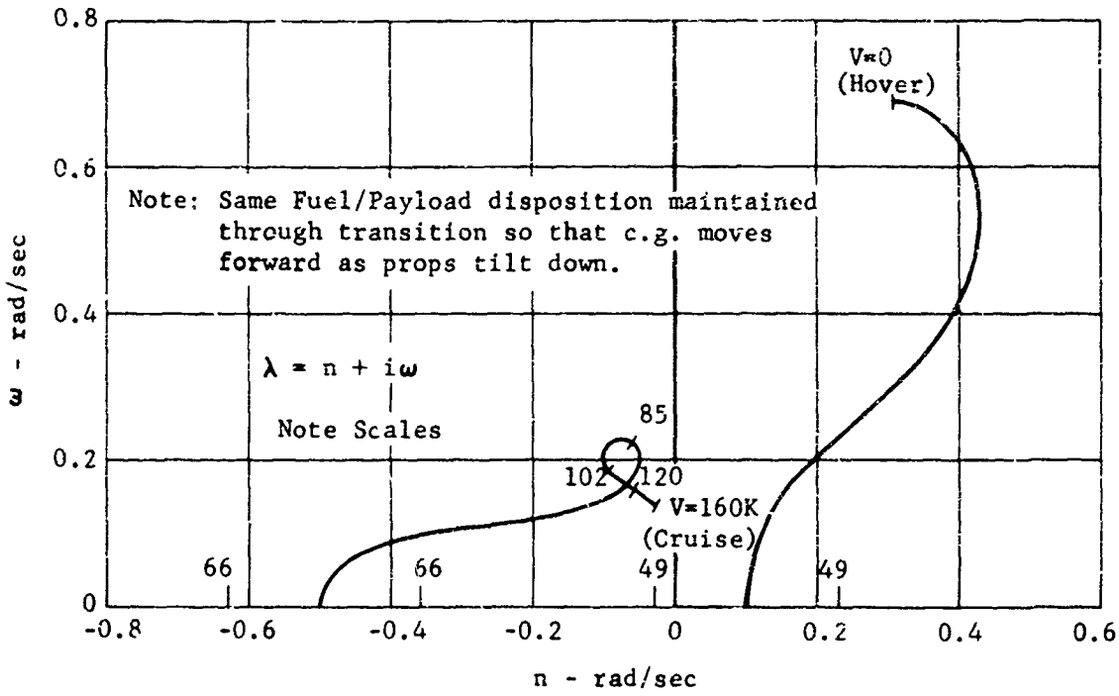

Figure 183. X-19, migration of the longitudinal Phugoid mode roots through transition with S.A.S. off; W = 12,300 pounds, height = sea level, start cruise/end transition c.g. = 42% lift chord.

"FURNISHED UNDER UNITED STATES GOVERNMENT CONTRACT No. AF33(615)-3940. SHALL NOT BE EITHER RELEASED OUTSIDE THE GOVERNMENT, OR USED, DUPLICATED, OR DISCLOSED IN WHOLE OR IN PART FOR MANUFACTURE OR PROCUREMENT, WITHOUT THE WRITTEN PERMISSION OF CURTISS-WRIGHT CORPORATION, EXCEPT FOR (i) EMERGENCY REPAIR OR OVERHAUL WORK BY OR FOR THE GOVERNMENT, WHERE THE ITEM OR PROCESS IS NOT OTHERWISE REASONABLY AVAILABLE TO ENABLE TIMELY PERFORMANCE OF THE WORK, OR (ii) RELEASE TO A FOREIGN GOVERNMENT, AS THE INTERESTS OF THE UNITED STATES MAY REQUIRE. PROVIDED THAT IN EITHER CASE THE RELEASE, USE, DUPLICATION OR DISCLOSURE HEREOF SHALL BE SUBJECT TO THE FOREGOING LIMITATIONS. THIS LEGEND SHALL BE MARKED ON ANY REPRODUCTION HEREOF IN WHOLE OR IN PART."

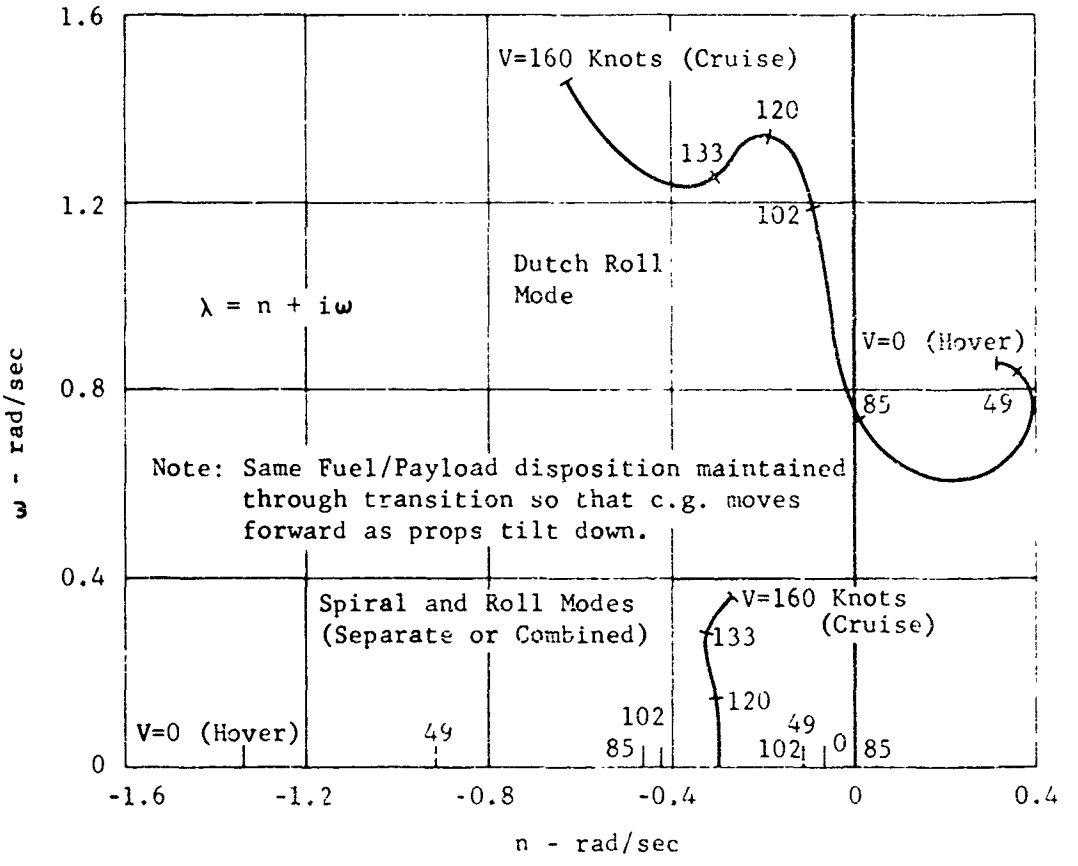

Figure 184. X-19, migration of the roots of the lateral directional modes through transition with S.A.S. off; W = 12,300 pounds, height = sea level, start cruise/end transition c.g. = 42% lift chord.

FURNISHED UNDER UNITED STATES GOVERNMENT CONTRACT NO. AF33(600)-41940. SHALL NOT BE EITHER RELEASED OUTSIDE THE GOVERNMENT, OR USED, DUPLICATED, OR DISCLOSED IN WHOLE OR IN PART FOR MANUFACTURE OR PROCUREMENT, WITHOUT THE WRITTEN PERMISSION OF CURTISS-WRIGHT CORPORATION, EXCEPT FOR (i) EMERGENCY REPAIR OR OVERHAUL WORK BY OR FOR THE GOVERNMENT, WHERE THE ITEM OR PROCESS IS NOT OTHERWISE REASONABLY AVAILABLE TO ENABLE TIMELY PERFORMANCE OF THE WORK, OR (ii) RELEASE TO A FOREIGN GOVERNMENT, AS THE INTERESTS OF THE UNITED STATES MAY REQUIRE, PROVIDED THAT IN EITHER CASE THE RELEASE, USE, DUPLICATION OR DISCLOSURE HEREOF SHALL BE SUBJECT TO THE FOREGOING LIMITATIONS. THIS LEGEND SHALL BE MARKED ON ANY REPRODUCTION HEREOF IN WHOLE OR IN PART.

moment from the propellers. The rudder itself, however, will produce some rolling moment.

A detailed discussion of the hover/transition control systems is included in Section VI.

(b) Pitch Control

Available pitching moment from full stick deflection, together with required moments for trim at W = 12,300 lb and two c.g.'s are shown in Figure 185.

Propeller contribution is phased out at 160 knots.

(c) Roll Control

Available rolling moment from full stick deflection is shown in Figure 186.

Propeller contribution is phased out at 160 knots.

(d) Yaw Control

Available yawing moment from full pedal deflection is shown in Figure 187.

Propeller contribution is phased out at 100 knots.

b. Cruise Flight Regime

(1) Introduction

Cruise is defined as the flight region in which the propellers are fully tilted down (i.e., $\emptyset_P$ = -3.0° and $\emptyset_R$ = -2.54°). This normally corresponds to a speed range from 160 knots E.A.S. to maximum speed.

(2) Assumptions

See Section VII, paragraph 1. a. (2).

(3) Stability

(a) General Procedure

The linearized aircraft equations of motion of (45) were used to determine the stick fixed characteristic modes of motion and are written in Table XVI for reference.

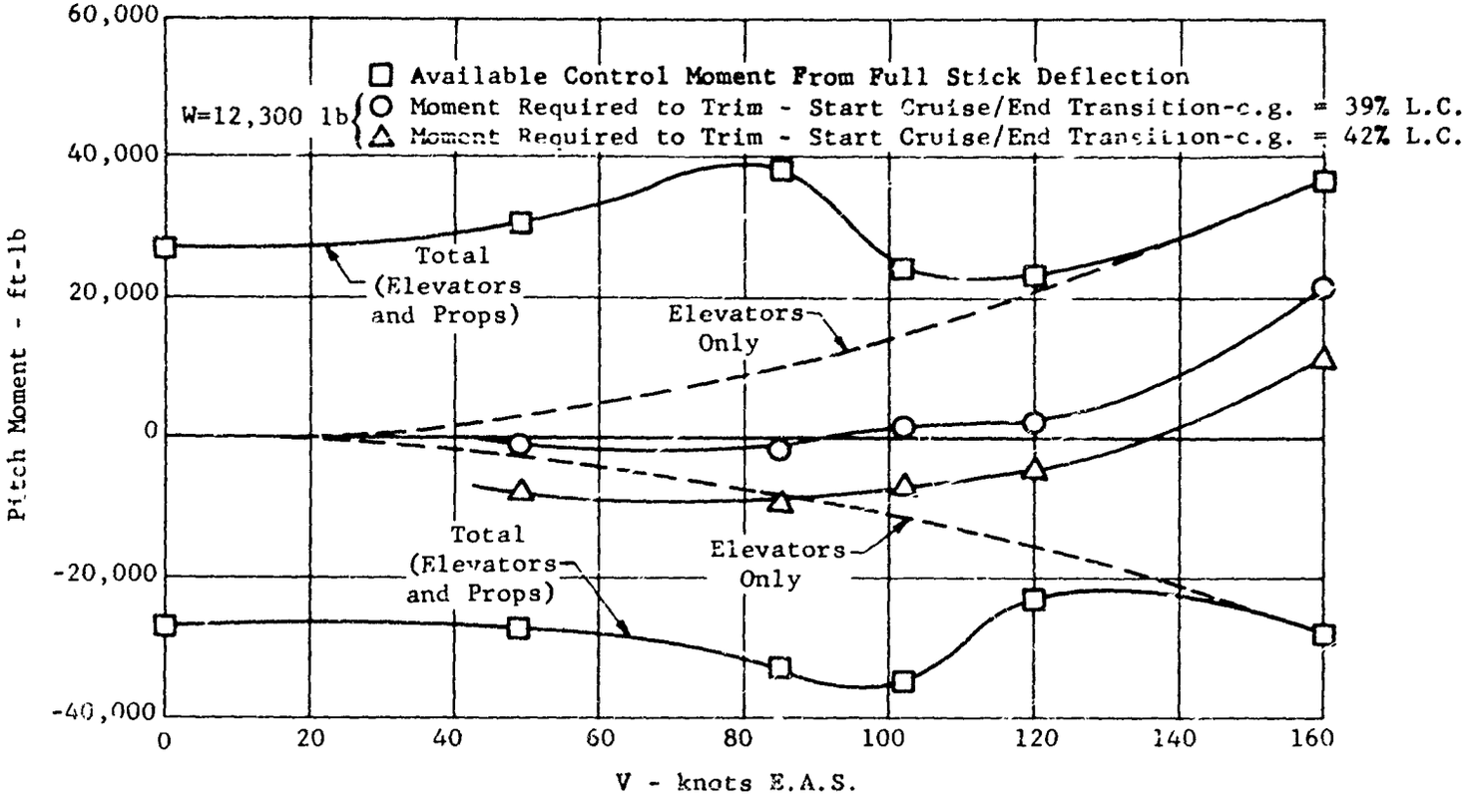

Figure 185. X-19, variation of available pitch control power and required trim moments through transition.

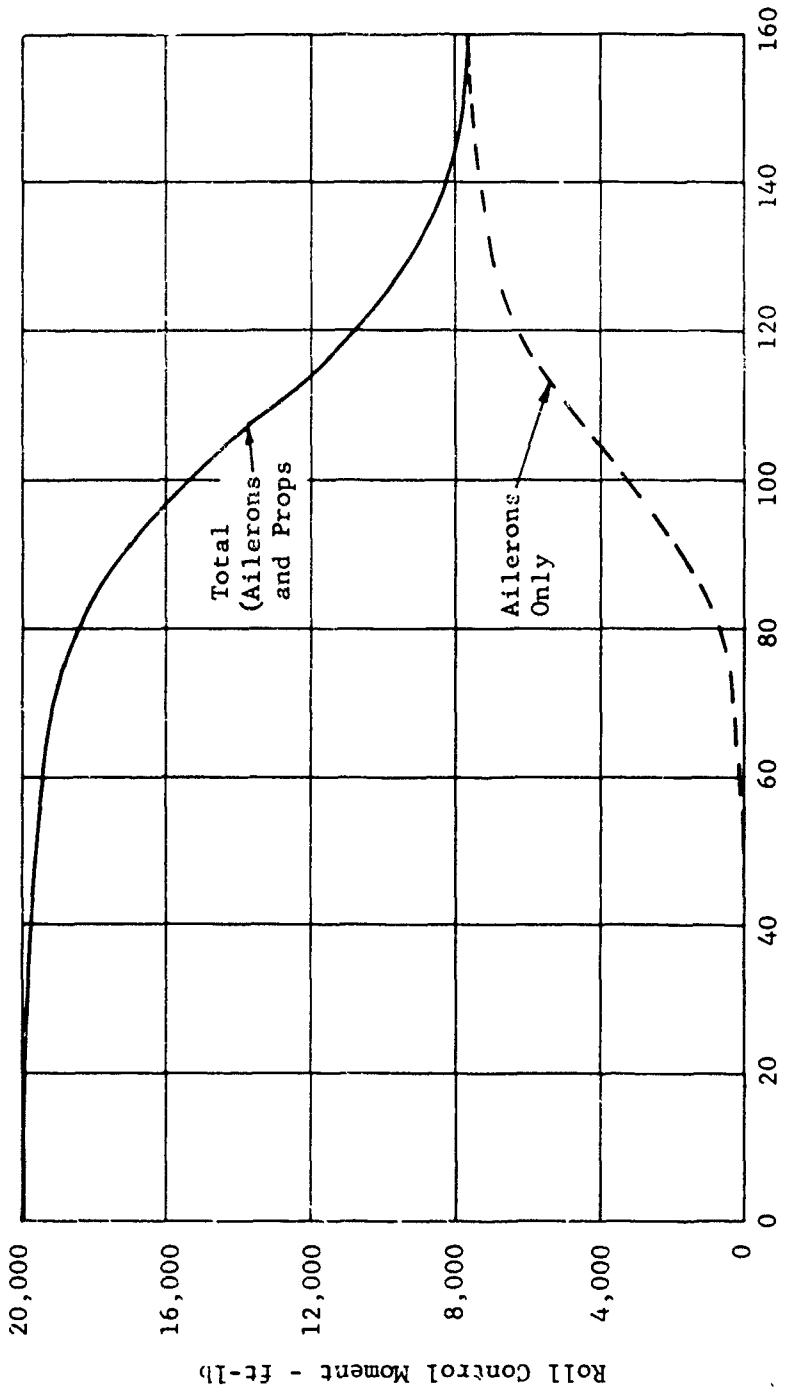

Figure 186. X-19, variation of available roll control power through transition.

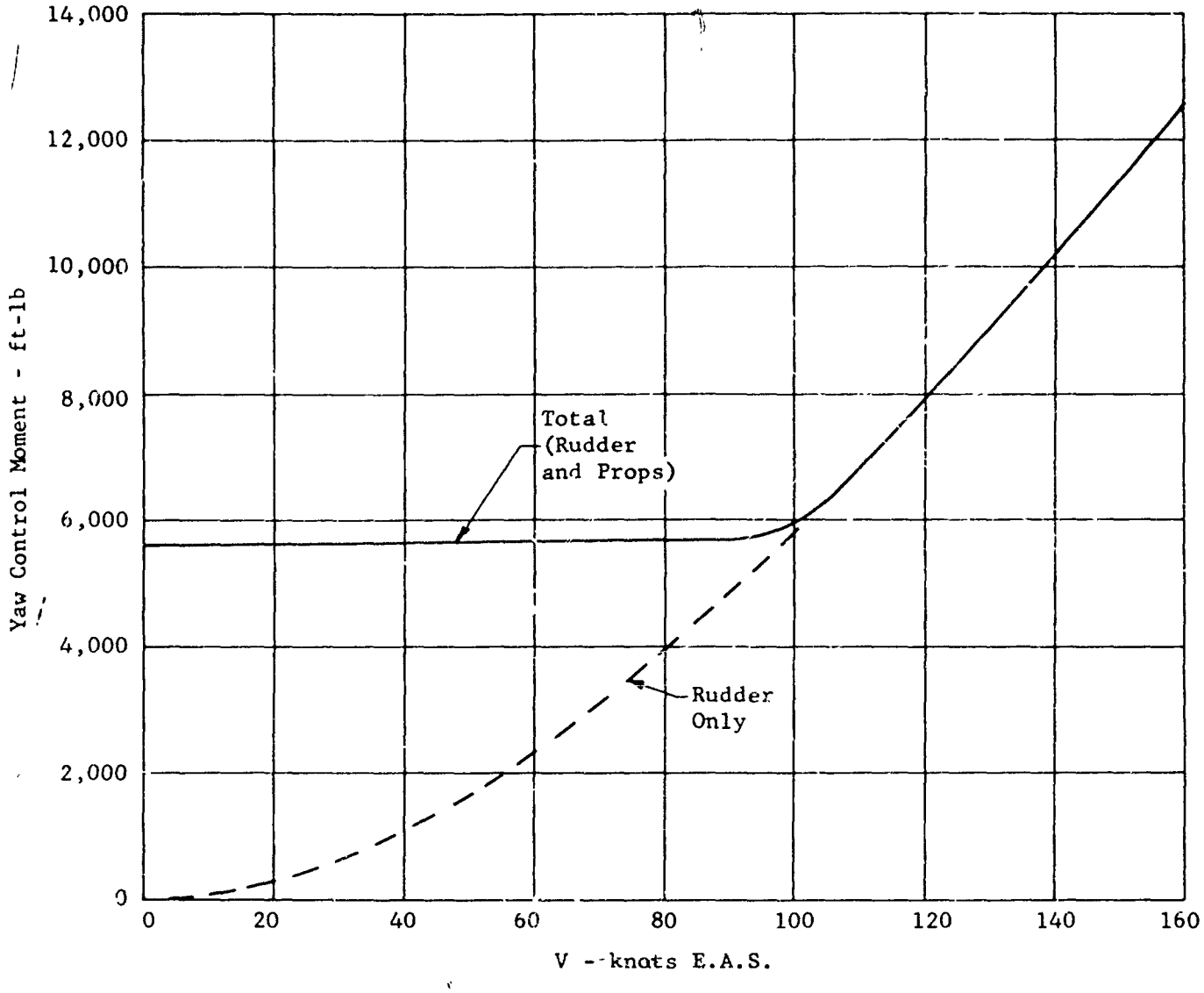

Figure 187. X-19, variation of available yaw control power through transition.

Solution of these equations (together with the determination of the stick-fixed stability derivatives), was accomplished with the aid of digital computer techniques. Rigid airplane stick fixed normal mode characteristics and stability derivatives (longitudinal and lateral) were determined for the allowable weight, c.g., altitude and speed range. The stability augmentation system does not provide any damping in the cruise regime.

Longitudinal stick free stability has not been considered since the elevator system is irreversible (see paragraph 1. b. (4) (b)).

The basic power-on derivatives C_{L_α}, C_{m_α}, C_{y_β}, C_{n_β} and C_{ℓ_β} were determined through the wind-tunnel tests of (48) through (52) and are shown in Figures 188, 189, 190, and 191.

(b) Normal Modes

The degree of compliance with (47) requirements of longitudinal short period mode damping and Dutch Roll damping are shown in Figures 192 and 193 and 194 through 196, respectively.

It is seen that for the weight, c.g., altitude and speed range shown, the requirement that the longitudinal short period oscillation damp to one-tenth amplitude in less than one cycle is easily met. This is also true for weights of 10,400 lbs (minimum flying weight) and 14,750 lbs (maximum overload) which are not included herein.

For a similar range of weight, c.g., altitude and speed, Dutch Roll damping exceeds the (47) requirement. At 10,400 lbs the sole point at which (47) is not met is 160 knots at 25,000 ft. The 10,400 lb and 14,750 lb data again are not included herein.

Over the airplane's entire operating range the Phugoid mode is stable and adequately damped. Under most conditions the other two 'usual' lateral modes (spiral and roll convergence) combine to form a second oscillatory mode which is virtually an oscillation in roll. It is very well damped and of rather long period.

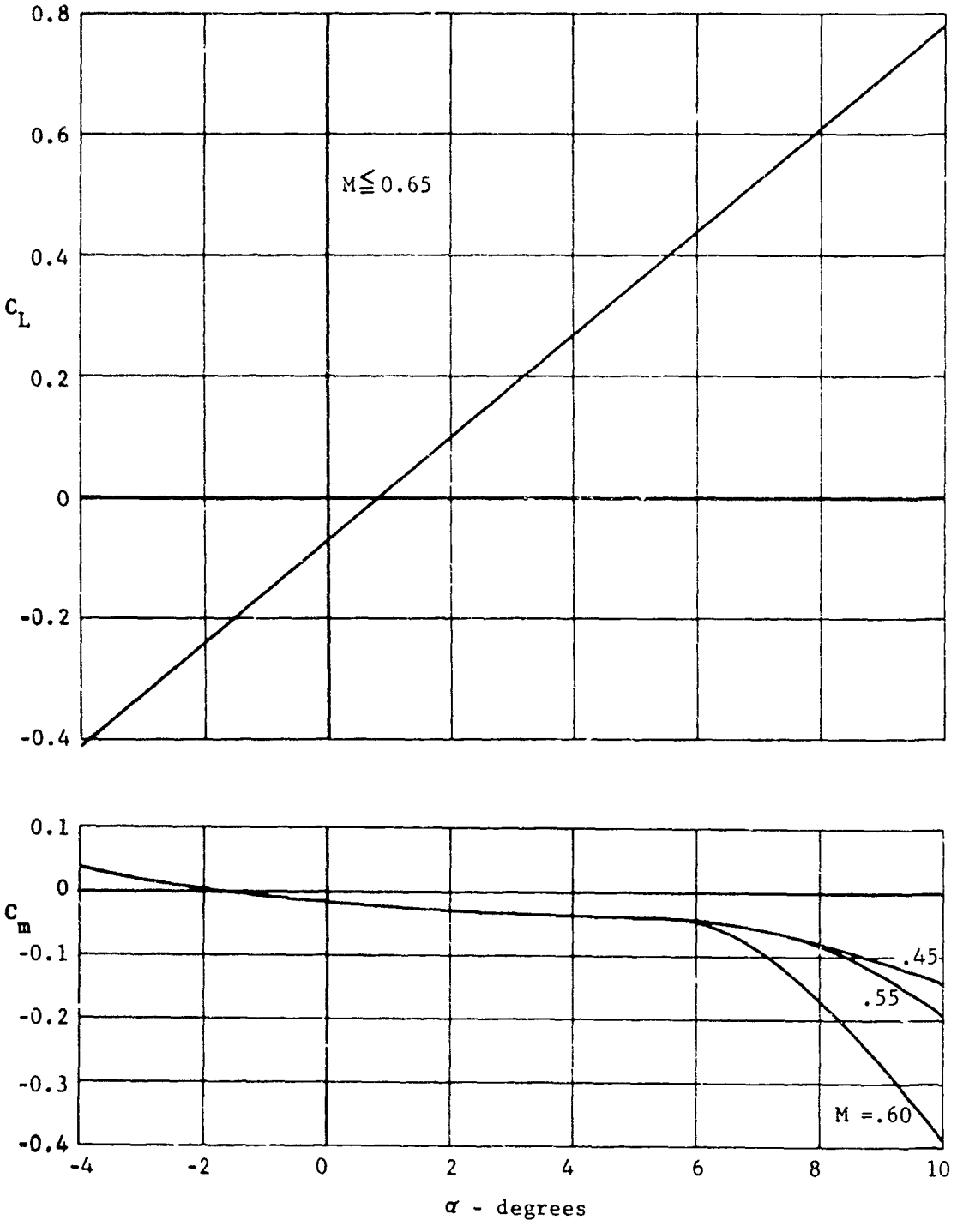

Figure 188. X-19, power on lift and pitching moment characteristics in cruise configuration based on wind tunnel data; c.g. = 42.9% lift chord.

FURNISHED UNDER UNITED STATES GOVERNMENT CONTRACT No. AF33(615)-1940. SHALL NOT BE EITHER RELEASED OUTSIDE THE GOVERNMENT, OR USED, DUPLICATED, OR DISCLOSED IN WHOLE OR IN PART FOR MANUFACTURE OR PROCUREMENT, WITHOUT THE WRITTEN PERMISSION OF CURTISS-WRIGHT CORPORATION, EXCEPT FOR (i) EMERGENCY REPAIR OR OVERHAUL WORK BY OR FOR THE GOVERNMENT WHERE THE ITEM OR PROCESS IS NOT OTHERWISE REASONABLY AVAILABLE TO ENABLE TIMELY PERFORMANCE OF THE WORK, OR (ii) RELEASE TO A FOREIGN GOVERNMENT, AS THE INTERESTS OF THE UNITED STATES MAY REQUIRE. PROVIDED THAT IN EITHER CASE THE RELEASE, USE, DUPLICATION OR DISCLOSURE HEREOF SHALL BE SUBJECT TO THE FOREGOING LIMITATIONS. THIS LEGEND SHALL BE MARKED ON ANY REPRODUCTION HEREOF IN WHOLE OR IN PART.

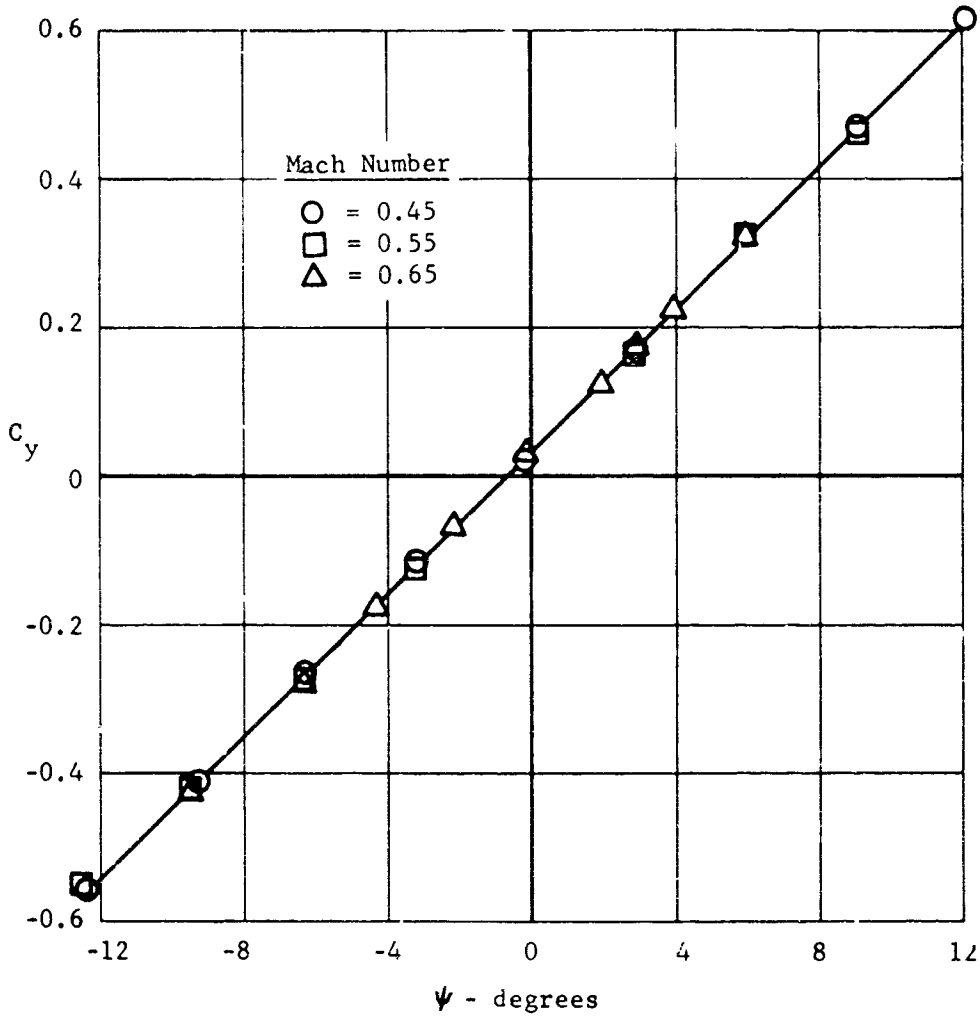

Figure 189. X-19, power on sideforce characteristics in cruise configuration based on wind tunnel data; $\alpha = 0$.

FURNISHED UNDER UNITED STATES GOVERNMENT CONTRACT No. AF33(615)-1940. SHALL NOT BE EITHER RELEASED OUTSIDE THE GOVERNMENT, OR USED, DUPLICATED, OR DISCLOSED IN WHOLE OR IN PART FOR MANUFACTURE OR PROCUREMENT WITHOUT THE WRITTEN PERMISSION OF CURTISS-WRIGHT CORPORATION, EXCEPT FOR (i) EMERGENCY REPAIR OR OVERHAUL WORK BY OR FOR THE GOVERNMENT WHERE THE ITEM OR PROCESS IS NOT OTHERWISE REASONABLY AVAILABLE TO ENABLE TIMELY PERFORMANCE OF THE WORK, OR (ii) RELEASE TO A FOREIGN GOVERNMENT, AS THE INTERESTS OF THE UNITED STATES MAY REQUIRE, PROVIDED THAT IN EITHER CASE THE RELEASE, USE, DUPLICATION OR DISCLOSURE HEREOF SHALL BE SUBJECT TO THE FOREGOING LIMITATIONS. THIS LEGEND SHALL BE MARKED ON ANY REPRODUCTION HEREOF IN WHOLE OR IN PART.

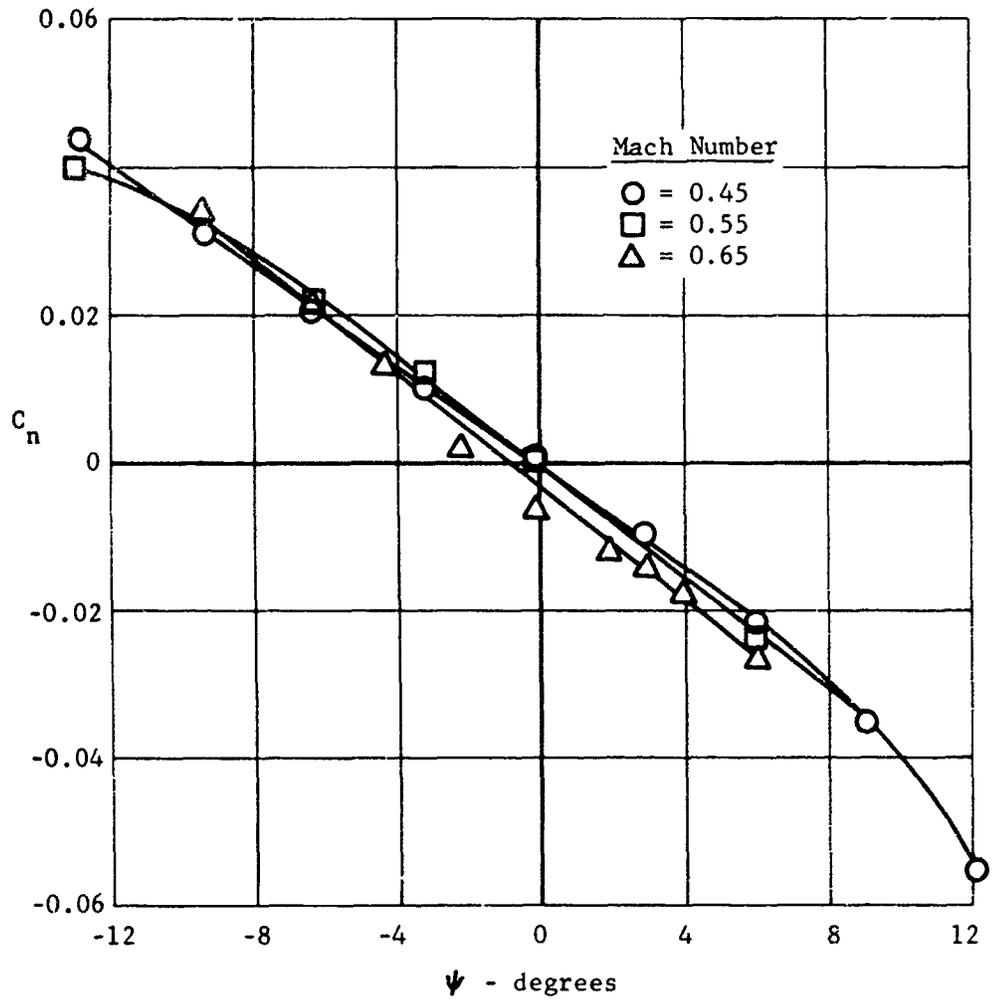

Figure 190. X-19, power on yawing moment characteristics in cruise configuration based on wind tunnel data. cg = 42.9% lift chord, α = 0.

'FURNISHED UNDER UNITED STATES GOVERNMENT CONTRACT No. AF33(615)-3940. SHALL NOT BE EITHER RELEASED OUTSIDE THE GOVERNMENT, OR USED, DUPLICATED, OR DISCLOSED IN WHOLE OR IN PART FOR MANUFACTURE OR PROCUREMENT, WITHOUT THE WRITTEN ' MISSION OF CURTISS-WRIGHT CORPORATION, EXCEPT FOR (i) EMERGENCY REPAIR OR OVERHAUL WORK BY OR FOR THE GOVERNMENT, WHERE THE ITEM OR PROCESS IS NOT OTHERWISE REASONABLY AVAILABLE TO ENABLE TIMELY PERFORMANCE OF THE WORK. OR (ii) RELEASE TO A FOREIGN GOVERNMENT, AS THE INTERESTS OF THE UNITED STATES MAY REQUIRE PROVIDED THAT IN EITHER CASE THE RELEASE, USE, DUPLICATION OR DISCLOSURE HEREOF SHALL BE SUBJECT TO THE FOREGOING LIMITATIONS THIS LEGEND SHALL BE MARKED ON ANY REPRODUCTION HEREOF IN WHOLE OR IN PART.'

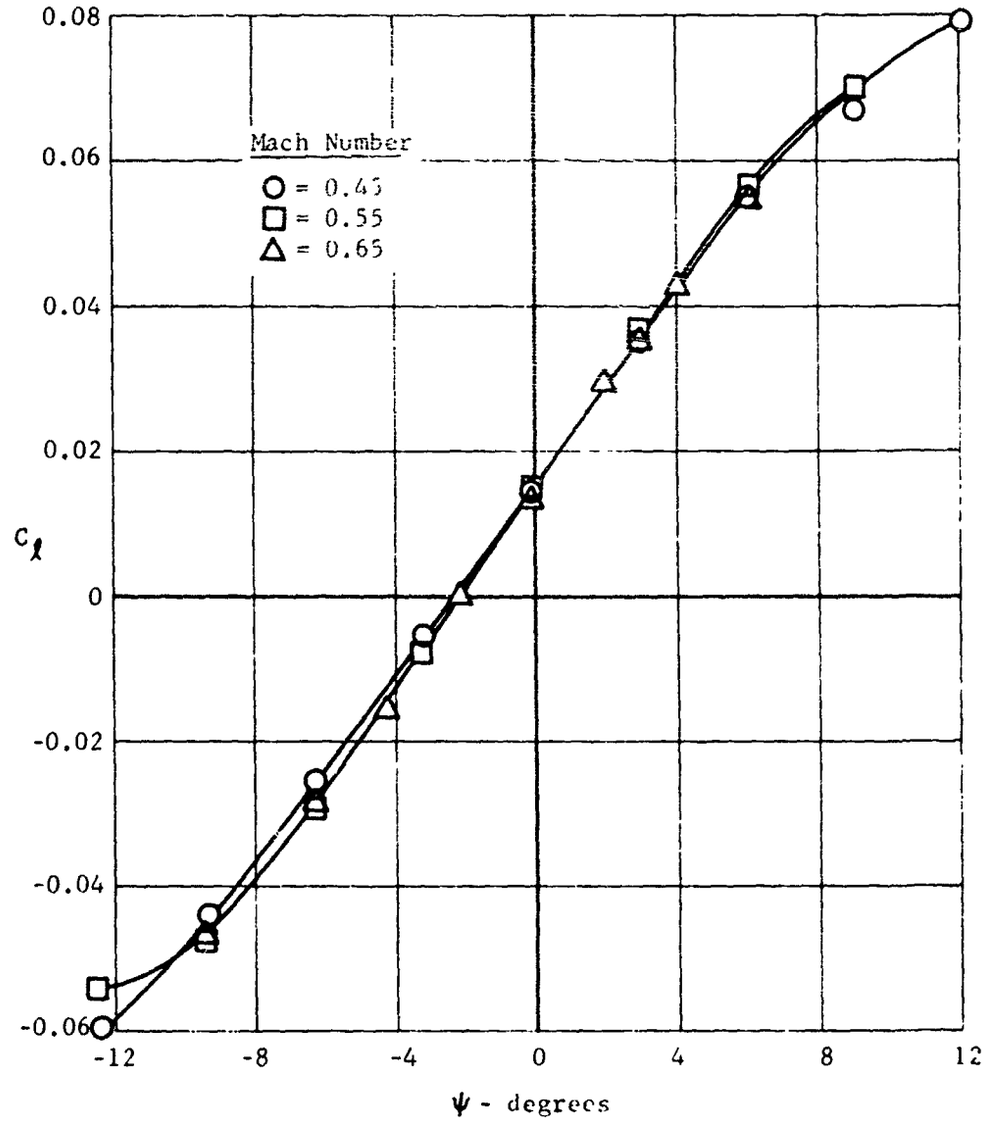

Figure 191. X-19, power on rolling moment characteristics in cruise configuration based on wind tunnel data; cg = 42.9% lift chord, α = 0.

"FURNISHED UNDER UNITED STATES GOVERNMENT CONTRACT No. AF33(615)-3940. SHALL NOT BE EITHER RELEASED OUTSIDE THE GOVERNMENT, OR USED, DUPLICATED, OR DISCLOSED IN WHOLE OR IN PART FOR MANUFACTURE OR PROCUREMENT, WITHOUT THE WRITTEN PERMISSION OF CURTISS-WRIGHT CORPORATION, EXCEPT FOR (i) EMERGENCY REPAIR OR OVERHAUL WORK BY OR FOR THE GOVERNMENT, WHERE THE ITEM OR PROCESS IS NOT OTHERWISE REASONABLY AVAILABLE TO ENABLE TIMELY PERFORMANCE OF THE WORK, OR (ii) RELEASE TO A FOREIGN GOVERNMENT, AS THE INTERESTS OF THE UNITED STATES MAY REQUIRE. PROVIDED THAT IN EITHER CASE THE RELEASE, USE, DUPLICATION OR DISCLOSURE HEREOF SHALL BE SUBJECT TO THE FOREGOING LIMITATIONS. THIS LEGEND SHALL BE MARKED ON ANY REPRODUCTION HEREOF IN WHOLE OR IN PART."

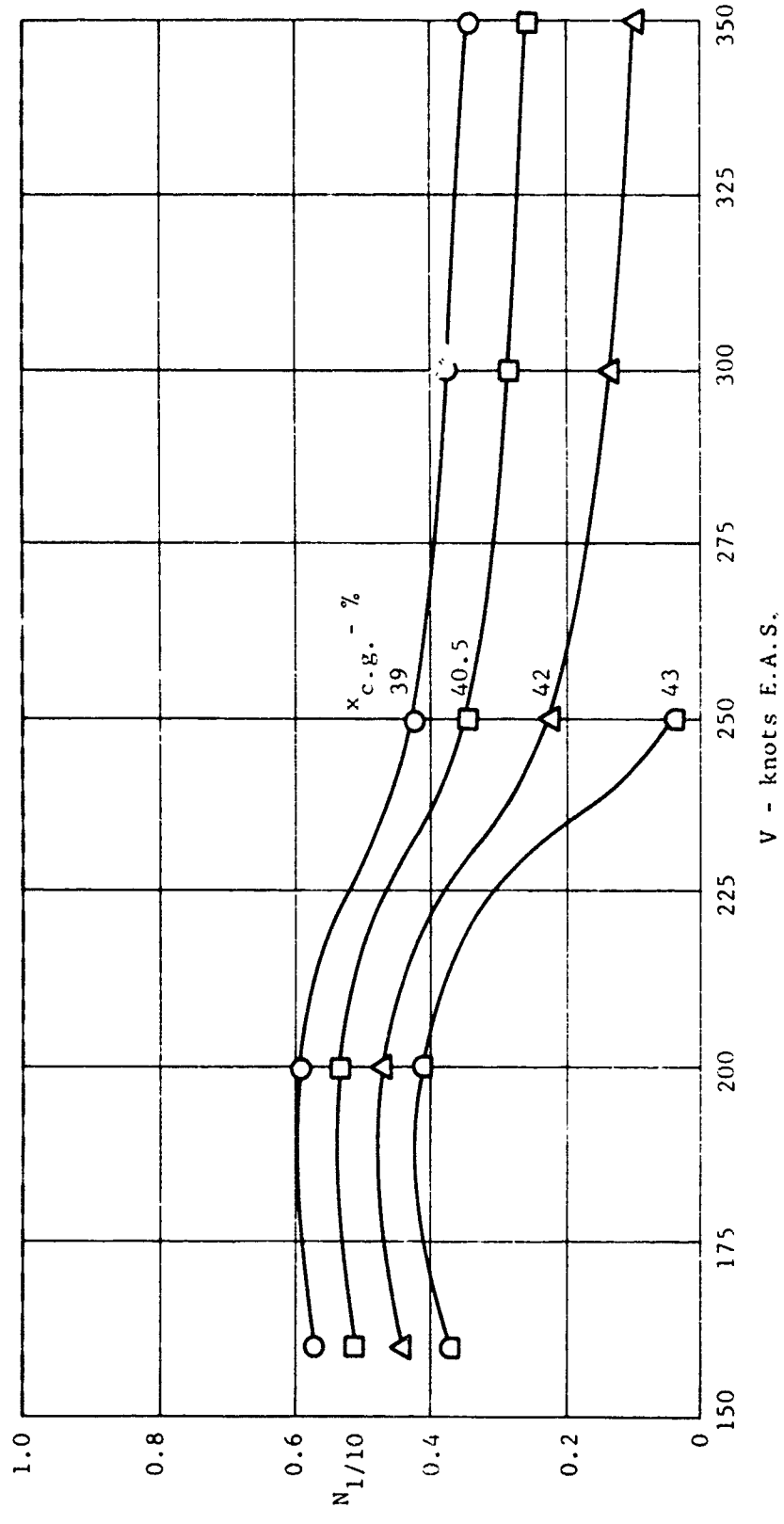

Figure 192. X-19, damping characteristics of the longitudinal short period mode in cruise; W = 12,300 pounds, height = sea level.

"FURNISHED UNDER UNITED STATES GOVERNMENT CONTRACT No. AF33(615)-3940. SHALL NOT BE EITHER RELEASED OUTSIDE THE GOVERNMENT, OR USED, DUPLICATED, OR DISCLOSED IN WHOLE OR IN PART FOR MANUFACTURE OR PROCUREMENT, WITHOUT THE WRITTEN PERMISSION OF CURTISS-WRIGHT CORPORATION, EXCEPT FOR (i) EMERGENCY REPAIR OR OVERHAUL WORK BY OR FOR THE GOVERNMENT, WHERE THE ITEM OR PROCESS IS NOT OTHERWISE REASONABLY AVAILABLE TO ENABLE TIMELY PERFORMANCE OF THE WORK, OR (ii) RELEASE TO A FOREIGN GOVERNMENT, AS THE INTERESTS OF THE UNITED STATES MAY REQUIRE. PROVIDED THAT IN EITHER CASE THE RELEASE, USE, DUPLICATION OR DISCLOSURE HEREOF SHALL BE SUBJECT TO THE FOREGOING LIMITATIONS. THIS LEGEND SHALL BE MARKED ON ANY REPRODUCTION HEREOF IN WHOLE OR IN PART."

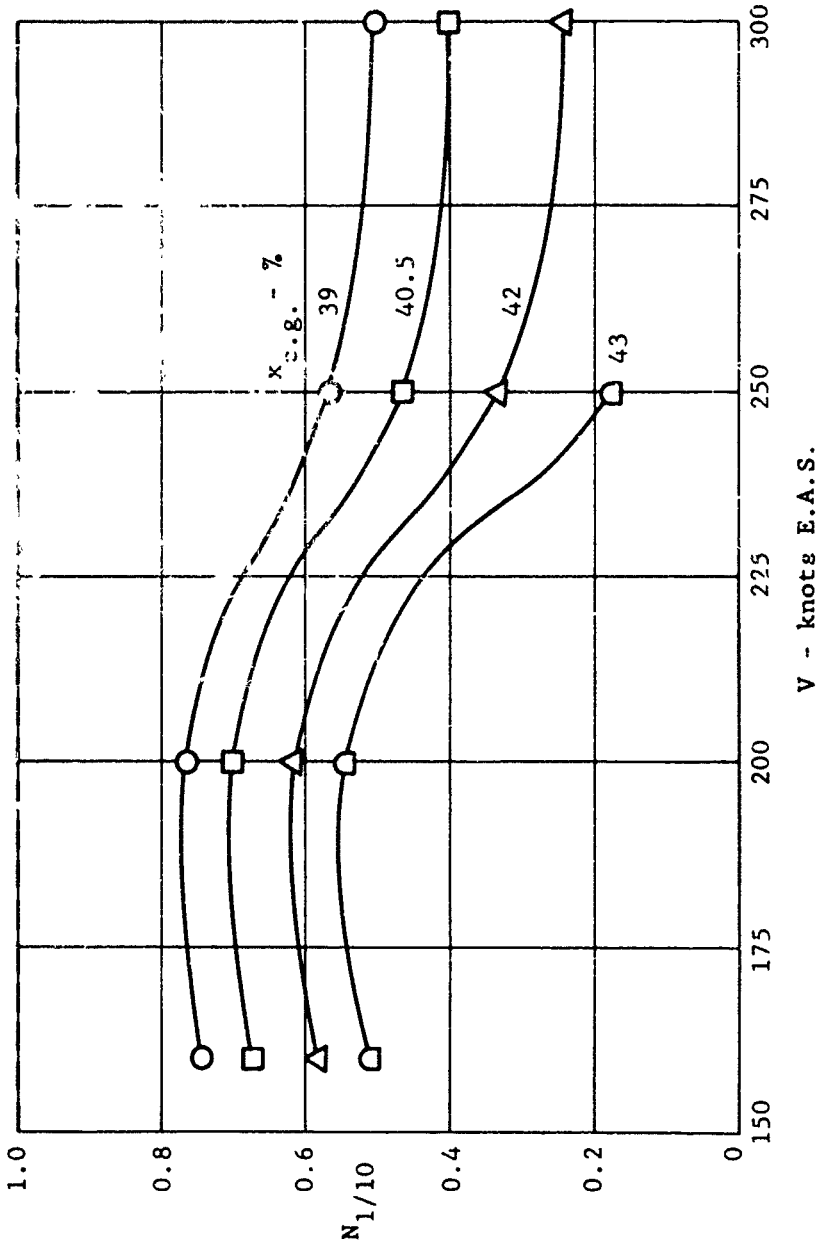

Figure 193. X-19, damping characteristics of the longitudinal short period mode in cruise; W = 12,300 pounds, height = 15,000 feet.

FURNISHED UNDER UNITED STATES GOVERNMENT CONTRACT No. AF33(615)-3940 SHALL NOT BE EITHER RELEASED OUTSIDE THE GOVERNMENT, OR USED, DUPLICATED, OR DISCLOSED IN WHOLE OR IN PART FOR MANUFACTURE OR PROCUREMENT, WITHOUT THE WRITTEN PERMISSION OF CURTISS-WRIGHT CORPORATION, EXCEPT FOR (i) EMERGENCY REPAIR OR OVERHAUL WORK BY OR FOR THE GOVERNMENT, WHERE THE ITEM OR PROCESS IS NOT OTHERWISE REASONABLY AVAILABLE TO ENABLE TIMELY PERFORMANCE OF THE WORK, OR (ii) RELEASE TO A FOREIGN GOVERNMENT, AS THE INTERESTS OF THE UNITED STATES MAY REQUIRE PROVIDED THAT IN EITHER CASE THE RELEASE, USE, DUPLICATION OR DISCLOSURE HEREOF SHALL BE SUBJECT TO THE FOREGOING LIMITATIONS. THIS LEGEND SHALL BE MARKED ON ANY REPRODUCTION HEREOF IN WHOLE OR IN PART.

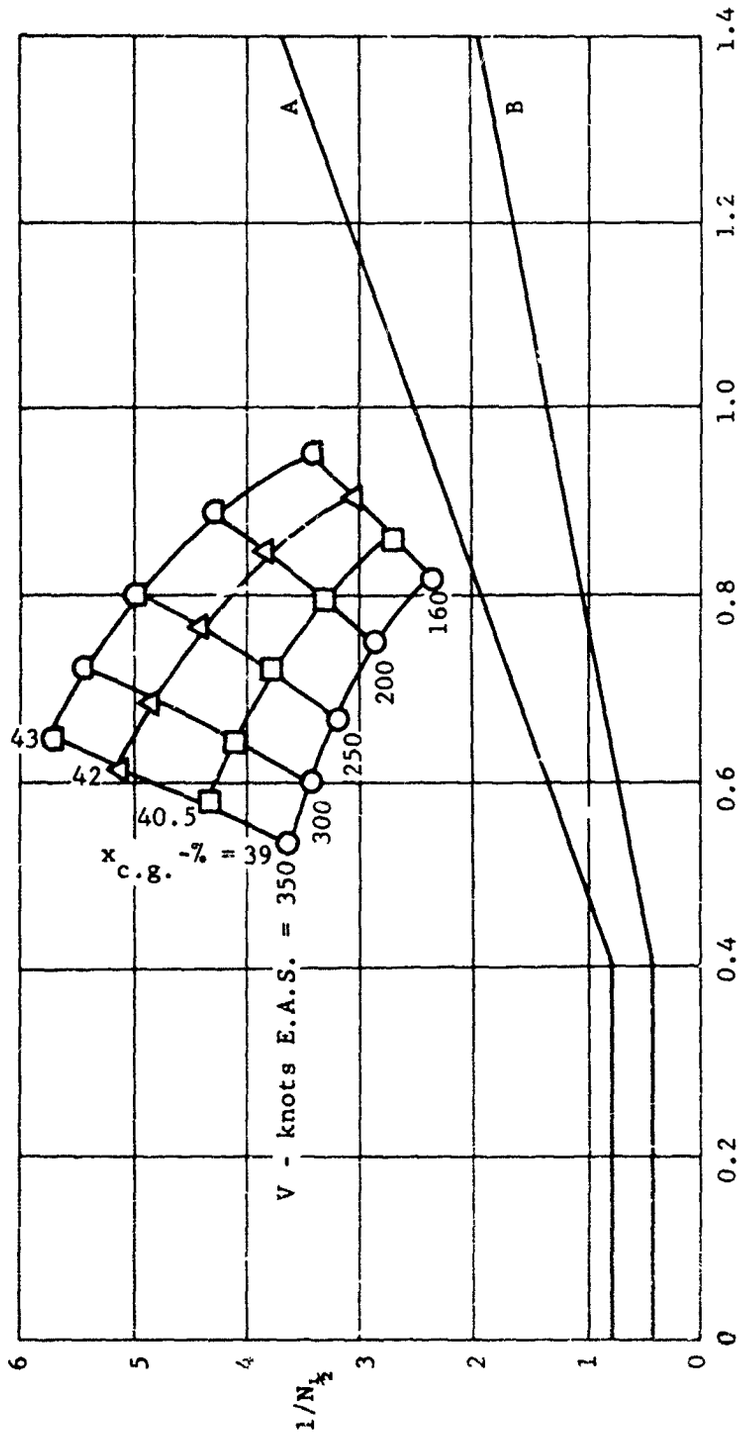

Figure 194. X-19, damping characteristics of the Dutch Roll mode in cruise; W = 12,300 pounds, height = sea level.

FURNISHED UNDER UNITED STATES GOVERNMENT CONTRACT No. AF33(615)-3940. SHALL NOT BE EITHER RELEASED OUTSIDE THE GOVERNMENT, OR USED, DUPLICATED, OR DISCLOSED IN WHOLE OR IN PART FOR MANUFACTURE OR PROCUREMENT, WITHOUT THE WRITTEN PERMISSION OF CURTISS-WRIGHT CORPORATION, EXCEPT FOR (i) EMERGENCY REPAIR OR OVERHAUL WORK BY OR FOR THE GOVERNMENT, WHERE THE ITEM OR PROCESS IS NOT OTHERWISE REASONABLY AVAILABLE TO ENABLE TIMELY PERFORMANCE OF THE WORK, OR (ii) RELEASE TO A FOREIGN GOVERNMENT, AS THE INTERESTS OF THE UNITED STATES MAY REQUIRE. PROVIDED THAT IN EITHER CASE THE RELEASE, USE, DUPLICATION OR DISCLOSURE HEREOF SHALL BE SUBJECT TO THE FOREGOING LIMITATIONS. THIS LEGEND SHALL BE MARKED ON ANY REPRODUCTION HEREOF IN WHOLE OR IN PART

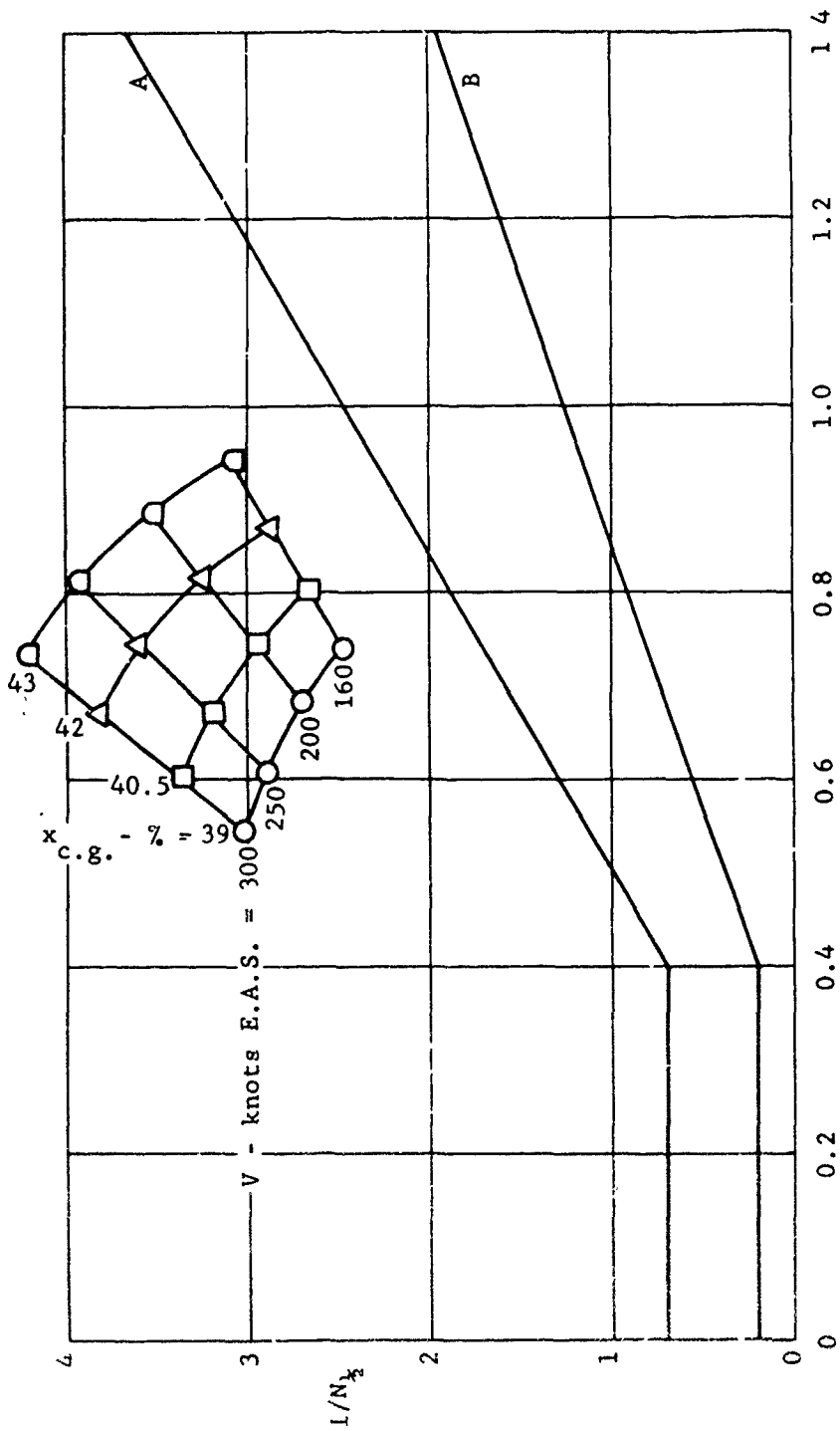

Figure 195. X-19, damping characteristics of the Dutch Roll mode in cruise; W = 12,300 pounds, height = 15,000 feet.

FURNISHED UNDER UNITED STATES GOVERNMENT CONTRACT No. AF33(600)-39460 SHALL NOT BE EITHER RELEASED OUTSIDE THE GOVERNMENT, OR USED DUPLICATED OR DISCLOSED IN WHOLE OR IN PART FOR MANUFACTURE OR PROCUREMENT WITHOUT THE WRITTEN PERMISSION OF CURTISS-WRIGHT CORPORATION, EXCEPT FOR (i) EMERGENCY REPAIR OR OVERHAUL WORK BY OR FOR THE GOVERNMENT, WHERE THE ITEM OR PROCESS IS NOT OTHERWISE REASONABLY AVAILABLE TO ENABLE TIMELY PERFORMANCE OF THE WORK, OR (ii) RELEASE TO A FOREIGN GOVERNMENT, AS THE INTERESTS OF THE UNITED STATES MAY REQUIRE, PROVIDED THAT IN EITHER CASE THE RELEASE, USE, DUPLICATION OR DISCLOSURE HEREOF SHALL BE SUBJECT TO THE FOREGOING LIMITATIONS. THIS LEGEND SHALL BE MARKED ON ANY REPRODUCTION HEREOF IN WHOLE OR IN PART.

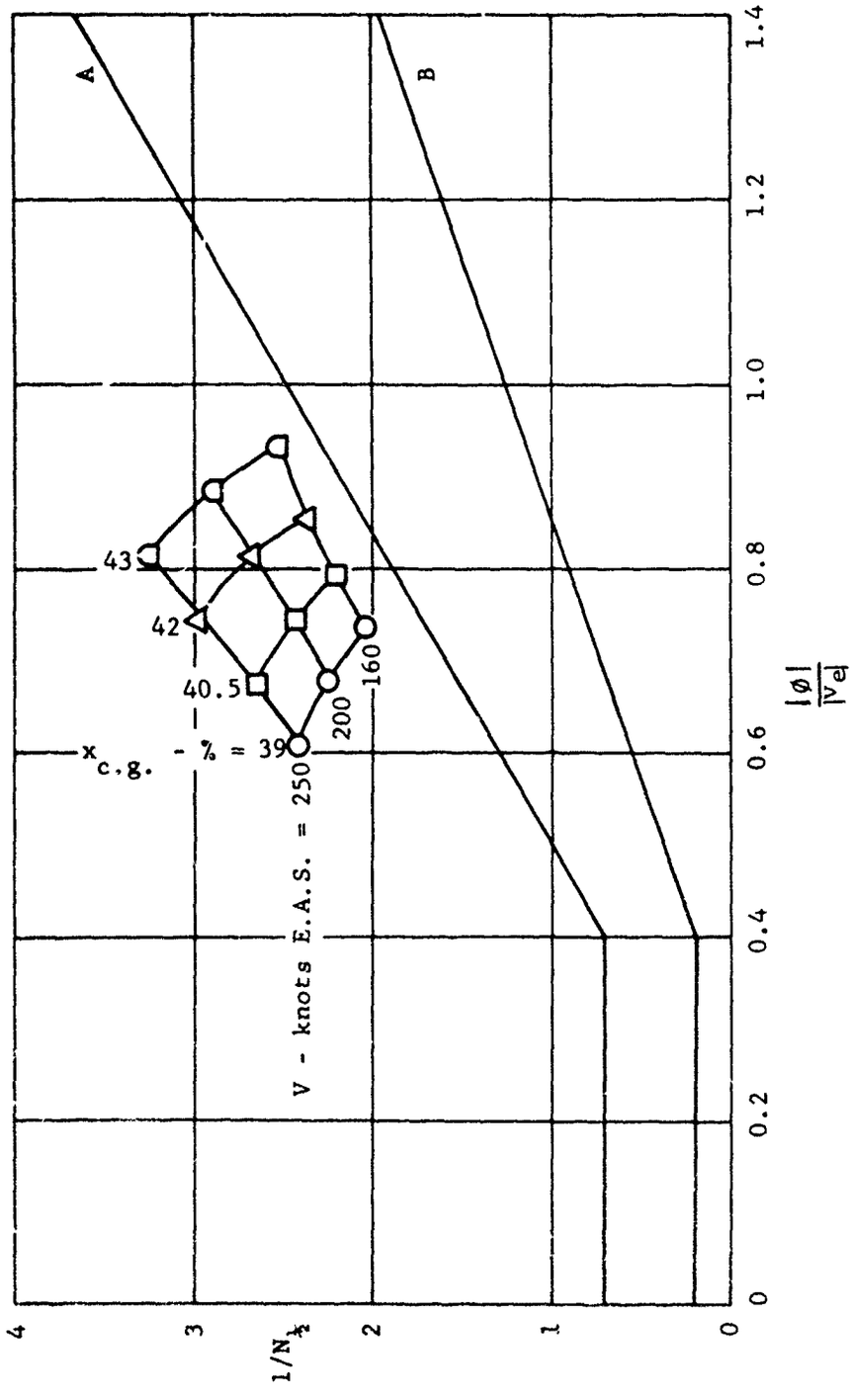

Figure 196. X-19, damping characteristics of the Dutch Roll mode in cruise; W = 12,300 pounds, height = 25,000 feet.

FURNISHED UNDER UNITED STATES GOVERNMENT CONTRACT No. AF33(615)-3940. SHALL NOT BE EITHER RELEASED OUTSIDE THE GOVERNMENT, OR USED DUPLICATED, OR DISCLOSED IN WHOLE OR IN PART FOR MANUFACTURE OR PROCUREMENT, WITHOUT THE WRITTEN PERMISSION OF CURTISS-WRIGHT CORPORATION, EXCEPT FOR (i) EMERGENCY REPAIR OR OVERHAUL WORK BY OR FOR THE GOVERNMENT, WHERE THE ITEM OR PROCESS IS NOT OTHERWISE REASONABLY AVAILABLE TO ENABLE TIMELY PERFORMANCE OF THE WORK, OR (ii) RELEASE TO A FOREIGN GOVERNMENT, AS THE INTERESTS OF THE UNITED STATES MAY REQUIRE. PROVIDED THAT IN EITHER CASE THE RELEASE, USE, DUPLICATION OR DISCLOSURE HEREOF SHALL BE SUBJECT TO THE FOREGOING LIMITATIONS. THIS LEGEND SHALL BE MARKED ON ANY REPRODUCTION HEREOF IN WHOLE OR IN PART."

(4) Controls and Control Systems

(a) General

In Cruise the X-19 utilizes conventional control surfaces only, viz. elevators, ailerons and rudder. No additional control power is obtained from the propellers as in transition.

(b) Elevators and Elevator System

The non-linear and, at large deflections, high hinge moments shown in Figure 197, taken from (52), make necessary the incorporation of an irreversible hydraulic power system. The power system provides up to the equivalent of 250 lbs at the stick. A hydraulic back up system provides up to 50% of the primary system power. Under either primary or back up system operation the hydraulic power may be supplemented by pilot effort, should a force greater than the actuator capacity be required. This situation is not expected to arise under primary system operation. With the back up system operating, additional pilot effort will be required under certain flight conditions in order to pull maximum allowable 'g'. Under such circumstances the additional stick forces will be stable.

The initial cruise stick feel system consisted only of the hover feel spring (1.06 lb/inch of stick). This has been replaced by a manually adjusted system that provides more reasonable stick forces in cruise. An indicator in the cockput displays stick force gradient setting relative to a nominal level equivalent to 15 lb/g, for all air speeds down to 120 knots.

The feel spring unit may be centered in such a manner that the stick force is zero at any trim elevator setting. System break-out force is 0.75 lb. No elevator trim tabs are fitted.

Elevator deflection range is 20° up and 15° down; full stick deflection is 4.06 inches forward and 5 42 inches aft. Resulting gear ratio is 0.773 rad/ft.

(c) Ailerons and Aileron System

A hydraulic actuator is incorporated in the aileron system which provides force up to the equivalent of 78 lbs at the stick. This modest boost is required primarily to reduce system friction to a low level in hover and

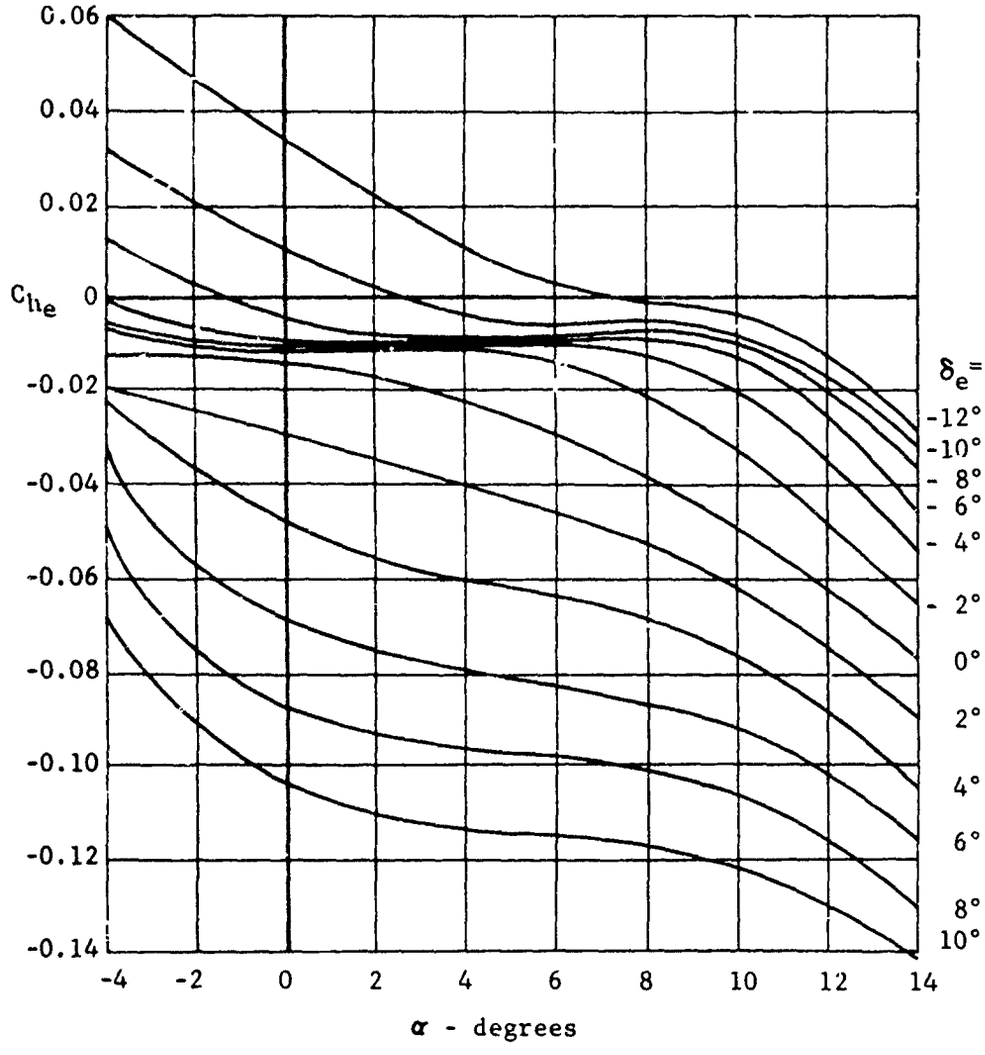

Figure 197. X-19, elevator hinge moment characteristics in cruise.

FURNISHED UNDER UNITED STATES GOVERNMENT CONTRACT No. AF33(615)-1940. SHALL NOT BE EITHER RELEASED OUTSIDE THE GOVERNMENT, OR USED DUPLICATED, OR DISCLOSED IN WHOLE OR IN PART FOR MANUFACTURE OR PROCUREMENT, WITHOUT THE WRITTEN PERMISSION OF CURTISS-WRIGHT CORPORATION, EXCEPT FOR (i) EMERGENCY REPAIR OR OVERHAUL WORK BY OR FOR THE GOVERNMENT, WHERE THE ITEM OR PROCESS IS NOT OTHERWISE REASONABLY AVAILABLE TO ENABLE TIMELY PERFORMANCE OF THE WORK, OR (ii) RELEASE TO A FOREIGN GOVERNMENT, AS THE INTERESTS OF THE UNITED STATES MAY REQUIRE. PROVIDED THAT IN EITHER CASE THE RELEASE, USE, DUPLICATION OR DISCLOSURE HEREOF SHALL BE SUBJECT TO THE FOREGOING LIMITATIONS. THIS LEGEND SHALL BE MARKED ON ANY REPRODUCTION HEREOF IN WHOLE OR IN PART.

in cruise is supplemented by pilot effort. The back up system is manual. Aileron hinge moments, taken from (52) are shown in Figure 198.

A position feel spring of gradient 1.25 lb/in. is incorporated and system break-out force is 1 lb Aileron deflection range is 15° up, and 11° down; stick travel is ± 5 inches. No trim tabs are fitted.

The ailerons are mechanically linked to the rear nacelles such that both ailerons droop progressively as the nacelles tilt up. The maximum deflection of 60° is reached at approximately $\emptyset_F$ = 80°. Differential aileron movement is maintained throughout the droop schedule. This technique serves to reduce download on the rear wing in hover and to increase rear wing lift throughout transition.

(d) Rudder and Rudder System

The rudder is actuated manually through a system of cables connected to conventional rudder pedals. To provide the pilot with feel in hover, a spring of gradient 5 lb/in. is incorporated in the system. This spring remains operative in cruise. System break-out force is 13 lb.

Figure 199. Rudder deflection range is ± 33°; pedal travel ± 3 inches. The rudder trim tab has ± 8° of travel

(e) Flaps and Flap System

The flaps are mechanically linked to the front nacelles and move only in conjunction with the nacelles. In a like fashion to the ailerons, the flaps droop (as the nacelles tilt up) to a maximum deflection of 60° and serve the same purposes of reducing download in hover and increasing lift through transition.

(5) Maneuvering Flight

(a) Elevator Angle to Trim

Elevator trim settings for level flight at 15,000 ft are shown in Figure 200 for W = 12,300 lbs. and

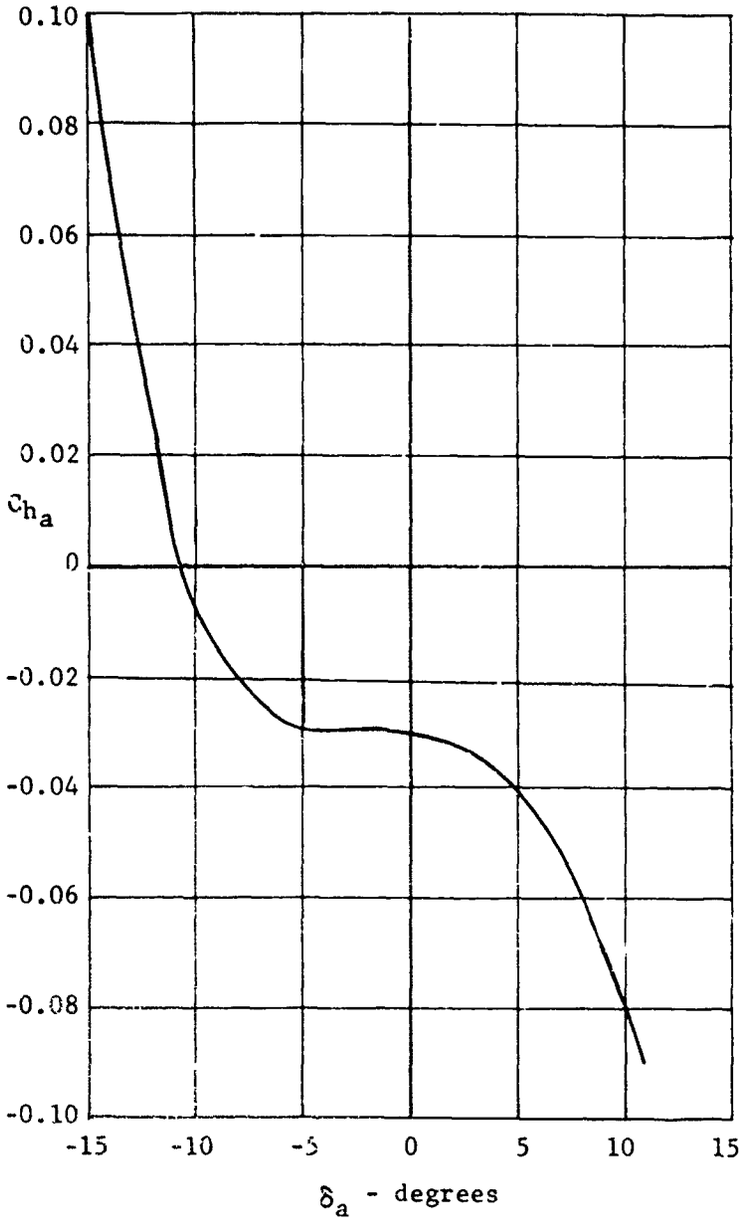

Figure 198. X-19, aileron hinge moment characteristic in cruise, $\alpha = 0$.

FURNISHED UNDER UNITED STATES GOVERNMENT CONTRACT No. AF33(615)-1940 SHALL NOT BE EITHER RELEASED OUTSIDE THE GOVERNMENT, OR USED DUPLICATED, OR DISCLOSED IN WHOLE OR IN PART FOR MANUFACTURE OR PROCUREMENT, WITHOUT THE WRITTEN PERMISSION OF CURTISS-WRIGHT CORPORATION, EXCEPT FOR (i) EMERGENCY REPAIR OR OVERHAUL WORK BY OR FOR THE GOVERNMENT, WHERE THE ITEM OR PROCESS IS NOT OTHERWISE REASONABLY AVAILABLE TO ENABLE TIMELY PERFORMANCE OF THE WORK, OR (ii) RELEASE TO A FOREIGN GOVERNMENT AS THE INTERESTS OF THE UNITED STATES MAY REQUIRE PROVIDED THAT IN EITHER CASE THE RELEASE, USE DUPLICATION OR DISCLOSURE HEREOF SHALL BE SUBJECT TO THE FOREGOING LIMITATIONS THIS LEGEND SHALL BE MARKED ON ANY REPRODUCTION HEREOF IN WHOLE OR IN PART.

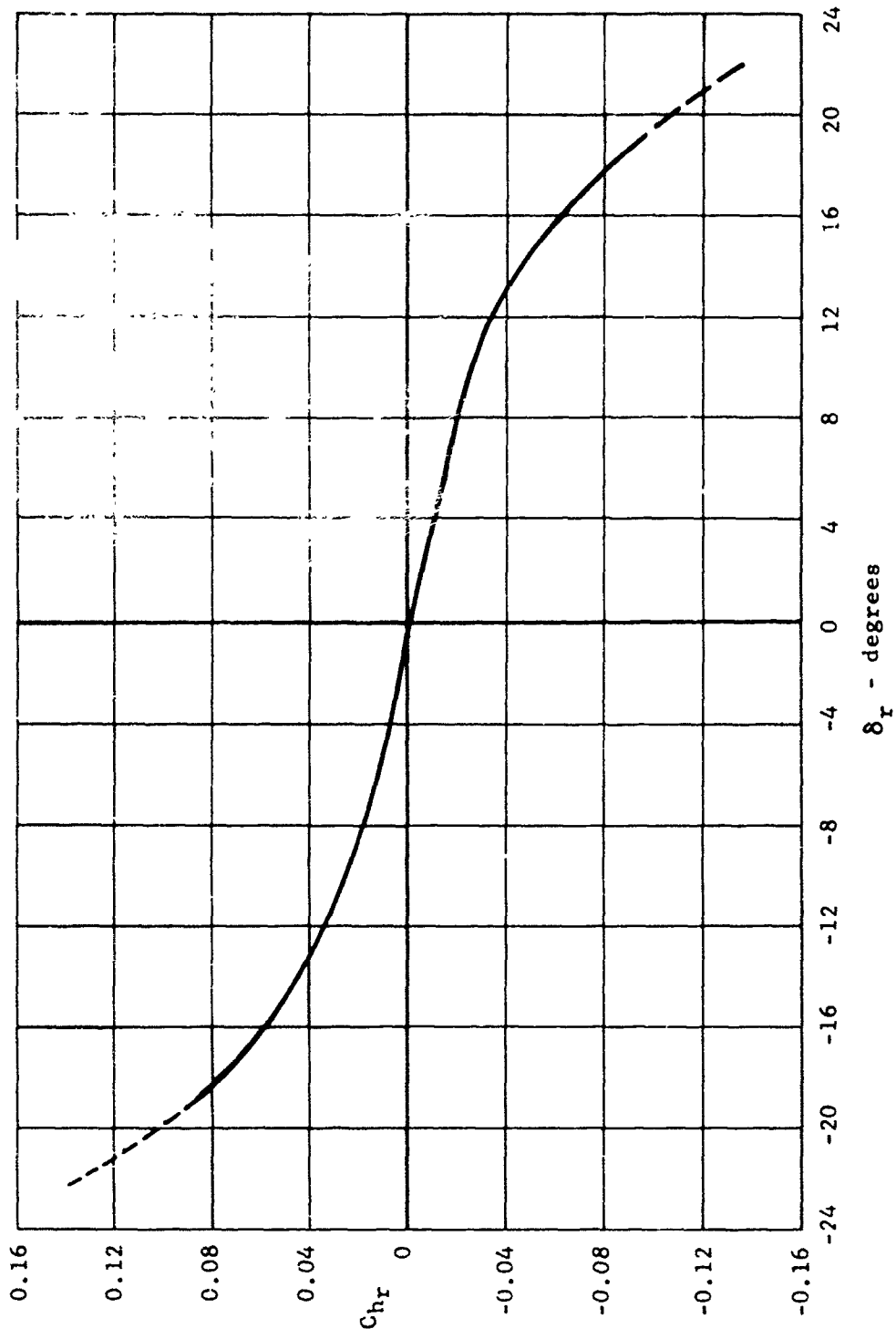

Figure 199. X-19, rudder hinge moment characteristics in cruise; $\alpha = 0$

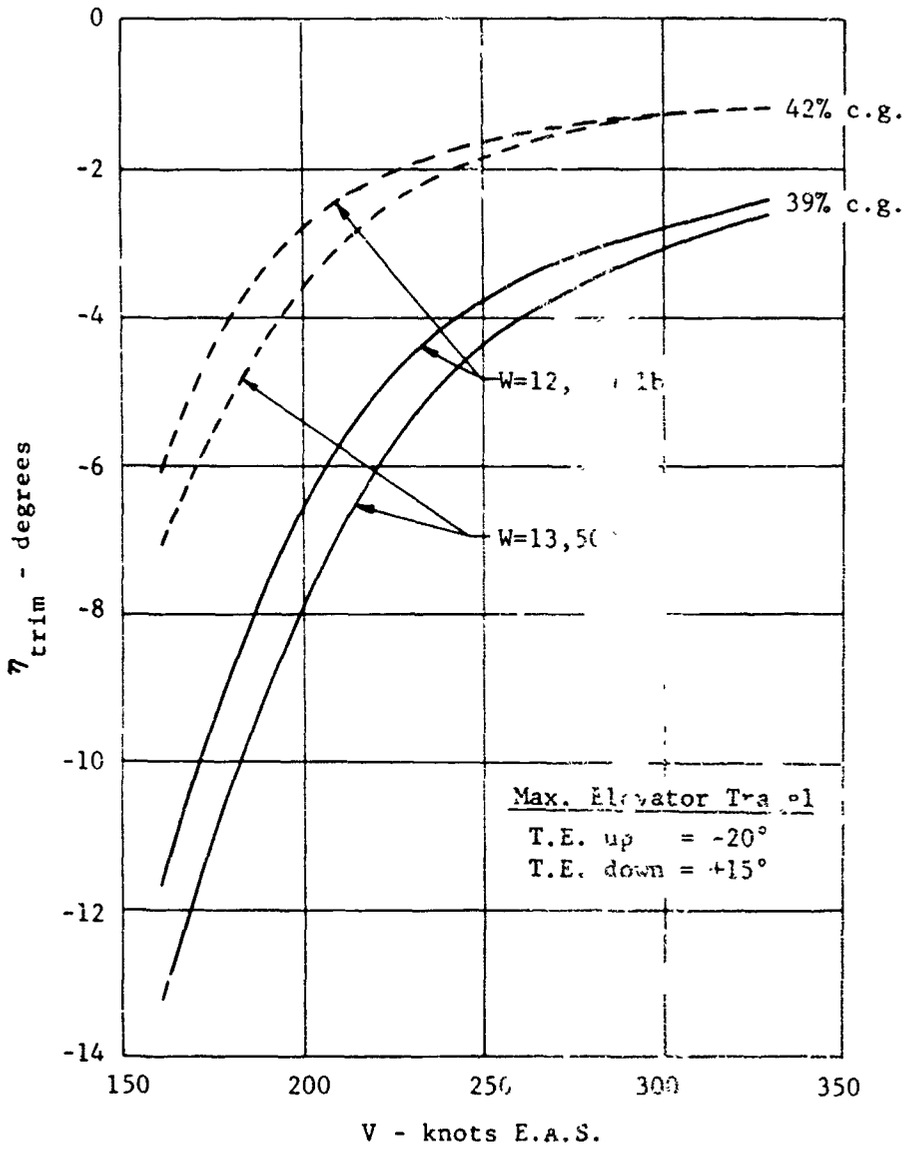

Figure 200. X-19, cruise elevator trim settings in level flight at 15,000 feet; W = 12,300 and 13,500 pounds, c.g. = 39% and 42% lift chord.

13,500 lbs at 39% and 42% c.g. All trim settings are trailing edge up since C_m at $\alpha = 0°$ is nose-down.

(b) Elevator Angle per 'g'

The variation of elevator angle per 'g' with forward speed is shown in Figure 201. This is a measure of the elevator control effectiveness in pulling normal load factors lesser or greater than 1g (level flight).

The reflexes in the curves are due to the non-linear $C_m \sim \alpha$ characteristic of the airplane. (See figure 203.)

(c) Stick Force per 'g'

Covered in paragraph 1.b. (4) (b) above.

(d) Roll Performance

Data are presented for the performance in a pure roll only. The effects of sideslipping and yawing motions have been neglected. Maximum aileron control has been defined as that available with a lateral stick force of 25 lbs. This is the criterion for assessing handling qualities as given in (47). The roll power derivative (C_{l_ξ}) used has been corrected for aeroelastic distortion of the rear wing.

Results are plotted as a function of forward speed and describe the characteristics of the pure roll transient following instantaneous deflection of the ailerons.

The amount of aileron available is influenced by control cable stretch and the stick force limitation defined above. Maximum steady roll rates range from 40°/sec at S.L. to 63°/sec at 25,000 ft as shown in Figure 202. Bank angle excursions at the end of 1 sec are plotted in Figure 203. The variation of the time constant of pure rolling motion is shown in Figure 204.

(e) Steady Sideslips

For steady sideslips, the lateral equations 4.15.8 of (45) are used, by letting the angular velocities and accelerations be zero. The modified equations are presented as follows:

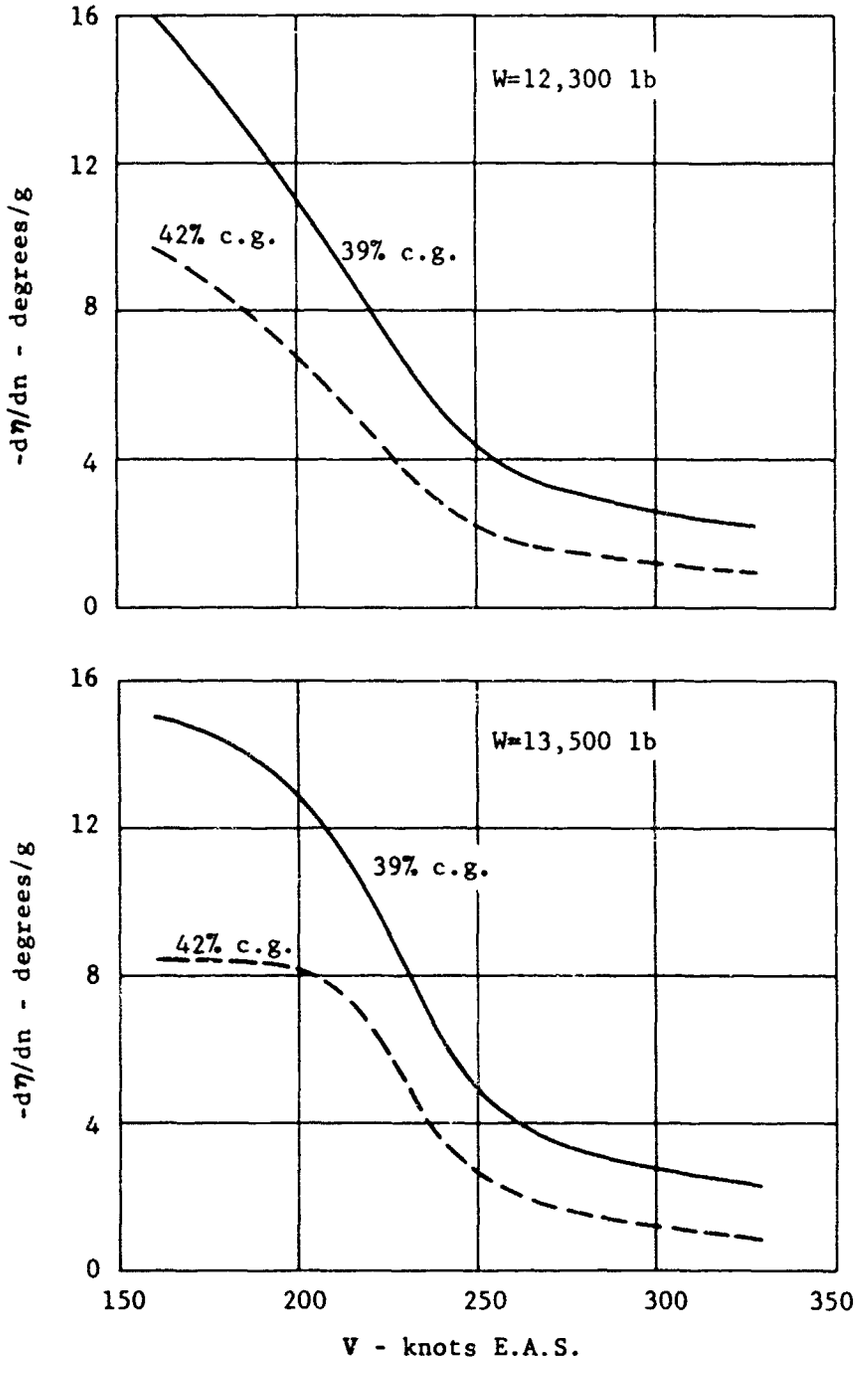

Figure 201. X-19, cruise elevator angle per 'g' at 15,000 feet; W = 12,300 and 13,500 pounds, c.g. = 39%, 42% lift chord.

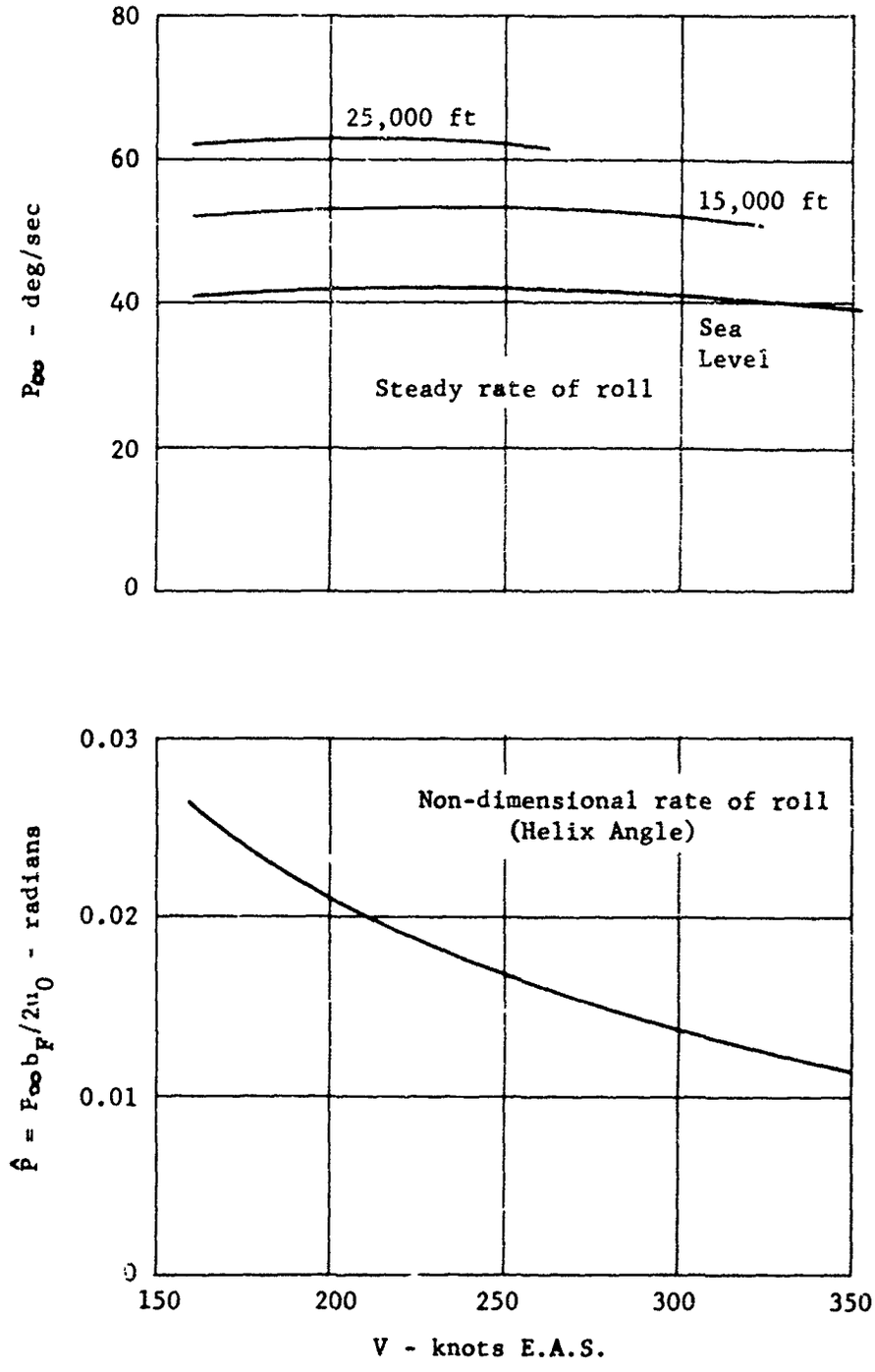

Figure 202. X-19, roll performance in cruise, steady roll rate and wing tip helix angle with a stick force of 25 pounds.

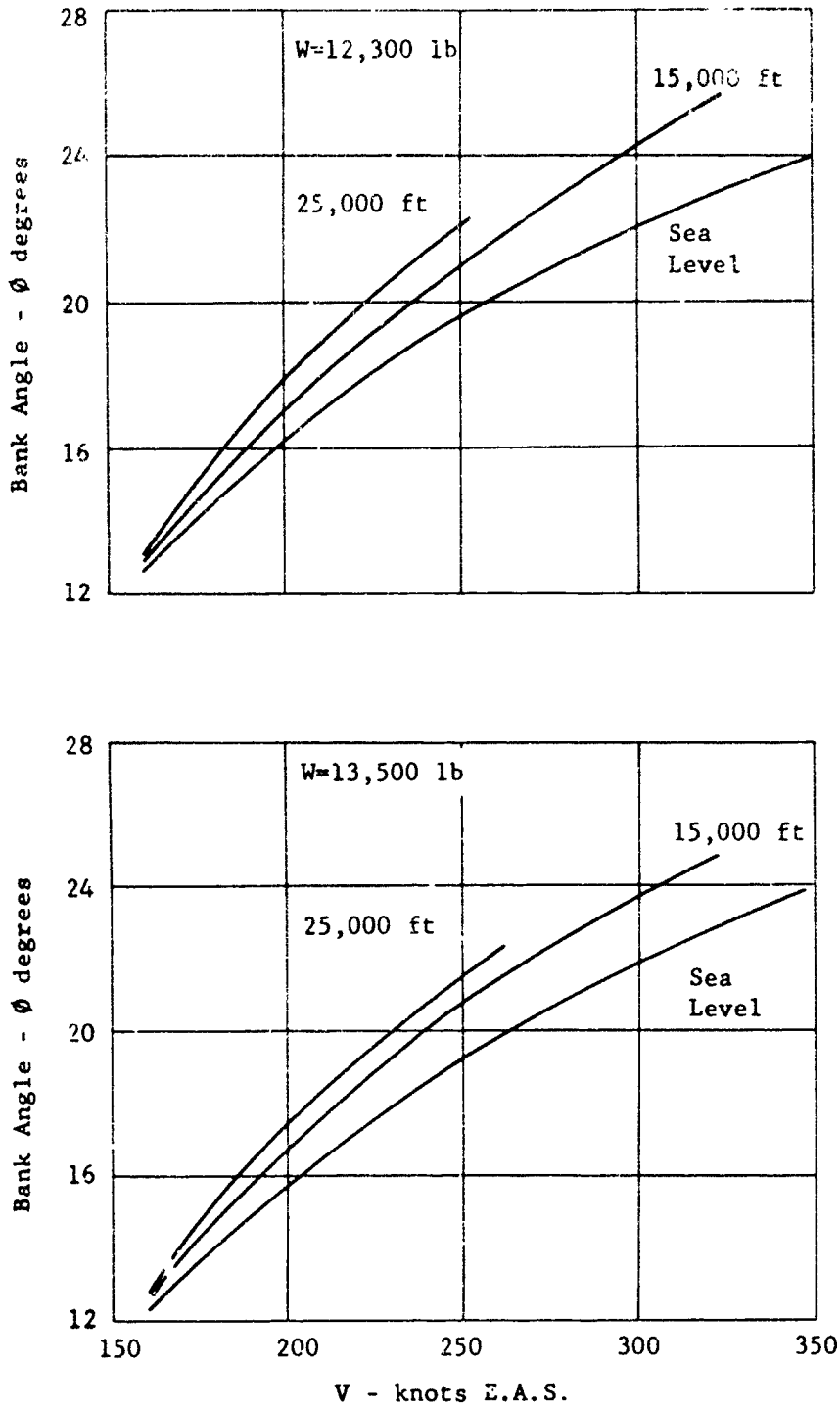

Figure 203. X-19, roll performance in cruise, bank angle attained one second after an instantaneous aileron deflection with a stick force of 25 pounds.

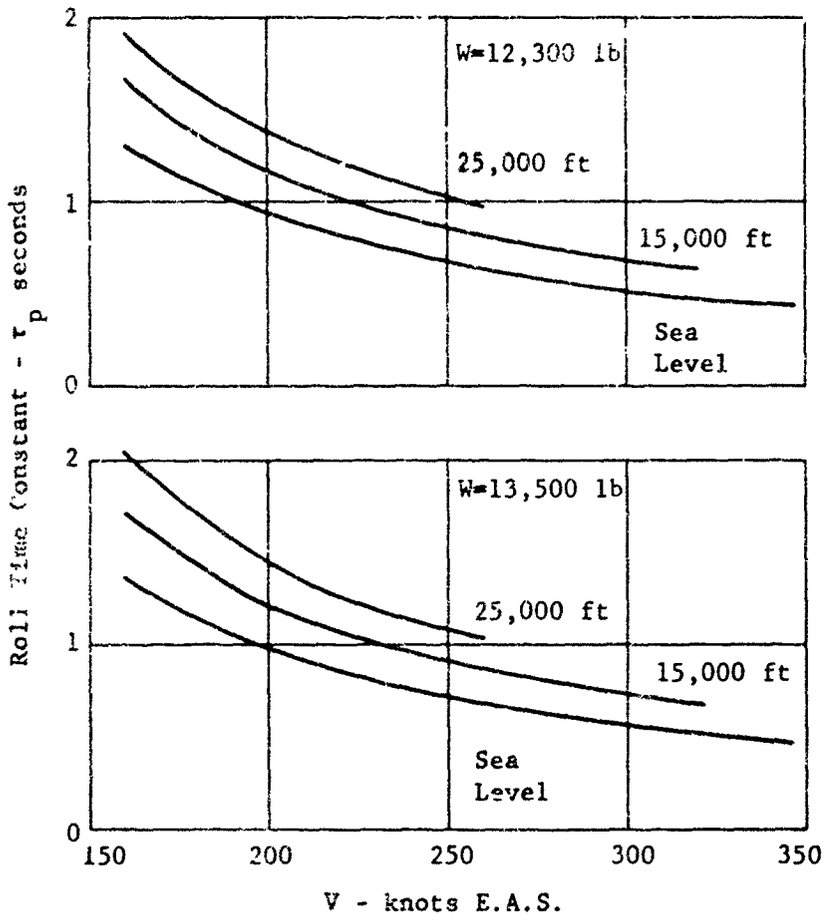

Figure 204. X-19, roll performance in cruise, roll time constant.

$$- C_{y_\beta}\beta \qquad - C_{y_{\delta_r}}\delta_r \qquad - C_{L_o}\phi = 0$$

$$- C_{\ell_\beta}\beta \qquad - C_{\ell_{\delta_a}}\delta_a \qquad - C_{\ell_{\delta_r}}\delta_r = 0$$

$$- C_{n_\beta}\beta \qquad - C_{n_{\delta_a}}\delta_a \qquad - C_{n_{\delta_r}}\delta_r = 0$$

Solution of these equations yields the following relationships for an aircraft weight of 12,300 lbs at 160 knots EAS and 347 knots EAS.

	160 knots EAS	347 knots EAS
δ_r	1.40β	2.08β
δ_a	-3.12β	-3.69β
ϕ	2.81β	12.71β

For both flight conditions, the maximum sideslip angle attainable is limited by aileron angle available. The results are:

	160 knots EAS	347 knots EAS
$\delta_{a_{max}}$	10.45	7.50
β°	-3.45	-2.03
ϕ°	-9.70	-25.80
$\delta^\circ_{r_{req'd}}$	-4.83	-4.22

2. TANDEM WING AIRPLANE AERODYNAMIC CHARACTERISTICS

a. Basic Data

The aerodynamic characteristics of wings in tandem were studied in theories of Munk (53) and Glauert (54). The results indicated that lift and induced drag would be similar to those of a single wing having a chord distribution corresponding to the sum of the local chords of the two wings.

However, the effects of body-wing interference are such that at the rear wing a highly distorted load distribution is encountered. Also, the propeller effects are considerable, so that the analytical estimation of the lift and drag characteristics was found to be of considerable complexity.

The basic aerodynamic data used were therefore based on a series of wind-tunnel tests of powered and unpowered models. Included was one of a model in which the geometry could be changed by use of various wings and fuselage sections. These tests are considered to give good data for lift and induced drag although the profile drags are not valid, due to the low Reynolds number.

b. Drag Estimate

The estimated total drag of the X-19 is based on the use of standard methods utilizing data obtained from (55) and (56) combined with results from wind tunnel tests of a powered 12% scale model. See (50), (51), and (52). The composition of the total drag coefficient is summarized in Figure 207.

c. Propellers-Off Incompressible Profile Drag Coefficient, C_{D_o}

The basic fuselage and airfoil drags were obtained from (56) with boundary layer transition assumed to occur at 10% chord of the airfoils and at 5% of the fuselage length, a point just aft of the end of the smooth fiberglass nose cap. The drag of the wings and tail were increased by 10% to allow for control gaps.

The canopy drag increment was taken from (57) and the external drag of the engine air inlet was based on data from (55) and some early Curtiss wind tunnel tests. Nacelle drag was taken from (56) assuming fully turbulent flow, while interference contributions were based on (55). As an allowance for external fittings, roughness, waviness, leaks, etc., 15% of the sum of the component drags was added. A check of a number of the external fittings indicated that this is a reasonable value, given a satisfactory surface finish overall.

Table XVII gives a breakdown of the component contributions to the profile drag at a Reynolds number of 2.5 million per foot, typical cruise value.

d. Effects of Lift, Power, and Compressibility

The configuration of the X-19 is such that analytical estimation of lift, power and compressibility effects is not feasible; it is necessary to base estimates on wind tunnel test data. It is generally assumed that Reynolds Number effects on these

FURNISHED UNDER UNITED STATES GOVERNMENT CONTRACT No. AF33(615)-3940 SHALL NOT BE EITHER RELEASED OUTSIDE THE GOVERNMENT, OR USED, DUPLICATED, OR DISCLOSED IN WHOLE OR IN PART FOR MANUFACTURE OR PROCUREMENT, WITHOUT THE WRITTEN PERMISSION OF CURTISS-WRIGHT CORPORATION, EXCEPT FOR (i) EMERGENCY REPAIR OR OVERHAUL WORK BY OR FOR THE GOVERNMENT, WHERE THE ITEM OR PROCESS IS NOT OTHERWISE REASONABLY AVAILABLE TO ENABLE TIMELY PERFORMANCE OF THE WORK, OR (ii) RELEASE TO A FOREIGN GOVERNMENT, AS THE INTERESTS OF THE UNITED STATES MAY REQUIRE. PROVIDED THAT IN EITHER CASE THE RELEASE USE, DUPLICATION OR DISCLOSURE HEREOF SHALL BE SUBJECT TO THE FOREGOING LIMITATIONS. THIS LEGEND SHALL BE MARKED ON ANY REPRODUCTION HEREOF IN WHOLE OR IN PART."

Table XVII. Incompressible power-off profile drag breakdown. Reynolds number = 2.5×10^6 per foot.

Component	$\Delta C_{D_o} S$	ΔC_{D_o} (Based on 154.6 ft^2)
Fuselage	2.092	0.0135
Front Wing	0.492	0.0032
Rear Wing	0.852	0.0055
Vertical Tail	0.407	0.0026
Nacelles*	0.598	0.0039
Minor Fittings, etc.	0.666	0.0043
Interference	0.187	0.0012
Total	5.294	0.0342

Note (*) Includes wing-nacelle interference

"FURNISHED UNDER UNITED STATES GOVERNMENT CONTRACT No. AF33(615)-3940 SHALL NOT BE EITHER RELEASED OUTSIDE THE GOVERNMENT, OR USED, DUPLICATED, OR DISCLOSED IN WHOLE OR IN PART FOR MANUFACTURE OR PROCUREMENT, WITHOUT THE WRITTEN PERMISSION OF CURTISS-WRIGHT CORPORATION, EXCEPT FOR (i) EMERGENCY REPAIR OR OVERHAUL WORK BY OR FOR THE GOVERNMENT WHERE THE ITEM OR PROCESS IS NOT OTHERWISE REASONABLY AVAILABLE TO ENABLE TIMELY PERFORMANCE OF THE WORK, OR (ii) RELEASE TO A FOREIGN GOVERNMENT, AS THE INTERESTS OF THE UNITED STATES MAY REQUIRE, PROVIDED THAT IN EITHER CASE THE RELEASE, USE, DUPLICATION OR DISCLOSURE HEREOF SHALL BE SUBJECT TO THE FOREGOING LIMITATIONS. THIS LEGEND SHALL BE MARKED ON ANY REPRODUCTION HEREOF IN WHOLE OR IN PART."

contributions will be of minor importance, thus, the wind tunnel test results should give a satisfactory indication of full-scale values.

The best wind tunnel data available are those obtained with the model sting-mounted in the Cornell 8 ft Transonic Wind Tunnel, (51) and (52). These data were used to establish the basic variation of drag with lift for the propellers-off case, and the elevator pitching moment and lift contributions for trimming. Also, in combination with the results from the M.I.T. tunnel tests (50), they served as a basis for the power on pitching moment curves. The propeller force data from the Cornell tests were unsatisfactory, however, so it was necessary to take increments of lift and drag due to power from M.I.T. tests. This was done by subtracting the thrust components, measured by strain gauges in the model wings, from the balance measurements in order to get the actual lift and drag with power on. Then the difference between these and the propellers-off values, from the same tunnel, were taken. These increments, added to the propellers-off Cornell data, had the effect shown in Figure 205, where the C_D at $C_L = 0$ was reduced by 0.008 and the slope increased from 0.124 to 0.180.

In the absence of usable power-on data at higher Mach numbers and considering the fact that the basic propeller performance does not change greatly up to M = 0.65 the increment is not varied with Mach number. The compressibility effects were therefore taken from the propellers-off tests of (51) and (52) which showed that the C_D at $C_{L_2} = 0$ increased steadily above M = 0.45 but the value of $\partial C_D / \partial C_L^2$ remained constant up to M = 0.65.

Bringing all these contributions together gives a total power-on trimmed, compressible drag coefficient:

$$C_D = C_{D_{Min}} + \Delta C_{D_M} + C_L^2 \frac{\partial C_D}{\partial C_L^2}$$

where $C_{D_{MIN}}$ = minimum drag coefficient
= C_{D_o} - 0.008 (Figure 206)

C_{D_o} = power off, incompressible, profile drag coefficient

ΔC_{D_M} = increase in C_{D_o} due to Mach Number

$\partial C_D / \partial C_L^2$ = power on, trimmed, compressible induced drag slope
= $(\partial C_D / \partial C_L^2)$ props off + 0.056.

"FURNISHED UNDER UNITED STATES GOVERNMENT CONTRACT No AF33(615)-3940 SHALL NOT BE EITHER RELEASED OUTSIDE THE GOVERNMENT, OR USED, DUPLICATED, OR DISCLOSED IN WHOLE OR IN PART FOR MANUFACTURE OR PROCUREMENT, WITHOUT THE WRITTEN PERMISSION OF CURTISS-WRIGHT CORPORATION, EXCEPT FOR (i) EMERGENCY REPAIR OR OVERHAUL WORK BY OR FOR THE GOVERNMENT, WHERE THE ITEM OR PROCESS IS NOT OTHERWISE REASONABLY AVAILABLE TO ENABLE TIMELY PERFORMANCE OF THE WORK, OR (ii) RELEASE TO A FOREIGN GOVERNMENT, AS THE INTERESTS OF THE UNITED STATES MAY REQUIRE. PROVIDED THAT IN EITHER CASE THE RELEASE, USE, DUPLICATION OR DISCLOSURE HEREOF SHALL BE SUBJECT TO THE FOREGOING LIMITATIONS. THIS LEGEND SHALL BE MARKED ON ANY REPRODUCTION HEREOF IN WHOLE OR IN PART."

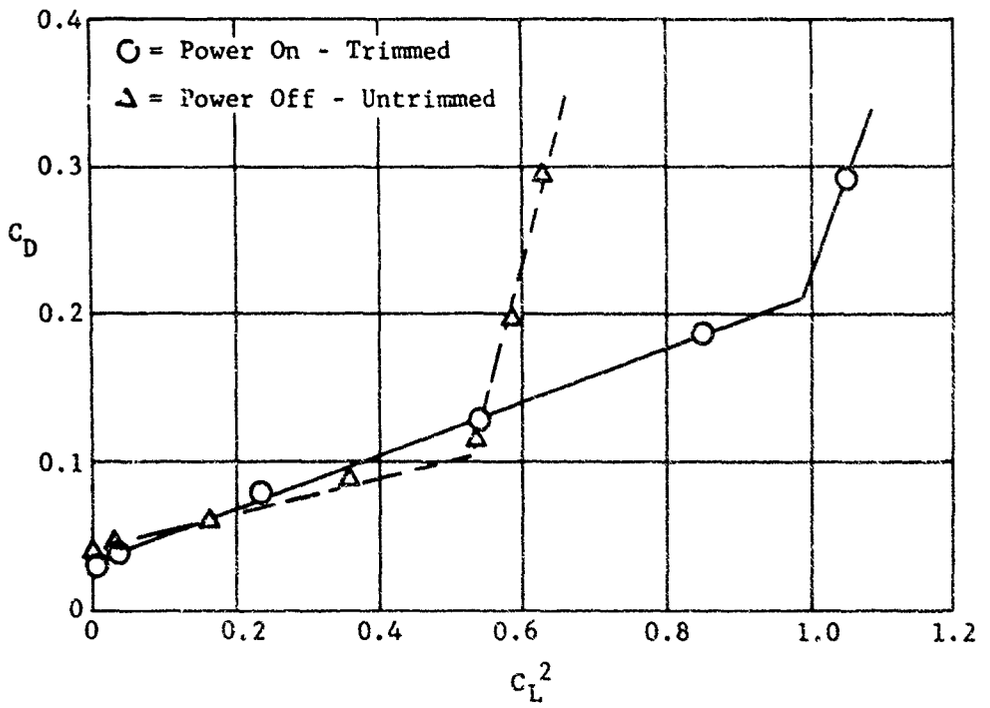

Figure 205. X-19, effect of power and trim on the induced drag factor $(\partial C_D/\partial C_L^2)$ in cruise.

'FURNISHED UNDER UNITED STATES GOVERNMENT CONTRACT No. AF33(615)-1940 SHALL NOT BE EITHER RELEASED OUTSIDE THE GOVERNMENT, OR USED DUPLICATED, OR DISCLOSED IN WHOLE OR IN PART FOR MANUFACTURE OR PROCUREMENT, WITHOUT THE WRITTEN PERMISSION OF CURTISS-WRIGHT CORPORATION, EXCEPT FOR (i) EMERGENCY REPAIR OR OVERHAUL WORK BY OR FOR THE GOVERNMENT, WHERE THE ITEM OR PROCESS IS NOT OTHERWISE REASONABLY AVAILABLE TO ENABLE TIMELY PERFORMANCE OF THE WORK, OR (ii) RELEASE TO A FOREIGN GOVERNMENT, AS THE INTERESTS OF THE UNITED STATES MAY REQUIRE, PROVIDED THAT IN EITHER CASE THE RELEASE, USE, DUPLICATION OR DISCLOSURE HEREOF SHALL BE SUBJECT TO THE FOREGOING LIMITATIONS. THIS LEGEND SHALL BE MARKED ON ANY REPRODUCTION HEREOF IN WHOLE OR IN PART "

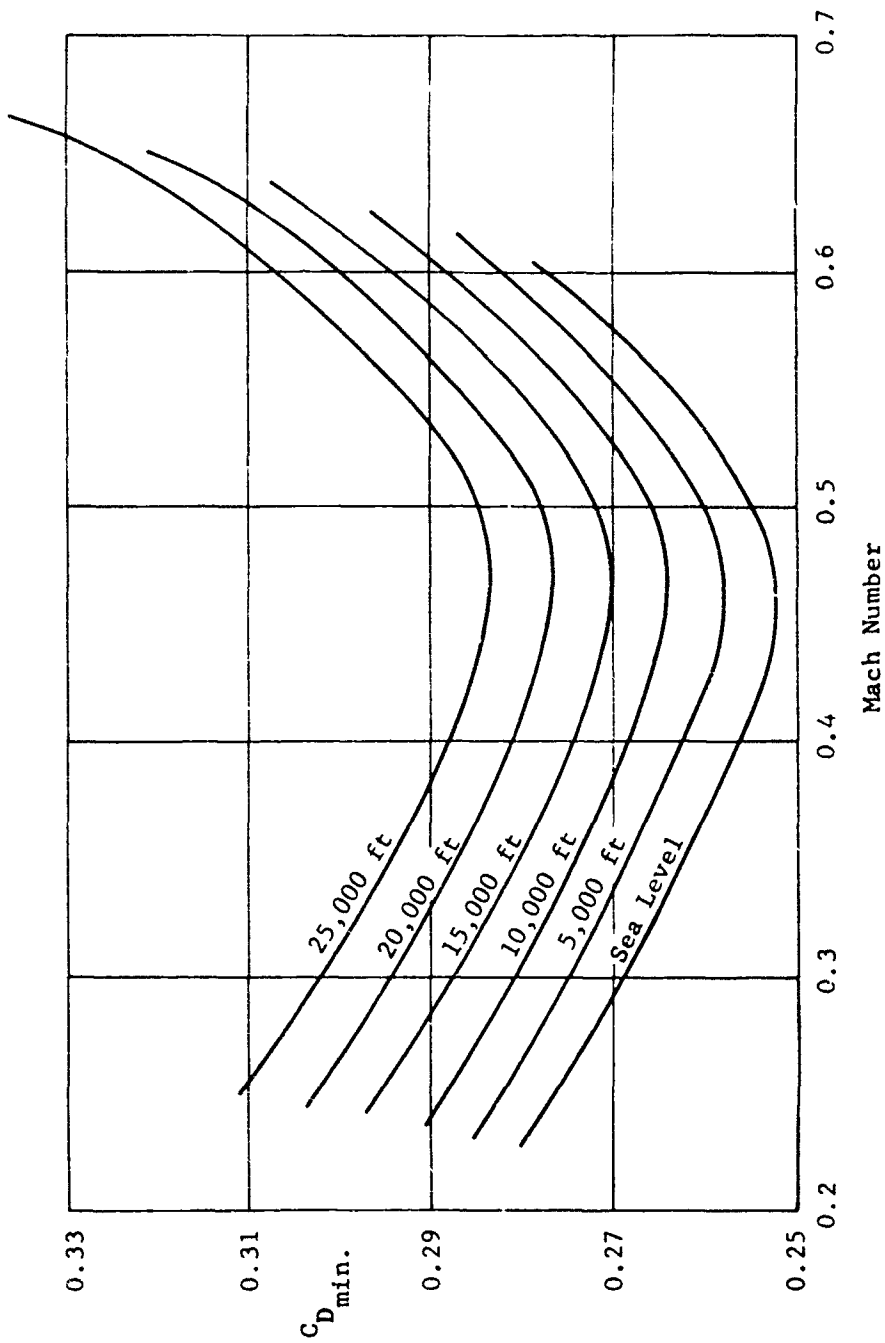

Figure 206. X-19, effect of Mach Number and altitude on minimum cruise drag coefficient.

"FURNISHED UNDER UNITED STATES GOVERNMENT CONTRACT No. AF33(615)-3940. SHALL NOT BE EITHER RELEASED OUTSIDE THE GOVERNMENT, OR USED, DUPLICATED, OR DISCLOSED IN WHOLE OR IN PART FOR MANUFACTURE OR PROCUREMENT, WITHOUT THE WRITTEN PERMISSION OF CURTISS-WRIGHT CORPORATION, EXCEPT FOR (i) EMERGENCY REPAIR OR OVERHAUL WORK BY OR FOR THE GOVERNMENT, WHERE THE ITEM OR PROCESS IS NOT OTHERWISE REASONABLY AVAILABLE TO ENABLE TIMELY PERFORMANCE OF THE WORK, OR (ii) RELEASE TO A FOREIGN GOVERNMENT, AS THE INTERESTS OF THE UNITED STATES MAY REQUIRE. PROVIDED THAT IN EITHER CASE THE RELEASE, USE, DUPLICATION OR DISCLOSURE HEREOF SHALL BE SUBJECT TO THE FOREGOING LIMITATIONS. THIS LEGEND SHALL BE MARKED ON ANY REPRODUCTION HEREOF IN WHOLE OR IN PART."

$(\partial C_D / \partial C_L^2)$ Props Off = measured induced drag slope from propellers-off clean model test of (51). These contributions to the total drag coefficient are shown in the summary plot of Figure 207.

e. Lift/Drag Ratio

Figure 208 shows the variation of lift/drag ratio with speed for the normal gross weight of 13,660 lbs. The maximum value of just under 7.4 is seen to occur at about 270 knots at sea level, with the peak value decreasing as the altitude increases. The cruise speed of 325 knots at 15,000 ft gives the best L/D of 7.1 for that altitude. Figure 209 shows L/D at 300 knots T.A.S. as a function of weight.

3. TEST AND THEORY COMPARISON OF AERODYNAMIC AND FLIGHT CONTROL CHARACTERISTICS

a. Aerodynamic

Theoretical estimation of the basic static stability derivatives was in general quite unsuccessful. Undoubtedly one of the main reasons for this was due to the difficulty in estimating the interference effects between propellers and airframe, and between airframe components. An example of the flow complexity involved is the case of the rear wing which is subject to the effects of the fuselage, the front wing, the front propellers and the rear propellers. Poor correlation between theoretical estimates and wind tunnel data on the original X-200 airplane led to the situation finally adopted for the X-19 wherein values used for all the static stability derivatives, both in cruise and transition, were wind tunnel measured.

All the rate derivatives were estimated. One has more confidence in these estimates since much of the input data could be extracted from the wind tunnel tests. A good example is the installed rear wing lift curve slope (a significant contribution to most of the rate derivatives), wherein rear wing "on" and rear wing "off" runs yield the required information. This method unfortunately only provides the gross answer and does not determine individually the numerous contributions to the whole.

Hinge moment derivatives used were also based on wind tunnel model data, again as a result of poor theory and test data correlation. The non-linear nature of the control surface hinge moment is shown in Figures 197, 198 and 199, which in the case of elevators and ailerons is probably a characteristic of thick wings.

"FURNISHED UNDER UNITED STATES GOVERNMENT CONTRACT No. AF33(615)-3940 SHALL NOT BE EITHER RELEASED OUTSIDE THE GOVERNMENT, OR USED, DUPLICATED, OR DISCLOSED IN WHOLE OR IN PART FOR MANUFACTURE OR PROCUREMENT, WITHOUT THE WRITTEN PERMISSION OF CURTISS-WRIGHT CORPORATION, EXCEPT FOR (1) EMERGENCY REPAIR OR OVERHAUL WORK BY OR FOR THE GOVERNMENT, WHERE THE ITEM OR PROCESS IS NOT OTHERWISE REASONABLY AVAILABLE TO ENABLE TIMELY PERFORMANCE OF THE WORK, OR (2) RELEASE TO A FOREIGN GOVERNMENT, AS THE INTERESTS OF THE UNITED STATES MAY REQUIRE: PROVIDED THAT IN EITHER CASE THE RELEASE, USE, DUPLICATION OR DISCLOSURE HEREOF SHALL BE SUBJECT TO THE FOREGOING LIMITATIONS. THIS LEGEND SHALL BE MARKED ON ANY REPRODUCTION HEREOF IN WHOLE OR IN PART."

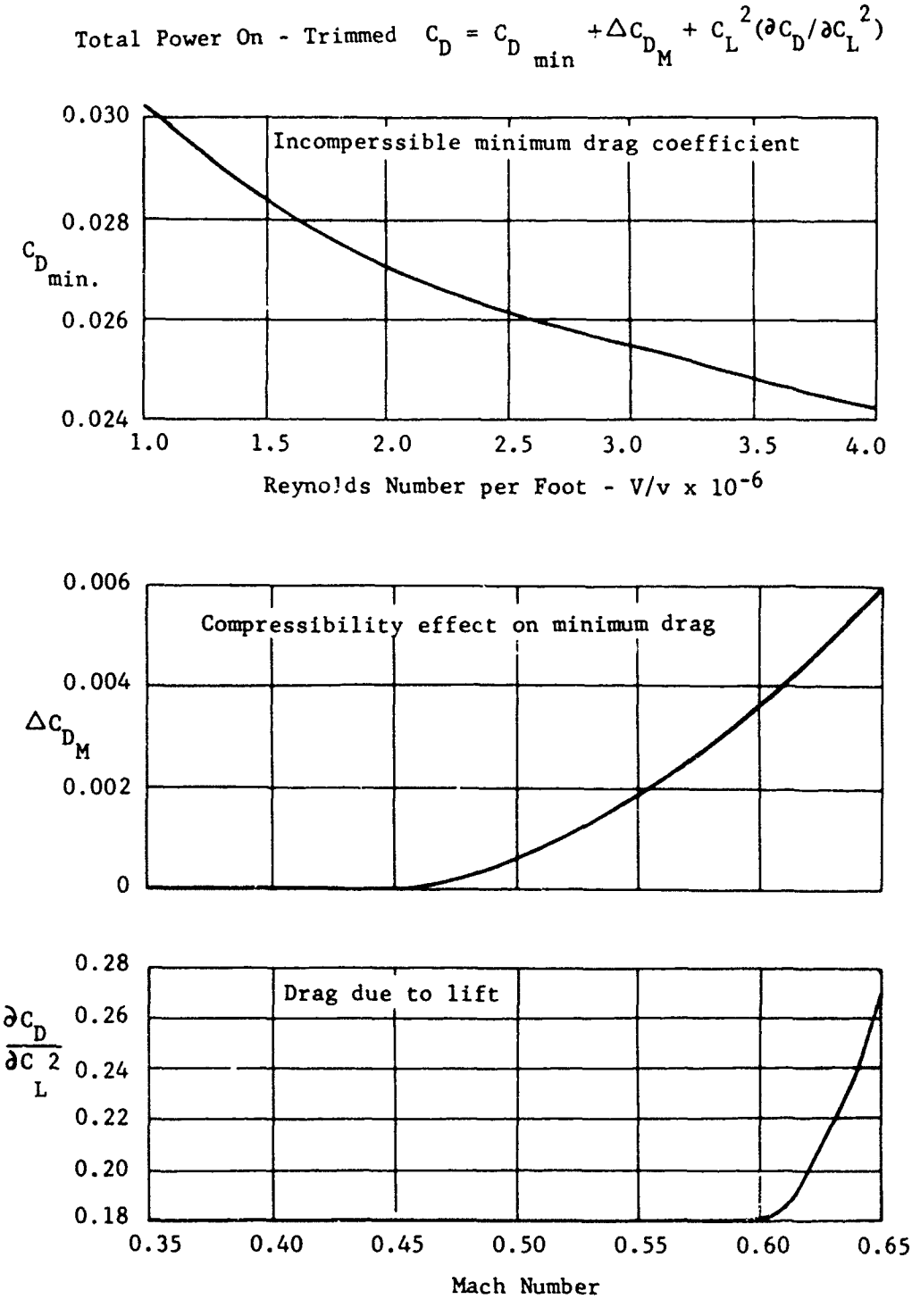

Figure 207. X-19, components of total cruise drag coefficient.

"FURNISHED UNDER UNITED STATES GOVERNMENT CONTRACT No AF33(615)-3940. SHALL NOT BE EITHER RELEASED OUTSIDE THE GOVERNMENT OR USED, DUPLICATED, OR DISCLOSED IN WHOLE OR IN PART FOR MANUFACTURE OR PROCUREMENT, WITHOUT THE WRITTEN PERMISSION OF CURTISS-WRIGHT CORPORATION, EXCEPT FOR (i) EMERGENCY REPAIR OR OVERHAUL WORK BY OR FOR THE GOVERNMENT, WHERE THE ITEM OR PROCESS IS NOT OTHERWISE REASONABLY AVAILABLE TO ENABLE TIMELY PERFORMANCE OF THE WORK, OR (ii) RELEASE TO A FOREIGN GOVERNMENT, AS THE INTERESTS OF THE UNITED STATES MAY REQUIRE. PROVIDED THAT IN EITHER CASE THE RELEASE, USE, DUPLICATION OR DISCLOSURE HEREOF SHALL BE SUBJECT TO THE FOREGOING LIMITATIONS. THIS LEGEND SHALL BE MARKED ON ANY REPRODUCTION HEREOF IN WHOLE OR IN PART."

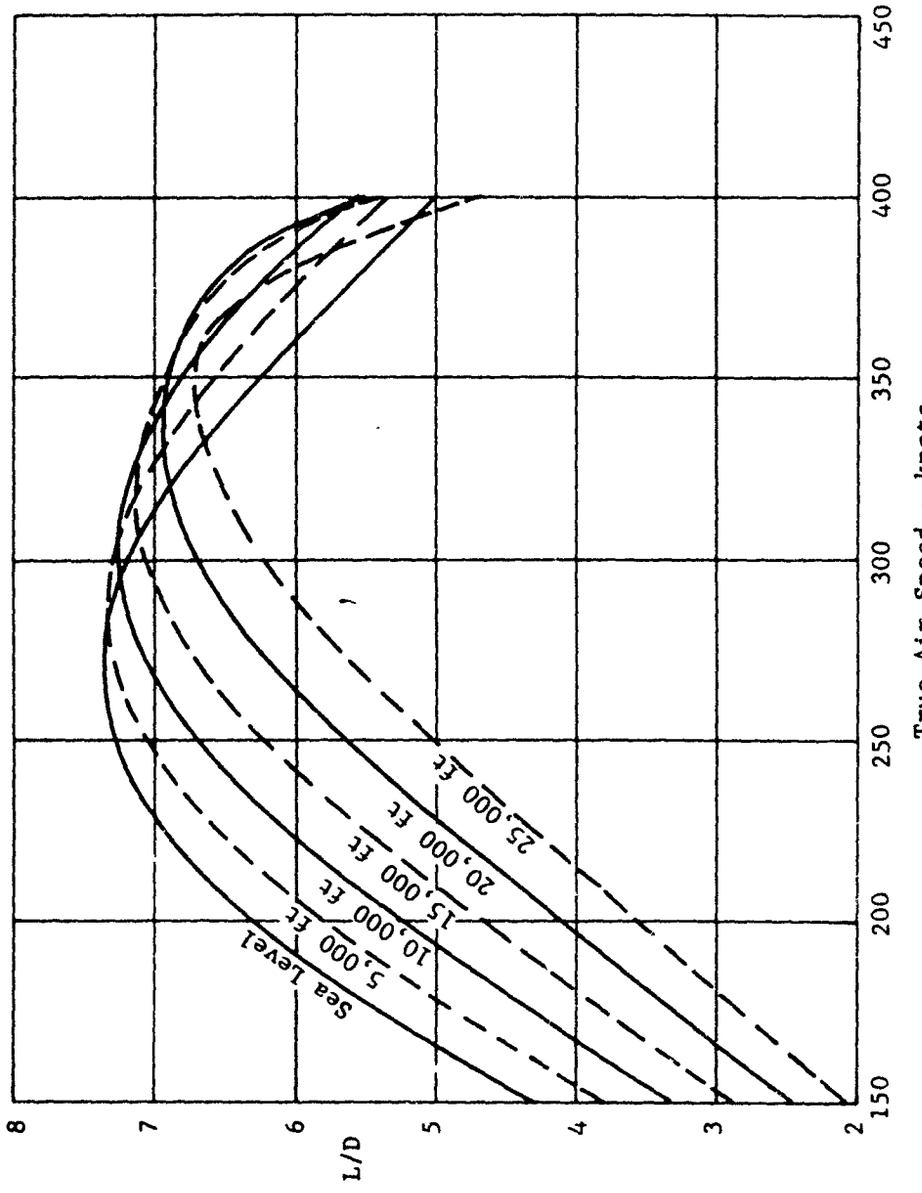

Figure 208. X-19, effect of speed and altitude on cruise lift-drag ratio; W = 13,660 pounds.

"FURNISHED UNDER UNITED STATES GOVERNMENT CONTRACT No. AF33(615)-3940. SHALL NOT BE EITHER RELEASED OUTSIDE THE GOVERNMENT, OR USED, DUPLICATED, OR DISCLOSED IN WHOLE OR IN PART FOR MANUFACTURE OR PROCUREMENT, WITHOUT THE WRITTEN PERMISSION OF CURTISS-WRIGHT CORPORATION, EXCEPT FOR (i) EMERGENCY REPAIR OR OVERHAUL WORK BY OR FOR THE GOVERNMENT, WHERE THE ITEM OR PROCESS IS NOT OTHERWISE REASONABLY AVAILABLE TO ENABLE TIMELY PERFORMANCE OF THE WORK, OR (ii) RELEASE TO A FOREIGN GOVERNMENT, AS THE INTERESTS OF THE UNITED STATES MAY REQUIRE: PROVIDED THAT IN EITHER CASE THE RELEASE, USE, DUPLICATION OR DISCLOSURE HEREOF SHALL BE SUBJECT TO THE FOREGOING LIMITATIONS. THIS LEGEND SHALL BE MARKED ON ANY REPRODUCTION HEREOF IN WHOLE OR IN PART."

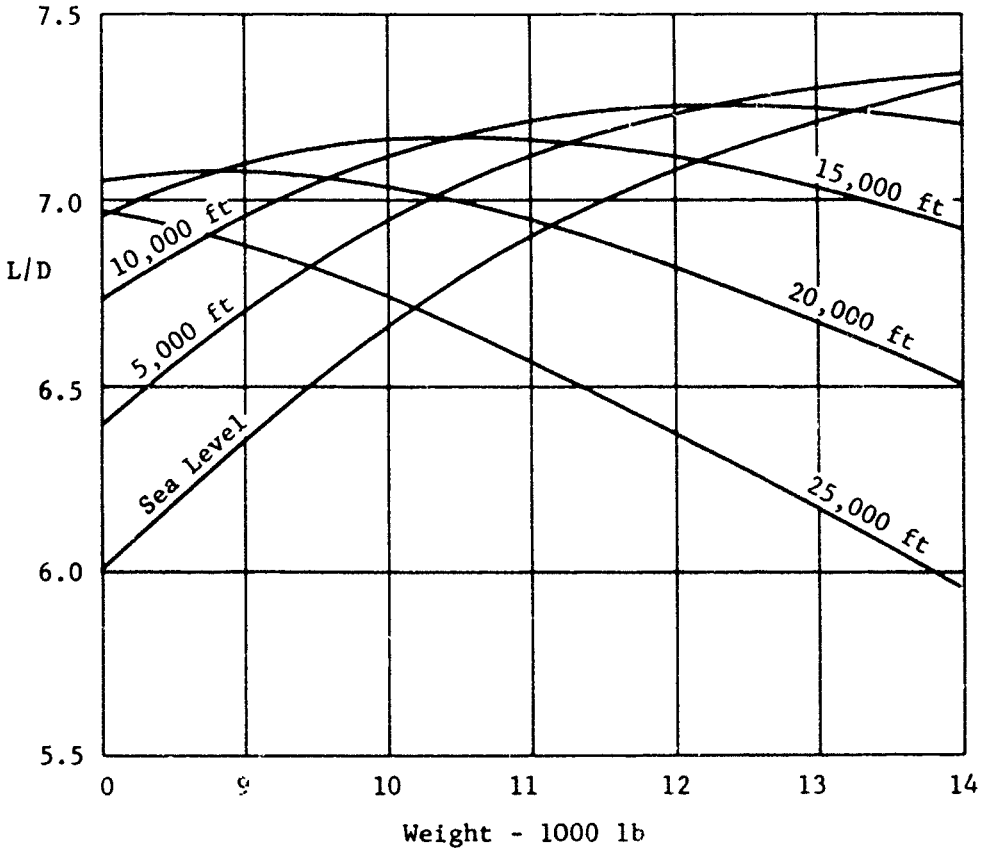

Figure 209. X-19, effect of weight and altitude on cruise lift-drag ratio; V = 300 knots T.A.S.

"FURNISHED UNDER UNITED STATES GOVERNMENT CONTRACT No. AF33(615)-3940. SHALL NOT BE EITHER RELEASED OUTSIDE THE GOVERNMENT, OR USED, DUPLICATED, OR DISCLOSED IN WHOLE OR IN PART FOR MANUFACTURE OR PROCUREMENT, WITHOUT THE WRITTEN PERMISSION OF CURTISS-WRIGHT CORPORATION, EXCEPT FOR (i) EMERGENCY REPAIR OR OVERHAUL WORK BY OR FOR THE GOVERNMENT, WHERE THE ITEM OR PROCESS IS NOT OTHERWISE REASONABLY AVAILABLE TO ENABLE TIMELY PERFORMANCE OF THE WORK, OR (ii) RELEASE TO A FOREIGN GOVERNMENT, AS THE INTERESTS OF THE UNITED STATES MAY REQUIRE. PROVIDED THAT IN EITHER CASE THE RELEASE, USE, DUPLICATION OR DISCLOSURE HEREOF SHALL BE SUBJECT TO THE FOREGOING LIMITATIONS. THIS LEGEND SHALL BE MARKED ON ANY REPRODUCTION HEREOF IN WHOLE OR IN PART."

b. Flight Control

Sufficient flight test data were available to extract the full scale values of a number of hover derivatives. These data are shown below, together with the original estimates.

Derivative		Estimated	Flight Test
M_u	ft-lb/ft/sec	+128	+605
X_u	lb/ft/sec	-13.2	-11.4
L_v	ft-lb/ft/sec	-195	-368
Y_v	lb/ft/sec	-10.8	-19.3
N_ψ	ft-lb/rad/sec	-3415	-3415

The poor correlation between the flight measured and estimated values of M_u and L_v is attributed to a large interference effect between leading and trailing pairs of propellers, not accounted for in the theoretical estimates. The measured value of L_v is an average of widely scattered results, the scatter being a result of the rather unsteady airplane attitude during lateral translations.

The good agreement on N_ψ verifies the assumption of "free propellers" (i.e., no interference effects) at least in yaw.

4. AIRCRAFT BEHAVIOR IN GROUND EFFECT

Section VIII is devoted entirely to the Ground Effect behavior of the X-19. Rather than deviate from the statement of work, this paragraph has been included to avoid confusion and to note that all pertinent discussions will be continued in the appropriate sections.

5. FLIGHT CONTROL DEFICIENCIES

a. Transition Flight Regime

(1) Introduction

Due to the lack of any generally accepted flying qualities specifications for VTOL aircraft in the transition regime, a strictly quantitative assessment of the X-19's (or any other VTOL airplane) transition flying qualities is difficult to present. Basically however with X-19, comparisons were made with MIL-F-8785 (ASG) requirements for speeds above 50 knots, while low speed characteristics were compared with the requirements of MIL-H-8501A, AGARD 408 and the numerous other handling qualities criteria available. In addition, a fair

amount of flight simulation work was performed to help resolve the many conflicting situations that arose.

It is pointed out that essentially all the transition data presented herein is estimated; unfortunately no quantitative stability and control testing was performed at other than hover propeller tilt angle.

(2) Stability

(a) Longitudinal

Here the greatest concern was the static instability, measured in the wind tunnel tests of (46), at a full scale peed of approximately 50 knots ($\emptyset_F$ = 82.5°).

Figure 182 shows that with SAS off the short period mode becomes unstable at approximately 75 knots and splits into two aperiodic modes at 55 knots. At around 50 knots the one aperiodic root is rapidly convergent, the other rapidly divergent. At lower speeds this divergent root approaches zero and becomes zero at hover. From Figure 183 it is seen that the Phugoid mode breaks down into two stable real roots at approximately 70 knots. At around 50 knots one of these real roots has become unstable and as speed is further reduced the mode again becomes oscillatory to eventually appear as the familiar dynamically unstable oscillation in hover.

Probably very little could be done to improve the clearly unsatisfactory basic airframe stability characteristics in this low speed regime. It was indeed left to the pitch rate plus attitude SAS to provide the necessary levels of stability. With SAS on, the airplane is hands-off stable in this low speed regime. Note however, that no severe problems were encountered during the limited "SAS Off" flying.

As shown in Figure 180, the MIL-F-8785 (ASG) requirements on short period mode damping are met at speeds greater than approximately 133 knots with SAS off.

(b) Lateral - Directional

The spiral and roll modes (separate or combined) are stable or neutrally stable for the whole speed range; but the Dutch Roll oscillation becomes divergent below approximately 85 knots. This is illustrated in Figure 184. The roll rate plus attitude SAS provides hands-off stability in this regime. Again it is felt that little

could be done to improve the low speed lateral-directional stability deficiencies other than with the addition of a SAS.

As shown in Figure 181, the SAS–off Dutch Roll characteristics comply with MIL-F-8785 (ASG) requirements at speeds above 100 knots

(3) Control

The final transition control characteristics were largely dictated, in pitch and roll, by the final SAS configuration. The hover control accelerations of $\ddot{\theta} = 0.68$ rad/sec^2 and $\ddot{\phi} = 1.75$ rad/sec^2 were considered satisfactory. However, the pitch and roll SAS's, each 30% of total control authority, reduced somewhat the maneuverability capabilities of the airplane. Despite this, flight test Cooper ratings of Satisfactory ($\leq$ 3-1/2) were recorded in pitch and roll, with SAS on, for the whole speed range flown. (See Section VI, paragraph 3.)

An area of possible concern was that of yaw control wherein it was thought that the low control power at low speed might be troublesome. Referring to Section XII, paragraph 3, however, it is seen that, although Cooper ratings of 4-1/2 were recorded in hover, the directional characteristics rapidly improve until Cooper ratings of "satisfactory" are achieved for all speeds above 35 knots.

It is therefore reasonable to say that there were no obvious control deficiencies in the transition regime actually flown. Bear in mind, however, that only very mild maneuvers were deliberately performed. The transition corridor was explored to a degree, in that mismatches between schedule tilt angle and speed frequently occurred during flight testing.

Pitch, roll and yaw moments through transition are shown in Figures 185, 186, and 187.

b. Cruise Flight Regime

(1) Introduction

Most of the X-19 cruise stability and control problems may be attributed to the geometric relationships inherent in the tandem wing configuration, namely the short moment arms of the rear wing and vertical tail, plus the shoulder mounted position of the wings.

Although the estimated stick fixed stability characteristics show compliance with the requirements of MIL-F-8785 (ASG) as reported in Section VII, paragraph 1.b.(3)(b), it is felt

that certain undesirable lateral directional characteristics exist. These characteristics are discussed below. Many of these deficiencies came to light during the course of a Curtiss-Wright sponsored study of the lateral directional handling qualities of V/STOL airplanes in cruising flight, performed by Cornell Aeronautical Laboratory (58). This study used the X-19 as a base point for a typical V/STOL airplane and thus was of direct benefit to the X-19 program.

In referring to this report however, care should be exercised in using the results since the basic X-19 data therein is for a c.g. location of 43% lift chord and with early estimates of the stability derivatives. The final aft c.g. limit was set at 42% lift chord and the final estimates of the derivatives differed somewhat from those early values.

Longitudinal stability characteristics are considered to be generally satisfactory.

(2) Stability

(a) Longitudinal: Generally satisfactory.

(b) Lateral - Directional:

In order to provide sufficient static directional stability (C_{n_β}), the short tail arm necessitated a relatively large area vertical tail of rather high aspect ratio. This coupled with the shoulder mounted wings and the high radial force propellers located an appreciable vertical distance from the c.g. resulted in a high level of static lateral stability (C_{ℓ_β}). Typically, in cruise, $|C_{\ell_\beta}| \simeq |2\ C_{n_\beta}|$ for the X-19.

As discussed in Section VII, paragraph 1.b.(3)(b) the resulting stick fixed normal modes are: a well damped Dutch Roll and a second oscillatory mode instead of the usual spiral mode and roll convergence mode. The second oscillatory mode is practically a pure oscillation in roll, is well damped and of rather long period. It has been referred to as the "Lateral Phugoid" mode and is mainly due to the high value of C_{ℓ_β} and to a lesser degree to the large positive value of C_{n_β}. Cruise flight simulation studies have indicated a distinct pilot distaste for the presence of this "Lateral Phugoid" mode during lateral maneuvers such as simple coordinated turns. The objection is over the "apparent" destabilizing effect the mode has on bank angle.

An example is the case of a banked turn. Here the pilot sets up the required bank angle, the Dutch Roll oscillation damps out, but then, unexpectedly, the "Lateral

Phugoid" (being of much longer period than the Dutch Roll), proceeds to further increase the bank angle in a fashion that is interpreted by the pilot as lateral instability.

This characteristic is more pronounced at high speed than at low speed. A recent unpublished study of the lateral-directional closed loop characteristics showed that high pilot gains would drive the "Lateral Phugoid" mode close to neutrally stable. In this study the pilot was represented by a simple gain. In (58) the closed loop "Lateral Phugoid" is shown to be unstable at certain pilot gains. This is due to the 43% c.g. location and early derivatives used in the study of (58). This is an example of the possible misinterpretation of results unless it is borne in mind that the basic data used were preliminary.

A further outcome of the high C_{ℓ_β} derivative is that relatively large bank angle excursions would be expected when flying in gusty air. For example, the roll to sideslip ratio ($|\theta/\beta|$) for the Dutch Roll mode approaches 6 at high speed cruise conditions.

A derivative which does not have an important effect on the normal modes but does affect the airplane's ride quality is C_{Y_β}. For the X-19, C_{Y_β} is high. This is primarily due to the large propeller radial force contribution which amounts to approximately 50% of the total C_{L_α}. High C_{Y_β} implies high lateral acceleration (load factor) due to sideslip. This imposes critical coordination requirements on the pilot in rolling maneuvers to minimize sideslip and hence lateral "g".

Studies of X-19 response to random side gusts (58), showed that the peak gust sensitivity was about the same as for current jet airliners, but that this sensitivity level is spread over a wide range of gust frequencies (with the maximum sensitivity occurring at the Dutch Roll undamped natural frequency). For conventional aircraft the sensitivity band is much narrower, with a sharp peak around the undamped natural frequency of the Dutch Roll mode.

The attenuation of lateral acceleration due to random turbulence may be more difficult with the X-19 than with conventional aircraft because of the broad band of frequencies involved. This includes a larger proportion of higher frequencies which the pilot would be unable to counter.

(3) Control

(a) Longitudinal:

This is generally satisfactory, except at low airspeeds somewhat large negative elevator settings are required for trim (see Figure 200). Also elevator angle per "g" becomes large (see Figure 201). Both items are a result of the non-linear C_m vs α characteristic (see Figure 188), the slope of which becomes rapidly more negative as angle of attack increases (or as speed decreases).

An improvement would be seen were the elevator and aileron linked to form an elevon. Such a system was not studied for X-19 but was given consideration in numerous other Curtiss tandem wing preliminary designs.

(b) Lateral:

In cruise the X-19 does not comply with the roll performance requirements of MIL-F-8785 (ASG) in terms of the roll rate parameter pb/2v. The wing tip helix angle however, was not considered to be too applicable to X-19, since the specified values of pb/2v are based in part on typical wing spans; X-19 is clearly not typical in this respect. It has been recognized, however, that better roll performance than that shown in Figures 202 and 203 would be desirable. This could be achieved by the aforementioned linking of aileron and elevator to form an elevon. Of course the intrinsic problem is the low wing span which results in short aileron moment arms.

An unanswered problem with the existing ailerons concerned the value of the derivative $C_{n_{\delta_a}}$. The 12% complete model wind tunnel test yielded a rather large negative value for this derivative (proverse aileron yaw) while single wing panel larger scale wind tunnel tests and theoretical estimates showed a positive value (adverse aileron yaw). (58) showed that with the strong proverse aileron yaw, a rather objectionable time history of rudder deflection was required for entry into, and recovery from, a coordinated turn.

With conventional adverse aileron yaw, entry into, say, a left turn (negative bank angle), will require initially positive aileron and positive rudder (i.e. left stick, left rudder) followed by some in-phase stick and rudder pedal motions until the steady state deflections that give the required bank angle are reached. To perform a similar meneuver with large negative $C_{n_{\delta_a}}$ (proverse aileron yaw), initially positive aileron and

negative rudder (i.e., left stick, right rudder) are required. The right rudder is necessary to balance out the nose left yawing moment generated by the ailerons. Recovery from a banked turn to level flight entails similar control surface time histories but in reverse.

(c) Directional:

Due primarily again to the large value of C_{l_β}, relatively large bank angles develop following a rudder input, particularly at high airspeeds. Simulator studies showed that a substantial improvement in lateral-directional handling qualities would be realized were the rudder power reduced at high speed.

6. AVAILABLE C.G. RANGE

Figure 210 shows the horizontal center of gravity envelope as a function of weight for the basic 13,660 lb. design gross weight aircraft.

The diagram is constructed as follows:

(1) Weight Empty + Pilot
(2) Weight Empty + Pilot + Co-pilot
(3) Weight Empty + Pilot + Co-pilot + Payload
(4) Weight Empty + Pilot + Co-pilot + Payload + Fuel Fwd.
(5) Weight Empty + Pilot + Co-pilot + Payload + Fuel Fwd. + Fuel Aft = W_{max}
(6) W_{max} - Co-pilot
(7) W_{max} - Co-pilot - Payload
(8) W_{max} - Co-pilot - Payload - Fuel Fwd.
(1) W_{max} - Co-pilot - Payload - Fuel Fwd - Fuel Aft

Note: Empty Weight includes oil.

The two lines of constant horsepower shown indicate the maximum hover lift capability (at S.L. standard conditions, σ = 1.0) as a function of c.g. for two values of front propeller horsepower (860 and 780 SHP per propeller).

Also shown are the forward and aft cruise c.g. limits. The aft limit of 42% lift chord is dictated by longitudinal stability considerations while the 38.9% c.g. represents the most forward c.g. at which structural analyses were conducted. Longitudinal control power, with the hydraulic boost system, is sufficient to permit a 38.9% c.g. limit.

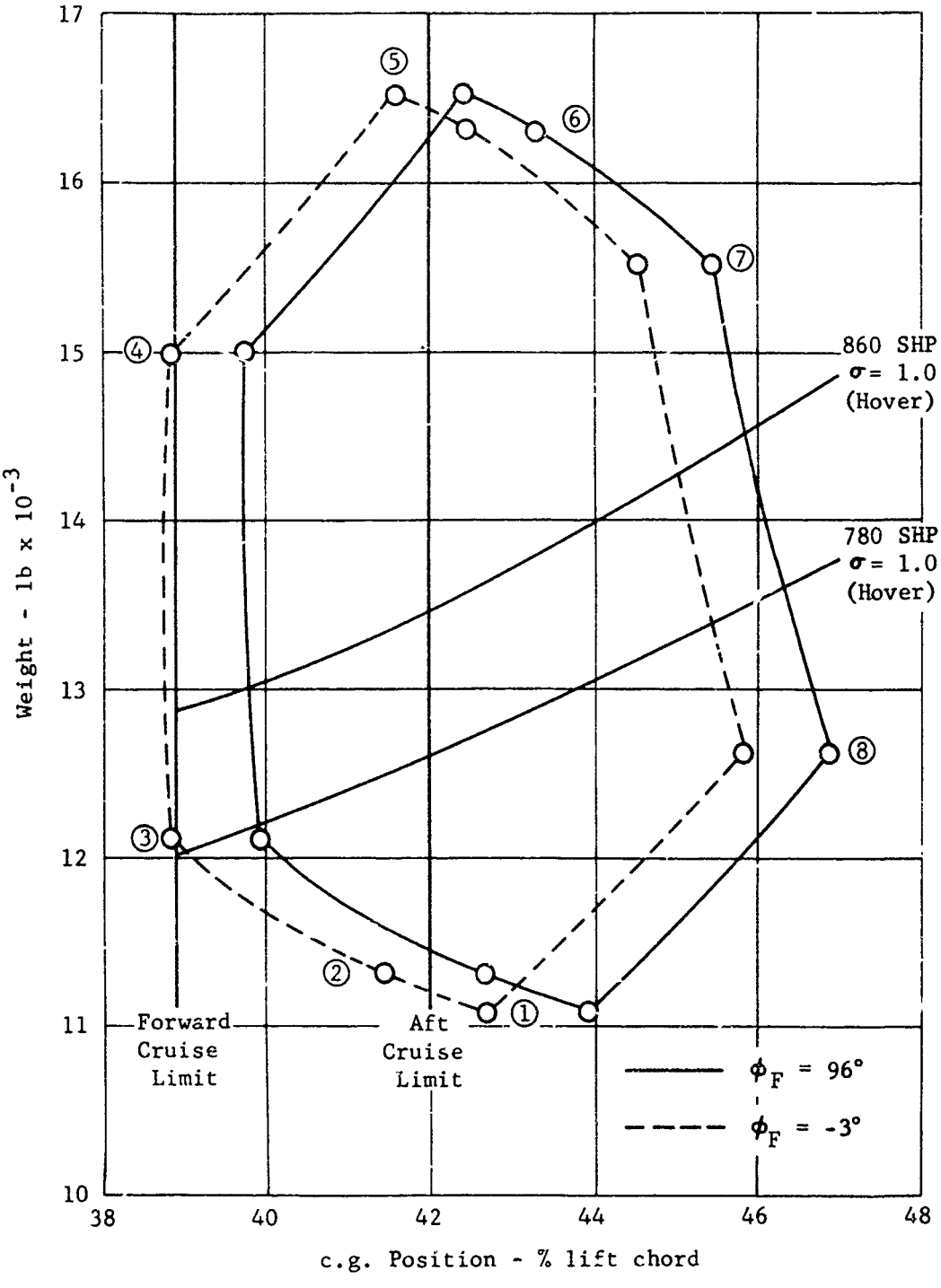

Figure 210. Horizontal c.g. envelope for the basic 13,560 pound design gross weight aircraft.

7. TILT, FLAP AND BLADE ANGLE PHASING

a. Nacelle Tilt Phasing

This discussion relates to the recommended tilt - velocity schedule. Early in the design phase of the X-19, it was decided to give transition phasing control to the pilot rather than to automatic sensing mechanisms . The simplest readout available to accomplish this end was of course, the nacelle tilt angle. It was decided that mechanisms such as the flaps, collective ailerons and all coordinator phasing would be geared to the tilt angle. The aerodynamic contributions of these mechanisms was related to the aircraft weight in search for a reasonable flight corridor. The aircraft was to hover at zero fuselage attitude, and by the end of transition, was to fly roughly at 10 degrees of attitude. Thus a tilt velocity schedule was to be obtained which would provide:

(1) a reasonable attitude variation.

(2) a minimum horsepower requirement.

(3) a minimum propeller "Aq" throughout the transition.

Without regard to control requirements, a very early analytical investigation showed that all three requirements could be met with a "toed-in" [4] configuration.

Furthermore, the power required was less than that of other fore-aft tilt configurations. However, without the benefit of wind tunnel data there was little else to confirm these findings.

Some basic characteristics of the control system were investigated following this analysis. Hover yaw control power was low, and an effort to increase this was in progress. It was found that a 50 percent increase [5] in hover yaw control power could be realized with a toed-in propeller configuration provided propeller rotation was properly fixed. The required arrangement of propeller rotation was (and continued throughout the program to be) right hand rotation for propellers 2 and 4, and left hand rotation for propellers 1 and 3. This arrangement satisfied another desired characteristic; namely to have the front propellers wash up past the front wing.

---

[4] This arrangement requires the front propeller to be consistently at a higher tilt angle than the rear propeller.

[5] This increase is the result of torque reaction added to the thrust generated jawing moment.

The only other configuration that would have delivered the desired hover yaw control was a "toed-Out" [6] configuration. This required the direction of rotation on all four propellers to be reversed from the "toed-In" configuration. At about this time, wind tunnel data on the cruise stability model had become available. The data indicated a slight stability increase, and less up elevator for trim, for the rotations required on the toed-in configuration.

Thus, the information available at the time favored a toed-in configuration. The final schedule called for a rear propeller $\emptyset_R$ equal to 84.5 percent of the front propeller $\emptyset_F$. On the basis of a 12,300 pound airplane the tilt-velocity schedule was generated, see Figure 211. Note, in cruise, the front tilt angle is $\emptyset_F = -3$ degrees, and $\emptyset_R = -2.5$ degrees. Originally, the tilt schedule was phased to zero degrees front and rear. However, for reasons of load reduction as well as better cruise efficiency, the cruise tilt angle was later revised to the values now shown. So as not to affect the fixed gearing between the front and rear propellers, the rear tilt angle remains at 84.5 percent of the front.

b. Flap and Collective Aileron Phasing

The flap and collective aileron schedules were established using simple criteria. For hover, the flaps and ailerons were deflected to decrease download. Deflections beyond 60 degrees effected little change in downloads. Consequently a target value of 60 degrees deflection subject to linkage idiosyncracies, was established. The deflections were to be phased to zero degrees in cruise. The full range of aileron deflection was to be maintained at all tilt angles. The flaps and ailerons were to be phased during transition to give maximum lift and thus a high negative pitching moment as possible. This is desirable as the torque requirements of the rear propellers during conversion tends to approach a peak and any reduction of lift produced by the wing will reduce the lift that must be generated by the rear propellers and thus their torque load requirements.

---

[6] Toed-out configuration requires the front propeller to be consistently at a lower tilt angle than the rear propeller.

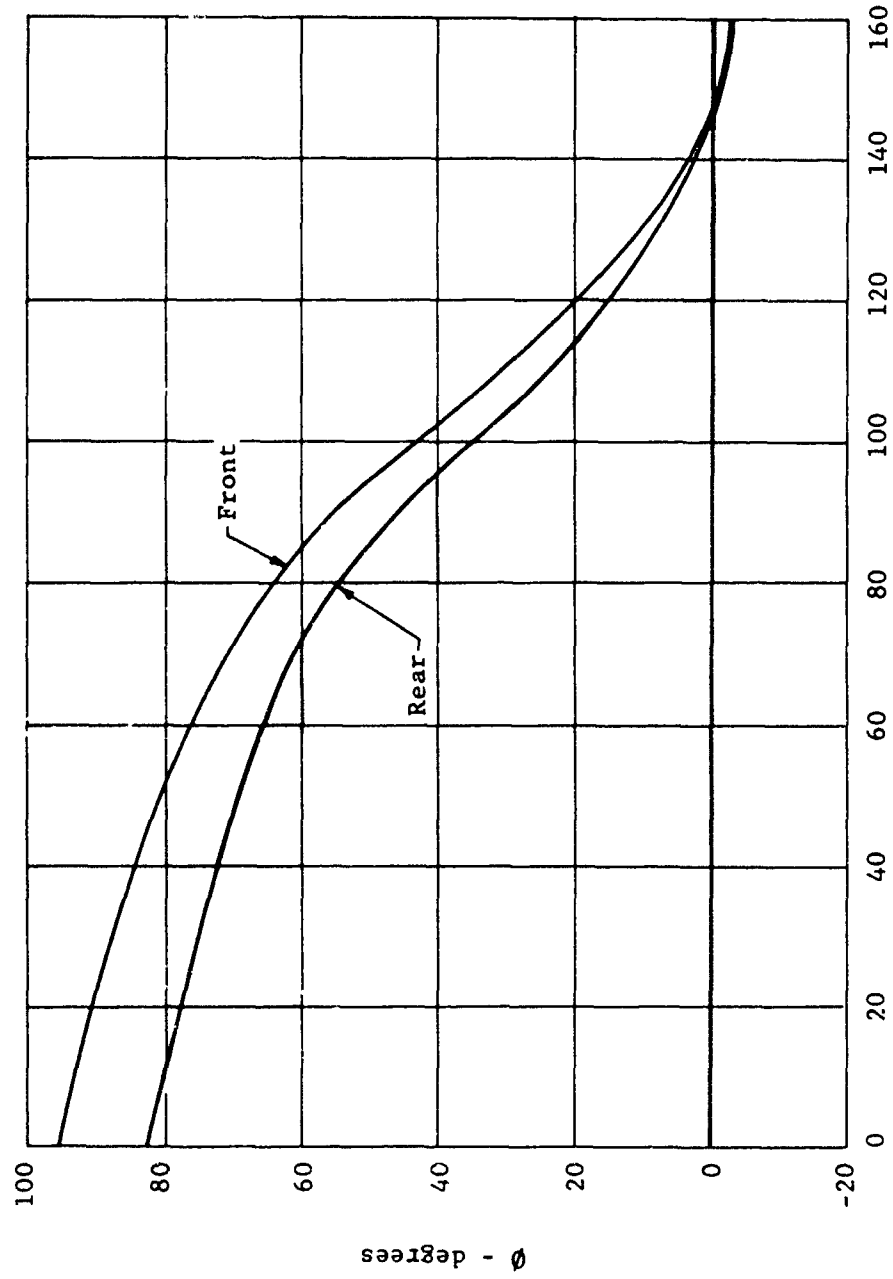

Figure 211. X-19, recommended tilt velocity schedule.

FURNISHED UNDER UNITED STATES GOVERNMENT CONTRACT No. AF33(615)-3940 SHALL NOT BE EITHER RELEASED OUTSIDE THE GOVERNMENT, OR USED, DUPLICATED, OR DISCLOSED IN WHOLE OR IN PART FOR MANUFACTURE OR PROCUREMENT, WITHOUT THE WRITTEN PERMISSION OF CURTISS-WRIGHT CORPORATION, EXCEPT FOR (i) EMERGENCY REPAIR OR OVERHAUL WORK BY OR FOR THE GOVERNMENT, WHERE THE ITEM OR PROCESS IS NOT OTHERWISE REASONABLY AVAILABLE TO ENABLE TIMELY PERFORMANCE OF THE WORK, OR (ii) RELEASE TO A FOREIGN GOVERNMENT, AS THE INTERESTS OF THE UNITED STATES MAY REQUIRE. PROVIDED THAT IN EITHER CASE THE RELEASE, USE, DUPLICATION OR DISCLOSURE HEREOF SHALL BE SUBJECT TO THE FOREGOING LIMITATIONS. THIS LEGEND SHALL BE MARKED ON ANY REPRODUCTION HEREOF IN WHOLE OR IN PART."

When using the ailerons for the dual purpose of increasing lift as a flap and for roll control the maximum flap angle is dictated by the requirements for roll control. This limited the flap angle due to the roll control power requirements at the end of conversion. The final schedule built into the aircraft are shown on Figures 211 and 212.

c. Propeller Blade Angle Phasing

(1) Auto-trim schedule

The auto-trim schedule defines the difference between the front and rear propeller blade angle as a function of tilt angle, at zero stick position. It is equivalent to adjusting the front and rear wing incidences to give near zero moment for the stick neutral. Although the propeller moment is sensitive to horsepower, advance ratio, angle of attack, center of gravity and tilt angle, only one auto-trim schedule can be used. The final compromise was to adjust the schedule as an average between the extreme moments that might be encountered at any given tilt angle. Figure 214 gives the schedule which was built into the aircraft. The large negative gradient [7] coming off the hover point created some concern early in the development. It was the result of small scale wind tunnel testing. Flight tests of the X-19 have shown control deflections to be quite close to the predicted values. That the stick deflections are as predicted implies a close agreement between flight test and small scale tunnel results.

(2) Pitch-gain schedule

The pitch-gain schedule relates to the phaseout of propeller pitch control with tilt angle. It was generated with the intent of maintaining constant control moment through transition. Thus as elevator power builds up, propeller pitch power is phased out. Figure 215 describes the pitch gain variation with tilt angle.

---

[7] This reflects the large pitch up moment with velocity off the hover point. The interference effects which contribute to this are discussed in Section III, 4.

'FURNISHED UNDER UNITED STATES GOVERNMENT CONTRACT No. AF33(615)-3940. SHALL NOT BE EITHER RELEASED OUTSIDE THE GOVERNMENT, OR USED, DUPLICATED, OR DISCLOSED IN WHOLE OR IN PART FOR MANUFACTURE OR PROCUREMENT, WITHOUT THE WRITTEN PERMISSION OF CURTISS-WRIGHT CORPORATION, EXCEPT FOR (i) EMERGENCY REPAIR OR OVERHAUL WORK BY OR FOR THE GOVERNMENT, WHERE THE ITEM OR PROCESS IS NOT OTHERWISE REASONABLY AVAILABLE TO ENABLE TIMELY PERFORMANCE OF THE WORK, OR (ii) RELEASE TO A FOREIGN GOVERNMENT, AS THE INTERESTS OF THE UNITED STATES MAY REQUIRE. PROVIDED THAT IN EITHER CASE THE RELEASE, USE, DUPLICATION OR DISCLOSURE HEREOF SHALL BE SUBJECT TO THE FOREGOING LIMITATIONS. THIS LEGEND SHALL BE MARKED ON ANY REPRODUCTION HEREOF IN WHOLE OR IN PART.'

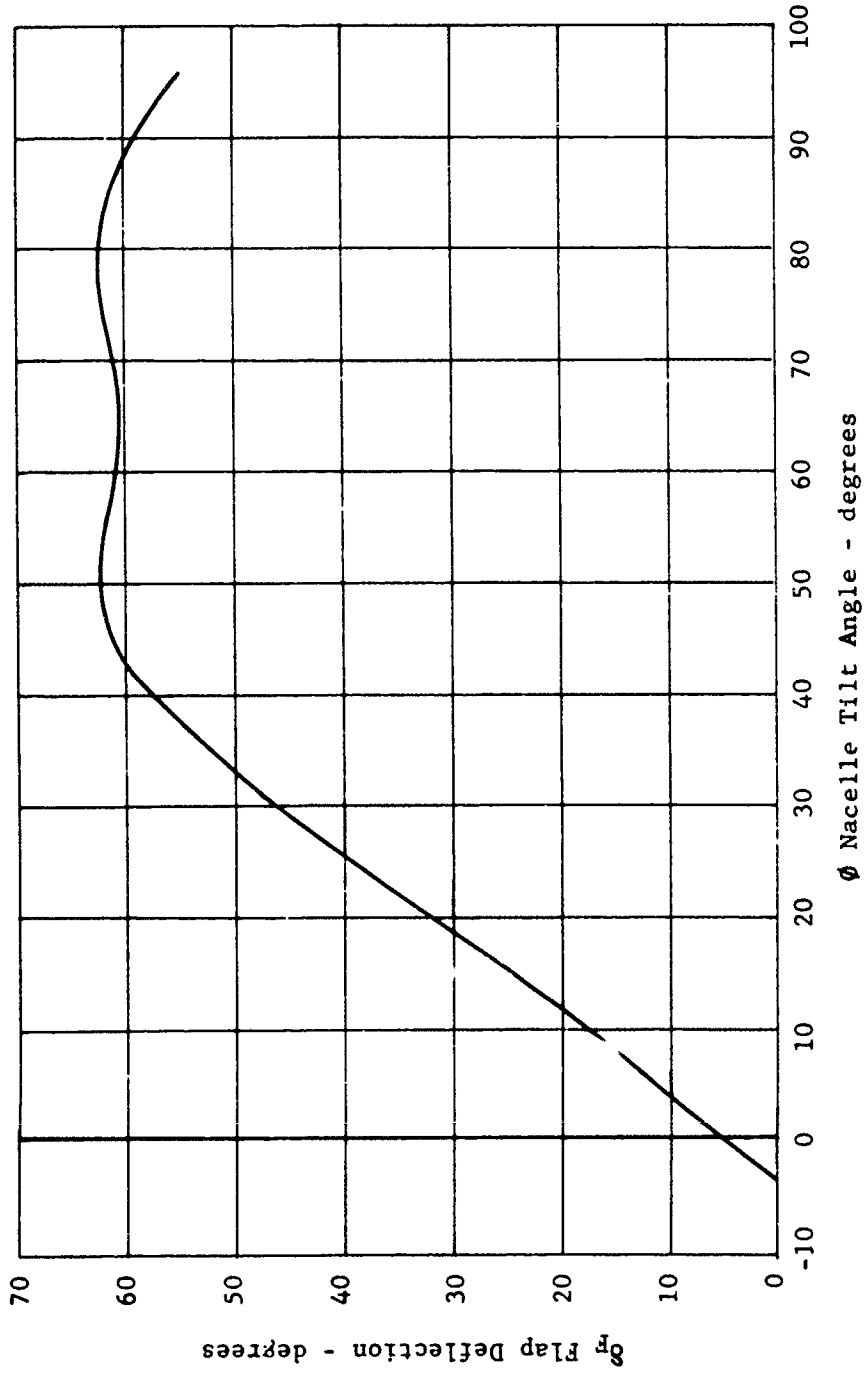

Figure 212. X-19, flap deflection schedule, forward lift strut.

FURNISHED UNDER UNITED STATES GOVERNMENT CONTRACT No. AF33(615)-3940. SHALL NOT BE EITHER RELEASED OUTSIDE THE GOVERNMENT OR USED, DUPLICATED, OR DISCLOSED IN WHOLE OR IN PART FOR MANUFACTURE OR PROCUREMENT, WITHOUT THE WRITTEN PERMISSION OF CURTISS-WRIGHT CORPORATION, EXCEPT FOR (i) EMERGENCY REPAIR OR OVERHAUL WORK BY OR FOR THE GOVERNMENT, WHERE THE ITEM OR PROCESS IS NOT OTHERWISE REASONABLY AVAILABLE TO ENABLE TIMELY PERFORMANCE OF THE WORK, OR (ii) RELEASE TO A FOREIGN GOVERNMENT, AS THE INTERESTS OF THE UNITED STATES MAY REQUIRE. PROVIDED THAT IN EITHER CASE THE RELEASE, USE, DUPLICATION OR DISCLOSURE HEREOF SHALL BE SUBJECT TO THE FOREGOING LIMITATIONS. THIS LEGEND SHALL BE MARKED ON ANY REPRODUCTION HEREOF IN WHOLE OR IN PART.

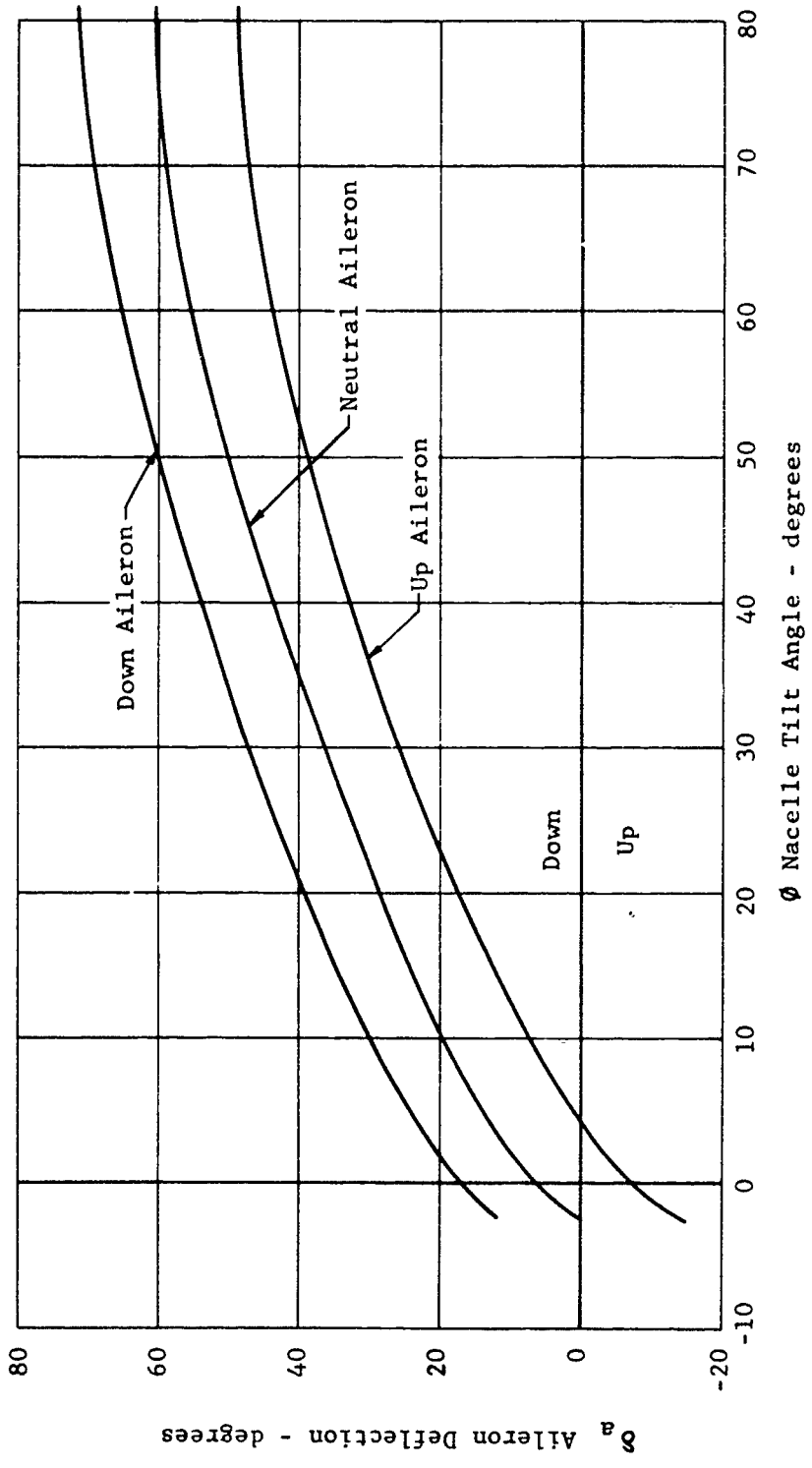

Figure 213. Collective aileron schedule, rear lift strut.

"FURNISHED UNDER UNITED STATES GOVERNMENT CONTRACT No. AF33(615)-3940. SHALL NOT BE EITHER RELEASED OUTSIDE THE GOVERNMENT, OR USED, DUPLICATED, OR DISCLOSED IN WHOLE OR IN PART FOR MANUFACTURE OR PROCUREMENT, WITHOUT THE WRITTEN PERMISSION OF CURTISS-WRIGHT CORPORATION, EXCEPT FOR (i) EMERGENCY REPAIR OR OVERHAUL WORK BY OR FOR THE GOVERNMENT, WHERE THE ITEM OR PROCESS IS NOT OTHERWISE REASONABLY AVAILABLE TO ENABLE TIMELY PERFORMANCE OF THE WORK. & (ii) RELEASE TO A FOREIGN GOVERNMENT, AS THE INTERESTS OF THE UNITED STATES MAY REQUIRE: PROVIDED THAT IN EITHER CASE THE RELEASE, USE, DUPLICATION OR DISCLOSURE HEREOF SHALL BE SUBJECT TO THE FOREGOING LIMITATIONS. THIS LEGEND SHALL BE MARKED ON ANY REPRODUCTION HEREOF IN WHOLE OR IN PART."

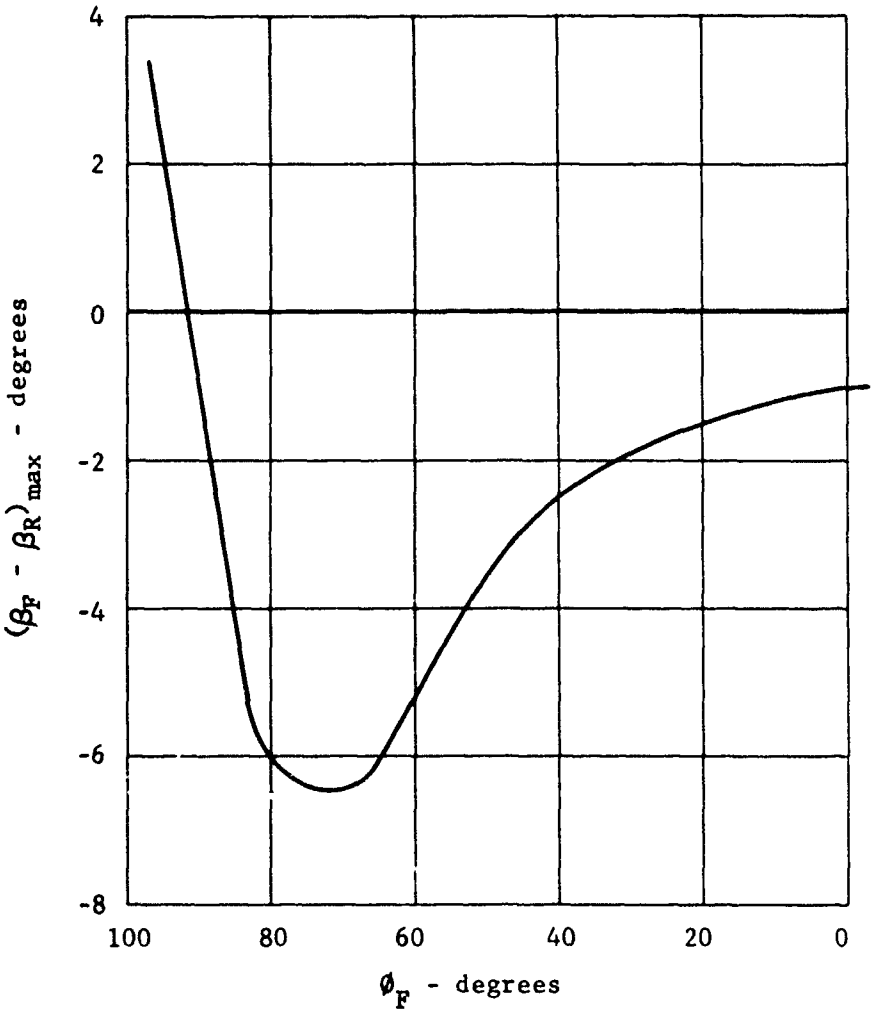

Figure 214. X-19, coordinator auto-trim schedule.

FURNISHED UNDER UNITED STATES GOVERNMENT CONTRACT No. AF33(615)-3940 SHALL NOT BE EITHER RELEASED OUTSIDE THE GOVERNMENT, OR USED DUPLICATED, OR DISCLOSED IN WHOLE OR IN PART FOR MANUFACTURE OR PROCUREMENT, WITHOUT THE WRITTEN PERMISSION OF CURTISS-WRIGHT CORPORATION, EXCEPT FOR (i) EMERGENCY REPAIR OR OVERHAUL WORK BY OR FOR THE GOVERNMENT, WHERE THE ITEM OR PROCESS IS NOT OTHERWISE REASONABLY AVAILABLE TO ENABLE TIMELY PERFORMANCE OF THE WORK, OR (ii) RELEASE TO A FOREIGN GOVERNMENT, AS THE INTERESTS OF THE UNITED STATES MAY REQUIRE PROVIDED THAT IN EITHER CASE THE RELEASE, USE, DUPLICATION OR DISCLOSURE HEREOF SHALL BE SUBJECT TO THE FOREGOING LIMITATIONS THIS LEGEND SHALL BE MARKED ON ANY REPRODUCTION HEREOF IN WHOLE OR IN PART."

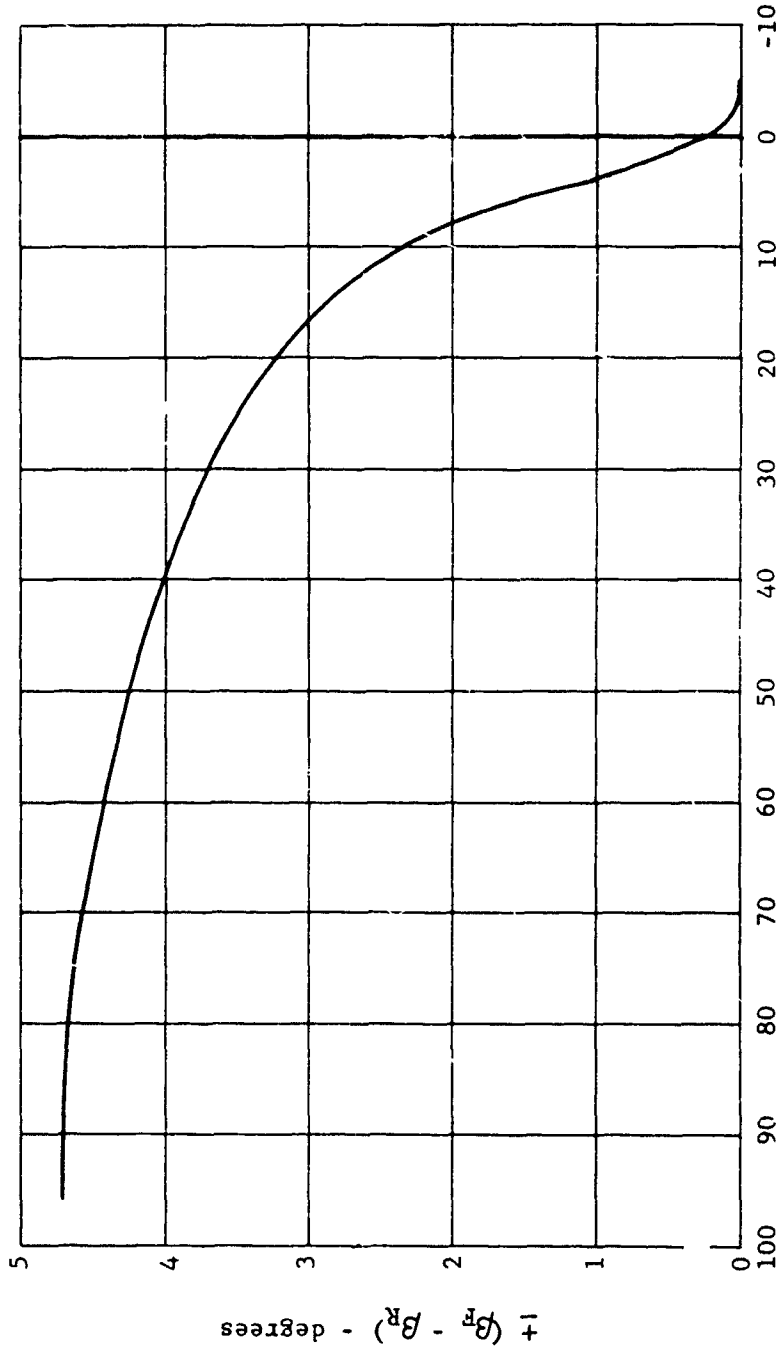

Figure 215. X-19, coordinator pitch-gain schedule.

"FURNISHED UNDER UNITED STATES GOVERNMENT CONTRACT No. AF33(615)-3940. SHALL NOT BE EITHER RELEASED OUTSIDE THE GOVERNMENT, OR USED, DUPLICATED, OR DISCLOSED IN WHOLE OR IN PART FOR MANUFACTURE OR PROCUREMENT, WITHOUT THE WRITTEN PERMISSION OF CURTISS-WRIGHT CORPORATION, EXCEPT FOR (i) EMERGENCY REPAIR OR OVERHAUL WORK BY OR FOR THE GOVERNMENT, WHERE THE ITEM OR PROCESS IS NOT OTHERWISE REASONABLY AVAILABLE TO ENABLE TIMELY PERFORMANCE OF THE WORK, OR (ii) RELEASE TO A FOREIGN GOVERNMENT, AS THE INTERESTS OF THE UNITED STATES MAY REQUIRE PROVIDED THAT IN EITHER CASE THE RELEASE, USE, DUPLICATION OR DISCLOSURE HEREOF SHALL BE SUBJECT TO THE FOREGOING LIMITATIONS. THIS LEGEND SHALL BE MARKED ON ANY REPRODUCTION HEREOF IN WHOLE OR IN PART."

(3) Roll-gain schedule

The roll-gain schedule is used to phase the propellers out of the roll control with tilt angle. As with the pitch control, the phase out is not complete until the cruise tilt angle is achieved. Originally, a roll control of 13,000 ft-lbs. (hover) was designed into the aircraft. Flight test experience indicated a desire for greater control. The coordinator gains were increased to provide 20,000 foot-pounds of rolling moment (maximum).

The roll gain schedule shown in Figure 216 corresponds to this requirement. A look at the roll gain schedule indicates a negative gain on the rear propellers at the lower tilt angles. As this gain corresponds to a right roll deflection, one finds that a large adverse roll has been inserted solely to remove the yaw coupling.

(4) Yaw-gain Schedule

The yaw schedule is presented in Figure 217. Unlike the pitch and roll schedules, the yaw gain is phased out at $\emptyset_F$ = 40 degrees. With this phasing, the yaw control is always greater than the hover value. The yaw control is positive about all four propellers in the hover configuration. Below $\emptyset_F$ = 90°, one notes the front propeller thrust will subtract from the positive yaw moments. Again, this is the result of removing the roll couple.

8. CONTROL MIXING

The variation with speed of propeller and aerodynamic surface contributions to total pitch, roll and yaw control moments through transition is shown in Figures 185, 186 and 187. It should be noted that the airspeeds shown in these figures correspond to prescribed propeller tilt angles according to the transition tilt schedule shown in Figure 211. If at some fixed tilt angle airspeed deviates from the specified schedule, total available control moment will vary in conventional fashion; namely, if speed increases (at fixed tilt angle) then maximum available control moment increases, and vice versa.

FURNISHED UNDER UNITED STATES GOVERNMENT CONTRACT No. AF33(615)-3940. SHALL NOT BE EITHER RELEASED OUTSIDE THE GOVERNMENT, OR USED, DUPLICATED, OR DISCLOSED IN WHOLE OR IN PART FOR MANUFACTURE OR PROCUREMENT, WITHOUT THE WRITTEN PERMISSION OF CURTISS-WRIGHT CORPORATION, EXCEPT FOR (i) EMERGENCY REPAIR OR OVERHAUL WORK BY OR FOR THE GOVERNMENT WHERE THE ITEM OR PROCESS IS NOT OTHERWISE REASONABLY AVAILABLE TO ENABLE TIMELY PERFORMANCE OF THE WORK, OR (ii) RELEASE TO A FOREIGN GOVERNMENT, AS THE INTERESTS OF THE UNITED STATES MAY REQUIRE PROVIDED THAT IN EITHER CASE THE RELEASE, USE, DUPLICATION OR DISCLOSURE HEREOF SHALL BE SUBJECT TO THE FOREGOING LIMITATIONS THIS LEGEND SHALL BE MARKED ON ANY REPRODUCTION HEREOF IN WHOLE OR IN PART

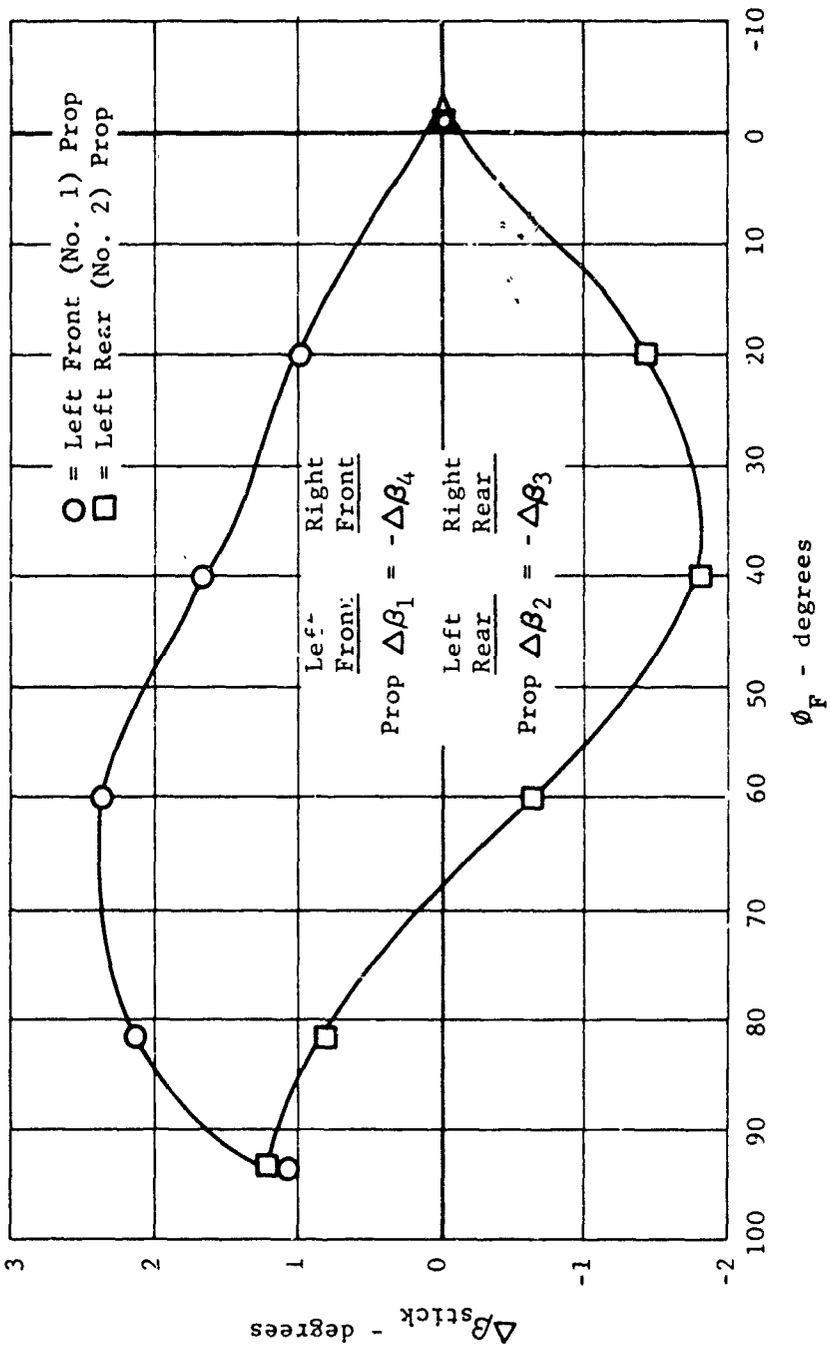

Figure 216. X-19, coordinator roll-gain schedule.

"FURNISHED UNDER UNITED STATES GOVERNMENT CONTRACT No AF33(615)-3940. SHALL NOT BE EITHER RELEASED OUTSIDE THE GOVERNMENT, OR USED, DUPLICATED, OR DISCLOSED IN WHOLE OR IN PART FOR MANUFACTURE OR PROCUREMENT, WITHOUT THE WRITTEN PERMISSION OF CURTISS-WRIGHT CORPORATION, EXCEPT FOR (i) EMERGENCY REPAIR OR OVERHAUL WORK BY OR FOR THE GOVERNMENT, WHERE THE ITEM OR PROCESS IS NOT OTHERWISE REASONABLY AVAILABLE TO ENABLE TIMELY PERFORMANCE OF THE WORK, OR (ii) RELEASE TO A FOREIGN GOVERNMENT, AS THE INTERESTS OF THE UNITED STATES MAY REQUIRE. PROVIDED THAT IN EITHER CASE THE RELEASE, USE, DUPLICATION OR DISCLOSURE HEREOF SHALL BE SUBJECT TO THE FOREGOING LIMITATIONS. THIS LEGEND SHALL BE MARKED ON ANY REPRODUCTION HEREOF IN WHOLE OR IN PART."

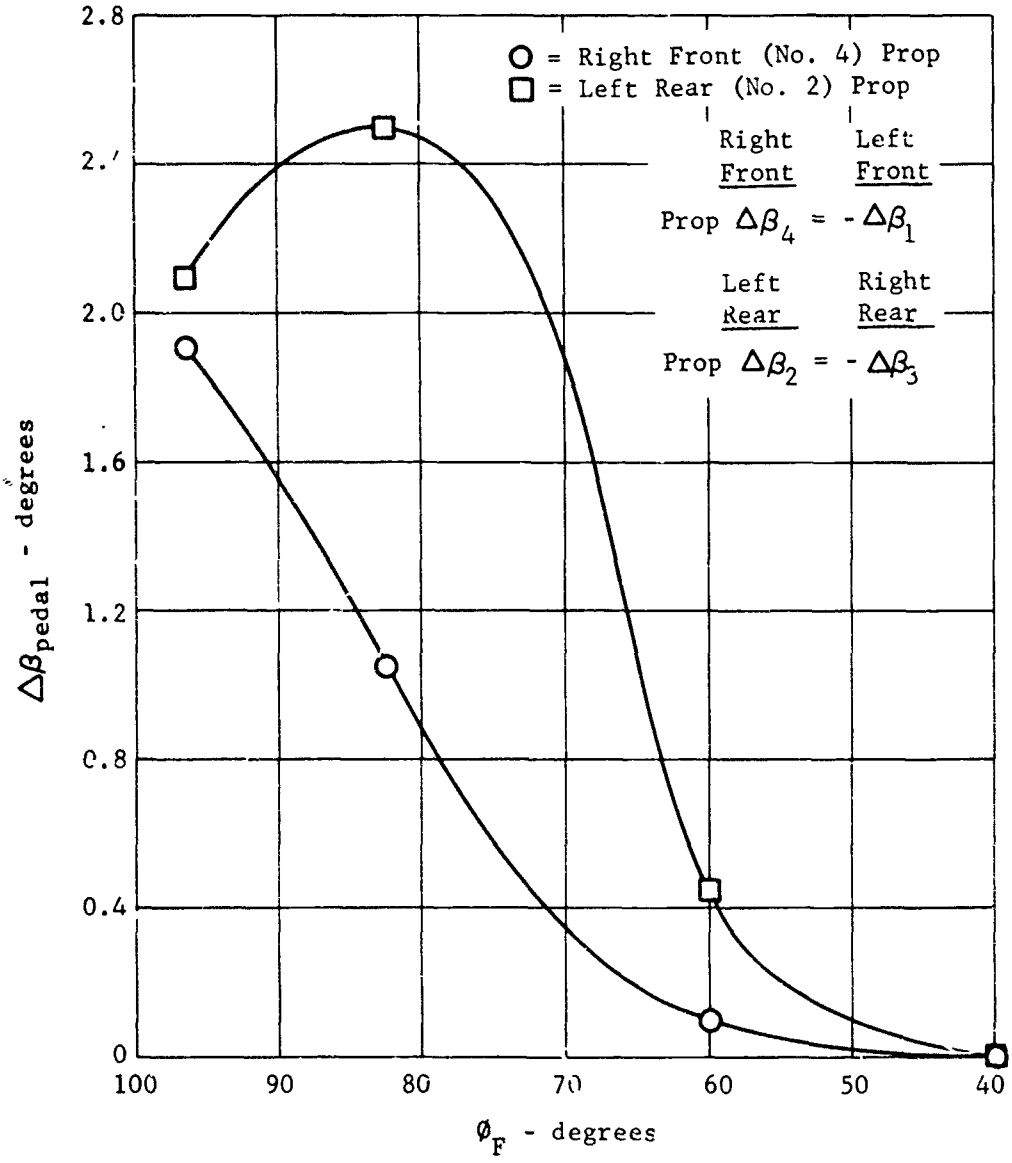

Figure 217. X-19, coordinator yaw-gain schedule.

FURNISHED UNDER UNITED STATES GOVERNMENT CONTRACT No. AF33(615)-1940. SHALL NOT BE EITHER RELEASED OUTSIDE THE GOVERNMENT, OR USED, DUPLICATED, OR DISCLOSED IN WHOLE OR IN PART FOR MANUFACTURE OR PROCUREMENT, WITHOUT THE WRITTEN PERMISSION OF CURTISS-WRIGHT CORPORATION, EXCEPT FOR (i) EMERGENCY REPAIR OR OVERHAUL WORK BY OR FOR THE GOVERNMENT, WHERE THE ITEM OR PROCESS IS NOT OTHERWISE REASONABLY AVAILABLE TO ENABLE TIMELY PERFORMANCE OF THE WORK, OR (ii) RELEASE TO A FOREIGN GOVERNMENT, AS THE INTERESTS OF THE UNITED STATES MAY REQUIRE. PROVIDED THAT IN EITHER CASE THE RELEASE, USE, DUPLICATION OR DISCLOSURE HEREOF SHALL BE SUBJECT TO THE FOREGOING LIMITATIONS. THIS LEGEND SHALL BE MARKED ON ANY REPRODUCTION HEREOF IN WHOLE OR IN PART.

REFERENCES

45. Etkin, Bernard, Dynamics of Flight - Stability and Control , John Wiley and Sons, Inc., 1959.

46. North American Aviation, Inc., Low Speed Wind Tunnel Tests of a .12 Scale Model of the C-W M-200 VTOL Airplane to Evaluate Longitudinal, Lateral and Directional Stability Characteristics, NACAL 93, Report No. NA62H-719, October 2, 1962.

47. MIL-F-8785 (AG), Military Specification, Flying Qualities of Piloted Airplanes , September, 1, 1954 and including Amendment-4, April 17, 1959.

48. Rogers, K. J., Curtiss-Wright Corporation, X-200 Turbine Stability Model , MIT Wind Tunnel Report No. 1005, November, 1960.

49. Rogers, K. J., Curtiss-Wright Corporation, X-200 Turbine Stability Model , MIT Wind Tunnel Report No. 1006, January 1961.

50. Rogers, K. J., Curtiss-Wright Corporation, M-200 Turbine Stability Model , MIT Wind Tunnel Report No. 1019, March 1962.

51. Hauser, R. J. Wind Tunnel Tests of a .12 Scale Model of the Curtiss-Wright Corporation X-19 Airplane , Cornell Aeronautical Laboratory, Inc. Report No. AA-1709-W-1, January 23, 1963.

52. Hauser, R. J., Wind Tunnel Tests of a .12 Scale Model of the Curtiss-Wright X-19, Series II, Cornell Aeronautical Laboratory, Inc. , Report No. AA-1771-W-1, May 27, 1963.

53. Munk Max M General Biplane Theory , NACA Report 151, 1922.

54. Glauert, H The Performance of Tandem Systems , British Aeronautical Research Council R & M 949, 1922.

55. Hoerner, S.F., Fluid Dynamic Drag .

56. Royal Aeronautical Society, Data Sheets, Aerodynamics, Volumes 2 and 4.

57. Robinson, R.C. and Delano, J.B. An Investigation of the Drag of Windshields in the 8 foot High Speed Tunnel , NACA Report 730.

58. Dolbin, B.H.Jr., Echart, F.H., Investigation of Lateral - Directional Handling Qualities of V/STOL Airplanes in Cruising Flight , Cornell Aeronautical Laboratory, Inc., CAL Report No. TB-1794-F-3, December 1963.

SECTION VIII NOMENCLATURE

C_m	Rate of change of pitching moment coefficient with angle of attack	
D	Propeller diameter,	ft
h	Mean height of propeller disks above ground,	ft
L_ϕ	Rate of change of rolling moment with roll attitude,	ft-lb/deg
M_θ	Rate of change of pitching moment with pitch attitude	ft-lb/deg
I.G.E.	In ground effect	
O.G.E.	Out of ground effect	
L	Lift,	lb
C_D	Coefficient of fuselage drag	
C_D'	Coefficient of landing gear door drag	
$q_{\bar{V}}$	Wake stream dynamic pressure,	lb/ft^2
A_f	Fuselage reference area,	ft^2
A_d	Landing gear door reference area,	ft^2

SECTION VIII

GROUND EFFECTS

1. INTRODUCTION

The amount of data accumulated on the X-19, relating to ground effects, is not very large. However some notable comments are made based on the limited tests run during the program. The introduction discusses some of the informal findings made by the pilot in the course of the hover and low speed flights.

To begin with, the first hover flights of the X-19 were performed within 2 or 3 feet of the ground. Reflecting, the normal learning curve, the pilot was capable of steady hovering after about 10 minutes of accumulated flying. In all of these flights, the pilot felt that stick activity was high. This was said to be a frequency rather than magnitude effect. In later hover flights, the pilot increased altitude above the nominal "ground level" hovering. The pilot reported that above about 3 feet of altitude, stick activity diminished. What is more, the general vibration and noise level were also reduced. Thereafter, hovering was performed at the higher heights. This low level ground effect is presumed to be an oscillatory shifting of the propeller wake, which is aggravated even by low intensity gusts. Further comments concerning the wash upon the fuselage are given in the following section.

Another characteristic which the pilot observed was the difference in stick activity at velocities greater than the hover point. For example, below about 15 knots, the pilot observed large oscillations on the boom-mounted airspeed pickup. Consistent with these oscillations was a reasonably active stick motion. Above 15 knots however, stick motion [8] eased considerably; so too did the gyrations on the boom. This behaviour appears related to the bending of the propeller wake. Above 15 knots the wake shifts aft; whereas below 15 knots a portion of the wake shifts forward, and recirculates sufficiently to agitate the velocity pick up. This characteristic has been found in the Curtiss-Wright X-100 as well as in other types of VTOL machines. Further comments concerning this behaviour are given in this section under inlet recirculation.

2. GROUND EFFECTS UPON STABILITY AND CONTROL

Information gathered in a ground proximity test on a 12% scale X-19 model is consistent with test pilots' comments regarding the full scale airplane's hover stability and control characteristics in ground effect.

---

8 By stick motion is meant an oscillatory motion of the stick about the required trim position. Forward trim increases with speeds above 15 knots if no down tilt is initiated.

The model tests show that in close ground proximity there are significant variations in aircraft pitching moment as a function of pitch angle, and in rolling moment as a function of roll angle (i.e. $M_\theta \neq 0$, $L_\phi \neq 0$, as is the case for O.G.E. hover). Average values obtained from these tests were, M_θ = -1000 ft. lb/deg. and L_ϕ = +150 ft.lb/deg. at h/D = 1.2 (where h = mean height of propeller diameters above ground, and D = propeller diameter). This h/D value is equivalent to a full scale wheel height above ground of approximately 9 feet. It will be noted that the M_θ is stable while L_θ is unstable.

The validity of these data is verified, at least qualitatively, through observations made by the pilots who flew in the aircraft.

The Curtiss-Wright test pilot frequently commented on the need for increased roll stick activity in close ground proximity, but made no adverse comments on pitch stick requirement. The point is well illustrated by the military co-pilot's observation on Flight No. 37: "Moderate upsetting lateral moments were encountered just before the aircraft touched the ground. Stick activity was noticeably high ..."

The following hypotheses are presented as explanations for the nature of M_θ and L_ϕ.

M_θ : a negative, or stabilizing term. The negative value may be explained by the effect of ground on front and rear pairs of propellers. Consider for example the case where the aircraft pitches nose down (negative pitch angle); the front propellers move closer to the ground and the rear propellers move further away, which due to normal ground effect produces an increase in thrust of the front propellers and a decrease in thrust of the rear propellers; or in total, a nose up pitching moment (i.e. negative M_θ).

L_ϕ : a positive, or destabilizing term. The same argument would seem to apply to L_ϕ as to M_θ, which would imply a stable value for L_ϕ also. However, consider for example the case where the aircraft rolls right (positive roll angle). As the right roll proceeds, the center of pressure of the recirculating propeller wash impinging on the underside of the aircraft fuselage moves to the left (or toward the "open" side) producing a right, or positive, rolling moment (i.e. acting in the direction of the roll angle perturbation).

It is suggested that this moment is larger than the stabilizing moment due to ground effect on the individual propellers (as with M_θ). The net result is that L_ϕ is destabilizing. This explanation is further substantiated by the tendency (as measured in the model tests) for L_ϕ to change sign (become stabilizing) at roll angles greater than approximately 5 degrees. This indicates that the center of pressure of the recirculating wash has passed beyond the bounds of the fuselage underside and the situation becomes almost identical to that in pitch. In pitch the recirculating wash effect is felt to be minor.

At aircraft heights greater than h/D = 3 (wheel height approximately 30 feet), ground effects on stability and control are considered insignificant.

A very limited amount of additional data applicable to low speed forward flight, in ground effect, is available from (59). This report contains the results of a 12% model X-19 wind tunnel test at a few selected transition configurations (at large propeller tilt angles). The conclusions drawn from these data regarding the effects of ground and velocity on lift and drag are discussed in Section III. Here it is mentioned that these data indicated very little change in the value of the static stability derivative C_{m_α}, I.G.E., compared with O.G.E. values. However, a nose up pitching moment is generated when climbing out of ground effect at constant speed and angle of attack. It is pointed out that no such trim changes were observed by the pilot during the STOL phase of the flight test program.

(59) also indicates that at low forward speeds, control power is unaffected by ground proximity.

3. FLOW FIELD RECIRCULATION - ENGINE INLET

a. General

Flow distortion tests within engine limits were accomplished on the Curtiss-Wright half-system rig. It was determined that less than 2% pressure drop and less than 4 degrees F temperature change (including oil cooler and engine cooler gear box) was attributable to ground effect. This represents a 2% power decrement from standard day O.G.E. values.

b. Recirculation

There was no supportable evidence in these tests of recirculation of engine exhaust into the inlet. Neither was there any known ingestion of exhaust due to tail winds or rapid rearward movement of the aircraft, although specific tests were not performed.

c. Reverse Flow

For the case with dead engine, tested in both rigs, no recirculation from operating engine exhaust through dead engine (reverse flow) was observed or measured. However, a secondary effect, where the live engine exhaust sucks air through the dead engine in parallel flow, did exist. No quantitive data were taken to demonstrate the magnitude of this effect.

d. Foreign Object Ingestion

The ever present problem of foreign objects being sucked into the engine inlet was also considered during ground testing. Both the

X-19 and the X-100 encountered minor problems of this nature, especially where the propeller flow whipped loose terrain (small stones) into the air during ground runs. There was evidence of stone ingestion during such a test. However, most foreign objects did settle at the bottom of the inlet plenum.

Damage to engines from foreign objects is costly and needless. Some damage to the first few stages of the engine compressor did occur due to small stone ingestion. A retractable 3/16 to 1/4" mesh screen with .060 wire grid in the plenum chamber would certainly prove its worth. Consideration was also given to some form of "egg-crating" (vertical baffling) to be installed in this area. Such baffling had not previously been installed; however it is believed that all but perhaps 10% of the ingestion without baffling would be trapped by its use.

e. Dust Clouds

Experience with X-19 and X-100 flights has shown that at speeds below 15 knots in normal operation a dust cloud is generated around the airplane on unprepared runways. At speeds in excess of 15 knots this cloud was observed to shift behind the airplane and effectively out of the province of objectionable interference. Other VTOL aircraft manufacturers have encountered the same effect. There appears to be little that can be done about this, short of having a "white room" flight test area.

4. HOVER POWER REQUIREMENT WITH GROUND HEIGHT

It has been shown experimentally with both the X-100 and X-19 aircraft and substantiated qualitatively by theoretical means that a multi-propeller VTOL hovering in ground proximity experiences a beneficial lifting augmentation. To the VTOL pilot this is a vitally important factor, particularly in its application to engine-out landings; and accurate prediction of this beneficial ground interference effect must be paramount in a program such as the X-19 development.

In the case of X-100 flight tests, it was evident that a positive pressure field was created on the bottom of the fuselage. The wake leaving the two propellers impinged on the ground and then spread radially. A plane of symmetry was generated along the centerline where the flow of the two props met and turned upward to press on the lower fuselage. This gave local pressures above one atmosphere thereby inducing an upload on the airplane. Velocity survey measured at ground level beneath the propellers and under the fuselage gave quantitative credence to this premise. It should be noted that this beneficial X-100 lift increment acts at the c.g., and thus required no change in control stick position.

The X-100 test pressure data has been applied to the X-19 configuration to estimate its ground effect. Since this configuration utilized four propellers, the law of super-position was applied. The predicted pressure distribution is shown in Figure 218. It can be seen that the front two

FURNISHED UNDER UNITED STATES GOVERNMENT CONTRACT No. AF33(615)-1940. SHALL NOT BE EITHER RELEASED OUTSIDE THE GOVERNMENT, OR USED, DUPLICATED, OR DISCLOSED IN WHOLE OR IN PART FOR MANUFACTURE OR PROCUREMENT, WITHOUT THE WRITTEN PERMISSION OF CURTISS-WRIGHT CORPORATION, EXCEPT FOR (i) EMERGENCY REPAIR OR OVERHAUL WORK BY OR FOR THE GOVERNMENT, WHERE THE ITEM OR PROCESS IS NOT OTHERWISE REASONABLY AVAILABLE TO ENABLE TIMELY PERFORMANCE OF THE WORK OR (ii) RELEASE TO A FOREIGN GOVERNMENT, AS THE INTERESTS OF THE UNITED STATES MAY REQUIRE. PROVIDED THAT IN EITHER CASE THE RELEASE, USE, DUPLICATION OR DISCLOSURE HEREOF SHALL BE SUBJECT TO THE FOREGOING LIMITATIONS. THIS LEGEND SHALL BE MARKED ON ANY REPRODUCTION HEREOF IN WHOLE OR IN PART

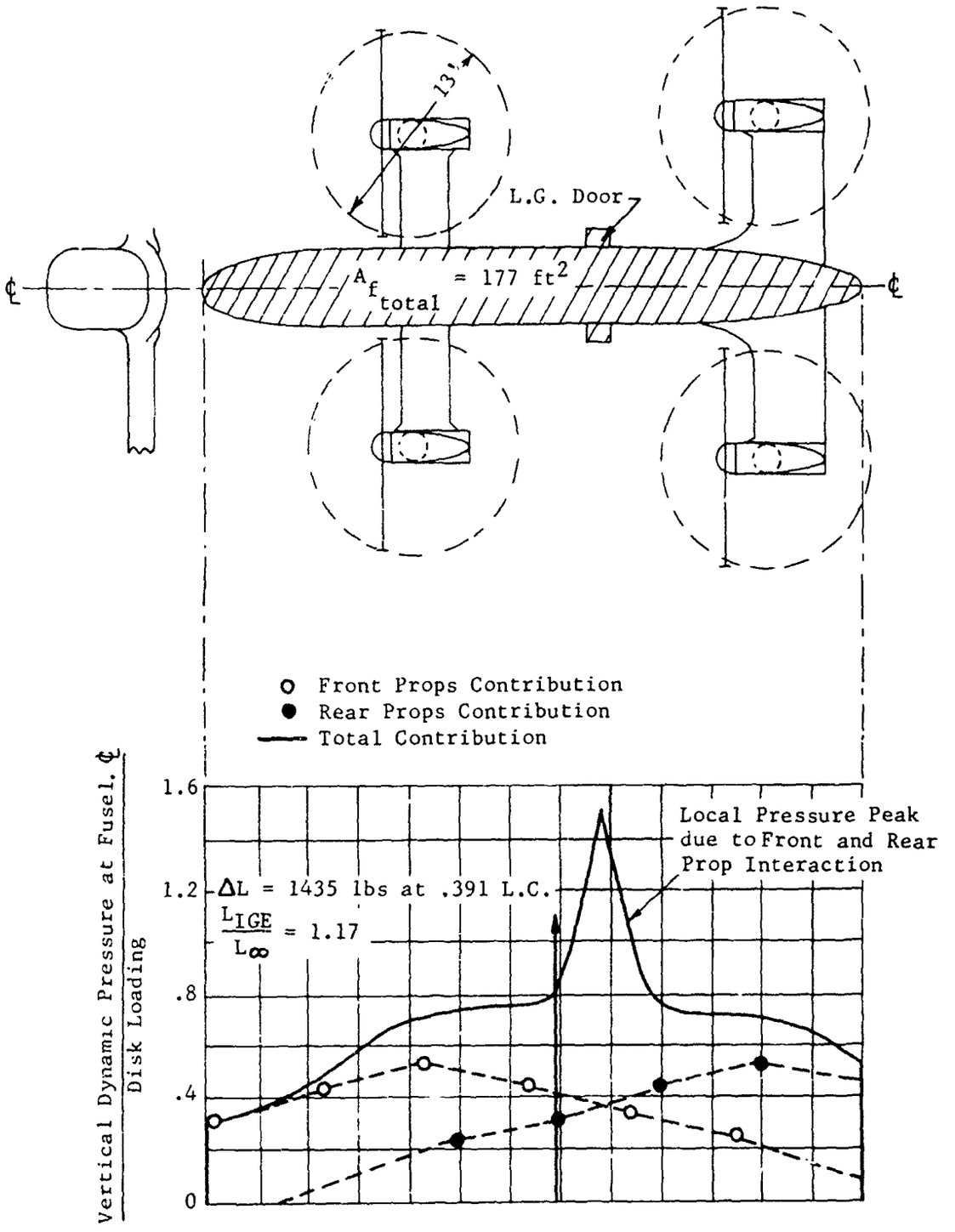

Figure 218. Estimated hover ground effect pressure distribution for the X-200 configuration.

"FURNISHED UNDER UNITED STATES GOVERNMENT CONTRACT No. AF33(615)-3940 SHALL NOT BE EITHER RELEASED OUTSIDE THE GOVERNMENT, OR USED, DUPLICATED, OR DISCLOSED IN WHOLE OR IN PART FOR MANUFACTURE OR PROCUREMENT, WITHOUT THE WRITTEN PERMISSION OF CURTISS-WRIGHT CORPORATION, EXCEPT FOR (i) EMERGENCY REPAIR OR OVERHAUL WORK BY OR FOR THE GOVERNMENT, WHERE THE ITEM OR PROCESS IS NOT OTHERWISE REASONABLY AVAILABLE TO ENABLE TIMELY PERFORMANCE OF THE WORK, OR (ii) RELEASE TO A FOREIGN GOVERNMENT, AS THE INTERESTS OF THE UNITED STATES MAY REQUIRE PROVIDED THAT IN EITHER CASE THE RELEASE, USE, DUPLICATION OR DISCLOSURE HEREOF SHALL BE SUBJECT TO THE FOREGOING LIMITATIONS. THIS LEGEND SHALL BE MARKED ON ANY REPRODUCTION HEREOF IN WHOLE OR IN PART."

propellers create a vertical velocity along the fuselage line of symmetry, and the two rear propellers contribute in a like manner. There is also a third contribution that occurs from interaction of the two front propellers with those at the rear causing a local high pressure peak halfway between the front and rear propellers. By coincidence this area of high pressure appears at the open landing gear doors which, because of the high pressure, contributes greatly to the overall ground effect lifting increment.

This lift increase has been computed as:

$$\Delta L = C_D \Sigma q_V A_f + C_D' \Sigma q_V A_D$$

where the first term is the fuselage contribution (for Reynolds number and the geometry, a $C_D = 0.45$ was used). The second term is the landing gear door contribution (use $C_D' = 1.0$, and A_D is the profile door area).

The fuselage contributes 10% lift augmentation and the doors seven per cent, giving precisely the same ground effect increment of 17 per cent as the X-100. The resultant force due to ground effect occurs at about 39 of the lift chord, which again is very close to the aircraft center of gravity. Figure 219 is included here to compare X-100/X-200 lift augmentation due to ground effect, as defined above, with similar data for the Hiller Aircraft Corp.'s X-18 tilt high-wing test aircraft. The higher lift augmentation of the latter aircraft can be attributed to its high disk loading and flat bottom fuselage. In hover, it was found that ground effect falls off appreciably with height off the ground, becoming zero at about 2.5 propeller diameters.

Subsequent X-19 model ground effect tests were conducted in November 1964, and are reported in Paragraph IX,2.e.(2) over ground, and in tests a year earlier over water in Paragraph IX,2.e.(1). The data obtained in those tests have essentially confirmed the above results.

For further detailed discussion of ground effects, see Section III,4. of this report.

FURNISHED UNDER UNITED STATES GOVERNMENT CONTRACT No. AF33(615)-1940. SHALL NOT BE EITHER RELEASED OUTSIDE THE GOVERNMENT, OR USED, DUPLICATED, OR DISCLOSED IN WHOLE OR IN PART FOR MANUFACTURE OR PROCUREMENT, WITHOUT THE WRITTEN PERMISSION OF CURTISS-WRIGHT CORPORATION, EXCEPT FOR (i) EMERGENCY REPAIR OR OVERHAUL WORK BY OR FOR THE GOVERNMENT, WHERE THE ITEM OR PROCESS IS NOT OTHERWISE REASONABLY AVAILABLE TO ENABLE TIMELY PERFORMANCE OF THE WORK, OR (ii) RELEASE TO A FOREIGN GOVERNMENT, AS THE INTERESTS OF THE UNITED STATES MAY REQUIRE. PROVIDED THAT IN EITHER CASE THE RELEASE, USE, DUPLICATION OR DISCLOSURE HEREOF SHALL BE SUBJECT TO THE FOREGOING LIMITATIONS. THIS LEGEND SHALL BE MARKED ON ANY REPRODUCTION HEREOF IN WHOLE OR IN PART.

Figure 219. Comparison of ground effect augmentation of hover lift of two different types of VTOL testbed aircraft.

"FURNISHED UNDER UNITED STATES GOVERNMENT CONTRACT No. AF33(615)-3940. SHALL NOT BE EITHER RELEASED OUTSIDE THE GOVERNMENT, OR USED, DUPLICATED, OR DISCLOSED IN WHOLE OR IN PART FOR MANUFACTURE OR PROCUREMENT, WITHOUT THE WRITTEN PERMISSION OF CURTISS-WRIGHT CORPORATION, EXCEPT FOR (i) EMERGENCY REPAIR OR OVERHAUL WORK BY OR FOR THE GOVERNMENT, WHERE THE ITEM OR PROCESS IS NOT OTHERWISE REASONABLY AVAILABLE TO ENABLE TIMELY PERFORMANCE OF THE WORK, OR (ii) RELEASE TO A FOREIGN GOVERNMENT, AS THE INTERESTS OF THE UNITED STATES MAY REQUIRE. PROVIDED THAT IN EITHER CASE THE RELEASE, USE, DUPLICATION OR DISCLOSURE HEREOF SHALL BE SUBJECT TO THE FOREGOING LIMITATIONS. THIS LEGEND SHALL BE MARKED ON ANY REPRODUCTION HEREOF IN WHOLE OR IN PART."

59. Low Speed Wind Tunnel Tests of a 0.12 Scale Model of the Curtiss-Wright X-19 Aircraft, North American Aviation Report NA 64H-837, (NACAL 120), August 1964

SECTION IX NOMENCLATURE

A = propeller angle of attack

C_D = drag coefficient - D/qS

C_L = lift coefficient = L/qS

CG = center of gravity

C_l = rolling moment coefficient

C_L = airplane lift coefficient

C_M = pitching moment coefficient

C_N = propeller normal force coefficient

C_p = power coefficient - propeller

C_{R_L} = rolling moment coefficient

C_T = propeller thrust coefficient

C_{Y_M} = yawing moment coefficient

C_y = side force coefficient

D = propeller diameter

h/D = height to diameter

J = advance ratio = $V/n\ D_p$

N = propeller RPM

T.S. = tunnel speed

q = dynamic pressure

MODEL DESIGNATIONS

F = fuselage

N = nacelle

P = power

V = vertical tail

W = wings

Subscripts

B = bow

A = aft

α_f = fuselage angle

β = propeller blade angle

δ = surface deflection angle

ψ = yaw angle

SECTION IX

WIND TUNNEL TESTS

1. INTRODUCTION

The history of the Curtiss-Wright X-19 configuration development, beginning with proving the concept of tilting propellers and of radial lift from the propellers, has been adequately covered earlier in this report. Suffice it to say here the evolution of the tandem tilt propeller VTOL aircraft, culminating in the ultimate construction and flight and ground testing of two X-19 aircraft, Air Force S/N 62-12197 and 62-12198, came about as a result of considerable wind tunnel testing, including full-scale Model X-100 testing in the NASA Ames Research Center 40 by 80 foot tunnel. This design evaluation backup was instrumental in critically defining many of the design and control parameters which went into the X-100 and X-19 flight test vehicles. It is the purpose of this section to elaborate on these tests and their contribution to the ultimate flight articles.

The objective of conducting wind-tunnel tests is, of course, to provide data on the actual configuration to supplement calculated data for predicting performance, loads, stability and control. Wind tunnel tests are planned and executed so as to duplicate as nearly as possible full-scale conditions so that corrections to the data will be minimized. Unfortunately this is generally not the case. It then becomes necessary to run the model tests and develop corrections for scale effects so that reliable estimates of the full-scale performance can be made.

2. TESTS IN SUPPORT OF X-19 AND X-100 AIRCRAFT

a. General

A large quantity and variety of data were taken on a substantial number of scale models during the wind tunnel testing phase of the X-19 development program. These data were reported in a series of wind tunnel test reports, in which the nature of the tests run and their results are catalogued.

It would not be appropriate in this Technology report to delve in any great detail into each individual test run, but rather to establish the significant characteristics and parameters derived from such testing.

Curtiss-Wright Corporation does not have its own wind tunnel test facilities, and therefore all testing of the X-19 concept configuration was accomplished in five commercial or U.S. Government wind tunnels, as follows: The MIT Wright Brothers Memorial Wind Tunnel, Cambridge, Massachusetts; Cornell Aeronautical Laboratory, Transonic Tunnel, Buffalo, New York; North American Aviation Corporation, NACAL Facility, Columbus, Ohio; University of Mary-

land, Wind Tunnel, College Park, Maryland; and the NASA Ames Research Center 40 by 80 foot full-scale tunnel, Moffett Field, California.

b. Test Models

The models tested varied in size, arrangement and purpose. Six specific models of the four-tilt-propeller type were used at various times during the test programs. However, one in particular, the 12% scale X-200 tandem wing stability model, was the basic model and was used extensively for determining the X-19 characteristics. One other model, that depicting the Curtiss-Wright Model 90 AAFSS Proposal configuration, was also devised and tested in 1964; its results were only qualitatively applicable to the X-19 program, and were unrelated to the first X-200 test program six years earlier.

The models used in these wind tunnel tests are identified as follows:

(1) 12% Scale X-200 Tandem Wing Stability Model

(2) 11.54% Scale X-200 Tandem Nacelle Radiator Model

(3) 25% Scale X-200 Semi-Span Rear Wing Model (64_3-418 modified)

(4) 50% Scale X-200 Half-Wing Model (NACA 64_4-421 modified)

(5) 7.15% Scale X-300 Tandem Wing and Propeller Model

(6) 12% Scale X-200 Fuselage Pressure Distribution Model

c. Test Uses of Models

These in turn had as their main purposes:

(1) The primary stability and control investigation of the Curtiss-Wright Model X-200, the aerodynamic properties of propellers mounted in tandem on nacelles at wing's extremity; various tail configurations; simulated transition flight; variation of nacelle angles; alternate rotation of propellers; blade angle variations; and wing incidence variation.

(2) To test the cooling capabilities and external aerodynamic forces of nacelle mounted radiator.

(3) To determine power-off control surface hinge moments together with force and moment characteristics of wing alone for clean conditions.

(4) To determine wing and flap, force, moment and pressure distribution at various flap deflections, and angle of attack variation.

(5) Unconventional configuration (single wing with nacelle pods at wing tips) with tandem propellers at opposite extremities of each nacelle; ascertainment of the propeller wash effects.

(6) Determination of pressure and flow patterns about the entire fuselage.

d. Model Variations

Except for the tests on the model of X-300 aircraft configuration, all other wind tunnel tests in the X-19 simulation program were conducted with models made for, or derived from, X-200 configuration.

This latter aircraft design configuration differed from the X-19 flight configuration essentially by its 18 inch shorter fuselage and consequent lift-chord length. The X-19 model also incorporated a 9 inch shorter nose section, a change in windshield configuration, and modifications to the flap and elevator arrangements of the original 12% scale X-200 model.

All tests reported in the MIT Reports 1006 or earlier (pre-1962) are specifically the X-200 original configuration, with some inlet variations early in that program to account for change of aircraft engine type from Wankel to gas turbine propulsion means. While these models do not truly represent the final X-19 configuration, tests run with the X-200 models were instrumental in establishing fruitful test data in later test programs at MIT, CAL and NACAL for the X-19 type.

Wind tunnel tests reported in MIT Report No. 1019, (60), and in the later CAL and NACAL series were conducted only with the 12% scale X-200 tandem wing stability model. These were modified by the addition of a proportionately scaled 18 inch fuselage section and reshaped nose, as well as the windshield and control surface changes, to represent the X-19 configuration. Therefore, data derived in tests reported in MIT-1019 and in subsequent tests are in fact X-19 data.

The fuselage of the latter model was composed of a steel frame to which the other components were attached, and a mahogany shell which gives it aerodynamic shape. A 30 horsepower electric motor was mounted in the fuselage and supplied power to the propellers for power-on tests. The air intake scoop (sealed) was situated on the upper surface of the fuselage in front of the rear wing.

The four wing-panels used in the MIT - 1019 tests were made of machined aluminum and housed power shafts to the propellers.

The bow wing was shaped to represent a modified NACA 2421 airfoil section, and the aft wing was made as a modified NACA 64_3-418 section. These smooth wings were also tested with a surface-roughness grit material included. The K90 grit number used in the MIT-1019 tests had an average size of 0.007 inch and was applied along the span at the quarter-chord of both wings and tail, as well as at designated points on the other components of the airplane. Other grit sizes were investigated in the CAL series of tests.

Power nacelles made of steel were used in the X-19 model version. These are 10% larger in diameter than the scale nacelles and contain the gearing and drive shafts for the propeller.

The steel sleeves which carry the power shafts to the propellers were strain-gage instrumented to record the thrust on both the bow and aft propellers on the left side. A Baldwin torque cell was installed on the forward drive shaft to determine the power absorbed by both front props. The strain gage and torque cell data were noted on a Brown Recorder. The propeller blades were of fiberglass construction. The blades were statically balanced and their blade angle was preadjustable.

For the CAL tests, CAL relocated the propeller gear train drive system, recut and refinished the model core, and fabricated new forward and aft wings and vertical tail of steel. Also seven instrumented, remotely actuated control surfaces were fabricated as integral components in the wing and tail panels to measure hinge moments produced by panel loads. A model electric motor located in the fuselage was used to drive the four propellers through a drive belt and gear train, producing clockwise rotation of the forward right and aft left (pilot's view) propellers, and counterclockwise rotation for the remaining propellers.

For one CAL run only, boundary layer transition strips (No. 120 grit) which has the average grain size of .0049 inch were applied on the fuselage nose and aft of the engine inlet, as well as the 10% chord on all wing and tail surfaces. A photograph of the X-19 model is shown in Figure 220, although not as mounted in the CAL tunnel. The only other model modifications were those necessitated to facilitate tripod mounting in the MIT tunnel, sting mounting in the CAL tunnel, and post-mounted in the NACAL tunnel (as in Figure 220).

e. Wind Tunnel Test Facilities Used

The test series and their detailed objectives and accomplishments

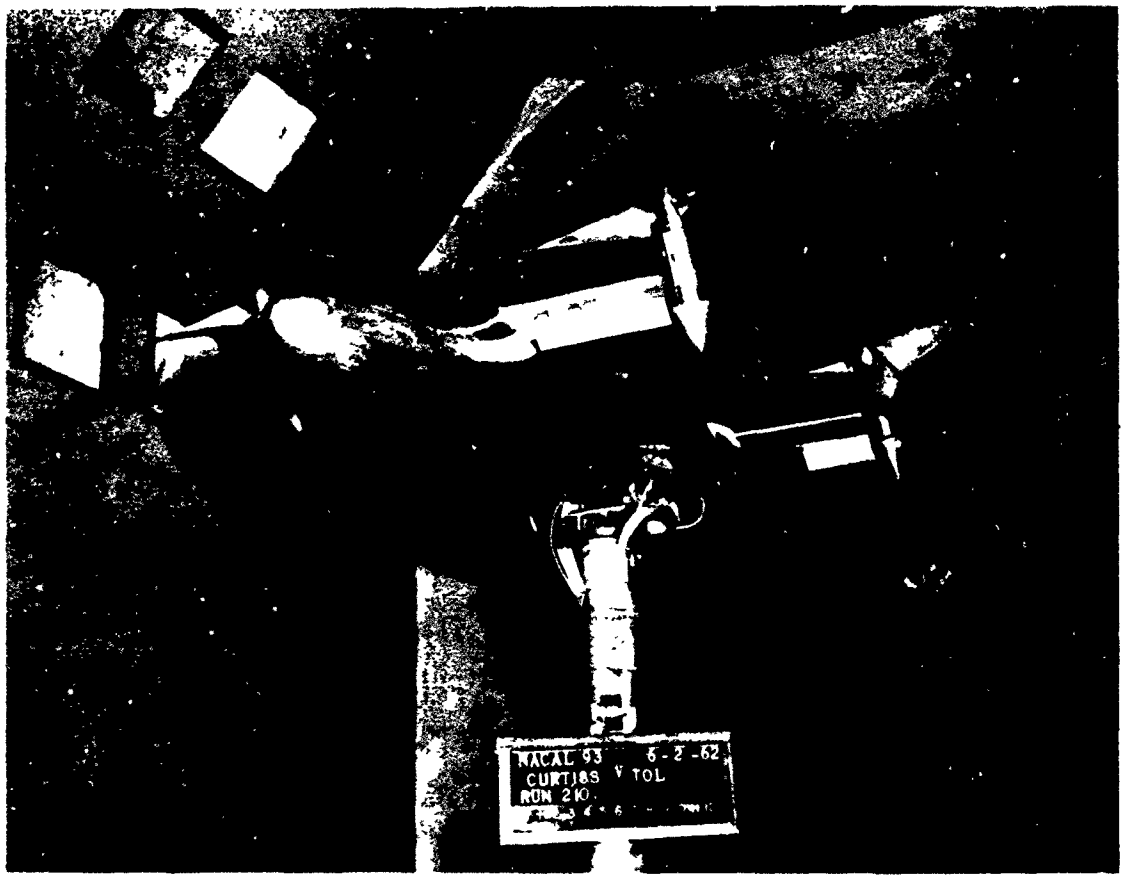

Figure 220. 0.12 scale model of the Curtiss-Wright X-19 configuration mounted in the NACAL wind tunnel.

are as follows:

(1) Early MIT Tests

The earliest applicable Curtiss-Wright tandem wing configuration wind tunnel tests were those run at The Massachusetts Institute of Technology Wright Brothers Memorial 10 by 7.5 foot elliptical-section Wind Tunnel during the latter part of 1958 thru 1960.

All six scale models previously described were used only during this test series. Because these tests were not specifically representative of the final X-19 configuration, only brief summations of these 15 early MIT test series with X-200 and X-300 models are given hereafter.

(a) MIT Report 979. These runs investigated the aerodynamic properties of two propellers mounted in tandem in the influence of nacelles and wings. Wing incidence was varied over the range from - 8 to + 8 degrees; nacelle gimbal angle was set variously from - 15 to + 90 (full-up) degrees; and propeller blade angle set at specific values from 10 to 38 degrees. Force and power coefficients, as well as propeller wake pressure data, were recorded for the wing, nacelle and propeller, the settings consistent with the 12% scale X-200 model, with non-scale power nacelles incorporated.

(b) MIT Report 984. This report covers the extension of the previous tests to supplement the data over greater angular ranges than were tested earlier, using the same model.

(c) MIT Report 985. With the substitution of scale nacelles for the previous power nacelles, the basic aerodynamic stability and control characteristics of the 12% scale X-200 model were tested, with the nacelles, ailerons, elevators, rudder and flaps deflected as required for the specified control study. In this test series, boundary layer trips, in the form of strands of thread of various diameters, were used.

(d) MIT Report 989. Tests were made to ascertain the stability and control characteristics of the 12% scale X-200 model as affected by a variety of tail configurations, nacelle-mounted vertical fins, simulated transition flight, and a variation in nacelle gimbal angle, not to mention alternate locations for a carburetor scoop. These tests were conducted with and without power, and provided pressure distribution data over the left rear wing of the model at various control surface deflections.

(e) MIT Report 991. A similar test procedure was performed on still other vertical and horizontal tail components on the 12 scale X-200 stability model. In addition, reversed rotation of the rear propellers, simulated transition, rudder deflection and autorotation, were tested for a range of propeller blade angle, nacelle angle and wing incidence with power on and off. The data taken were in the form of force and moment measurements and power measurements.

(f) MIT Report 992. Using the half-scale wing model having a total of 116 pressure orifices located at four spanwise stations, tests were run to determine wing and flap force, moment and pressure distribution at various flap deflections, and through an α range from - 8 to + 16 degrees.

(g) MIT Reports 995 and 997. The only tests of the X-300 tandem propeller model, consisting of the right wing and tip nacelle of the proposed airplane, are reported therein. While this unorthodox configuration has no bearing on the X-19 configuration technology, the tests provided data concerning pitching moment vectors in transition as well as propeller wash data not previously available for this wing-nacelle-propeller combination.

(h) MIT Reports 996 and 998. Using the 11.54% tandem nacelle radiator model, tests were performed to test the cooling capabilities and external aerodynamic forces of an X-200 nacelle radiator configuration in the flight modes of hover, hover with ground plane, and cruise (inner door removed). Again, the test data recorded were values of pressure, force and power.

(i) MIT Report 999. Returning to the 12% stability model again, tests to study the reliability of nacelle coolers or various combinations of wing coolers rather than fuselage engine coolers were investigated, as well as devising means to improve the stability characteristics of the X-200.

(j) MIT Report 1003. Bow and aft wing-nacelle-propeller lift, drag, propeller power and pitching moment data simultaneously and in close proximity to the fuselage during transition flight were obtained in this test series. The force and moment contribution of the propellers, alone as tested above, were also measured. The propeller contribution to the longitudinal stability,

and propeller efficiency in the cruise configuration, were also valuable outputs of these test runs. Cruise data were taken at 100 mph tunnel speed, and transition results were recorded at various tunnel speeds from 40 to 100 mph; the propeller rpm range varied from 3318 to 6900 during these tests.

(k) MIT Report 1004. A 25% scale X-200-T semi-span rear-wing model provided the means for determining the power-off control surface hinge moments, together with force and moment characteristics of wing alone for clean conditions.

Aileron deflection ranged from + 11 to - 15 degrees, whereas collective aileron deflections covered angles from + 10 to + 40 degrees. Elevators were deflected variously from + 15 to -20 degrees in these tests, while the model angle of attack was set from - 9 to + 16 degrees.

(l) MIT Report 1005. Returning to the 12% stability model, further tests to determine the aerodynamic stability and control characteristics of the X-200-T aircraft were made. The model underwent some minor changes in this series principally to reduce aerodynamic interference. Also the effect of front-wing roughness (K_{70}) (0.0098 inch maximum grit size) on longitudinal stability was investigated. Rear wing area was further increased with the attachment of a piece of sheet metal, and three variants of vertical fin to evaluate its height effects were also tested.

(m) MIT Report 1006. The last report of this test series at MIT recorded supplementary stability and control characteristics tests with the 12% X-200-T model. Tests of the rear wing enlargements, per the MIT Report 1005, were extended in this report to represent two different spans and various wing fairings. A front-wing flap variation and a different vertical fin were also tested here. The drag test involved the use of a K_{280} roughness (0.0011 maximum grit size) applied to all components of the complete configuration.

(2) Later MIT Tests

The tests and results of the second MIT test program, using the 12% scale X-19 configuration tandem wing model, are contained in their entirety in (60). These tests were performed during March, 1962, to determine the longitudinal, lateral and directional stability characteristics over a

range of simulated full-scale flight conditions. Included in that program were specific tests to determine the effect of power, the aerodynamic contributions of various aircraft components, and a props-off drag study. Pressure data on the flat-panel windshield and the windmilling propeller characteristics of the aircraft, both in and out of ground effect, were also investigated.

The relative comparisons within the results are more accurate than either absolute values or the comparisons between reports. This is due to scale effects and wind tunnel influences unaccounted for by the standard data correction methods.

Since this test series was the first to investigate the X-19 configuration it would be useful to present some graphical results of the MIT Report 1019 tests as a basis for comparison with other tests run later in the X-19 program.

(a) Longitudinal Characteristics

As in the previous MIT tests a free-floating, counterbalanced fairing was installed over the juncture between the support system and the model to decrease turbulence at the model support. During the early running this airfoil hung up occassionally, and the data (especially lift) is subject to some scatter.

In an attempt to reduce the area requirement of the rear wing and obtain a more aft allowable C.G. a floating flap on the front wing was investigated. This flap was designed to float and reduce the slope of the lift curve of the front wing and so improve longitudinal stability. Unfortunately the flap would float at two different angles and therefore was not practical. For this reason the idea was abandoned.

The modifications to the X-200 model necessary to obtain X-19 model configuration (increased fuselage length and flat panel windshield) increased the longitudinal stability only slightly. Figure 221 (runs 28 and 100) presents the longitudinal characteristics, props on and off, of the basic cruise configuration of the X-19. This compares favorably with the earlier MIT Report 1006 test data for the original X-200 configuration.

The drag data for the runs with free-floating flap on the front wing are presented in Figure 222, combining in one illustration all such data, since the difference in the data is less than the accuracy of the balance.

(b) Directional and Lateral Stability

The directional stability (yaw) and lateral stability (roll) of the cruise configuration at the cruise angle of attack (about 4°) may be seen for propellers on and off, in Figure 223 (runs 70 to 95). The yawing moment and rolling moment derivatives differ considerably from

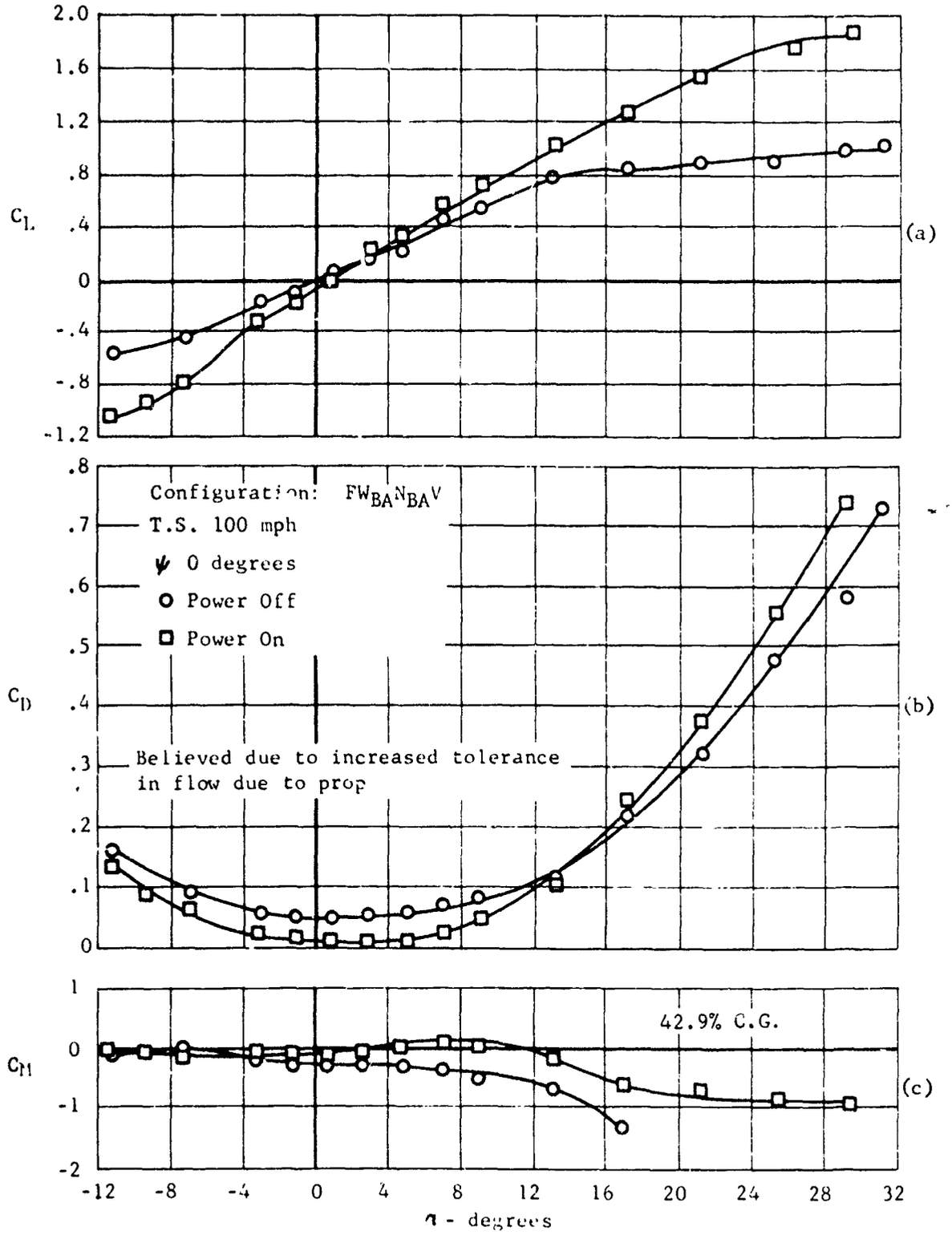

Figure 221. Longitudinal aerodynamic characteristics of the 0.12 scale model of the Curtiss-Wright X-19, power on and power off, MIT-1019 runs 9 and 100.

FURNISHED UNDER UNITED STATES GOVERNMENT CONTRACT No. AF33(615)-3940. SHALL NOT BE EITHER RELEASED OUTSIDE THE GOVERNMENT OR USED, DUPLICATED, OR DISCLOSED IN WHOLE OR IN PART FOR MANUFACTURE OR PROCUREMENT, WITHOUT THE WRITTEN PERMISSION OF CURTISS-WRIGHT CORPORATION, EXCEPT FOR (i) EMERGENCY REPAIR OR OVERHAUL WORK BY OR FOR THE GOVERNMENT, WHERE THE ITEM OR PROCESS IS NOT OTHERWISE REASONABLY AVAILABLE TO ENABLE TIMELY PERFORMANCE OF THE WORK, OR (ii) RELEASE TO A FOREIGN GOVERNMENT, AS THE INTERESTS OF THE UNITED STATES MAY REQUIRE. PROVIDED THAT IN EITHER CASE THE RELEASE, USE, DUPLICATION OR DISCLOSURE HEREOF SHALL BE SUBJECT TO THE FOREGOING LIMITATIONS. THIS LEGEND SHALL BE MARKED ON ANY REPRODUCTION HEREOF IN WHOLE OR IN PART.

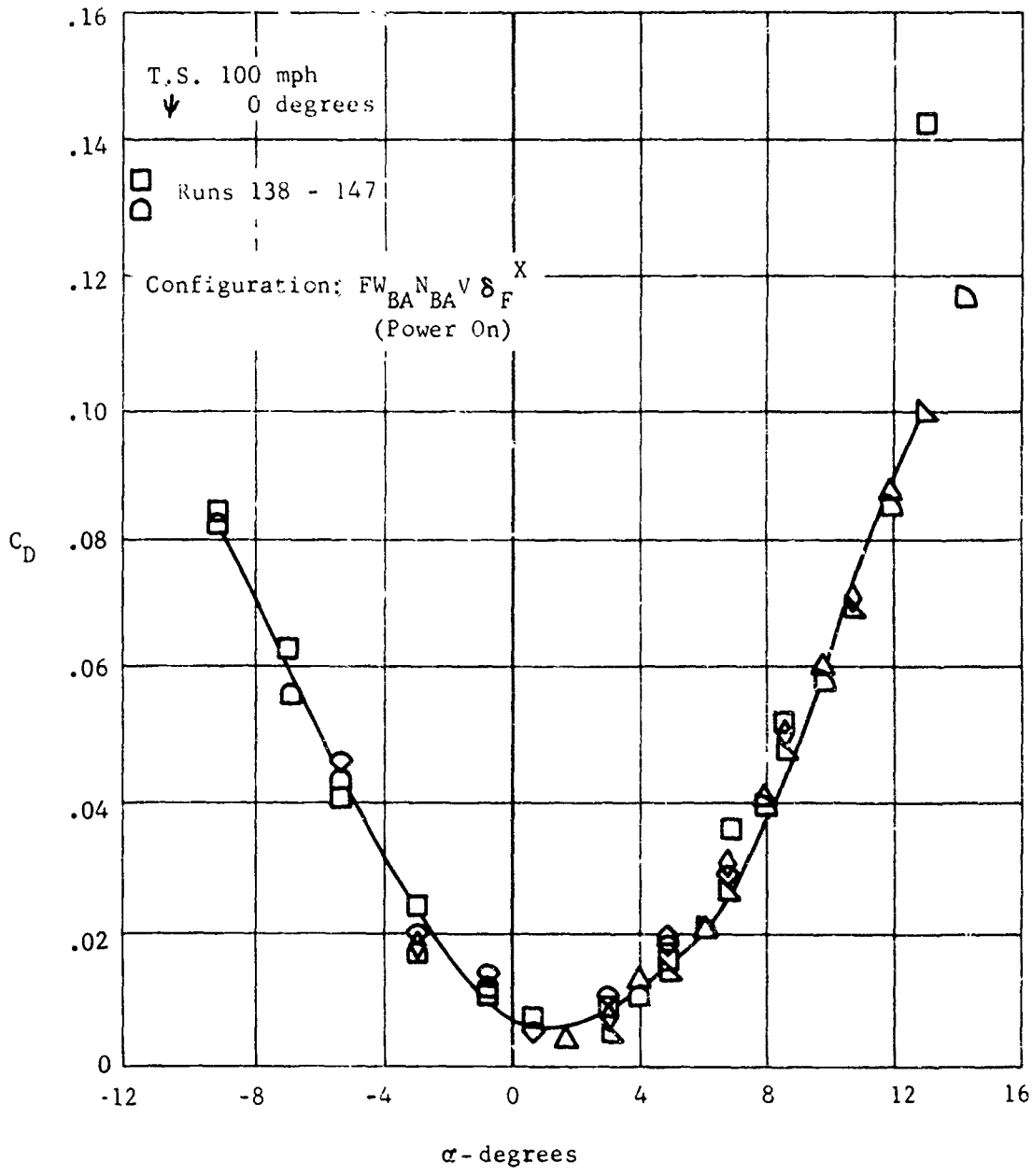

Figure 222. Drag characteristics of the 0.12 scale model of the Curtiss Wright X-19.

"FURNISHED UNDER UNITED STATES GOVERNMENT CONTRACT No. AF33(615)-3940. SHALL NOT BE EITHER RELEASED OUTSIDE THE GOVERNMENT, OR USED, DUPLICATED, OR DISCLOSED IN WHOLE OR IN PART FOR MANUFACTURE OR PROCUREMENT, WITHOUT THE WRITTEN PERMISSION OF CURTISS-WRIGHT CORPORATION, EXCEPT FOR (i) EMERGENCY REPAIR OR OVERHAUL WORK BY OR FOR THE GOVERNMENT, WHERE THE ITEM OR PROOF IS NOT OTHERWISE REASONABLY AVAILABLE TO ENABLE TIMELY PERFORMANCE OF THE WORK, OR (ii) RELEASE TO A FOREIGN GOVERNMENT, AS THE INTERESTS OF THE UNITED STATES MAY REQUIRE PROVIDED THAT IN EITHER CASE THE RELEASE, USE, DUPLICATION OR DISCLOSURE HEREOF SHALL BE SUBJECT TO THE FOREGOING LIMITATIONS. THIS LEGEND SHALL BE MARKED ON ANY REPRODUCTION HEREOF IN WHOLE OR IN PART."

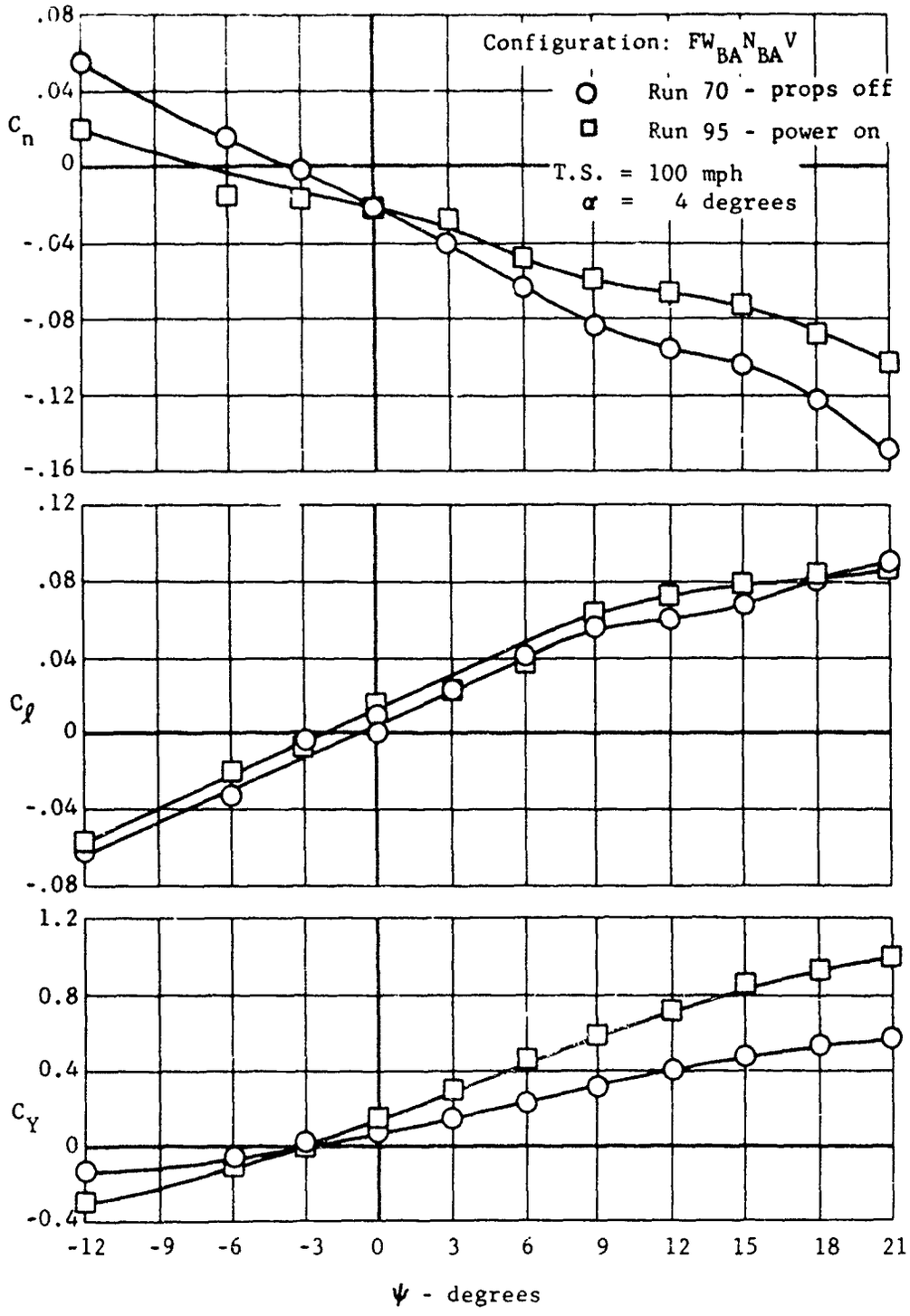

Figure 223. Directional and lateral stability characteristics of the 0.12 scale model X-19 in MIT-1019 cruise simulation.

FURNISHED UNDER UNITED STATES GOVERNMENT CONTRACT No. AF33(615)-1940. SHALL NOT BE EITHER RELEASED OUTSIDE THE GOVERNMENT, OR USED DUPLICATED, OR DISCLOSED IN WHOLE OR IN PART FOR MANUFACTURE OR PROCUREMENT, WITHOUT THE WRITTEN PERMISSION OF CURTISS-WRIGHT CORPORATION, EXCEPT FOR (i) EMERGENCY REPAIR OR OVERHAUL WORK BY OR FOR THE GOVERNMENT, WHERE THE ITEM OR PROCESS IS NOT OTHERWISE REASONABLY AVAILABLE TO ENABLE TIMELY PERFORMANCE OF THE WORK, OR (ii) RELEASE TO A FOREIGN GOVERNMENT, AS THE INTERESTS OF THE UNITED STATES MAY REQUIRE. PROVIDED THAT IN EITHER CASE THE RELEASE, USE, DUPLICATION OR DISCLOSURE HEREOF SHALL BE SUBJECT TO THE FOREGOING LIMITATIONS. THIS LEGEND SHALL BE MARKED ON ANY REPRODUCTION HEREOF IN WHOLE OR IN PART.

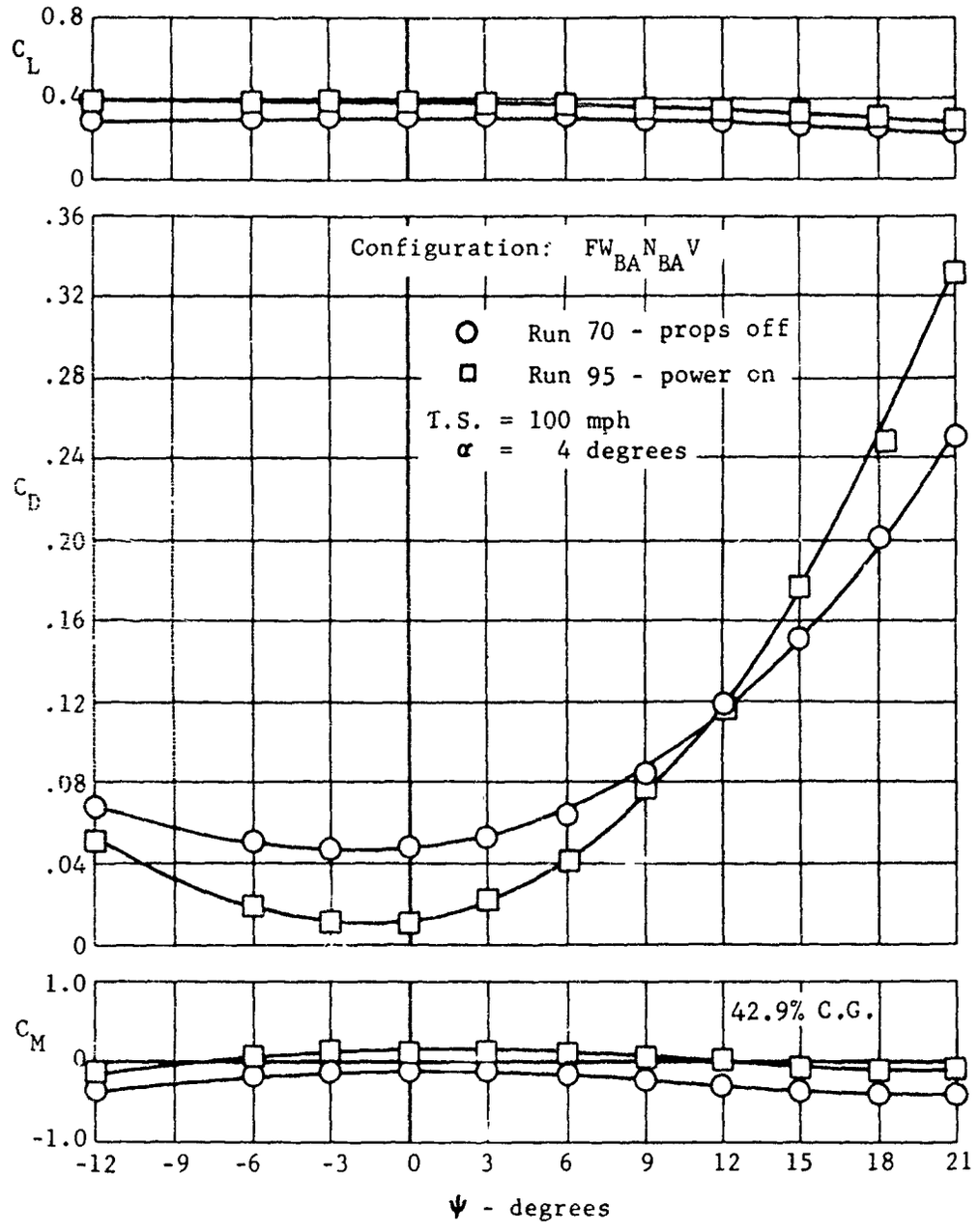

Figure 223. Concluded.

FURNISHED UNDER UNITED STATES GOVERNMENT CONTRACT No. AF33(615)-3940 SHALL NOT BE EITHER RELEASED OUTSIDE THE GOVERNMENT, OR USED, DUPLICATED, OR DISCLOSED IN WHOLE OR IN PART FOR MANUFACTURE OR PROCUREMENT, WITHOUT THE WRITTEN PERMISSION OF CURTISS-WRIGHT CORPORATION, EXCEPT FOR (i) EMERGENCY REPAIR OR OVERHAUL WORK BY OR FOR THE GOVERNMENT, WHERE THE ITEM OR PROCESS IS NOT OTHERWISE REASONABLY AVAILABLE TO ENABLE TIMELY PERFORMANCE OF THE WORK, OR (ii) RELEASE TO A FOREIGN GOVERNMENT, AS THE INTERESTS OF THE UNITED STATES MAY REQUIRE PROVIDED THAT IN EITHER CASE THE RELEASE, USE DUPLICATION OR DISCLOSURE HEREOF SHALL BE SUBJECT TO THE FOREGOING LIMITATIONS THIS LEGEND SHALL BE MARKED ON ANY REPRODUCTION HEREOF IN WHOLE OR IN PART.

previous data due to the stretch in the fuselage and consequent change in lift chord length. Directional and lateral stability were greatly improved due to the stretch in the fuselage.

(c) Other Test Data

The effects of power on the components of the aircraft in cruise were also investigated. The control surface data showed that adequate and reliable control power was available.

The particular values of area, span and chord used to define the coefficients are scaled values of the reference constants defined for the full-scale airplane, and are enumerated in (60).

(3) Cornell Test Series

At Cornell Aeronautical Laboratory, Buffalo, New York, the 8-foot transonic wind tunnel was utilized for its size (in relation to the 0.12 scale model size) ability to be pressurized to increase Reynolds number and tunnel speed. The purpose of these tests was to establish the aerodynamic characteristics of the X-19 airplane in the Mach [illegible] range, corresponding to that of the design cruise configuration; to determine propeller performance at the higher Reynolds number and Mach number and their contribution to the stability characteristics of the airplane; to ascertain the effects of fixing flow transition; and to evaluate the effects of adding tip extensions on the aft wing.

The tests thus required were conducted in two separate series, as recorded in detail in the CAL test reports, (61) and (62), the first being run in October 1962 and the other during the month of February, 1963. The model used for these tests was as modified (previously described), and mounted on the sting in the wind tunnel, but not as in Figure 220, in the 8 foot perforated-wall test section. Angles of attack were obtained with the pitch mechanism of the vertical strut system set for the model at 0° roll angle (for $\Psi = 0^{\circ}$ constant).

Variable yaw angles (at $\alpha_f = 0^{\circ}$ constant) were similarly obtained by rolling the model -90° from the position shown in Figure 220. Model rolling attitude was accomplished

remotely by utilizing the W60-0500 roll mechanism described in (61).

All instrumentation static outputs were read and recorded on the CAL automatic digital readout equipment. A vast amount of force and moment data, reduced to coefficient form, as well as propeller and nacelle data, were presented in (61), and (62). The latter data were presented in the nature of propeller thrust, speed and torque, and nacelle normal force, pitching and yawing moments in both wind axis and body axis systems. Data were taken with propellers on and propellers off in this series.

The overall force and moment data resulting from these CAL tests have been resolved to a wind axis system having its origin at a reference c.g. and plotted against angle of attack, α_f, and angle of yaw, ψ, for the required range of Mach number and control surface settings (at constant advance ratio, J).

Control surface hinge moment coefficients were plotted against α_f or ψ and tabulated relative to control surface setting angle. Propeller torque and power data, in addition to nacelle data, were presented tabulated in the referenced test reports; however, in the first CAL test series the nacelle data are regarded as suspect due to grounded gauges in the system. In the second test series, information was also presented for zero control angles and zero J for the range of Mach numbers tested. In addition, the effects of transition flow fixing were determined during the tests.

Because of the large mass of data obtained and plotted in these CAL test programs, none are shown here, but are available in (61) and (62). Later in this section, comparisons of data taken from all the X-19 test programs will be made which is more fruitful than any presentation here of specific test data plots from the Cornell Test series.

(4) NACAL Tunnel Tests

Subsequent tests of the 0.12 scale X-19 configuration model tandem wing VTOL airplane were conducted in the North American Aviation, Inc., NACAL 16 by 14 ft. low speed wind tunnel located at Columbus, Ohio. These tests occurred between the Spring of 1962 and Fall 1965 in three separately identified series, known as NACAL -93, -120 and -142. The results of these tests were the last specifically X-19 configuration data obtained by model simulation before the VTOL Division terminated this program.

The definition of each of these test series programs is given separately hereafter, and in a later paragraph of this section a comparison is made of the various test programs. The correlation of their results is then also discussed. The NACAL wind tunnel programs represent the largest percentage of X-19 model test data available and were instrumental in predicting the full scale transition flight characteristics of the flight test X-19 vehicle.

The mounting of the aircraft model in the 16 by 14 ft. wind tunnel test section is shown in Figure 220 for NACAL -93 tests. It is also depicted schematically in Figure 224 as a typical installation for all three NACAL test programs.

One other test program in the NACAL tunnel was conducted using the X-19 model. This test program is known as NACAL-121 and is a North American Aviation Inc. test series for which the Curtiss-Wright Corporation was not responsible or billed. It involved repeating some of the NACAL-120 tests at high tilt nacelle angles with the model mounted in the smaller 7 by 10 foot test section (see Figure 224) as a means of comparing the results for tests in two different-sized test sections of the same tunnel. No report was issued to Curtiss-Wright for this test series but some information concerning the results was conveyed to CW personnel for reference purposes only. No discussion of these data are included in this report.

(a) In the first of these tests (NACAL-93) conducted during May 1962, the aerodynamic characteristics of the M 200 powered 12% scale model were evaluated through the transition flight regime.

The data obtained covered the effects of thrust resulting from variation of propeller blade angle and rotational speed, effects of forward and aft propeller disk incidence and flap deflection on pitch control and trim. Aileron roll control effectiveness data were also investigated at that time. The test results for NACAL-93 are presented in detail in (63).

The test model was mounted on the post balance and a single support strut as shown in Figures 220 and 224. The HH-263 six component strain gauge balance and integral windshield were keyed to the tip of the variable height strut and attached to the model. A large under-fuselage fairing was used to provide a clean aerodynamic surface in the area of the strut and balance. This fairing covered the pressure tubes, electrical lines, and a portion of the linear actuator. Beginning with Run 56 the fuselage fairing and pressure

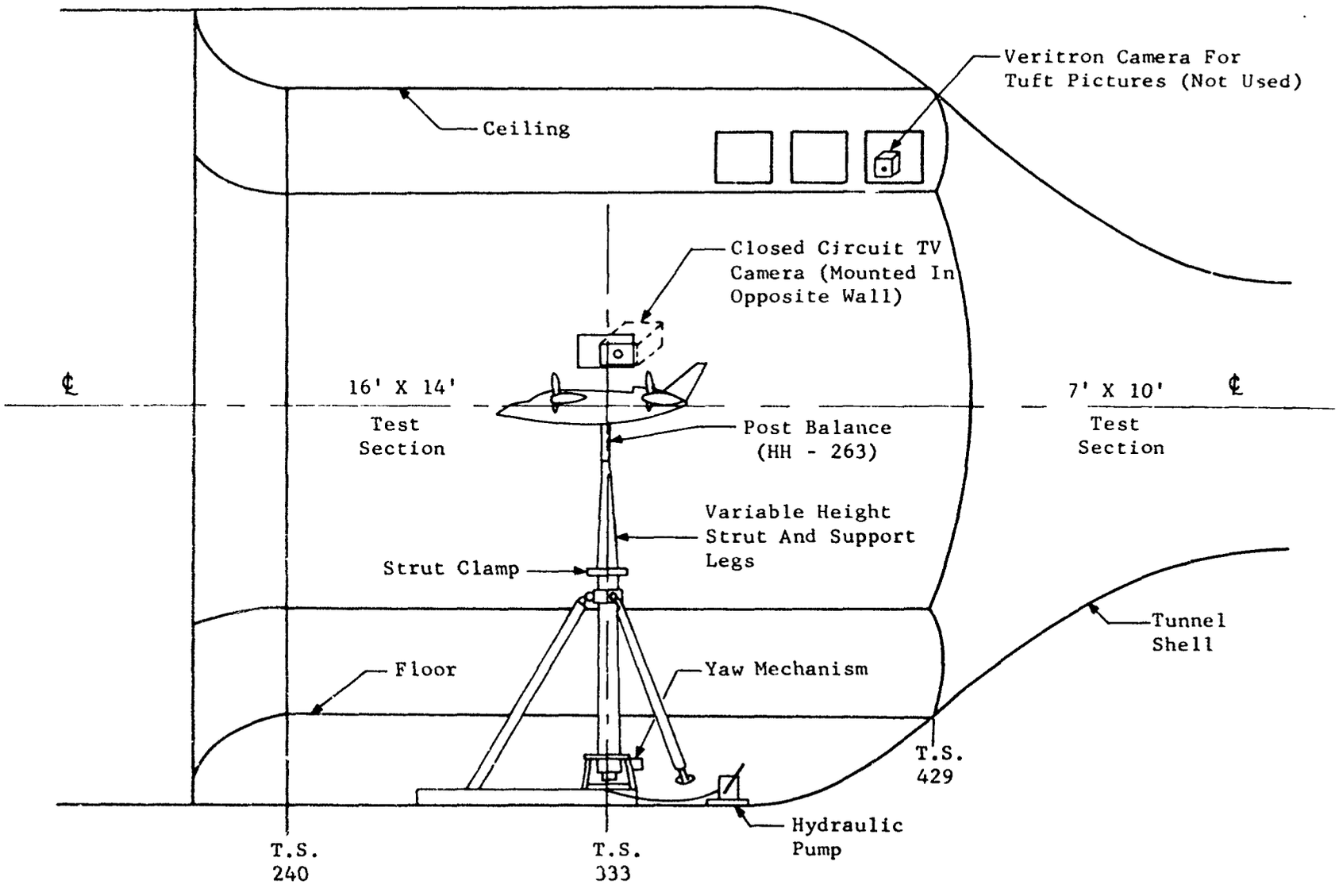

Figure 224. NACAL low speed tunnel X-19 type model installation for NACAL-93 wind tunnel tests.

lines were removed to improve data repeatability and general data accuracy.

Throughout the test program primary six-component data recording accuracy and repeatability was adversely affected by model dynamics, balance flexibility and interference of test apparatus leads across the balance.

The stiffness of the leads was found to be the primary contribution to this problem. The effect was largest on the drag data. The effect on pitching moment data error was also large. Because of this problem the data from a large number of runs had to be eliminated and further tests conducted. The effect on all lateral-directional components was considered satisfactory.

Model propeller force and moment instrumentation evidenced inadequate sensitivity for accurate metering of test loads. Some improvement in normal force was obtained in later runs of this series by replacing the initial recording instrument with one of greater dampening capability. Based on the poor repeatability of several check calibrations of this instrumentation, however, it was concluded that the desired accuracy was not obtained.

Longitudinal test results showing the effect of propeller and propeller speed in pitch attitude for typical cruise and transition conditions are shown in Figures 225 and 226 respectively, at appropriate blade angles and flight speeds.

Other data are presented in (63) for combinations of variations in dynamic pressure, blade angle, nacelle tilt angle, aileron deflection and flap deflection. Comparable directional characteristics test data are shown in Figures 227 and 228. Additional plots of the test results are presented in (63).

(b) The second series of North American Columbus Division wind tunnel tests (NACAL - 120) were conducted in April and June 1964, using the same model to obtain information of the static stability of the X-19 aircraft during translating flight at high propeller tilt angles, both in and out of ground effect. The tests are reported in their entirety in (64).

The test installation differed somewhat from that of the last series discussed in the preceding paragraph. Figure 229 shows how the balance was keyed to a short sting which was mounted on the standard NACAL single support strut trunnion block. The ground board was

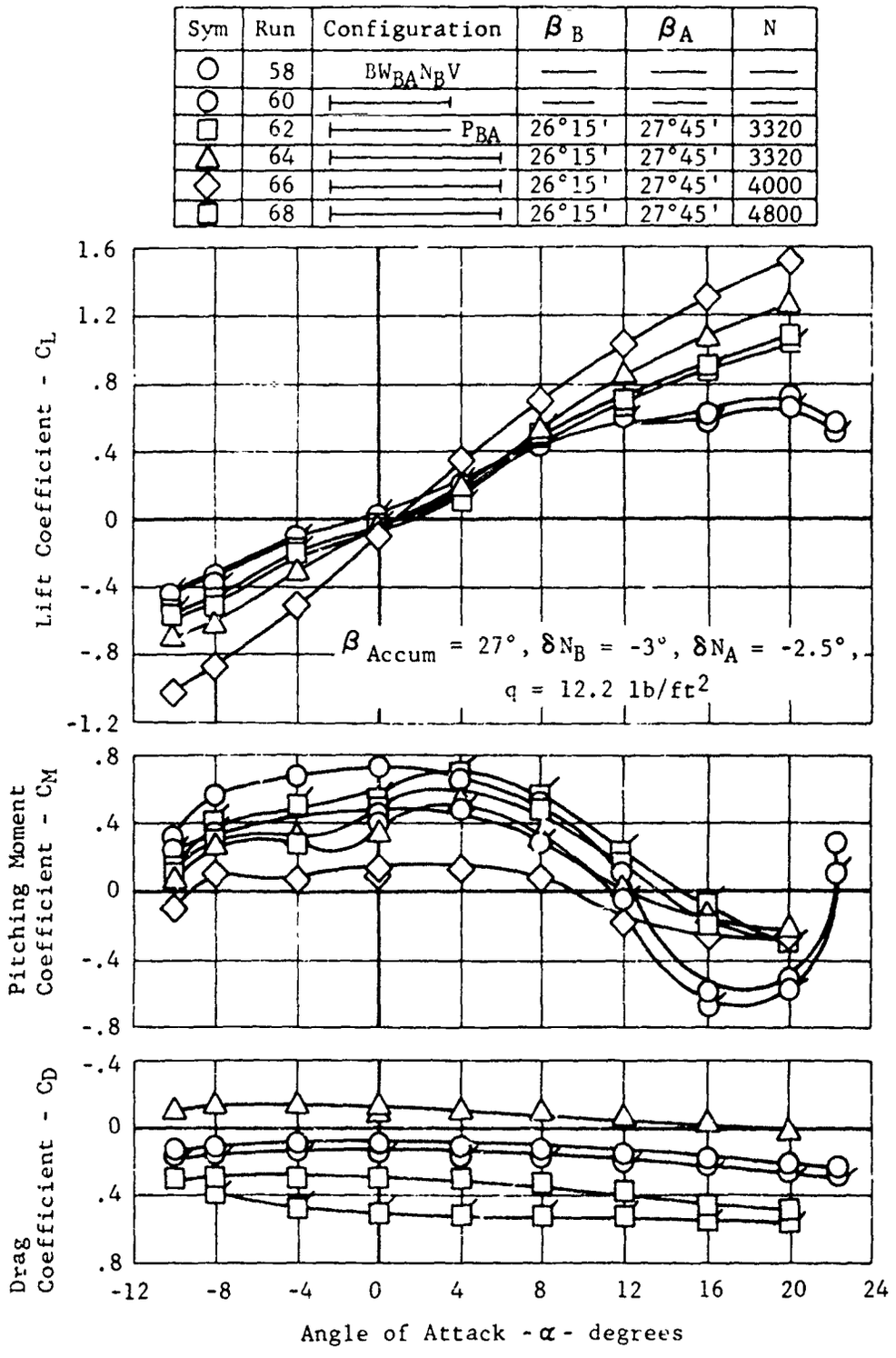

Figure 225. NACAL-93 test data to demonstrate the effect of propeller speed in pitch, X-19 cruise configuration.

"FURNISHED UNDER UNITED STATES GOVERNMENT CONTRACT No. AF33(615)-3940. SHALL NOT BE EITHER RELEASED OUTSIDE THE GOVERNMENT, OR USED, DUPLICATED, OR DISCLOSED IN WHOLE OR IN PART FOR MANUFACTURE OR PROCUREMENT, WITHOUT THE WRITTEN PERMISSION OF CURTISS-WRIGHT CORPORATION, EXCEPT FOR (i) EMERGENCY REPAIR OR OVERHAUL WORK BY OR FOR THE GOVERNMENT, WHERE THE ITEM OR PROCESS IS NOT OTHERWISE REASONABLY AVAILABLE TO ENABLE TIMELY PERFORMANCE OF THE WORK, OR (ii) RELEASE TO A FOREIGN GOVERNMENT, AS THE INTERESTS OF THE UNITED STATES MAY REQUIRE. PROVIDED THAT IN EITHER CASE THE RELEASE, USE, DUPLICATION OR DISCLOSURE HEREOF SHALL BE SUBJECT TO THE FOREGOING LIMITATIONS. THIS LEGEND SHALL BE MARKED ON ANY REPRODUCTION HEREOF IN WHOLE OR IN PART."

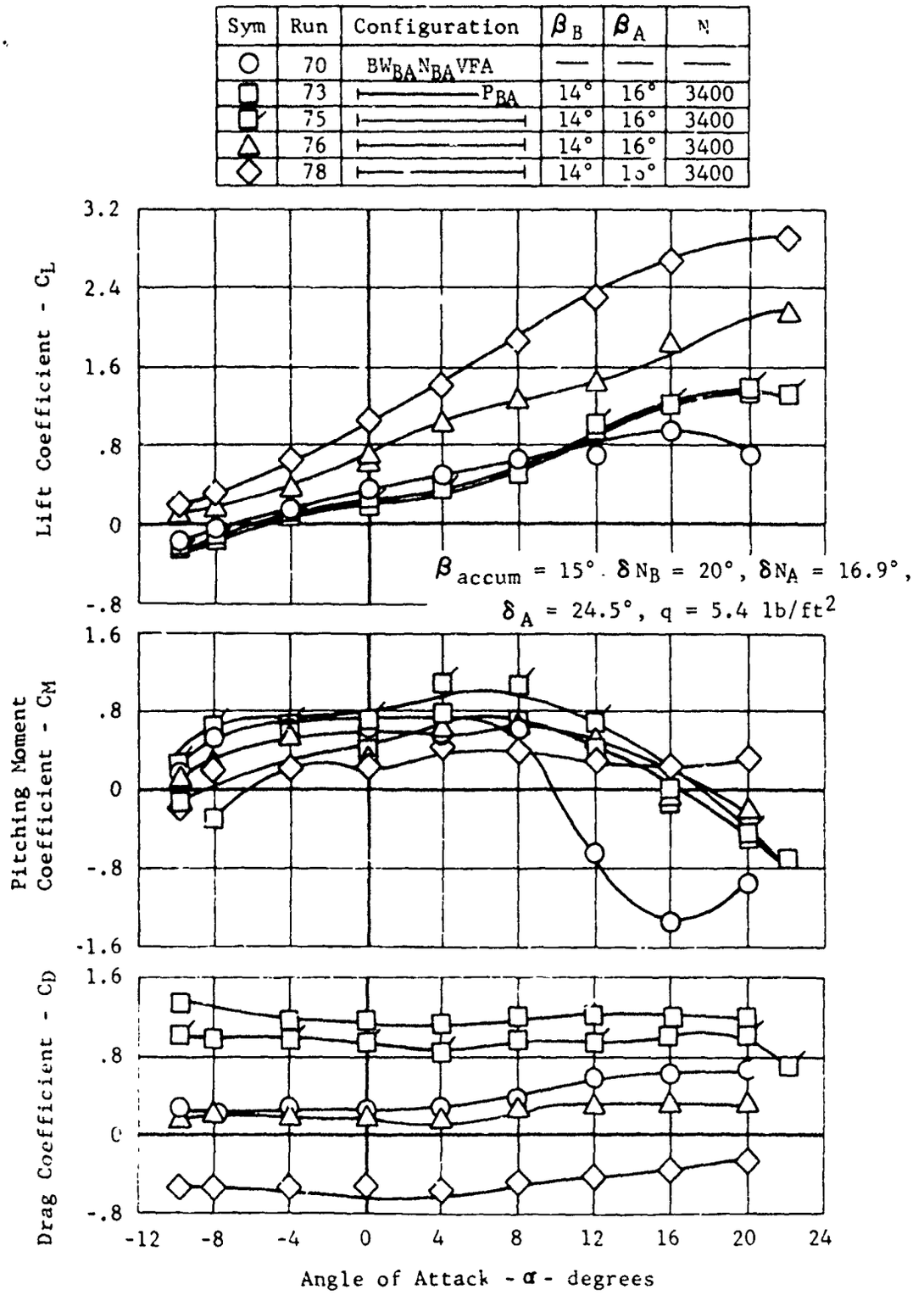

Figure 226. NACAL-93 test data to demonstrate the effect of propeller speed in pitch, X-19 transition configuration.

"FURNISHED UNDER UNITED STATES GOVERNMENT CONTRACT No. AF33(615)-3940. SHALL NOT BE EITHER RELEASED OUTSIDE THE GOVERNMENT, OR USED, DUPLICATED, OR DISCLOSED IN WHOLE OR IN PART FOR MANUFACTURE OR PROCUREMENT, WITHOUT THE WRITTEN PERMISSION OF CURTISS-WRIGHT CORPORATION, EXCEPT FOR (i) EMERGENCY REPAIR OR OVERHAUL WORK BY OR FOR THE GOVERNMENT, WHERE THE ITEM OR PROCESS IS NOT OTHERWISE REASONABLY AVAILABLE TO ENABLE TIMELY PERFORMANCE OF THE WORK; OR (ii) RELEASE TO A FOREIGN GOVERNMENT, AS THE INTERESTS OF THE UNITED STATES MAY REQUIRE; PROVIDED THAT IN EITHER CASE THE RELEASE, USE, DUPLICATION OR DISCLOSURE HEREOF SHALL BE SUBJECT TO THE FOREGOING LIMITATIONS. THIS LEGEND SHALL BE MARKED ON ANY REPRODUCTION HEREOF IN WHOLE OR IN PART."

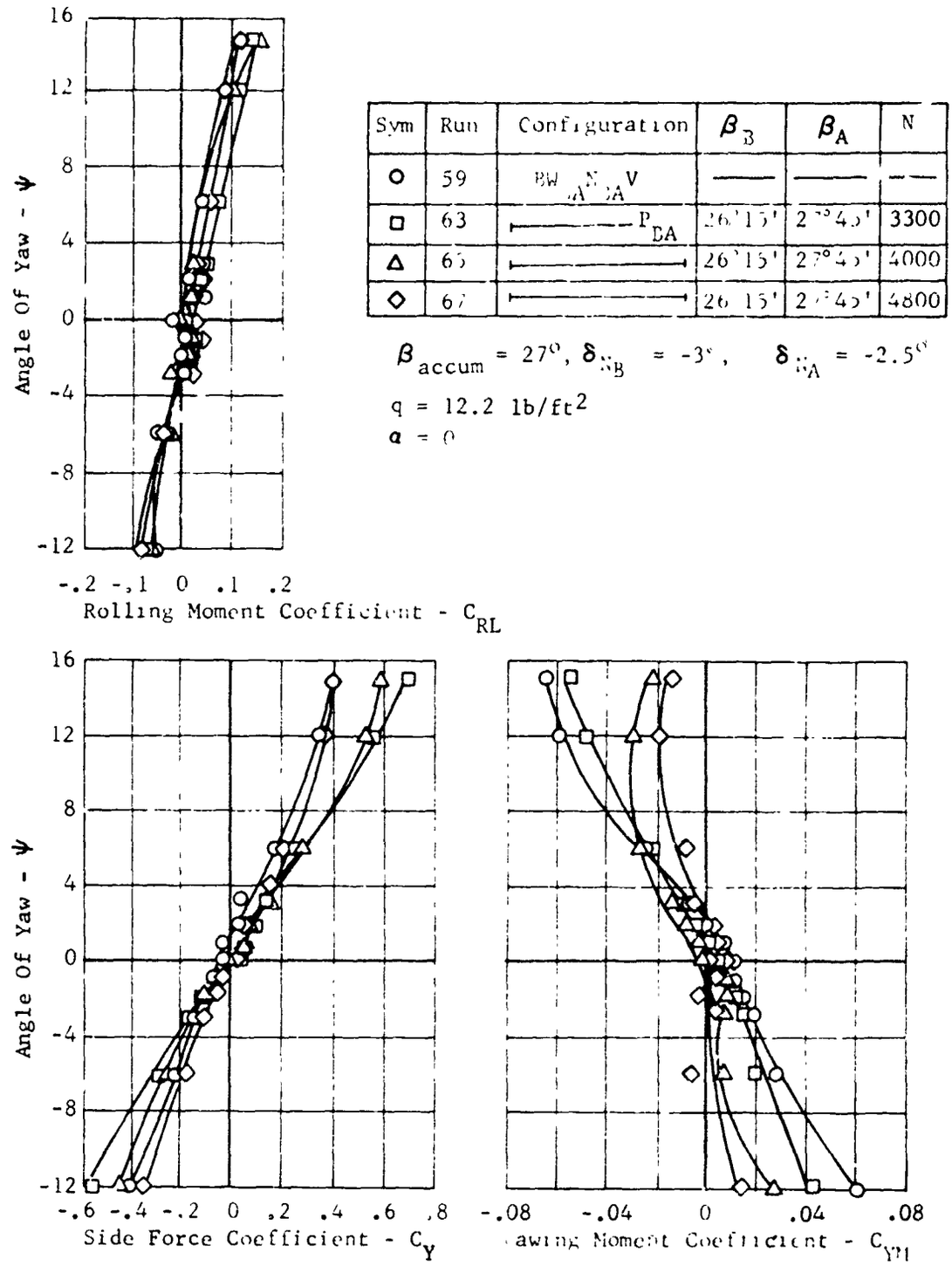

Figure 227. NACAL-93 test data to demonstrate the effect of propeller and propeller speed in yaw, X-19 cruise configuration.

FURNISHED UNDER UNITED STATES GOVERNMENT CONTRACT No. AF33(615)-3940. SHALL NOT BE EITHER RELEASED OUTSIDE THE GOVERNMENT, OR USED, DUPLICATED, OR DISCLOSED IN WHOLE OR IN PART FOR MANUFACTURE OR PROCUREMENT WITHOUT THE WRITTEN PERMISSION OF CURTISS-WRIGHT CORPORATION, EXCEPT FOR (i) EMERGENCY REPAIR OR OVERHAUL WORK BY OR FOR THE GOVERNMENT, WHERE THE ITEM OR PROCESS IS NOT OTHERWISE REASONABLY AVAILABLE TO ENABLE TIMELY PERFORMANCE OF THE WORK, OR (ii) RELEASE TO A FOREIGN GOVERNMENT, AS THE INTERESTS OF THE UNITED STATES MAY REQUIRE, PROVIDED THAT IN EITHER CASE THE RELEASE, USE, DUPLICATION OR DISCLOSURE HEREOF SHALL BE SUBJECT TO THE FORFGOING LIMITATIONS. THIS LEGEND SHALL BE MARKED ON ANY REPRODUCTION HEREOF IN WHOLE OR IN PART.

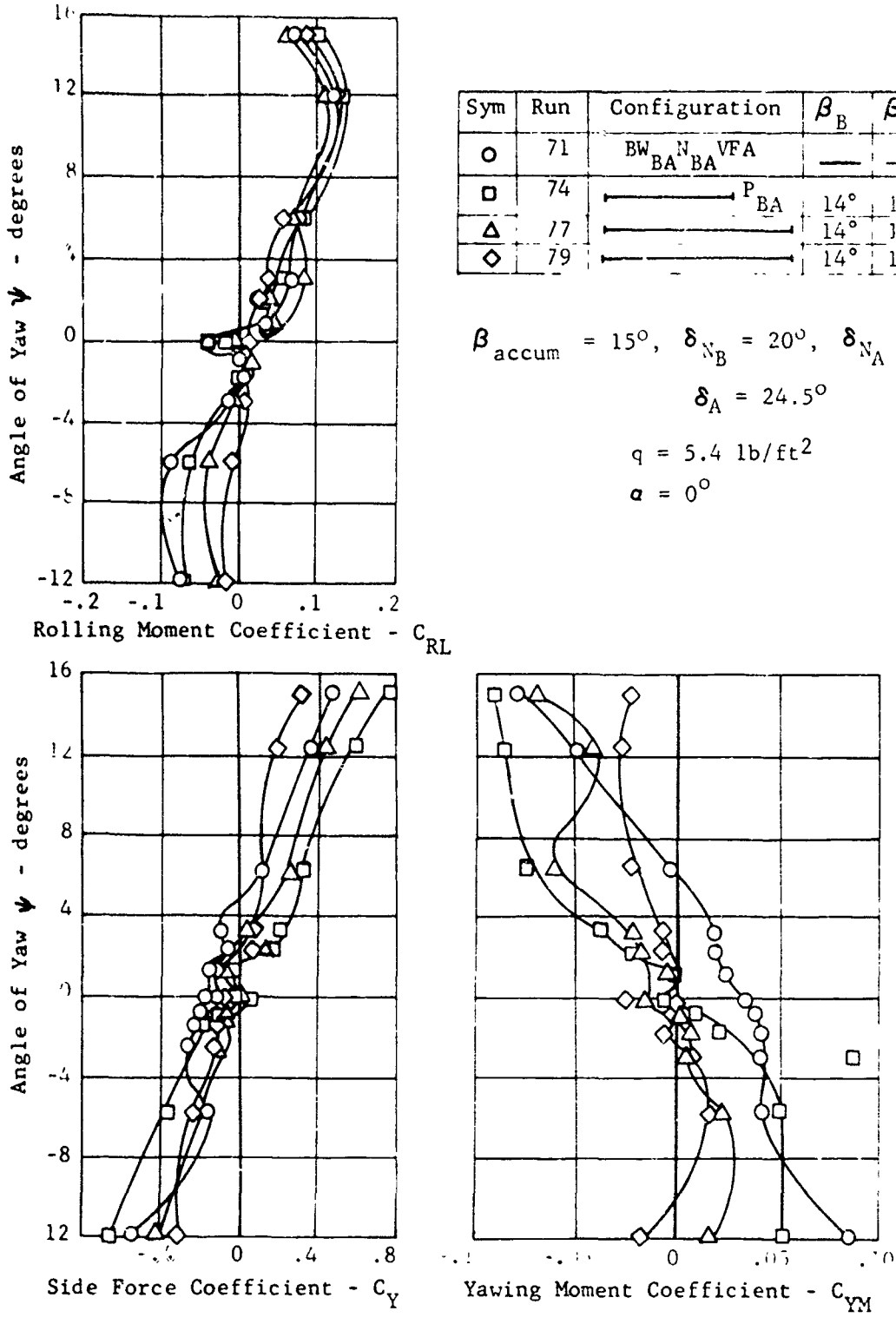

Figure 228. NACAL-93 test data to demonstrate the effect of propeller and propeller speed in yaw, X-19 transition configuration.

FURNISHED UNDER UNITED STATES GOVERNMENT CONTRACT No. AF33(615)-3940. SHALL NOT BE EITHER RELEASED OUTSIDE THE GOVERNMENT, OR USED DUPLICATED, OR DISCLOSED IN WHOLE OR IN PART FOR MANUFACTURE OR PROCUREMENT, WITHOUT THE WRITTEN PERMISSION OF CURTISS-WRIGHT CORPORATION, EXCEPT FOR (i) EMERGENCY REPAIR OR OVERHAUL WORK BY OR FOR THE GOVERNMENT WHERE THE ITEM OR PROCESS IS NOT OTHERWISE REASONABLY AVAILABLE TO ENABLE TIMELY PERFORMANCE OF THE WORK OR (ii) RELEASE TO A FOREIGN GOVERNMENT, AS THE INTERESTS OF THE UNITED STATES MAY REQUIRE PROVIDED THAT IN EITHER CASE THE RELEASE USE DUPLICATION OR DISCLOSURE HEREOF SHALL BE SUBJECT TO THE FOREGOING LIMITATIONS THIS LEGEND SHALL BE MARKED ON ANY REPRODUCTION HEREOF IN WHOLE OR IN PART.

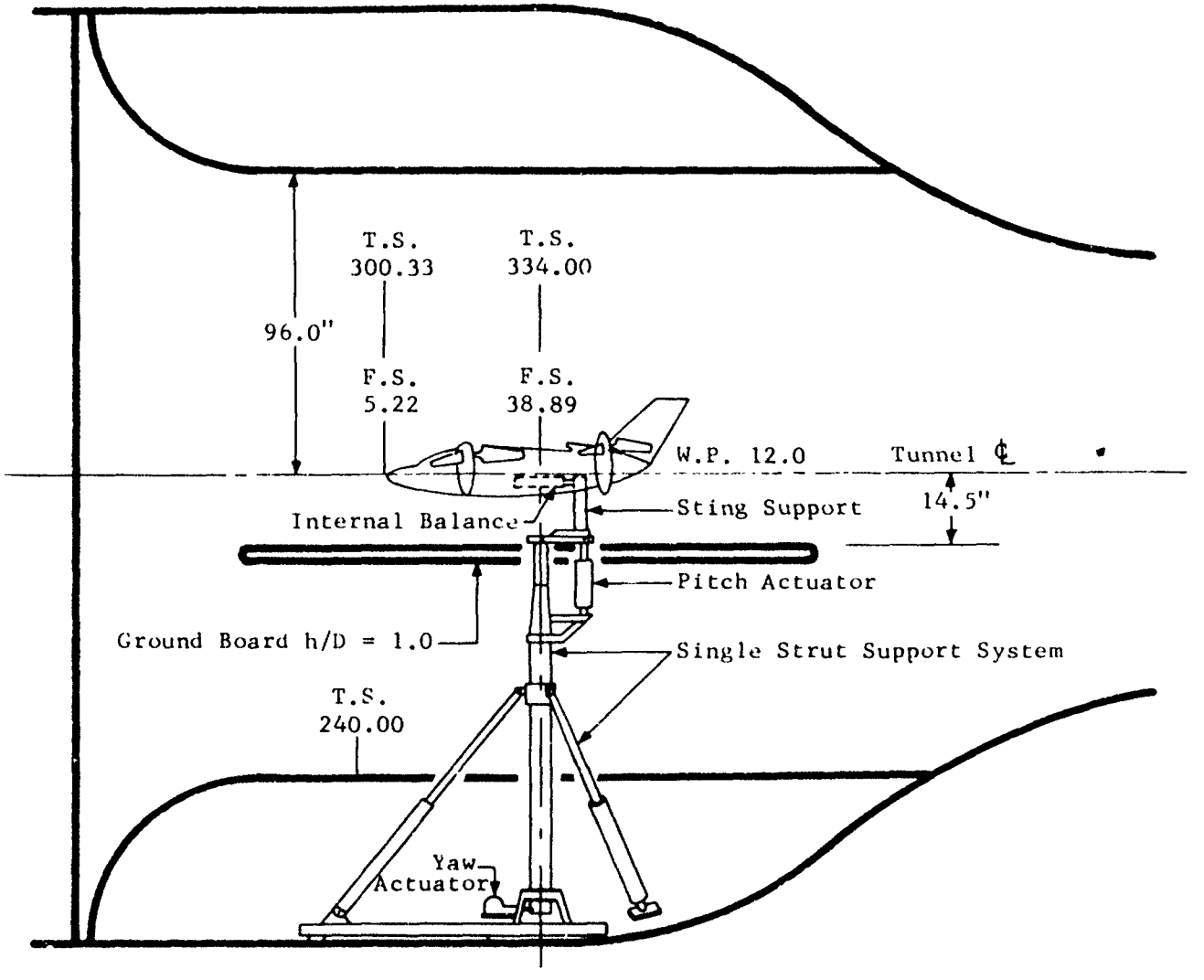

Figure 229. NACAL low speed tunnel X-19 model installation for NACAL-120 wind tunnel tests.

installed in two vertical positions to provide the required ground height ratios, h/D = 1.0, 2.0 and 5.34

As in the previous NACAL tests, because direct vision into the 16 x 14 foot test section from the control room was not possible, a closed circuit TV camera provided constant monitoring of the model condition during testing. In this series of tests the 3155B internal balance was provided for six-component force and moment data measurement.

In NACAL, all tests are conducted at one atmosphere pressure. The angle of attack range was -4 to +20 degrees and the angle of yaw range was +75 to +105 degrees. The model was run at yaw angles of 75 to 105 degrees to find the yaw moments for the case where the airplane is hovering in a cross wind. During these tests the model aft drive motor speeds were held constant throughout the run, as was the tunnel velocity. The flap and elevator settings were also constant throughout the test, the fore and aft flaps being set at 57° and the elevators at -2°. For all runs the model configuration remained the same.

The denominator of a data coefficient (based on free-stream q) for the 11 knot runs was very small compared with the load being non-dimensionalized. Hence, the coefficient comparisons in some cases were not realistic because recording accuracy and scatter tended to be greatly exaggerated.

Considering the fact that at 11 knots the aircraft is essentially in a hover condition it was decided to treat this speed case as hover data and base the coefficients on total thrust and propeller diameter. Coefficients for other than 11 knot data were non-dimensionalized with wing area, chord and span and with freestream dynamic pressure.

Aerodynamic characteristics data were obtained for a series of tunnel speeds from 11 to 70 knots at three high nacelle-incidence angles and at the prescribed ground-plane heights. The effect of the ground-plane presence on longitudinal characteristics for just the 11 knots case and one nacelle incidence is shown in Figure 230. The effect of nacelle angle on lateral-directional characteristics at the same speed and for the highest ground-plane height is shown in Figure 231. For all other plotted data see (64).

(c) Finally the X-19 0.12 scale powered model was subjected to further tests at North American Aviation Inc.'s Columbus Division, NACAL low speed wind tunnel during the months of October and November, 1965. The purpose

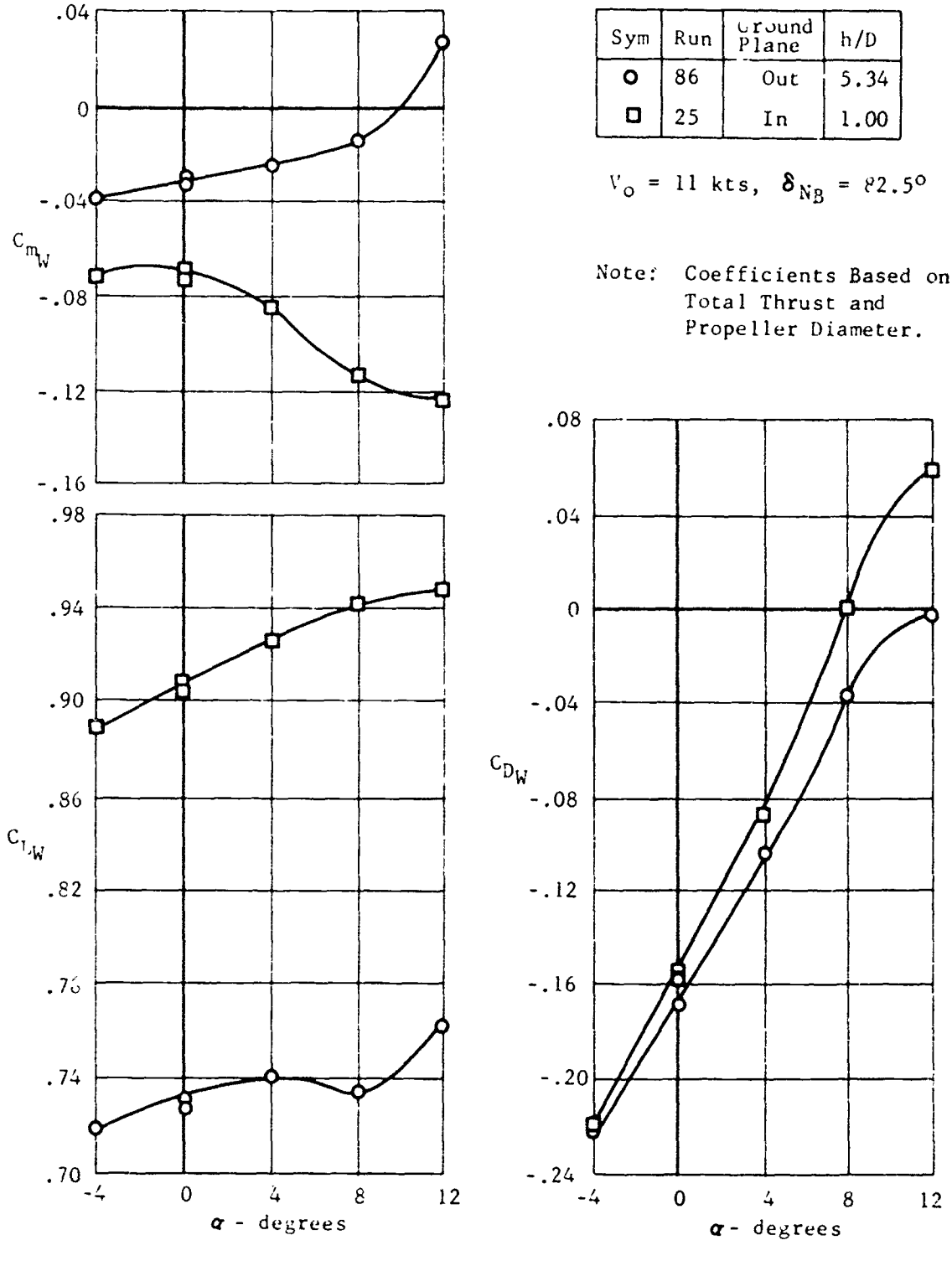

Sym	Run	Ground Plane	h/D
O	86	Out	5.34
□	25	In	1.00

V_o = 11 kts, δ_{NB} = 82.5°

Note: Coefficients Based on Total Thrust and Propeller Diameter.

Figure 230. NACAL-120 test data to demonstrate the effect of ground plane presence on longitudinal characteristics in hover of the X-19 model.

FURNISHED UNDER UNITED STATES GOVERNMENT CONTRACT No. AF33(615)-3940 SHALL NOT BE EITHER RELEASED OUTSIDE THE GOVERNMENT, OR USED, DUPLICATED, OR DISCLOSED IN WHOLE OR IN PART FOR MANUFACTURE OR PROCUREMENT, WITHOUT THE WRITTEN PERMISSION OF CURTISS-WRIGHT CORPORATION, EXCEPT FOR (i) EMERGENCY REPAIR OR OVERHAUL WORK BY OR FOR THE GOVERNMENT, WHERE THE ITEM OR PROCESS IS NOT OTHERWISE REASONABLY AVAILABLE TO ENABLE TIMELY PERFORMANCE OF THE WORK, OR (ii) RELEASE TO A FOREIGN GOVERNMENT, AS THE INTERESTS OF THE UNITED STATES MAY REQUIRE, PROVIDED THAT IN EITHER CASE THE RELEASEE, USE, DUPLICATION OR DISCLOSURE HEREOF SHALL BE SUBJECT TO THE FOREGOING LIMITATIONS. THIS LEGEND SHALL BE MARKED ON ANY REPRODUCTION HEREOF IN WHOLE OR IN PART."

Sym	Run	δ_{NB}	δ_{NA}
O	92	32 5	69.6
Δ	98	90.0	76.0

β_B = 10.5 V_c = 11 kts

β_A = 13.5 h/D = 5.34

Note: Coefficients Based on Total Thrust and Propeller Diameter

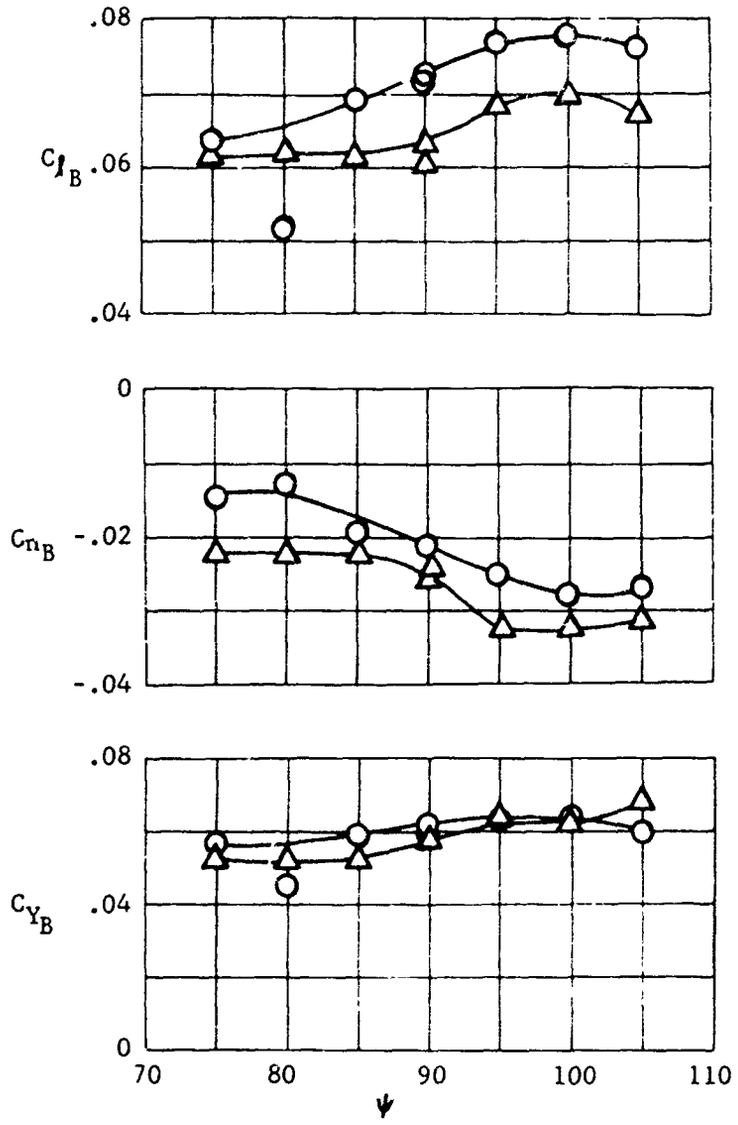

Figure 231. NACAL-120 test data to demonstrate the effect of nacelle angle on lateral-directional characteristics in hover of the X-19 model.

FURNISHED UNDER UNITED STATES GOVERNMENT CONTRACT No. AF33(616)-3940. SHALL NOT BE EITHER RELEASED OUTSIDE THE GOVERNMENT, OR BE DUPLICATED, OR DISCLOSED IN WHOLE OR IN PART FOR MANUFACTURE OR PROCUREMENT, WITHOUT THE WRITTEN PERMISSION OF CURTISS-WRIGHT CORPORATION, EXCEPT FOR (i) EMERGENCY REPAIR OR OVERHAUL WORK BY OR FOR THE GOVERNMENT, WHERE THE ITEM OR PROCESS IS NOT OTHERWISE REASONABLY AVAILABLE TO ENABLE TIMELY PERFORMANCE OF THE WORK, OR (ii) RELEASE TO A FOREIGN GOVERNMENT AS THE INTERESTS OF THE UNITED STATES MAY REQUIRE. PROVIDED THAT IN EITHER CASE THE RELEASE, USE, DUPLICATION OR DISCLOSURE HEREOF SHALL BE SUBJECT TO THE FOREGOING LIMITATIONS. THIS LEGEND SHALL BE MARKED ON ANY REPRODUCTION HEREOF IN WHOLE OR IN PART.

of these tests is to determine the optimum propeller tilt schedule in transition from vertical to horizontal flight. The effect of differential nacelle tilt angle, direction of propeller rotation, propeller blade angle, propeller rotational speed and propeller downwash were also considered. This test series is known as NACAL-142, and the results of these tests were published as (65).

The model was mounted in the 16 x 14 foot V/STOL test section on an internal strain gauge balance and single strut support, in a manner similar to that shown in Figure 229 for NACAL-120, except minus the ground board. During these tests the model aft drive motor speed and tunnel velocity were held constant throughout a run, and the model attitude was varied. The angle of attack range was -11° to +20° and the angle of yaw range was -15° to +15°

Data are graphically presented in (65) in more than 200 plots describing the effects of nacelle tilt angle, propeller rotation direction, flap deflection, aileron deflection, differential aileron deflection, flap and aileron deflection taken together, propeller rotational speed, bow and aft propellers at various propeller speeds, aft propeller blade angle and downwash distribution. Tests for data repeatability were also included.

(5) University of Maryland Tests

The first of the University of Maryland series of wind tunnel tests of the tandem wing, tilt propeller configuration similar to the X-19 VTOL aircraft were tested in the 7.75 x 11 foot test section of the Glenn L. Martin Institute of Technology Low Speed Wind Tunnel during late February and early March 1963. Its purpose was to ascertain the aerodynamic characteristics of the X-19 type aircraft for varying geometry.

The model used in these tests was a generalized model constructed in such a manner that numerous configurations and variables could be evaluated by changing individual components such as nacelles, sponsons, inlet systems, and nose sections. There were three nose sections, two types of nacelles, four inlet and dorsal configurations and two types of sponsons. These components were constructed of wood and could be fastened to the basic fuselage section which was also made of wood. Numerous wing combinations were available for the tandem wing configuration. Basic front and rear wings of constant chord were constructed of metal.

Constant chord extensions, also of metal, could be attached to the outboard ends of the basic wings to change the span and area. The basic fuselage was constructed with removable filler blocks so that the front and rear wings could be mounted in any of a number of locations. The model was mounted on a three-support system through a bayonet-dowel attachment in the side of the fuselage.

A large metal wing and a small metal stub wing were attached to the basic fuselage during one portion of this test program to form the "Horned Toad" configuration, discussed separately in a later paragraph.

For most runs the tests were conducted at a dynamic pressure so as to represent 150 MPH indicated airspeed. Additional tests were also made to simulate 100 and 200 MPH tunnel indicated speeds on the tandem wing model to determine Reynolds number effects.

Six component force and moment data were recorded on all runs and reduced to dimensionless coefficient form. The span of the rear wing, which was always larger than the front wing, was used as the reference. The reference wing area depended on the combination of front and rear wings used for a given configuration. The results of these tests are documented in (66).

A second series of tests in the University of Maryland low speed wind tunnel were conducted during early June 1964, using the same model as in the preceding paragraph. The main objectives of this test series were to obtain the stability and control characteristics of various vertical and ventral fins, to determine aileron effectiveness, and to acquire the aerodynamic characteristics of two twisted rear wings.

The model described in (66) was modified to substitute a new vertical fin and ventral fins, to add ailerons to the basic rear wing, and to provide two new twisted wings to accomplish the specified objective of this test program. In addition, pressure orifices were installed in the rear of the fuselage in the vicinity of the rear wing.

Six component force and moment data, obtained from the tunnel balance system, were recorded during the test runs. Pressure data were recorded for the side ventral configuration and during the aileron effectiveness runs. Aerodynamic loads on the portion of the pressure tubing exposed to the air stream were transmitted to the balances and included in the model force and moment data. Runs were made using a fluorescent oil technique to study the flow

around the aft portion of the fuselage, and one run was made to investigate the flow from the engine exhausts.

In addition to the twisted wings, various front and rear wing anhedral combinations were tested as well. The results of all the test runs appear in (67).

The University of Maryland program for testing three-blade VTOL scale model propellers is discussed in a later section.

f. Other Applicable Test Programs

Under a separate contract with the U. S. Navy Bureau of Naval Weapons, an investigation of the over-water aspects of VTOL airplanes at high disk loading was conducted at the Curtiss-Wright Corporation VTOL Systems Division during September and October, 1963. Both the X-100 and the X-19 configurations were tested in this program to investigate the disturbance and spray caused by high disk loading aircraft hovering above water, and to determine downwash effects on objects floating below the X-19 model.

In these tests the 15% scale X-100 and the 0.12 scale X-19 powered wind tunnel models were utilized to obtain the results. However, the X-19 propellers were fitted to the X-100 in these tests since the disk loading as a function of RPM of these propellers had been previously calibrated. A photograph of the test apparatus, including the specially built 30 by 15 by 3 foot deep water tank, is included herein as Figure 232 showing the X-19 model in test position.

Excellent agreement was achieved between the full-scale results of the X-100 VTOL research aircraft tests over water and the spray height predicted from model test for this aircraft. This confirmed that model tests can be used to predict the spray characteristics for hovering aircraft. Results indicate a relationship between disk loading and spray height, and also indicate the minimum heights for hovering above floating objects without causing them to capsize.

Approximately a year later, in October and November 1964, a study of ground proximity effects on and from a hovering four-propeller tandem-wing VTOL aircraft was conducted at the Curtiss-Wright VTOL Systems Test Facility. In these tests the 12% scale powered X-19 model was again employed to investigate both the effect of ground proximity on the overall characteristics of a VTOL aircraft and the effect of the downwash from the aircraft on the ground.

The propeller blade angles and power input during the tests were adjusted to represent a range of disk loadings and a range of fore and aft power splits (i.e., c.g. locations).

Figure 232. Curtiss-Wright test facility for the investigation of over-water aspects of high disk loading VTOL airplane.

Overall forces and moments, auxiliary forces and moments and ground board surface measurements were taken over a range of ground clearances from contact to clear of ground effect, for a range of pitch and roll attitudes.

All information obtained was reduced to coefficient form in terms of mean propeller disk loading and the usual reference areas and lengths. Pressure data recorded as surface pressure coefficients on both the model undersurface and on the ground board were also included in the information taken during these tests.

From the data taken, it was concluded that normal force coefficient is sensitive to ground clearance and nacelle tilt angle but not to attitude, disk loading or c.g. location. On the other hand pitching moment coefficient is sensitive to ground clearance, nacelle tilt, attitude and power split, but not significantly so to disk loading. However, the side force, yawing moment and rolling moment coefficients were affected in varying degrees by ground clearance, roll angle and power split. All of the auxiliary measurements of thrust and nacelle torque were affected by ground clearance negligibly or not at all.

A test program was performed full-scale with the X-100 VTOL testbed aircraft in the 40 by 80 foot wind tunnel at the NASA Ames Research Center, Moffett Field, California, during March and April 1963. The tests were performed in order to obtain propeller aerodynamic performance data and propeller blade load distribution data. Since the allowed wind tunnel time was reduced to just one week, not all of the test objectives were met. However, by establishing a test program priority schedule, the prime objectives were completed so that most of the desired data were obtained. Total aircraft running time in the tunnel was 12.27 hours.

Prior to the tunnel test, the aircraft and instrumentation were satisfactorily ground checked and then installed on an outdoor static test stand at Ames, in order to obtain force and moment data with the aircraft in the hover condition at zero q or wind velocity. Load cells were used at the three mount points to measure lift, drag and pitching moment. The propeller gimbal angle was 90°, flaps zero, fuselage level, engine power was varied from 70% N_I to military power, and propeller tip speed was varied from 650 to 500 fps.

Installation of the aircraft in the wind tunnel was accomplished as shown in Figure 233. Aircraft and instrumentation electrical conduits were run down the landing gear, through the tunnel struts, under the tunnel floor and then connected to the control console and recording instruments in the control room. Besides the recording of wind tunnel balance data, propeller thrust, normal force, pitching moment, yawing moment, power absorbed and blade

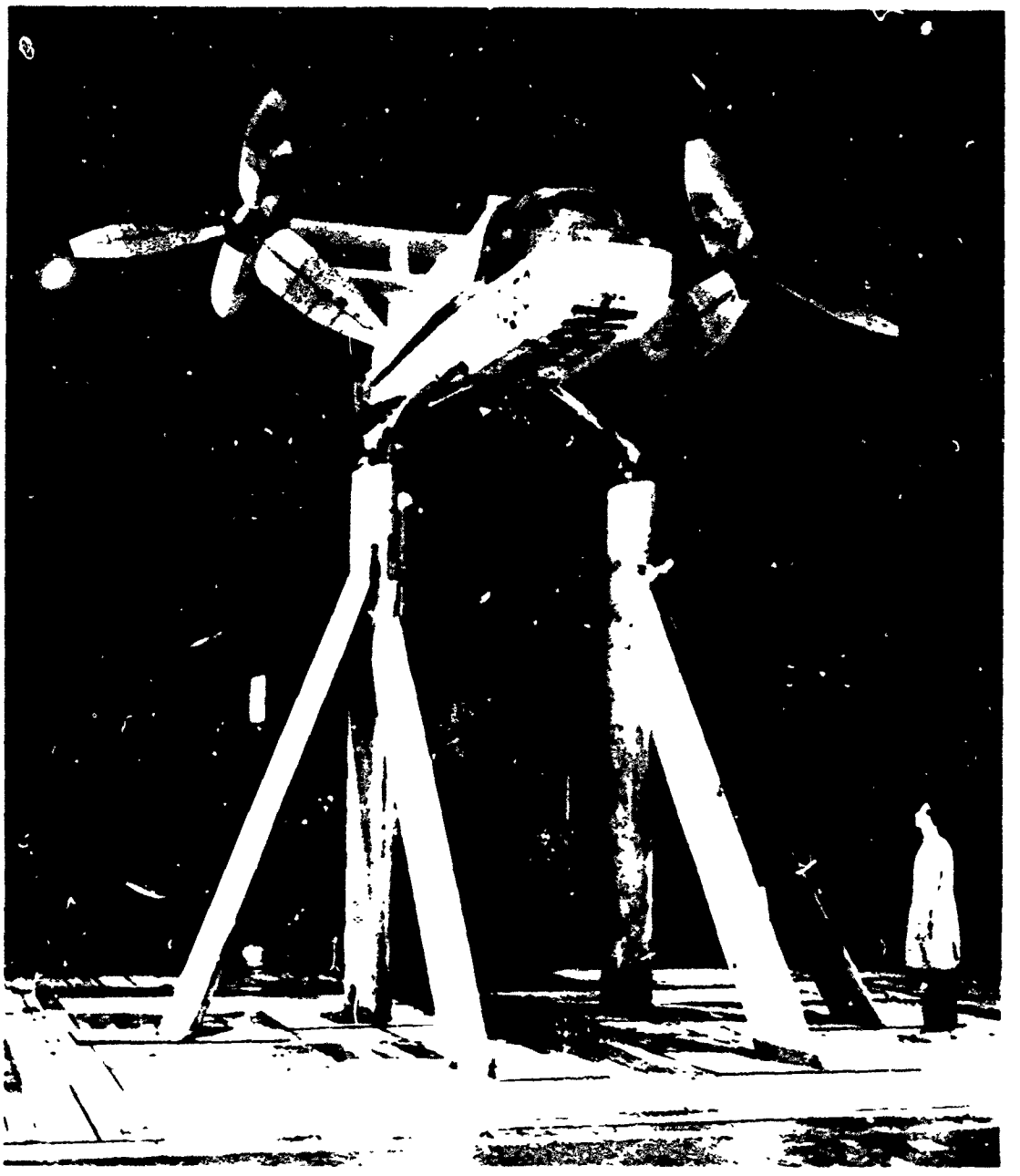

Figure 233. Installation of the X-100 research aircraft on the NASA 40 x 80 wind tunnel mounts at Ames Research Center.

load distribution data were recorded. The data were taken at various power settings ranging from 70% N_I to military and at propeller tip speeds ranging from 500 to 600 fps. Wind tunnel speed throughout the test varied from q = 0 to q = 37 psf. At q = 0 the wind tunnel overhead doors were opened for the test. Props-off data were obtained at gimbal angles from 3° to 90° and aircraft angle of attack from - 12° to 16°. Wing flaps were also deflected down in increments to 45°. See (72).

The evaluation of the results of this test program, as pertains to the evaluation of propeller aerodynamic performance is presented in a later paragraph.

3. TESTS IN SUPPORT OF ADVANCED TANDEM WING CONCEPTS

Considerable test data have been published on the various types of VTOL aircraft systems, but the tandem-wing tilt-propeller variety has been investigated in depth only by Curtiss-Wright Corporation's VTOL Systems Division. The tilt propeller concept had been first tested using its single-short-span-wing vehicle, the X-100, before going on to the tandem-wing four-tilt propeller X-200 and its derivative test vehicle, the X-19 VTOL Airplane. However other aircraft manufacturers have devised and tested low disk loading tilting rotor test aircraft in the past, but always with only two rotors and a single cruise-lift wing. The only other VTOL aircraft to reach test status with tandem wings (of sorts) is a four-tilt-duct type whose forward "wing" is in reality more of a pylon for the duct than a lift producing wing. Thus, as a VTOL aircraft configuration, Curtiss-Wright's tandem wing X-19 test vehicle is somewhat an aerodynamic phenomenon not found elsewhere in this technology. In this context, then, germain wind tunnel tests of the tandem wing VTOL concept are only those enumerated in this report.

Only one test program was conducted, subsequent to the X-19 series tests listed in the previous paragraph, in which the tandem-wing tilt-propeller VTOL concept was the dominating theme. This was in the NACAL-126 tests of the CW Model 90 AAFSS competition aircraft. The specialized requirements of this U. S. Army specified aircraft compelled drastic rearrangement of the interior and nose sections, a different crew seating configuration, the addition of weapons packages at strategic external locations, and a twin-vertical-tail arrangement in place of the X-19's single central vertical control surface. Various mechanical changes were also necessary in defining that configuration, but all the essential elements of the X-19 concept were retained in that proposed aircraft. An entirely new 0.10 scale powered model was built and tested in October of 1964.

The purpose of this test program was to determine the trimmed lift and drag coefficients and the static stability characteristics in the cruise configuration. These tests were conducted in the 7 x 10 foot test section of the NACAL subsonic wind tunnel for pitch angles ranging from -8° to +20° and yaw angles ranging from - 12 to + 12 degrees. Trim points were

obtained from flap effectiveness studies performed in five increments from 0 to + 60 degrees. All runs were made with a transition strip applied to the bow wing upper surface. The resultant data are recorded and plotted in (68).

During the time period of the development of the X-19 configuration of the tandem-wing tilt-propeller aircraft, one other configuration was tested at the University of Maryland in February and March 1963, the "Horned Toad" configuration. This concept differed from the X-19 type VTOL primarily in its conventional single wing for normal cruise rather than the tandem arrangement discussed heretofore. Its four tilting propellers were disposed at the extremeties of the horizontal tail in the rear and a stub wing at the nose, retaining the essentials of the X-19's vertical flight thrusting vector dispersion about the aircraft c.g. Further information and data on this test program may be found in (66).

4. TRANSITION WIND TUNNEL WALL CORRECTIONS

All wind tunnel testing data taken, described in the preceding sub-paragraphs for X-19 model testing in the several commercial wind tunnel test facilities used, necessarily bears the imprint of the test circumstances under which they were obtained. The size of the model in the tunnel, size of test section in the tunnel, the type of mounting utilized for holding and adjusting aircraft attitude, and the nature of the wall effect on the model parameters recorded, as well as the reading accuracies of the instrumentation systems affect the results obtained. Since the model was essentially the same throughout the test programs at the various tunnels, an opportunity is presented here for showing how the test data compare.

The matter of wind tunnel corrections applied to the data are as reported in (60) through (69). In those documents it can be seen that the MIT and Cornell tunnel corrections were essentially negligible, and those of the NACAL and University of Maryland were manageable and reasonable as represented in the appropriate test reports.

The greater tunnel effects lie in the fact that the same 0.12 scale stability model of the X-19 VTOL test aircraft configuration was used in all the tunnels, but the data are not always compatable with one another. All the test programs have the common parameter of being subject to the accuracies of the respective six component balance systems recording extremely low loads due to the low speeds of transition flight tested. Therefore the relative comparisons within the results are more accurate than absolute values which are subject to scale and other effects. In each test program also, testing problems were encountered which rendered some of the data either useless or at best suspect. Likewise, the test parameters and conditions set for each test program were not necessarily the same, making precise comparisons of results from the various tunnels and tests more difficult. An attempt to make such fruitful comparison was made in (70), which applies only to the tests through the NACAL-93 series. There the NACAL results have been compared with the previous

FURNISHED UNDER UNITED STATES GOVERNMENT CONTRACT No. AF33(615)-1940. SHALL NOT BE EITHER RELEASED OUTSIDE THE GOVERNMENT, OR USED, DUPLICATED, OR DISCLOSED IN WHOLE OR IN PART FOR MANUFACTURE OR PROCUREMENT, WITHOUT THE WRITTEN PERMISSION OF CURTISS-WRIGHT CORPORATION, EXCEPT FOR (i) EMERGENCY REPAIR OR OVERHAUL WORK BY OR FOR THE GOVERNMENT, WHERE THE ITEM OR PROCESS IS NOT OTHERWISE REASONABLY AVAILABLE TO ENABLE TIMELY PERFORMANCE OF THE WORK, OR (ii) RELEASE TO A FOREIGN GOVERNMENT, AS THE INTERESTS OF THE UNITED STATES MAY REQUIRE. PROVIDED THAT IN EITHER CASE THE RELEASE, USE, DUPLICATION OR DISCLOSURE HEREOF SHALL BE SUBJECT TO THE FOREGOING LIMITATIONS. THIS LEGEND SHALL BE MARKED ON ANY REPRODUCTION HEREOF IN WHOLE OR IN PART.

MIT and Cornell tests to determine the corrections required to accurately interpret the NACAL data. Figures 234 through 239 are taken from said Reference and show the six component data of the X-19 stability model, props off, as recorded at the MIT, Cornell and NACAL (-93) tunnels.

In essence these are the findings in this comparison of the test results: The lift curve slopes of the MIT and Cornell tests are about the same. Reynolds Number is a weak parameter in this respect. The considerably reduced slope in the NACAL-93 low gimbal angle data is attributed, therefore, to interference between the post suspension and the rear wing. The standard tare and interference corrections have not been applied to the NACAL-93 results since it was impossible to mount the model in an inverted position. These corrections if known would produce a better agreement amoung the CAL, MIT, and NACAL lift, drag and pitching moment data.

The yaw data from the NACAL-93 tests compare favorably with the Cornell results, while the MIT data differs slightly due to the interferences in its support system. The MIT model is mounted on bayonets attached to the side of the fuselage; therefore, the side force data is more greatly affected. The pressure distribution data, though limited in scope, verified the belief that the rear wing was not generating sufficient lift in the NACAL-93 tests.

A subsequent comparative study was undertaken late in 1965 to correlate all existing transition tunnel tests on the X-19. Correlation of all tunnel tests simultaneously was begun. It was aimed at a general aerodynamic analysis, with performance, stability, control and loads uninfluenced by the previous analyses. From the results achieved at the time of program stoppage it was apparent that the approach used for the analysis was correct and would have provided aerodynamic data suitable for general use.

5. CORRECTIONS OF MODEL PROPELLERS TO FULL SCALE RESULTS

In the course of the development of the X-100 aircraft, a considerable amount of aerodynamic testing was done. This testing included power model wind tunnel testing, and full scale propeller testing. The actual propellers of the X-100 aircraft were tested in the NASA Ames Research Center 40 x 80 foot wind tunnel for the complete range of power, tilt angle, RPM and speed that was expected on the X-100 aircraft (72). The aerodynamic and structural data were than used as a basis for calculating the performance, stability and control of the X-100 aircraft. These data were later shown to be in agreement with actual flight test results.

The MIT Wright Brothers Wind Tunnel 7.5 x 100 foot test section was used to test a 0.15 scale powered model of the X-100 at speeds up to 100 MPH over a complete range of gimbal angles, control deflections, power settings, angle of attack, and yaw angles. The tests were run to obtain performance information and stability derivatives. The results are reported in (73), including the test findings of the undesirable flow conditions at the "T" tail.

"FURNISHED UNDER UNITED STATES GOVERNMENT CONTRACT No. AF33(615)-3940. SHALL NOT BE EITHER RELEASED OUTSIDE THE GOVERNMENT, OR USED, DUPLICATED, OR DISCLOSED IN WHOLE OR IN PART FOR MANUFACTURE OR PROCUREMENT, WITHOUT THE WRITTEN PERMISSION OF CURTISS-WRIGHT CORPORATION, EXCEPT FOR (i) EMERGENCY REPAIR OR OVERHAUL WORK BY OR FOR THE GOVERNMENT, WHERE THE ITEM OR PROCESS IS NOT OTHERWISE REASONABLY AVAILABLE TO ENABLE TIMELY PERFORMANCE OF THE WORK, OR (ii) RELEASE TO A FOREIGN GOVERNMENT, AS THE INTERESTS OF THE UNITED STATES MAY REQUIRE. PROVIDED THAT IN EITHER CASE THE RELEASE, USE, DUPLICATION OR DISCLOSURE HEREOF SHALL BE SUBJECT TO THE FOREGOING LIMITATIONS. THIS LEGEND SHALL BE MARKED ON ANY REPRODUCTION HEREOF IN WHOLE OR IN PART."

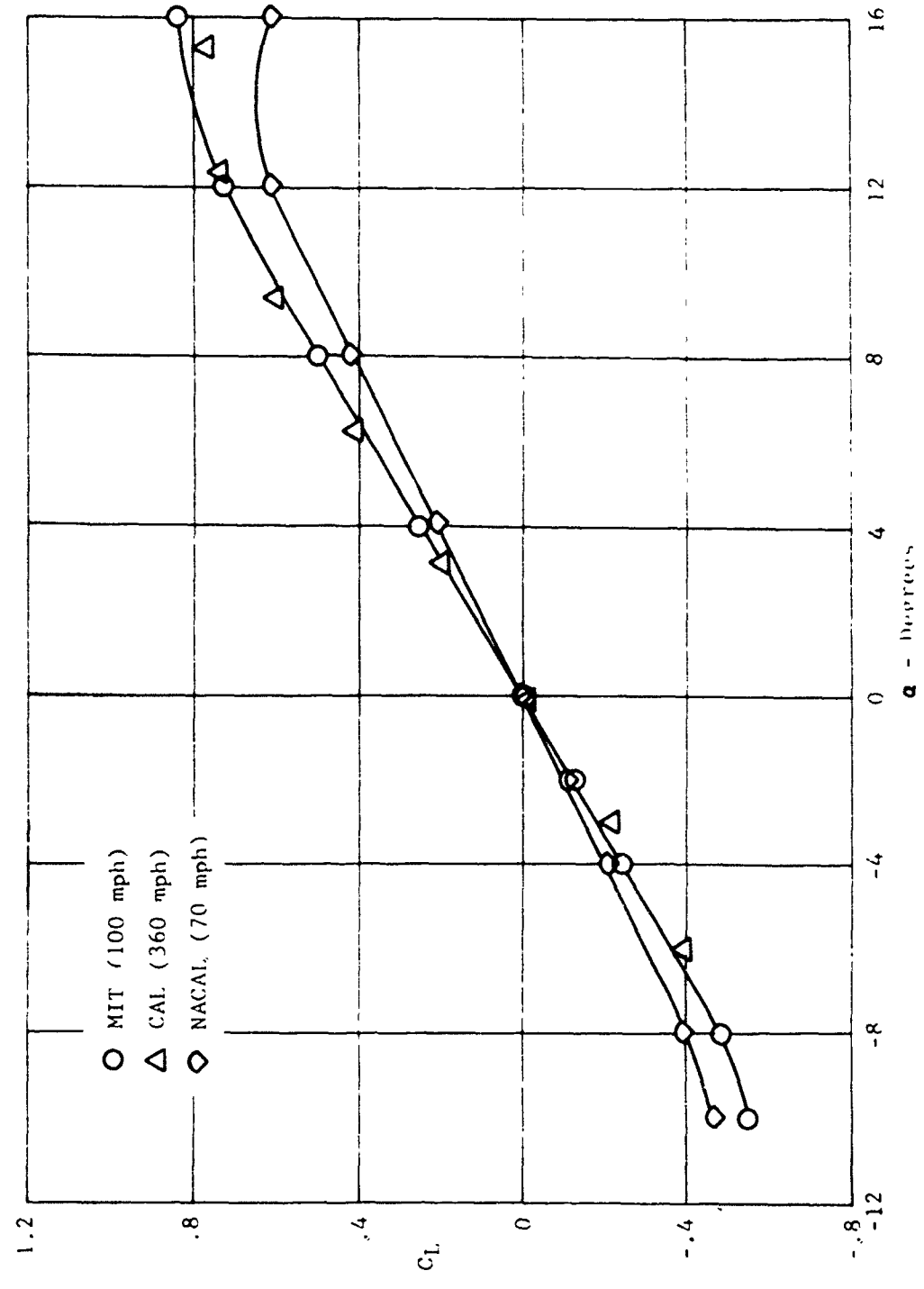

Figure 234. Comparison of similar test configurations of the 0.12 scale X-19 model in three different wind tunnels - C_L vs α, power off.

FURNISHED UNDER UNITED STATES GOVERNMENT CONTRACT No. AF33(615)-1940. SHALL NOT BE EITHER RELEASED OUTSIDE THE GOVERNMENT, OR USED, DUPLICATED, OR DISCLOSED IN WHOLE OR IN PART FOR MANUFACTURE OR PROCUREMENT, WITHOUT THE WRITTEN PERMISSION OF CURTISS-WRIGHT CORPORATION, EXCEPT FOR (i) EMERGENCY REPAIR OR OVERHAUL WORK BY OR FOR THE GOVERNMENT, WHERE THE ITEM OR PROCESS IS NOT OTHERWISE REASONABLY AVAILABLE TO ENABLE TIMELY PERFORMANCE OF THE WORK, OR (ii) RELEASE TO A FOREIGN GOVERNMENT, AS THE INTERESTS OF THE UNITED STATES MAY REQUIRE. PROVIDED THAT IN EITHER CASE THE RELEASE, USE, DUPLICATION OR DISCLOSURE HEREOF SHALL BE SUBJECT TO THE FOREGOING LIMITATIONS. THIS LEGEND SHALL BE MARKED ON ANY REPRODUCTION HEREOF IN WHOLE OR IN PART.

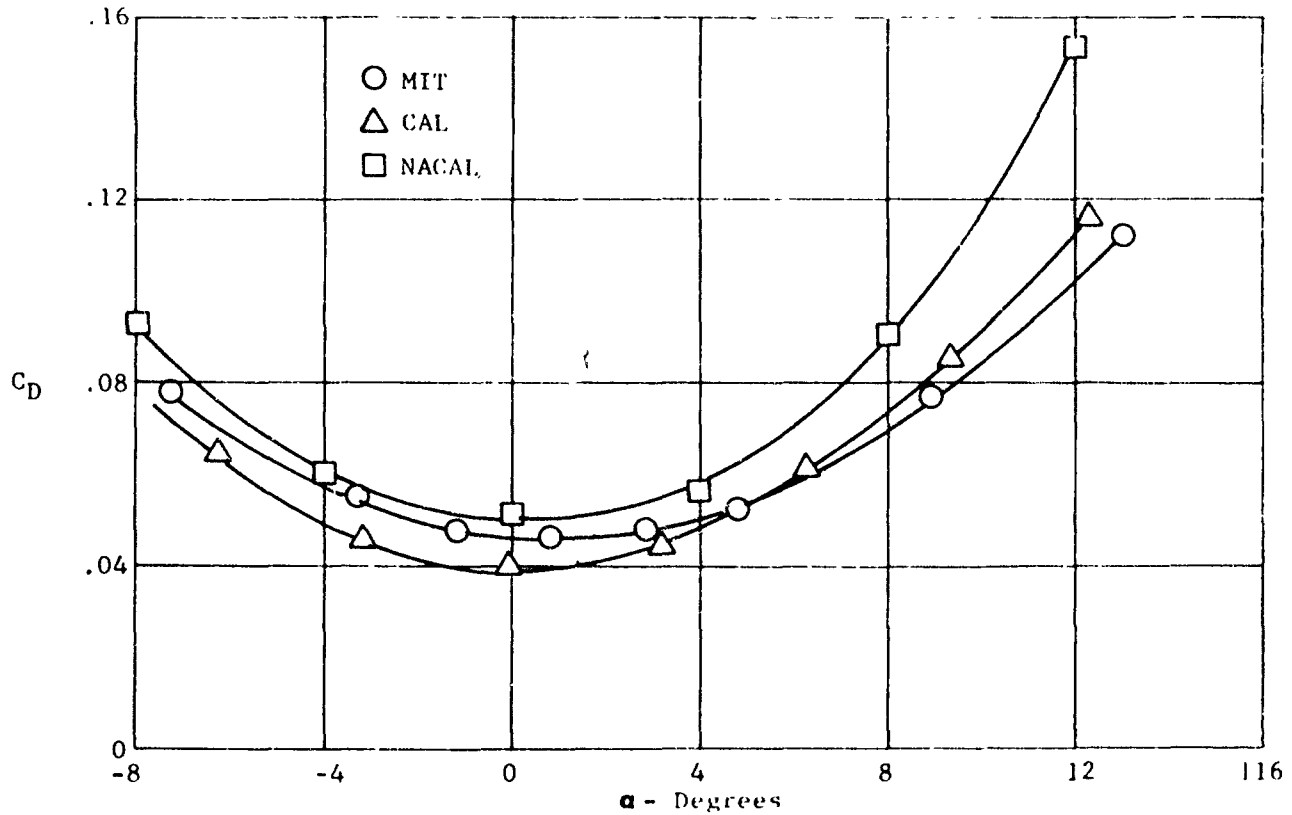

Figure 235. Comparison of similar test configurations of the 0.12 scale X-19 model in three different wind tunnels - C_D vs α, power off.

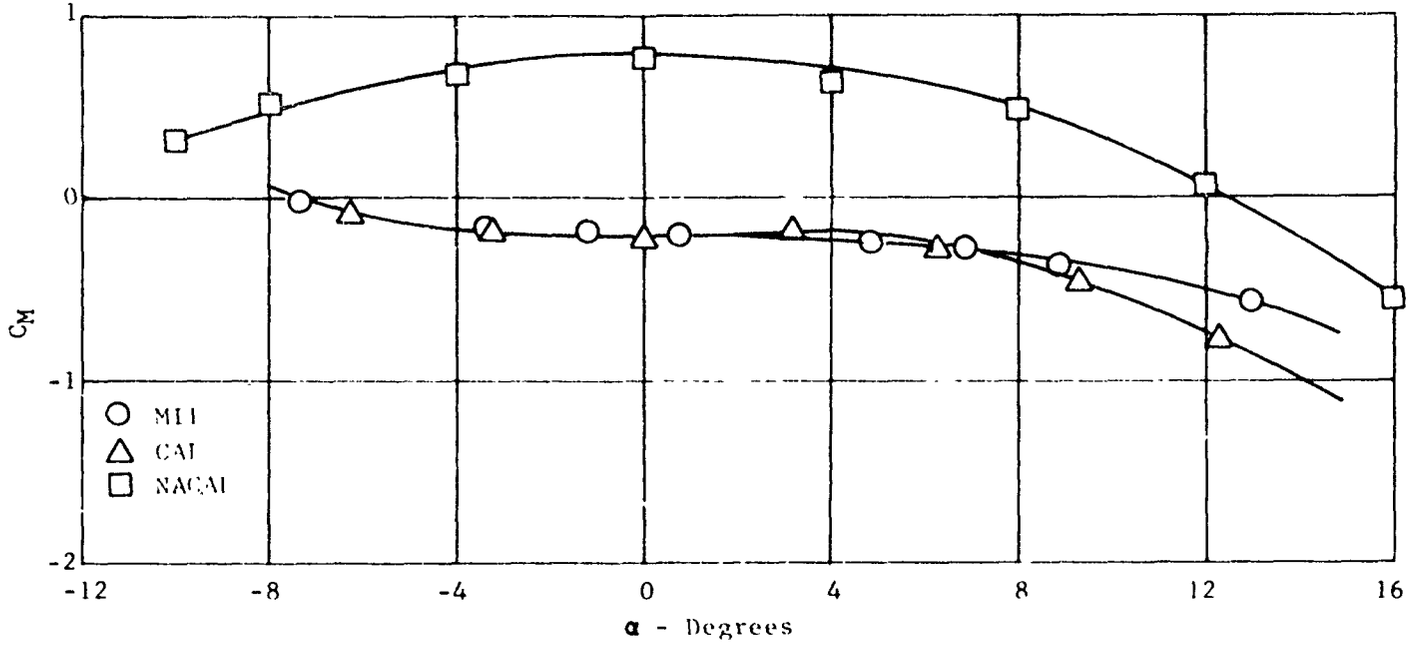

Figure 236. Comparison of similar test configurations of the 0.12 scale X-19 model in three different wind tunnels - C_M vs α, power off.

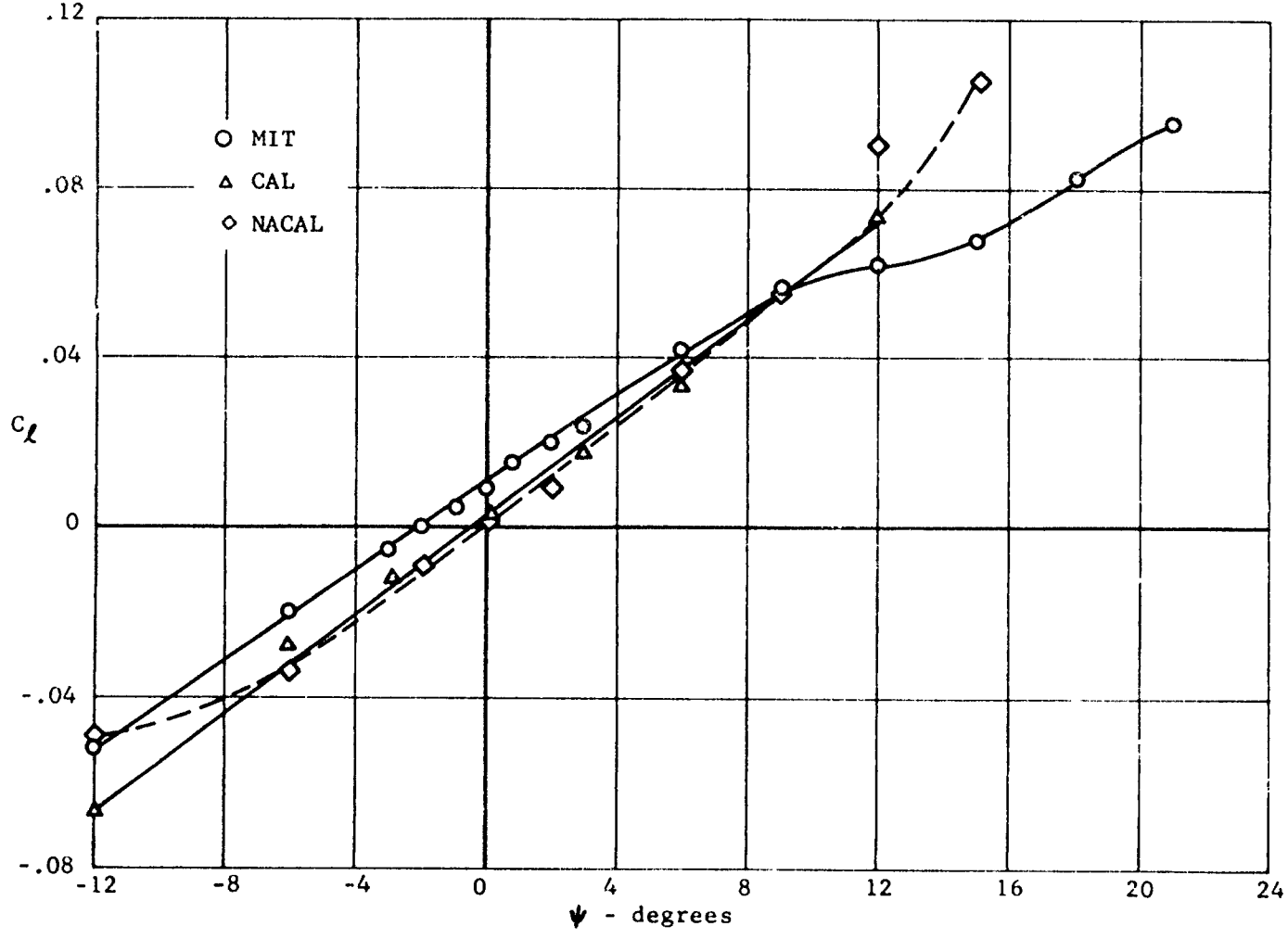

Figure 237. Comparison of similar test configurations of the 0.12 scale X-19 model in three different wind tunnels - C_ℓ vs ψ, power off.

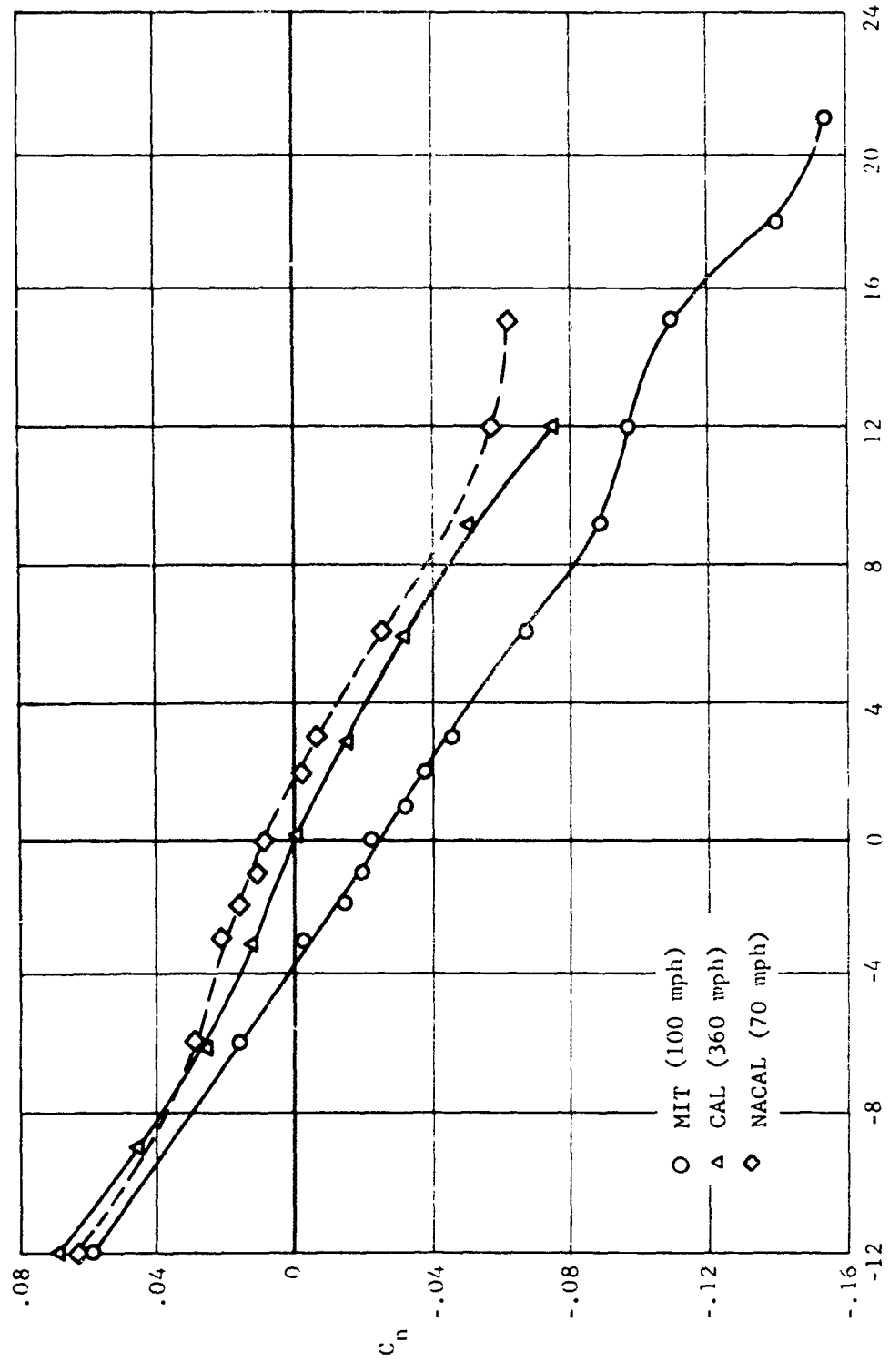

Figure 238. Comparison of similar test configurations of the 0.12 scale X-19 model in three different wind tunnels - C_n vs ψ, power off.

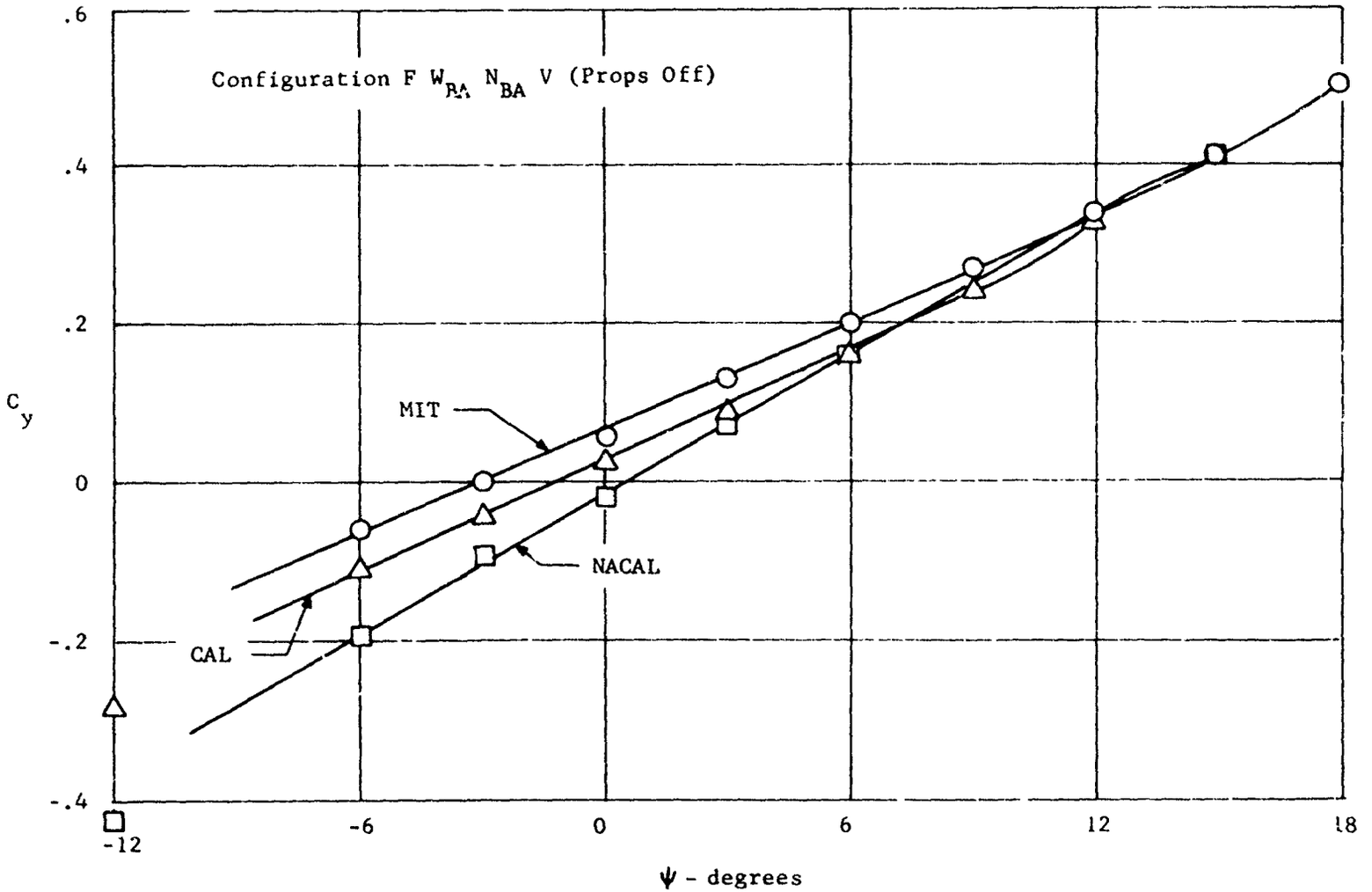

Figure 239. Comparison of similar test configurations of the 0.12 scale X-19 model in three different wind tunnels - C_y vs Ψ power off.

The full-scale X-100 type propellers were tested in the NASA Ames Research Center 40 x 80 foot wind tunnel over a speed range of 0 to 150 MPH for the full range of gimbal angle to obtain propeller blade load distribution data and propeller performance data. The results of these tests are reported in (71) and (72). They are comparable with other NASA full scale propeller data operating at similar test conditions reported in (74) and (75).

Because of the importance in obtaining predicted take-off performance, the 15% scale propellers were run at the static condition outside the wind tunnel. The results of these tests were 15 to 20 percent lower than predicted full scale values, as shown in Figure 240, but close to the performance expected when the effects of Reynolds number were considered. This is further borne out by the results of other tests and comparisons shown in Figures 241 and 242.

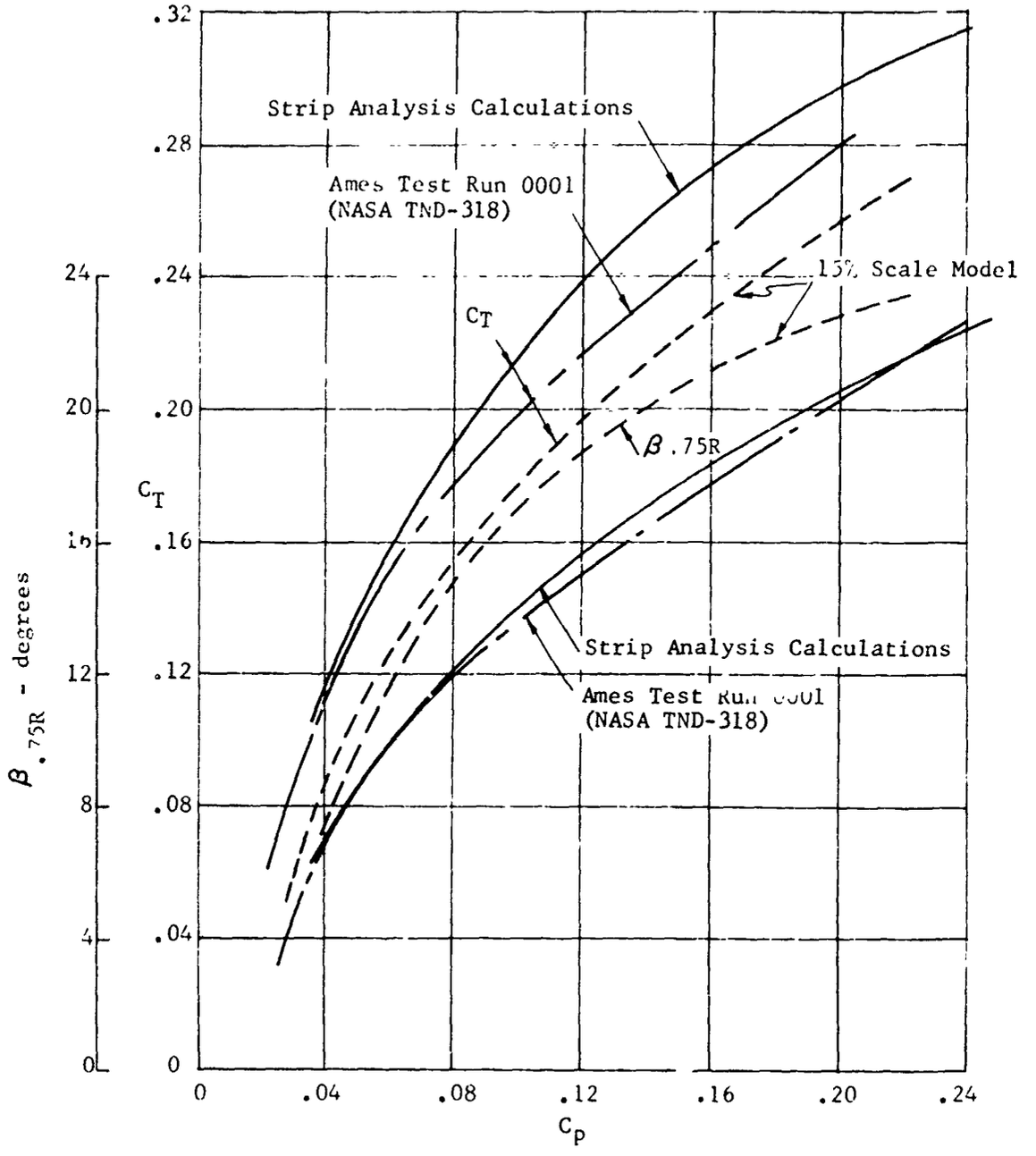

Figure 24C. Comparison of calculated and test data of X-100 propeller blade angle and thrust coefficient versus power coefficient at static condition.

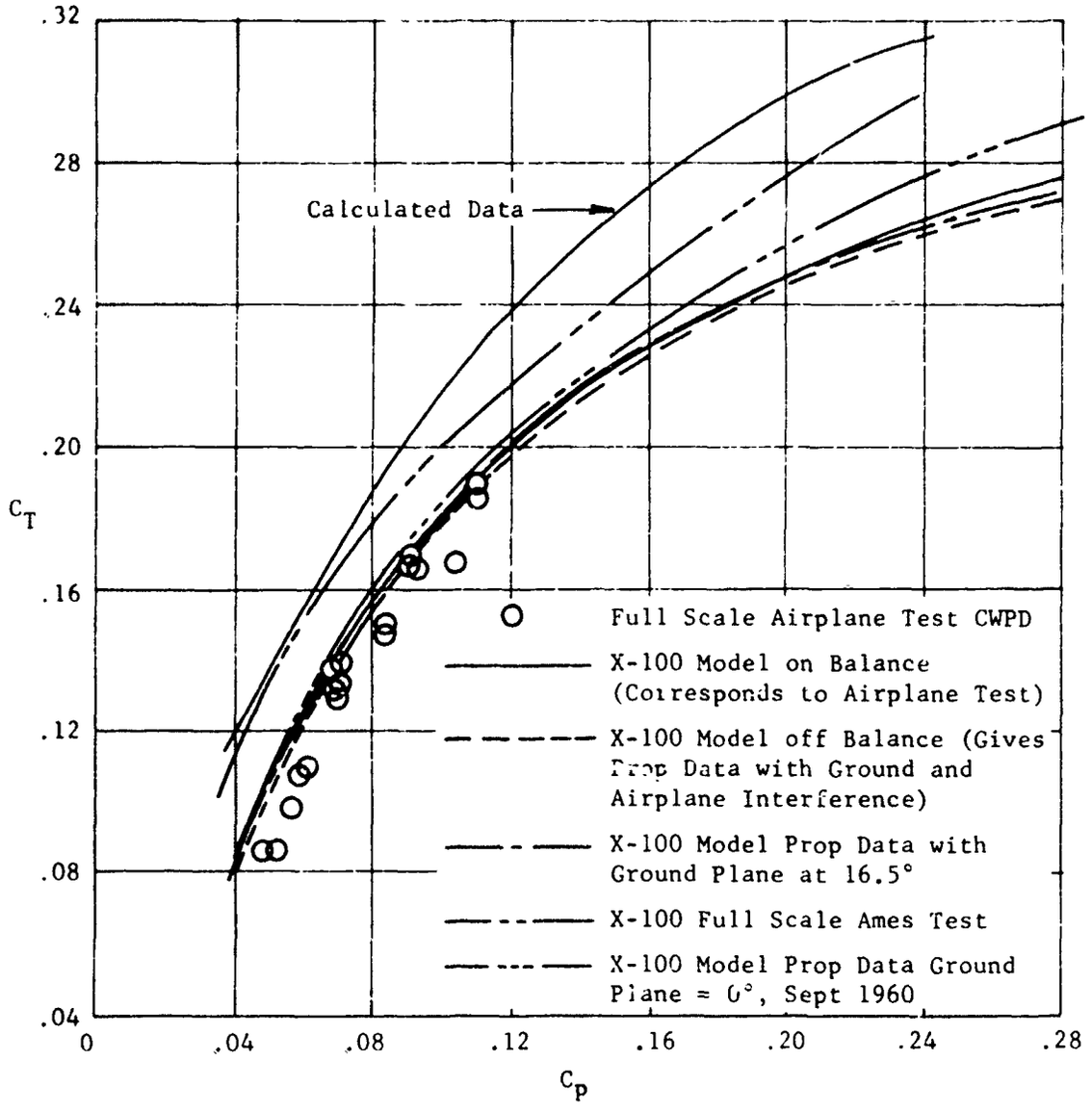

Figure 241. Comparison of X-100 full scale and model propeller data in terms of C_T and C_p.

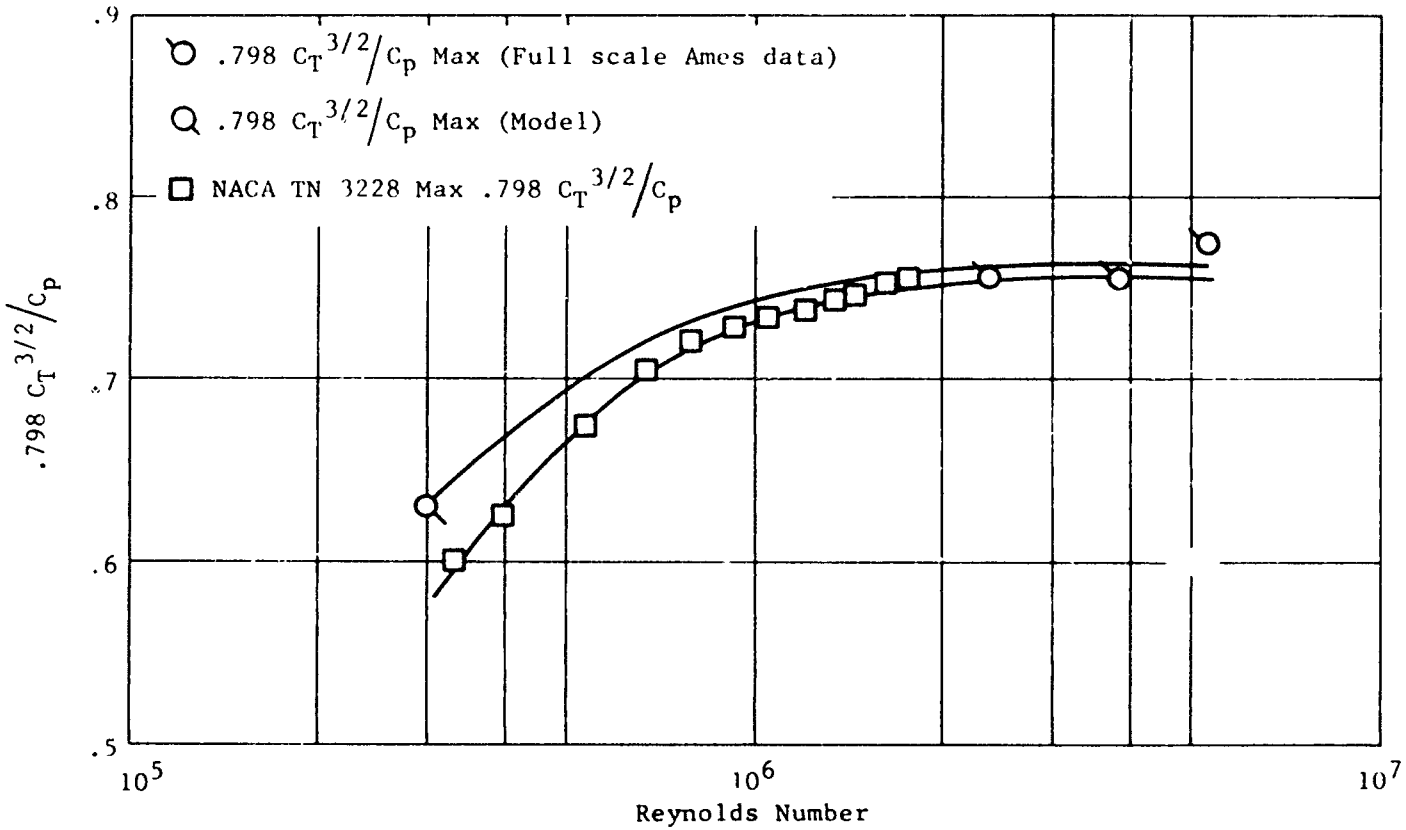

Figure 242. X-100 maximum values of propeller figure of merit at various Reynolds numbers based on blade chord at .75 radius full-scale and model test data.

60. K. J. Rogers, MIT Wind Tunnel Report 1019, M200 Turbine Stability Model Curtiss-Wright Corp. Report No. 014-36, dated 5 September 1962.

61. K. J. Rogers, and R. J. Hauser, Cornell Aero Lab. Report No. AA-1709-W-1, Wind Tunnel Tests of a 0.12 Scale Model of the Curtiss-Wright X-19 Airplane Curtiss-Wright Report No. 014-583, dated 23 January 1963.

62. K. J. Rogers and R. J. Hauser, Cornell Aero Lab. Report No. AA-1771-W-1, Wind Tunnel Tests of a 0.12 Scale Model of the Curtiss-Wright X-19 Series II, Curtiss-Wright Report No. 014-584, dated 24 May 1963.

63. K. J. Rogers, NACAL Test No. 93, Low Speed Tunnel Test of a 0.12 Scale Model of the Curtiss-Wright M-200 VTOL Airplane to Evaluate Longitudinal, Lateral and Directional Stability Characteristics, North American Aviation Report No. NA 62H-719, filed under Curtiss-Wright Report No. 014-582, dated 2 October 1962.

64. K. J. Rogers, NACAL Test No. 120, Low Speed Wind Tunnel Tests of a 0.12 Scale Model of the Curtiss-Wright X-19 Aircraft, North American Aviation Report No. NA 64H-837, filed under Curtiss-Wright Report No. 014-585, dated 21 August 1964.

65. K. J. Rogers, NACAL Test No. 142, Low Speed Wind Tunnel Test of a 0.12 Scale Powered Model of the Curtiss-Wright X-19 Aircraft to Determine the Optimum Propeller Tilt Schedule in Transition, North American Aviation Report No. NA 66H-43, dated 25 February 1966.

66. R. I. Windsor, Wind Tunnel Test of Curtiss-Wright Variable Configuration Model, University of Maryland Wind Tunnel Report No. 367, dated June 1963.

67. R. I. Windsor, Wind Tunnel Test of Curtiss-Wright Variable Configuration Model, University of Maryland Wind Tunnel Report No. 410, dated July 1964.

68. K. J. Rogers, NACAL Test No. 126, Low Speed Wind Tunnel Tests of a 0.10 Scale Model of a Curtiss-Wright Research V/STOL Airplane, North American Aviation Report No. NA 65H-130, filed under Curtiss-Wright Report No. 012-70, dated 16 February 1965.

69. W. S Sekscienski, Wind Tunnel Tests of Curtiss-Wright Propellers, 156, 958 and 109, University of Maryland Wind Tunnel Test No. 418, dated February 1965.

70. K. J. Rogers, Transition Test of the X-19 Stability Model in the Low Speed Section of the NACAL Wind Tunnel, Appendix to NACAL Report 93, Curtiss-Wright Report No. 014-102, dated 1 February, 1963.

71. H. V. Borst, Design and Performance of the Lifting Propeller X-100 VTOL Airplane , Curtiss-Wright Report No. C-2798, dated 8 October 1959.

72. J. Vander Hoven, Test of X-100 Aircraft at Ames Research Center Wind Tunnel , Curtiss-Wright Report No. 014-200, dated 3 June 1963.

73. E. R. Flemig, and J. Bicknell, Curtiss-Wright Corp. Model X-100 Tests, Massachusetts Institute of Technology Aerodynamic Laboratory Report No. 973, dated June 1958.

74. P. F. Yaggy and V. L. Rogallo, A Wind Tunnel Investigation of Three Propellers through an Angle of Attack Range from 0° to 85°, NASA TN D-318 dated May 1960.

75. H. C. McLemore and M. D. Cannon, Aerodynamic Investigation of a Four Blade Propeller Operating through an Angle of Attack Range from 0° to 180°, NACA TN 3228, dated 1954.

SECTION X NOMENCLATURE

A	Propeller angle of attack (∢ between thrust vector and relative wind),	degrees
b	Wing span,	ft
C_D	Total drag coefficient, D/qS	
C_L	Lift coefficient, L/qS or nW/qS	
C_{L_o}	Lift coefficient - zero angle of attack	
$C_{L_{\delta_a}}$	Aileron lift slope,	per degree
$C_{L_{\delta_e}}$	Elevator lift slope,	per degree
C_{m_o}	Pitching moment coefficient - zero angle of attack	
C_m	Pitching moment coefficient	
C_H	Propeller pitching moment coefficient, $H/\rho n^2 D_p^5$	
C_N	Propeller normal force coefficient, $N/\rho n^2 D_p^4$	
C_P	Propeller power coefficient, $550\ HP/\rho n^3 D_p^5$	
C_Q	Propeller torque coefficient, $Q/\rho n^2 D_p^5$	
C_S	Propeller side force coefficient, $S/\rho n^2 D_p^4$	
C_T	Propeller thrust coefficient, $T/\rho n^2 D_p^4$	
C_X	Net thrust coefficient, F_n/qS	
C_Y	Propeller yawing moment coefficient $Y/\rho n^2 D_p^5$	
D	Drag, $C_D qS$,	lb
D_p	Propeller diameter,	ft
D_i	Induced drag, $C_{D_i} qS$,	lb
D L	Wing download - % of thrust,	lb
$\partial C_L/\partial \alpha$	Lift coefficient slope,	per degree
$\partial C_m/\partial \alpha$	Pitching moment coefficient slope,	per degree
$d\theta/d\alpha$	Rate of wing twist with angle of attack	
$d\theta/d\delta_a$	Rate of wing twist with aileron angle	
EAS	Equivalent airspeed,	knots
EHP	Engine horsepower	
F_n	Net accelerating thrust,	lb
g	Gravitational constant,	ft/sec/sec
GJ	Wing stiffness constant	lb/ft^2
J	Advance ratio, V/nD_p	
l_{ξ_e}-$C_{l_{\delta_{a_e}}}$	Rate of change of airplane rolling moment coefficient with mean aileron angle for elastic wing - negative for positive aileron angle,	per radian
l_{ξ_r}-$C_{l_{\delta_{a_r}}}$	Rate of change of airplane rolling moment coefficient with mean aileron angle for rigid wing - negative for positive aileron angle,	per radian
L	Lift,	lb
LC	Lift chord (distance from front to rear tilt center),	inches
M	Mach number	
M	Moment, M	ft lb
M_c	Propeller pitching moment coefficient, $q\ W/4\ D_p^3$	
n	Load factor, L/W	
n	Revolutions per second,	rps
p	Roll rate,	rad/sec
pb/2V	Non-dimensional roll rate	
PHP, SHP	Propeller, or shaft horsepower	
q	Dynamic pressure, $\frac{1}{2}\rho V^2$,	lb/ft^2
Q	Torque	ft-lb
R/C	Rate of climb,	ft/min
ReN	Reynolds number	
S	Propeller side force, reference area,	lb/ft^2
T	Propeller thrust, T	lb
T_c	Propeller thrust coefficient, $q\ W/4\ D_p^3$	
V	Velocity	
V_c	Design cruise speed	
V_D	Design dive speed	
W	Weight,	lb
W/S	Wing loading,	lb/ft^2
X	Moment arm from c.g.,	ft
Y	Propeller yawing moment Y	ft-lb
Y_c	Propeller yawing moment coefficient, $q\ W/4\ D_p^3$	
α	Angle of attack (∢ between fuselage ref., WL100 and relative wind),	degrees
α_o	Angle of zero lift,	degrees
α_{o_f}	Angle of zero lift -front wing,	degrees
α_{o_r}	Angle of zero lift -rear wing,	degrees
$\beta_{.75R}$	Propeller blade angle at 75% radius,	degrees
β_c or β_{coll}	Propeller collective blade angle (at 75% radius if unmarked), $\frac{1}{2}(2\beta_y + 2\beta_R)$,	degrees
δ_a	Aileron deflection - starboard aileron positive down,	degrees
$\delta_{a_{coll}}$	Collective aileron angle (droop) positive down,	degrees
δ_e	Elevator deflection positive down,	degrees
δ_f	Flap deflection positive down,	degrees
δ_S	Stick deflection push force positive,	degrees
$\Delta\beta$	Differential blade angle, β_y-β_R = $\Delta\beta_o$+ $\Delta\beta_\delta$,	degrees
$\Delta\beta_o$	Differential blade angle zero stick position,	degrees
$\Delta\beta_\delta$	Differential blade angle due to stick motion, $\Delta\beta_y$- $\Delta\beta_R$,	degrees
ϵ	Downwash angle,	degrees
$d\epsilon/d\alpha$	Downwash derivative	
$d\sigma/d\phi$	Sidewash derivative	
ϕ	Yaw angle,	degrees
θ	Angle of twist,	degrees
vnb	Propeller tip speed,	ft/sec
θ	Tilt angle (∢ between thrust vector and fuselage reference, WL100, line),	degrees

Subscripts

c.g.	Center of gravity
f, fus	Fuselage
F	Front
max	Maximum
N	Nacelle
P	Propeller
R	Rear
S	Stick
tot	Total
w	Wing
δ_a	Due to aileron
δ_e	Due to elevator
r	Rigid

SECTION X

STRUCTURAL LOADS

1. INTRODUCTION

The entire loads analysis of the X-19 has been broken into three parts: 1. hover, 2. transition, and 3. cruise. In the hover and transition regime there is no specification upon which a set of aerodynamic loads can be based. However, (76) was used in determining gust loadings, in which horizontal or vertical gusts of 30 fps intensity must be withstood. A maneuvering load factor envelope in the hover-transition regime has not been drawn because of the inability to develop load factors greater than 1.0 without excessive power excursions. This requires the pilot to fly near-steady maneuvers during transition. These are limited to equilibrium, steady climbs or descents, and moderate accelerations. Therefore, the loads for steady flight, gusts, loadings due to stick excursions, and angular accelerations have been determined.

Loads in the cruise regime (propellers fully tilted down) are determined in the conventional manner. Both the gust and maneuver envelopes are prepared for the design weight of 13,660 pounds. Limit load factors, n, are + 2.7 and -1. An approximate, but conservative, theory accounts for front and rear wing twist as a function of wings, nacelles and propeller loads. The guiding specification is the Civil Air Regulations Part 4, (77), where applicable. Vertical tail loads were generated using (78) as a guide. This was necessitated by the rudder limitation (due to large yaw-roll coupling) and the added definition given in (78).

The cruise loads will be discussed first, as they represent the least departure from conventional methods. Following these, the hover loads will be discussed pointing out the pecularities of this regime. Lastly, the transition regime will be discussed, this being the most difficult and least defined region of flight. Specific aerodynamic loads will not be given, as this definition has been provided in (74).

2. CRUISE LOADS

a. General

A brief description of the basic force distribution data defining the aircraft is given. A more detailed discussion is given in (79).

b. Propeller-off distributions.

For convenience in the analysis of the power-off (propellers off) data, it was assumed that the total lift on the aircraft was made up of fuselage lift, front wing lift and rear wing lift. These lifts are defined as follows:

(a) Fuselage lift = Fuselage lift without wings present but with vertical tail

(b) Front wing lift = Wing lift plus nacelle lift and including fuselage and rear wing interferences (i.e. tip-to-tip)

(c) Rear wing lift = Wing lift plus nacelle lift and including fuselage and front wing interferences (i.e. tip-to-tip)

Using this breakdown and the data given in (80) through (84), an analysis was made which enabled the values of

$$\frac{\partial C_L}{\partial \alpha}, \; C_{L_o}, \; \frac{\partial C_m}{\partial \alpha} \text{ and } C_{m_o}$$

to be obtained for each of the above generating surfaces.

Figures 243 through 251 describe both the lift and the moment distributions so obtained. These curves are based on the wind tunnel data of a 12% model.

c. Effects of Power

The propellers contribute a C_L and C_m in the longitudinal plane and a C_y and C_s in the lateral plane. The former contributions are given in Figures 252 and 253 and the latter in Figures 254 and 255. The slipstream effects upon the wing aerodynamic forces and moments have been found to be negligible at the cruise values of J_o. Tunnel tests, (81) and (85), indicate that a delayed stall is present on that portion of the wing covered by the propeller wash. This added lift is apparent at $\alpha_{fus} > 10°$ and is found to exist on the front wing only. It is believed that the low Reynolds Number results in a laminar stall (low α_{fus}) which is eliminated when the propeller energizes the flow, thereby delaying the stall angle. Consequently, the added lift due to propeller wash is considered realistic in the full scale and has been used in subsequent analyses.

d. Effects of Mach Number

Compressibility effects on lift and moment coefficients have been assumed zero, although later tunnel tests show that an effect is present on the overall moment at higher angles of attack.

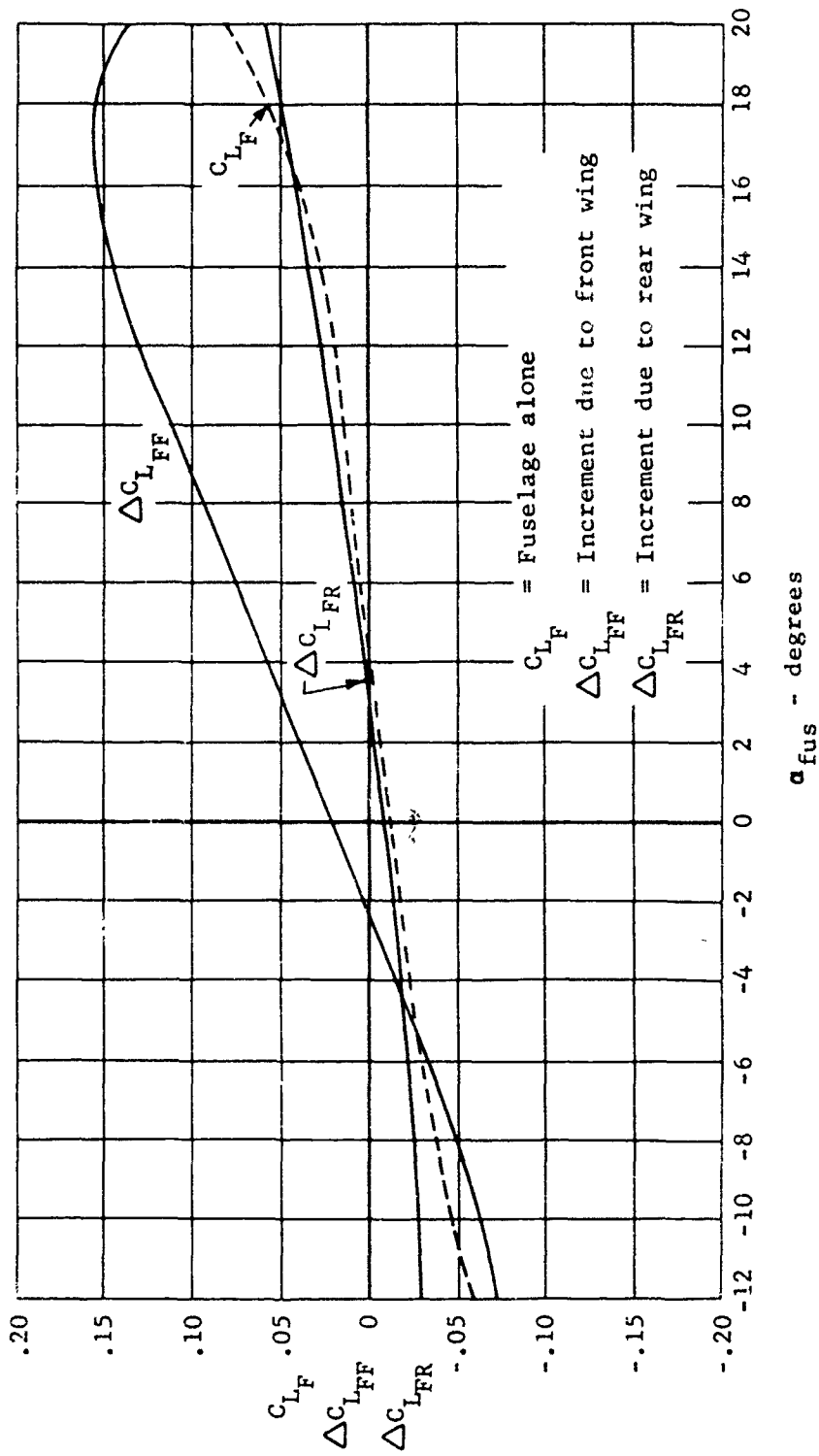

Figure 243. X-19, fuselage lift coefficient characteristics; S_{ref} = 154.6 square feet.

FURNISHED UNDER UNITED STATES GOVERNMENT CONTRACT No. AF33(615)-3940 SHALL NOT BE EITHER RELEASED OUTSIDE THE GOVERNMENT, OR USED, DUPLICATED, OR DISCLOSED IN WHOLE OR IN PART FOR MANUFACTURE OR PROCUREMENT, WITHOUT THE WRITTEN PERMISSION OF CURTISS-WRIGHT CORPORATION, EXCEPT FOR (i) EMERGENCY REPAIR OR OVERHAUL WORK BY OR FOR THE GOVERNMENT, WHERE THE ITEM OR PROCESS IS NOT OTHERWISE REASONABLY AVAILABLE TO ENABLE TIMELY PERFORMANCE OF THE WORK, OR (ii) RELEASE TO A FOREIGN GOVERNMENT, AS THE INTERESTS OF THE UNITED STATES MAY REQUIRE. PROVIDED THAT IN EITHER CASE THE RELEASE, USE, DUPLICATION OR DISCLOSURE HEREOF SHALL BE SUBJECT TO THE FOREGOING LIMITATIONS. THIS LEGEND SHALL BE MARKED ON ANY REPRODUCTION HEREOF IN WHOLE OR IN PART."

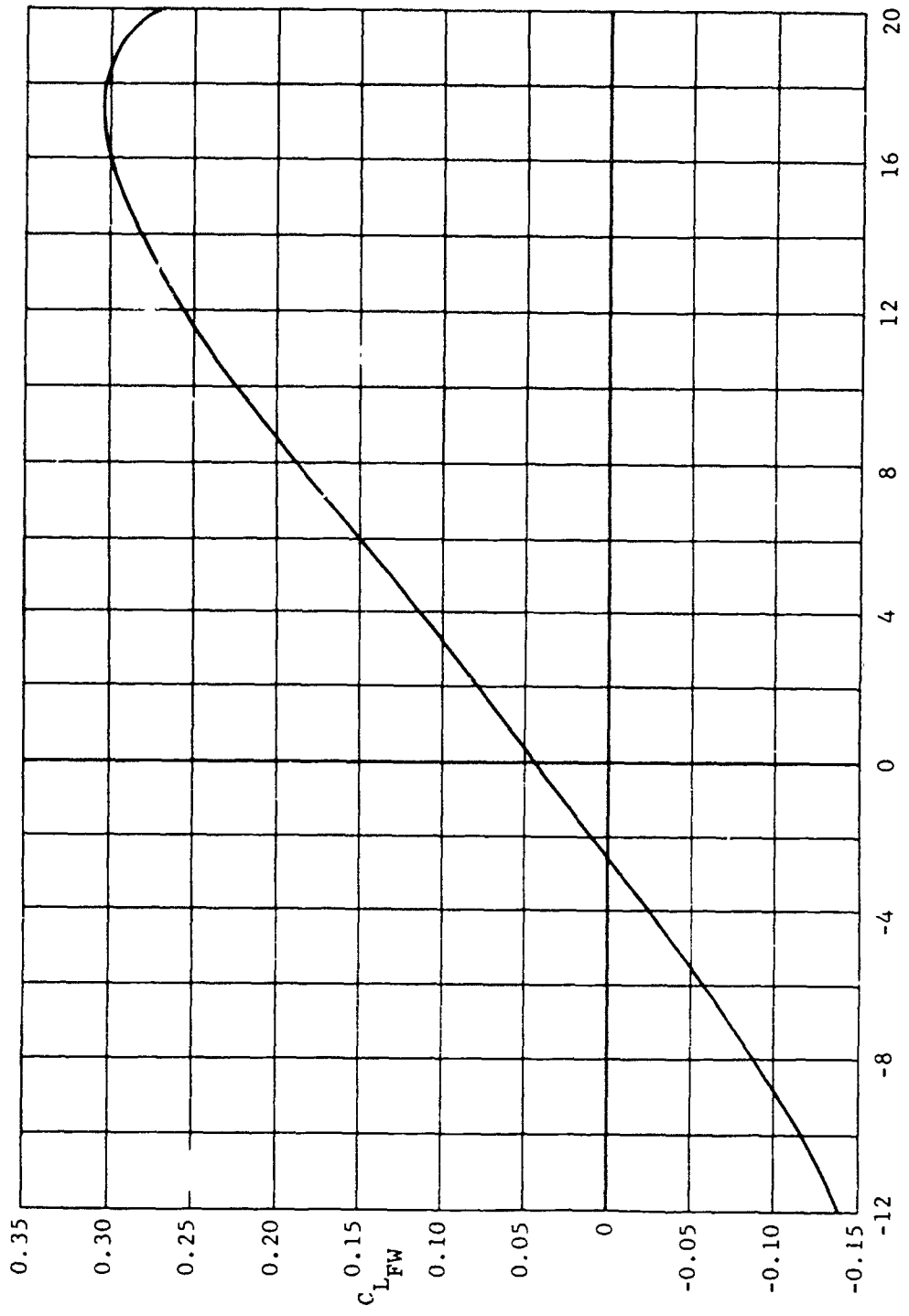

Figure 244. X-19, exposed front wing lift coefficient; S_{ref} = 154.6 square feet.

FURNISHED UNDER UNITED STATES GOVERNMENT CONTRACT No. AF33(615)-3940. SHALL NOT BE EITHER RELEASED OUTSIDE THE GOVERNMENT, OR USED DUPLICATED, OR DISCLOSED IN WHOLE OR IN PART FOR MANUFACTURE OR PROCUREMENT, WITHOUT THE WRITTEN PERMISSION OF CURTISS-WRIGHT CORPORATION, EXCEPT FOR (i) EMERGENCY REPAIR OR OVERHAUL WORK BY OR FOR THE GOVERNMENT WHERE THE ITEM OR PROCESS IS NOT OTHERWISE REASONABLY AVAILABLE TO ENABLE TIMELY PERFORMANCE OF THE WORK, OR (ii) RELEASE TO A FOREIGN GOVERNMENT, AS THE INTERESTS OF THE UNITED STATES MAY REQUIRE. PROVIDED THAT IN EITHER CASE THE RELEASE, USE, DUPLICATION OR DISCLOSURE HEREOF SHALL BE SUBJECT TO THE FOREGOING LIMITATIONS. THIS LEGEND SHALL BE MARKED ON ANY REPRODUCTION HEREOF IN WHOLE OR IN PART."

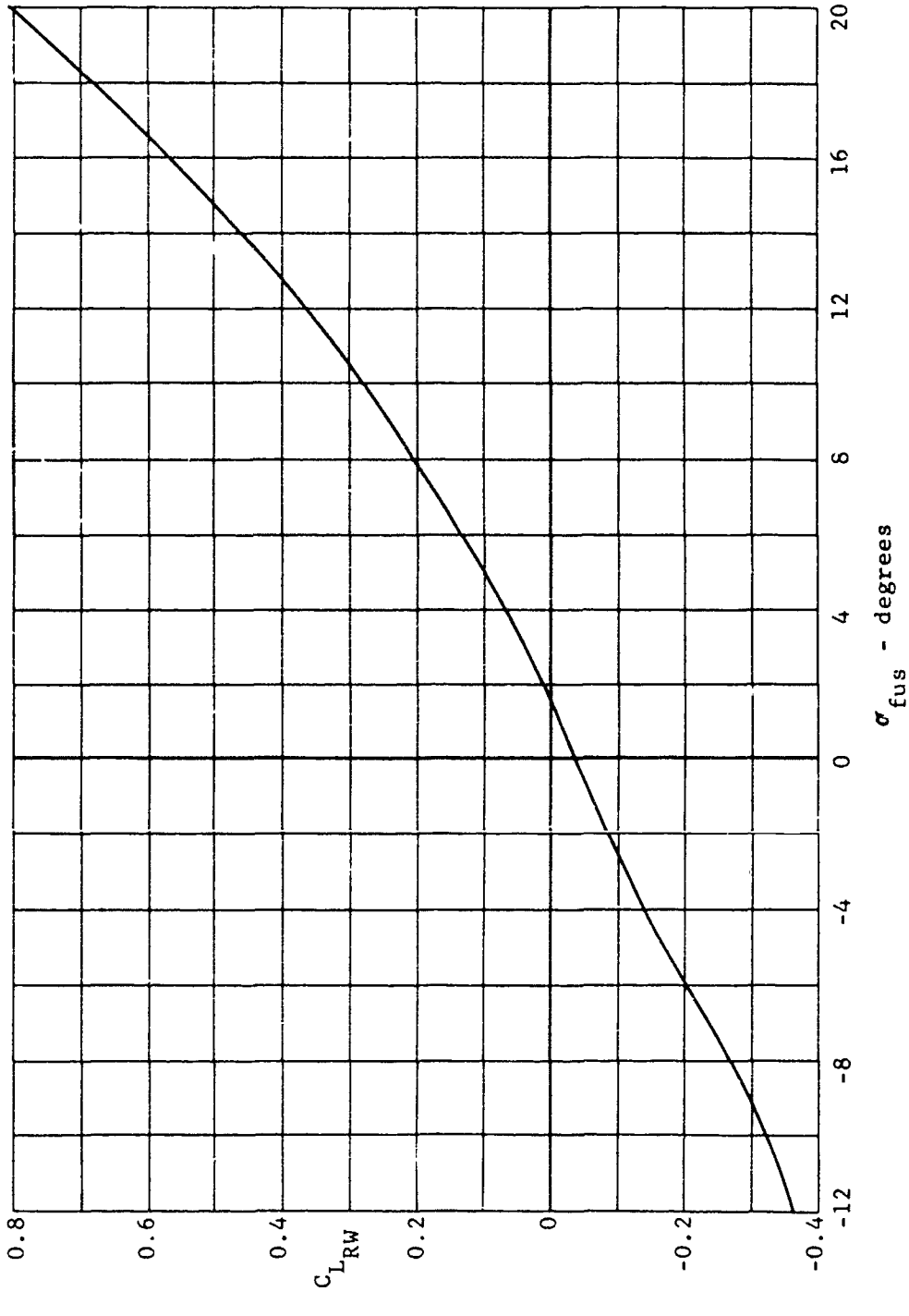

Figure 245. X-19, exposed rear wing lift coefficient; S_{ref} = 154.6 square feet, (external to BL 16.7 inches).

"FURNISHED UNDER UNITED STATES GOVERNMENT CONTRACT No. AF33(615)-3940. SHALL NOT BE EITHER RELEASED OUTSIDE THE GOVERNMENT OR USED DUPLICATED, OR DISCLOSED IN WHOLE OR IN PART FOR MANUFACTURE OR PROCUREMENT, WITHOUT THE WRITTEN PERMISSION OF CURTISS-WRIGHT CORPORATION, EXCEPT FOR (i) EMERGENCY REPAIR OR OVERHAUL WORK BY OR FOR THE GOVERNMENT, WHERE THE ITEM OR PROCESS IS NOT OTHERWISE REASONABLY AVAILABLE TO ENABLE TIMELY PERFORMANCE OF THE WORK, OR (ii) RELEASE TO A FOREIGN GOVERNMENT AS THE INTERESTS OF THE UNITED STATES MAY REQUIRE PROVIDED THAT IN EITHER CASE THE RELEASE, USE, DUPLICATION OR DISCLOSURE HEREOF SHALL BE SUBJECT TO THE FOREGOING LIMITATIONS THIS LEGEND SHALL BE MARKED ON ANY REPRODUCTION HEREOF IN WHOLE OR IN PART."

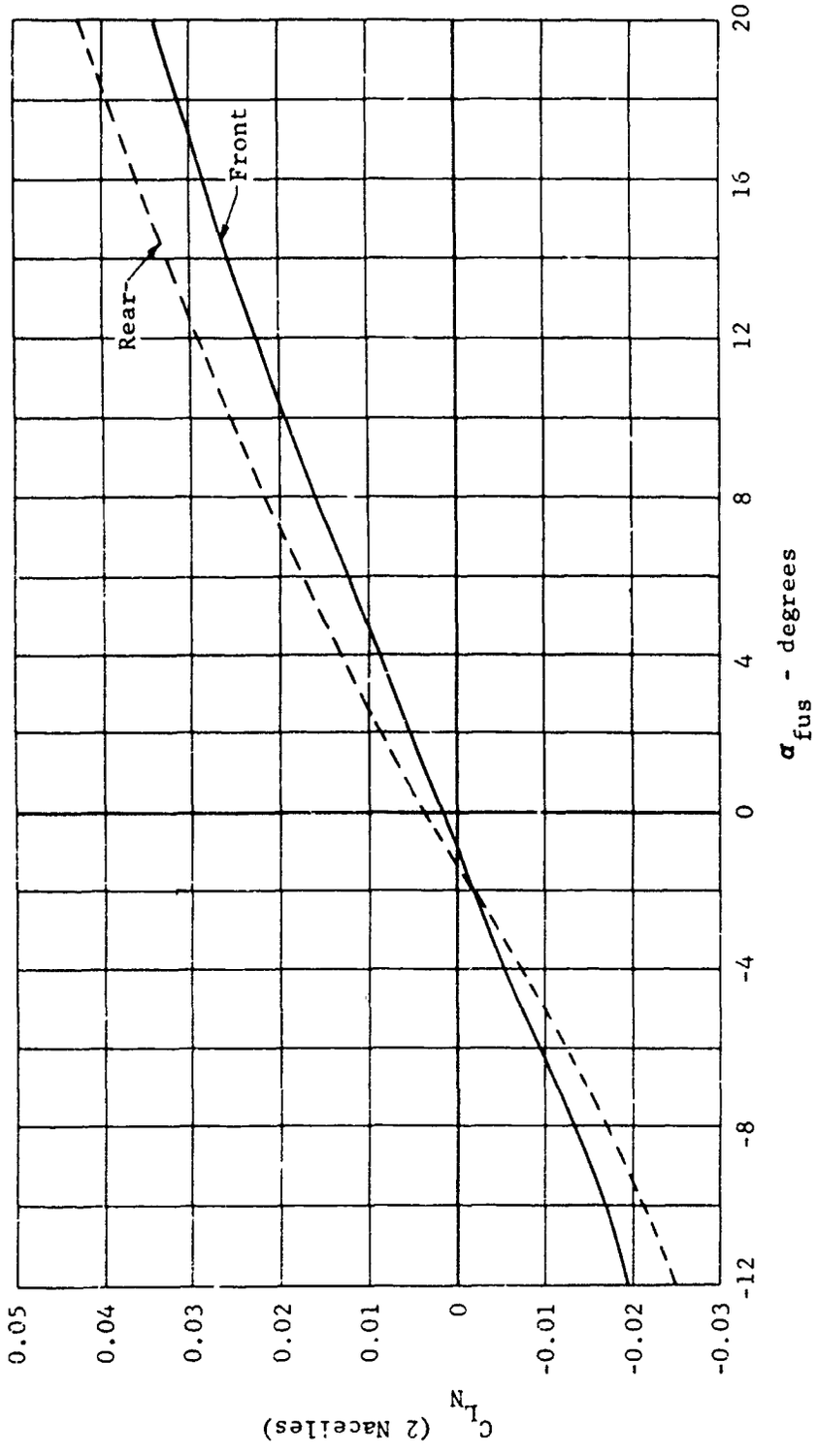

Figure 246. X-19, nacelle lift coefficients; S_{ref} = 154.6 square feet.

FURNISHED UNDER UNITED STATES GOVERNMENT CONTRACT No. AF33(615)-3940 SHALL NOT BE EITHER RELEASED OUTSIDE THE GOVERNMENT OR USED, DUPLICATED, OR DISCLOSED IN WHOLE OR IN PART FOR MANUFACTURE OR PROCUREMENT, WITHOUT THE WRITTEN PERMISSION OF CURTISS-WRIGHT CORPORATION, EXCEPT FOR (i) EMERGENCY REPAIR OR OVERHAUL WORK BY OR FOR THE GOVERNMENT, WHERE THE ITEM OR PROCESS IS NOT OTHERWISE REASONABLY AVAILABLE TO ENABLE T MELY PERFORMANCE OF THE WORK, OR (ii) RELEASE TO A FOREIGN GOVERNMENT, AS THE INTERESTS OF THE UNITED STATES MAY REQUIRE, PROVIDED THAT IN EITHER CASE THE RELEASE, USE DUPLICATION OR DISCLOSURE HEREOF SHALL BE SUBJECT TO THE FOREGOING LIMITATIONS THIS LEGEND SHALL BE MARKED ON ANY REPRODUCTION HEREOF IN WHOLE OR IN PART."

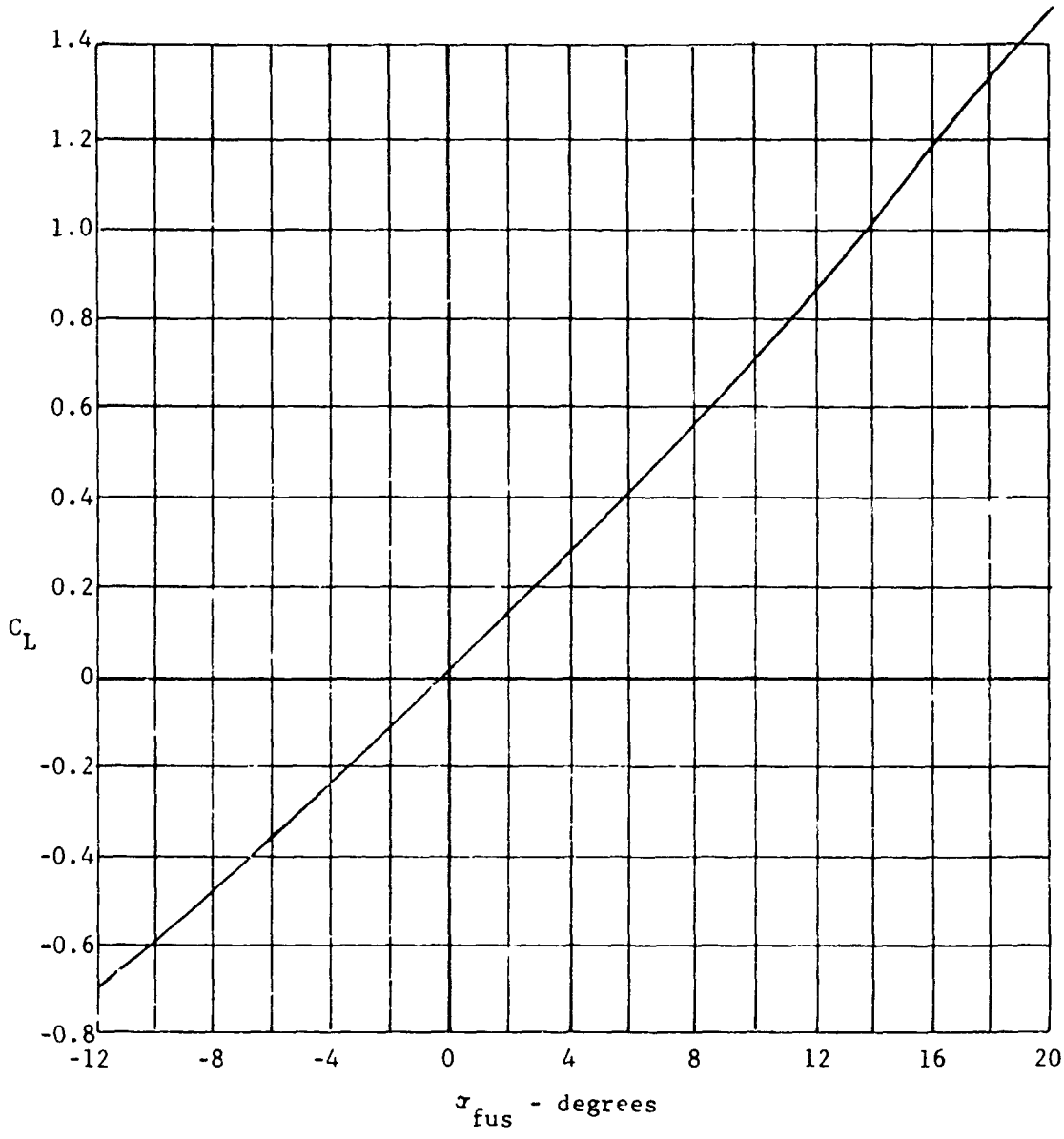

Figure 247. X-19, lift coefficient of complete airplane - propellers off; S_{ref} = 154.6 square feet.

"FURNISHED UNDER UNITED STATES GOVERNMENT CONTRACT No. AF33(615)-3940. SHALL NOT BE EITHER RELEASED OUTSIDE THE GOVERNMENT, OR USED, DUPLICATED, OR DISCLOSED IN WHOLE OR IN PART FOR MANUFACTURE OR PROCUREMENT, WITHOUT THE WRITTEN PERMISSION OF CURTISS-WRIGHT CORPORATION, EXCEPT FOR (i) EMERGENCY REPAIR OR OVERHAUL WORK BY OR FOR THE GOVERNMENT, WHERE THE ITEM OR PROCESS IS NOT OTHERWISE REASONABLY AVAILABLE TO ENABLE TIMELY PERFORMANCE OF THE WORK, OR (ii) RELEASE TO A FOREIGN GOVERNMENT, AS THE INTERESTS OF THE UNITED STATES MAY REQUIRE. PROVIDED THAT IN EITHER CASE THE RELEASE, USE, DUPLICATION OR DISCLOSURE HEREOF SHALL BE SUBJECT TO THE FOREGOING LIMITATIONS. THIS LEGEND SHALL BE MARKED ON ANY REPRODUCTION HEREOF IN WHOLE OR IN PART."

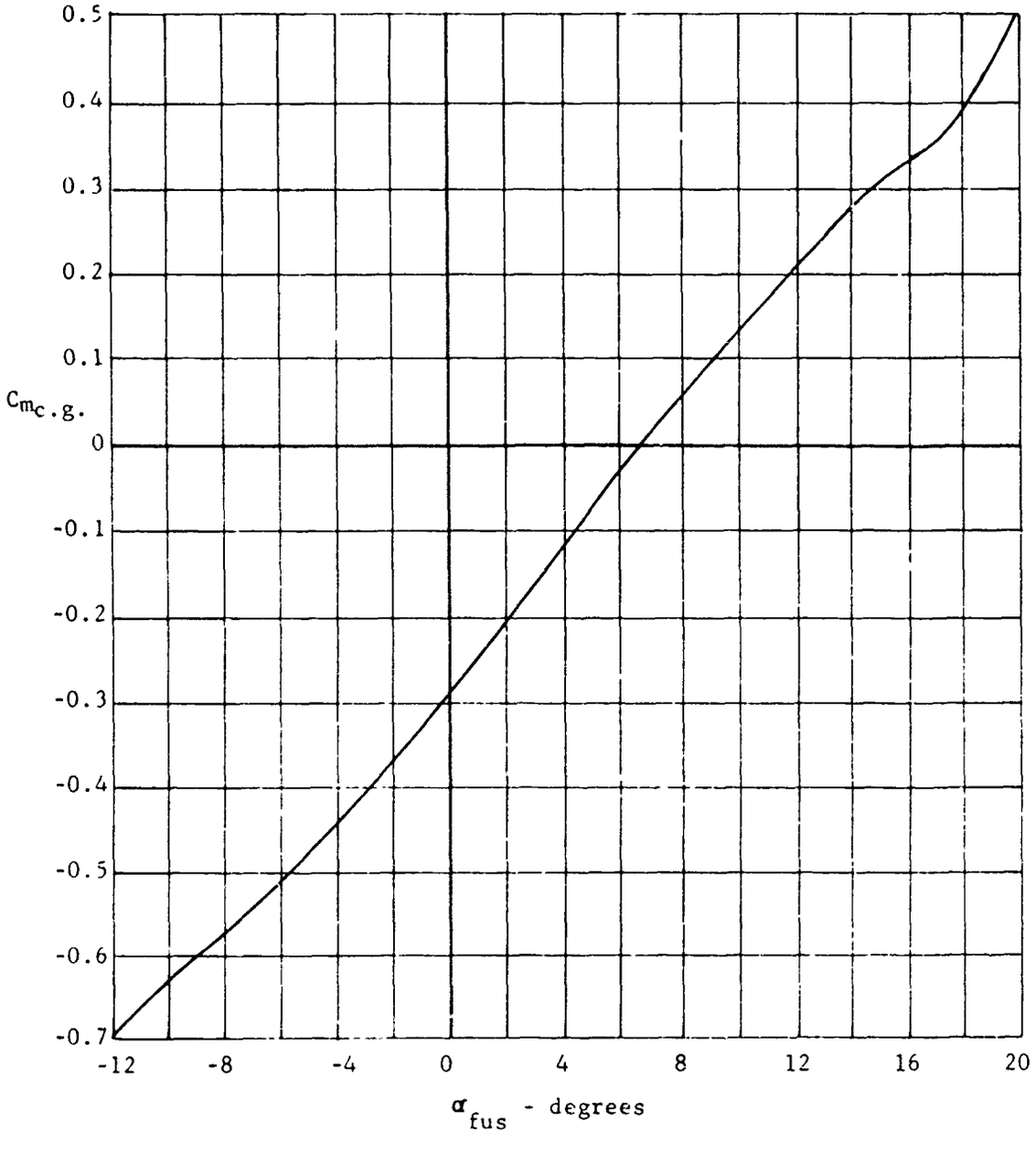

Figure 248. X-19, pitching moment coefficient of fuselage alone about the 42.9% c.g.; S_{ref} = 154.6 squre feet, $\bar{c}$ = 2.875 feet.

FURNISHED UNDER UNITED STATES GOVERNMENT CONTRACT No AF33(615)-3940 SHALL NOT BE EITHER RELEASED OUTSIDE THE GOVERNMENT OR USED, DUPLICATED, OR DISCLOSED IN WHOLE OR IN PART FOR MANUFACTURE OR PROCUREMENT, WITHOUT THE WRITTEN PERMISSION OF CURTISS-WRIGHT CORPORATION. EXCEPT FOR (i) EMERGENCY REPAIR OR OVERHAUL WORK BY OR FOR THE GOVERNMENT, WHERE THE ITEM OR PROCESS IS NOT OTHERWISE REASONABLY AVAILABLE TO ENABLE TIMELY PERFORMANCE OF THE WORK, OR (ii) RELEASE TO A FOREIGN GOVERNMENT AS THE INTERESTS OF THE UNITED STATES MAY REQUIRE PROVIDED THAT IN EITHER CASE THE RELEASE, USE, DUPLICATION OR DISCLOSURE HEREOF SHALL BE SUBJECT TO THE FOREGOING LIMITATIONS THIS LEGEND SHALL BE MARKED ON ANY REPRODUCTION HEREOF IN WHOLE OR IN PART."

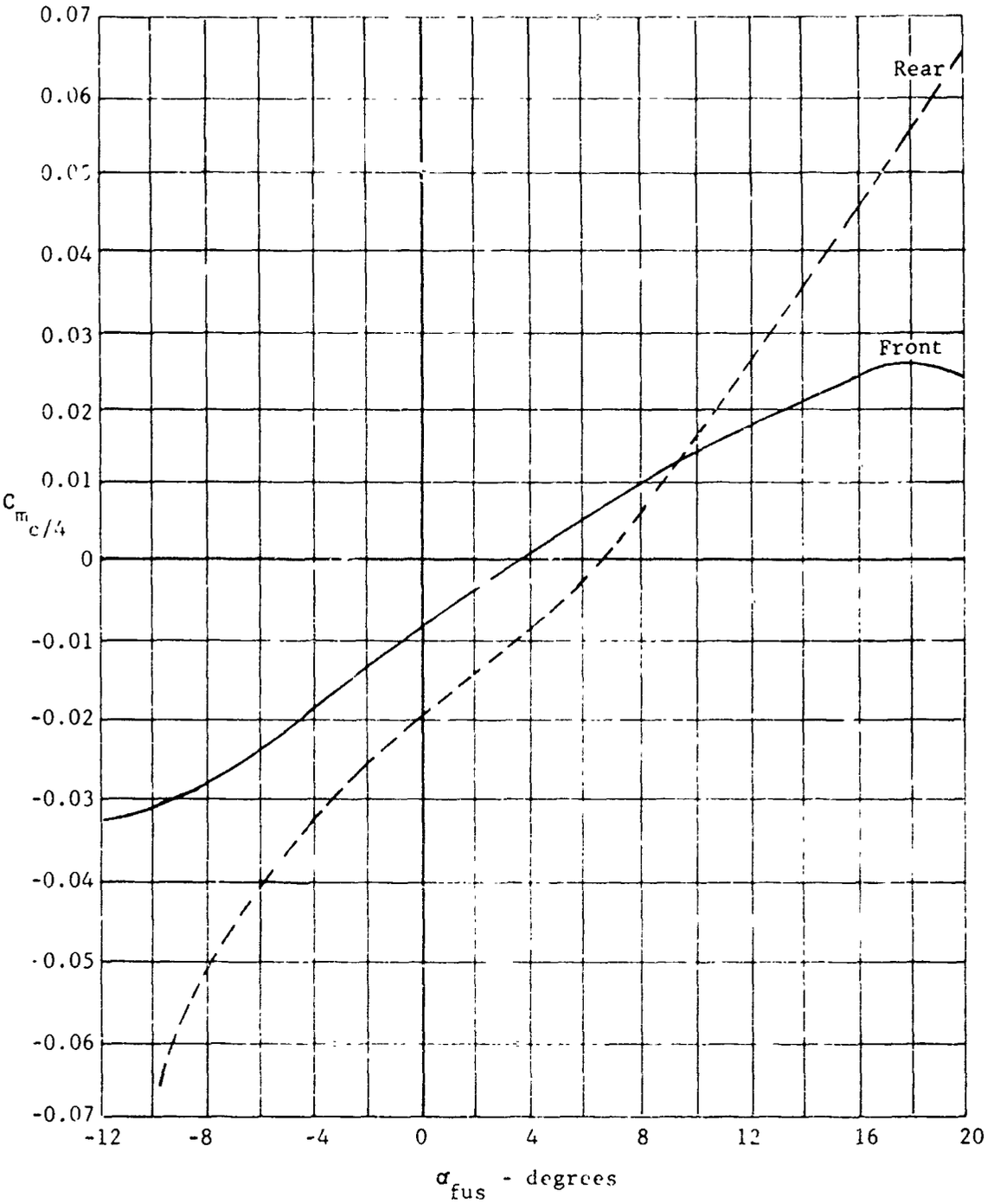

Figure 249. X-19, exposed front and rear wing pitching moments about respective quarter chords; S_{ref} = 154.6 square feet, $\bar{c}$ = 2.875 feet.

"FURNISHED UNDER UNITED STATES GOVERNMENT CONTRACT No. AF33(615)-3940. SHALL NOT BE EITHER RELEASED OUTSIDE THE GOVERNMENT, OR USED, DUPLICATED, OR DISCLOSED IN WHOLE OR IN PART FOR MANUFACTURE OR PROCUREMENT, WITHOUT THE WRITTEN PERMISSION OF CURTISS-WRIGHT CORPORATION, EXCEPT FOR (i) EMERGENCY REPAIR OR OVERHAUL WORK BY OR FOR THE GOVERNMENT, WHERE THE ITEM OR PROCESS IS NOT OTHERWISE REASONABLY AVAILABLE TO ENABLE TIMELY PERFORMANCE OF THE WORK, OR (ii) RELEASE TO A FOREIGN GOVERNMENT, AS THE INTERESTS OF THE UNITED STATES MAY REQUIRE. PROVIDED THAT IN EITHER CASE THE RELEASE, USE, DUPLICATION OR DISCLOSURE HEREOF SHALL BE SUBJECT TO THE FOREGOING LIMITATIONS. THIS LEGEND SHALL BE MARKED ON ANY REPRODUCTION HEREOF IN WHOLE OR IN PART."

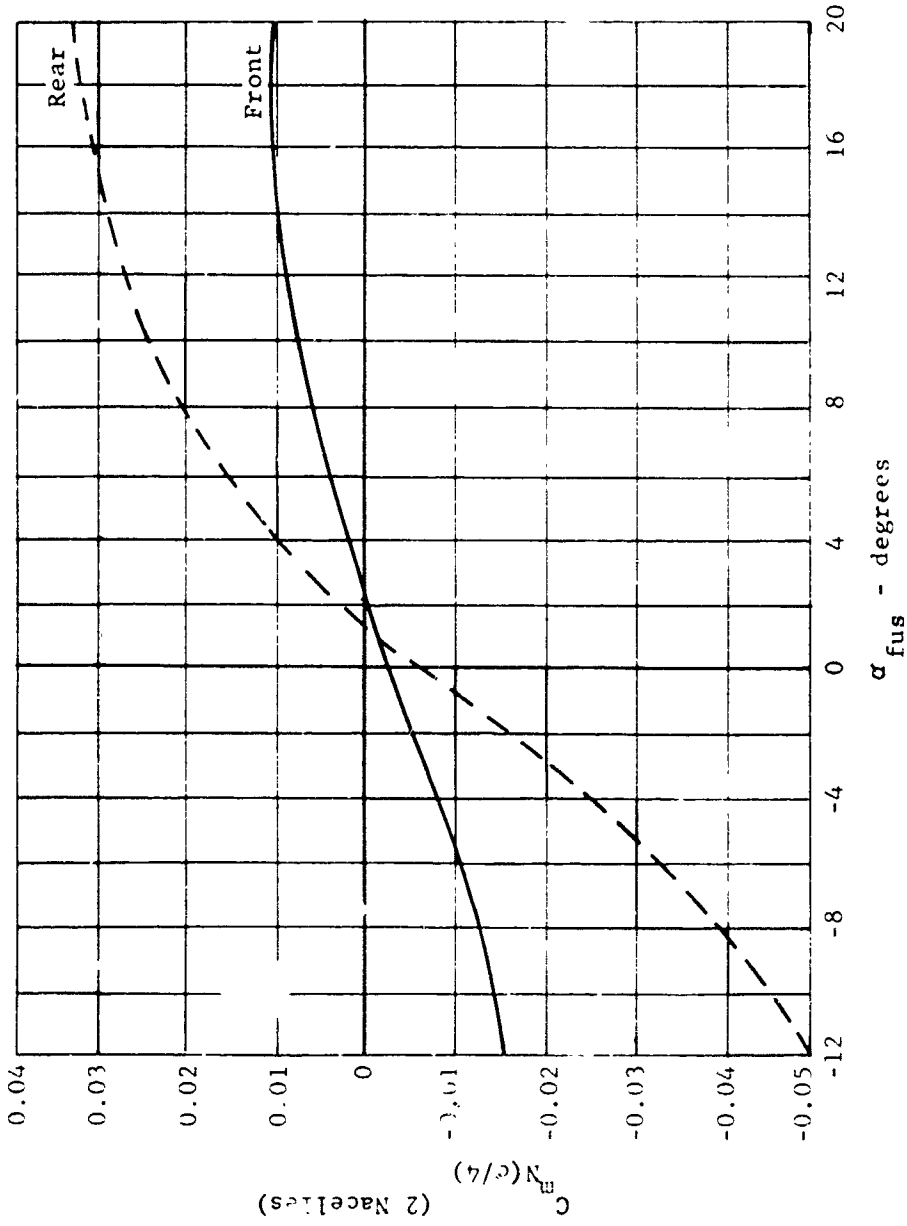

Figure 250. X-19, nacelle pitching moments about respective wing quarter chords; S_{ref} = 154.6 square feet, $\bar{c}$ = 2.875 feet.

FURNISHED UNDER UNITED STATES GOVERNMENT CONTRACT No. AF3 (615)-3940. SHALL NOT BE EITHER RELEASED OUTSIDE THE GOVERNMENT OR USED, DUPLICATED, OR DISCLOSED IN WHOLE OR IN PART FOR MANUFACTURE OR PROCUREMENT, WITHOUT THE WRITTEN PERMISSION OF CURTISS-WRIGHT CORPORATION, EXCEPT FOR (i) EMERGENCY REPAIR OR OVERHAUL WORK BY OR FOR THE GOVERNMENT, WHERE THE ITEM OR PROCESS IS NOT OTHERWISE REASONABLY AVAILABLE TO ENABLE TIMELY PERFORMANCE OF THE WORK, OR (ii) RELEASE TO A FOREIGN GOVERNMENT, AS THE INTERESTS OF THE UNITED STATES MAY REQUIRE, PROVIDED THAT IN EITHER CASE THE RELEASE, USE, DUPLICATION OR DISCLOSURE HEREOF SHALL BE SUBJECT TO THE FOREGOING LIMITATIONS. THIS LEGEND SHALL BE MARKED ON ANY REPRODUCTION HEREOF IN WHOLE OR IN PART."

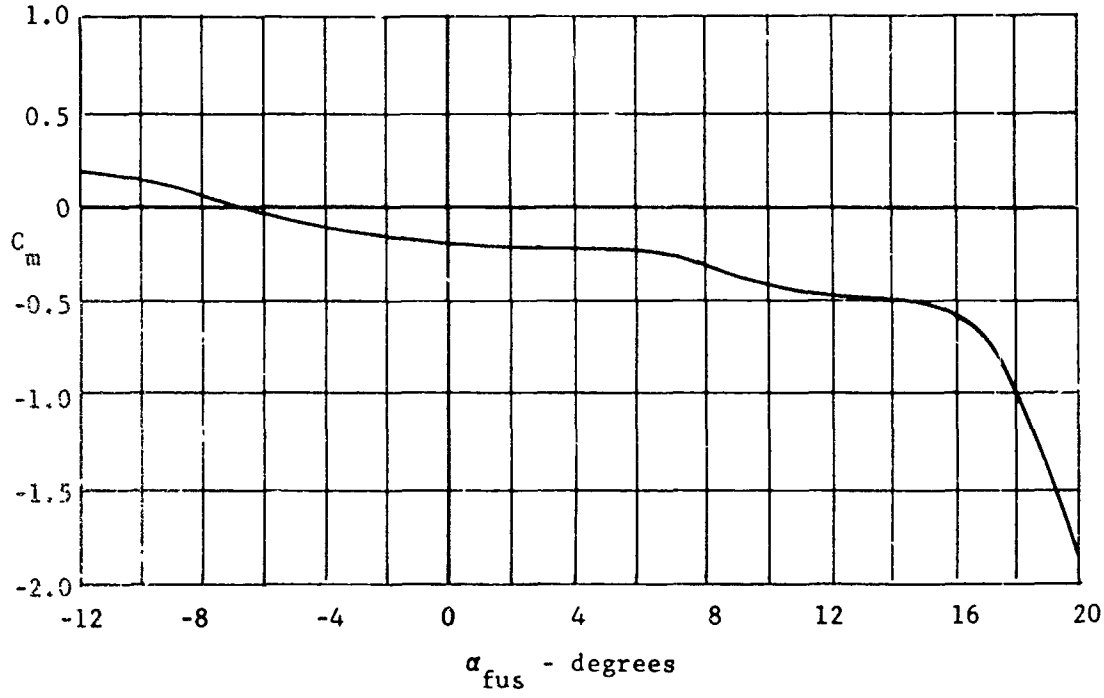

Figure 251. X-19, pitching moment of complete airplane about the 42.9% c.g., propellers off; S_{ref} = 154.6 square feet, $\bar{c}$ = 2.875 feet.

FURNISHED UNDER UNITED STATES GOVERNMENT CONTRACT No. AF33(615)-3940. SHALL NOT BE EITHER RELEASED OUTSIDE THE GOVERNMENT, OR USED, DUPLICATED, OR DISCLOSED IN WHOLE OR IN PART FOR MANUFACTURE OR PROCUREMENT, WITHOUT THE WRITTEN PERMISSION OF CURTISS-WRIGHT CORPORATION, EXCEPT FOR (i) EMERGENCY REPAIR OR OVERHAUL WORK BY OR FOR THE GOVERNMENT, WHERE THE ITEM OR PROCESS IS NOT OTHERWISE REASONABLY AVAILABLE TO ENABLE TIMELY PERFORMANCE OF THE WORK, OR (ii) RELEASE TO A FOREIGN GOVERNMENT, AS THE INTERESTS OF THE UNITED STATES MAY REQUIRE. PROVIDED THAT IN EITHER CASE THE RELEASE, USE, DUPLICATION OR DISCLOSURE HEREOF SHALL BE SUBJECT TO THE FOREGOING LIMITATIONS. THIS LEGEND SHALL BE MARKED ON ANY REPRODUCTION HEREOF IN WHOLE OR IN PART.

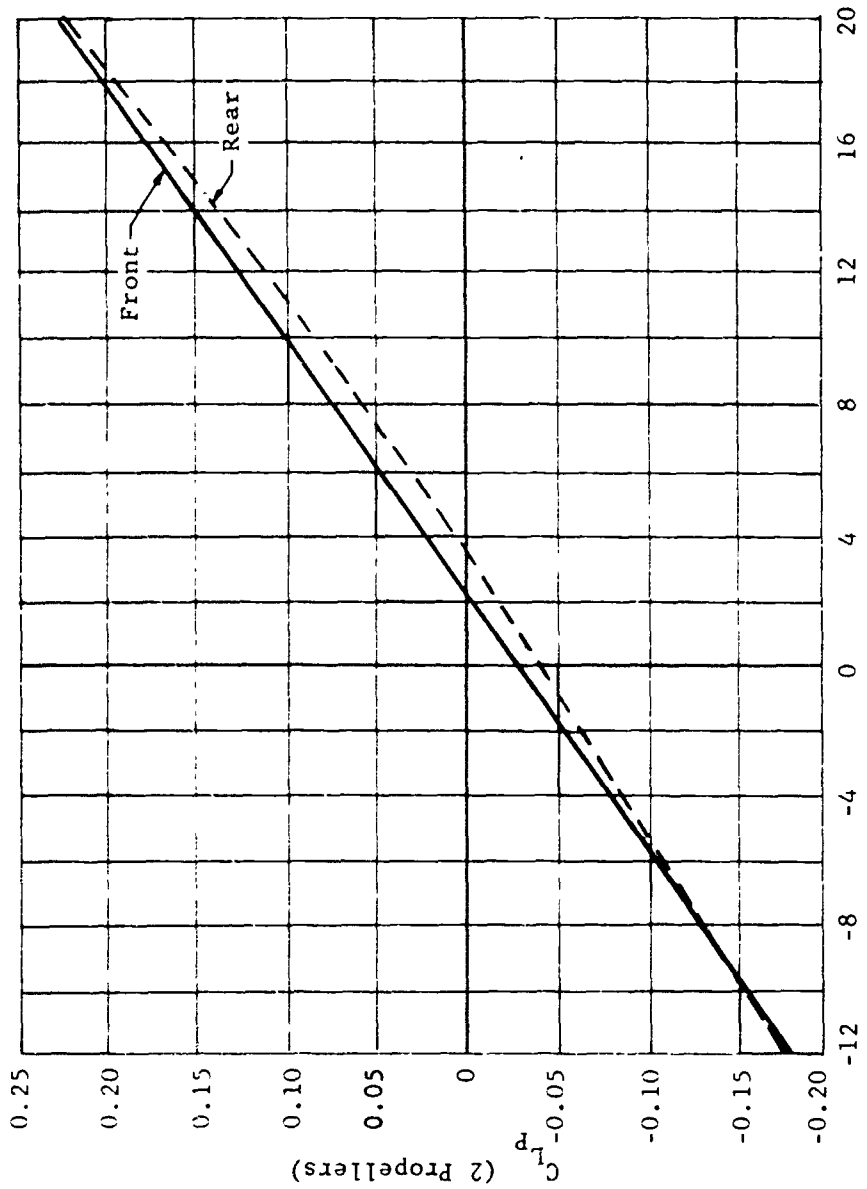

Figure 252. X-19, propeller lift coefficients, front and rear; S_{ref} = 154.6 square feet.

FURNISHED UNDER UNITED STATES GOVERNMENT CONTRACT No. AF33(615)-3940. SHALL NOT BE EITHER RELEASED OUTSIDE THE GOVERNMENT OR USED, DUPLICATED, OR DISCLOSED IN WHOLE OR IN PART FOR MANUFACTURE OR PROCUREMENT, WITHOUT THE WRITTEN PERMISSION OF CURTISS-WRIGHT CORPORATION, EXCEPT FOR (i) EMERGENCY REPAIR OR OVERHAUL WORK BY OR FOR THE GOVERNMENT, WHERE THE ITEM OR PROCESS IS NOT OTHERWISE REASONABLY AVAILABLE TO ENABLE TIMELY PERFORMANCE OF THE WORK, OR (ii) RELEASE TO A FOREIGN GOVERNMENT, AS THE INTERESTS OF THE UNITED STATES MAY REQUIRE. PROVIDED THAT IN EITHER CASE THE RELEASE, USE, DUPLICATION OR DISCLOSURE HEREOF SHALL BE SUBJECT TO THE FOREGOING LIMITATIONS. THIS LEGEND SHALL BE MARKED ON ANY REPRODUCTION HEREOF IN WHOLE OR IN PART.

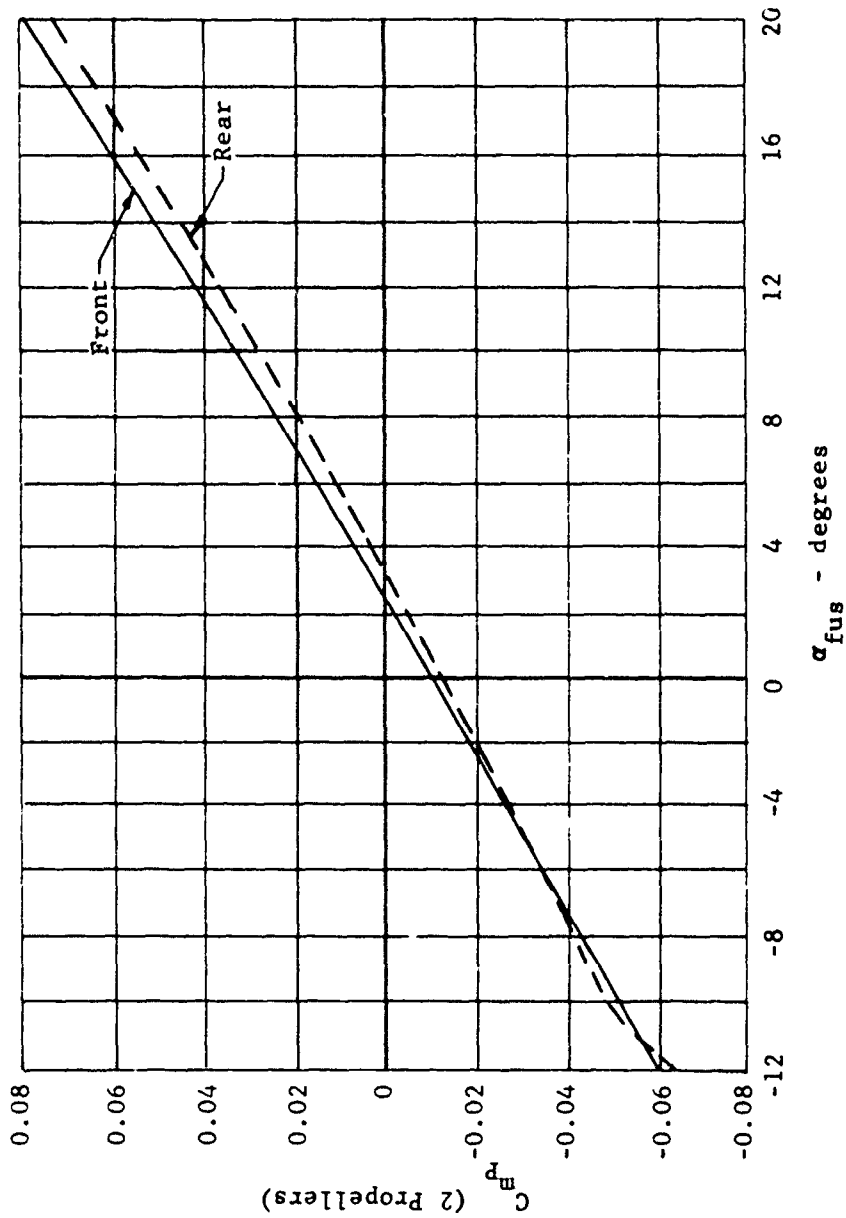

Figure 253. X-19, propeller pitching moment coefficients, front and rear; S_{ref} 154.6 square feet, $\bar{c}$ = 2.875 feet.

FURNISHED UNDER UNITED STATES GOVERNMENT CONTRACT No. AF33(615)-3940. SHALL NOT BE EITHER RELEASED OUTSIDE THE GOVERNMENT, OR USED, DUPLICATED, OR DISCLOSED IN WHOLE OR IN PART FOR MANUFACTURE OR PROCUREMENT, WITHOUT THE WRITTEN PERMISSION OF CURTISS-WRIGHT CORPORATION, EXCEPT FOR (i) EMERGENCY REPAIR OR OVERHAUL WORK BY OR FOR THE GOVERNMENT, WHERE THE ITEM OR PROCESS IS NOT OTHERWISE REASONABLY AVAILABLE TO ENABLE TIMELY PERFORMANCE OF THE WORK, OR (ii) RELEASE TO A FOREIGN GOVERNMENT, AS THE INTERESTS OF THE UNITED STATES MAY REQUIRE. PROVIDED THAT IN EITHER CASE THE RELEASE, USE, DUPLICATION OR DISCLOSURE HEREOF SHALL BE SUBJECT TO THE FOREGOING LIMITATIONS. THIS LEGEND SHALL BE MARKED ON ANY REPRODUCTION HEREOF IN WHOLE OR IN PART.

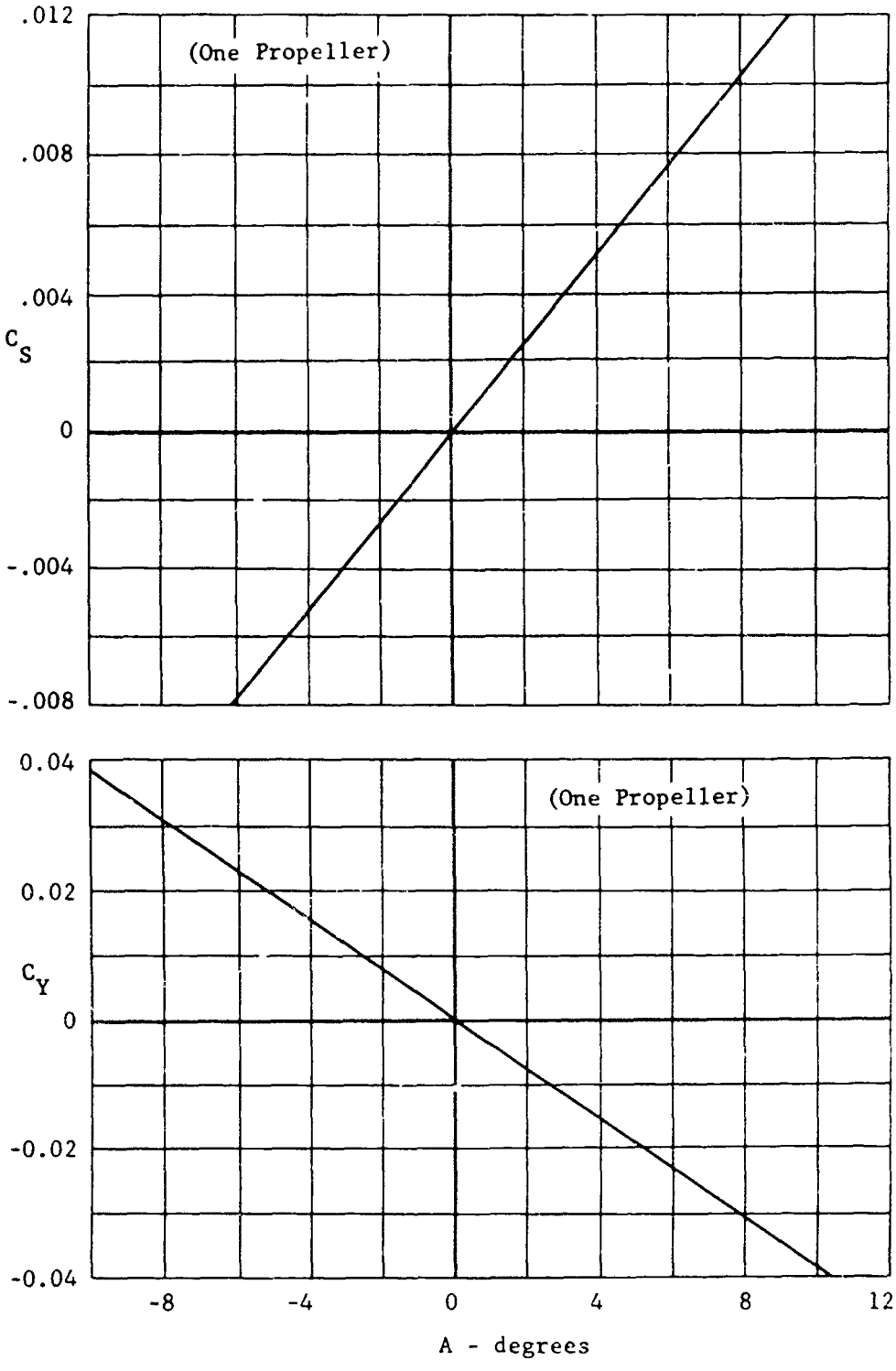

Figure 254. X-19, propeller side force and yawing moment coefficient; S_{ref} = 154.6 square feet, $\bar{c}$ = 2.875 feet.

FURNISHED UNDER UNITED STATES GOVERNMENT CONTRACT No. AF33(615)-3940. SHALL NOT BE EITHER RELEASED OUTSIDE THE GOVERNMENT OR USED, DUPLICATED, OR DISCLOSED IN WHOLE OR IN PART FOR MANUFACTURE OR PROCUREMENT, WITHOUT THE WRITTEN PERMISSION OF CURTISS-WRIGHT CORPORATION, EXCEPT FOR (i) EMERGENCY REPAIR OR OVERHAUL WORK BY OR FOR THE GOVERNMENT, WHERE THE ITEM OR PROCESS IS NOT OTHERWISE REASONABLY AVAILABLE TO ENABLE TIMELY PERFORMANCE OF THE WORK, OR (ii) RELEASE TO A FOREIGN GOVERNMENT, AS THE INTERESTS OF THE UNITED STATES MAY REQUIRE. PROVIDED THAT IN EITHER CASE THE RELEASE, USE, DUPLICATION OR DISCLOSURE HEREOF SHALL BE SUBJECT TO THE FOREGOING LIMITATIONS. THIS LEGEND SHALL BE MARKED ON ANY REPRODUCTION HEREOF IN WHOLE OR IN PART.

1. The Propeller Rotation Will be Viewed From the Rear of the Airplane Looking Forwards.

2. The Right Hand "Corkscrew Rule" Will be Applied, Thus Rotation in a Clockwise Sense is Positive, and Rotation in an Anti-Clockwise Sense is Negative.

3. The Following Rotations Exist on the Airplane,

	Front Propellers	Rear Propellers
Left	Negative Rotation	Positive Rotation
Right	Positive Rotation	Negative Rotation

4. The Coefficients Given on Figure 254 are for Positive Rotations.

Figure 255. Propeller sign convention.

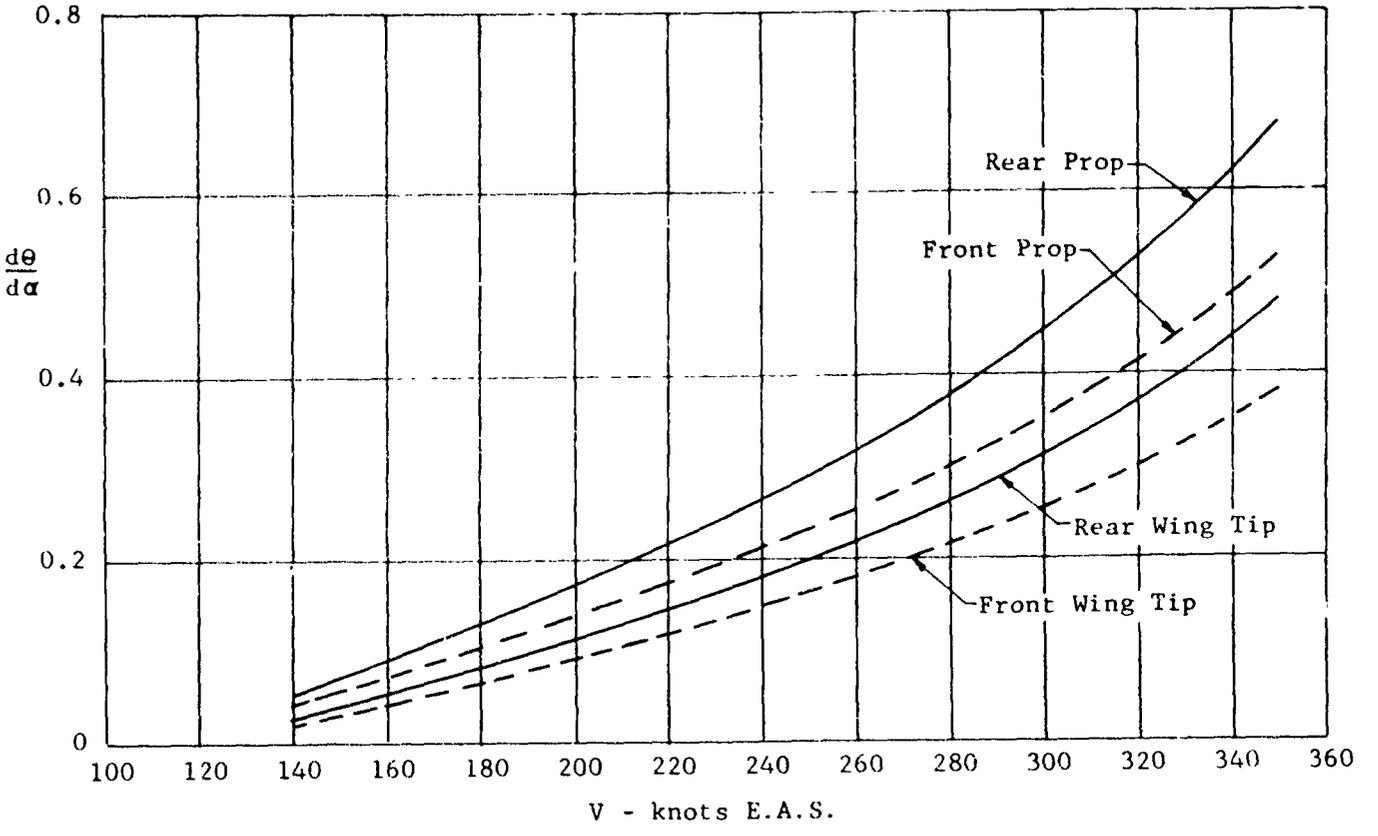

Figure 256. X-19, aeroelastic wing and propeller twist derivatives.

e. Effects of Reynolds Number

The tunnel tests on the X-19 configuration were performed at Reynolds Numbers considerably less than those expected under cruise conditions (i.e. 0.75×10^6 compared with 6×10^6), (86) through (89). These tests indicate that an increase in $C_{L_{max}}$, coupled with no change in lift curve slope, will result from an increase in Re from test values to cruise values for isolated wings.

By applying this correction to the tunnel results for the front wing, an allowance was made for Re change. Comparing C_{L_α} curves of front and rear wing, an adjustment was made to the rear wing to allow for the new front wing C_L curve. A change in downwash results from a change in front wing lift. No Reynolds Number correction was applied to the fuselage.

f. Effects of Aeroelastic Twist

(1) Due to Angle of Attack

In (90) a method has been derived for the evaluation of wing twist due to aerodynamic and inertial loads. This method presents the twist of the nacelle centerline as a function of angle of attack in the form of a derivative $d\theta/d\alpha$. In this analysis, the wing torsional stiffness and the lift distribution have been assumed constant along the wing span, which then resulted in considerable analytical simplification, These assumptions are justifiable and the $d\theta/d\alpha$ is expected to be a fairly close estimation.

Subsequent to this analysis, an allowance was made for added flexibility between nacelle and wing, and these results are shown in Figure 278.

(2) Due to Aileron Deflection

A Curtiss-Wright study was made which developed a theoretical estimate of the wing twist due to aileron deflection and the corresponding loss in rolling effectiveness. The results of this study are based upon linear aerodynamic derivatives and assume a constant G.J. along the wing semi-span (G.J. = 2.5×10^6 lb ft.^{2}). A typical spanwise load distribution due to aileron deflection was approximated in this analysis with the essential loading characteristics being utilized (see Figure 279).

Figure 280 gives the wing twist due to aileron deflection and

Figure 281 the loss in rolling effectiveness.

g. Drag Distribution

(1) Induced Drag Breakdown

The induced drag of the complete airplane, power-on, trimmed, is given as

$$D_i = \left\{ C_L^2 \quad \left(\frac{\partial C_D}{\partial C_L^2}\right) \right\} qS$$

where $\left(\frac{\partial C_D}{\partial C_L^2}\right)$ is given in Figure 282

and $C_L = \left(\frac{nW}{qS}\right)$

This drag is assumed to be distributed between front wing, rear wing and fuselage as follows:

(a) Exposed front wing including nacelles = 35%

(b) Exposed rear wing including nacelles = 45%

(c) Fuselage = 20%

100%

The drags may be distributed on the wings and nacelles according to the spanwise lift distribution on each wing.

(2) Profile Drag Breakdown

The total profile drag of the aircraft is given in Figure 282, which has been derived from a profile drag buildup analysis based on the aircraft exterior configuration drawing.

This drag is assumed to be distributed as follows:

Fuselage	= 39.5%
Front Wing	= 9.3%
Rear Wing	= 16.1%
Vertical Tail	= 7.6%
Nacelles	= 11.4%
Minor Fittings	= 12.6%
Interference	= 3.5%
	100.0%

h. Flight Envelope

(1) Design Speeds

The flight envelope as defined in C.A.R. 4b.211 Figure 4.b2 in (72) has been assumed applicable to the X-19 in cruise, where the design dive speed, V_D, and the design crusing speed, V_c, have been chosen as follows:

Design dive speed, V_D = 347 knots E.A.S.

Design cruising speed, V_c = 271 knots E.A.S.

(2) Maximum Positive Maneuvering Load Factor

The maximum positive maneuvering load factor for W = 13,660 lb has been derived from + 3.0 g at W = 12,300 lb such that the product nW (i.e. the gross lift) remains unaltered.

Maximum positive maneuvering n = 2.70g

(3) Minimum Negative Maneuvering Load Factor

The minimum negative maneuvering load factor is as defined in (77), Paragraph 4b.211 (a) (2), thus,

Minimum negative n = -1.0g

(4) Flight Envelope 'Stall' Curve

Power off data indicates that the front wing stalls at an angle of attack of approximately 17°. This angle of attack has been used to establish the positive 'stall' curve on the flight envelope. Up to an angle of attack of -12°, neither the front wing nor the rear wing stalls in the negative direction and so, to complete the flight envelope, it has been assumed that the negative stall curve is the mirror image of the positive stall curve.

In the estimation of these curves, due allowance has been made for the large elevator induced loads, and the propeller normal force upon the total aerodynamic lift forces.

The resulting flight envelope is shown in Figure 257.

i. Symetrical Gust Envelope

The symetrical vertical gust envelope as recommended in (77),

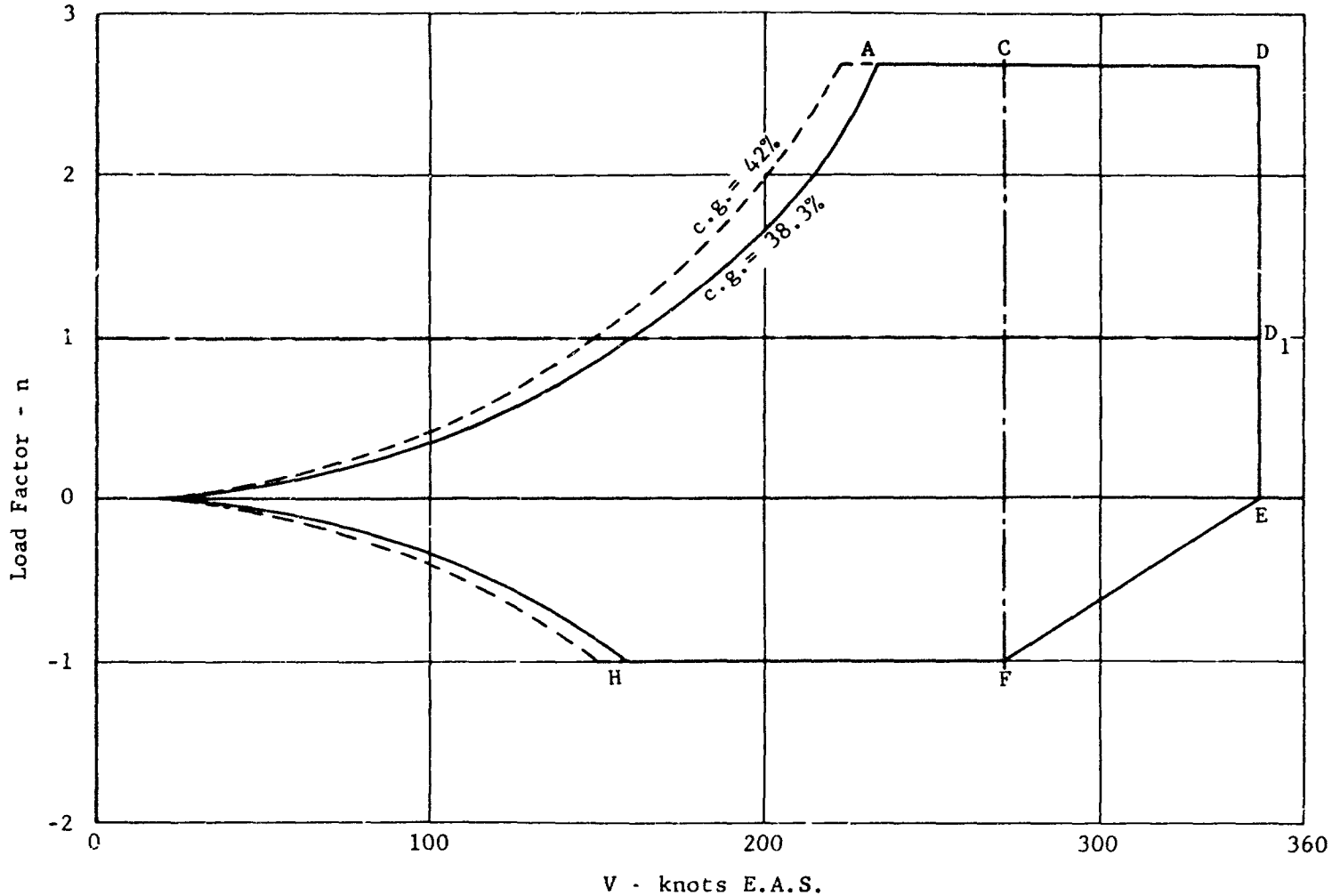

Figure 257. X-19, V-N diagram; W = 13,660 pounds.

Paragraph 4b.211 (b), Figure 4b-3, has been assumed applicable to the X-19 aircraft.

The gust load factors have been calculated by the following formula which is based upon a simple static analysis:

$$n_{gust} = 1 \pm \frac{K.U.V.a}{575(W/S)}$$

where K = Factor to convert a sharp-edged gust into an equivalent sharp-edged gust

$$= 1.33 - \frac{2.67}{(W/S)^{3/4}} \quad \text{for } (W/S) > 16 \text{ lb/sq}^2$$

and U = nominal gust velocity in feet per sec.,E.A.S.

V = aircraft speed in m.p.h., E.A.S.

a = aircraft lift slope per radian (including propeller effects).

W = aircraft weight, lb

S = aircraft total wing area = 154.6 ft^2

Nominal gust intensities of 15, 30 and 40 feet per second E.A.S. have been investigated and the results are shown in Figure 258.

From an analysis of the transient response of the X-19 to a vertical sharp-edged gust, it was found that the maximum load factor reached, following the gust impact, will be slightly less than that given by the expression above.

From this analysis, it is also apparent that the X-19 behaves like a conventional airplane in a vertical gust and therefore no special gust envelope need be considered for stressing purposes.

j. Balance Equations

As stated in Paragraph 2 (b) of this Section, the aerodynamic forces acting on the aircraft have been broken down into numerous components, and these are shown diagrammatically on Figure 259.

These forces are distributed in a rational manner so that two equations have been derived and are shown on the following pages. Equation 10.1 represents the total lift, and Equation 10.2 represents the total moment on the aircraft.

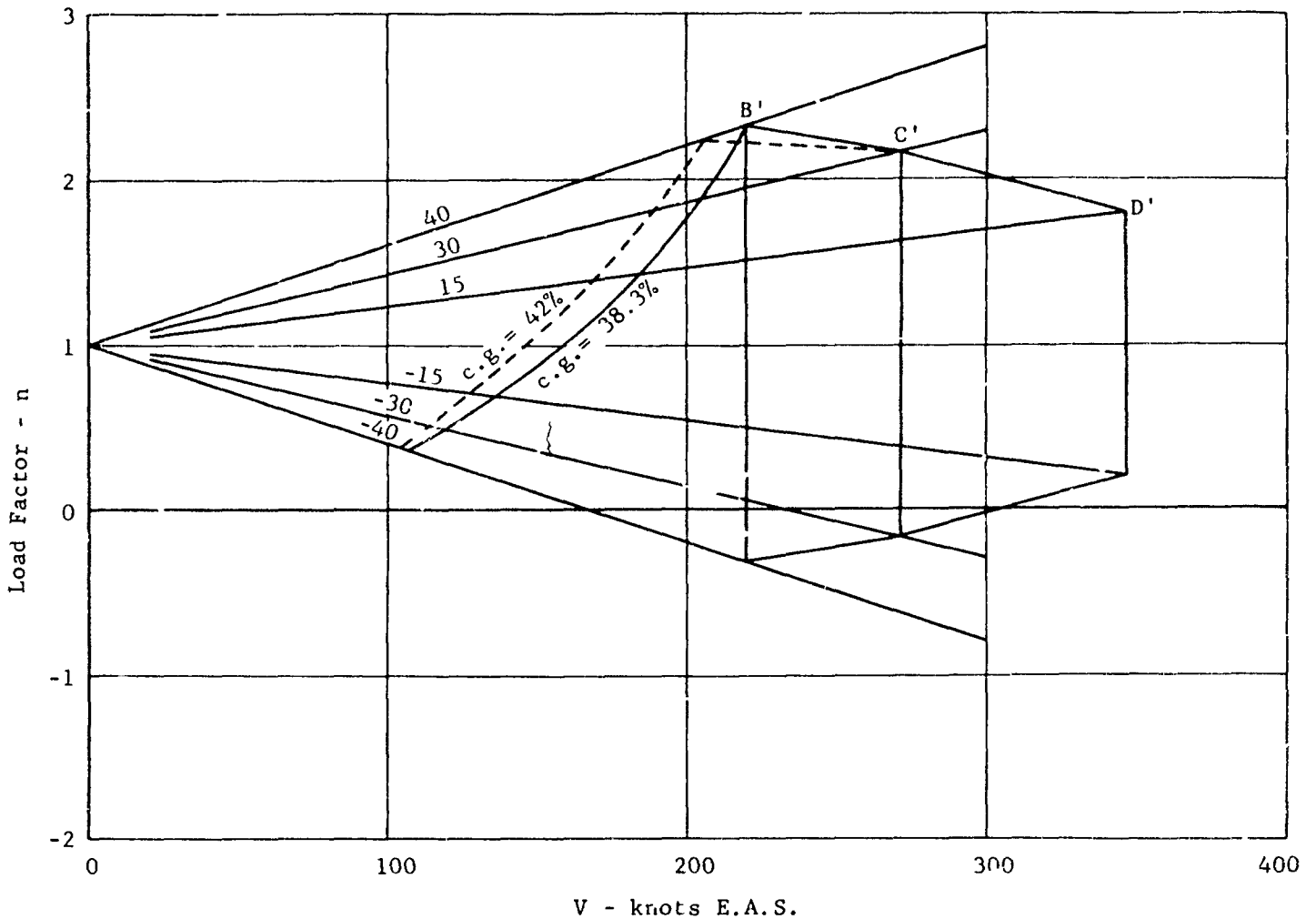

Figure 258. X-19, gust envelope; W = 13,660 pounds.

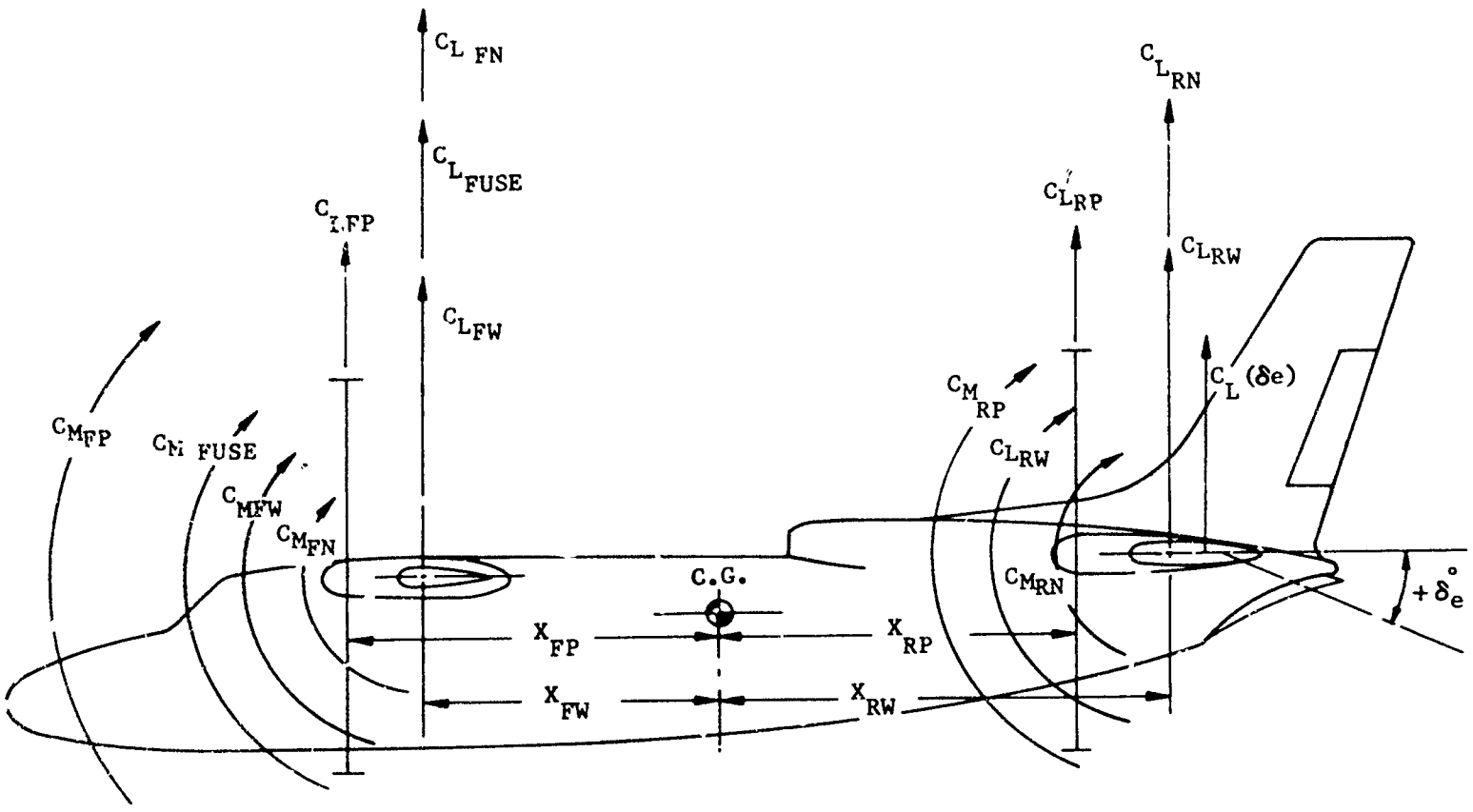

Positive forces and movements shown.
Moment arms are positive forward of the c.g. and negative behind the c.g.

Figure 259. Diagramatic representation of aerodynamic cruise loads.

$$C_L = C_{L_{FUSE}} + C_{L_{FW}} + C_{L_{RW}} + C_{L_{FN}} + C_{L_{RN}} + C_{L_{FP}} + C_{L_{RP}} + C_{L_{\delta_e}} \delta_e + C_{L_{\delta_a}} \delta_a \quad (1)$$

$$C_M = C_{M_{FUSE}} + \frac{x_{FW}}{C}\left[C_{L_{fuse}} + C_{L_{FW}} + C_{L_{FN}}\right] - \frac{x_{RW}}{C}\left[C_{L_{RW}} + C_{L_{RN}} + C_{L_{\delta_a}} \delta_a\right] \quad (2)$$

$$+ \frac{x_{FP}}{C} C_{L_{FP}} - \frac{x_{RP}}{C} C_{L_{RP}} - C_{L_{\delta_e}} \delta_e \left[\frac{x_{RW}}{C} - \frac{C_{M_{\delta_e}}}{C_{L_{\delta_e}}}\right] + C_{M_{\delta_a}} \delta_a$$

$$+ C_{M_{FW}} + C_{M_{RW}} + C_{M_{FN}} + C_{M_{RN}} + C_{M_{FP}} + C_{M_{RP}}$$

These equations are solved simultaneously, the governing criteria being the magnitude of the required pitching moment.

By selecting a given elevator lift slope, for these results, assumed as $C_{L_\alpha} = + 0.012/\text{deg.}$, an elevator angle required for each condition was derived and checked against data obtained in stability and control calculations.

In deriving the equations it was assumed that:

a. Drag equals thrust

b. Drag pitching moment equals thrust pitching moment.

c. No distinction has been drawn between lift, which is at right angles to the free-stream direction, and normal force which is at right angles to the fuselage reference axis (Waterline 100).

To allow for wing flexibility, the single value of angle of attack, α_{fus}, usually associated with equations of the form of Equations 10.1 and 10.2, has been replaced by component angles of attack varying from α_{fus} by the magnitude of the component flexibility. The analysis for this component angle approach is given in (90) and the results can be summarized as follows:

The wing operates at an effective angle of attack of α_{fus} plus one-half the magnitude of the wing tip twist, while the propeller reaches the α_{fus} plus the full value of wing tip twist which includes a nacelle/wing added flexibility.

k. Load Breakdowns

Specific loads and distributions are omitted from this report as this information is highly detailed, the particulars of which are given in (79).

l. Spanwise Lift Distribution

An area which has received considerable attention in the X-19 is the rear wing lift distribution. Normally, a wing lift distribution is approached with the knowledge that the fuselage covers a small span of the wing in the presence of a uniform free stream. Not so in the X-19. The rear wing, by far the larger of the two, surprisingly is no larger than a horizontal stabilizer with respect to the fuselage length. Yet this rear wing is expected to provide stability and trim to the configuration. It is easy to see that small changes in $(\partial C_L/\partial \alpha)$ or in α_{o_L} will effect large changes in the stability and trim of the aircraft. This is highly magnified in a tandem machine as the stability is given by the expression,

$$C_{m_{\alpha_{c.g.}}} = C_{m_{\alpha_{fus}}} + C_{m_{\alpha_{props}}} + C_{L_{\alpha_{FW}}}\left(\frac{x_F}{c}\right) - C_{L_{\alpha_{RW}}}\left(\frac{x_R}{c}\right) \qquad (11)$$

and a small change in $C_{L_{\alpha_{RW}}}$ (on the moment arm x_R/c) is large.

Early tests of the configuration showed a considerable downwash on the rear wing, thereby resulting in a larger rear span than originally intended. One of the early loads efforts shows the magnitude of the wash effects in Figure 260. Note the fuselage contribution to the downwash is of the same order as that of the front wing. This has been further substantiated from later tunnel tests, the results of which are given in Figure 261. The unusual lift distribution shows the unloading influence of the fuselage. From a loads point of view, the problem reduces to one of greater root bending. The design loads were based on such a distribution.

Considerable importance was placed on this characteristic especially as it affected the design of tandem configurations. Accordingly a theoretical study was embarked upon to learn more about fuselage wash. The published information appeared to be limited to a wing, mounted through the center line of a fuselage,

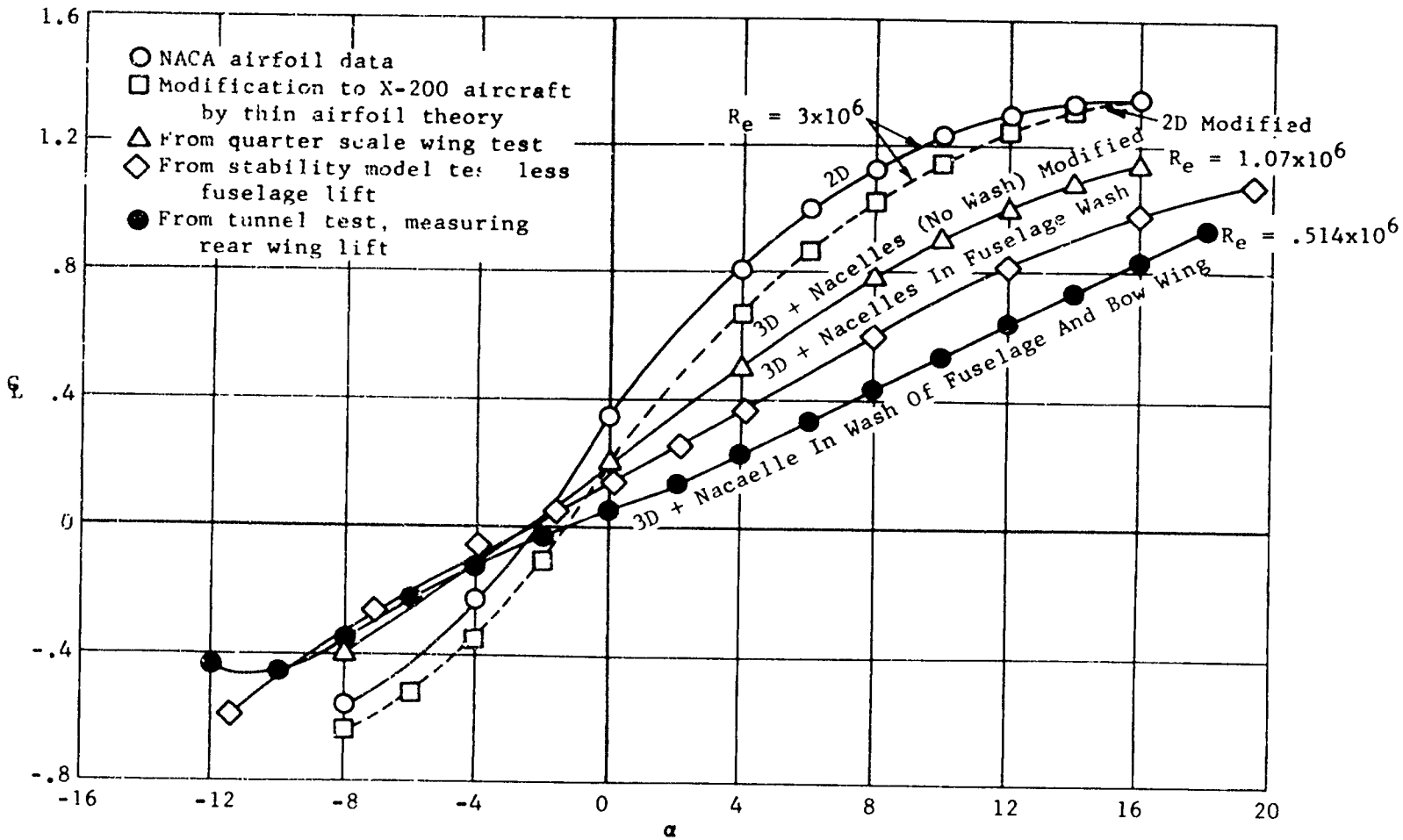

Figure 260. X-19, rear wing lift coefficient, based on S = 84.75 square feet (exposed) area; NACA 64_3-418 airfoil modified.

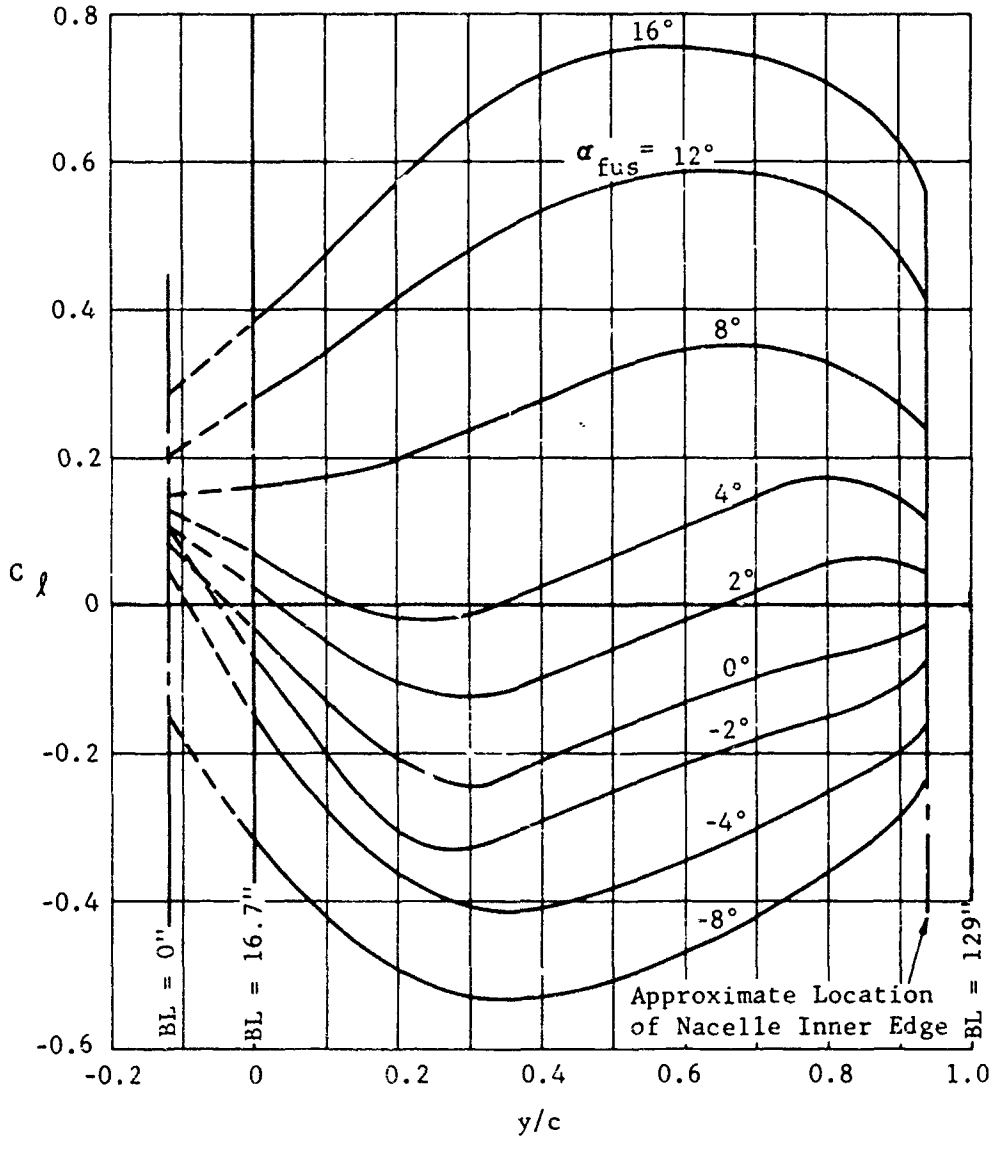

Figure 261. X-19, rear wing spanwise lift distribution - propellers off.

The component angles are expressed as follows:

$$\alpha_{FWD} = \left\{1 + \tfrac{1}{2}\left(\frac{d\theta}{d\alpha}\right)_F\right\}\left\{\alpha_f + 57.3\left[\frac{-x_{FW}(n-1)g}{V^2} + \tfrac{1}{2}\left(\frac{pb_F}{2V}\right)\right]\right\} - \tfrac{1}{2}\left(\frac{d\theta}{d\alpha}\right)_F \alpha_{o_F} \tag{3}$$

$$\alpha_{FWU} = \left\{1 + \tfrac{1}{2}\left(\frac{d\theta}{d\alpha}\right)_F\right\}\left\{\alpha_f + 57.3\left[\frac{-x_{FW}(n-1)g}{V^2} - \tfrac{1}{2}\left(\frac{pb_F}{2V}\right)\right]\right\} - \tfrac{1}{2}\left(\frac{d\theta}{d\alpha}\right)_F \alpha_{o_F} \tag{4}$$

$$\alpha_{RWD} = \left\{1 + \tfrac{1}{2}\left(\frac{d\theta}{d\alpha}\right)_R\right\}\left\{\alpha_f + 57.3\left[\frac{x_{RW}(n-1)g}{V^2} + \tfrac{1}{2}\left(\frac{pb_F}{2V}\right)\frac{b_R}{b_F}\right]\right\} - \tfrac{1}{2}\left(\frac{d\theta}{d\alpha}\right)_R \alpha_{o_R} + \tfrac{1}{2}\left(\frac{d\theta}{d\delta_{a_u}}\right)\delta_{a_u} \tag{5}$$

$$\alpha_{RWU} = \left\{1 + \tfrac{1}{2}\left(\frac{d\theta}{d\alpha}\right)_R\right\}\left\{\alpha_f + 57.3\left[\frac{x_{RW}(n-1)g}{V^2} - \tfrac{1}{2}\left(\frac{pb_F}{2V}\right)\frac{b_R}{b_F}\right]\right\} - \tfrac{1}{2}\left(\frac{d\theta}{d\alpha}\right)_R \alpha_{o_R} + \tfrac{1}{2}\left(\frac{d\theta}{d\delta_{a_D}}\right)\delta_{a_D} \tag{6}$$

$$\alpha_{FPD} = \left\{1 + \left(\frac{d\theta}{d\alpha}\right)_F\right\}\left\{\alpha_f + 57.3\left[\frac{-x_{FP}(n-1)g}{V^2} + \left(\frac{pb_F}{2V}\right)\right]\right\} - \left(\frac{d\theta}{d\alpha}\right)_F \alpha_{o_F} \tag{7}$$

$$\alpha_{FPU} = \left\{1 + \left(\frac{d\theta}{d\alpha}\right)_F\right\}\left\{\alpha_f + 57.3\left[\frac{-x_{FP}(n-1)g}{V^2} - \left(\frac{pb_F}{2V}\right)\right]\right\} - \left(\frac{d\theta}{d\alpha}\right)_F \alpha_{o_F} \tag{8}$$

$$\alpha_{RPD} = \left\{1 + \left(\frac{d\theta}{d\alpha}\right)_R\right\}\left\{\alpha_f + 57.3\left[\frac{x_{RP}(n-1)g}{V^2} + \left(\frac{pb_F}{2V}\right)\frac{b_R}{b_F}\right]\right\} - \left(\frac{d\theta}{d\alpha}\right)_R \alpha_{o_R} + \left(\frac{d\theta}{d\delta_{a_u}}\right)\delta_{a_u} \tag{9}$$

$$\alpha_{RPU} = \left\{1 + \left(\frac{d\theta}{d\alpha}\right)_R\right\}\left\{\alpha_f + 57.3\left[\frac{x_{RP}(n-1)g}{V^2} - \left(\frac{pb_F}{2V}\right)\frac{b_R}{b_F}\right]\right\} - \left(\frac{d\theta}{d\alpha}\right)_R \alpha_{o_R} + \left(\frac{d\theta}{d\delta_{a_D}}\right)\delta_{a_D} \tag{10}$$

without regard to fuselage station. Additional empirical studies, performed at Curtiss-Wright, had shown that wing location within fuselage station had significant effects upon the $(\partial C_L/\partial \alpha)$ as well as α_{QL} (see Figures 262 and 263). These curves were extracted from (91).

A method has been evolved which defines the wash field from the fuselage, based on potential theory. The findings of this study have not been completed, however, a large amount of information has been derived, some of which is given here. To start with, the theory shows that the wash field has two contributions from the fuselage. The first is a general wash due to the shape of the fuselage at zero angle of attack. The second is a wash derivative which varies with fuselage angle of attack. The parameters of importance are: (1) position of wing in fuselage both in waterline and station, and (2) the fuselage width to wing span ratio. The fuselage shape must be known. Using this method, the fuselage-induced wash on the rear wing was computed for the X-19. The results are shown in Figure 264. Note the general downwash field both in ϵ and $d\epsilon/d\alpha$ near the fuselage.

The large upwash derivative near the tip of the wing is generated by the nacelle. This distribution was to be fed into a computer program for determining the spanwise lift distribution.

Figure 287 is included to show the difference in local effective angle of attack (not ϵ) along the wing. The implication is that the inboard section of the wing sees approximately 5 degrees of downwash more than the outboard section. This is consistent with the theory shown in Figure 290. Figure 293 is included to show how the wing actually becomes unloaded. One can see that the upper surface pressure is fairly constant along the span. It is the leading edge of the lower surface which is so strongly affected by the spanwise downwash. Butt Line 27 passes through the leading edge fairing at the root of the wing (which explains the negative (x/c). Figures 261, 265, and 266 are taken from the test results of (93).

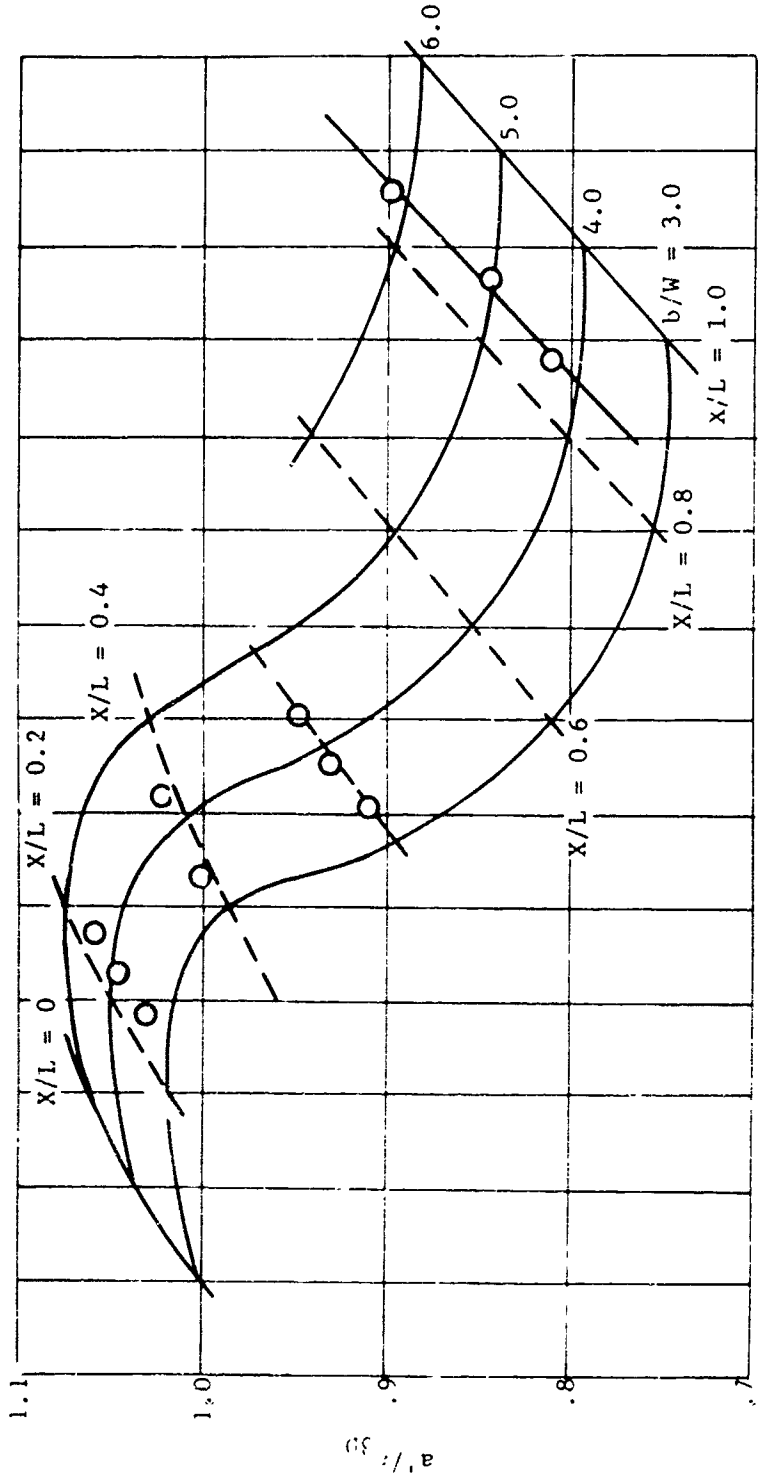

Figure 262. Effects of fuselage upon the wing ($\partial C_L/\partial a$); parameters: wing location along fuselage X/L, body width ratios, $Z/h = 0.907$; based on clear through wing area.

FURNISHED UNDER UNITED STATES GOVERNMENT CONTRACT No. AF33(615)-3940. SHALL NOT BE EITHER RELEASED OUTSIDE THE GOVERNMENT, OR USED, DUPLICATED, OR DISCLOSED IN WHOLE OR IN PART FOR MANUFACTURE OR PROCUREMENT, WITHOUT THE WRITTEN PERMISSION OF CURTISS-WRIGHT CORPORATION, EXCEPT FOR (i) EMERGENCY REPAIR OR OVERHAUL WORK BY OR FOR THE GOVERNMENT, WHERE THE ITEM OR PROCESS IS NOT OTHERWISE REASONABLY AVAILABLE TO ENABLE TIMELY PERFORMANCE OF THE WORK, OR (ii) RELEASE TO A FOREIGN GOVERNMENT, AS THE INTERESTS OF THE UNITED STATES MAY REQUIRE, PROVIDED THAT IN EITHER CASE THE RELEASE, USE, DUPLICATION OR DISCLOSURE HEREOF SHALL BE SUBJECT TO THE FOREGOING LIMITATIONS. THIS LEGEND SHALL BE MARKED ON ANY REPRODUCTION HEREOF IN WHOLE OR IN PART.

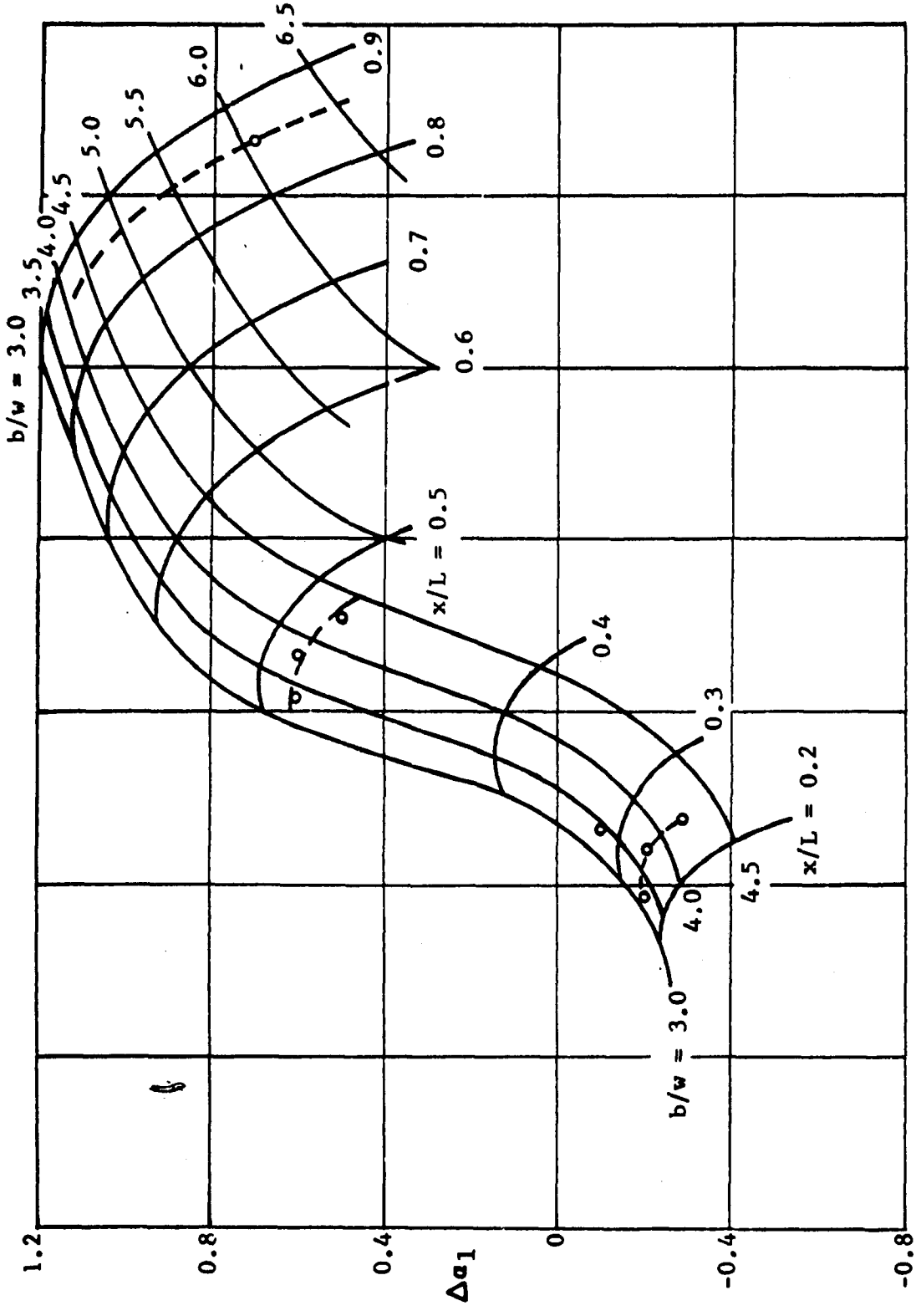

Figure 263. Effects of fuselage upon wing angle of zero lift; parameters: X/L, b/W, X/H = 0.907.

"FURNISHED UNDER UNITED STATES GOVERNMENT CONTRACT No. AF33(615)-3940. SHALL NOT BE EITHER RELEASED OUTSIDE THE GOVERNMENT, OR USED, DUPLICATED, OR DISCLOSED IN WHOLE OR IN PART FOR MANUFACTURE OR PROCUREMENT, WITHOUT THE WRITTEN PERMISSION OF CURTISS-WRIGHT CORPORATION, EXCEPT FOR (i) EMERGENCY REPAIR OR OVERHAUL WORK BY OR FOR THE GOVERNMENT, WHERE THE ITEM OR PROCESS IS NOT OTHERWISE REASONABLY AVAILABLE TO ENABLE TIMELY PERFORMANCE OF THE WORK; OR (ii) RELEASE TO A FOREIGN GOVERNMENT, AS THE INTERESTS OF THE UNITED STATES MAY REQUIRE; PROVIDED THAT IN EITHER CASE THE RELEASE, USE, DUPLICATION OR DISCLOSURE HEREOF SHALL BE SUBJECT TO THE FOREGOING LIMITATIONS. THIS LEGEND SHALL BE MARKED ON ANY REPRODUCTION HEREOF IN WHOLE OR IN PART."

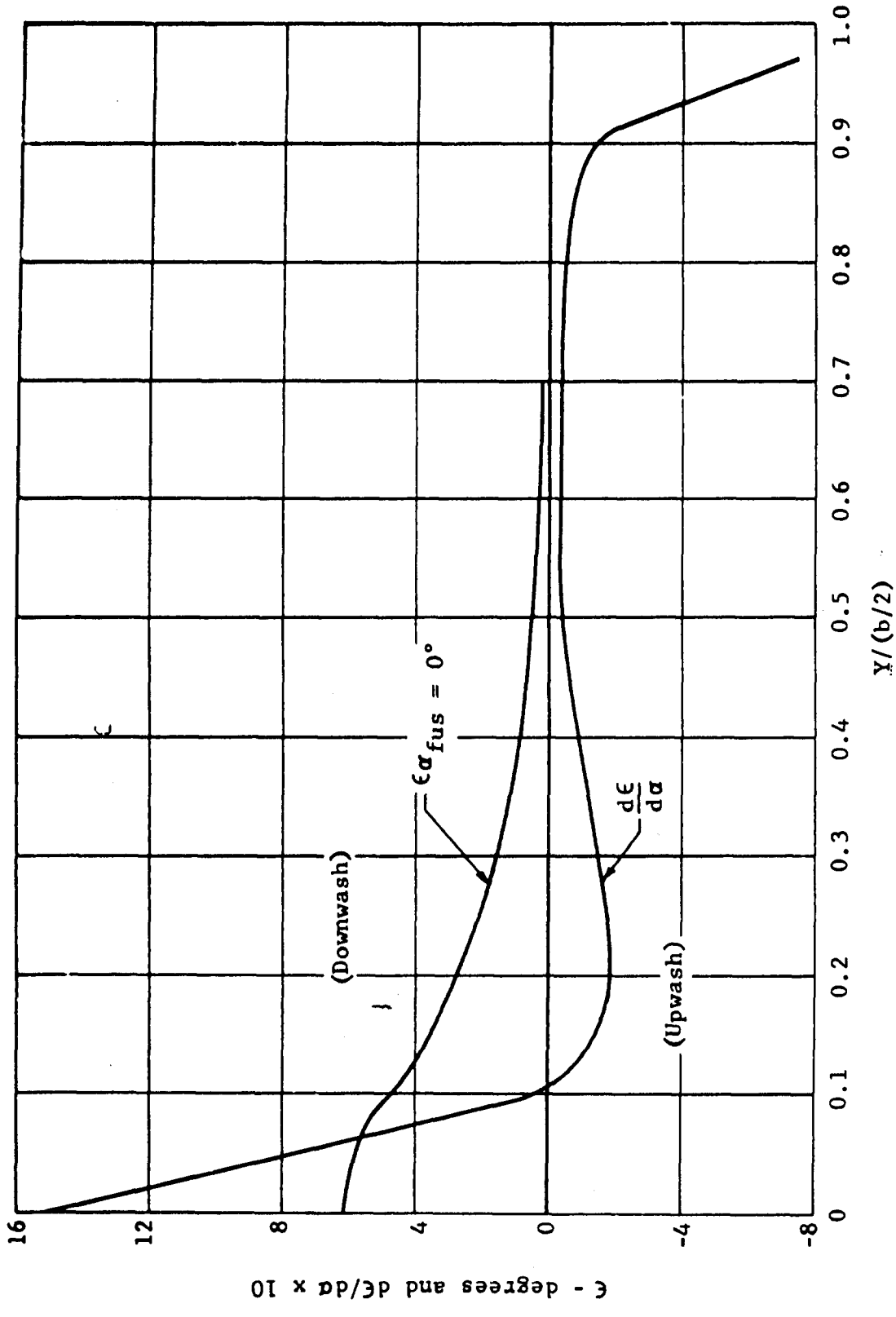

Figure 264. X-19, fuselage and nacelle wash effects on the rear wing at 77% chord position.

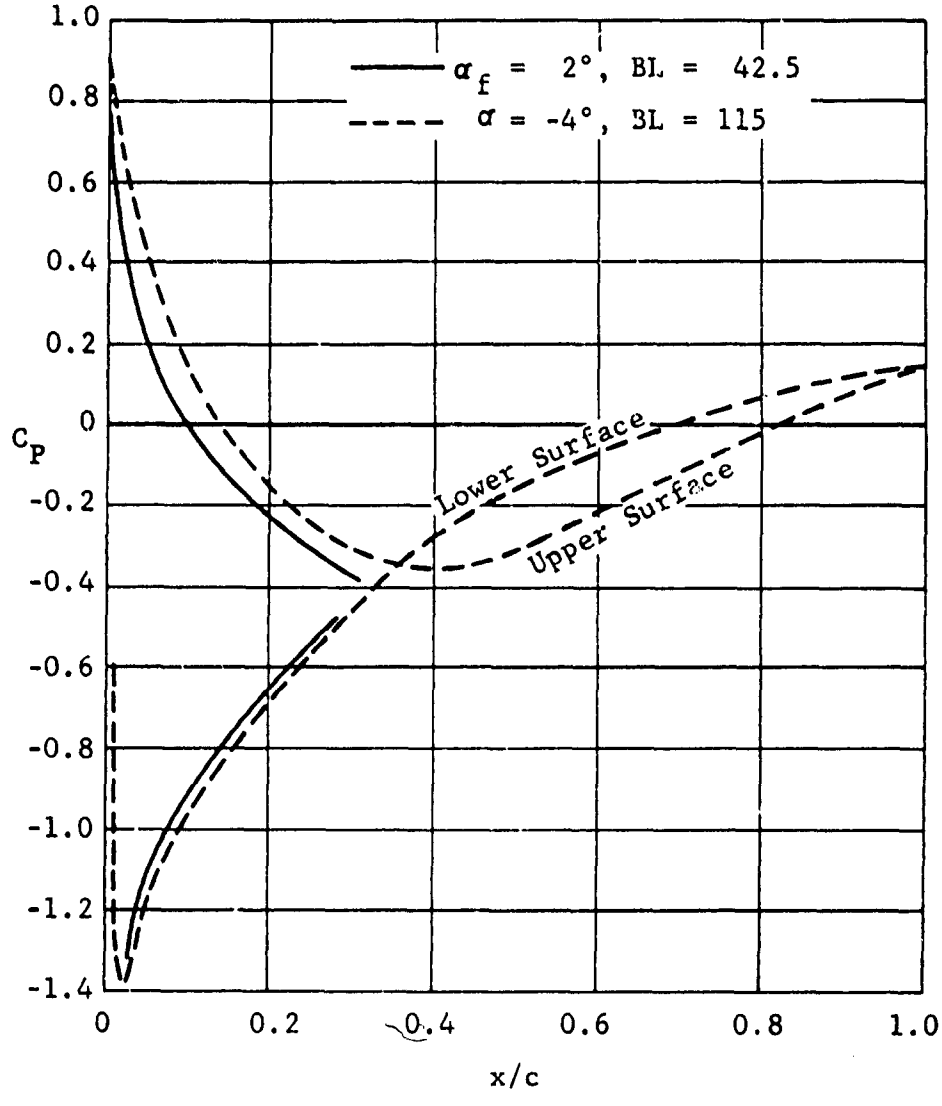

Figure 265. X-19, rear wing chordwise pressure distribution - propellers off; ϕ_F = -3°.

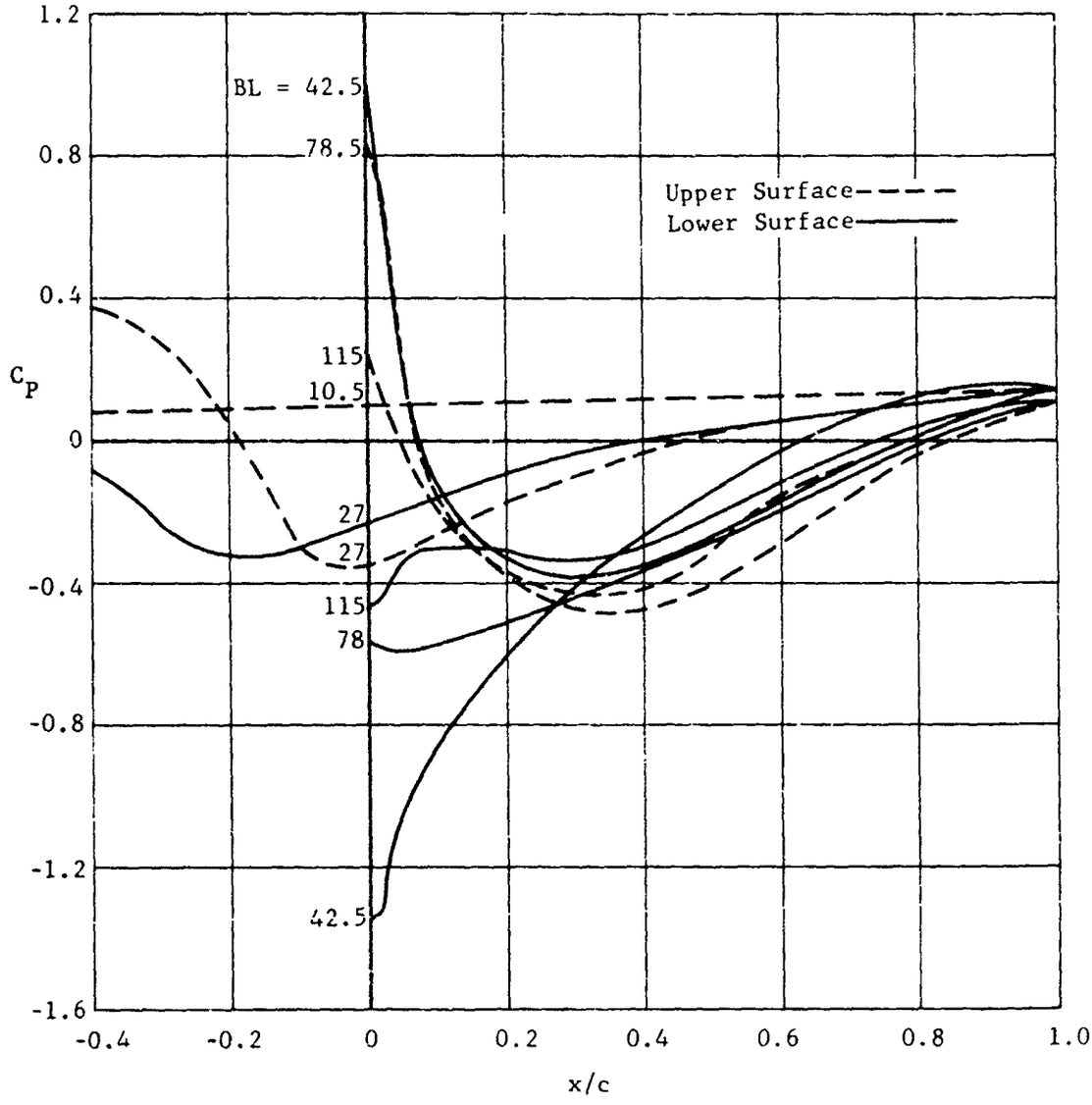

Figure 266. X-19, rear wing chordwise pressure distribution - propellers off; $\phi_F = -3^\circ$, $\alpha_{fus} = +2^\circ$.

As a matter of interest, the method was extended to the yaw plane. A distribution of $d\epsilon/d\psi$ was computed for the rear wing. The general trend of wash is as one would expect. The results are given in Figure 267. Thus a theoretical method exists for computing fuselage induced longitudinal and lateral wash characteristics, with application in loads, stability and configuration analysis. It remains to demonstrate how well the method compares with experimental results.

3. HOVER LOADS

a. General

Hover loads are closely related to the control and transmission systems. Consequently, such a discussion will thread between these areas. To start with, the hover loads are strictly propeller point loads directed at the wingtips. Secondary loads include wing down loads and are of the order of ten percent of the propeller loads. The process of establishing hover loads requires determining the range of:

(1) Symmetrical trimmed Thrusts - all c.g.s.

(2) Use of trim button.

(3) Throttle and stick excursions.

b. Symmetrical Trimmed Thrusts

The range of powers required to trim the airplane for steady hover is obtained from a simultaneous solution of the lift and moment equations yielding:

$$T_R = T_F \left(\frac{x_F}{x_R}\right)\left(\frac{1 - DL_F}{1 - DL_R}\right) \tag{12}$$

$$\frac{V}{\sigma} = \frac{2T_F(1 - DL_F)\sin \phi_F}{(T/w)}\left(1 + \frac{x_F}{x_R}\frac{\sin \phi_R}{\sin \phi_F}\right) \tag{13}$$

Thus the center of gravity, as it affects the moment arms, strongly influences the thrust and consequently the torque distribution.

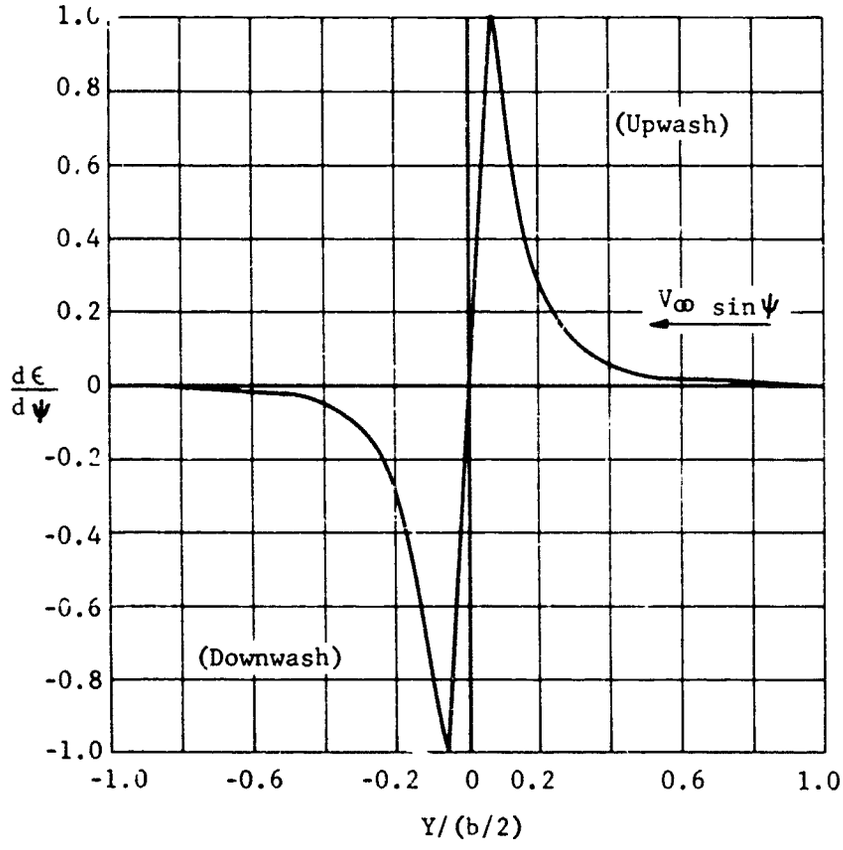

Figure 267. X-19, fuselage induced wash derivative on rear wing due to side slip at 77% chord position.

It is desirable to place the c.g. at 50% of the lift-chord, as this equalizes and minimizes the torque to the propellers at the hover condition. Unfortunately, at the 50% c.g. position, an unstable C_{m_α} is encountered[9] in cruise, and large trim shifts are obtained in transition.[10] To eliminate these problems, a c.g. forward of the mid-lift chord is used. From transmission consideration the criteria are such that maximum steady-hover torque on front propellers equals the maximum steady transition torque on the rear propellers. There is the need to provide a reasonable c.g. operating range. In the case of the X-19, a forward hover c.g. of 39.3% and aft cruise c.g. of 42% were established as initial achievable flight test values, but the aircraft was capable of a wider range (see Figure 268 and (79).

For a given permissible gear box torque level, decreasing the density requires a further aft c.g. position. This is a powerful effect, as can be seen on Figure 269, generated for a front propeller horsepower equal to 730 HP at 819 πnD. This curve reflects the interchanges between aircraft weight, relative density, center of gravity and propeller speed. The definition of a steady horsepower limit is not to be confused with a maximum power limitation, as this would be given in the following expression:

$$HP_{max} = HP_{control\ neutral} + \Delta HP_{trim} + \Delta HP_{throttle} + \Delta HP_{control}$$

c. Trim Button

The trim button was installed on the aircraft to permit the stick to be held neutral throughout the range of c.g., weight and density conditions. In effect, the trim button is additive to the stick, so that from any trimmed hover condition, a full stick displacement is available to generate the maximum control moment.

Thus when a maximum steady horsepower (front propeller) is attained, it is implied that stick is neutral while the trim button zeroes the moment. Or therefore:

$$HP_{max.\ steady} = HP_{control\ neutral} + \Delta HP_{trim}$$

---

9 A stable C_{m_α} is obtained by increasing the rear wing area (meaning higher structural weight).

10 The center of pressure moves forward with low forward speed resulting in a demand for increased trimming torque on the rear propellers.

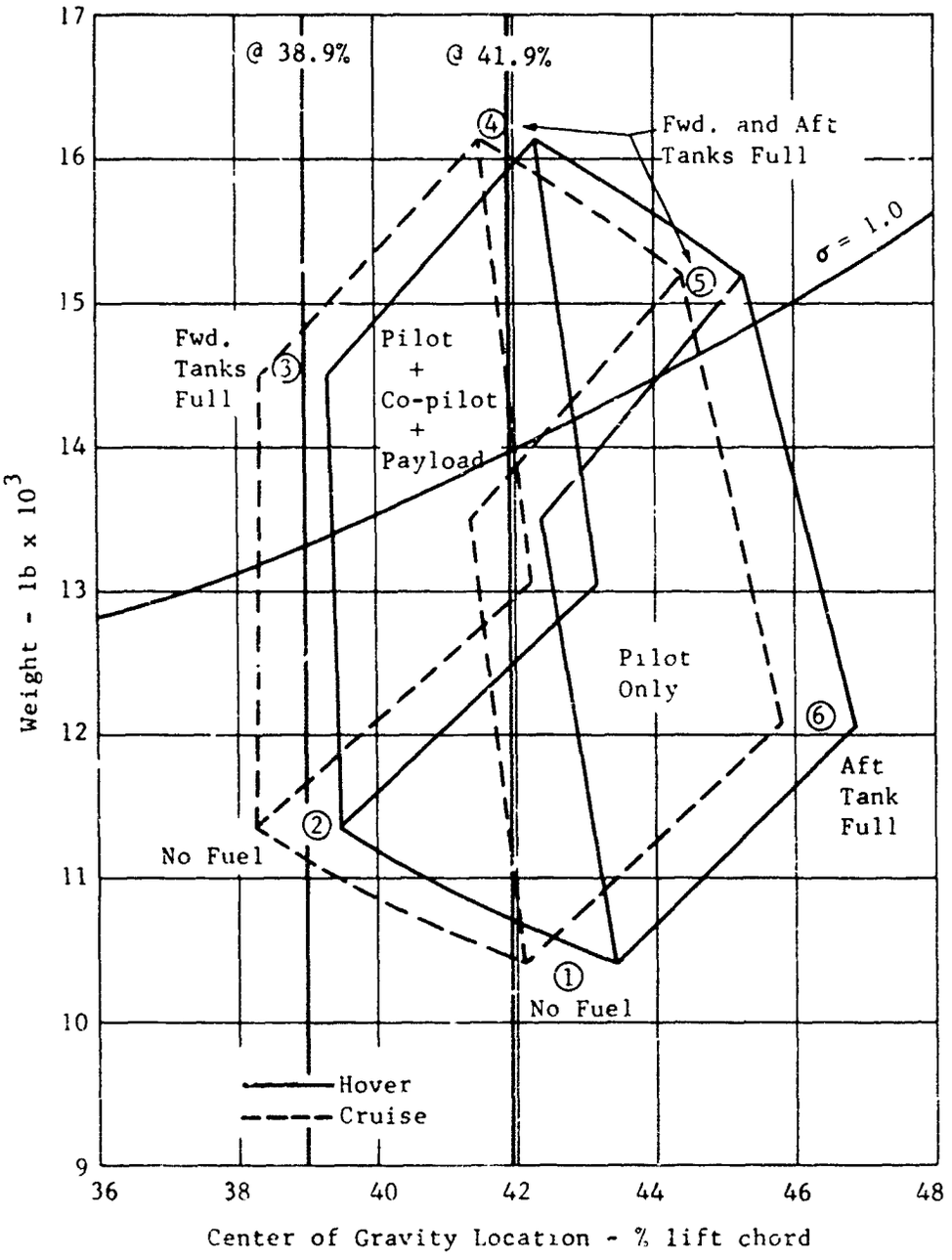

Figure 268. X-19, center of gravity envelope based on empty weight.

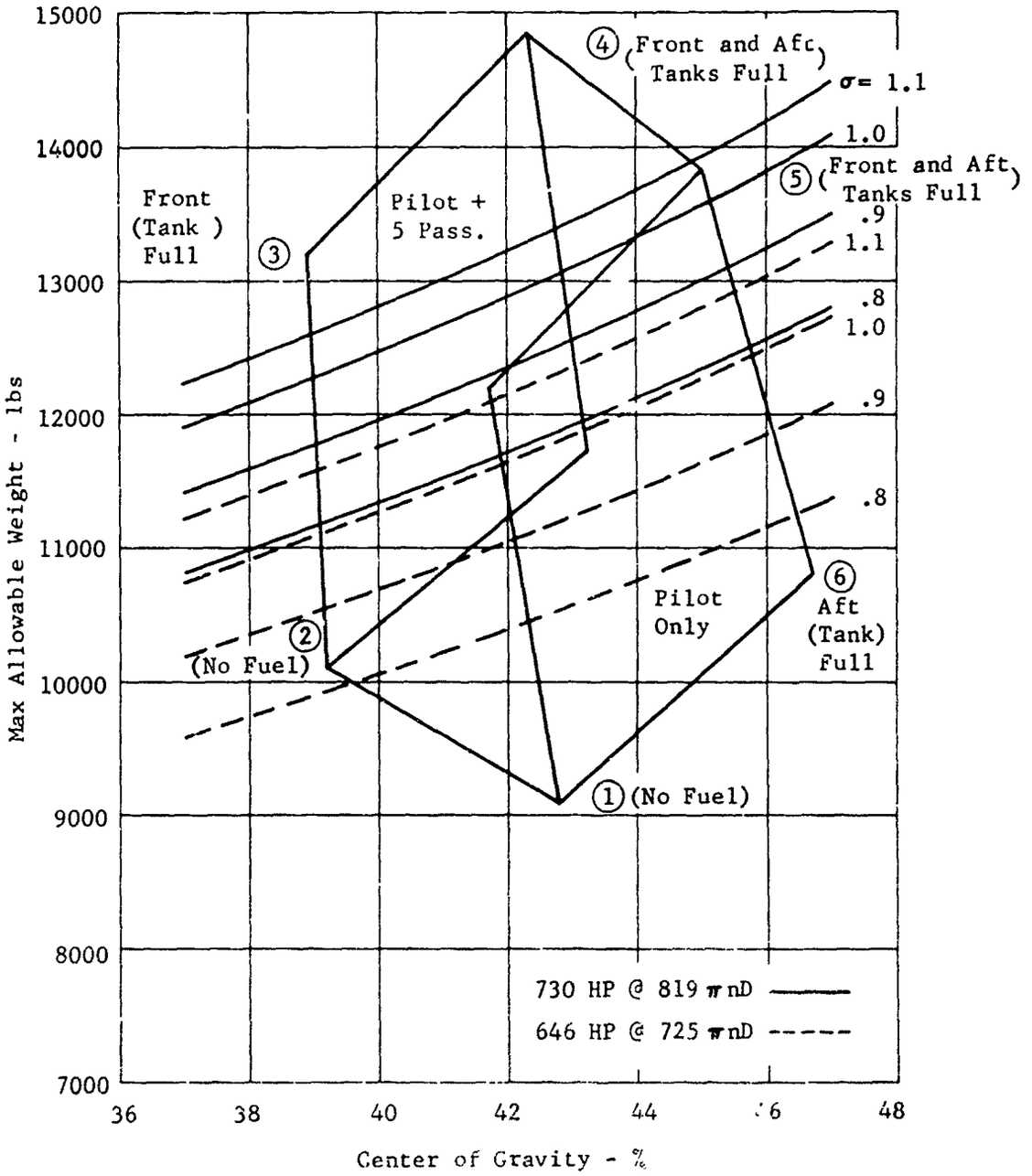

Figure 269. X-19, hover transmission limit - allowable forward center of gravity position at thrust to weight = 1.0.

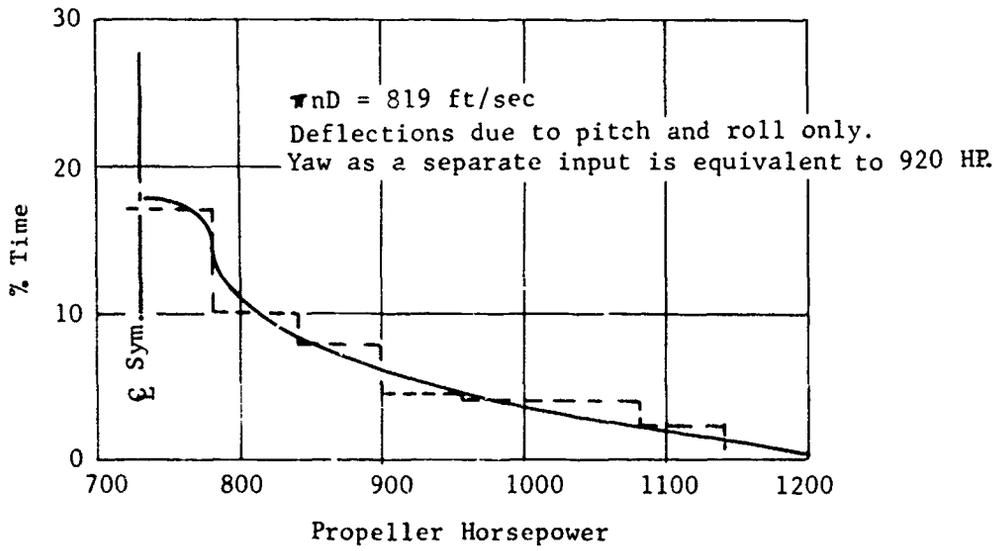

Figure 270. X-19, propeller horsepower histogram (hover).

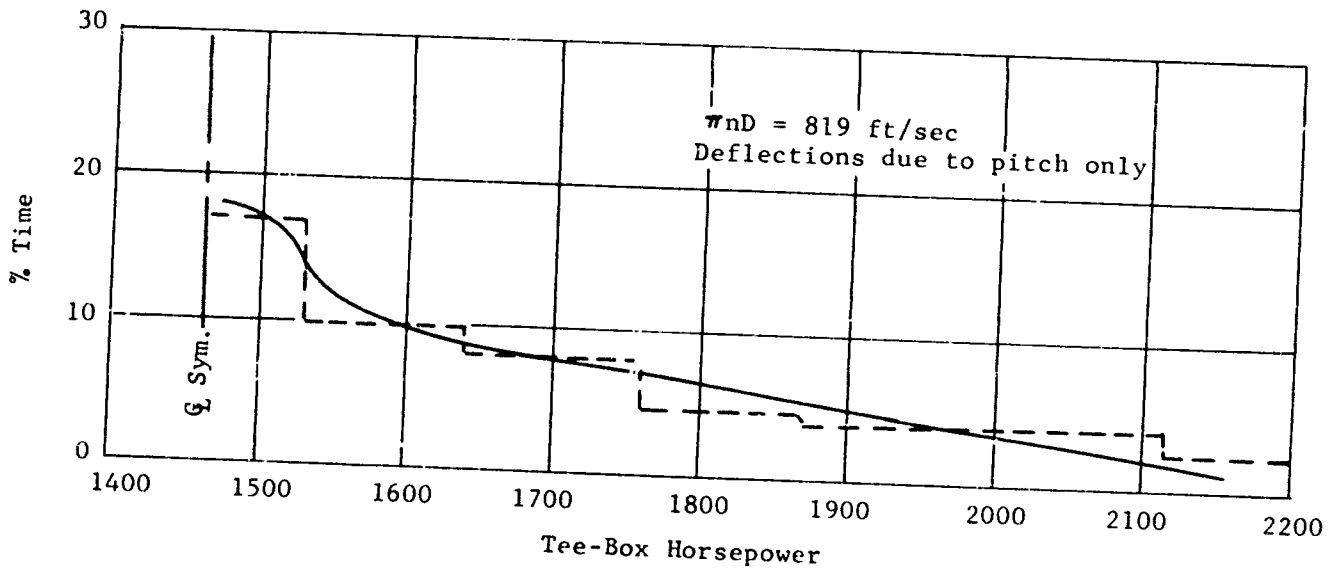

Figure 271. X-19, tee-box horsepower histogram (hover).

d. Throttle and Control Excursions

The pilot exercises the throttle and control stick as the maneuver demands. The maximum incremental power that could be generated by the control column was used for stressing the airframe. Likewise, the transmission was required to accept these peak loadings. However it was recognized that maximum transmission loadings would exist for a short period of time only. Consequently, it was decided to generate power histograms reflecting the time spent at various levels of power. These histograms were used to establish the projected life of the transmission. Figures 270 and 271 reflect some earlier histograms used for the X-19. These were obtained from an analog simulation under gusty conditions. Histograms generated from the X-19 flights reasonably corroborate the predicted values.

e. Design Criteria

The hover loads problem is basically one of defining the thrust and torque loadings resulting from gusts or maneuvering. The previous discussion has dwelt on the maneuvering induced loads, predominantly through the transmission. Obviously, the knowledge of a thrust, torque curve and the movements of torque will define the thrusts.

This was the method used for establishing the thrust and consequent airframe loadings. The dynamics of the governor system as it affected propeller speed and torque was mostly a function of throttle rather than stick motion; and as stick-induced loads were far greater than throttle-induced loads, as discussed in the preceding paragraph number, the dynamics of the governor were considered secondary. The height control system introduced towards the end of the program was intended to give a rapid thrust response (throttle motion) with small torque overshoot. From the little data gleaned from flight test, indications are that torque and thrust response were close to a step input. Consequently, the dynamics of the governor circuit would appear to contribute little to the loads.

The control power was such that considerable pitch or roll acceleration could be experienced through the center of gravity. Angular inertia load factors were easily computed and added to the direct thrust and torque loadings.

The linear load factors due to throttle motion were close to $T/W = 1.0$. Of course for $T/W > 1$, the linear inertia load factor is relieving and for this reason was neglected. Gyroscopic loads were available from a knowledge of the roll and pitch rates. These are the criteria which were used for maneuvering loads in hover

Gusts are specified in (76) for 30 fps gust velocities. The effects of gust are less than that of maneuvering in the hover regime, and consequently no effort was expended in this area.

4. TRANSITION LOADS

a. General

Transition is the flight regime in which the interchange between propeller and wing forces is very large. At low speeds the propellers dominate. At the higher speeds and lower tilt angles wing forces predominate. Obviously at low speeds, the propeller lift is predominantly a function of the power. At the higher speeds, wing loading is sufficiently high (W/S $\simeq$ 80 psf) that load factor is limited. This feature, plus the fact that stick deflection, propeller speed and tilt-velocity corridor can strongly influence individual component loads without strongly influencing load factor, makes the V-n diagram a less useful tool. Consequently, the V-n diagram was never generated for the transition regime.

The approach taken was to determine how all of the control, maneuver and gust parameters would affect the aircraft, and from that compute the loads. As a preliminary, the loads were determined along the tilt-velocity schedule with variations in throttle, stick deflection (max pitch, roll, or yaw), angle of attack, propeller speed and center of gravity. Following this, it was intended to open the tilt-velocity corridor as a further load-checking condition. In many instances, checks showed small effects due to the velocity extension.

In general, transition loads consist of high propeller loadings, and thrust-power distributions between the fore and aft that are highly unsymmetric. By contrast, the cruise loadings are approximately 70 percent on the wings, the remainder being a propeller lift force. Stick deflection and power have relatively smaller influence on airframe loads in cruise.

b. Airplane Characteristics

In transition, the airplane characteristics should be thought of as a new configuration at each tilt angle. One then matches each configuration to obtain the proper flight characteristics. Basic airplane characteristics are shown in the following figures, as a function of the tilt angle.

Figures 272 through 276 describe the lift characteristics. Note at $\phi_F = 82.5^\circ$, the extreme dependence of lift upon the horsepower with a relatively small dependence upon angle of attack. Note further that the maximum lift coefficient occurs at about σ_{fus} = 8 degrees. At a tilt angle of $\phi_F = 20^\circ$, one finds lift to be far more sensitive to angle of attack.

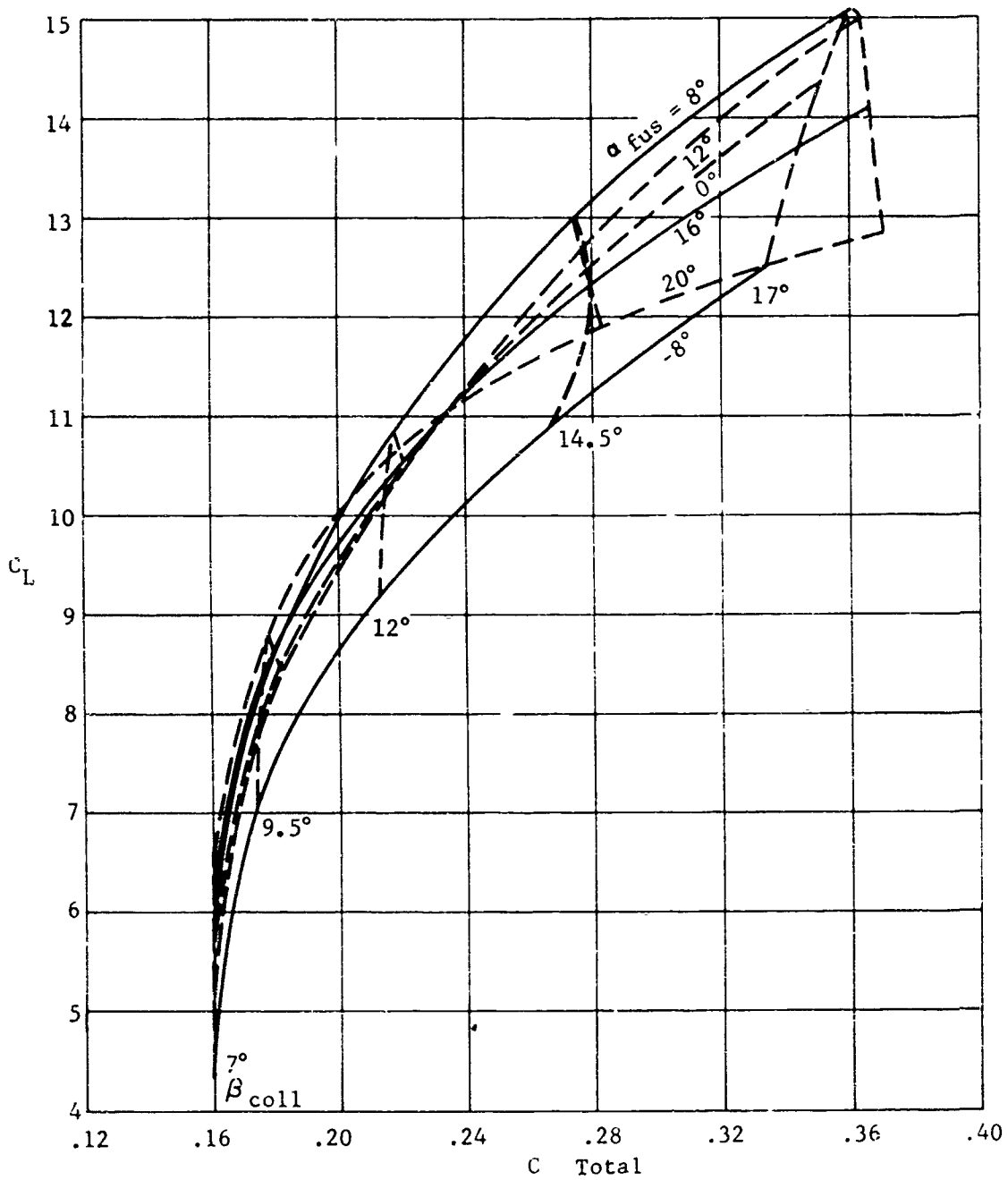

Figure 272. X-19, transition lift coefficient characteristics; ϕ_F = 82.5°, V = 49 knots, 819 rnD, neutral stick.

FURNISHED UNDER UNITED STATES GOVERNMENT CONTRACT No AF33(615)-3940 SHALL NOT BE EITHER RELEASED OUTSIDE THE GOVERNMENT OR USED DUPLICATED, OR DISCLOSED IN WHOLE OR IN PART FOR MANUFACTURE OR PROCUREMENT, WITHOUT THE WRITTEN PERMISSION OF CURTISS-WRIGHT CORPORATION, EXCEPT FOR (i) EMERGENCY REPAIR OR OVERHAUL WORK BY OR FOR THE GOVERNMENT WHERE THE ITEM OR PROCESS IS NOT OTHERWISE REASONABLY AVAILABLE TO ENABLE TIMELY PERFORMANCE OF THE WORK, OR (ii) RELEASE TO A FOREIGN GOVERNMENT AS THE INTERESTS OF THE UNITED STATES MAY REQUIRE PROVIDED THAT IN EITHER CASE THE RELEASE USE, DUPLICATION OR DISCLOSURE HEREOF SHALL BE SUBJECT TO THE FOREGOING LIMITATIONS. THIS LEGEND SHALL BE MARKED ON ANY REPRODUCTION HEREOF IN WHOLE OR IN PART.

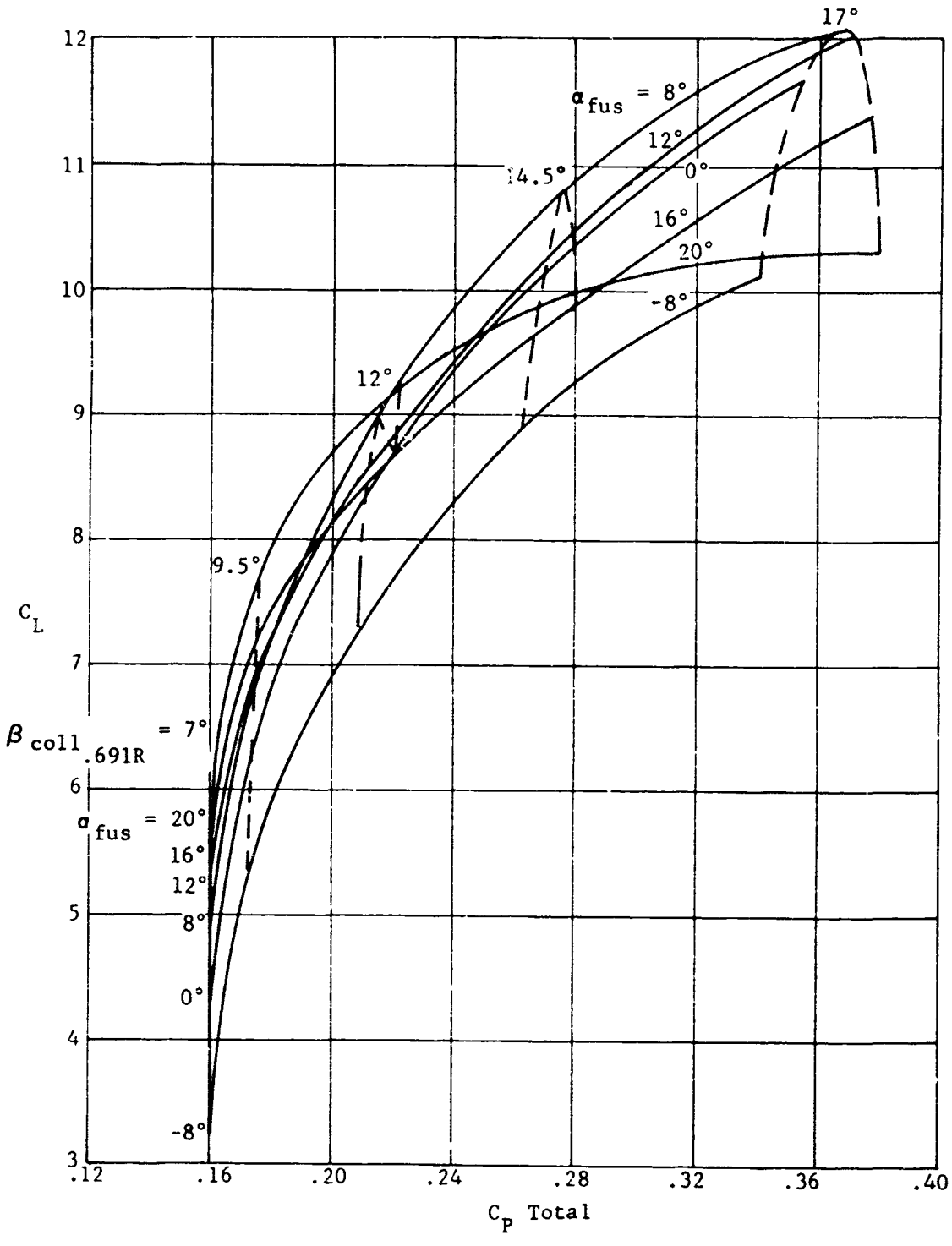

Figure 273. X-19, transition lift coefficient characteristics; $\emptyset_F$ = 82.5°, V = 49 knots, 725 rnD, neutral stick.

FURNISHED UNDER UNITED STATES GOVERNMENT CONTRACT No. AF33(615)-1940 SHALL NOT BE EITHER RELEASED OUTSIDE THE GOVERNMENT, OR USED DUPLICATED, OR DISCLOSED IN WHOLE OR IN PART FOR MANUFACTURE OR PROCUREMENT, WITHOUT THE WRITTEN PE MISSION OF CURTISS-WRIGHT CORPORATION, EXCEPT FOR (i) EMERGENCY REPAIR OR OVERHAUL WORK BY OR FOR THE GOVERNMENT, WHERE THE ITEM R PROCESS IS NOT OTHERWISE REASONABLY AVAILABLE TO ENABLE TIMELY PERFORMANCE OF THE WORK, OR (ii) RELEASE TO A FOREIGN GOVERNMENT, A THE INTERESTS OF THE UNITED STATES MAY REQUIRE PROVIDED THAT IN EITHER CASE THE RELEASE, USE DUPLICATION OR DISCLOSURE HEREOF SHA BE SUBJECT TO THE FOREGOING LIMITATIONS. THIS LEGEND SHALL BE MARKED ON ANY REPRODUCTION HEREOF IN WHOLE OR IN PART."

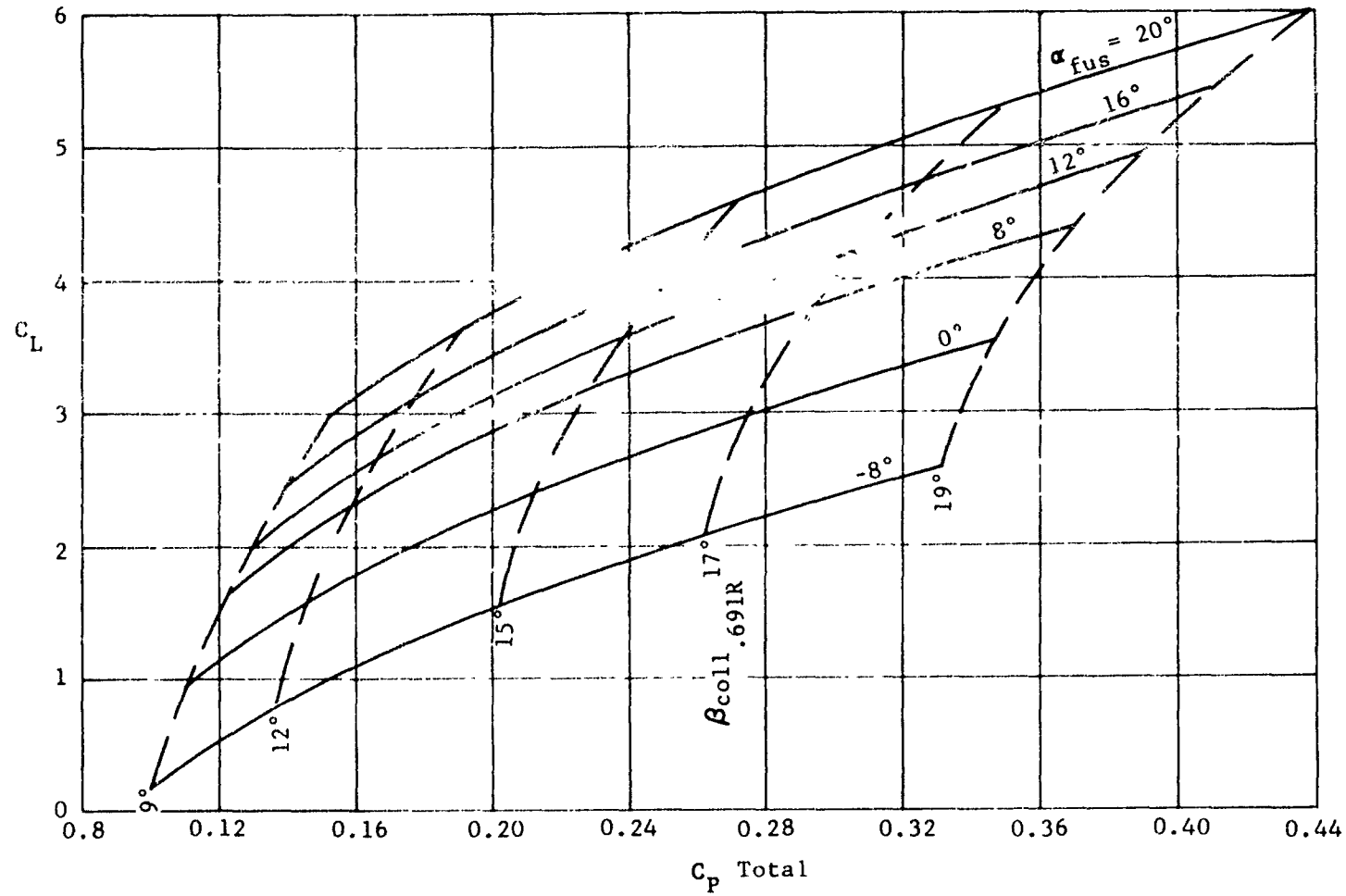

Figure 274. X-19, transition lift coefficient characteristics; ϕ_F = 60°, V = 85 knots, 725 πnD, neutral stick.

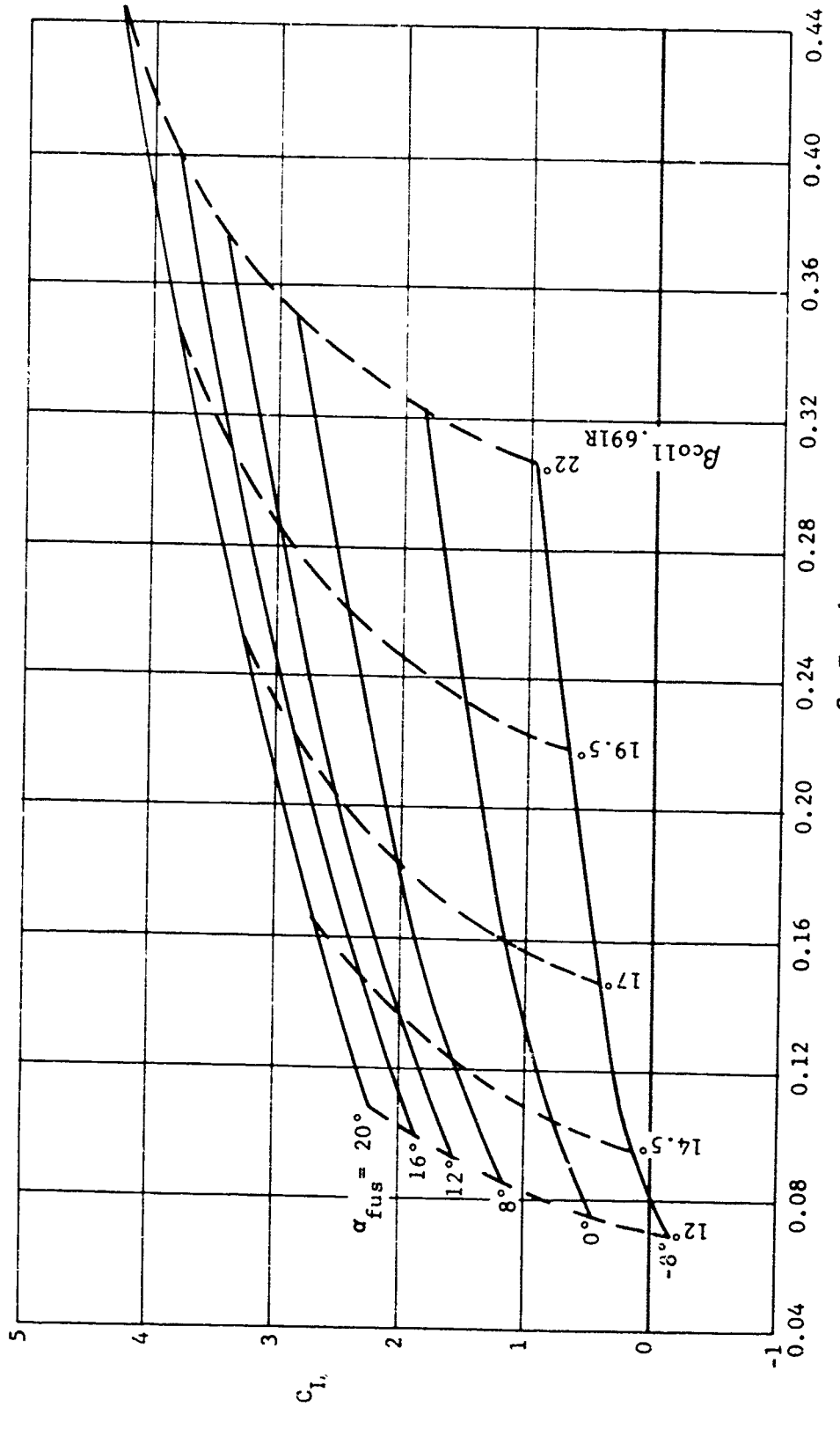

Figure 275. X-19, transition lift coefficient characteristics; ϕ_F = 40°, V = 102 knots, 725 rnD, neutral stick.

67-2218

FURNISHED UNDER UNITED STATES GOVERNMENT CONTRACT No AF33(615)-3940. SHALL NOT BE EITHER RELEASED OUTSIDE THE GOVERNMENT OR USED DUPLICATED, OR DISCLOSED IN WHOLE OR IN PART FOR MANUFACTURE OR PROCUREMENT, WITHOUT THE WRITTEN PERMISSION OF CURTISS-WRIGHT CORPORATION, EXCEPT FOR (i) EMERGENCY REPAIR OR OVERHAUL WORK BY OR FOR THE GOVERNMENT WHERE THE ITEM OR PROCESS IS NOT OTHERWISE REASONABLY AVAILABLE TO ENABLE TIMELY PERFORMANCE OF THE WORK OR (ii) RELEASE TO A FOREIGN GOVERNMENT, AS THE INTERESTS OF THE UNITED STATES MAY REQUIRE. PROVIDED THAT IN EITHER CASE THE RELEASE, USE, DUPLICATION OR DISCLOSURE HEREOF SHALL BE SUBJECT TO THE FOREGOING LIMITATIONS. THIS LEGEND SHALL BE MARKED ON ANY REPRODUCTION HEREOF IN WHOLE OR IN PART.

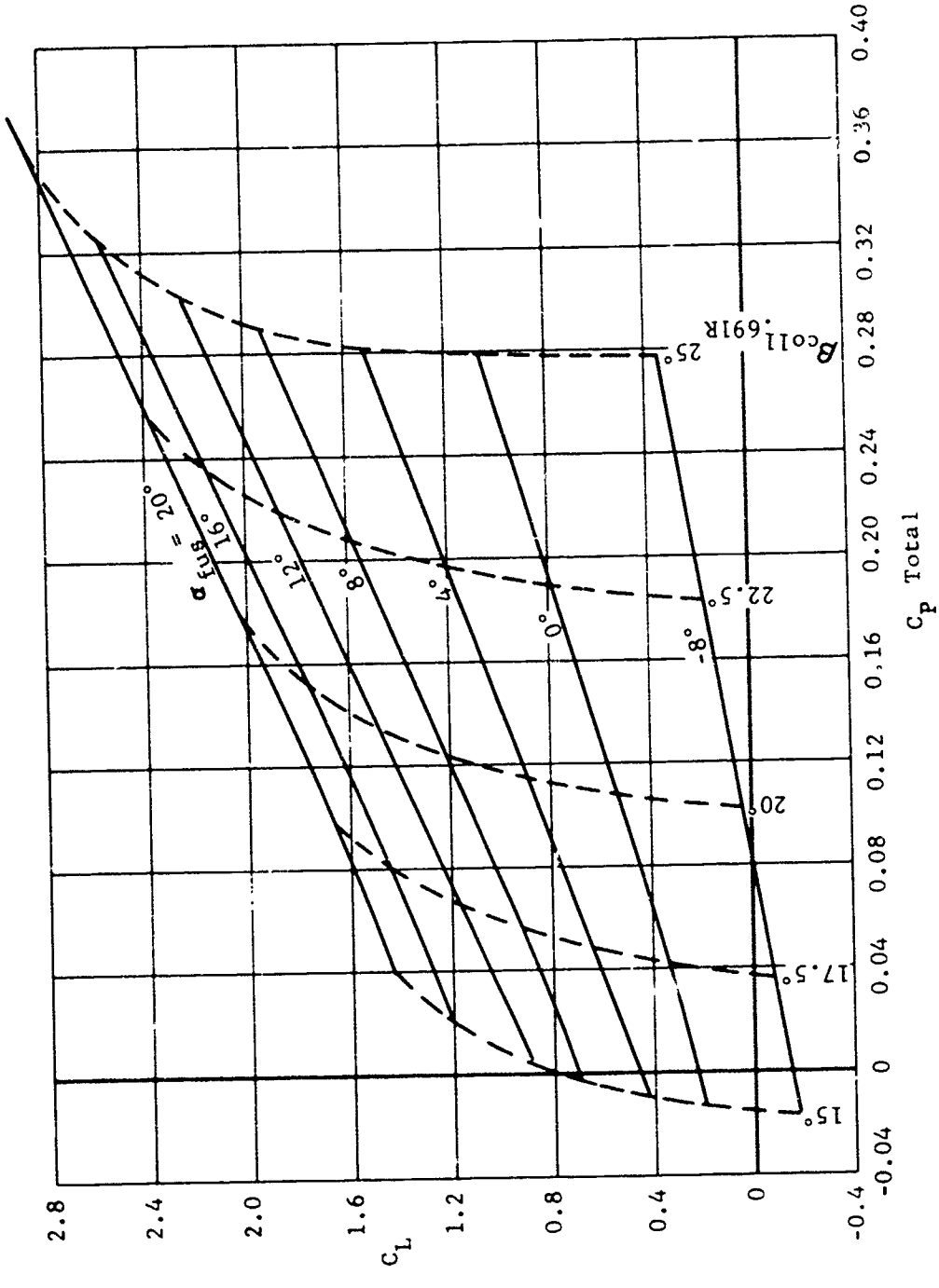

Figure 276. X-19, transition lift coefficient characteristics; ϕ_F = 20°, V = 120 knots, 725 rnD, neutral stick.

"FURNISHED UNDER UNITED STATES GOVERNMENT CONTRACT No. AF33(615)-3949 SHALL NOT BE EITHER RELEASED OUTSIDE THE GOVERNMENT, OR USED, DUPLICATED, OR DISCLOSED IN WHOLE OR IN PART FOR MANUFACTURE OR PROCUREMENT, WITHOUT THE WRITTEN PERMISSION OF CURTISS-WRIGHT CORPORATION, EXCEPT FOR (i) EMERGENCY REPAIR OR OVERHAUL WORK BY OR FOR THE GOVERNMENT, WHERE THE ITEM OR PROCESS IS NOT OTHERWISE REASONABLY AVAILABLE TO ENABLE TIMELY PERFORMANCE OF THE WORK, OR (ii) RELEASE TO A FOREIGN GOVERNMENT, AS THE INTERESTS OF THE UNITED STATES MAY REQUIRE. PROVIDED THAT IN EITHER CASE THE RELEASE, USE, DUPLICATION OR DISCLOSURE HEREOF SHALL BE SUBJECT TO THE FOREGOING LIMITATIONS. THIS LEGEND SHALL BE MARKED ON ANY REPRODUCTION HEREOF IN WHOLE OR IN PART."

Figures 277 through 281 illustrate the drag characteristics. It appears that there exists an opposite behaviour with respect to angle of attack and horsepower. For example, at the high tilt angles the drag is highly sensitive to angle of attack, with a strong but less important reliance upon horsepower. On the other hand at $\phi_F = 20^\circ$, power is the dominant parameter affecting drag. The significance of this, is that an equilibrium condition will be dependent both on power and angle of attack. During flight test, at tilt angles above 75 degrees the pilot appeared able to match the tilt-velocity schedule, through power and attitude manipulations, with reasonable ease. No experience at tilt angles as low as $\phi_F = 60^\circ$ was obtained (except for Flight 50). However analog studies indicated a greater difficulty in attaining equilibrium flight at $\phi_F = 60^\circ$ compared with the higher tilt angles. For example, a small change in attitude or power would result in a changing velocity and altitude.

The pitching moment curves are given in Figures 282 through 285. As expected, pitching moment is significantly related to angle of attack, either in the unstable or stable regions. Horsepower appears to have a lesser influence on the moment throughout. This effect has not gone unnoticed, however. In the final phase of Flight 50, following the full throttle input, the co-pilot commented that the aircraft pitched up without an application of back stick. Figure 283 shows the pitch up moment due to power characteristic to which reference is made.

c. Design Control Loads Criteria

Design control loads have been treated in a manner similar to that of conventional cruise. A trim equilibrium condition is first established, from which control deflections are superimposed to define the resultant loads. In cruise, maximum control deflections are generally imposed about a single axis. In some instances a combined control loading, such as in a rolling pull out, are determined. However, this is generally less than a full control deflection about both axis. In the X-19, the approach taken was to allow a full control deflection about a single axis in the transition regime. In hover, full three axis deflections were allowed, completely additive, for the airframe analysis. The base point was a trimmed hover at W = 13,660 pounds. For the transmission, a combination of pitch and roll was allowed in the hover regime for establishing maximum torque. This was obtained from analog equipment with various gust effects superimposed.

If one includes throttle deflections as part of the control deflection, the following comments are applicable. The engine topping governors were set to prevent overspeeds in excess of 3 percent.

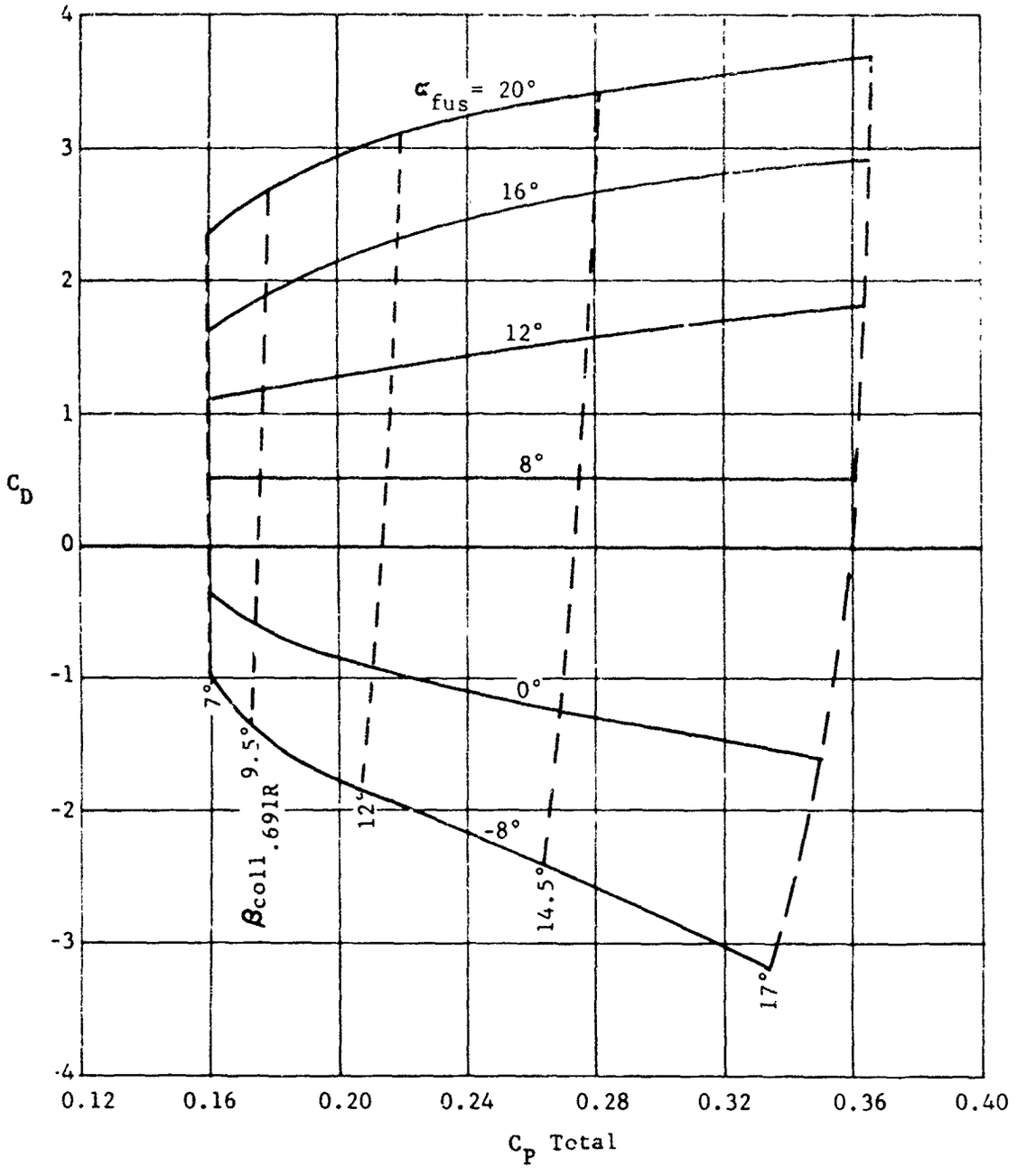

Figure 277. X-19, transition drag coefficient characteristics; ϕ_F = 82.5°, V = 49 knots, 819 rpm D, neutral stick.

FURNISHED UNDER UNITED STATES GOVERNMENT CONTRACT No. AF33(615)-3940. SHALL NOT BE EITHER RELEASED OUTSIDE THE GOVERNMENT, OR USED DUPLICATED, OR DISCLOSED IN WHOLE OR IN PART FOR MANUFACTURE OR PROCUREMENT, WITHOUT THE WRITTEN PERMISSION OF CURTISS-WRIGHT CORPORATION, EXCEPT FOR (i) EMERGENCY REPAIR OR OVERHAUL WORK BY OR FOR THE GOVERNMENT, WHERE THE ITEM OR PROCESS IS NOT OTHERWISE REASONABLY AVAILABLE TO ENABLE TIMELY PERFORMANCE OF THE WORK, OR (ii) RELEASE TO A FOREIGN GOVERNMENT, AS THE INTERESTS OF THE UNITED STATES MAY REQUIRE, PROVIDED THAT IN EITHER CASE THE RELEASE, USE, DUPLICATION OR DISCLOSURE HEREOF SHALL BE SUBJECT TO THE FOREGOING LIMITATIONS. THIS LEGEND SHALL BE MARKED ON ANY REPRODUCTION HEREOF IN WHOLE OR IN PART.

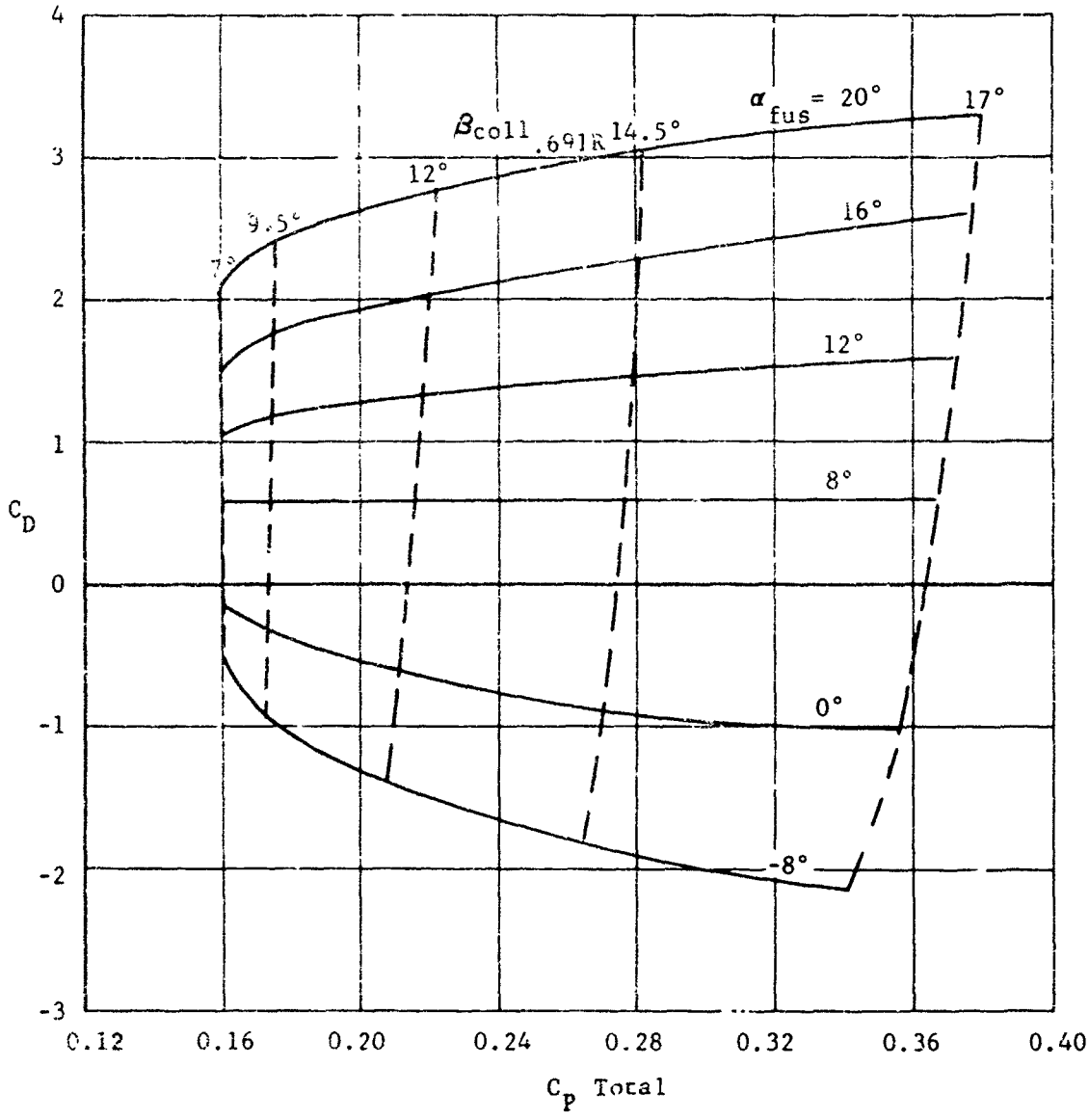

Figure 278. X-19, transition drag coefficient characteristics; $\emptyset_p$ = 82.5°, V = 49 knots, 725 πnD, neutral stick.

FURNISHED UNDER UNITED STATES GOVERNMENT CONTRACT No. AF33(616)-3940. SHALL NOT BE EITHER RELEASED OUTSIDE THE GOVERNMENT, OR USED, DUPLICATED, OR DISCLOSED IN WHOLE OR IN PART FOR MANUFACTURE OR PROCUREMENT, WITHOUT THE WRITTEN PERMISSION OF CURTISS-WRIGHT CORPORATION, EXCEPT FOR (i) EMERGENCY REPAIR OR OVERHAUL WORK BY OR FOR THE GOVERNMENT, WHERE THE ITEM OR PROCESS IS NOT OTHERWISE REASONABLY AVAILABLE TO ENABLE TIMELY PERFORMANCE OF THE WORK, OR (ii) RELEASE TO A FOREIGN GOVERNMENT, AS THE INTERESTS OF THE UNITED STATES MAY REQUIRE. PROVIDED THAT IN EITHER CASE THE RELEASEE, USE, DUPLICATION OR DISCLOSURE HEREOF SHALL BE SUBJECT TO THE FOREGOING LIMITATIONS. THIS LEGEND SHALL BE MARKED ON ANY REPRODUCTION HEREOF IN WHOLE OR IN PART.

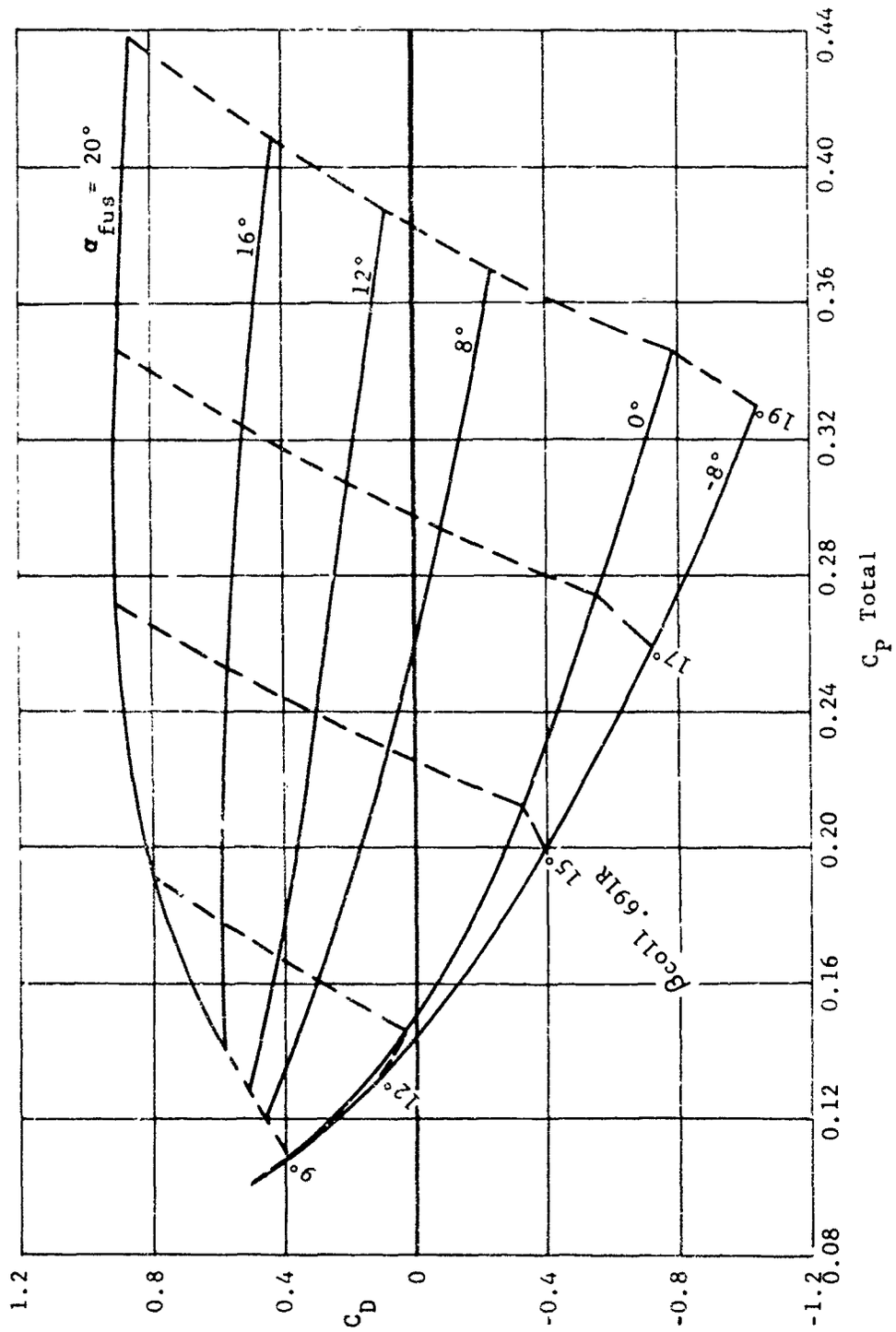

Figure 279. X-19, transition drag coefficient characteristics; ϕ_F = 60°, V = 85 knots, 725 rnD, neutral stick.

'FURNISHED UNDER UNITED STATES GOVERNMENT CONTRACT No AF33(615)-3940 SHALL NOT BE EITHER RELEASED OUTSIDE THE GOVERNMENT, OR USED DUPLICATED, OR DISCLOSED IN WHOLE OR IN PART FOR MANUFACTURE OR PROCUREMENT, WITHOUT THE WRITTEN PERMISSION OF CURTISS-WRIGHT CORPORATION, EXCEPT FOR (i) EMERGENCY REPAIR OR OVERHAUL WORK BY OR FOR THE GOVERNMENT, WHERE THE ITEM OR PROCESS IS NOT OTHERWISE REASONABLY AVAILABLE TO ENABLE TIMELY PERFORMANCE OF THE WORK, OR (ii) RELEASE TO A FOREIGN GOVERNMENT, AS THE INTERESTS OF THE UNITED STATES MAY REQUIRE, PROVIDED THAT IN EITHER CASE THE RELEASE, USE, DUPLICATION OR DISCLOSURE HEREOF SHALL BE SUBJECT TO THE FORGOING LIMITATIONS. THIS LEGEND SHALL BE MARKED ON ANY REPRODUCTION THEREOF IN WHOLE OR IN PART.'

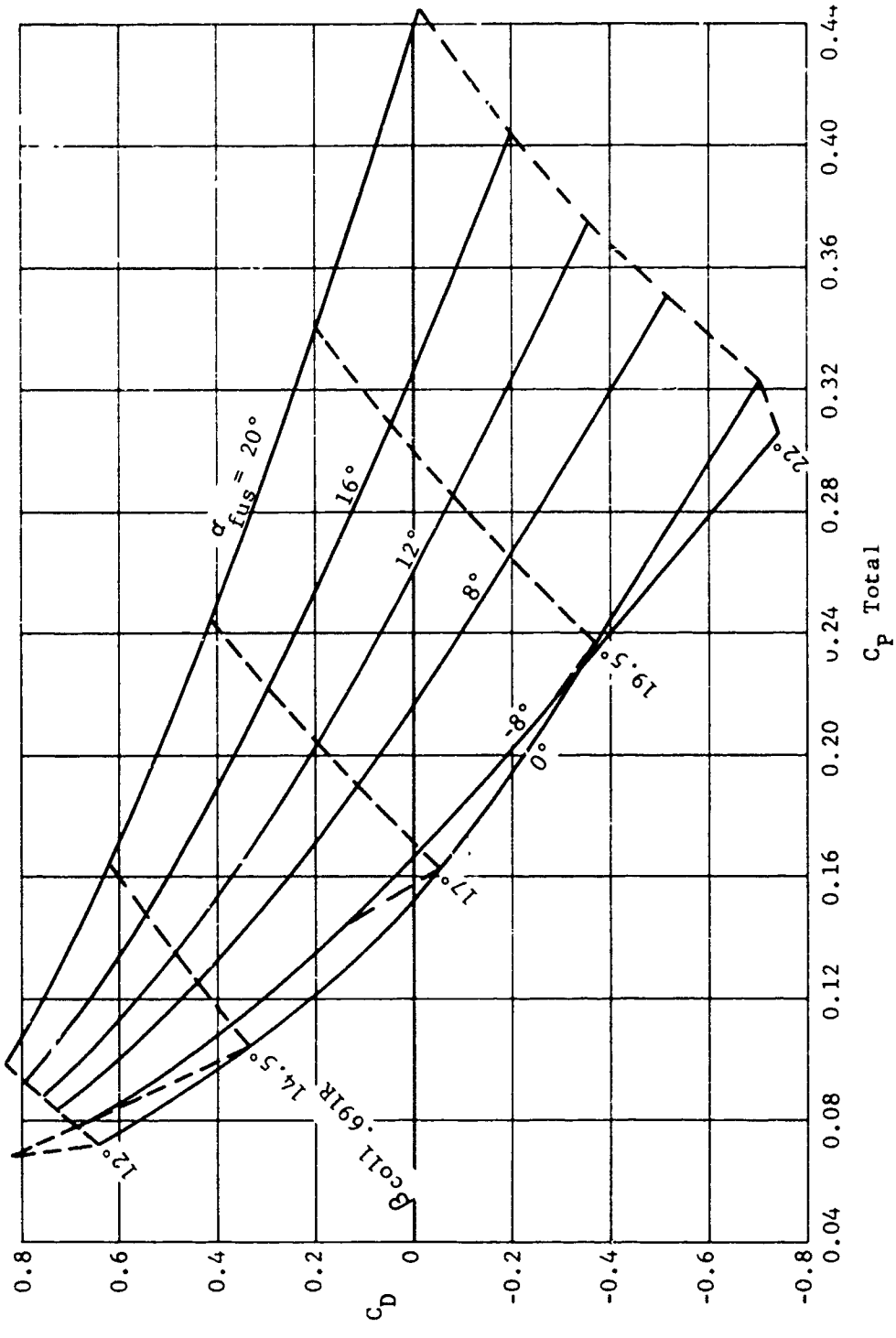

Figure 280. X-19, transition drag coefficient characteristics, ϕ_F = 40°, V = 102 knots, 725 rnD, neutral stick.

'FURNISHED UNDER UNITED STATES GOVERNMENT CONTRACT No. AF33(615)-3940 SHALL NOT BE EITHER RELEASED OUTSIDE THE GOVERNMENT, OR USED, DUPLICATED, OR DISCLOSED IN WHOLE OR IN PART FOR MANUFACTURE OR PROCUREMENT, WITHOUT THE WRITTEN PERMISSION OF CURTISS-WRIGHT CORPORATION, EXCEPT FOR (i) EMERGENCY REPAIR OR OVERHAUL WORK BY OR FOR THE GOVERNMENT, WHERE THE ITEM OR PROCESS IS NOT OTHERWISE REASONABLY AVAILABLE TO ENABLE TIMELY PERFORMANCE OF THE WORK, OR (ii) RELEASE TO A FOREIGN GOVERNMENT, AS THE INTERESTS OF THE UNITED STATES MAY REQUIRE PROVIDED THAT IN EITHER CASE THE RELEASE, USE, DUPLICATION OR DISCLOSURE HEREOF SHALL BE SUBJECT TO THE FOREGOING LIMITATIONS. THIS LEGEND SHALL BE MARKED ON ANY REPRODUCTION HEREOF IN WHOLE OR IN PART."

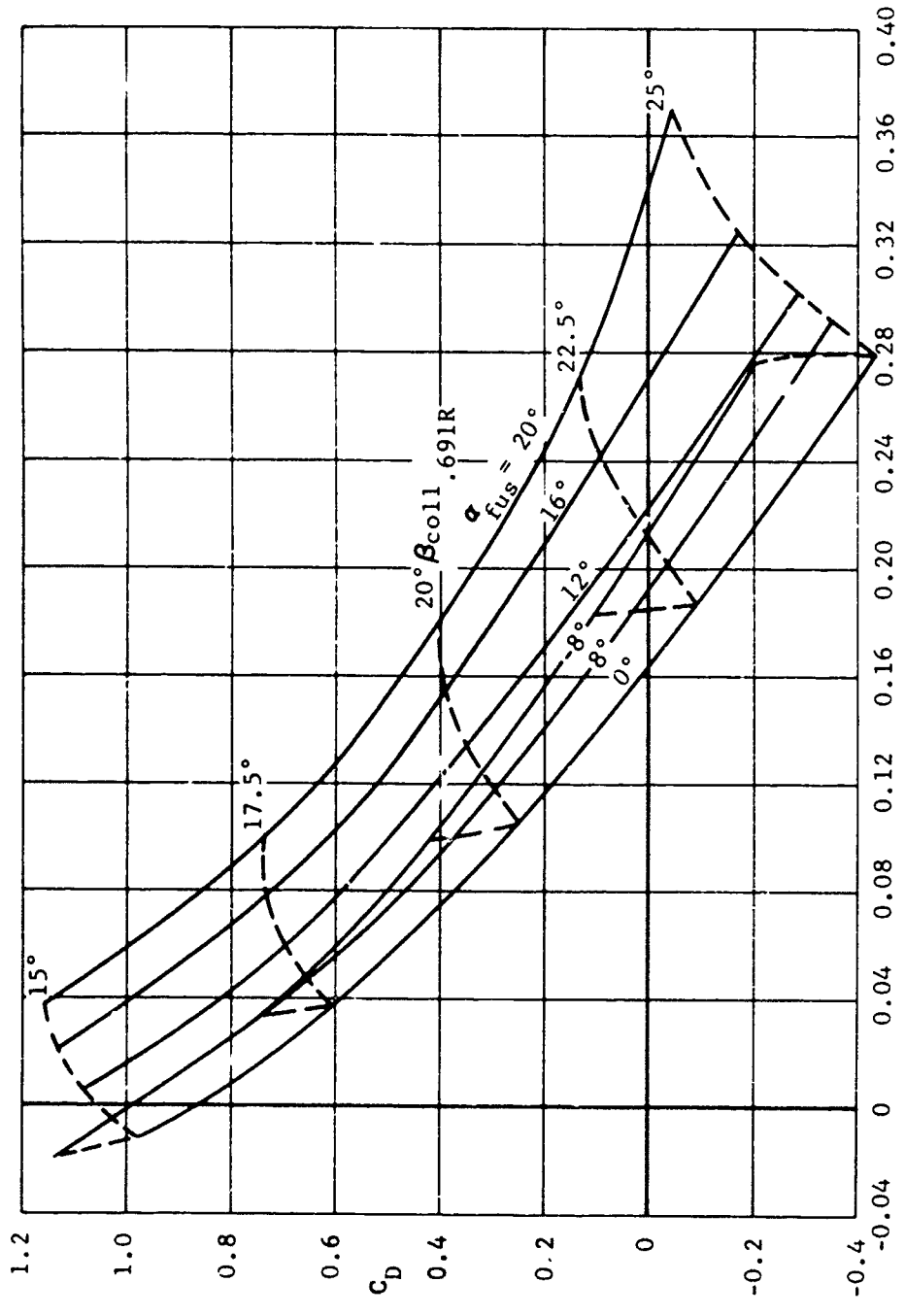

Figure 281. X-19, transition drag coefficient characteristics; ϕ_F = 20°, V = 120 knots, 725 πnD, neutral stick.

FURNISHED UNDER UNITED STATES GOVERNMENT CONTRACT No. AF33(615)-3940. SHALL NOT BE EITHER RELEASED OUTSIDE THE GOVERNMENT OR USED DUPLICATED, OR DISCLOSED IN WHOLE OR PART FOR MANUFACTURE OR PROCUREMENT, WITHOUT THE WRITTEN PERMISSION OF CURTISS-WRIGHT CORPORATION, EXCEPT FOR (i) EMERGENCY REPAIR OR OVERHAUL WORK BY OR FOR THE GOVERNMENT, WHERE THE ITEM OR PROCESS IS NOT OTHERWISE REASONABLY AVAILABLE TO ENABLE TIMELY PERFORMANCE OF THE WORK, OR (ii) RELEASE TO A FOREIGN GOVERNMENT, AS THE INTERESTS OF THE UNITED STATES MAY REQUIRE. PROVIDED THAT IN EITHER CASE THE RELEASE, USE, DUPLICATION OR DISCLOSURE HEREOF SHALL BE SUBJECT TO THE FOREGOING LIMITATIONS. THIS LEGEND SHALL BE MARKED ON ANY REPRODUCTION HEREOF IN WHOLE OR IN PART."

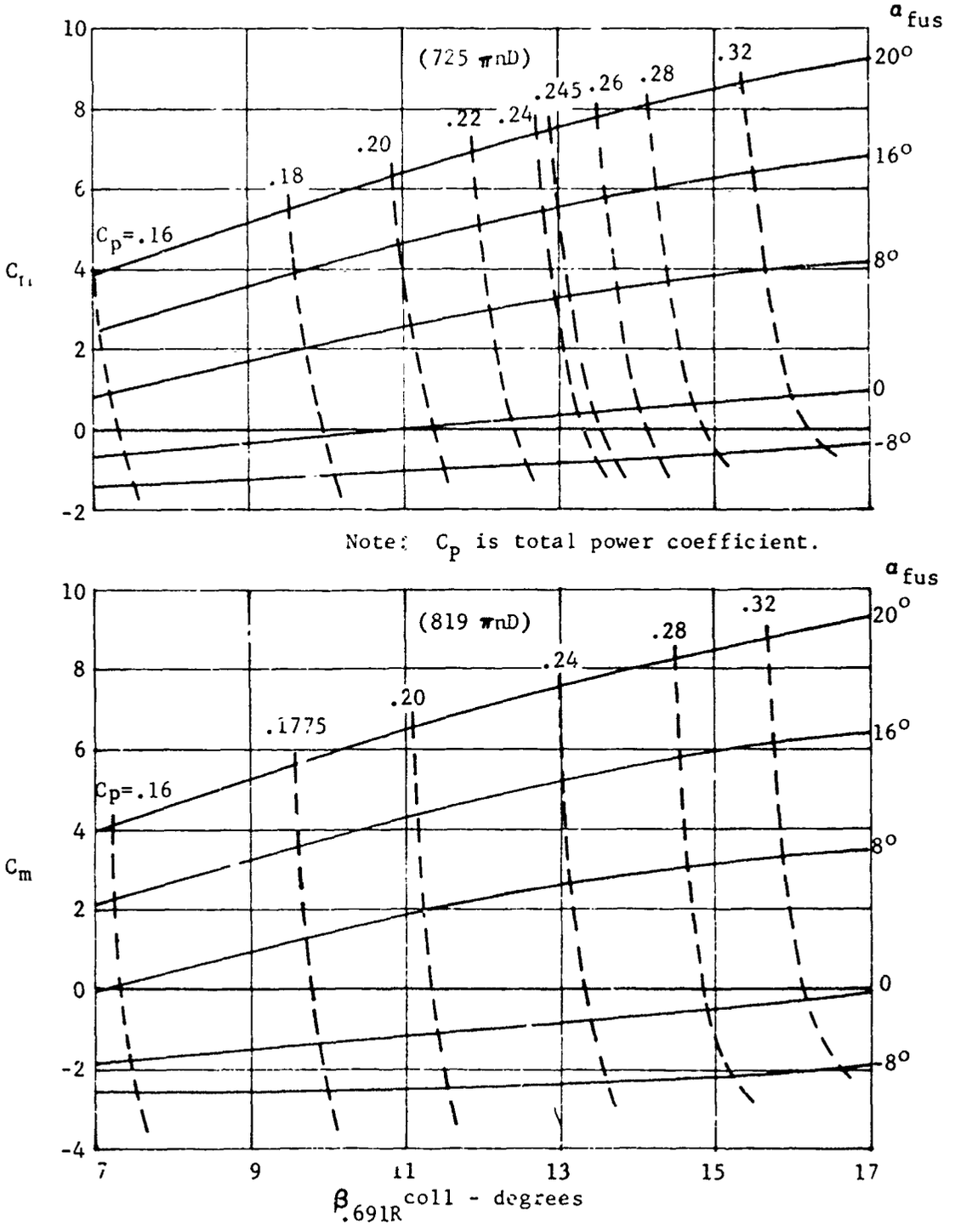

Figure 282. X-19 transition pitching moment coefficient characteristics; ϕ_F = 82.5°, V = 49 knots, c.g. = 42.8%, neutral stick, 725 and 819 πnD.

FURNISHED UNDER UNITED STATES GOVERNMENT CONTRACT No. AF33(615)-3940 SHALL NOT BE EITHER RELEASED OUTSIDE THE GOVERNMENT, OR USED, DUPLICATED, OR DISCLOSED IN WHOLE OR IN PART FOR MANUFACTURE OR PROCUREMENT, WITHOUT THE WRITTEN PERMISSION OF CURTISS-WRIGHT CORPORATION, EXCEPT FOR (i) EMERGENCY REPAIR OR OVERHAUL WORK BY OR FOR THE GOVERNMENT, WHERE THE ITEM OR PROCESS IS NOT OTHERWISE REASONABLY AVAILABLE TO ENABLE TIMELY PERFORMANCE OF THE WORK, OR (ii) RELEASE TO A FOREIGN GOVERNMENT AS THE INTERESTS OF THE UNITED STATES MAY REQUIRE PROVIDED THAT IN EITHER CASE THE RELEASE, USE, DUPLICATION OR DISCLOSURE HEREOF SHALL BE SUBJECT TO THE FOREGOING LIMITATIONS. THIS LEGEND SHALL BE MARKED ON ANY REPRODUCTION HEREOF IN WHOLE OR IN PART."

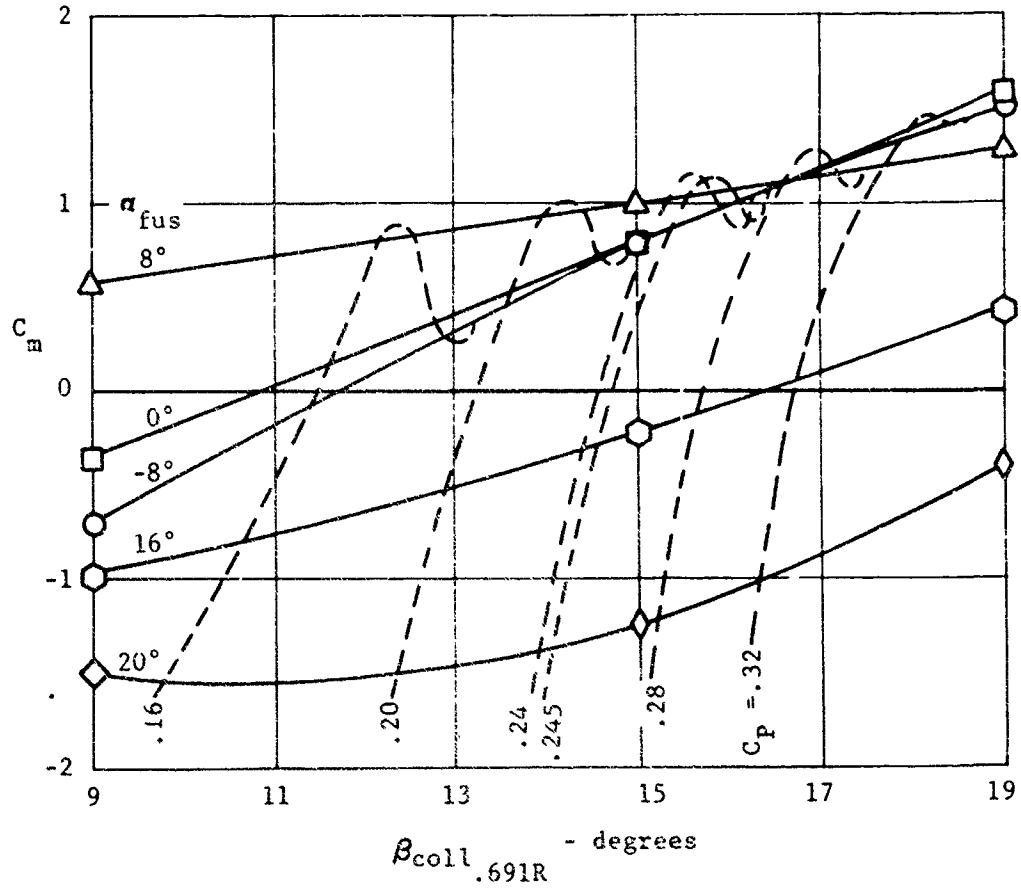

Figure 283. X-19, transition pitching moment characteristics; ϕ_F = 60°, V = 85 knots, c.g. = 42.8%, neutral stick, 725 rpm.

FURNISHED UNDER UNITED STATES GOVERNMENT CONTRACT No. AF33(615)-3940. SHALL NOT BE EITHER RELEASED OUTSIDE THE GOVERNMENT, OR USED DUPLICATED, OR DISCLOSED IN WHOLE OR IN PART FOR MANUFACTURE OR PROCUREMENT, WITHOUT THE WRITTEN PERMISSION OF CURTISS-WRIGHT CORPORATION, EXCEPT FOR (i) EMERGENCY REPAIR OR OVERHAUL WORK BY OR FOR THE GOVERNMENT, WHERE THE ITEM OR PROCESS IS NOT OTHERWISE REASONABLY AVAILABLE TO ENABLE TIMELY PERFORMANCE OF THE WORK, OR (ii) RELEASE TO A FOREIGN GOVERNMENT, AS THE INTERESTS OF THE UNITED STATES MAY REQUIRE. PROVIDED THAT IN EITHER CASE THE RELEASE, USE, DUPLICATION OR DISCLOSURE HEREOF SHALL BE SUBJECT TO THE FOREGOING LIMITATIONS. THIS LEGEND SHALL BE MARKED ON ANY REPRODUCTION HEREOF IN WHOLE OR IN PART.

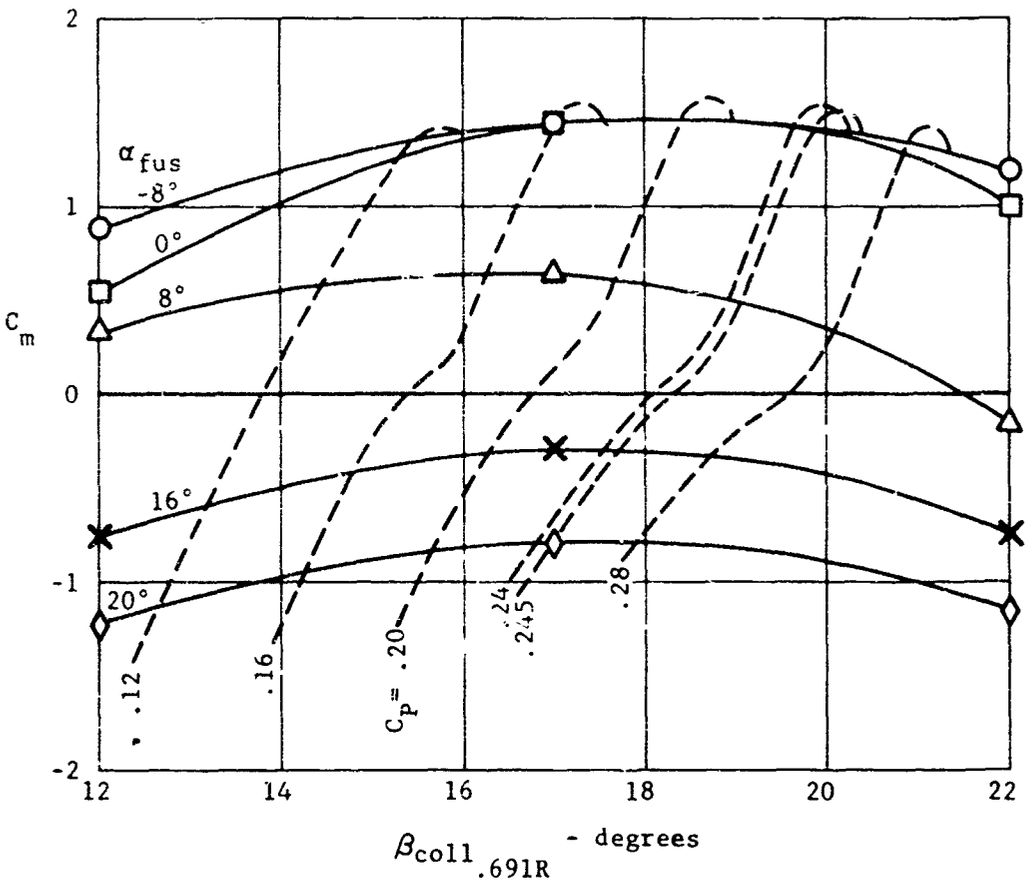

Figure 284. X-19, transition pitching moment coefficient characteristics; $\emptyset_F$ = 40°, V = 102 knots, c.g. = 42.8%, neutral stick, 725 rpD.

FURNISHED UNDER UNITED STATES GOVERNMENT CONTRACT No. AF33(615)-3940. SHALL NOT BE EITHER RELEASED OUTSIDE THE GOVERNMENT, OR USED, DUPLICATED, OR DISCLOSED IN WHOLE OR IN PART FOR MANUFACTURE OR PROCUREMENT, WITHOUT THE WRITTEN PERMISSION OF CURTISS-WRIGHT CORPORATION, EXCEPT FOR (i) EMERGENCY REPAIR OR OVERHAUL WORK BY OR FOR THE GOVERNMENT, WHERE THE ITEM OR PROCESS IS NOT OTHERWISE REASONABLY AVAILABLE TO ENABLE TIMELY PERFORMANCE OF THE WORK, OR (ii) RELEASE TO A FOREIGN GOVERNMENT, AS THE INTERESTS OF THE UNITED STATES MAY REQUIRE. PROVIDED THAT IN EITHER CASE THE RELEASE, USE, DUPLICATION OR DISCLOSURE HEREOF SHALL BE SUBJECT TO THE FOREGOING LIMITATIONS. THIS LEGEND SHALL BE MARKED ON ANY REPRODUCTION HEREOF IN WHOLE OR IN PART.

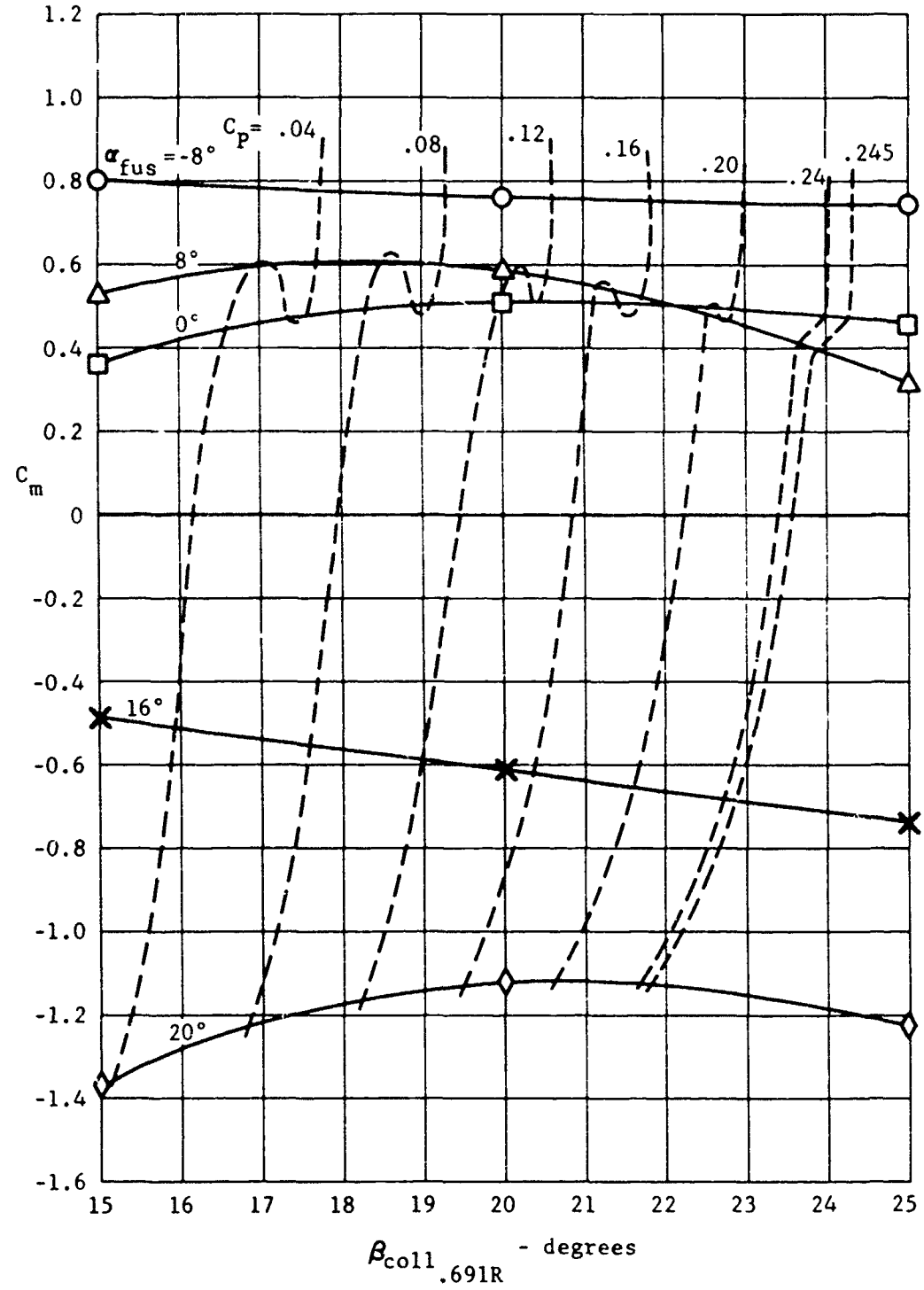

Figure 285. X-19, transition pitching moment coefficient characteristics; ϕ_F = 20°, V = 120 knots, c.g. = 42.8%, neutral stick, 725 rnD.

FURNISHED UNDER UNITED STATES GOVERNMENT CONTRACT No. AF33(615)-3940. SHALL NOT BE EITHER RELEASED OUTSIDE THE GOVERNMENT OR USED DUPLICATED, OR DISCLOSED IN WHOLE OR IN PART FOR MANUFACTURE OR PROCUREMENT, WITHOUT THE WRITTEN PERMISSION OF CURTISS-WRIGHT CORPORATION, EXCEPT FOR (i) EMERGENCY REPAIR OR OVERHAUL WORK BY OR FOR THE GOVERNMENT, WHERE THE ITEM OR PROCESS IS NOT OTHERWISE REASONABLY AVAILABLE TO ENABLE TIMELY PERFORMANCE OF THE WORK, OR (ii) RELEASE TO A FOREIGN GOVERNMENT, AS THE INTERESTS OF THE UNITED STATES MAY REQUIRE. PROVIDED THAT IN EITHER CASE THE RELEASE, USE, DUPLICATION OR DISCLOSURE HEREOF SHALL BE SUBJECT TO THE FOREGOING LIMITATIONS. THIS LEGEND SHALL BE MARKED ON ANY REPRODUCTION HEREOF IN WHOLE OR IN PART."

The free zone in the propeller governor circuit was set so that a maximum power increment of 20 percent would result from large throttle motions. The airframe would not be designed by loads of this magnitude. Likewise, the transmission loads from a pure throttle impulse would not be critical. Combinations of throttle and control deflection were not used for design.

d. Design Maneuvers and Flight Envelopes

Figures 286 through 289 illustrate the fore-aft power distribution for trimmed flight. It is apparent, for the most part, that the rear propeller is consistently at a higher power level than the front propeller in trimmed flight. At low tilt angles and high angles of attack (high descent rate) this trend is reversed. Some flight test data have confirmed the general trend.

Figures 290 through 293 illustrate the effects of deviating from the prescribed tilt schedule, at tilt angle of $\emptyset_F$ = 60 degrees.

A flight-loads program must reflect all of the curves and characteristics discussed throughout this section. Actually these do not reflect the full gamut of conditions. The data presented here are used solely to generate trim loads at various rates of climb or acceleration, throughout the transition corridor. Some small load factor loadings can be obtained with throttle. However, component loadings, which are quite substantial, are generated by control deflections or by gusts.

e. Design Gust Loads Criteria

Gust loads have been treated in a manner similar to the cruise criteria; i.e., the gust velocity is superimposed on the free stream velocity. In the cruise regime, vertical gusts are generally considered, with no effective change in velocity. In transition, the 30 fps gust has been superimposed upon the trimmed equilibrium condition. In this case, however, the vertical gust does not necessarily design the machine. Therefore horizontal and side gusts have also been investigated. As the forward speed is not very high in transition, a 30 ft/sec gust can alter both the propeller angle of attack and the resultant velocity. Both have been taken into consideration in the final load determination. For the vertical or horizontal gust, a simple two-dimensional computation was made. In the case of side gusts, the resultant velocity vector is skewed to the propeller body axis. The method evolved was to establish the propeller loads (six components) in the skewed plane. Then the loads were resolved back into the body axis system.

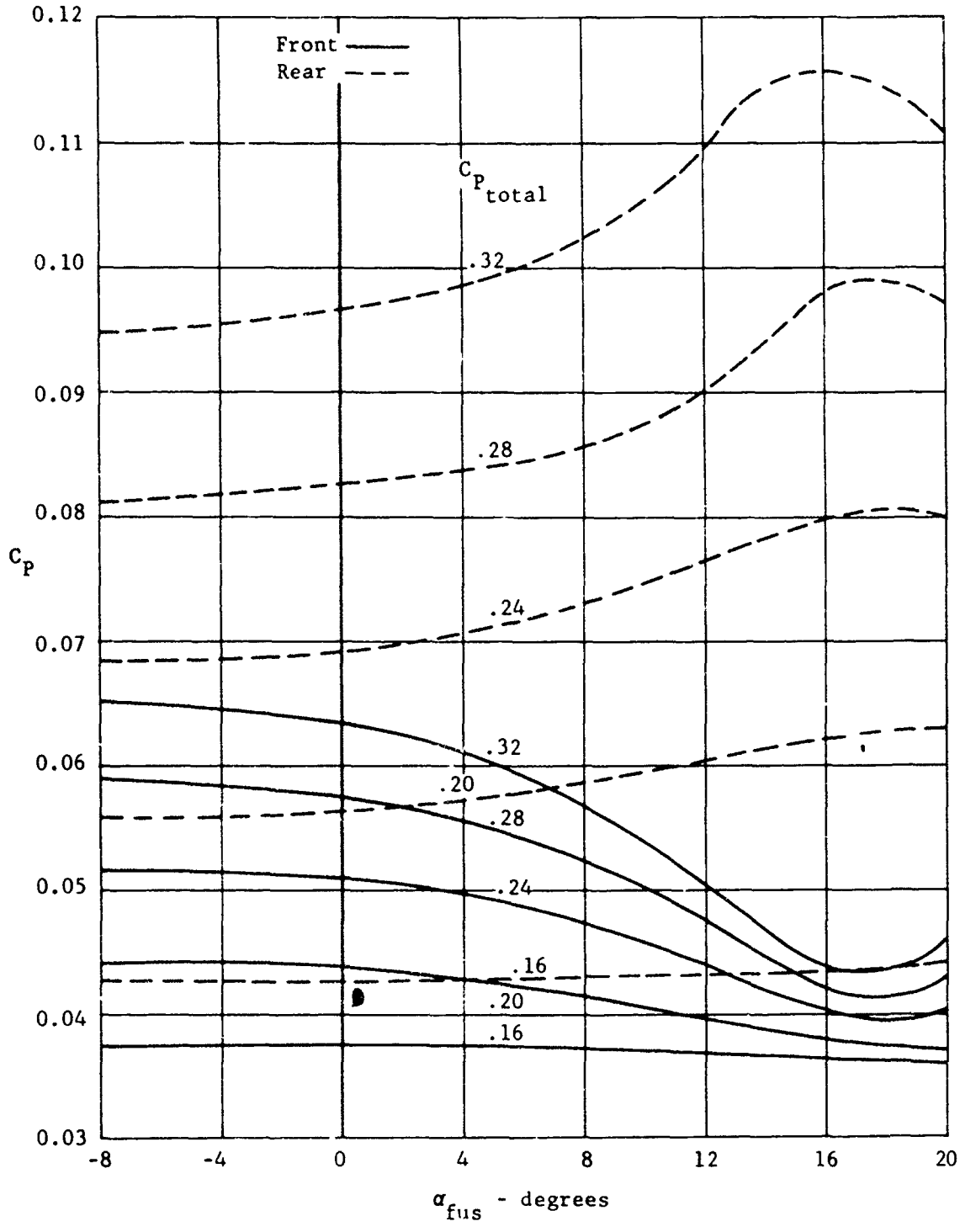

Figure 286. X-19, transition front and rear propeller trim powers; ϕ_F = 82.5°, V = 49 knots, 725 πnD, c.g. = 42.8%.

FURNISHED UNDER UNITED STATES GOVERNMENT CONTRACT No. AF33(615)-3940 SHALL NOT BE EITHER RELEASED OUTSIDE THE GOVERNMENT, OR USED, DUPLICATED, OR DISCLOSED IN WHOLE OR IN PART FOR MANUFACTURE OR PROCUREMENT, WITHOUT THE WRITTEN PERMISSION OF CURTISS-WRIGHT CORPORATION, EXCEPT FOR (i) EMERGENCY REPAIR OR OVERHAUL WORK BY OR FOR THE GOVERNMENT, WHERE THE ITEM OR PROCESS IS NOT OTHERWISE REASONABLY AVAILABLE TO ENABLE TIMELY PERFORMANCE OF THE WORK, OR (ii) RELEASE TO A FOREIGN GOVERNMENT, AS THE INTERESTS OF THE UNITED STATES MAY REQUIRE, PROVIDED THAT IN EITHER CASE THE RELEASE, USE, DUPLICATION OR DISCLOSURE HEREOF SHALL BE SUBJECT TO THE FOREGOING LIMITATIONS. THIS LEGEND SHALL BE MARKED ON ANY REPRODUCTION HEREOF IN WHOLE OR IN PART.

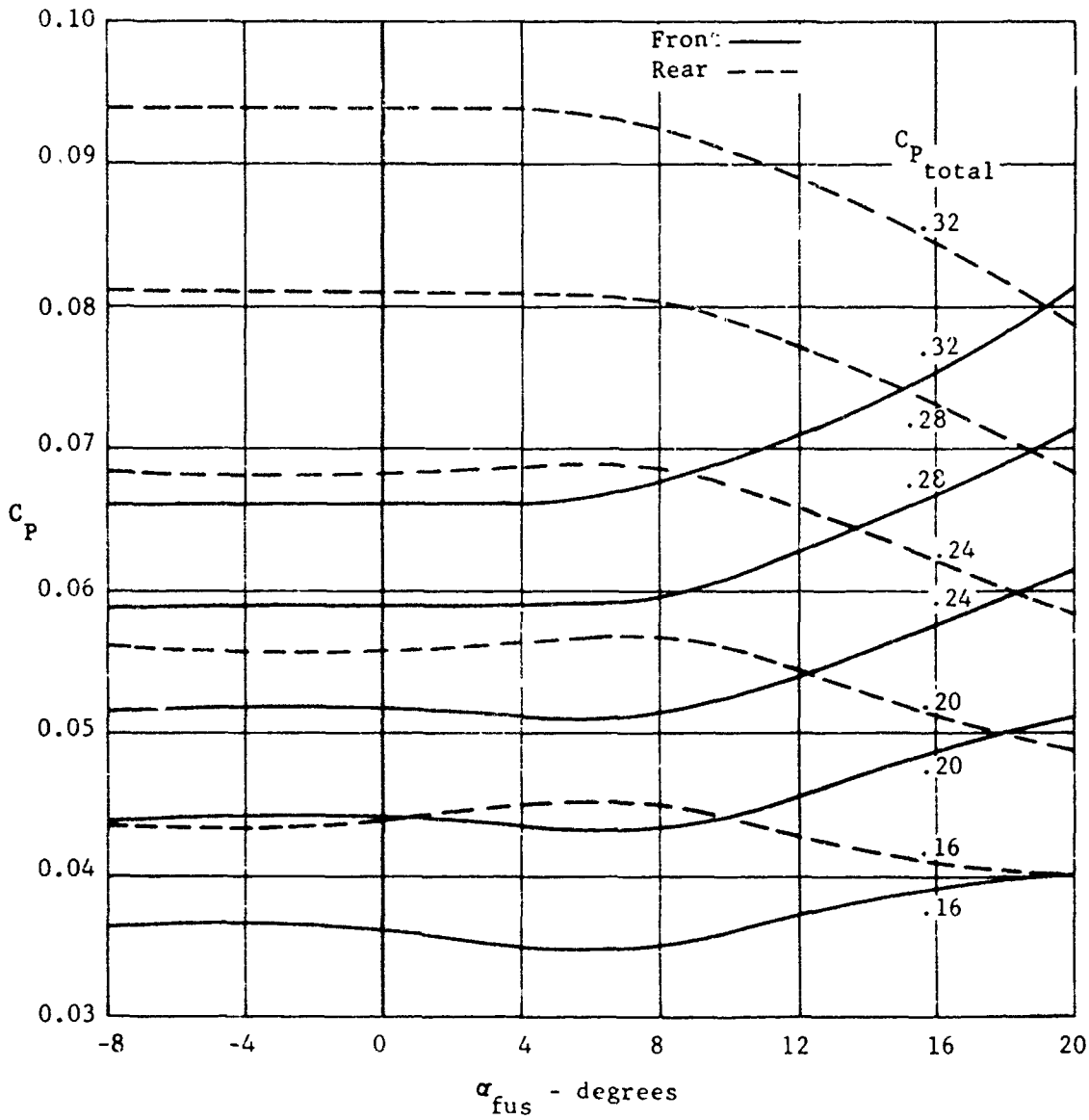

Figure 287. X-19, transition front and rear propeller trim powers; ϕ_F = 60°, V = 85 knots, 725 πnD, c.g. 42.8%.

FURNISHED UNDER UNITED STATES GOVERNMENT CONTRACT No. AF33(615)-3940. SHALL NOT BE EITHER RELEASED OUTSIDE THE GOVERNMENT OR USED, DUPLICATED, OR DISCLOSED IN WHOLE OR IN PART FOR MANUFACTURE OR PROCUREMENT, WITHOUT THE WRITTEN PERMISSION OF CURTISS-WRIGHT CORPORATION, EXCEPT FOR (i) EMERGENCY REPAIR OR OVERHAUL WORK BY OR FOR THE GOVERNMENT WHERE THE ITEM OR PROCESS IS NOT OTHERWISE REASONABLY AVAILABLE TO ENABLE TIMELY PERFORMANCE OF THE WORK, OR (ii) RELEASE TO A FOREIGN GOVERNMENT, AS THE INTERESTS OF THE UNITED STATES MAY REQUIRE. PROVIDED THAT IN EITHER CASE THE RELEASE, USE, DUPLICATION OR DISCLOSURE HEREOF SHALL BE SUBJECT TO THE FOREGOING LIMITATIONS. THIS LEGEND SHALL BE MARKED ON ANY REPRODUCTION HEREOF IN WHOLE OR IN PART."

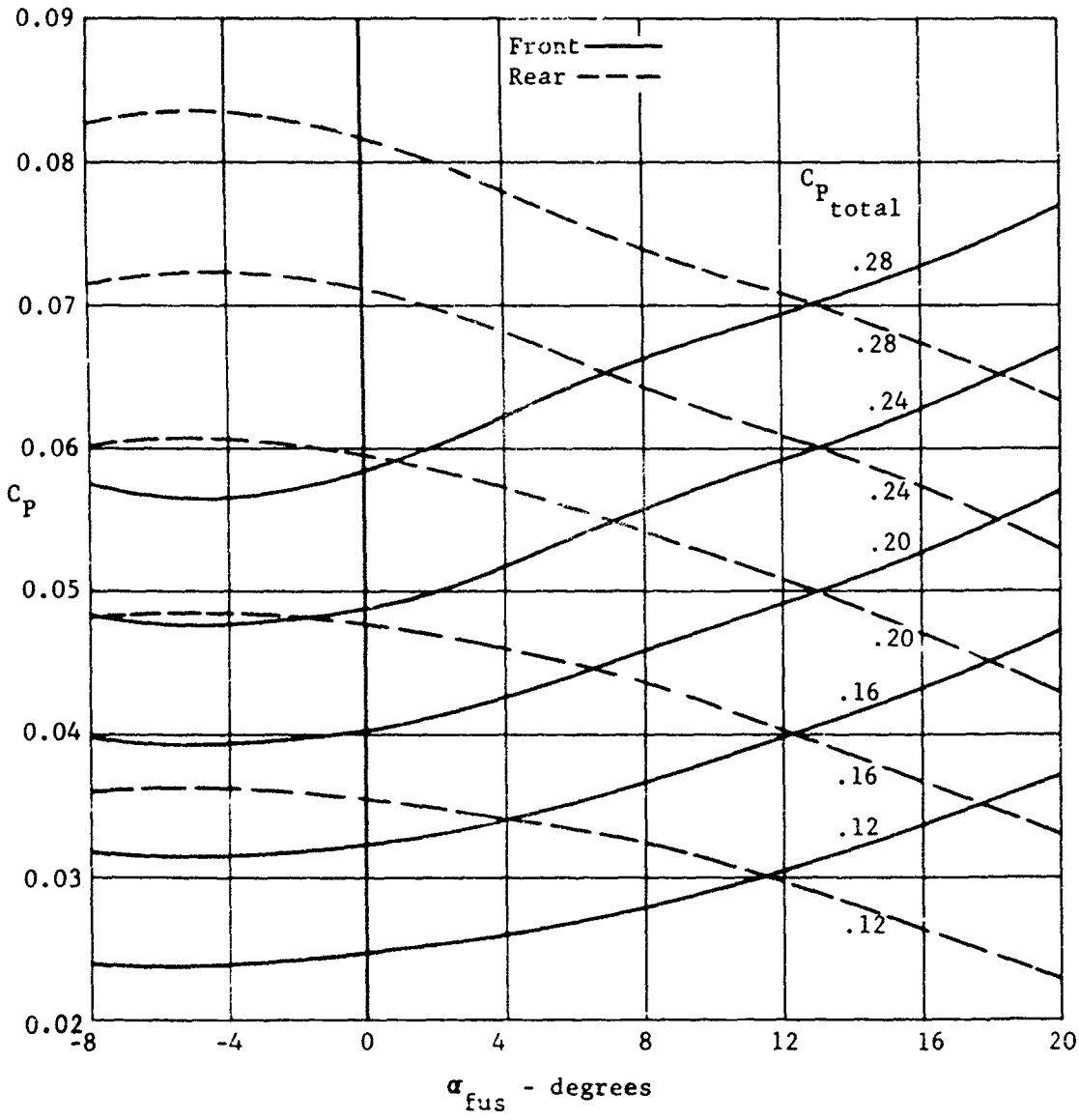

Figure 288. X-19, transition front and rear propeller trim powers; $\emptyset_F$ = 40°, V = 102 knots, 725 πnD, c.g. = 42.8%.

FURNISHED UNDER UNITED STATES GOVERNMENT CONTRACT No. AF33(615)-3940 SHALL NOT BE EITHER RELEASED OUTSIDE THE GOVERNMENT OR USED DUPLICATED, OR DISCLOSED IN WHOLE OR IN PART FOR MANUFACTURE OR PROCUREMENT, WITHOUT THE WRITTEN PERMISSION OF CURTISS-WRIGHT CORPORATION, EXCEPT FOR (i) EMERGENCY REPAIR OR OVERHAUL WORK BY OR FOR THE GOVERNMENT WHERE THE ITEM OR PROCESS IS NOT OTHERWISE REASONABLY AVAILABLE TO ENABLE TIMELY PERFORMANCE OF THE WORK OR (ii) RELEASE TO A FOREIGN GOVERNMENT, AS THE INTERESTS OF THE UNITED STATES MAY REQUIRE PROVIDED THAT IN EITHER CASE THE RELEASE, USE, DUPLICATION OR DISCLOSURE HEREOF SHALL BE SUBJECT TO THE FOREGOING LIMITATIONS. THIS LEGEND SHALL BE MARKED ON ANY REPRODUCTION HEREOF IN WHOLE OR IN PART.

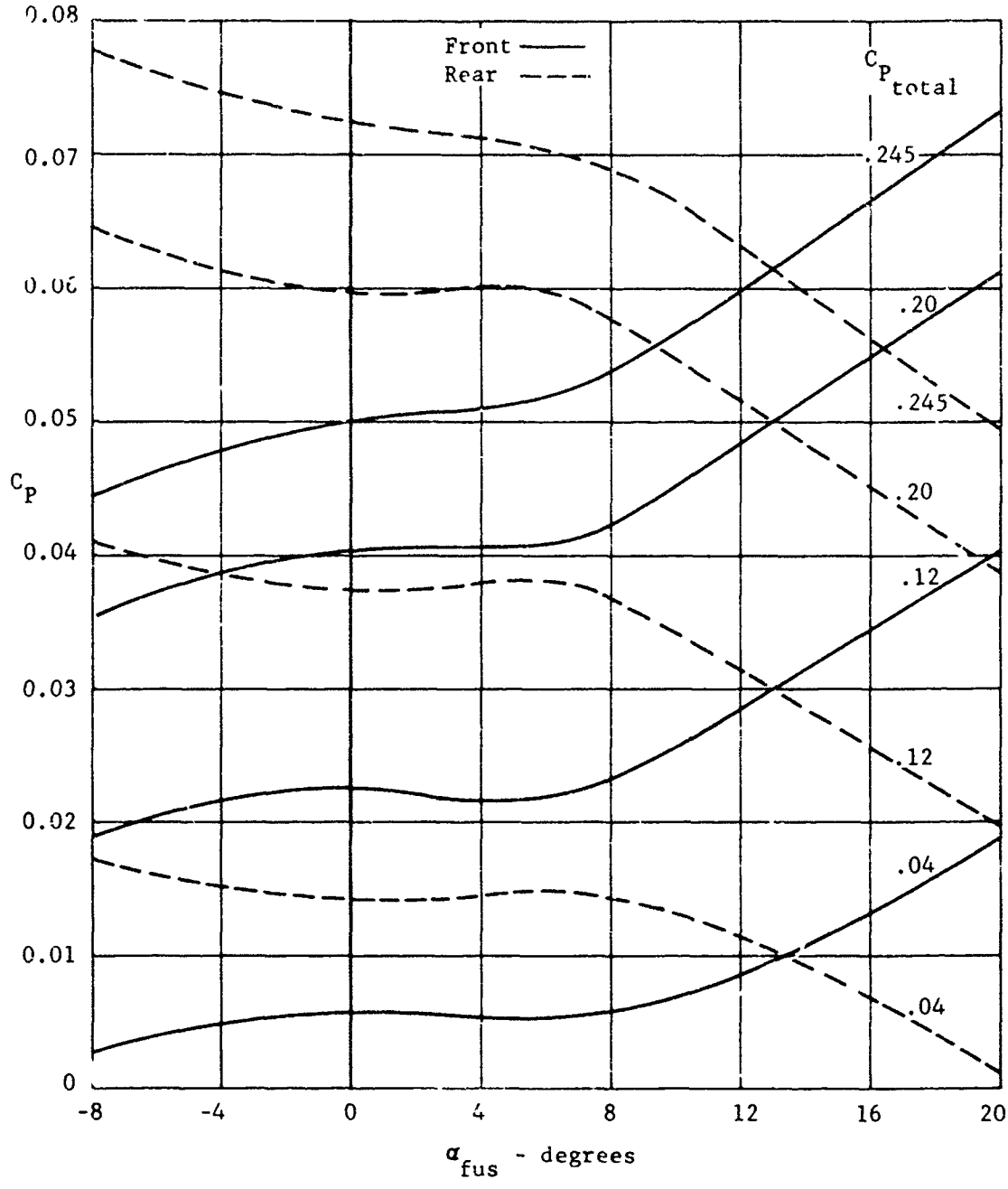

Figure 289. X-19, transition front and rear propeller trim powers; $\emptyset_F$ = 20°, V = 120 knots, 725 πnD, c.g. = 42.8%.

FURNISHED UNDER UNITED STATES GOVERNMENT CONTRACT No. AF33(615)-3940 SHALL NOT BE EITHER RELEASED OUTSIDE THE GOVERNMENT, OR USED, DUPLICATED, OR DISCLOSED IN WHOLE OR IN PART FOR MANUFACTURE OR PROCUREMENT, WITHOUT THE WRITTEN PERMISSION OF CURTISS-WRIGHT CORPORATION, EXCEPT FOR (i) EMERGENCY REPAIR OR OVERHAUL WORK BY OR FOR THE GOVERNMENT, WHERE THE ITEM OR PROCESS IS NOT OTHERWISE REASONABLY AVAILABLE TO ENABLE TIMELY PERFORMANCE OF THE WORK, OR (ii) RELEASE TO A FOREIGN GOVERNMENT, AS THE INTERESTS OF THE UNITED STATES MAY REQUIRE. PROVIDED THAT IN EITHER CASE THE RELEASE, USE, DUPLICATION OR DISCLOSURE HEREOF SHALL BE SUBJECT TO THE FOREGOING LIMITATIONS. THIS LEGEND SHALL BE MARKED ON ANY REPRODUCTION HEREOF IN WHOLE OR IN PART."

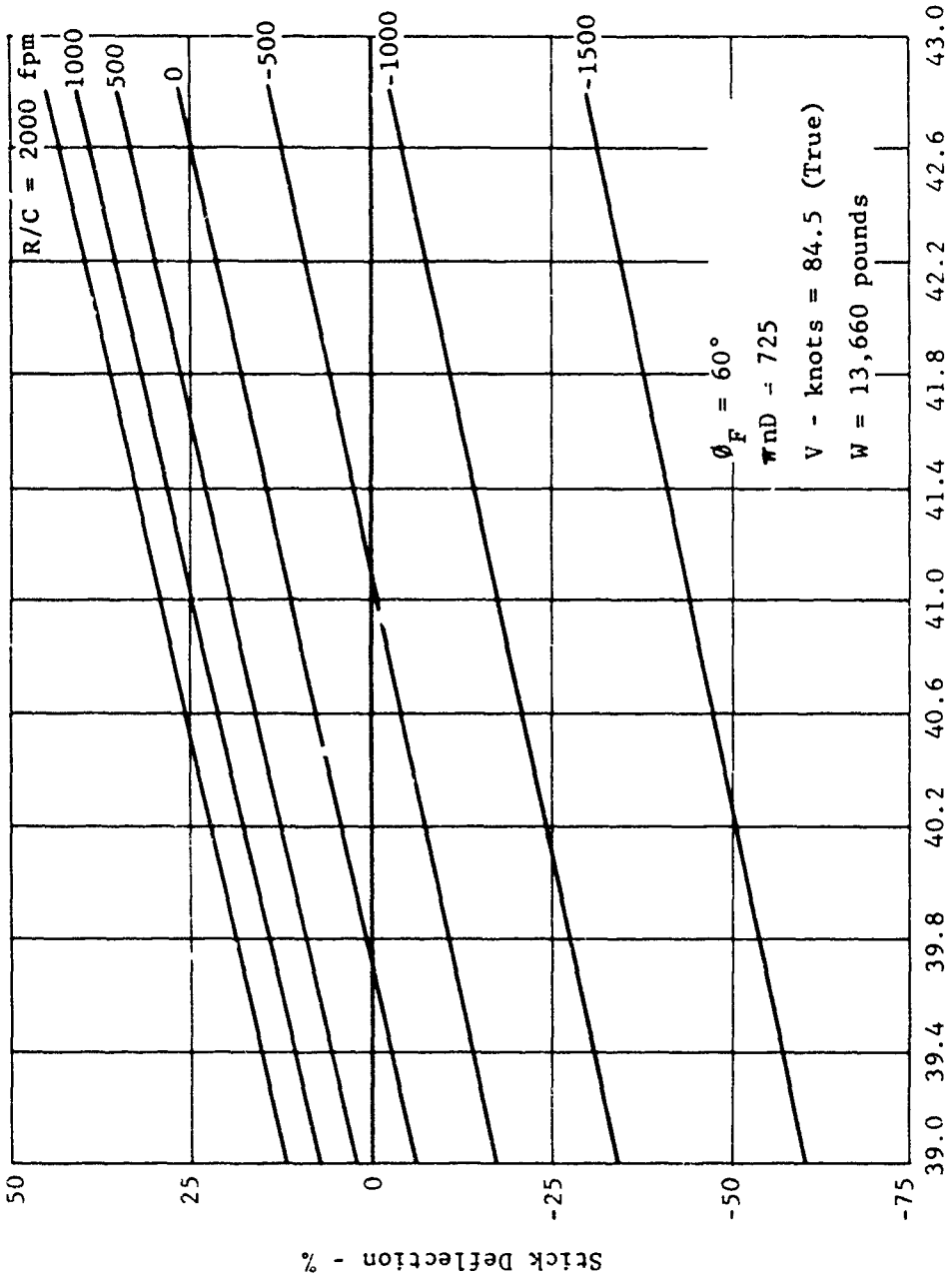

Figure 290. X-19, effects of c.g. location on stick position; ϕ_F = 60°, πnD = 725, V= 85 knots, W = 13,660 pounds.

'FURNISHED UNDER UNITED STATES GOVERNMENT CONTRACT No. AF33(615)-3940. SHALL NOT BE EITHER RELEASED OUTSIDE THE GOVERNMENT OR USED DUPLICATED, OR DISCLOSED IN WHOLE OR IN PART FOR MANUFACTURE OR PROCUREMENT, WITHOUT THE WRITTEN PERMISSION OF CURTISS-WRIGHT CORPORATION, EXCEPT FOR (i) EMERGENCY REPAIR OR OVERHAUL WORK BY OR FOR THE GOVERNMENT, WHERE THE ITEM OR PROCESS IS NOT OTHERWISE REASONABLY AVAILABLE TO ENABLE TIMELY PERFORMANCE OF THE WORK OR (ii) RELEASE TO A FOREIGN GOVERNMENT, AS THE INTERESTS OF THE UNITED STATES MAY REQUIRE PROVIDED THAT IN EITHER CASE THE RELEASE, USE, DUPLICATION OR DISCLOSURE HEREOF SHALL BE SUBJECT TO THE FOREGOING LIMITATIONS THIS LEGEND SHALL BE MARKED ON ANY REPRODUCTION HEREOF IN WHOLE OR IN PART.'

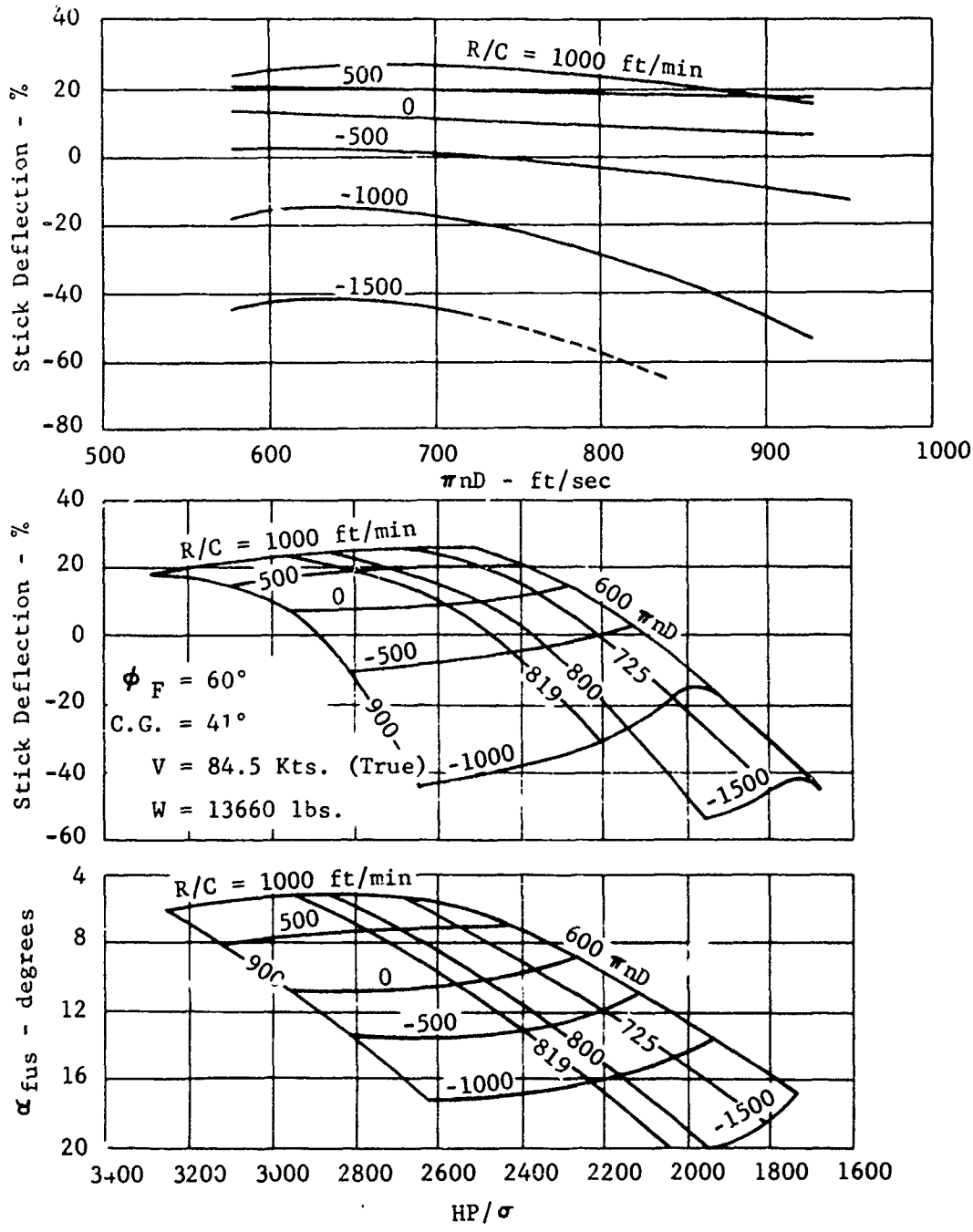

Figure 291. X-19, effects of πnD variation upon trim; ϕ_F = 60°, V = 85 knots, W = 13,660 pounds, c.g. = 41%.

"FURNISHED UNDER UNITED STATES GOVERNMENT CONTRACT No. AF33(615)-3940. SHALL NOT BE EITHER RELEASED OUTSIDE THE GOVERNMENT, OR USED, DUPLICATED, OR DISCLOSED IN WHOLE OR IN PART FOR MANUFACTURE OR PROCUREMENT, WITHOUT THE WRITTEN PERMISSION OF CURTISS-WRIGHT CORPORATION, EXCEPT FOR (i) EMERGENCY REPAIR OR OVERHAUL WORK BY OR FOR THE GOVERNMENT, WHERE THE ITEM OR PROCESS IS NOT OTHERWISE REASONABLY AVAILABLE TO ENABLE TIMELY PERFORMANCE OF THE WORK, OR (ii) RELEASE TO A FOREIGN GOVERNMENT, AS THE INTERESTS OF THE UNITED STATES MAY REQUIRE. PROVIDED THAT IN EITHER CASE THE RELEASE, USE, DUPLICATION OR DISCLOSURE HEREOF SHALL BE SUBJECT TO THE FOREGOING LIMITATIONS. THIS LEGEND SHALL BE MARKED ON ANY REPRODUCTION HEREOF IN WHOLE OR IN PART."

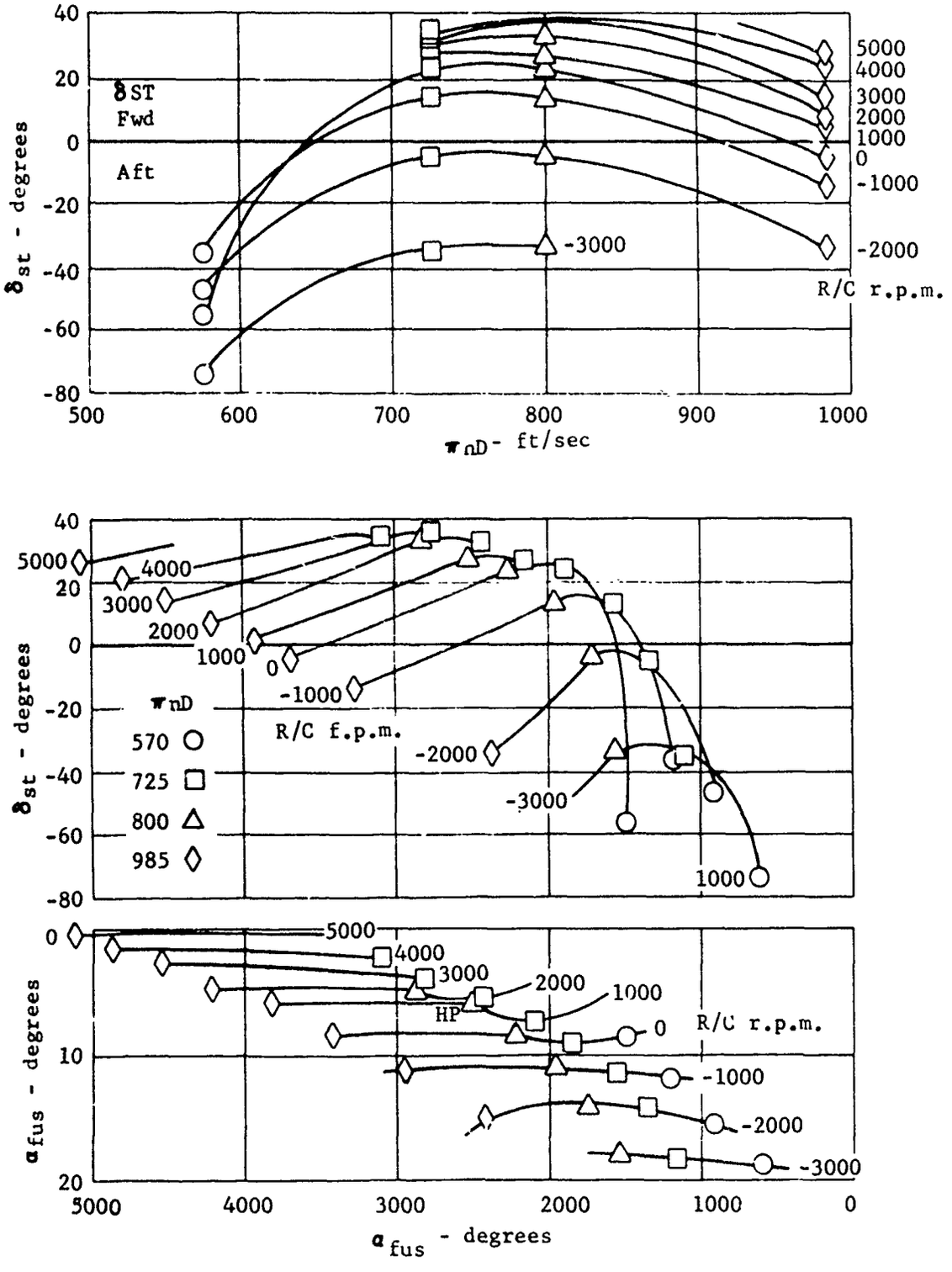

Figure 292. X-19, effects of πnD variation upon trim; ϕ_F = 40°, W = 12,300 pounds, V = 102 knots, c.g. = 42.8%.

FURNISHED UNDER UNITED STATES GOVERNMENT CONTRACT No. AF33(615)-3940. SHALL NOT BE EITHER RELEASED OUTSIDE THE GOVERNMENT, OR USED, DUPLICATED, OR DISCLOSED IN WHOLE OR IN PART FOR MANUFACTURE OR PROCUREMENT, WITHOUT THE WRITTEN PERMISSION OF CURTISS-WRIGHT CORPORATION, EXCEPT FOR (i) EMERGENCY REPAIR OR OVERHAUL WORK BY OR FOR THE GOVERNMENT, WHERE THE ITEM OR PROCESS IS NOT OTHERWISE REASONABLY AVAILABLE TO ENABLE TIMELY PERFORMANCE OF THE WORK, OR (ii) RELEASE TO A FOREIGN GOVERNMENT, AS THE INTERESTS OF THE UNITED STATES MAY REQUIRE. PROVIDED THAT IN EITHER CASE THE RELEASE, USE, DUPLICATION OR DISCLOSURE HEREOF SHALL BE SUBJECT TO THE FOREGOING LIMITATIONS. THIS LEGEND SHALL BE MARKED ON ANY REPRODUCTION HEREOF IN WHOLE OR IN PART.

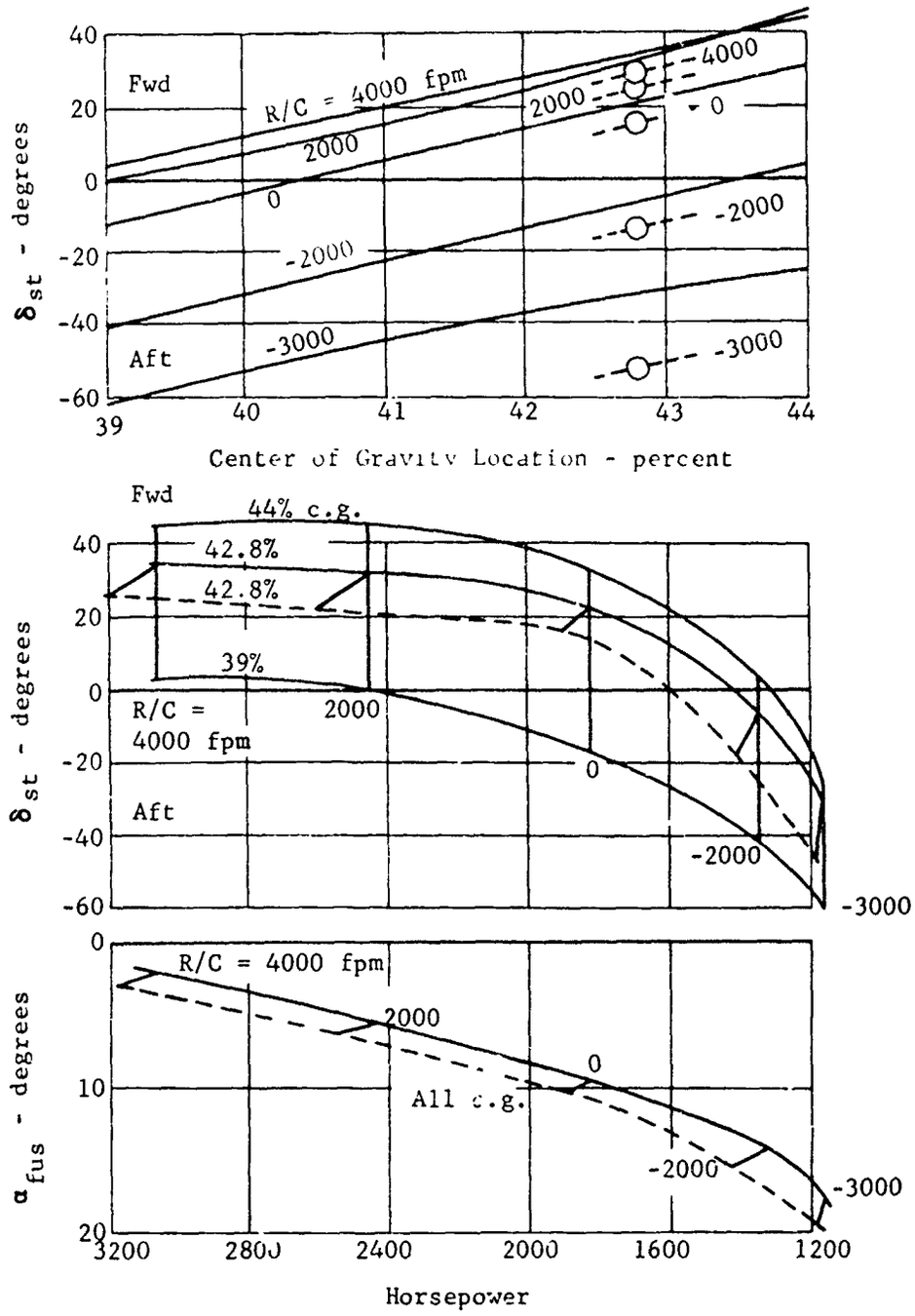

Figure 293. X-19, effects of c.g. location upon trim; $\emptyset_F$ = 40°, πnD = 725, V = 102 knots.

FURNISHED UNDER UNITED STATES GOVERNMENT CONTRACT No AF33(615)-1940 SHALL NOT BE EITHER RELEASED OUTSIDE THE GOVERNMENT, OR USED, DUPLICATED, OR DISCLOSED IN WHOLE OR IN PART FOR MANUFACTURE OR PROCUREMENT, WITHOUT THE WRITTEN PERMISSION OF CURTISS-WRIGHT CORPORATION, EXCEPT FOR (i) EMERGENCY REPAIR OR OVERHAUL WORK BY OR FOR THE GOVERNMENT, WHERE THE ITEM OR PROCESS IS NOT OTHERWISE REASONABLY AVAILABLE TO ENABLE TIMELY PERFORMANCE OF THE WORK, OR (ii) RELEASE TO A FOREIGN GOVERNMENT, AS THE INTERESTS OF THE UNITED STATES MAY REQUIRE PROVIDED THAT IN EITHER CASE THE RELEASE, USE, DUPLICATION OR DISCLOSURE HEREOF SHALL BE SUBJECT TO THE FOREGOING LIMITATIONS THIS LEGEND SHALL BE MARKED ON ANY REPRODUCTION HEREOF IN WHOLE OR IN PART."

5. DESIGN GROUND LOADS CRITERIA

The permissible landing loads are derived from specifications given in Civil Air Regulations Part 7 for Rotorcraft-Transport Category. To these requirements were added several loading conditions specified in ANC-2, as well as certain other conditions specified by Curtiss-Wright, as being desirable for anticipating probable ground loads. The various design conditions and their respective sources are collected in the following brief summary:

Design Condition	Wheels in Contact	c.g. Location % L.C.	Specification Reference
Level landing	3*	40,43	CAM-7, Para. 7.231a
	2,1	40	CAM-7, Para. 7.233
Rolling drag	3*,2	40	CAM-7, Para. 7.231b
Nose up 17.40	2	40	CAM-7, Para. 7.232
Lateral drift	3*,2	40	CAM-7, Para. 7.234
Braked roll	3*,2	40	CAM-7, Para. 7.235
Reversed braking	2	40	ANC-2 Sect. 3.214
Spinup and Springback	3,2	40	ANC-2 Sect. 7.3, p.4.1
Airborne side drift	1	40	Curtiss-Wright Spec. p.2.1
Aircraft at 30° roll	1	40	Curtiss-Wright Spec. p.2.1
Towing load, fwd & aft	3	43	ANC-2 Sect. 4.2, p.8

* Three-wheel loading for both forward and aft c.g. limit.

Limit loads were then calculated for these conditions for an aircraft GW of 12,300 lb to obtain the loads acting on the landing gear. The c.g. positions employed are the most aft or most forward, whichever gives the maximum load in the wheel considered. The limit gear load factor of 2.0 was used, having been determined from drop testing of the main landing gear in accordance with provisions in Paragraph 7.332 of CAR Part 7.

REFERENCES

76. Civil Air Regulations, Part 7, Rotor Air worthiness, Transport Categories, Civil Aeronautics Board, Aug. 1, 1956

77. Civil Air Regulations, Part 4b, Airplane Air worthiness, Transport Categories, Civil Aeronautics Board, Dec. 31, 1953

78. Airplane Strength and Rigidity, Flight Loads, Military Specification MIL-A-8861 (ASF), May 18, 1960

79. Fluk, H; Jenkins, M.W.M. X-19 Aerodynamic Loads Summary, Curtiss-Wright Report 014-253, March 31, 1964

80. Model X-200T Tandem Front and Rear Propeller-Nacelle-Wing Characteristics in the Presence of the Fuselage , MIT Report No. 1003, October 1960

81. Curtiss-Wright Corporation M200 Turbine Stability Model MIT Report No. 1019, March 1962

82. R.G. Locklin, Control Surface Hinge Moments and Overall Lift Effectiveness of the Model X-200T 25 percent Scale Semi-Span Rear Wing , MIT Report No. 1004, Oct., Nov. 1960

83. Curtiss-Wright Corporation X-200 Turbine Stability Model, MIT No. 1005, Nov. 1960

84. Cornell Aeronautical Laboratory Inc., Wind Tunnel Tests of A 0.12 Scale Model of The Curtiss-Wright X-19 Airplane, October 1962 Vol I of II

85. Richard E. Kuhn and John W. Draper, Investigation of the Aerodynamic Characteristics of a Model Wing-Propeller Combination and of a Wing and Propeller Separately at Angles of Attack Up to 90°, NACA Report 1263, 1956

86. Harry Goett and W. Kenneth Bulliant, Tests of NACA 0009, 0012 and 0018 Airfoils in the Full Scale Tunnel, NACA Report 647

87. L.K. Loftin, Jr. and W.J. Burnsall, The Effects of Variations in Re No. between 3×10^6 and 25×10^6 Upon the Aerodynamic Characteristics of a Number of 6 Series Airfoil Sections, NACA Report 964, 1950

88. George B. McCullough and Donald E. Garret, Examples of Three Representative Types of Airfoil - Section Stall at Low Speed, NACA TN 2502, September 1951

89. Ira H. Abott, Albert E. Von Doenhoff and Louis S. Stivers Jr., Summary of Airfoil Data, NACA Report 824, 1945

90. H. Fluk, Contribution of Aeroelastic Twist to Wing and Propeller Loads, Curtiss-Wright Report C-2870

91. W. McLean, Empirical Estimation of Aerodynamic Characteristics of a Single of Tandem-Winged Aircraft based on Wind Tunnel Tests of a Variable Geometry Model, Curtiss-Wright Report 001-63, December 15, 1964

92. W.G. Smith, and F.A. Lazzeroni, Experimental and Theoretical Study of a Rectangular Wing in a Vortical Wake, NASA TND 339, October 1960

93. Low Speed Wind Tunnel Tests of 0.12 Scale Model of the Curtiss-Wright M 200 VTOL airplane to Evaluate Longitudinal, Lateral and Directional Stability Characteristics, NA 62H-719, October 2, 1962, (NACAL 93).

SECTION XI

POWER-OFF CONSIDERATIONS

1. SAFE OPERATING ENVELOPE

The unsafe operating range of the X-19 aircraft for the case of failure of one engine is shown on Figure 348 for operating gross weights of 12,300 and 13,660 lb. The knee of the "avoid" region is approximately 50 to 70 knots respectively, and lowest altitude would be 20 ft above ground. When operating at the higher transition speeds and higher altitudes, it will be necessary to dive the airplane to gain the speed necessary to make a a safe landing, or maintain flight on the remaining engine. In any case, it will be necessary to land the X-19 with a velocity in excess of that indicated by the knee of the curve, as this is the minimum velocity at which flight can be maintained with one T55-L5 engine.

When operating at the higher altitudes and at speeds below the knee, it is necessary to tilt the propellers to a lower angle in accordance with the recommended tilt schedule while diving the airplane, to obtain the required speed. This requirement was one of the limits establishing the upper boundary of the curve

In cruise, when a complete engine power failure is experienced and the speed is above 160 knots, a safe landing can be accomplished provided a suitable area is immediately available. When determining the minimum speed and altitude for a safe power-off landing, it is assumed the airplane is operated near the correct tilt angle.

2. ENGINE FAILURE CONSIDERATIONS

The power-off and engine-failure characteristics of VTOL aircraft have been of prime concern to the industry's designers. This type of aircraft derives lift directly from power during the operation in hover and conversion and a power failure can thus result in a crash. The original design specification of the M-200 and X-19 aircraft called for power sufficient to maintain hover flight in the event of an engine failure. As the chances of a complete power failure in this two engine configuration were extremely remote, it was felt that an adequate safety margin had been provided.

Unfortunately, the ability to hover with one engine out does not in itself make for a safe airplane. The power must be transmitted to the propellers instantaneously and must be sufficient to reduce vertical acceleration to zero prior to touch-down. Because of the finite time required for the remaining engine to achieve full power, the concept of requiring hover with one engine out is an unrealistic criteria. Even if this level of power were available, there would be occasions when flight operation would be unsafe, due to time lags on the part of engine and pilot. Consequently, additional power to provide so called engine out hover safety, will still result in restricted envelopes. In the case of the X-19, the power available was nearly sufficient to hover the airplane with an engine out; but due to the time lag, in excess of 3 seconds, the aircraft could not be operated safely in hover at altitudes between 20 feet and 550 feet.

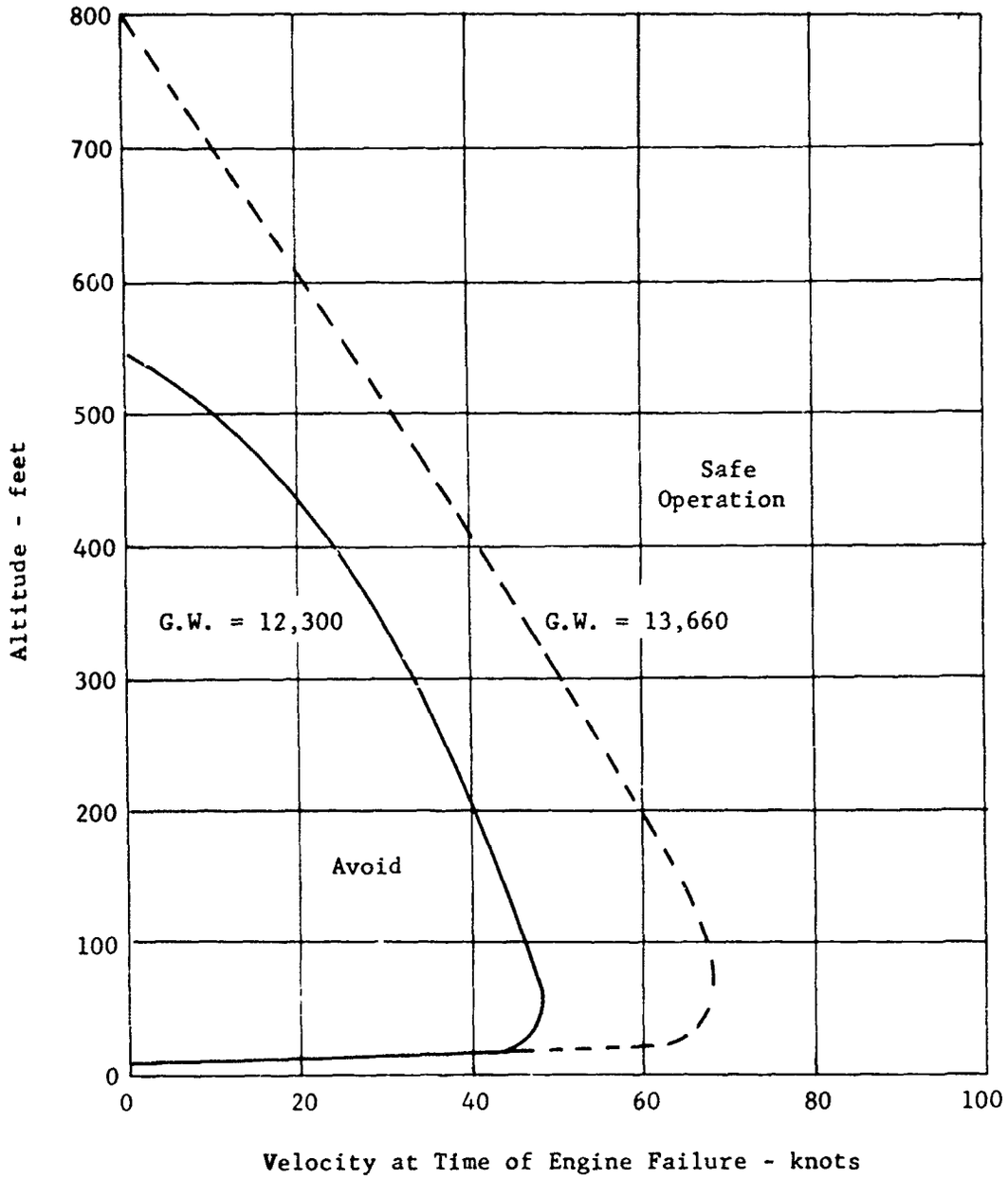

Figure 294. X-19, hover operating envelope, single engine failure.

In determining the engine-out safety design requirements, consideration must be given to how the airplane is used and what type of operating conditions may be encountered. It is believed that the landing gear requirements must be integrated with the engine-out requirements to obtain an acceptable compromise of landing gear and overall design. For example, assume a VTOL airplane is hovering at an altitude of 50 feet, has a landing gear capable of withstanding a 20 ft/sec sink, has a finite number of engines with equal ratings, and has an automatic device for detecting the failure of an engine and advancing the other throttles so that full remaining power is instantaneously available. If the power is directly proportional to thrust, the percent increase necessary to stay within the capacity of the landing gear is as follows:

Total No. of Engines	% Power Increase
2	74
4	16
6	5
8	0

Thus, with a four-engine airplane, only a 16 percent increase in power would be necessary to stay within the capacity of a 20 ft/sec landing gear. This compares with a 25% increase required to provide engine out power for maintaining hover thrust. This serves to illustrate how the landing gear and engine characteristics should be balanced to obtain the desired safety. The study also illustrates the point that an arbitrary design characteristic can actually defeat its intended goal.

3. POWER-OFF CHARACTERISTICS VS SPEED AND ALTITUDE (WINDMILLING)

As stated previously, the minimum cruise configuration approach speed and altitude are approximately 160 knots and 120 feet, respectively, following a steady power-off descent path. The technique of accomplishing the landing would be to let the propeller continue to windmill at the cruise rpm, tilt the propellers up to 16 degrees at which point the flap is 30 degrees, and set up a descent condition at an operating lift coefficient near L/D (lift drag ratio) maximum. The propellers windmill when the equivalent blade angle is slightly below the apparent wind angle so that the section is operating at a negative angle of attack. At this condition the blade lift coefficient is supplying torque in the direction of rotation, see figure A. The windmilling propellers operate at a blade angle slightly below that for cruise, and if they are governing, the blade angle would be quickly reached. In the event of a power failure at altitudes below that noted above, a safe landing can still be effected, because initial sink rate is zero.

Normal Propeller Section Absorbing Power

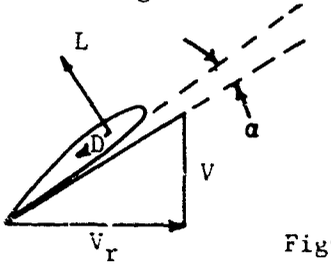

Windmilling Propeller Section Producing Power

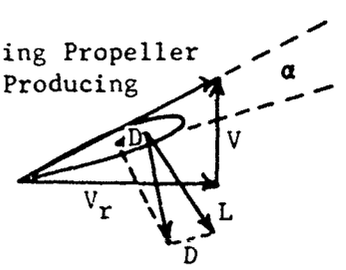

Figure A

Since the propellers can be assumed to be decoupled from the engine, little power must be absorbed and the negative thrust or drag produced is very low. Since the radial force is mainly a function of the variation of section angle of attack and relative velocity produced by the rotation and shaft angle, the propellers are generating nearly the same force as with power on (see Section II). This force is important and must be considered when determining the landing characteristics of the airplane. At the proper altitude, the pilot initiates a flare and performs a landing at a minimum speed of 120 knots. The details of this operation, and the methods and assumptions for calculating the descent and landing, are given in the following paragraphs.

In general, a typical descent and landing will consist of two parts, a steady descent followed by a final flare out. The first portion of descent is subject to the following assumptions:

a. Constant flight path velocity, V_o

b. Constant angle of descent, θ

The equations of motion for these conditions are:

$L = W \cos \theta$, (lift)
$D = W \sin \theta$, (drag)
$M = 0$, (pitching moment about c.g.)
where $W = 12{,}300$ lb

In Figures 295 to 297, required elevator deflection for pitch trim, fuselage angle of attack, angle of descent and rate of sink are plotted as functions of constant flight path velocity for the initial portion of descent, (shown as dashed curves).

Rate of sink is defined as

$$R/S = V_o \sin \theta = DV_o/W$$

These dashed curves then define the requirements needed to maintain a constant velocity, constant rate of sink. Referring to Figure 297, note that a minimum rate of sink is on the order of 48 ft/sec. Since this is well beyond the structural capabilities of the landing gear and/or the airplane, the second portion of the descent and landing technique, the final flare out, is quite necessary.

The equations of motion for the flare out are the same as previously shown, except for the addition of acceleration terms.

$$L - W \cos \theta = \frac{w}{g} V_o \frac{d\theta}{dt}$$

$$W \sin \theta - D = \frac{w}{g} \frac{dV_o}{dt}$$

Holding a constant airplane angle of attack, the equations are functions of only V_o and θ, and thus, numerical integration is possible. The effect of flare out was studied at three values of initial constant descent. These results are plotted as solid lines on Figures 295 to 297.

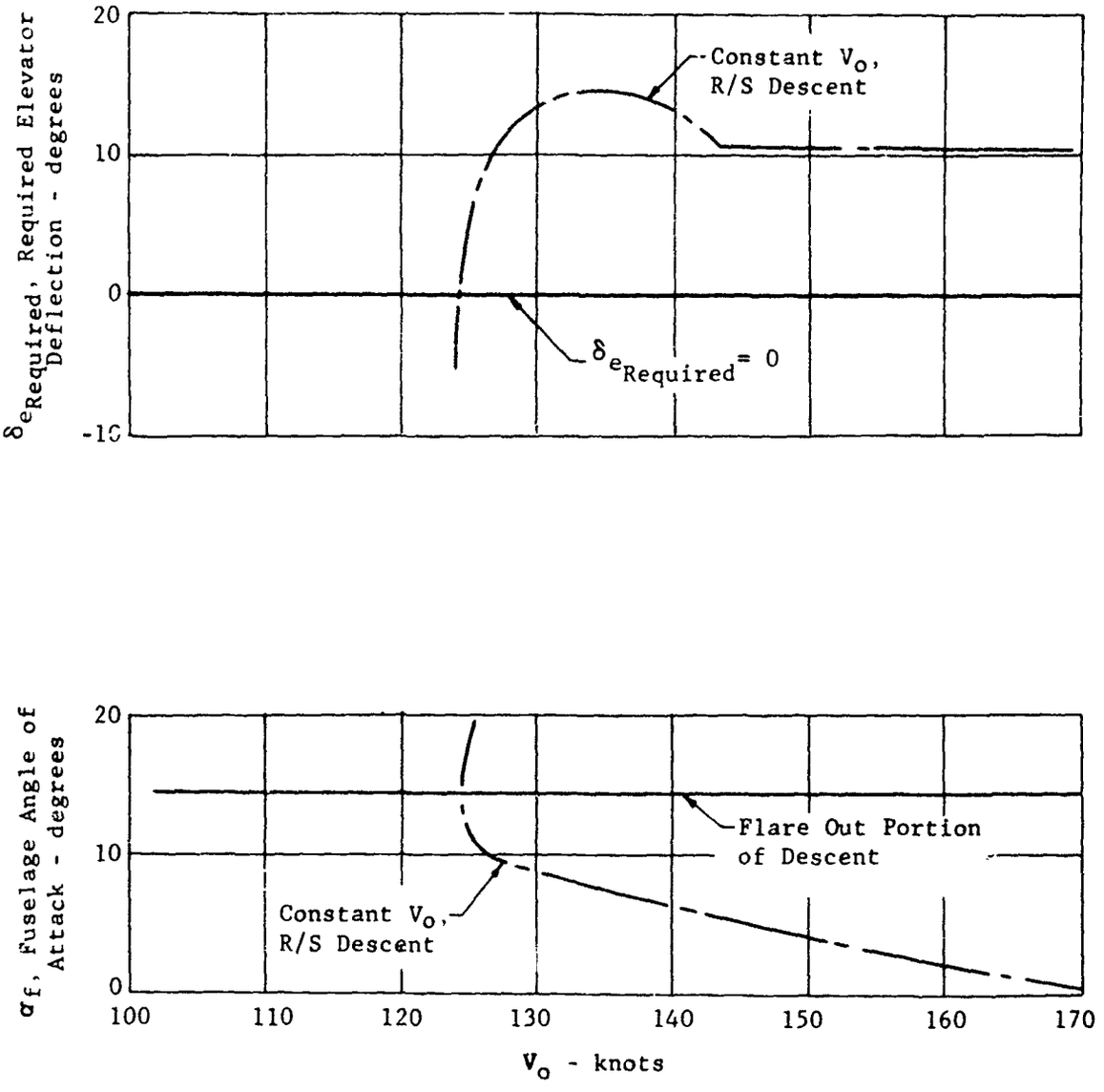

Figure 295. X-19, cruise windmilling descent, trim characteristics; W = 12,300 pounds, cg = 42.9 percent, ϕ_F = 16.3°, $\beta_{.75R}$ = 51 degrees.

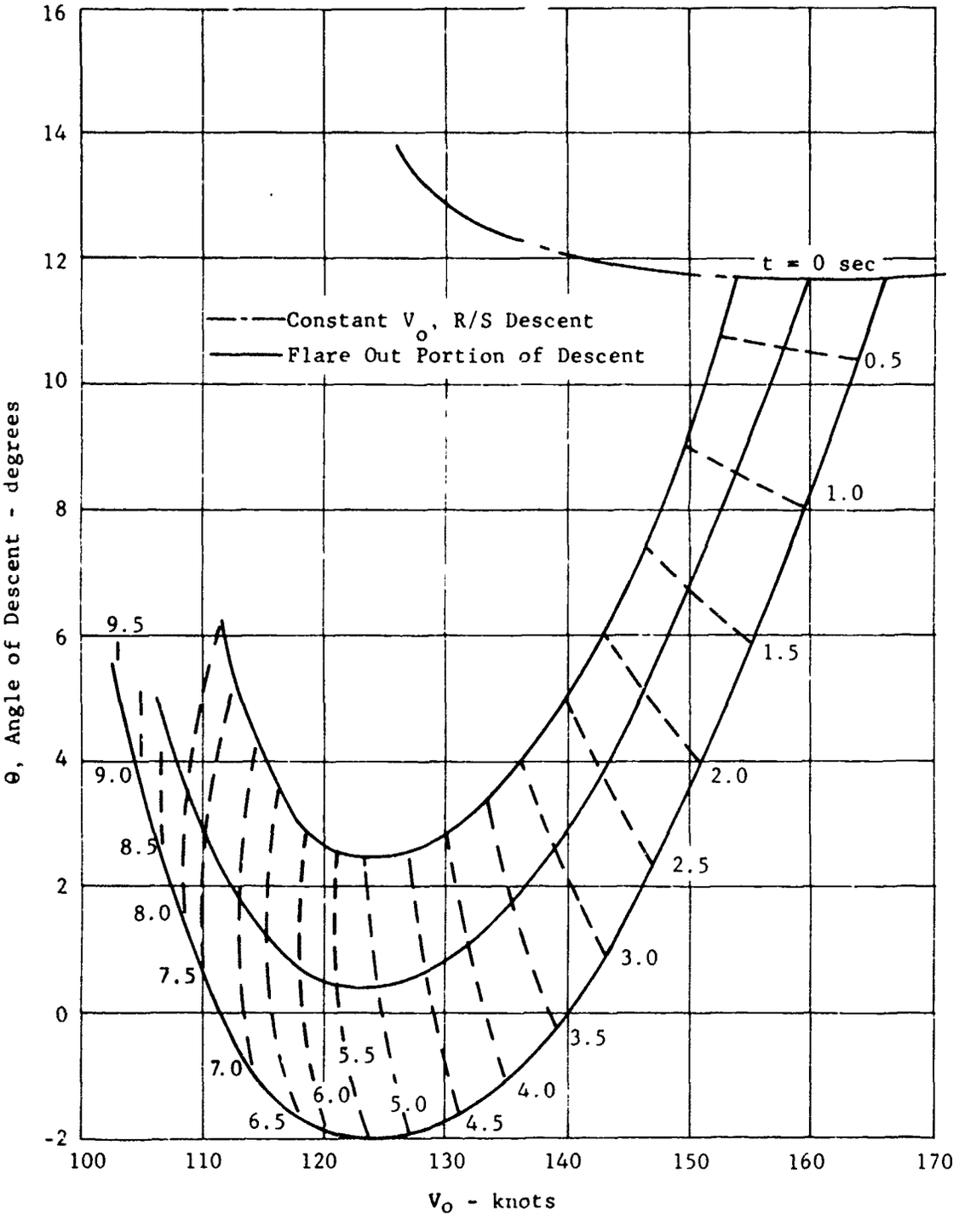

Figure 296. X-19, cruise windmilling descent angle; W = 12,300 pounds, cg = 42.9 percent, ϕ_F = 16.3°, $\beta_{.75R}$ = 51 degrees.

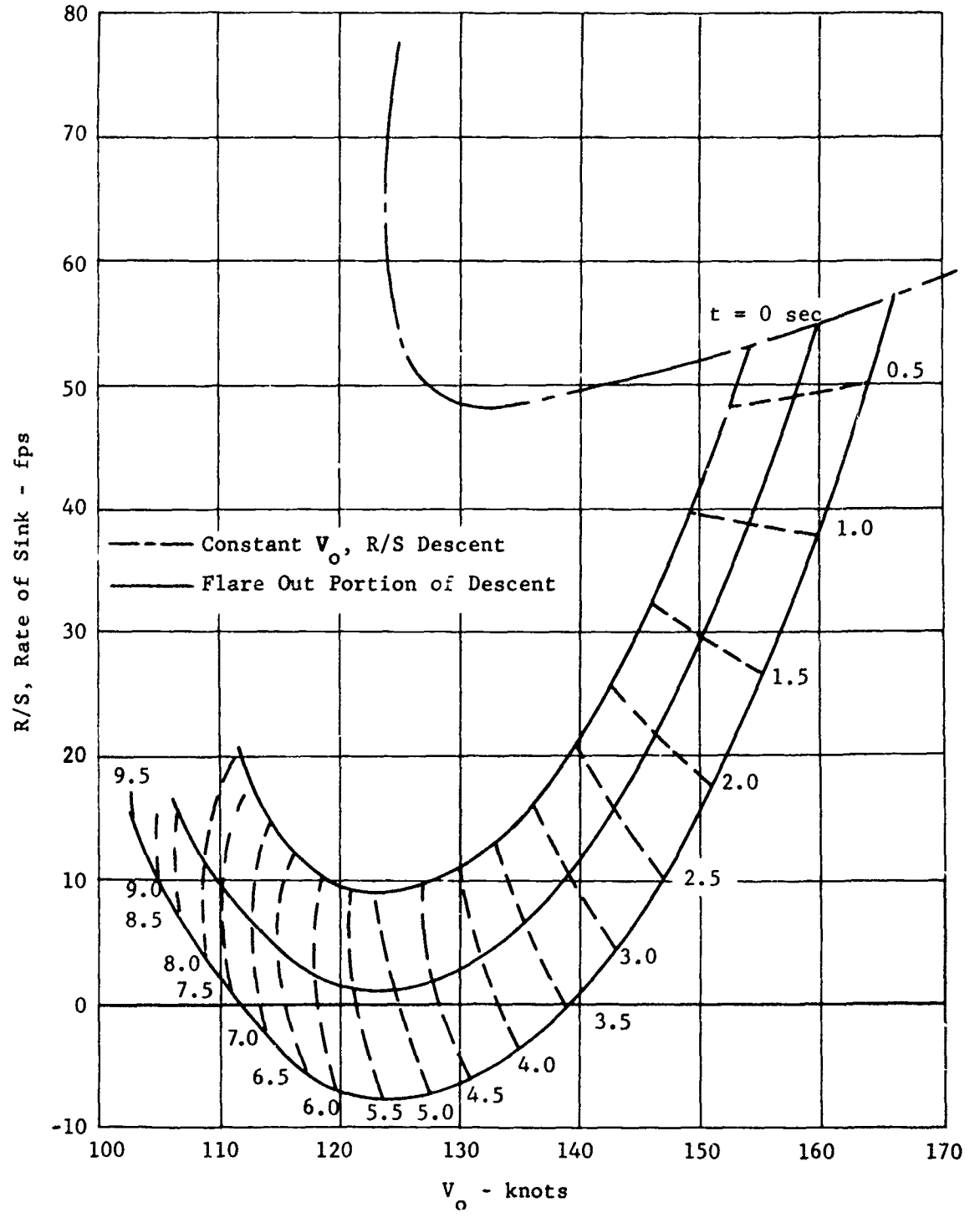

Figure 297. X-19, cruise windmilling rate of descent flares; W = 12,300 pounds, cg = 42.9 percent, ϕ_F = 16.3°, $\beta_{.75R}$ = 51 degrees.

Assuming a maximum desired rate of sink of 10 ft/sec, flare outs starting at speeds below 153 knots should not be attempted, as can be seen in Figure 297. Flaring started at velocities above 162 knots contain the possibility of climbing after $\theta = 0$ is reached.

Possible flight paths during flare are shown in Figure 298. Three paths, which are functions of the velocity at which the flare is initiated, are given. Also superimposed are the flight path velocity and rate of sink at points along the flight path. Because of the high decelerations encountered (0.3 to 0.4 g's) and the short period of time during flare (note times on Figures 295 to 297) it is necessary that the pilot gimbal to a proper tilt angle before initiating his flare. Values of $\phi_F = 25°$ [11] appear acceptable. When initiating the flare, the only pilot requirements will be to pull the stick back to neutral position, which corresponds to a fuselage angle of attack of 14.4°, at which $C_{L_{max}}$ including elevator requirement occurs. Referring to Figure 299 to 301, showing the M.I.T. scale data, corresponding values at $\alpha_f = 14.4°$ and $\beta_{.75R} = 51°$ are:

$C_L = 1.53$ = aircraft lift coefficient

$C_D = .515$ = total drag coefficient

$C_M = 0$ = moment coefficient

ϕ = tilt angle; the angle between thrust vector and fuselage reference line, WL100

The pilot should attempt a landing only within the landing envelope shown in Figure 298. This envelope is constrained by the following requirements and definitions.

a. Maximum allowable R/S = 10 ft/sec

b. Points above a constant R/S = 0 line are in fact rates of climb; this is the upper limit to the envelope.

c. For a flare which allows a rate of climb to occur (e.g., 166 knots flare) there is the possibility of two distinct safe landing points. However, the lower speed solution occurs at altitudes above the higher speed solution. The lower speed solution is ignored, thereby closing the envelope.

Another criterion which is not considered here is the combination of sink speed and tangential speed as it affects the landing gear (structurally). It may be that only low sink rates are allowable for the high speed touchdown. If this is so, it can reduce considerably the usable band of avail-

---

[11] $\phi_F = 25°$ is a minimum value for landing because of propeller ground clearance requirements. All calculations and plots have been calculated for $\phi_F = 16.3°$ because of lack of available windmill data at higher tilt angles.

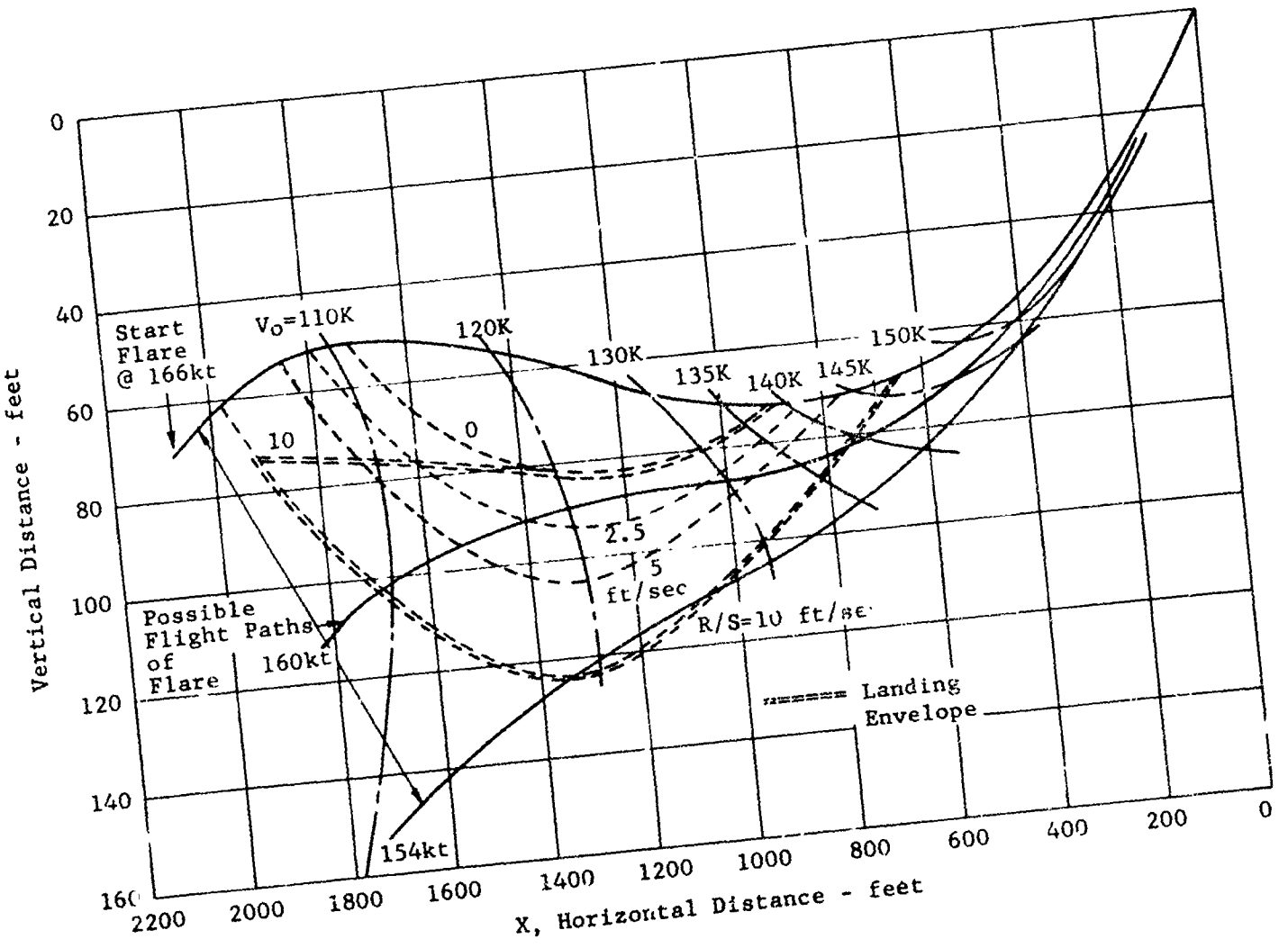

Figure 298. X-19, cruise windmilling flared flight paths; W = 12,300 pounds, cg = 42.9 percent, ϕ_F = 16.3°, $\beta_{.75R}$ = 51 degrees, α_{fus} = 14.4°.

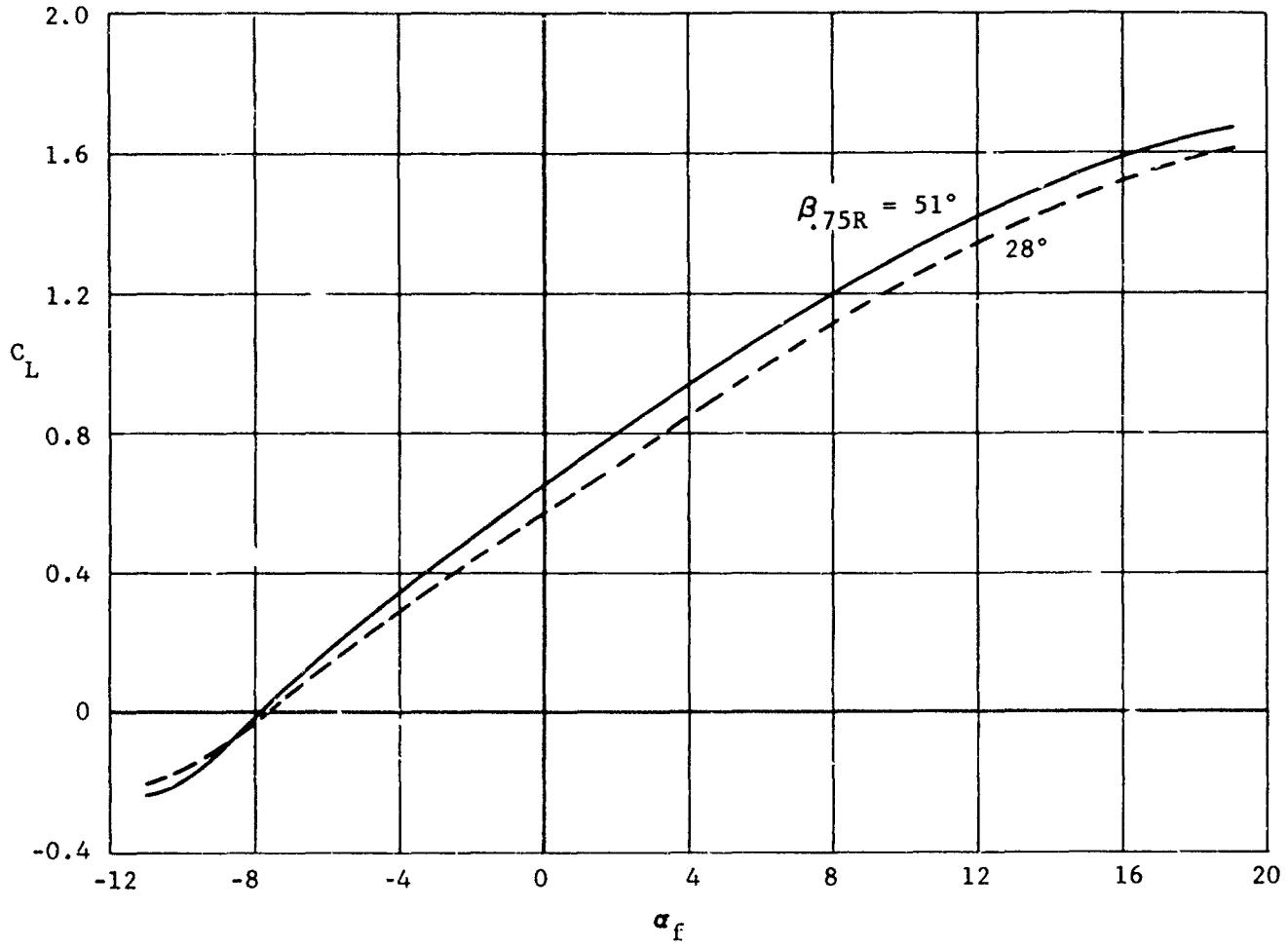

Figure 299. X-19, windmilling lift coefficient characteristics at ϕ_F = 16.25 degrees; S_{ref} = 154.6 sq ft., δ_F = 23.2 degrees, $\delta_{a_{coll}}$ = 21.5 degrees.

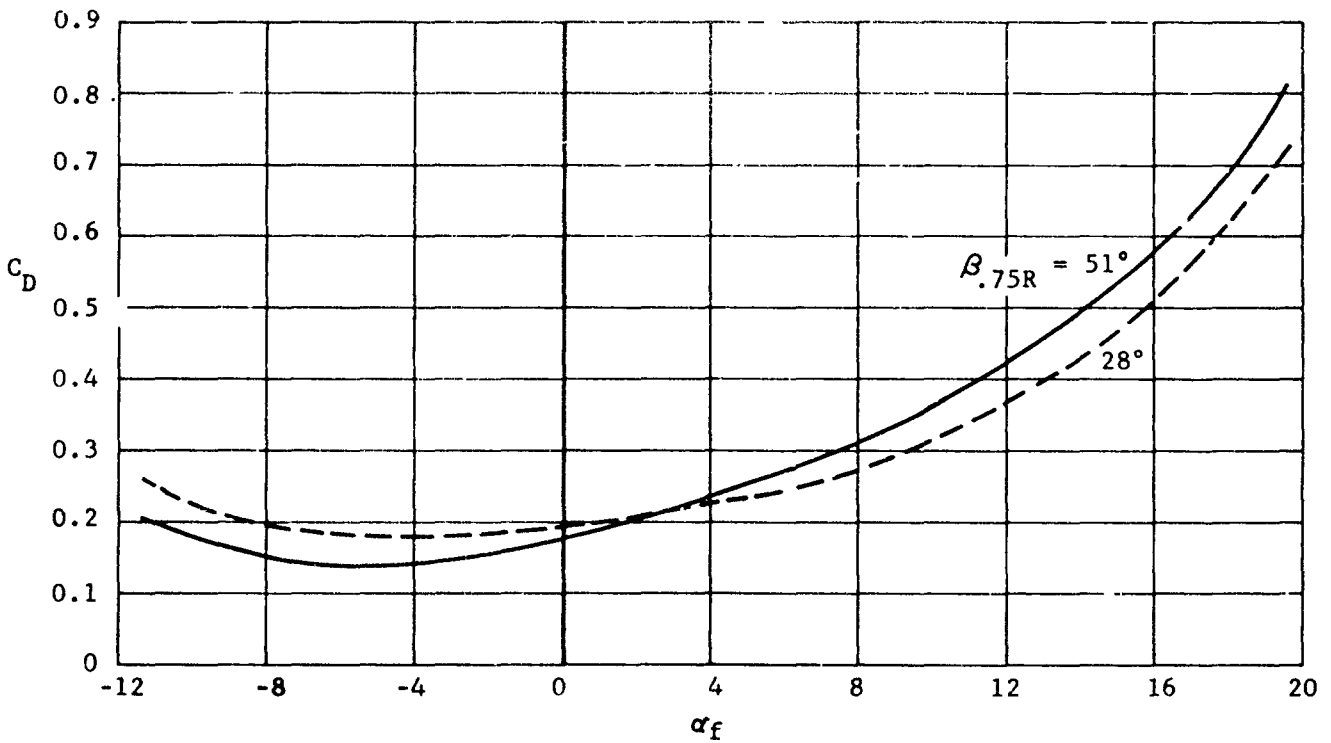

Figure 300. X-19, windmilling drag coefficient characteristics at ϕ_F = 16.25 degrees; S_{ref} = 154.6 sq ft., δ_F 23.2 degrees, $\delta_{a_{coll}}$ = 21.5 degrees.

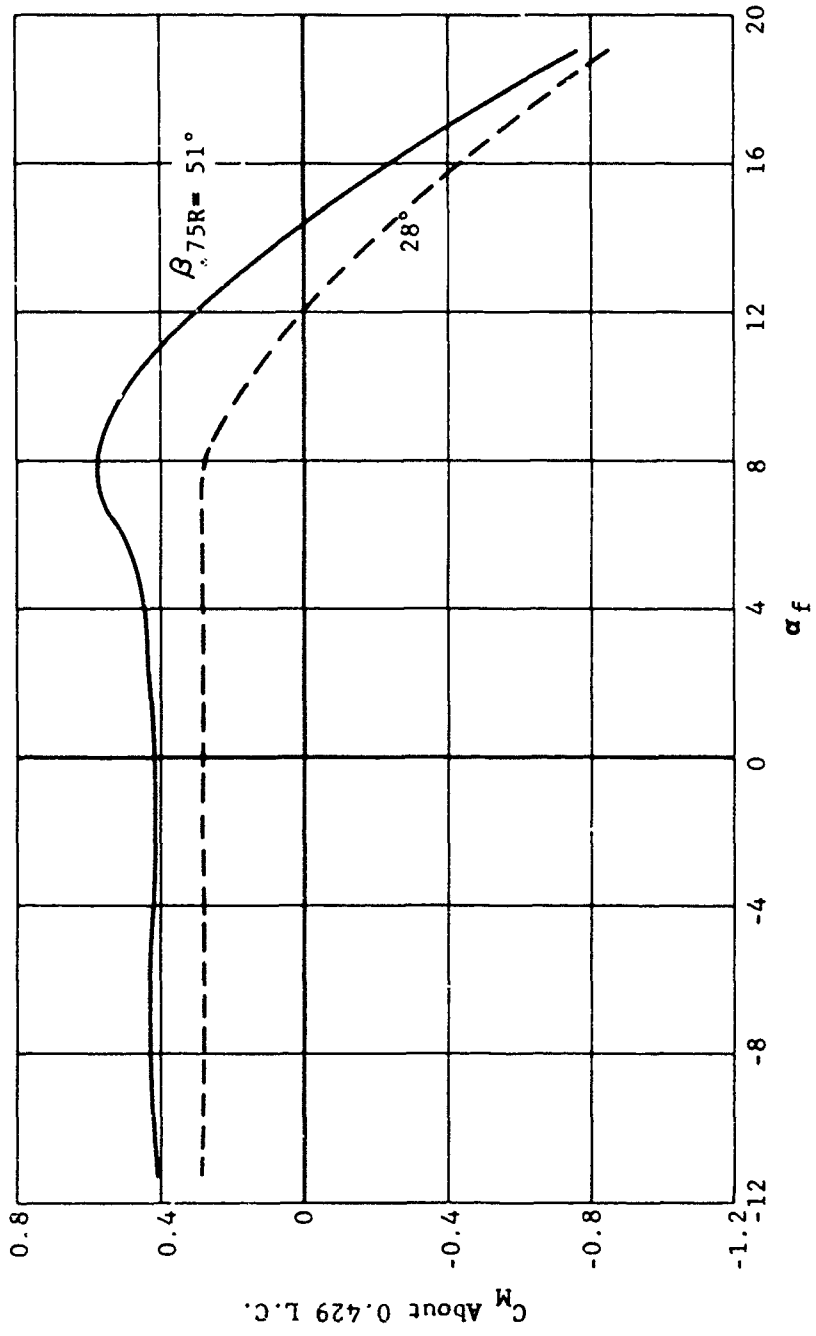

Figure 301. X-19, windmilling moment coefficient characteristics at ϕ_F = 16.25 degrees; S_{ref} = 154.6 sq ft., cg = 42.9 percent, δ_F = 23.2 degrees, $\delta_{a_{coll}}$ = 21.5 degrees.

able flareouts.

Actually, a simpler type of landing can be made at or near minimum R/S. In most cases, the pilot will not attempt to land in the low speed portion of the landing envelope. Touchdown velocities around 120 to 130 knots are expected to be typical.

The type of descent analyzed in this report is subject to the limitation of maintaining constant blade angle. This implies that the propeller governor is by-passed, allowing a constant J_o to be held. Thus, as forward speed diminishes, prop rpm must fall off.

Another limitation on the results, that should be mentioned, is in the interpretation of the drag data shown in Figure 300. Since the drag data were not run at true windmill conditions (the power coefficients were slightly negative), it is estimated that the drag readings are about 5% high.

The effect of Reynolds' number on drag also tends to give high drag readings. The magnitude of this effect is still unknown. However, it can be generalized that if the airplane experiences a lower drag than used in this analysis, the flare can be initiated at reduced speeds.

The emergency landing procedure assumes the pilot can fly the correct flight path, and that space for landing is available. Experience has been gained on landing lifting bodies which have lift drag ratios below that of the X-19, with power-off. These results indicate landings can be made. A study of the X-19 power-off landing characteristics was made based on the results of the tests with lifting bodies. This study indicated that higher speeds and altitudes would be necessary to land, in case of a complete power failure, than was indicated in the previous paragraphs. However, this study is not considered complete and further work was indicated.

4. AUTOROTATIVE CHARACTERISTICS

The autorotative characteristics of the propellers on the X-100 and X-19 airplane will result in a low level of thrust when the airplane is descending at a moderate descent speed. To produce thrust (windmilling drag) equal to aircraft weight for the high disk loading associated with the X-19 aircraft, sink speeds in excess of 100 ft/sec are required. Compared with helicopter rotors, propellers have very little kinetic energy available for slowing up the airplane to a safe landing. Thus, even if the velocity of an autorotational descent for thrust equal to weight could be reduced, the possibility of making a safe landing is remote. For this reason, the use of autorotation was rejected as a means of landing the aircraft in the event of engine failure.

Even if the thrust/advance ratio relationship of the propeller were the same as a helicopter rotor, the disk area difference would reduce the lift of the propeller to between one-fifth and one-seventh that of the helicopter. This is apparent, as the disk area of a helicopter is 5 to 7 times greater than that of an X-19 type VTOL aircraft of the same weight; and the lift is directly dependent on the disk area.

Due to the large amount of twist used in the blades of the X-19 propeller, the windmilling thrust at a given disk loading will be less than that of a helicopter rotor. Therefore, the autorotation characteristics are poorer than would be indicated by area considerations alone.

Data was run on thirty-inch-diameter model propellers to determine their characteristics when autorotating. These data are shown for the shaft angles of 140,160 and 180 degrees on Figures 302 to 304. The characteristics of the blade used is shown on Figure 305.

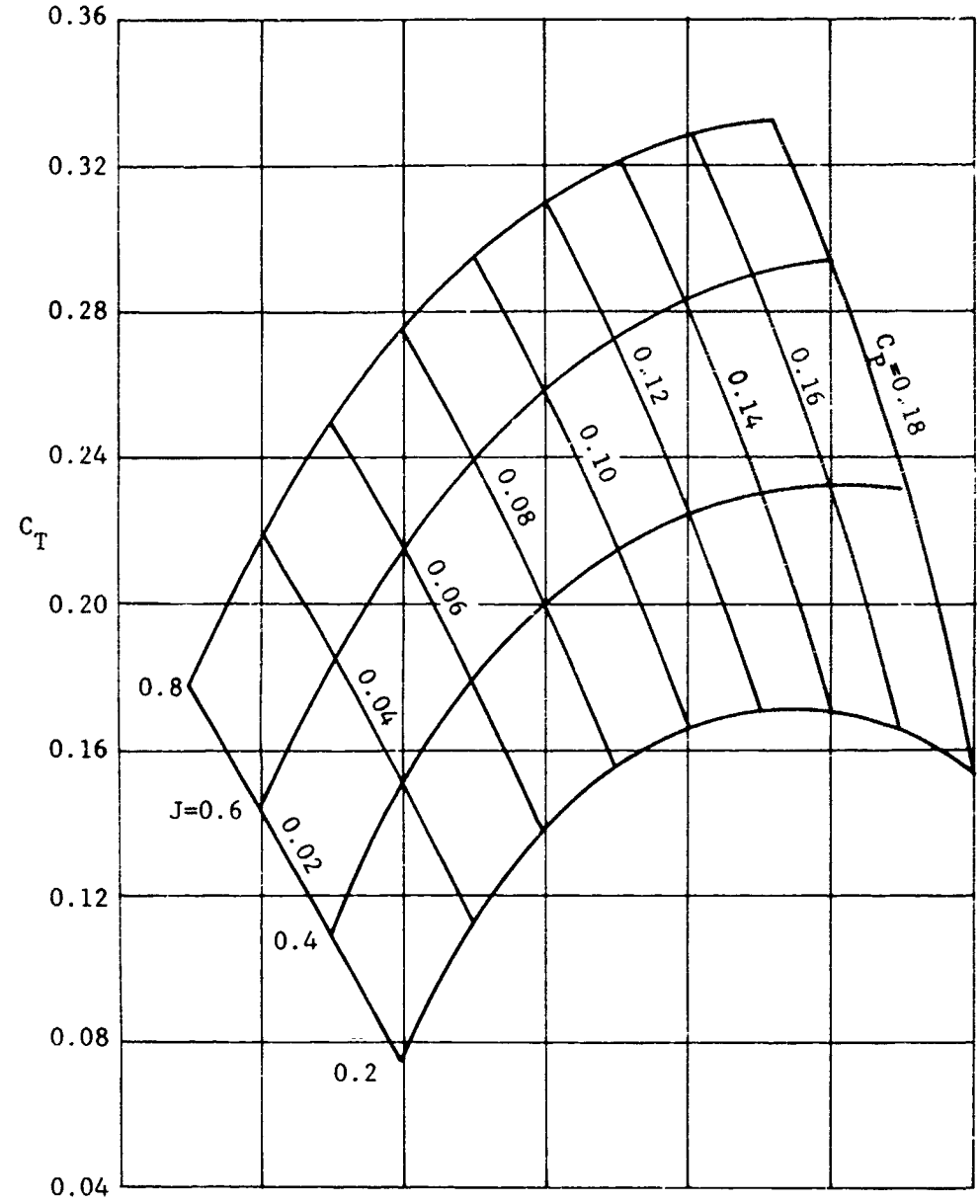

Figure 302. Thrust coefficient characteristics at tilt angle of 140 degrees; CWC blade 3(156109), AF = 115, IC_{L_i} = 0.482.

FURNISHED UNDER UNITED STATES GOVERNMENT CONTRACT No. AF33(615)-3940. SHALL NOT BE EITHER RELEASED OUTSIDE THE GOVERNMENT, OR USED, DUPLICATED, OR DISCLOSED IN WHOLE OR IN PART FOR MANUFACTURE OR PROCUREMENT, WITHOUT THE WRITTEN PERMISSION OF CURTISS-WRIGHT CORPORATION, EXCEPT FOR (i) EMERGENCY REPAIR OR OVERHAUL WORK BY OR FOR THE GOVERNMENT WHERE THE ITEM OR PROCESS IS NOT OTHERWISE REASONABLY AVAILABLE TO ENABLE TIMELY PERFORMANCE OF THE WORK, OR (ii) RELEASE TO A FOREIGN GOVERNMENT AS THE INTERESTS OF THE UNITED STATES MAY REQUIRE. PROVIDED THAT IN EITHER CASE THE RELEASE, USE, DUPLICATION OR DISCLOSURE HEREOF SHALL BE SUBJECT TO THE FOREGOING LIMITATIONS. THIS LEGEND SHALL BE MARKED ON ANY REPRODUCTION HEREOF IN WHOLE OR IN PART."

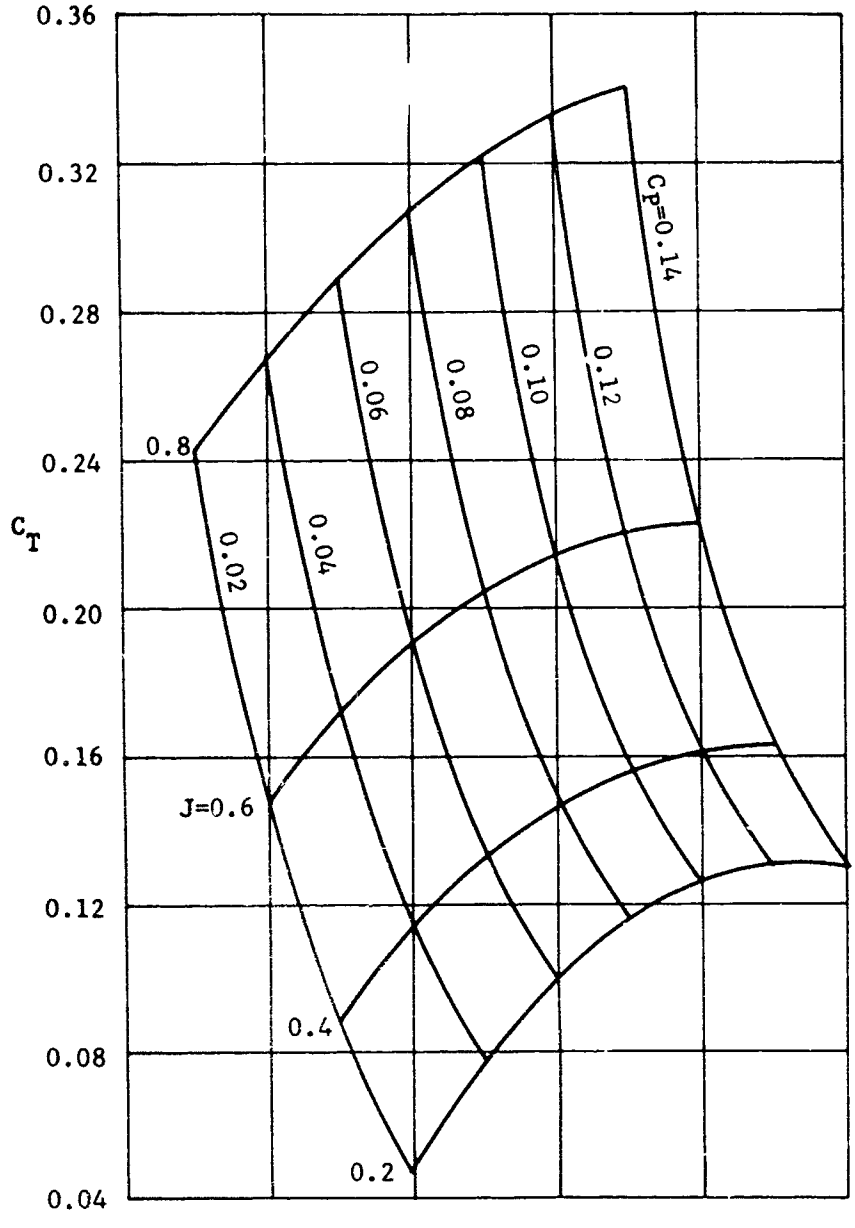

Figure 303. Thrust coefficient characteristics at tilt angle of 160 degrees; CWC blade 3(156109), AF = 115, IC_{L_i} = 0.482.

FURNISHED UNDER UNITED STATES GOVERNMENT CONTRACT No. AF33(615)-3940. SHALL NOT BE EITHER RELEASED OUTSIDE THE GOVERNMENT, OR USED, DUPLICATED, OR DISCLOSED IN WHOLE OR IN PART FOR MANUFACTURE OR PROCUREMENT, WITHOUT THE WRITTEN PERMISSION OF CURTISS-WRIGHT CORPORATION, EXCEPT FOR (i) EMERGENCY REPAIR OR OVERHAUL WORK BY OR FOR THE GOVERNMENT WHERE THE ITEM OR PROCESS IS NOT OTHERWISE REASONABLY AVAILABLE TO ENABLE TIMELY PERFORMANCE OF THE WORK, OR (ii) RELEASE TO A FOREIGN GOVERNMENT, AS THE INTERESTS OF THE UNITED STATES MAY REQUIRE, PROVIDED THAT IN EITHER CASE THE RELEASE, USE, DUPLICATION OR DISCLOSURE HEREOF SHALL BE SUBJECT TO THE FOREGOING LIMITATIONS. THIS LEGEND SHALL BE MARKED ON ANY REPRODUCTION HEREOF IN WHOLE OR IN PART.

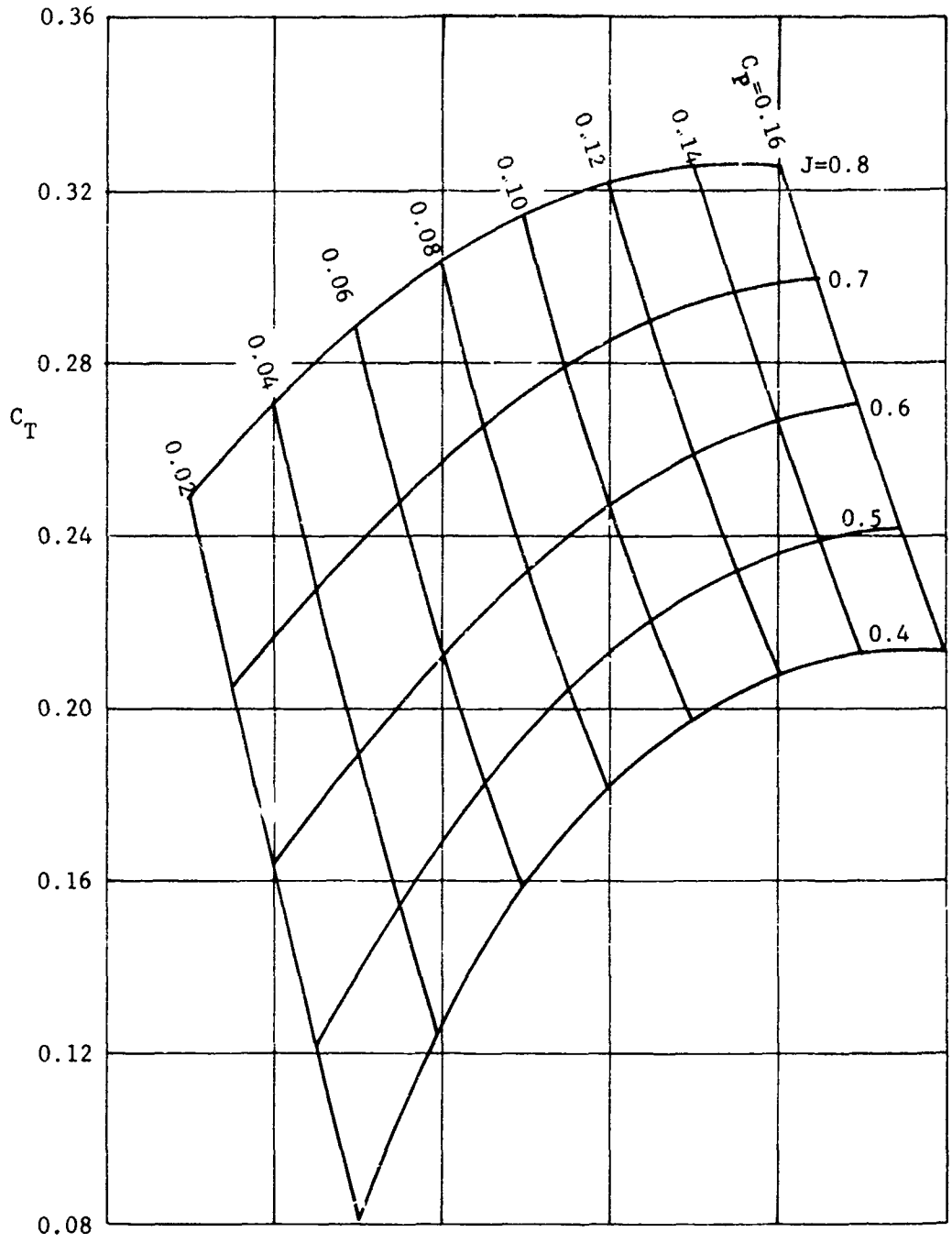

Figure 304. Thrust coefficient characteristics at tilt angle of 180 degrees; CWC blade 3(156109), AF = 115, IC_{L_1} = 0.482.

"FURNISHED UNDER UNITED STATES GOVERNMENT CONTRACT NO. AF33(615)-3940. SHALL NOT BE EITHER RELEASED OUTSIDE THE GOVERNMENT, OR USED, DUPLICATED, OR DISCLOSED IN WHOLE OR IN PART FOR MANUFACTURE OR PROCUREMENT, WITHOUT THE WRITTEN PERMISSION OF CURTISS-WRIGHT CORPORATION, EXCEPT FOR (i) EMERGENCY REPAIR OR OVERHAUL WORK BY OR FOR THE GOVERNMENT, WHERE THE ITEM OR PROCESS IS NOT OTHERWISE REASONABLY AVAILABLE TO ENABLE TIMELY PERFORMANCE OF THE WORK, OR (ii) RELEASE TO A FOREIGN GOVERNMENT, AS THE INTERESTS OF THE UNITED STATES MAY REQUIRE PROVIDED THAT IN EITHER CASE THE RELEASE, USE, DUPLICATION OR DISCLOSURE HEREOF SHALL BE SUBJECT TO THE FOREGOING LIMITATIONS THIS LEGEND SHALL BE MARKED ON ANY REPRODUCTION HEREOF IN WHOLE OR IN PART."

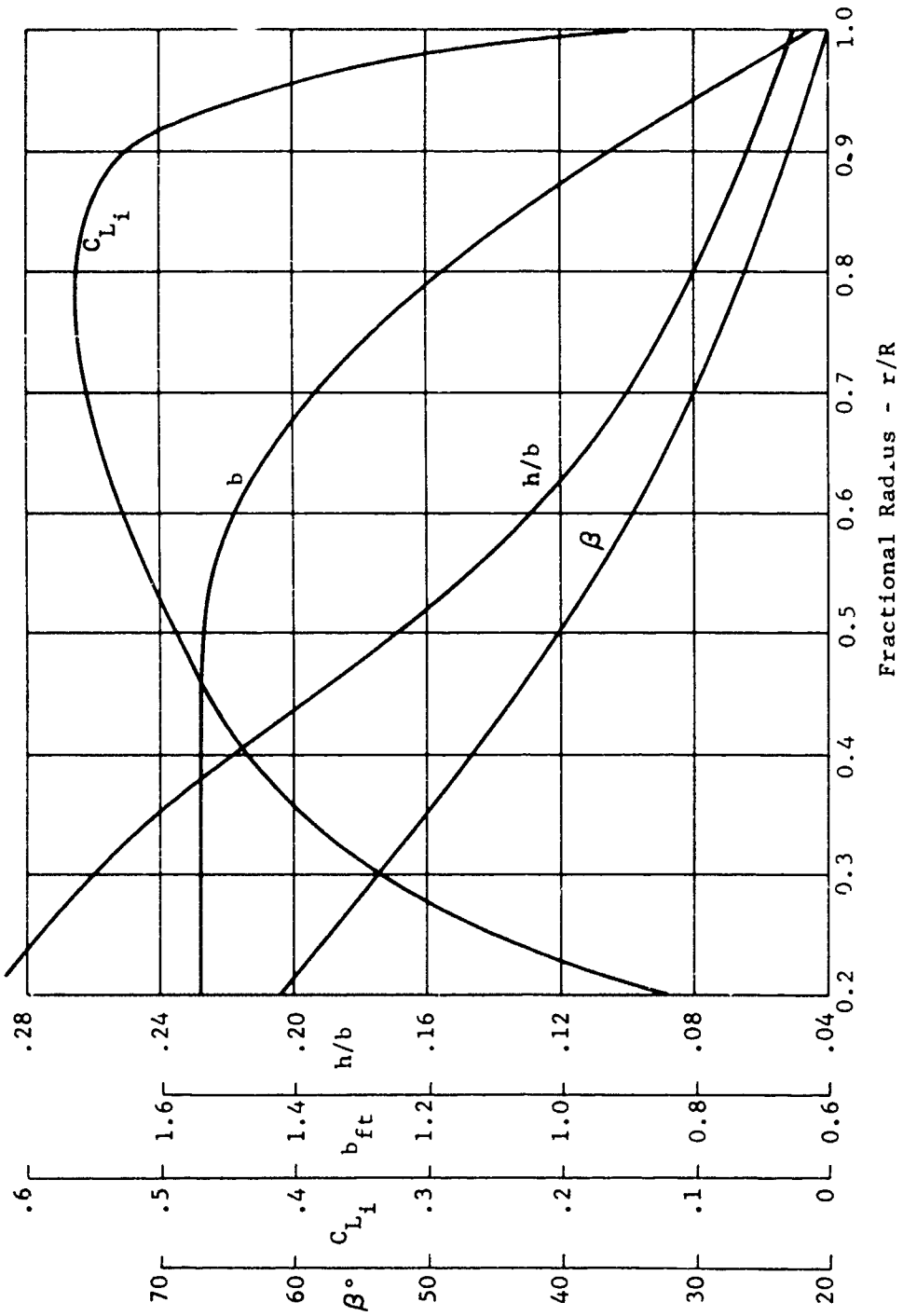

Figure 305. Blade characteristics of CWC 3(156109); AF = 109, IC_{L_i} = 0.482.

FURNISHED UNDER UNITED STATES GOVERNMENT CONTRACT No. AF33(615)-3940 SHALL NOT BE EITHER RELEASED OUTSIDE THE GOVERNMENT, OR USED DUPLICATED, OR DISCLOSED IN WHOLE OR IN PART FOR MANUFACTURE OR PROCUREMENT, WITHOUT THE WRITTEN PERMISSION OF CURTISS-WRIGHT CORPORATION, EXCEPT FOR (i) EMERGENCY REPAIR OR OVERHAUL WORK BY OR FOR THE GOVERNMENT, WHERE THE ITEM OR PROCESS IS NOT OTHERWISE REASONABLY AVAILABLE TO ENABLE TIMELY PERFORMANCE OF THE WORK, OR (ii) RELEASE TO A FOREIGN GOVERNMENT, AS THE INTERESTS OF THE UNITED STATES MAY REQUIRE PROVIDED THAT IN EITHER CASE THE RELEASE, USE, DUPLICATION OR DISCLOSURE HEREOF SHALL BE SUBJECT TO THE FOREGOING LIMITATIONS THIS LEGEND SHALL BE MARKED ON ANY REPRODUCTION HEREOF IN WHOLE OR IN PART.

SECTION XII NOMENCLATURE

BHP brake horsepower

C.G. center of gravity

C_P = power coefficient

C_T = thrust coefficient

fpm feet per minute

K = knots

L.C. lift chord (=274 in.), distance between front and rear tilt axis along fuselage water line.

L lift

N_2 power turbine rotational speed

SAS stability augmentation system

TAS true airspeed, knots

V_e equivalent airspeed, knots

V_t test airspeed

V_s schedule airspeed

W airplane weight, pounds

β blade angle

ϕ_p front propeller tilt angle, degrees

σ relative air density ratio

Subscripts

N at propeller nacelle, total N_R at a rear propeller t, test value

N_F at a front propeller nacelle S standard, and schedule

SECTION XII

FLIGHT TEST SUMMARY

1. INTRODUCTION

This section summarizes the activities of the X-19 Category 1 Flight Test Program under Item 2 of the Contract (94), which stipulates the flight demonstration and test requirements to be met by the X-19 aircraft. Fifty flights were completed in accordance with the planned procedures. Flight tests performed were all within the Flight Capability Demonstration as defined in the latter referenced report.

The purpose of the Flight Capability Demonstration flight tests is to demonstrate the ability of the airplane to make sustained, controlled hovering maneuvers and then to progress with gradually increasing nacelle tilt to demonstrate the transition to cruise flight.

In support of the flight test operation, two airplanes were operated during the vehicle test program. Ground Run and tie down tests took a total of 134 hours, 4½ hours on X-19 aircraft Serial No. 62-12198 and 129½ hours on X-19 aircraft Serial No. 62-12197. The latter aircraft was used in all flights. Its total flight time was 3 hours 45 minutes, of which 3 hours 38 minutes was under Item 2 of the subject contract.

During the series of test flights with X-19 Serial No. 62-12197 the Flight Capability Demonstration items in hovering flight were completed and successfully demonstrated. Also, the flight envelope in the conversion/reconversion mode had been extended to 100 knots with the nacelles tilted down to 45°. STOL tests were made at lift-off and touch-down airspeeds of up to 60 knots.

During Flight No. 50, on a flight programmed for conversion flight maneuvers up to 100 knots, failure on No. 2 propeller nacelle casting caused the loss of that propeller and the aircraft crashed and was destroyed. Both pilots ejected and landed safely by parachute.

The original plans for the flight test operation called for X-19 Serial No. 62-12198 to be the structural test airplane. Following the loss of X-19 Serial No. 62-12197 the flight test plan was revised so that the remaining airplane would combine all remaining flight test operations. At the conclusion of the program the available aircraft was in preparation for flight test, having completed its transmission green runs and preflight system tests; no test operations had been made against this revised plan.

2. HISTORY OF X-19 TEST FLIGHTS

a. Historical Progression

The historical progression of flight tests on X-19 Serial No. 62-12197 is shown in Table XVIII. This table lists the various flights made on the airplane and details in abbreviated form the achievements of each flight. Additional details of any flight are contained in Curtiss-Wright X-19 Flight Test Reports Nos. 8 through 50 pertaining to Flight Nos. 8 through 50 respectively. For historical completeness, data have been tabulated from Flight No. 1, and the tabulation includes a breakdown by Ground Run numbers for ground tests performed between flights. The ground tests supported the flight test program by basically serving as a pre-flight checkout of the airplane and its systems. The X-19 ground run reports for each specific run number list the alterations to the airplane prior to each run, the tests performed, qualitative test results, and the discrepancies discovered during the run.

b. Simplified Flight Test Schedule at Curtiss-Wright

A simplified schedule of flight tests is shown in Figure 306, which assigns tests against batches of flights in a calendar time versus Flight Number presentation. From this presentation it is convenient to consider the overall operation in several discrete phases:

(1) Flight Nos. 8 thru 19:

Initial development of Pilot's hovering ability, including limited translation maneuvers. These flights, totalling 70 minutes flying time and 25 lift-offs, were made without the S.A.S. operative.

As experience was developed and the airplane could be controlled in steady hovering flight, the duration of flights increased and simple local hovering maneuvers were performed experimentally. Hovering spot turns were made to left and right and the airplane translated, at hover nacelle angle, forwards, rearwards and sideways. The airplane was hovered at heights ranging from 5 to 25 feet to evaluate ground effects. Flight No. 19 was a summary flight during which all the maneuvers previously explored were performed successively.

(2) Flights No. 20 thru 22:

Commencing with Flight No. 20 the stability augmentation system was switched on and evaluations made of its influence on airplane handling and stability. Flights Nos. 20 and 21 were made with both pitch and roll S.A.S. channels activated selectively. The pilot was not able to detect any significant im-

Table XVIII. Historical breakdown X-19 S/N 62-12197.

DATE	FLIGHT NO.	FLIGHT TIME (MINS.)	BRIEF DESCRIPTION OF FLIGHT	INTERMEDIATE GROUND RUN NOS.	BRIEF DESCRIPTION OF GROUND RUN
9-18-63				1 Thru 70	a. Initial engine starts b. Correction of aircraft instrumentation and system discrepancies c. Establishing required gearbox oil levels d. Developing aft tee box lubrication system e. Transmission system green runs f. Airframe vibration and propeller balancing tests g. Propeller pitch control rigging and control response tests h. Low speed taxi, brake and steering evaluation
11-20-63	1	:01	Initial lift-off in hover, aircraft damaged when landing gear collapsed		
1-31-64				71 Thru 149	a. Several power transmission green runs b. Aerodynamic balancing of propeller assemblies c. Fire extinguisher system tests d. Propeller speed governor operation and response tests e. Propeller rigging tests f. Static performance and control response tests g. Simulated single engine failure tests h. Prop. pitch control system stress tests i. Aircraft vibration tests j. Noise level tests k. Nacelle tilt tests l. Carbon monoxide contamination tests m. Functional air conditioning tests n. Fuel system tests o. Engine acceleration and deceleration tests p. Pilot control force versus deflection tests q. Nose wheel steering evaluation r. Propeller coordinator vibratory force tests s. Prop. pitch control linkage resolution tests t. Check of hover trim positions with aircraft light on its wheels
6-25-64					
6-26-64	2	:01	Hover		
6-26-64	3	:01	Hover		

Table XVIII. Continued.

DATE	FLIGHT NOS.	FLIGHT TIME (MINS.)	BRIEF DESCRIPTION OF FLIGHT	INTERMEDIATE GROUND RUN NOS.	BRIEF DESCRIPTION OF GROUND RUN
6-26-64				150 Thru 155	a. S.A.S. ground checks b. Air conditioning system evaluation c. Pilots stick force versus deflection tests
7-7-64					d. Evaluate aircraft padding characteristics e. Maintenance checks
7-7-64	4	:01	Hover		
7-10-64	5	:01	Hover		
7-14-64				156 Thru 158	a. Propeller rigging checks b. Simulated single engine failure c. N.A.S.A. pilot familiarization
7-16-64					d. Maintenance checks
7-17-64	6	:01	Hover		
7-17-64	7	:01	Hover - Complete Flight Capability Item A.1		
7-21-64			(Note: Beginning Contract N_1 AF33(657)-13017, Item 2)	159	Maintenance Check
7-22-64	8	:04	Hover		
7-23-64	9	:03	Hover		
7-23-64				160	Maintenance
7-23-64	10	:10	Hover, spot turns		
7-23-64	11	.03	Hover and forward translation		
7-27-64				161	Maintenance check and air conditioning system evaluation
7-28-64	12	:09	Hover at various heights, forward translation		
7-28-64	13	:07	Hover, sideways and rearwards translation		

Table XVIII. Continued.

DATE	FLIGHT NO.	FLIGHT TIME (MINS.)	BRIEF DESCRIPTION OF FLIGHT	INTERMEDIATE GROUND RUN NOS.	BRIEF DESCRIPTION OF GROUND RUN
7-28-64				162	Maintenance check
7-29-64	14	:05	Hover, spot turn, rearward translation		
7-30-64	15	:02	Hover with minimum control activity		
7-30-64	16	:10	Hover, rearwards and sideways translation		
7-30-64	17	:06	Hover, sideways and quartering translation		
7-31-64	18	:07	Forward translation (20 Kt), hover at various heights		
7-31-64	19	:04	Flight capability summary flight		
7-31-64				163	Taxi runs
8-4-64	20	:06	Hover, pitch SAS on and off		
8-4-64	21	:05	Hover, roll SAS and pitch and roll SAS on		
8-6-64				164	a. Maintenance checks
Thru				Thru	b. TRI-SERVICE pilot familiarization
8-6-64				166	
8-7-64	22	:09	Hover, translation, SAS evaluation		
8-7-64				167	a. Propeller rigging checks
Thru				Thru	b. Nacelle tilt - propeller blade angle schedule tests
11-10-64				200	c. Propulsion system cooling tests
					d. Noise level tests
					e. Aft tee box cooling evaluation
					f. Engine acceleration and deceleration tests
					g. Coordinator "auto trim cam" schedule checks
					h. Stick force versus deflection tests
					i. Static and dynamic control response tests
					j. Propeller control linkage resolution tests
					k. Fuel boost pump effect on engine operation
					l. Functional hydraulic and air conditioning system checks
					m. Nose wheel steering evaluation taxi test
					n. Aileron hinge bracket strain evaluation

Table XVIII. Continued.

DATE	FLIGHT NO.	FLIGHT TIME (MINS.)	BRIEF DESCRIPTION OF FLIGHT	INTERMEDIATE GROUND RUN NOS.	BRIEF DESCRIPTION OF GROUND RUN
11-12-64	23	:03	Hover SAS evaluation Pitch SAS malfunction		
11-12-64	24	:06	Hover SAS off		
11-13-64	25	:05	Hover 15 Kt. wind		
11-13-64	26	:03	Hover spot n, Roll SAS n action		
11-19-64				201 Thru 212	a. Transmission system green run b. Functional and vibratory evaluation of SAS c. Nose wheel steering evaluation taxi tests d. Higher speed taxi runs evaluating stopping distances without brakes e. Fuel system tests
12-3-64	27	:06	Hover, pitch and roll SAS assessment		
12-3-64 12-10-64				213 Thru 221	a. Higher speed taxi runs to evaluate aircraft acceleration and deceleration characteristics b. Propeller rigging checks c. Nose wheel off taxi runs, for S.T.O.L. build-up
12-10-64	28	:07	Hover, SAS evaluation pitch SAS malfunction		
12-11-64	29	:04	Hover, forward translation for SAS evaluation		
12-19-64 12-22-64				222 Thru 227	a. Propeller rigging checks b. SAS system evaluation c. Nacelle tilt schedule tests d. Nose wheel off taxi runs, for S.T.O.L build-up
12-23-64	30	:06	Hover, SAS evaluation		
12-23-64	31	:08	Hover, forward and sideways translations, SAS on		
12-23-64 1-5-65				228 Thru 231	a. Nose wheel off taxi runs, for S.T.O.L. flying build-up b. Maintenance check c. Evaluation of control trim positions with aircraft light on its wheels d. Functional evaluation of S.A.S. system e. Functional evaluation revised nacelle tilt system, (tilt rate slowed down)

Table XVIII. Continued.

DATE	FLIGHT NO.	FLIGHT TIME (MINS.)	BRIEF DESCRIPTION OF FLIGHT	INTERMEDIATE GROUND RUN NOS.	BRIEF DESCRIPTION OF GROUND RUN
1-7-65	32	:07	Conversion/reconversion through 20 Kt.		
1-7-65	33	:01	Hover, terminated with propeller vibration		
1-7-65	34	:02	Conversion/reconversion to 37 Kt.		
1-7-65	35	:02	Conversion/reconversion to 37 Kt.		
1-20-65	36	:10	Hover, roll SAS evaluation Military pilot eval.		
1-29-65				240	a. Transmission system green runs
Thru				Thru	b. Propeller rigging checks
7-31 65				262	c. Nacelle tilt - propeller blade angle schedule tests
					d. Pitch trim schedule tests
					e. Fuel boost pump bypass system tests
					f. Wing down load pressure survey
					g. Hydraulic system tests
					h. Cabin ventilation evaluation
					i. Emergency gear extension tests
					j. S.A.S. functional tests
					k. Coordinator vibration checks
					l. Engine fuel inlet vapor/liquid ratio tests
					m. Height control- propeller speed governor tests
					n. Control response and resolution tests
					o. Fuel low level warning system tests
					p. Propeller pitch control trimmer system tests
					q. Aircraft light on its wheels control trim check
7-31-65	37	:07	Hover, SAS evaluation height control eval.		
8-10-65				263	a. Aircraft shake down run after reassembling aircraft at Atlantic City, New Jersey
Thru				Thru	
8-12-65				265	b. Maintenance checks
8-13-65	38	:08	Hover, forward and sideways translation (N.A.F.E.C.)		
8-13-65	39	:05	Hover, rearward and sideways translation		
8-14-65	40	:04	Conversion/reconversion to 22 Kt.		
8-14-65	41	:02	Conversion/reconversion to 37 Kt.		

Table XVIII. Concluded.

DATE	FLIGHT NO.	FLIGHT TIME (MINS.)	BRIEF DESCRIPTION OF FLIGHT	INTERMEDIATE GROUND RUN NOS.	BRIEF DESCRIPTION OF GROUND RUN
8-17-65				266 Thru 267	a. Maintenance checks
8-18-65					
8-18-65	42	:06	Conversion/reconversion to maximum of 62 Kt.		
8-18-65	43	:06	Conversion/reconversion to 45 Kt.		
8-19-65	44	:01	STOL take-off and landings, 30 through 60 Kt.		
8-19-65	45	:02	Conversion/reconversion to 71 Kt.		
8-21-65	46	:06	Conversion/reconversion to 60 Kt.		
8-21-65	47	:04	STOL take-off at 60 kt., turns right and left, reconversion to hover landing		
8-21-65	48	:04	STOL take off at 60 kt., conversion to 70 kt., reconversion to hover		
8-21-65	49	:02	STOL take-off at 60 kt., conversion to 80 kt., reconversion to hover		
8-24-65				268 Thru 269	a. Maintenance checks
8-24-65					
8-25-65	50	:07	STOL take-off, climb at 80 kt., conversion to 90 and 100 kt. No.2 nacelle failure caused airplane to crash. Crew ejected safely.		

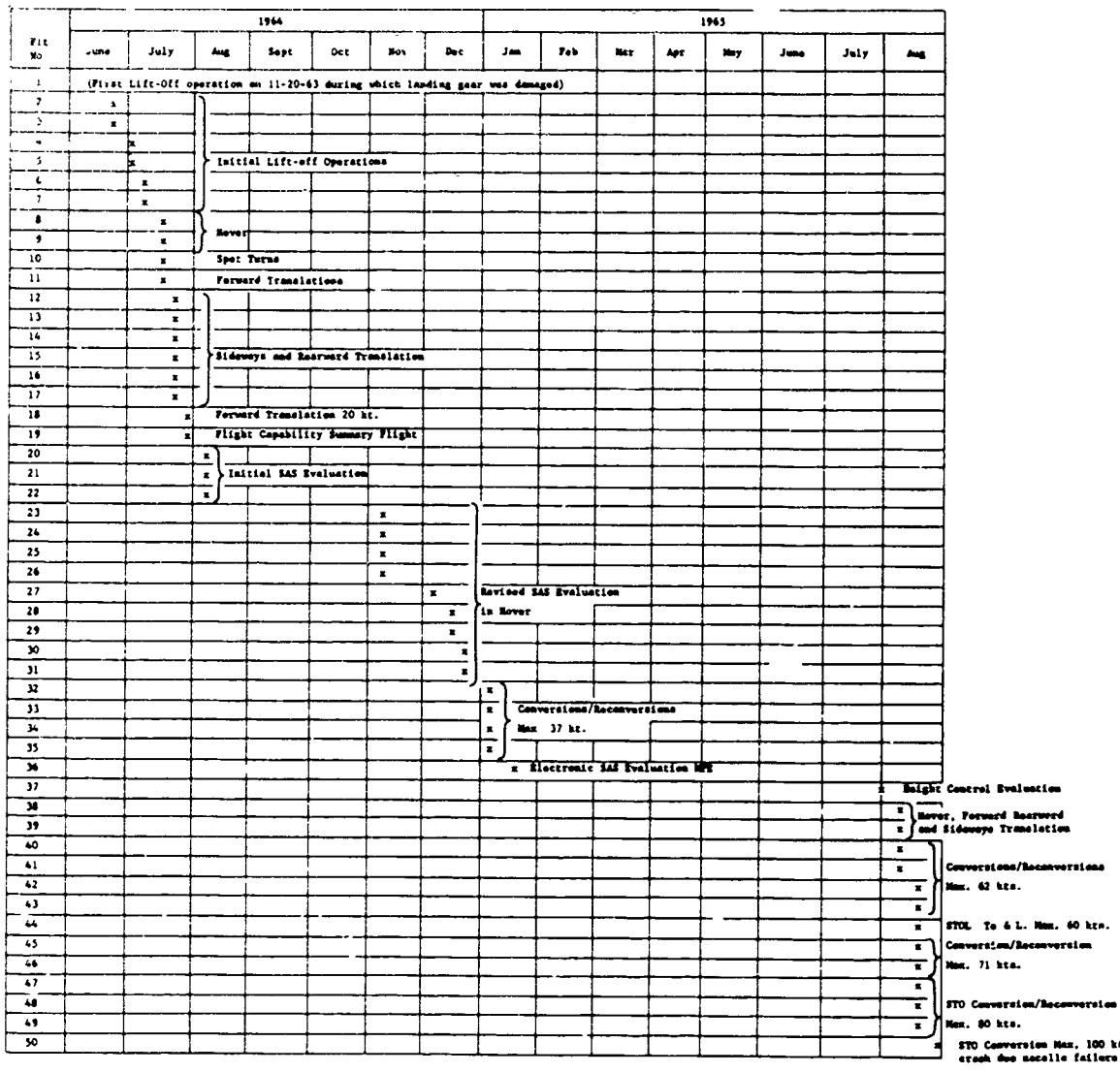

Figure 306. Flight test schedule, X-19 S/N 62-12197.

c. Flight Test Schedule at NAFEC

All of the above flights and the first 262 ground runs were made at the Caldwell-Wright Airport at Caldwell, New Jersey. In view of the limitations of this airport as a test site for cruise flight tests, the test program was transferred to the Federal Aviation Agency National Aviation Facilities Experimental Center at Pamona, New Jersey. At this facility there was a 10,000 foot runway available and test airspace allocation adjoining the airport.

During the ensuing flight tests at N.A.F.E.C. a company co-pilot was added to the flight crew, all previous flights having been made with one pilot only, except on Flights Nos. 36 and 37 when a military co-pilot was carried. Subsequent flight test phases were:

(1) Flight Nos. 38 and 39:

These flights were made to refamiliarize the pilot and evaluate the electronic S.A.S. performance in translation flight. It was established that airplane operation was normal after its rebuild following shipment to N.A.F.E.C.

(2) Flights No. 40 thru 43:

Conversion/reconversion maneuver runs were made along runways starting and finishing in hover flight, with the nacelles being tilted down to accelerate the airplane. Maximum airspeed reached was advanced on successive runs from 20 knots at 90° nacelle angle to 62 knots at 82° nacelle angle.

(3) Flight No. 44:

A series of STOL type take-offs and landings were performed at airspeeds from 20 to 60 knots. In each run the nacelle angle appropriate to the target airspeed was pre-set before take-off. As take-off power was applied the airplane was allowed to roll forward. As it accelerated through the target take-off speed the nose was raised and sufficient power added to take-off as near to the target airspeed as possible. After a brief stabilized period of level flight, power was reduced and a landing made. After landing the nose wheel was lowered onto the ground, a further power reduction made, the nacelles tilted up and the airplane braked to a stop.

(4) Flight No. 45 thru 49:

Further extension of the conversion/reconversion maximum airspeed was developed in Flights Nos. 45 through 49. This was accomplished via a STOL take-off at 60 knots and 77° nacelle tilt to achieve the initial acceleration.

Further in-flight nacelle tilt was performed, to accelerate to 70 and 80 knots airspeed on successive flights. The reconversion decelerating maneuver was made by tilting the nacelles up to hover, prior to a hovering landing. Turns were made at 60 knots, following the runway pattern 45° right, 90° left and 45° right again. Well coordinated turns at approximately 11° bank angle were made in both directions. On another run the propeller speed was changed in flight at 50-60 knots from hover speed 98.5% N_2, to transition speed 88% N_2, and back again. A reduction in power setting required for level flight was observed as the propeller speed was reduced. During Flight No. 49 a maximum stabilized airspeed of 80 knots was achieved with a nacelle angle of 65°.

(5) Flight No. 50:

This last, and catastrophic, flight of X-19 Serial No. 62-12197 is of special interest in a historical context. Therefore it is chronicled here in greater detail than the earlier flights for the sake of a complete record.

It was agreed with the Air Force that Flight No. 50, planned to extend conversion maneuvers to 90 and 100 knots, should be flown as an airfield circuit. Accordingly Flight No. 50, commencing with a 60 knot STOL take-off, was progressed with a climb to 1,000 feet at 80 knots. This was followed by runs down the field at 90 and 100 knots on a racetrack or oval pattern. The following description of Flight No. 50 is taken from (95):

"After checking all instruments, fuel, tilt position of 77°, trim, etc., power was advanced and the aircraft accelerated to 60 K, the predetermined take-off speed, using runway No.31. At this speed a small rotation was made, and the X-19 climbed to a height of 30 feet. The nose was then lowered, tilt changed to 65° to accelerate to 80 K.

"During this maneuver some altitude was lost, but otherwise the stability and control of the airplane was good. A steep climb was then started with the objective of reaching 1,000 feet altitude. The climb was actually made in four segments, the last phase in a 180° climbing turn. During the climb, power read was 950 foot-pounds and R/C was 800 to 1,000 fpm. This compared with a predicted value of 1,000 fpm for approximately 1,000 foot-pounds torque.

"At the top of the climb, power was reported to be reduced to approximately 800 foot-pounds torque and the nacelles reduced to an angle of 55 degrees, the values predicted to be the 90 K level flight speed. The airplane reached a speed of 90 K with the pilot estimating an angle of attack change from 7° at 80 K and 65° tilt, to 10° at 90 K at 55° tilt. Further,

the pilot stated that the stick position was 85 to 90 per cent forward. The trim was still believed to be neutral. Because of the 'uncomfortable feeling', tilt was brought back to an angle of 63 degrees with a reported reduction of angle of attack to 7 degrees, and the flight continued." It should be noted that the calculated steady state flight speed for 55° tilt is 90 K at 10° angle of attack with a neutral stick." This last note is incorrect. If on the tilt velocity schedule the stick should be at about 70% forward. If one accounts for the deviations in power, c.g. and velocity, the predicted position will fall in the vicinity of 85% to 90% forward.

Returning to the quoted text:

"During the 90 K downwind leg of the flight, the aircraft was maintained under good control, and its stability appeared to be satisfactory. The altitude varied from 1,000 to 1,300 feet with the speed varying from 95 K to 105 K. See Figure 307 and 308 for a time history of velocity and altitude.

"Due to positive indications from temperature warning lights, it was decided to terminate the flight. At this point the aircraft was operating at a speed of 105 K and an altitude of 1,100 ft. Power was reduced, and the aircraft descended with an ever-tightening right turn. During the right turn the runway was missed, and the turn was continued crossing runway No.31 at right angles, approximately 900 feet from its end. The turn and rate of descent were held until the aircraft was approximately 60 feet off the ground. It appeared to the co-pilot that a landing was intended at this point. The speed was approximately 85 K, and the rate of descent was 1,100 to 1,200 fpm. At this point the co-pilot applied nearly full power, the aircraft rotated approximately 10 to 15 degrees, and a climb rate of as high as 1,400 ft/min was encountered.

"During the climb, the power was apparently maintained, and the speed increased to 120 K. At the time of the power application the blade angle increased through the dead zone of the rate limiter so that the RPM increased. The RPM increased to approximately 103% N_2 and was then controlled by the fuel topping governor.

"The aircraft was levelled off at an altitude of 400 feet, and the right turn continued. Three to four seconds after the top of the turn, No. 2 propeller left the airplane. This caused the airplane to roll left and pitch up. After rolling approximately 40 degrees, the No. 1 propeller left, and the roll rate increased. Propellers No. 3 and 4 then were torn off the airplane due to the high rate of rotation at an angle of approximately 90° from the vertical. Then at a roll angle of 200 to 210 degrees measured clockwise from the front, and

with the aircraft at 400 ft. travelling at approximately 120 knots, the two pilots ejected, almost simultaneously, successfully. The aircraft continued to roll, finally ending up in a nearly vertical dive and crashing into a swamp with fire on impact. The pilots landed ahead of the aircraft with minor injuries probably received on ejecting."

Subsequent to the crash on Flight No. 50 an analysis of photo theodolite records and photographs indicated that the No. 2 propeller and part of the No. 2 propeller nacelle broke off and flew clear of the aircraft at the top of the climb-out. The aircraft commenced to roll to the left and pitch nose up, and in the ensuing maneuver all of the other propellers and/or nacelles broke off. Both parachutes of the crew deployed at approximately 250 feet and the pilots landed safely and essentially uninjured. The airplane crashed approximately 500 feet away from the crew landing point, in a dried out reservoir lake bed within the N.A.F.E.C. airport boundary fence. The airframe was completely destroyed by the crash impact and the resulting fire.

The track taken by the aircraft during Flight No. 50 and the details of the positioning of crashed airplane parts are shown in (96) and (97), and are also graphically presented with respect to time for climb velocity (Figure 309), resultant velocity (Figure 310), in-flight acceleration (Figure 311), vertical acceleration (Figure 312), bank angle (Figure 313), pitch angle (Figure 314), roll rate (Figure 315), front and rear nacelle angles (Figure 316) and excess thrust horsepower absorbed (Figure 317), all for the moments just before the crash. Additional theodolite data are plotted and presented in (95). These maps and photographs were supplied to the Air Force Accident Board of Inquiry immediately after the crash.

d. Aircraft Used in Flight Tests

The total flight time on X-19 Serial No. 62-12197 against subject contract (between Flights Nos. 8 and 50) was 3 hours 44 minutes. A total of 84 lift-offs were made. Figure 318 shows the airplane at approximately 1,000 feet at 90 knots during Flight No. 50. Further discussion of this flight appears in Sections XII,5. and XII,6. of this report. Flights No. 1 thru 7, conducted with this aircraft, were performed under Contract AF 33(657)-8665, Part I (a), Item 2.d, and are summarized in Curtiss-Wright Report 014-496. Figure 319 depicts the airplane hovering during one of these flights.

The second airplane X-19 Serial No. 62-12198 did not make any flights against the subject contract (94), but some significant ground tests, particularly those on updated components, were made during its ground runs.

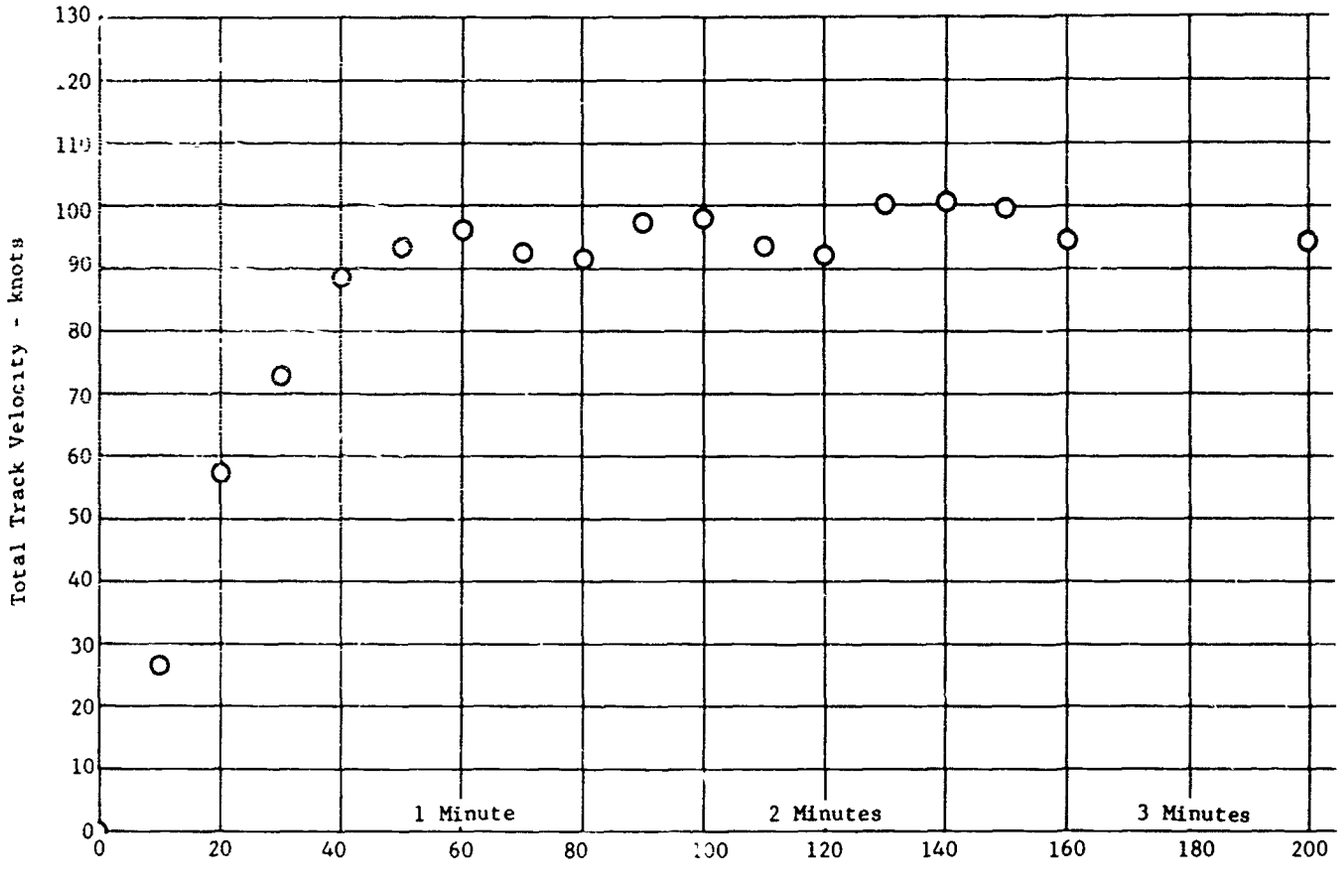
Total Track Velocity - knots
130
120
110
100
90
80
70
60
50
40
30
20
10
0
0
20
40
60
80
100
120
140
160
180
200
1 Minute
2 Minutes
3 Minutes

Fli

A

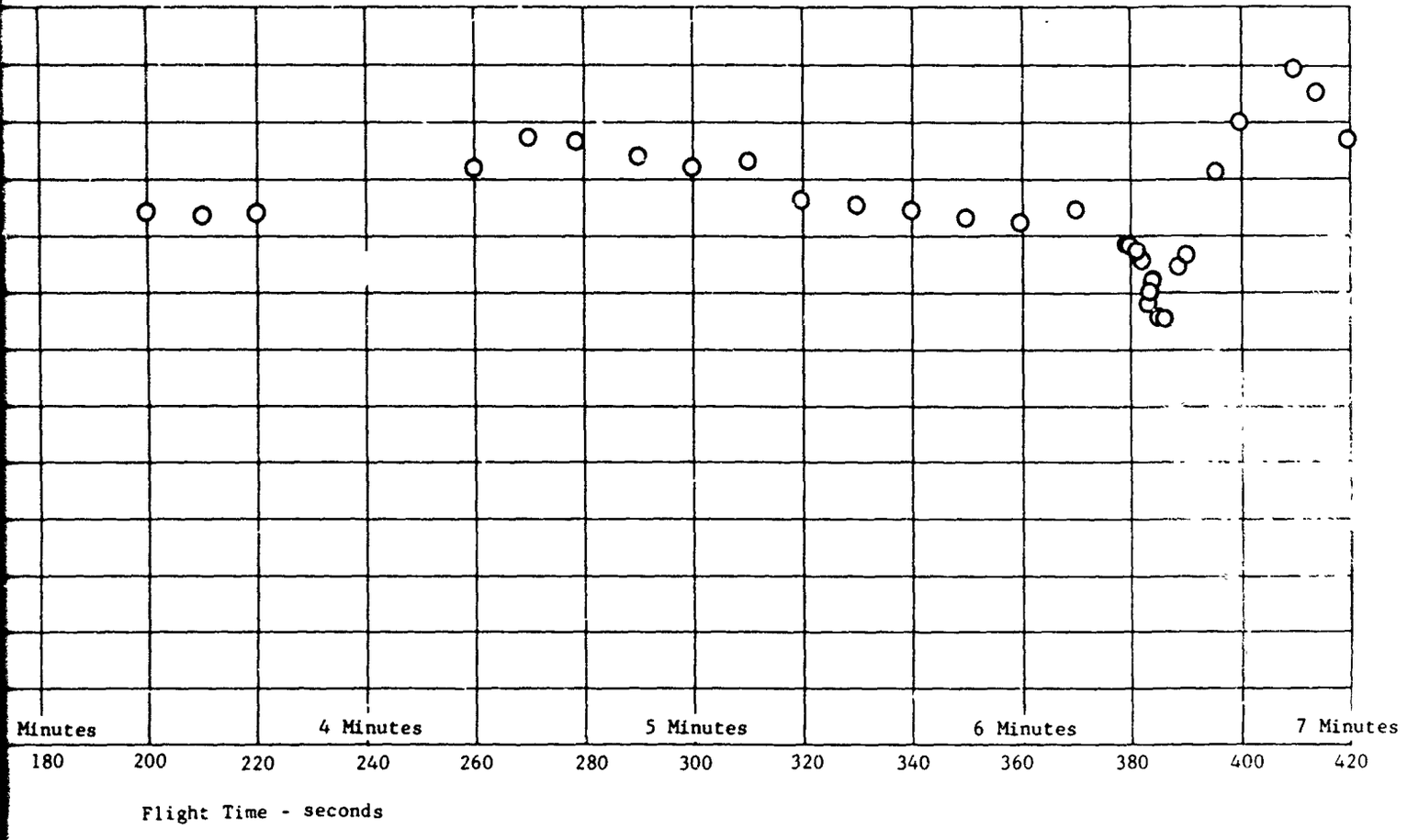

Figure 307. X-19 Flight No.50, track velocity history (Theodolite digital data).

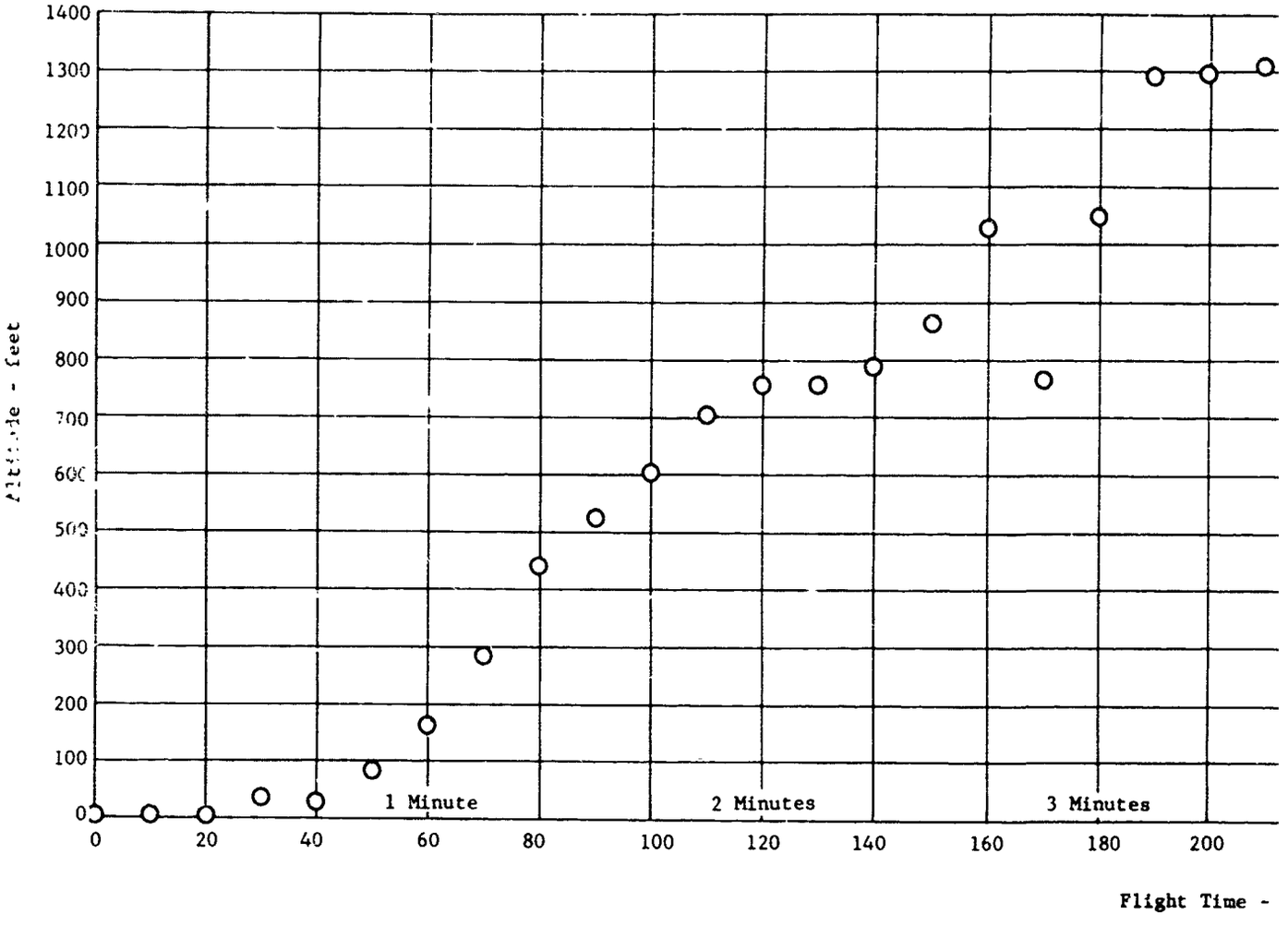
1400
1300
1200
1100
1000
900
800
700
600
500
400
300
200
100
0
0
20
40
60
80
100
120
140
160
180
200
1 Minute
2 Minutes
3 Minutes
Flight Time -

A

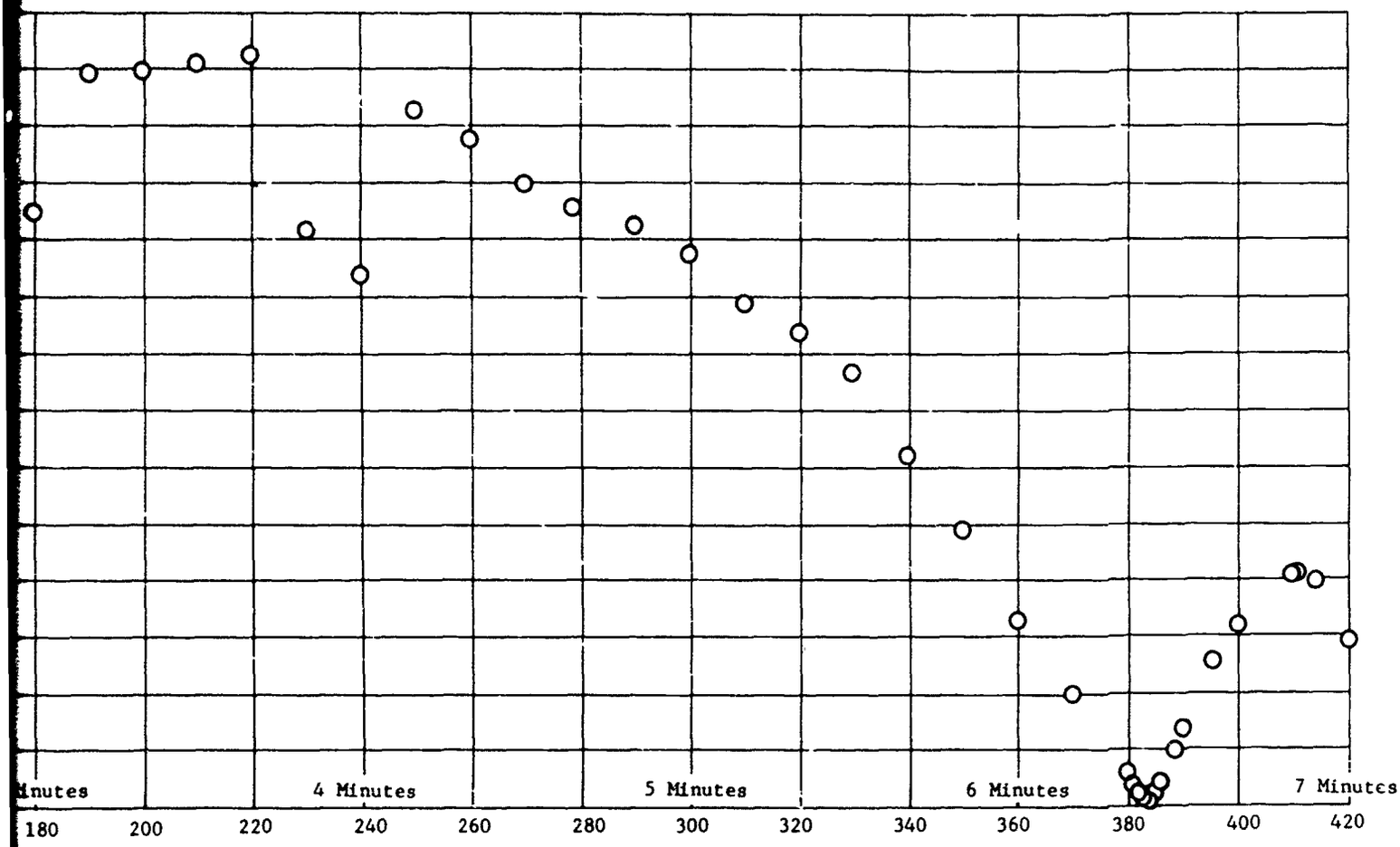

Figure 308. X-19 Flight No.50, altitude time history (Theodolite digital data).

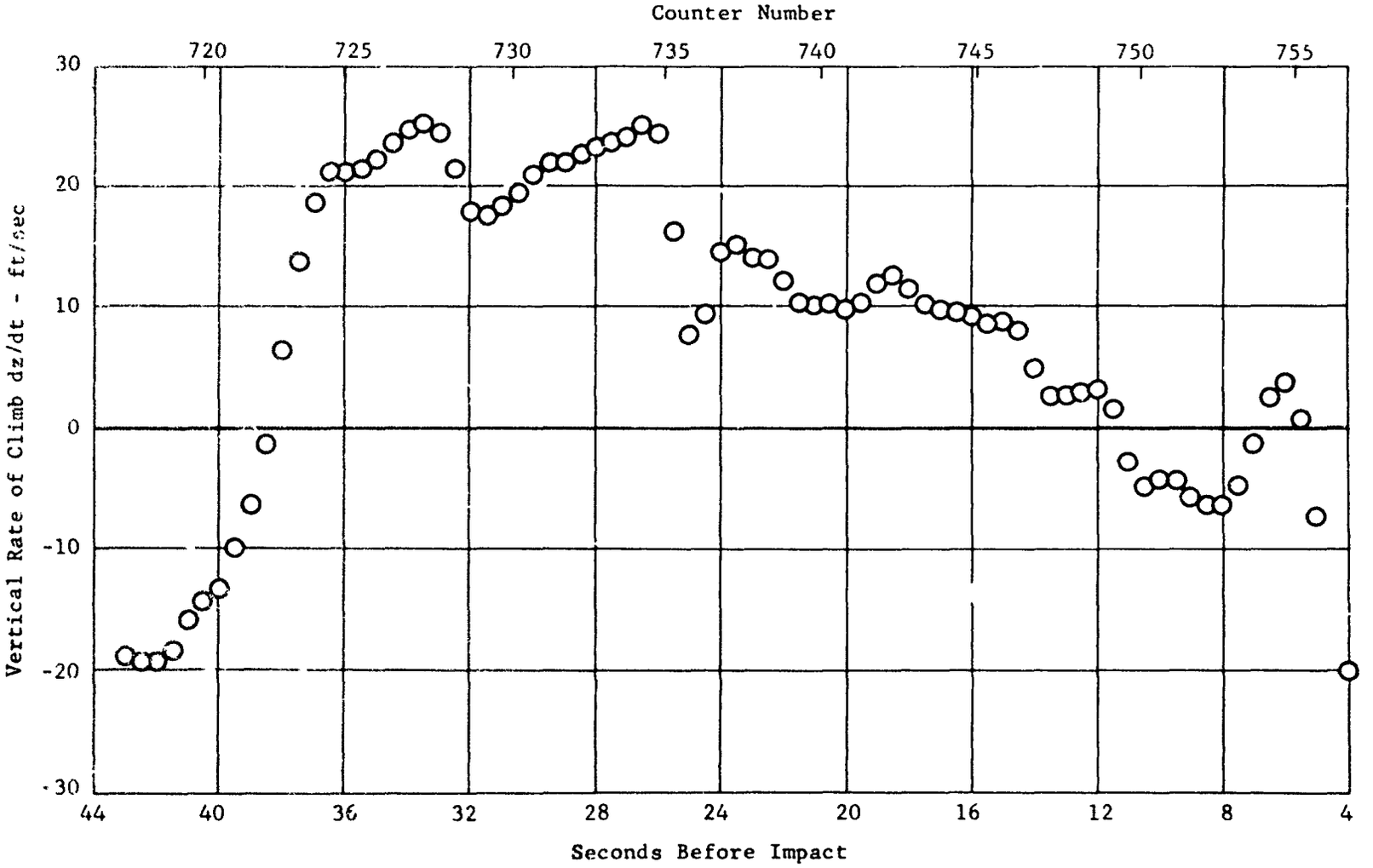

Figure 309. X-19 Flight No.50, climb velocity vs time (Theodolite Digital Data).

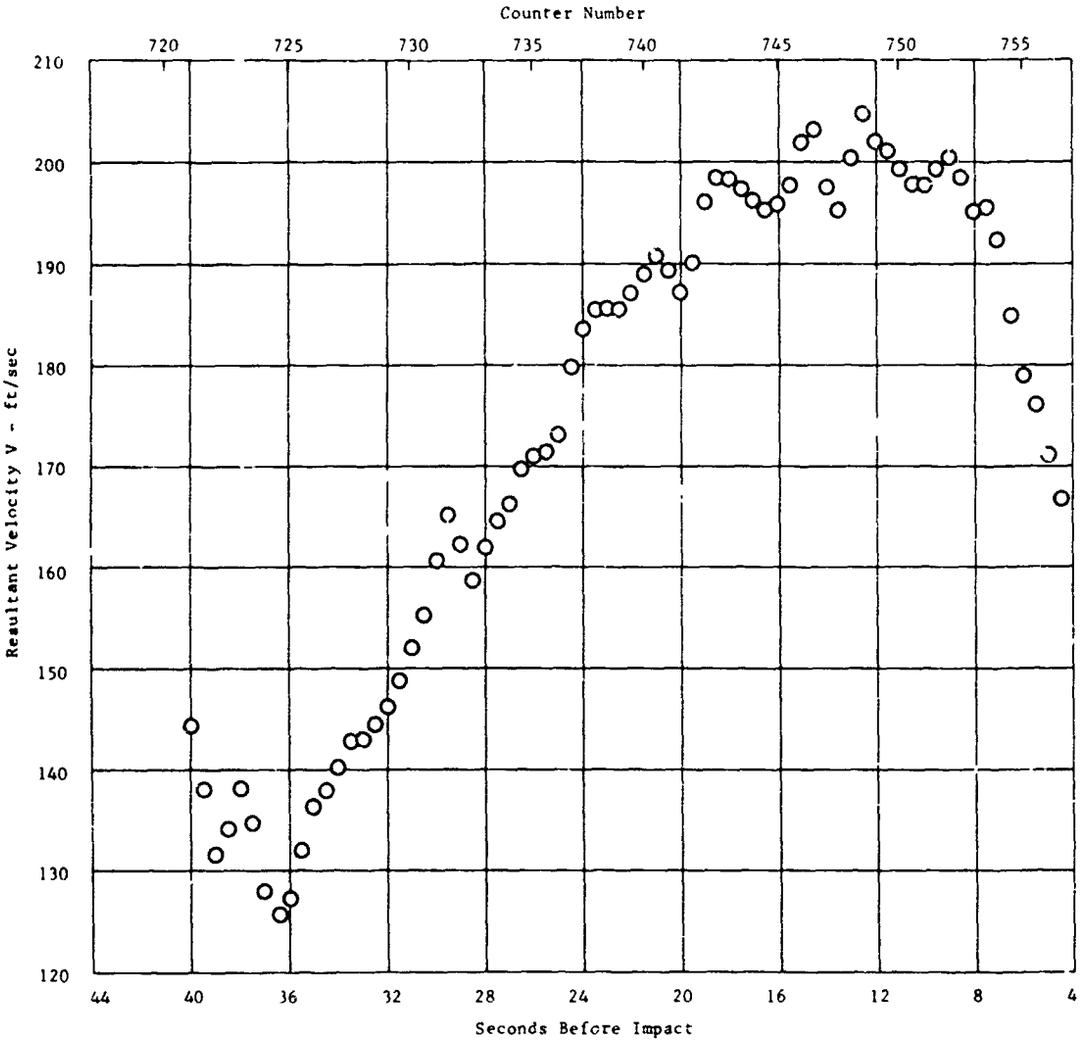

Figure 310. X-19 Flight No.50, resultant velocity vs time (Theodolite Digital Data).

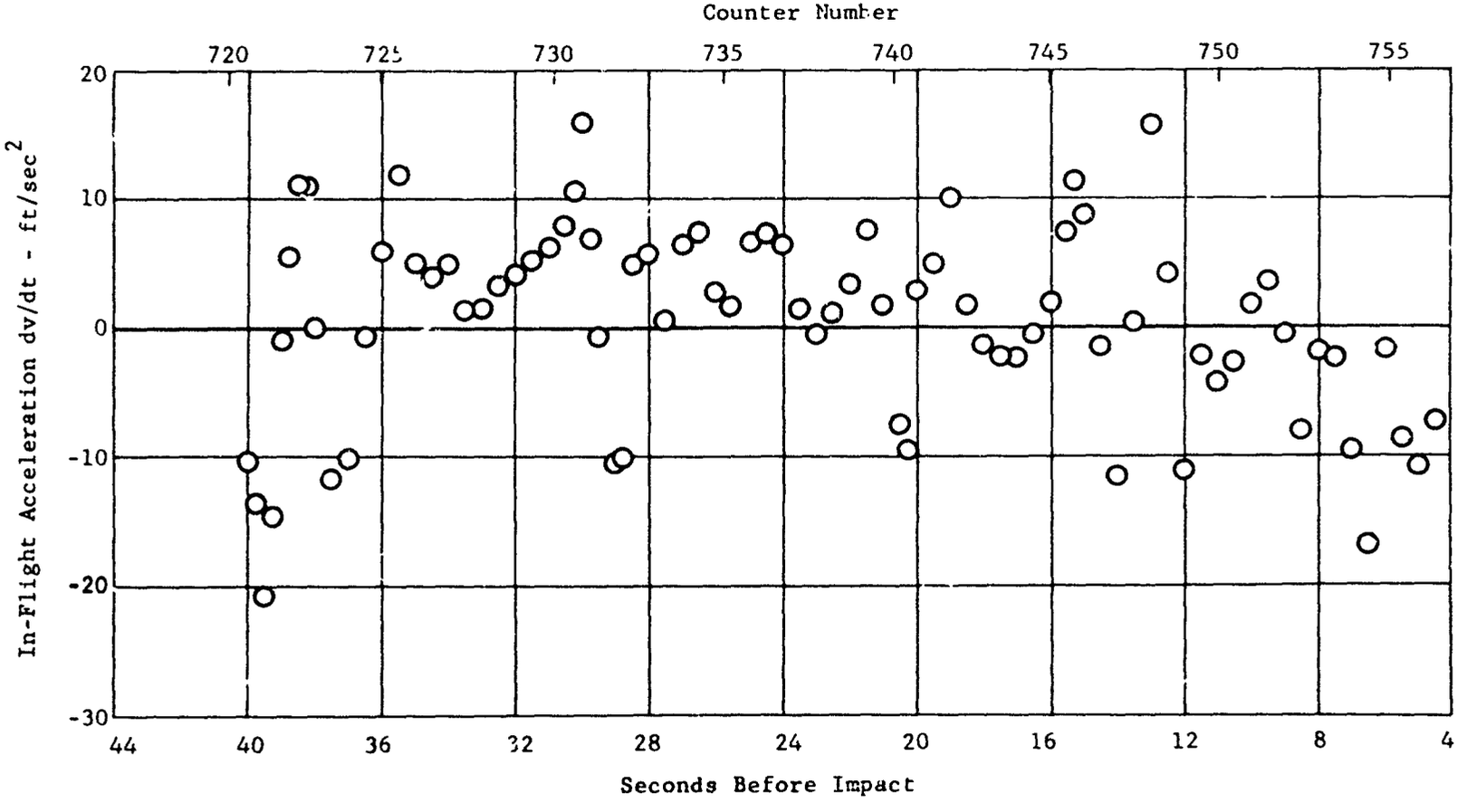

Figure 311. X-19 flight number 50, in-flight acceleration vs time (Theodlite Digital Data).

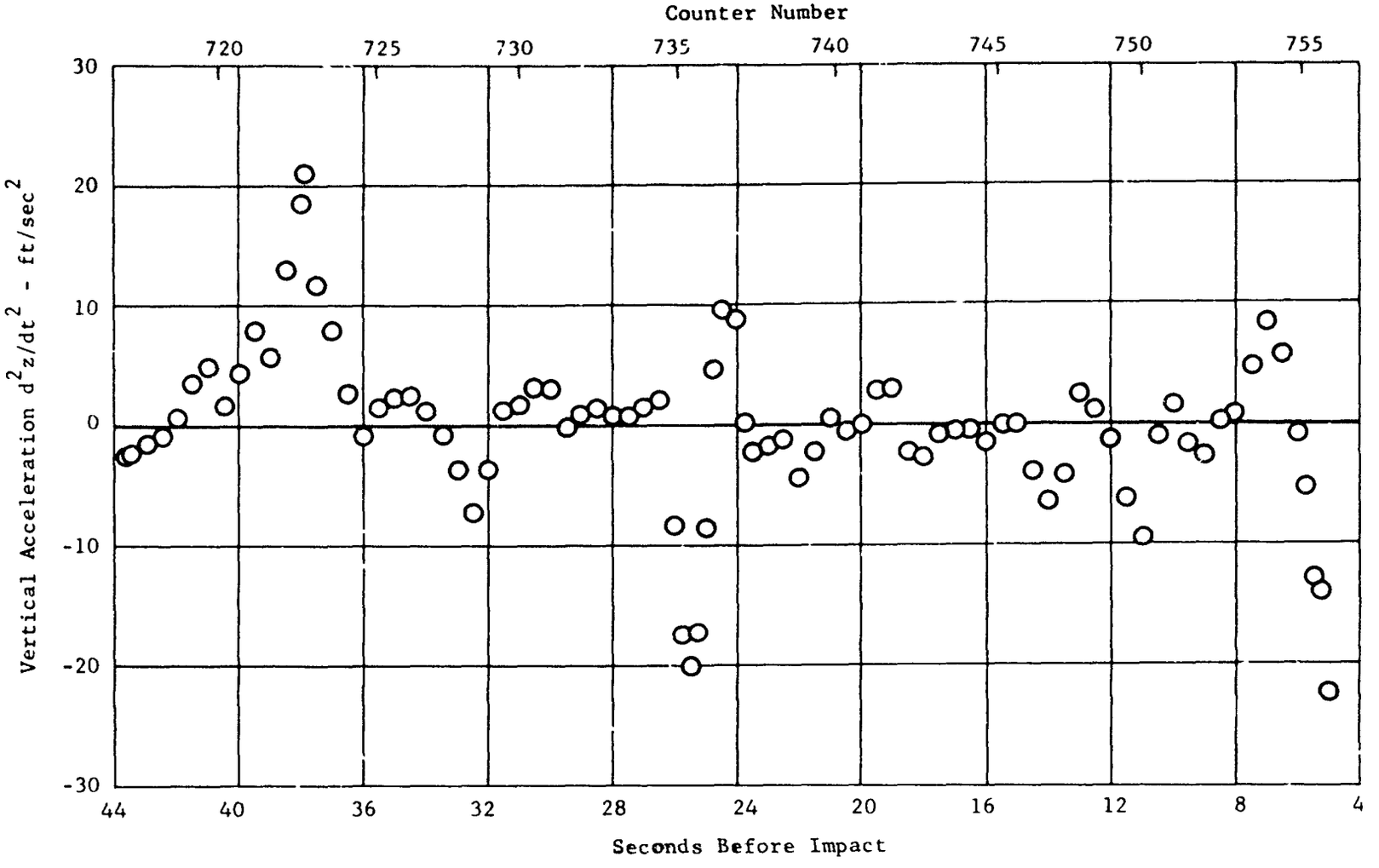

Figure 312. X-19 flight number 50, vertical acceleration vs time (Theodlite Digital Data).

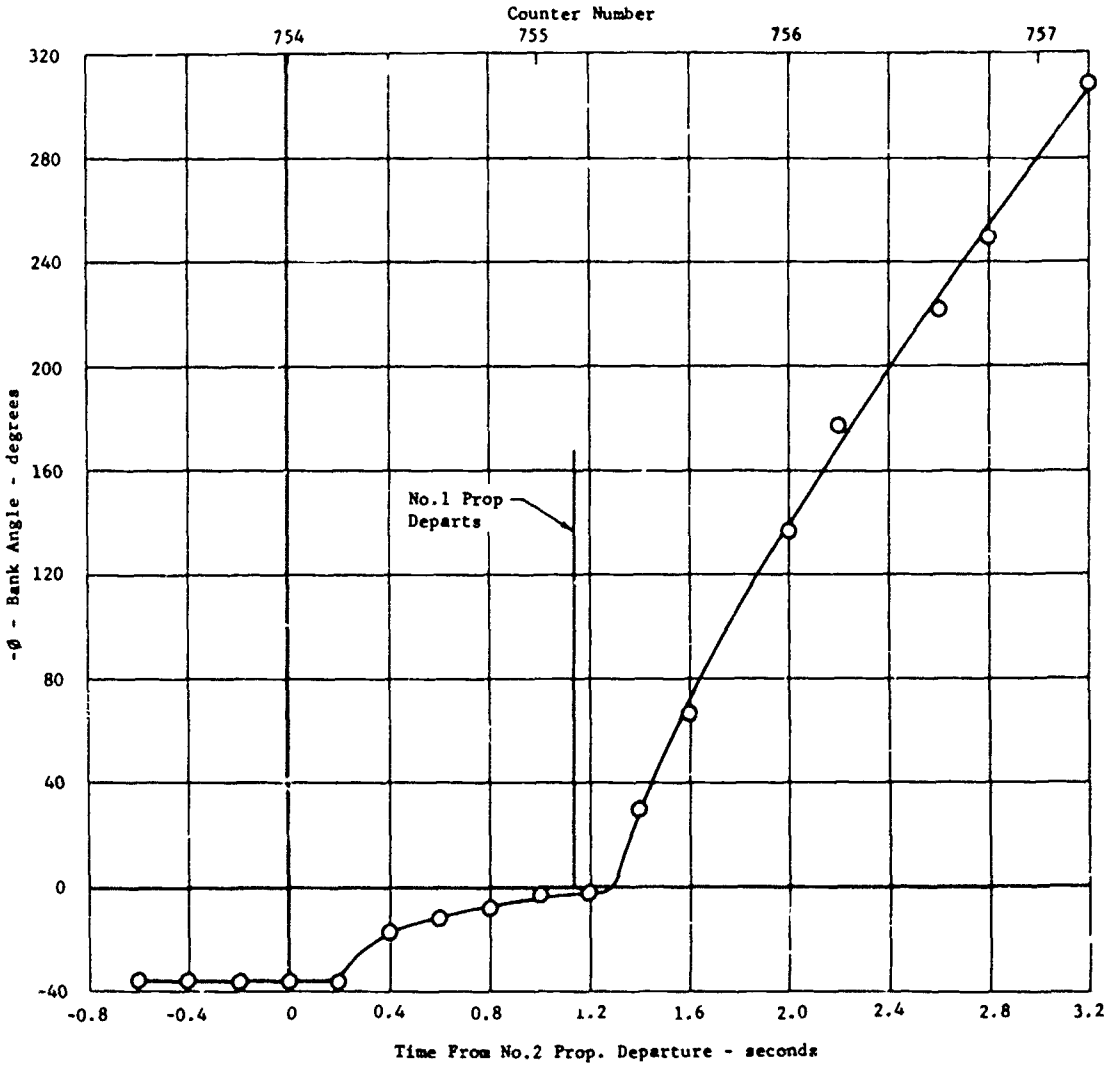

Figure 313. X-19 Flight No.50, bank angle (Theodolite film data).

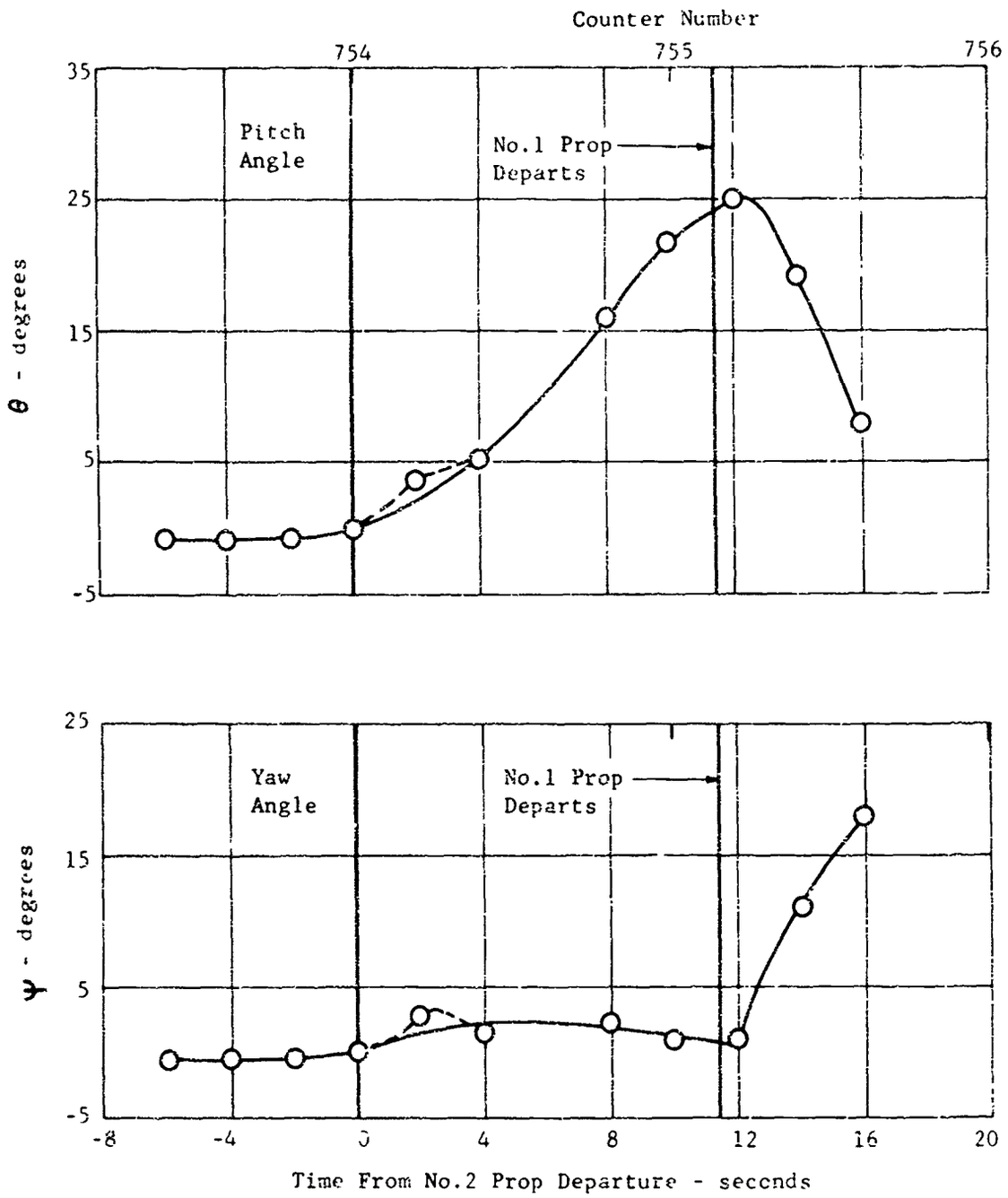

Figure 314. X-19 flight number 50, pitch angle and component of yaw angle (Theodlite Film Data).

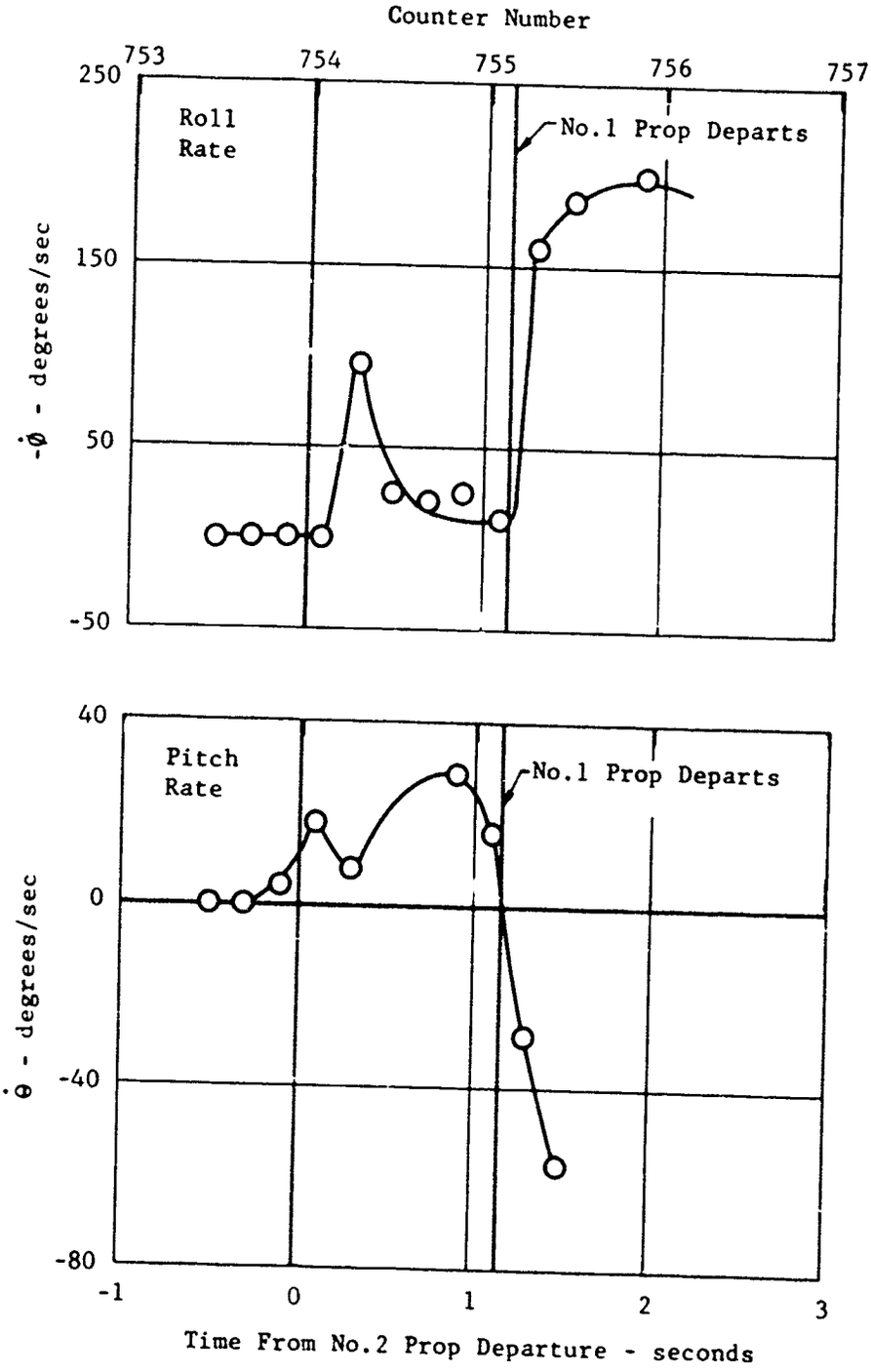

Figure 315. X-19 flight number 50, roll and pitch rate (Theodlite Digital Data).

67-2282

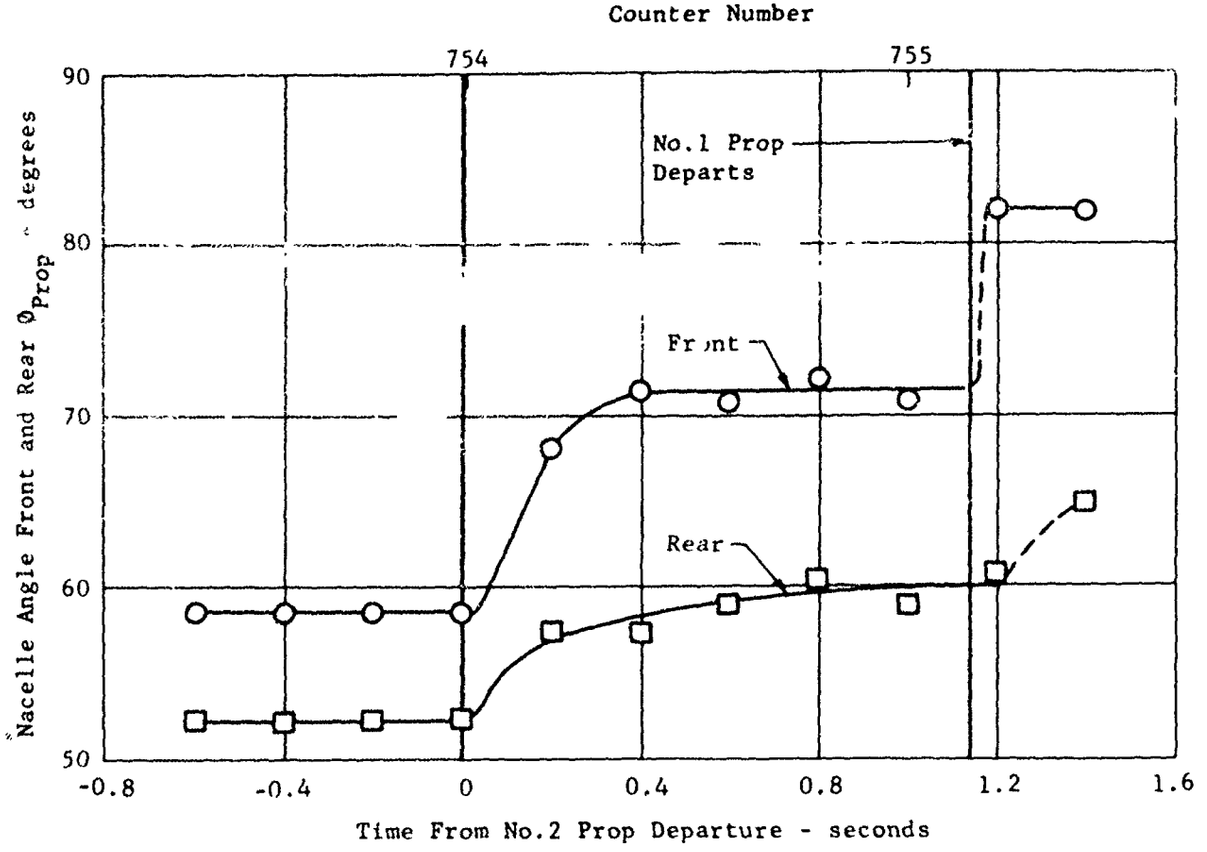

Figure 316. X-19 flight number 50, front and rear nacelle angles (Theodlite Film Data).

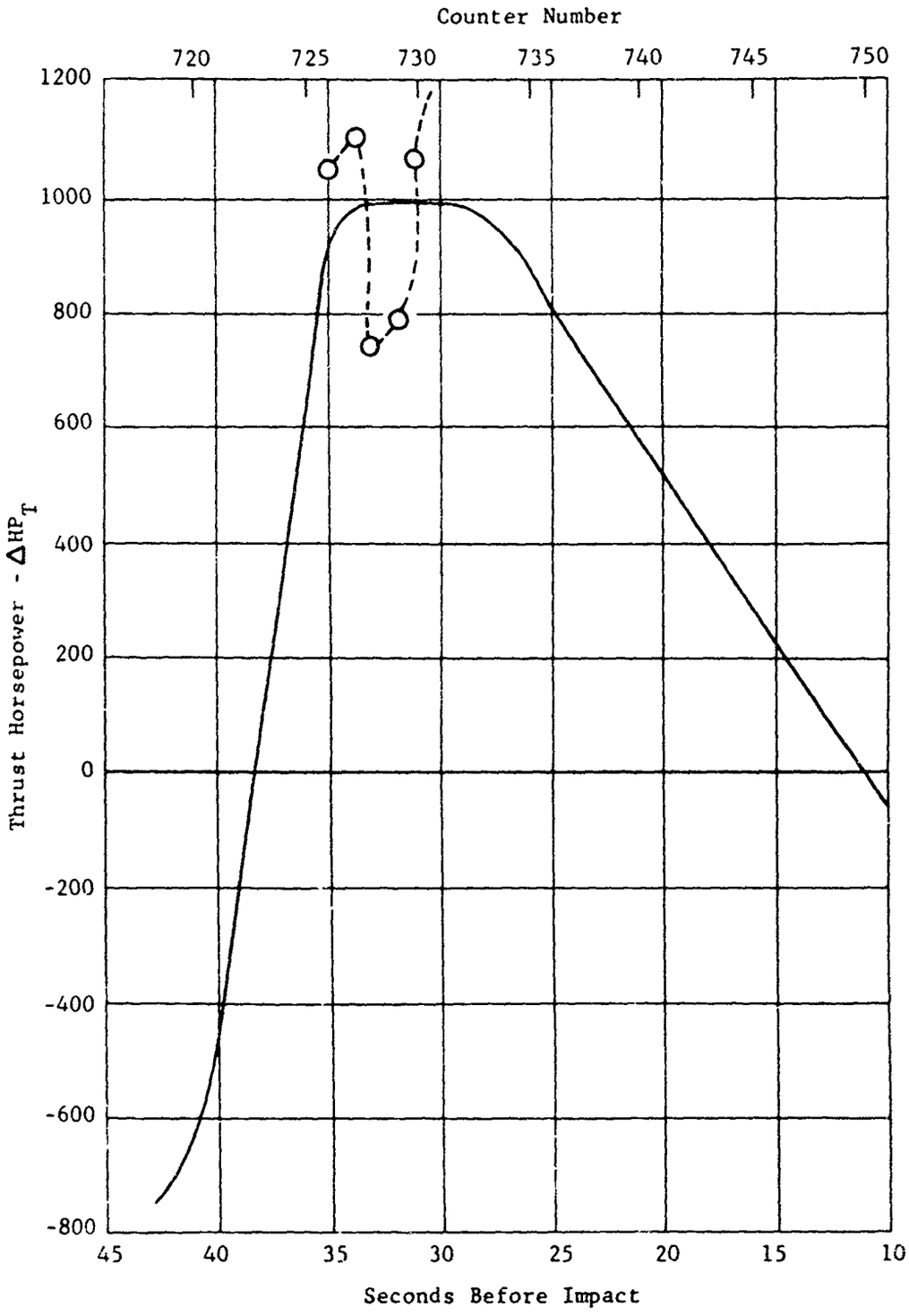

Figure 317. X-19 flight number 50, excess thrust horsepower absorbed along the vertical axis (Average Theodlite Trace and Digital Data).

Figure 318. X-19 S/N 62-12197 in conversion flight at 90 knots.

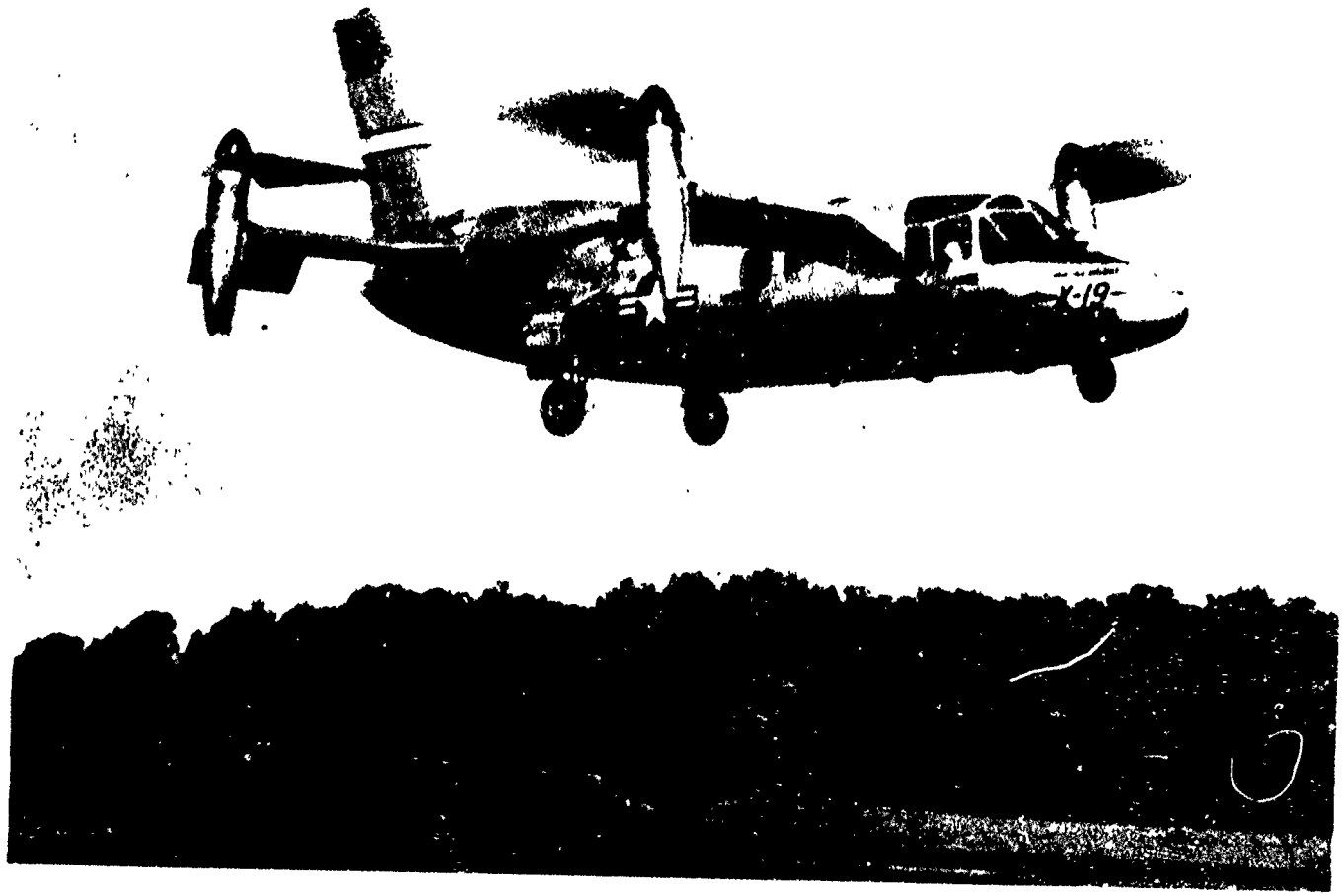

Figure 319. X-19 S/N 62-12197 in hover flight.

3. AIRCRAFT CONFIGURATION VS TIME

The X-19 flight test summary is contained and detailed in (98). Table XVIII of the present report lists the historical progression of flight tests on X-19 Serial No. 62-12197, as obtained from that reference. The test aircraft underwent successive modifications during the flight test program variously for correcting malfunctions and for improving upon its design. This section enumerates those configuration changes to the aircraft.

a. Aircraft at Beginning of Flight No. 8

The configuration of the test aircraft at the commencement of tests at Flight No. 8 was as defined below:

A. X-19 Serial No. 62-12197 built to Drawing No. 200-000001. B. Plus all VTOL Systems Division ECNs through 6338 which are applicable to X-19 Serial No. 62-12197 C. Plus all Curtiss Division ECNs through 30886 which are applicable to X-19 Serial No. 62-12197.	Defines what the airplane should be if current with the drawing system as of August 7, 1964.
D. Minus the VTOL Systems Division Quality Department's listing of "Open ECNs on X-19 Serial No. 62-12197 as of August 7, 1964"	Defines which airframe ECNs were unaccomplished as of August 7, 1964.
E. Minus all Curtiss Division ECNs and VTOL Systems Division Mechanical Systems ECNs applicable to X-19 Serial No. 62-12197 which were still unaccomplished at August 7, 1964.	Should define all mechanical systems ECNS which were still unaccomplished as of August 7, 1964.
F. Plus the changes prior to Ground Run or Flight listed in Ground Run Nos. 154 through 159.	Defines the Flight Test and ECN changes between August 7, 1964 and Flight No. 8.

c. Plus the changes other than ECNs listed in Ground Run Reports through No. 159 and Flights through No. 7. } Defines the Flight Test changes to the airplane prior to Flight No. 8.

b. Configuration Changes During Test Program

The changing configuration of the airplane between Flight No. 1 and Flight No. 59 is reported in chronologically successive Flight and Ground Run Reports. Most of the significant configuration changes may be considered as they occurred between the phases of flights listed in the preceding subsection. The changes considered most important with respect to their impact on the flight test program are listed below, as accomplished prior to the given Run numbers.

Prior to Ground Runs Nos. 1 - 70

(1) Modified aft tee box lubrication system.

(2) Repaired propeller pitch control coordinator nacelle tilt and collective functions.

(3) Installed improved engine inlet plenum chamber door hinges.

(4) Installed improved propeller pitch control bungees (Part No. 734085)

(5) Installed flight test debris screens over engine inlet plenum chamber doors.

(6) Temporarily stiffened left hand throttle levers.

(7) Replaced all propeller pitch control rod with new rods having 1/4 inch threaded ends.

Prior to Ground Runs Nos. 71 - 149

(1) Repaired damaged landing gear components and aircraft sheet metal parts damaged by collapse of the left hand main gear on Flight No. 1.

(2) Installed new design elevators.

(3) Modified elevator boost system.

(4) Replaced static inverters with rotary inverters.

(5) Modified all of the power transmission gear boxes.

(6) Installed improved power transmission shafts.

(7) Modified engine fuel controls.

(8) Modified fire extinguisher nozzles.

(9) Modified engine inlet plenum chamber doors.

(10) Modified wing flap droop schedule.

(11) Modified propeller-nacelle assemblies.

(12) Reworked main landing gear retraction system.

(13) Rotated pilot's stick grip 19°.

(14) Installed beefed up left hand throttles.

(15) Reworked nacelle tilt system.

(16) Stiffened aileron hinge bracket.

(17) Installed a secondary roll boost system.

(18) Installed beefed up propeller pitch control hangers.

(19) Modified nose wheel steering system.

(20) Modified pilot's stick feel spring mechanism.

(21) Reworked propeller pitch coordinator and roll trim assembly.

(22) Modified fuel system to feed both engines from the forward left hand tank.

(23) Modified primary hydraulic system relief valve.

(24) Modified aft tee box cooling air ducting.

(25) Increased lateral stick travel to $\pm$ 5 inches.

Prior to Ground Runs Nos. 150 - 155

(1) Repaired pitch S.A.S. gyro unit.

(2) Installed new pilot's stick roll feel spring.

(3) Removed dorsal fairing to improve aft tee box cooling.

Prior to Ground Runs Nos. 156 - 158

(1) Replaced the No. 2 propeller assembly.

(2) Replaced No. 2 engine fuel control to correct a fuel leak.

Prior to Ground Run No. 159

(1) Reduced pilot's roll feel spring breakout force to approximately one pound.

(2) Repaired damaged A.P.U. clutch assembly.

(3) Zero timed the accessory drive gear box.

Prior to Ground Run No. 160 - None

Prior to Ground Run No. 161 - None

Prior to Ground Run No. 162

(1) Reduced roll feel spring rate.

(2) Installed reworked roll S.A.S. gyro unit.

Prior to Ground Run No. 163 - None

Prior to Ground Runs Nos. 164 - 166

(1) Increased gain of roll S.A.S. by a factor of 2.5.

Prior to Ground Runs Nos. 167 - 200

(1) Installed an improved propeller coordinator.

(2) Re-rigged the propeller control linkage of all four nacelles in the laboratory whirl booth.

(3) Installed new propeller blades on Nos. 1, 3, and 4 propellers.

(4) Installed calibrated engines.

(5) Inspected transmission system.

(6) Modified fire extinguisher system.

(7) Modified the aft tee box cooling air inlet ducts and exhaust system.

(8) Swapped the aft tee box and several aft tee box cooling components around during the aft tee box cooling evaluation.

(9) Modified aileron droop linkage.

(10) Modified elevator control system.

(11) Modified landing gear retraction mechanism.

(12) Made electrical modifications to the control sticks.

(13) Improved the secondary hydraulic system.

(14) Installed new flaperon binge brackets.

(15) Modified roll control and pitch S.A.S. circuits in propeller coordinator.

(16) Installed modified roll and pitch stick feel springs.

(17) Installed the latest change pitch and roll S.A.S. gyro units.

(18) Repaired broken "auto trim cam" by replacing coordinator.

(19) Replaced the coordinator input roll trim assembly with a bungee assembly.

(20) Installed emergency nose gear extension system.

(21) Installed new nacelle gear sets.

Prior to Ground Runs Nos. 201 - 212

(1) Pitch and roll S.A.S. gyro units modified.

(2) Inspected transmission system gear boxes and replaced No. 3 nacelle gear set.

(3) Modified nose wheel steering system.

(4) Installed improved nacelle tilt drive shafts.

(5) Replumbed fuel system back to having both forward fuselage fuel tanks in operation.

(6) Stiffeners added to S.A.S. gyro units.

Prior to Ground Runs Nos. 213 - 221

(1) Modified nose wheel steering system.

Prior to Ground Runs Nos. 222 - 227

(1) Repaired broken "auto trim cam" and installed modified S.A.S. gyro units by replacing the coordinator.

Prior to Ground Runs Nos. 228 - 231

(1) Aft fuselage external skin repaired as a result of tail striking runway during high speed taxi runs.

(2) Installed additional restriction in the nacelle tilt hydraulic supply line to slow down nacelle tilt rate.

Prior to Ground Runs Nos. 232 - 239

(1) Installed a larger main gear retraction cylinder.

(2) Improved the decoupling portion of the electrical nacelle tilt system.

(3) Repaired broken A.P.U. clutch.

(4) Replaced the roll S.A.S. gyro with Part No. 170858-M unit.

(5) Removed damaged nose gear doors and set up landing gear for fixed gear operation.

Prior to Ground Runs Nos. 240 - 262

(1) Installed two new forward nacelle assemblies with "Standardized" propeller pitch control linkages.

(2) "Standardized" the propeller pitch control linkages on the two rear nacelles.

(3) Completed the addition of an emergency nose gear extension system (blowdown bottle).

(4) Installed redesigned aileron hinge bracket.

(5) Incorporated a fuel boost pump fuel bypass and pressure warning system in the two forward fuel tanks.

(6) Capped off the No. 2 fuel outlet, converting the fuel system back to a single sump tank (left hand forward) system.

(7) Due to propeller failure on Run No. 242, removed all four propeller assemblies and installed ground-test-only propeller on the rear nacelles. Run Nos. 243 through 246 were conducted with rear propellers only.

(8) Installed the main gear emergency extension system (blowdown bottle).

(9) Removed airconditioning system to save weight.

(10) Modified forward elevator boost actuator to improve stability.

(11) Installed steel throttle levers.

(12) Reworked aileron droop mechanism to eliminate free play and stiffen mechanism.

(13) Stiffened the aileron control system.

(14) Stiffened the main landing gear structure.

(15) Increased roll boost actuator output force.

(16) Modified nose gear emergency extension system.

(17) Incorporated modifications to provide retractable landing gear.

(18) Improved the electrical nacelle tilt system.

(19) Increased aileron travel.

(20) Installed electronic S.A.S. system.

(21) Installed propellers on forward nacelles (All runs subsequent to Run No. 246 had all four propellers installed).

(22) Installed propeller pitch control trimmers (for lateral torque balance).

(23) Incorporated variable stick force gradient system.

(24) Incorporated anti-surge tanks within the forward fuselage fuel tanks.

(25) Incorporated height control system.

(26) Prior to Run No. 254, replumbed the fuel system back to the normal two tank operation (both forward tanks feeding engines).

Prior to Ground Runs Nos. 263 - 265

(1) Aircraft was partially disassembled to truck it to Atlantic City, New Jersey, and then reassembled.

(2) Removed the instrumentation photo recorder.

(3) Increased the pilot's stick breakout forces to approximately 1.5 pounds in pitch and roll.

Prior to Ground Runs Nos. 266 - 267 - None

Prior to Ground Runs No. 268 - 2o9

(1) Removed the main gear doors.

c. Configuration at Flight No. 50.

At the conclusion of the flight tests, Flight No. 50, the configuration was as defined below:

A. X-19 Serial No. 62-12197 built to Drawing No. 200-000001.

B. Plus all VTOL Systems Division ECNs through 8546 which are applicable to X-19 Serial No. 62-12197.

C. Plus all Curtiss Division ECNs through 32185 which are applicable to X-19 Serial No. 62-12197.

D. Minus the VTOL Systems Division Quality Department's listing of "Open ECNs on X-19 Serial No. 62-12197 as of August 24, 1965."

E. Minus all Curtiss Division ECNs and VTOL System Division mechanical systems ECNs applicable to X-19 Serial No. 62-12197 which were still unaccomplished at August 24, 1965.

F. Plus the changes prior to Ground Run or Flight listed in Ground Run Reports Nos 268 and 269, and Flight Report No. 50.

G. Plus the changes, other than ECNs, listed in Ground Run Reports through No. 269 and Flight Reports through No. 50.

d. Flight Test Instrumentation Through Flight No. 37.

Flight test instrumentation carried on the airplane throughout the tests comprised one 50 channel CEC Type 5-119P3-50 oscillograph. Between Flights Nos. 23 and 36 a photo panel was carried. Parameters recorded were generally in accord with the instrumentation called out in the specifications. Typical instrumentation parameters recorded on the oscillograph are shown in Table XIX. The breakdown of the multiplexed temperature parameters which were recorded on one oscillograph channel is shown in Table XX. The photo panel was used to record the parameters listed in Table XXI

e. Flight Test Instrumentation at NAFEC

The majority of flights made at NAFEC were covered by the phototheodolite tracking system which is a local F.A.A. facility. From this system a readout was available of instantaneous airplane position and velocity components. In addition, a 35 mm movie

Table XIX. Typical multiplexed temperature record schedule.

X-19 S/N 62-12197

Curtiss-Wright Corporation
VTOL Systems Division

X-19 Serial Number 62-12197 Test Instrumentation: Parameter Locations
Oscillograph S/N 24027-Ch. #5 Temp. Recorder S/N #1 Lite Weight

Temperature Schedule #10

Position No.	Parameter	
1	No. 1 Nacelle Oil Temperature	T-41
2	No. 2 Nacelle Oil Temperature	T-42
3	No. 3 Nacelle Oil Temperature	T-43
4	No. 4 Nacelle Oil Temperature	T-44
5	Fwd. Tee Box Oil Temperature	T-45
6	Aft Tee Box Oil Temperature	T-46
7	No. 1 ECGB Oil Temperature	T-47
8	No. 2 ECGB Oil Temperature	T-48
9	Accessory Drive Gear Box	T-12
10	Engine No. 1 Fuel Temperature	T-55
11	Primary Hydraulic System "Hot Spot"	T-14
12	Secondary Hyd. System Temperature	T-57
13	Engine No. 2 Fuel Temperature	T-56
14	No. 1 Longitudinal Shaft Bearing	T-9
15	No. 2 Longitudinal Shaft Bearing	T-10
16	No. 3 Longitudinal Shaft Bearing	T-11
17	Fwd. Right Transverse Shaft Bearing	T-5
18	Fwd. Left Transverse Shaft Bearing	T-6
19		
20	Aft Right Transverse Shaft Bearing	T-7
21	Aft Left Travaverse Shaft Bearing	T-8
22	Front Wing Carry Over Structure	T-17
23	Engine Bay Shear Plate	T-18
24	Sta. 434 Outside Frame	T-19
25	Sta. 434 Inside Frame	T-20

Position No.	Parameter		Gnd. Test No.	Flt. Test No.	Date
26	Sta. 434 Vertical Strut	T-21			
27	Sta. 462 Frame Top, Center	T-22			
28	Sta. 462 Horizontal Strut	T-23			
29	Sta. 480 Top Of Frame	T-24			
30	Sta. 480 Outside, Low, Frame Flange	T-26			
31	Sta. 480 Inside Top Of Frame	T-25			
32	Sta. 480 Low, Inside Frame Flange	T-27			
33	Sta. 493.5 Inside Top Of Frame	T-28			
34	Sta. 493.5 Inside, Low, Frame Flange	T-29			
35	L. H. Eng. Front Comp. Hsg., Amb.	T-30			
36	L. H. Eng. Front Burner Chamb., Amb.	T-31			
37	L. H. Eng. Rear Burner Chamb., Amb.	T-32			
38	L. H. Eng. Exhaust Duct, Ambient	T-33			
39	R. H. Eng. Front Comp. Hsg., Amb.	T-36			
40	R. H. Eng. Front Burner Chamb., Amb.	T-37			
41	R. H. Eng. Rear Burner Chamb., Amb.	T-38			
42	R. H. Eng. Exhaust Duct Amb.	T-39			
43	Rear Tee Box Ambient Air	T-34			
44	Gen. No. 1 Inbd. Temperature	T-58			
45	Gen. No. 2 Outbd. Temperature	T-59			
46					
47					
48					
49					
50					

Table XX. Typical test instrumentation oscillograph schedule.

OSCILLOGRAPH S/N 2w027 SCHEDULE NO 18 DATE Rev 8/2/66

CK NO.	PARAMETER	Nominal TRACE ALL SENSITIVITY	TRANSDUCER S/N	TRACE SENSE	GALVO TYPE	REFERENCE (ELECTRICAL) TRACE POSITION
1	Collective Pitch	9° (Large)		Inc β (+)	7-315	Min β
2	No. 2 Prop Blade Angle (Actual)	3°		Inc β (+)	7-315	Big Position
3	Voltage Cal 7.5V Zener	5 volts		Inc V (+)	7-315	7.5 volts
4	S.G. No. 1 Prop Blade 1	15,200 psi			7-318	Static
5	A/C Temperatures (See Temp Sched No. 10)	32° F		Inc Temp (+)	7-315	32°F
6	No. 1 Prop Blade Angle	9° (.47" prt)		Inc β (+)	7-341	Big Position
7	Pitch Trim Post 1	60%		Inc β fwd prop (+)	7-315	Mid Stroke
8	S.G. No. 2 Prop 1 Blade 1	2,400 psi			7-318	Static
9	No. 2 Prop Blade Angle	1° (.47" prt)		Inc β (+)	7-341	Big Position
10	Vertical G Acceleration	1.13 G		up accel (+)	7-349	Static
11	S.G. No. 3 Prop 1 Blade 1	2500 psi			7-318	Static
12	No. 3 Prop Blade Angle	11° (.47" prt)		Inc β (+)	7-341	Big Position
13	S.G. No. 4 Prop 1 Blade 1	2400 psi			7-319	Static
14	SAS Position - Roll	3°		rt coll (+)	7-349	Big Position
15	No. 4 Prop Blade Angle	.7° (.47" prt)		Inc β (+)	7-341	Big Position
16	S.G. No. 5 Prop 2, Blade 1	15,200 psi			7-318	Static
17	Control Position - Roll	50%		right (+)	7-318	Control Centered
18	Control Position - Pitch	50%		stick fwd (+)	7-318	Control Centered
19	Control Position - Yaw	50%		rt pedal (+)	7-318	Control Centered
20	SAS Position - Pitch	3°		nose up (+)	7-315	Big Position
21	Elevator Position (L H)	20°		nose up (+)	7-315	Control Centered
22	S.G. No. 6 Prop 2, Blade 1	2500 psi			7-318	Static
23	Primary Hyd. Sys. Press.	1400 psi	21023	Inc P (+)	7-315	No Pressure
24	****** NOTE SENSITIVITIES ARE GIVEN IN TERMS OF					
25	****** UNIT GALVO DEFLECTION					
26	A/C Attitude - Roll	9°		rt turn (+)	7-349	A/C Level
27	A/C Angular Accel Roll	2.43 rad/sec^2	43	rt accel (+)	7-349	Static
28	A/C Attitude - Pitch	9°		nose up (+)	7-349	A/C Level
29	A/C angular Accel-Pitch	2.43 rad/sec^2	47	nose up accel (+)	7-349	Static
30	A/C Attitude - Yaw	73°		Rt Yaw (+)	7-315	Gyro Mid-range
31	No. 1 Trans Shaft Torque	10,000" LB		Inc. tor (-)	7-347	No Load
32	No. 2 Prop Coord Output Force	17,72 LB		Inc force inc (+)	7-315	Controls Centered
33	No. 2 Trans Shaft Torque	10,000" LB		Inc tor (-)	7-347	No Load
34	No. 2 Prop Coord Output Position	9°		Inc. β (+)	7-315	Controls Centered
35	No. 3 Trans Shaft Torque	10,000" LB		Inc tor (-)	7-347	No Load
36	No. 4 Prop Coord Output Force	16.90 LB		Inc force inc (+)	7-315	Controls Centered
37	No. 4 Trans Shaft Torque	10,000" LB		Inc tor (-)	7-347	No Load
38	No. 4 Prop Coord Output Position	9°		Inc β (+)	7-315	Controls Centered
39	Throttle Pos Eng No. 1	20°		Inc power (+)	7-315	Closed
40	Throttle Pos Eng No. 2	20°		Inc power (+)	7-315	Closed
41	N_1 RPM - Eng No. 1	10% (above 50%)		Inc RPM (+)	7-349	Static
42	No. 1 Nacelle Angle	22°		Inc α (+)	7-315	Hover Position
43	S.G. No. 7 Prop 2 Blade 1	2500 psi			7-318	Static
44	S.G. No. 8 Prop 2 Blade 1	1200 psi			7-319	Static
45	Governor Position	100%		Inc RPM (+)	7-315	Big Position
46	Prop No. 2 Phase Marker			Mark (-)	7-315	Static
47	Pitch Pip and L.O. Signal			Pip (+) L.O. ( )	7-318	Static A/C on ground
48	L.H. Aileron Position	20°		rt roll (+)	7-315	Hover Position
49	N_2 RPM - Eng No. 2	10% (above 5 %)		Inc RPM ( )	7-349	Static
50	Sec Hyd Sys Pressure	650 psi	1409	Inc P (+)	7-315	No Pressure

Ref Nacelle Tilt Switch Dec α (+) Static

** OSC CH NUMBERING GALVO INSTALLED IN CHANNELS 24 and 25 1/3 Oct 8.77

▲ DENOTES CHANGES FROM PREVIOUS SCHEDULE CHANGES PRIOR TO FLT FLIGHT NO

Table XXI. Typical X-19 S/N 62-12197 photo panel parameter schedule.

Layout No. 1 Date 9/15/64

Run No. 168 thru 174 Flight No. -

Hole No.	Description
1	No. 1 & No. 2 Nacelle Oil Pressure Indicator
2	No. 3 & No. 4 Nacelle Oil Pressure Indicator
3	No. 1 & No. 2 Location ECGB Pressure Indicator
4	Fwd. & Aft T-Box Oil Pressure Indicator
5	
6	
7	
8	APU Oil Pressure (Prior To Run 175)
9	Airspeed Low Range
10	Airspeed Standard
11	Altimeter
12	R/C Indicator
13	Fuel System Diff. Pressure
14	
15	
16	OAT Indicator
17	Camera Frame & Footage Counter
18	Flight Card
19	8 Day Clock & Stop Watch
20	Alighting Gear Lift-Off Lights
21	
22	
23	N_1 Tach. Indic. L. H. Eng.
24	N_2 Tach. Indic. L. H. Eng.
25	Torque L. H. Eng.
26	Fuel Flow L. H. Eng.
27	EGT L. H. Eng.
28	Fuel Pressure L. H. Eng.
29	
30	N_1 Tach. Indic. R. H. Eng.
31	N_2 Tach. Indic. R. H. Eng.
32	Torque R. H. Eng.
33	Fuel Flow R. H. Eng.
34	EGT R. H. Eng.
35	Fuel Pressure R. H. Eng.

film was taken through each of three tracking cameras, at five frames per second.

4. AIRCRAFT PERFORMANCE RESULTS USING STEADY STATE DATA

a. Overall Airplane Performance From Flight Tests

Overall airplane performance test data were derived from selected flights throughout the flight capability demonstrations. The aircraft was operated at weights ranging from 11500 lb. through 13000 lb. with the center of gravity between 40.8% and 44.1% of the aerodynamic chord. Most flight conditions suitable for use as performance data points were held for such short periods that the accuracy of derived data was poorer than would have been achieved by specific performance tests. These were scheduled for later sections of the Flight Test Program. Predicted overall aircraft performance was extensively documented in the X-19 Aerodynamic Performance Summary Report, (reference 99).

b. Hovering Performance

Hovering performance was found to substantiate data previously recorded during tiedown tests. Limited hovering at various heights in ground effect supported predictions of a favorable ground effect. However, operation within ground effect had unfavorable effects on airplane controlability.

c. Conversion/Reconversion Flight Maneuvers

Conversion/reconversion flight maneuvers have been analyzed to assess the variation of airplane performance with forward speed. These data have been presented as transient and steady powers required versus airspeed and may be compared with design estimates.

d. Power Required

In general there is good agreement with power estimates at low airspeeds when operating near the theoretical nacelle tilt-airspeed schedule, but as airspeed was increased above 50 kts. the power required tended to be less than estimated, by some 25% at 80 kts.

The split in total power between front and rear nacelles agrees with the estimates up to 5 knots, above which the front propellers require significantly less power than estimated, although the rear propellers data agree closely with estimates.

Analysis of X-19 Power Required based on Category 1 flight rest results was made. From this a useful prediction method is shown for determining: (1) total power required versus velocity, and (2) front and rear propeller power required versus velocity.

The data analyzed herein were obtained during Category 1 flight testing of X-19 S/N 12197 and covered the range of steady level flight speeds given in Figure 320. The accuracy of the basic flight test data is estimated as:

$$BHP = \pm\ 3\%$$

$$V_e = \pm\ 3\%$$

$$W_t = \pm\ 0.8\%$$

The Method of Analysis emplved is as follows:
The basic flight test data were in the form of transverse drive shaft torque for a variety of aircraft weights, ambient temperatures, ambient pressures, indicated airspeeds and propeller rotational speeds. It was desired to reduce these variable to normalized parameters for a clear and concise presentation of power required versus airspeed. That is, it was desired to produce a single curve that represents power required versus velocity at all weights, all altitudes and all temperatures.

The adopted approach to analysis was that of PIW-VIW format, where the indicated power and indicated airspeed parameter were defined as follows:

$$PIW = \frac{\sqrt{\sigma}\ BHP}{(W_t / W_s)^{1.5}},\ \text{horsepower}$$

$$VIW = \frac{V_e}{\sqrt{(W_t / W_s)}},\quad \text{knots}$$

Once the PIW versus VIW plot is determined for a specific airplane, the BHP vs. TAS plot for any weight, temperature or altitude may be found. Such a plot, however, applies only to subsonic speeds where the total drag is the sum of parasite and induced drag.

The following nomenclature is used within this paragraph:

Symbols

BHP	brake horsepower
L.C.	lift chord (= 274 in.), distance between front and rear tilt axis along a fuselage water line.
TAS	true airspeed, knots
V_e	equivalent airspeed, knots
W	airplane weight, pounds
σ	relative air density ratio
ϕ_p	front propeller tilt angle, degrees

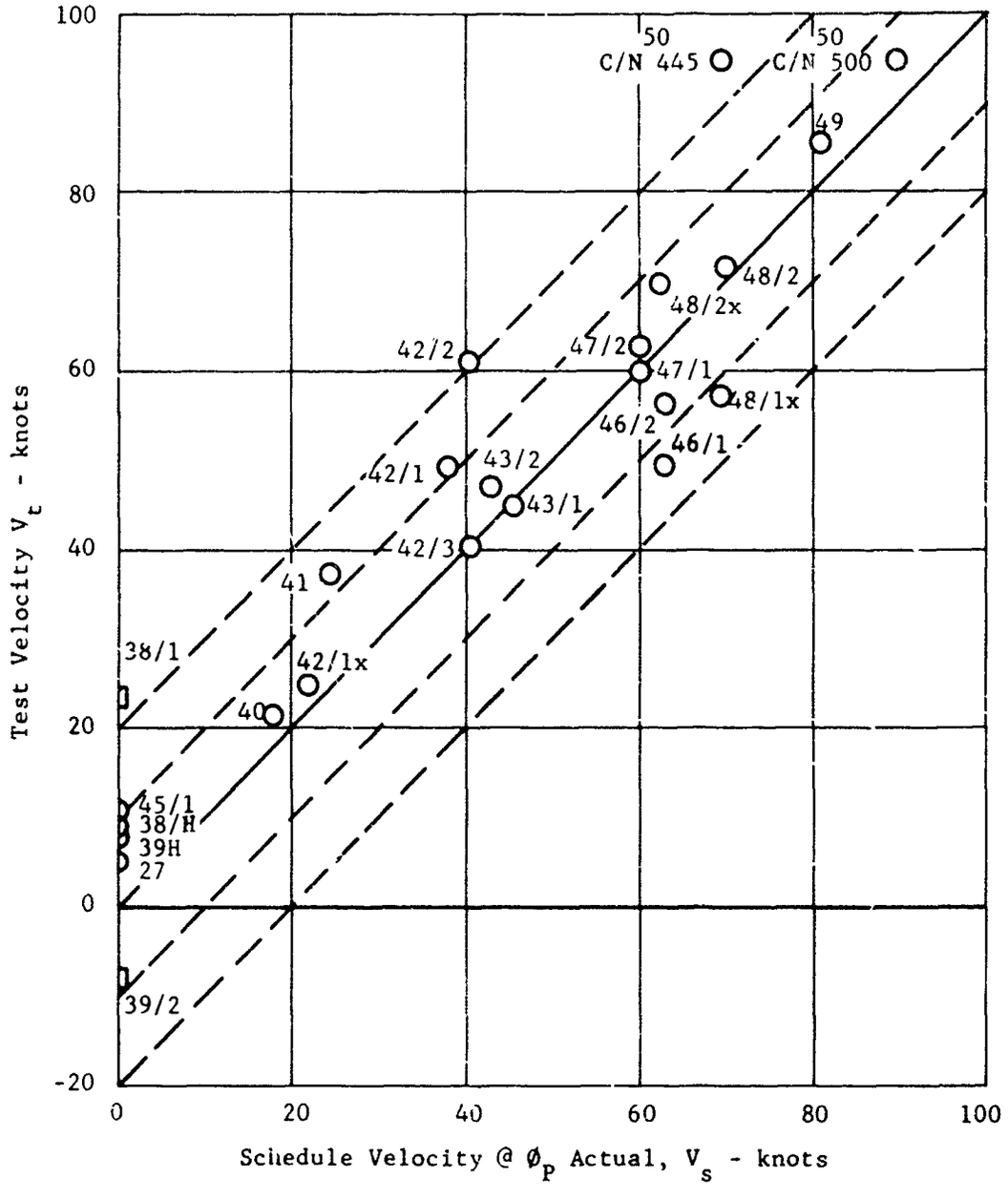

Figure 320. X-19, flight speed range tested for steady level flight, test velocity vs scheduled velocity.

Subscripts

N	at propeller nacelles, total
N_F	at a front propeller nacelle
N_R	at a rear propeller nacelle
S	standard, and schedule
t	test value

The interested reader is referred to AFFTC-TN-60-28 for a detailed derivation of the PIW-VIW theory.

The results of this analysis are shown plotted in Figures 321, 322, and 323 which give the variation with velocity of total propeller nacelle input power, front propeller nacelle input power and rear propeller nacelle input power, respectively. As noted, these plots are for a "standard" weight of 13,660 pounds, and cover a velocity range from zero to approximately 95 knots.

Inasmuch as total power required varies only slightly with c.g. location, within the permissible c.g. range of the X-19, Figure 321 can be applied to all c.g. locations. Front and rear propeller power requirements, however, are very largely dependent on longitudinal c.g. location. As noted on Figures 322 and 323, individual propeller powers are presented at only the 41.5% L.C. c.g. location.

For identification, all test points plotted are designated by listing the flight number followed by a slash and the run number.

(1) Total Power Required

Examination of Figure 321 shows that excellent correlation exists among the test results. Nearly all points for which the test airspeed was within six knots of that scheduled for the particular propeller tilt angle employed fall within $\pm$ 5% band of the curve shown. This is considered very satisfactory in view of the magnitude of the flight test data accuracy.

Test points such as 42/1, 42/2, and 50 C/N 445 fall substantially above the curve generated. This is expected and predictable inasmuch as they are approximately 10, 20 and 25 knots respectively, above the scheduled airspeed for the propeller tilt angles flown.

Also spotted on Figure 321 are the flight performance predictions based on propeller static thrust (whirl) tests obtained at both Wright Field and Curtiss-Wright VTOL Systems Division and from wind tunnel model test results at the scheduled 49 and 85 knot configurations.

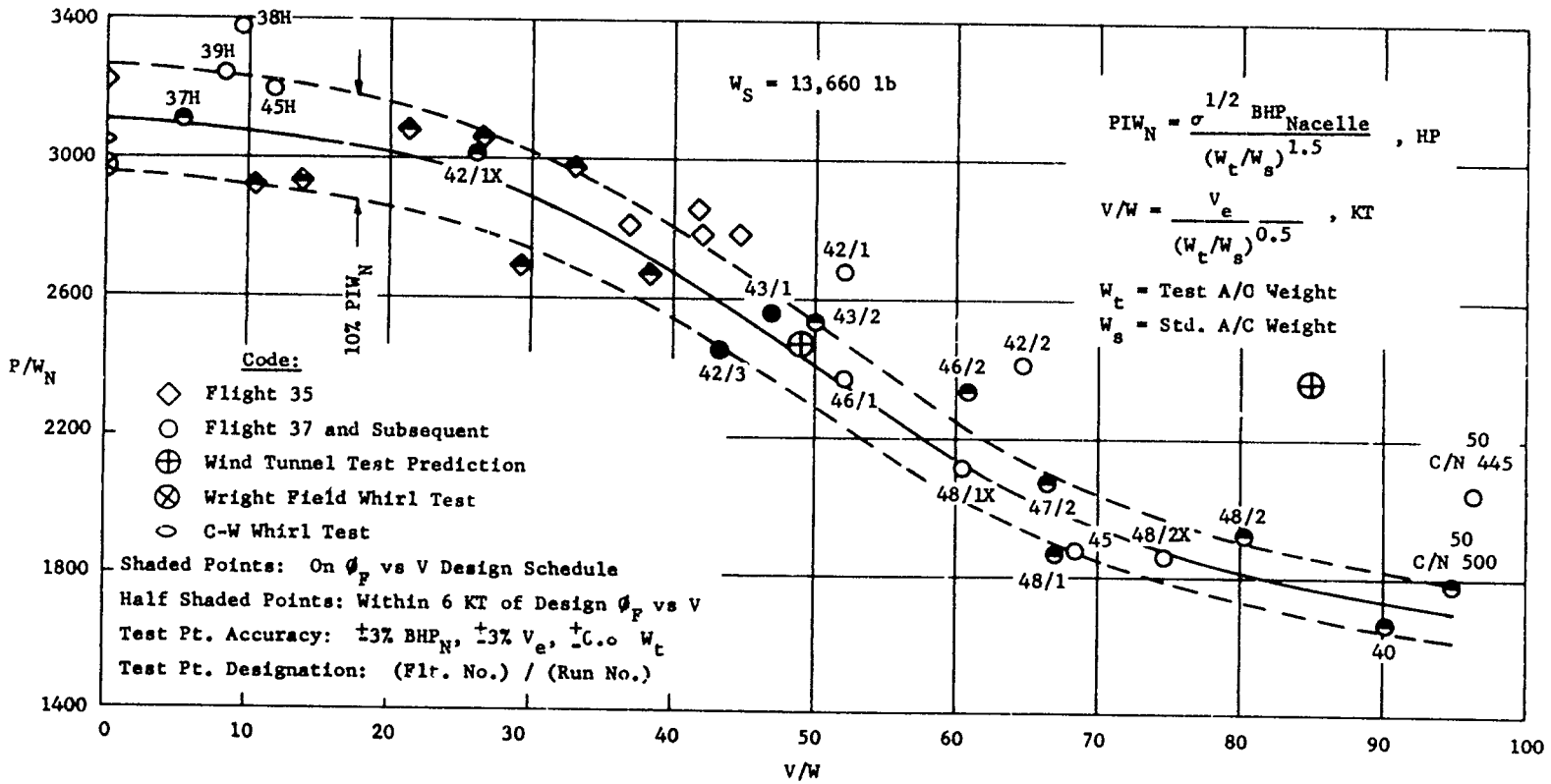

Fixture 321. X-19 test power required for steady level flight, PIW_N vs VIW.

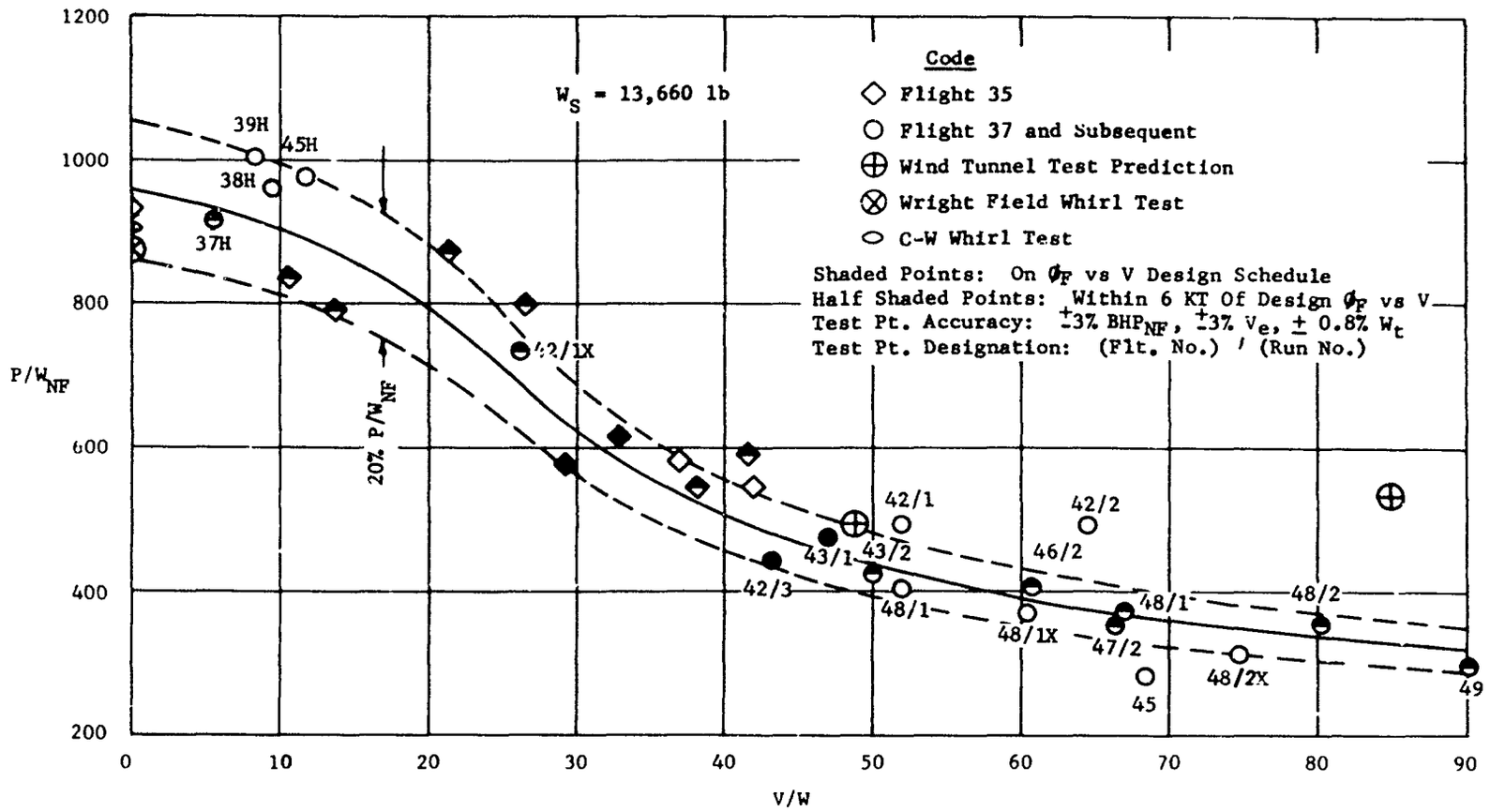

Figure 322. X-19, test front nacelle power required for steady level flight, PIW_{NF} vs VIW.

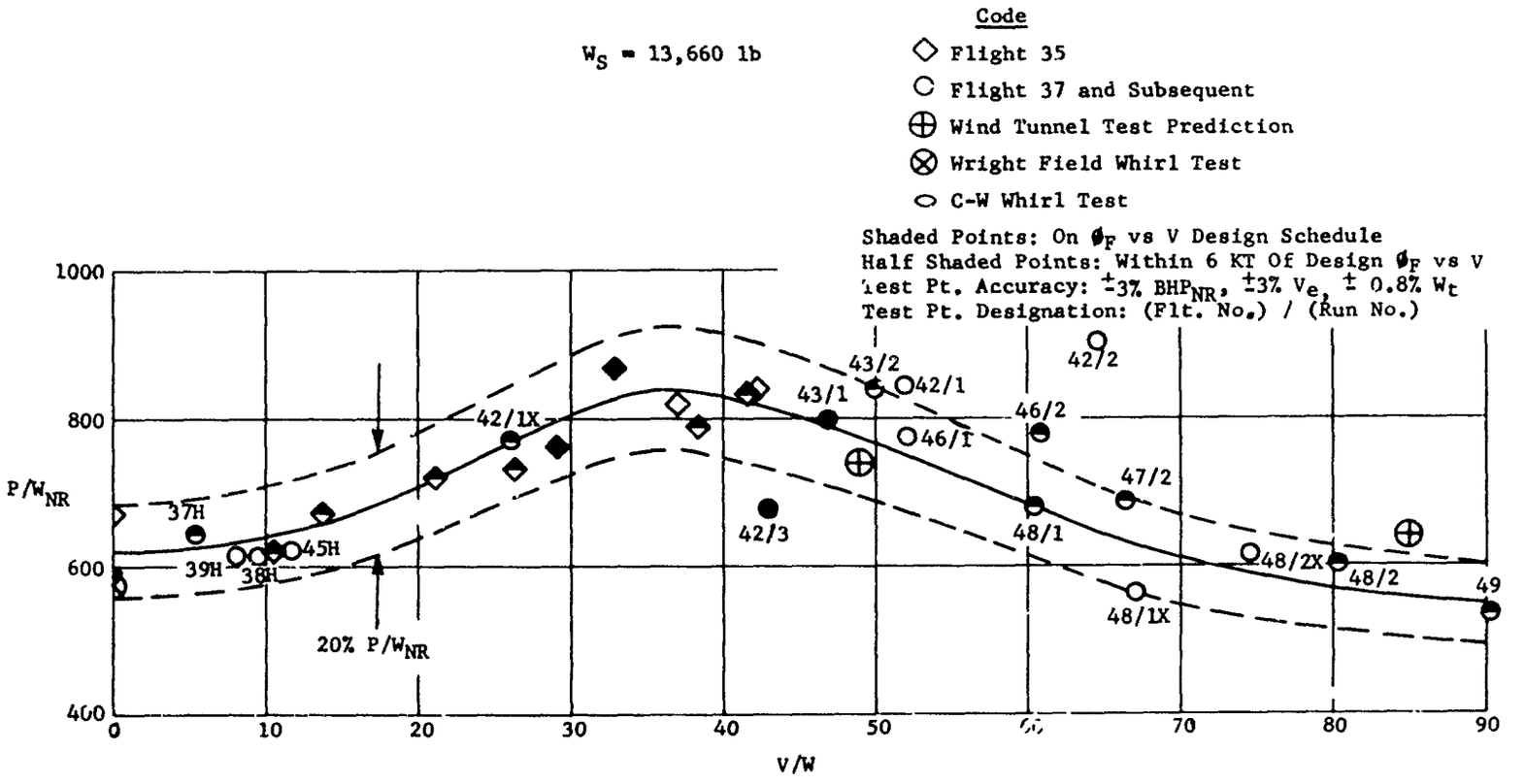

Figure 323. X-19, test rear nacelle power required for steady level flight, PIW_{NR} vs VIW.

As can be noted, the power required at hover is within 2% of the prediction based on Curtiss-Wright testing, a value within the range of flight test data accuracy. Wright Field data have always been thought to have a 1-2% blockage effect, which again seems borne out by this analysis.

The wind tunnel results show excellent agreement with flight test at 49 knots, but are poor agreement at 85 knots, indicating too great a total power required by some 33% over that measured by flight test results.

The disagreement between predictions and flight test at 85 knots is perhaps attributable to low Reynolds Number scale effects causing the model testing to to yield lower performance.

(2) Front Nacelle Power Required

Discussion with regard to the resulting front nacelle input power required shown in Figure 322 is essentially identical with that expressed regarding the total power required, Figure 321. It should be noted however, the envelope of correlation for test points within six knots of schedule speed has expanded to $\pm$ 10% rather than the $\pm$5% in the case of total power. This will also be noted when examining the rear nacelle powers of Figure 323.
This situation exists because flight is never completely smooth and free from atmospheric turbulence, causing the aircraft's stability augmentation system (SAS) to feed attitude control signals to the propeller. This is accomplished by varying propeller blade angle, thereby altering the power absorption of the individual propellers. It is felt that this SAS activity is the cause of the expanded correlation envelope.

e. Thrust - Power Download

Thrust data, obtained with the aircraft on the force measuring rig, does not isolate the contributions of wing download due to propeller slipstream impingement from the ground proximity effect. In order to reduce the recorded values to coefficient form and compare them with estimated data, it was assumed that the ground effect cancels the download and the recorded lift data is actually pure thrust data.

The incorporation of this assumption is based on the fact that, at the particular height of the aircraft on the force measuring rig, 3 feet, the estimated ground effect is approximately equal to the download, 11.5% ground effect, 8.8% download.

Figure 324 shows the results of ground run No. 96 reduced under the above assumption. The solid line is the isolated propeller performance predicted by Wright Field whirl test data. The front propeller thrust vs. power performance is seen to agree fairly well with the whirl test data while the rear propellers exhibit extensive scatter. The converse is true for the blade angle power relationship; that is, considerable scatter on the front propellers and good agreement is obtained on the rear. In addition, propeller No. 1 appears to be operating about 3 degrees below the expected value of blade angle.

This apparent contradiction, agreement between thrust and power and discrepancies between blade angle and power, or vice versa, indicates discrepancies due to instrumentation error. They are not deviations from expected values.

Additional thrust power data has been obtained from Flights No. 8, 11, 12, 14, 16, 18, 19, 21 and 22. These flights consisted of either steady hovers or low speed translations. Figure 325 presents the recorded values of total thrust and total power obtained from these tests, reduced to coefficient form and compared with Wright Field data. In determining the thrust coefficient the average download factor of 8.8% was applied. Since torque is measured at the transverse shafts, a 1.5% nacelle gearbox loss was accounted for in the power coefficient. Ground effect correction is not needed in Figure 325, since all test points were taken with the aircraft essentially out of its influence.

During the later stages of Flight No. 50 severe power variations were imposed on the airplane. No test data were reclaimed from this section of the flight but estimates of the performance and structural significances are given in (95).

f. Ground Effect

During the initial ground running on the force measuring rig, an attempt was made to obtain a qualitative analysis of ground effect characteristics through the use of tufts, suspended on wires, below the aircraft. Figure 326 shows the general test arrangement.

Testing with the tufts in place was limited to a single run (the wires restricted operations around the rig) during which the following characteristics were observed:

(1) The point of interaction of the washes on the fuselage from the front and rear propellers appeared to depend on the total output power level. At low total output power there was no evidence of an interaction of the washes under the fuselage; but instead,

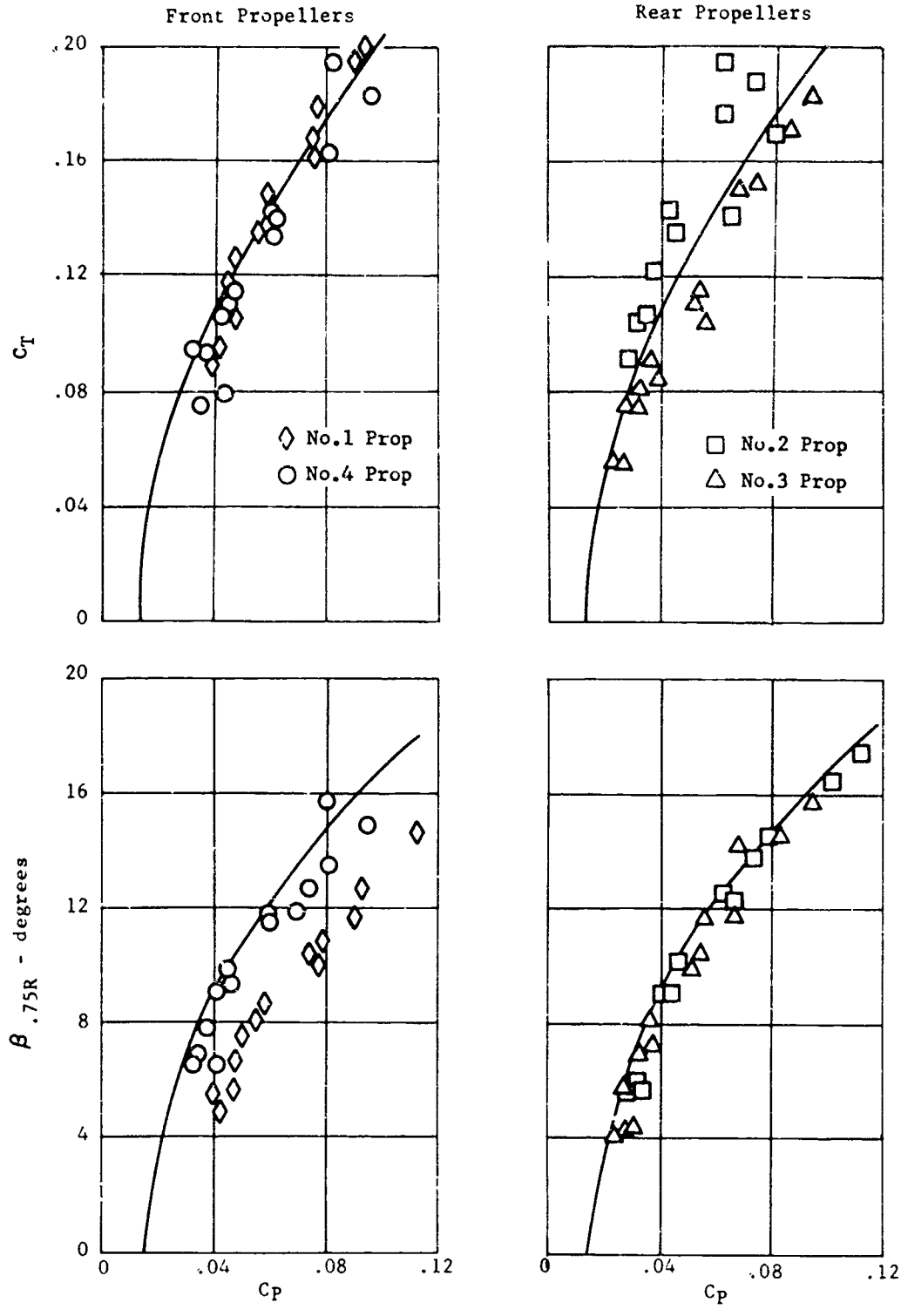

Figure 324. X-19, ground run number 96, thrust coefficient and blade angle vs power coefficient.

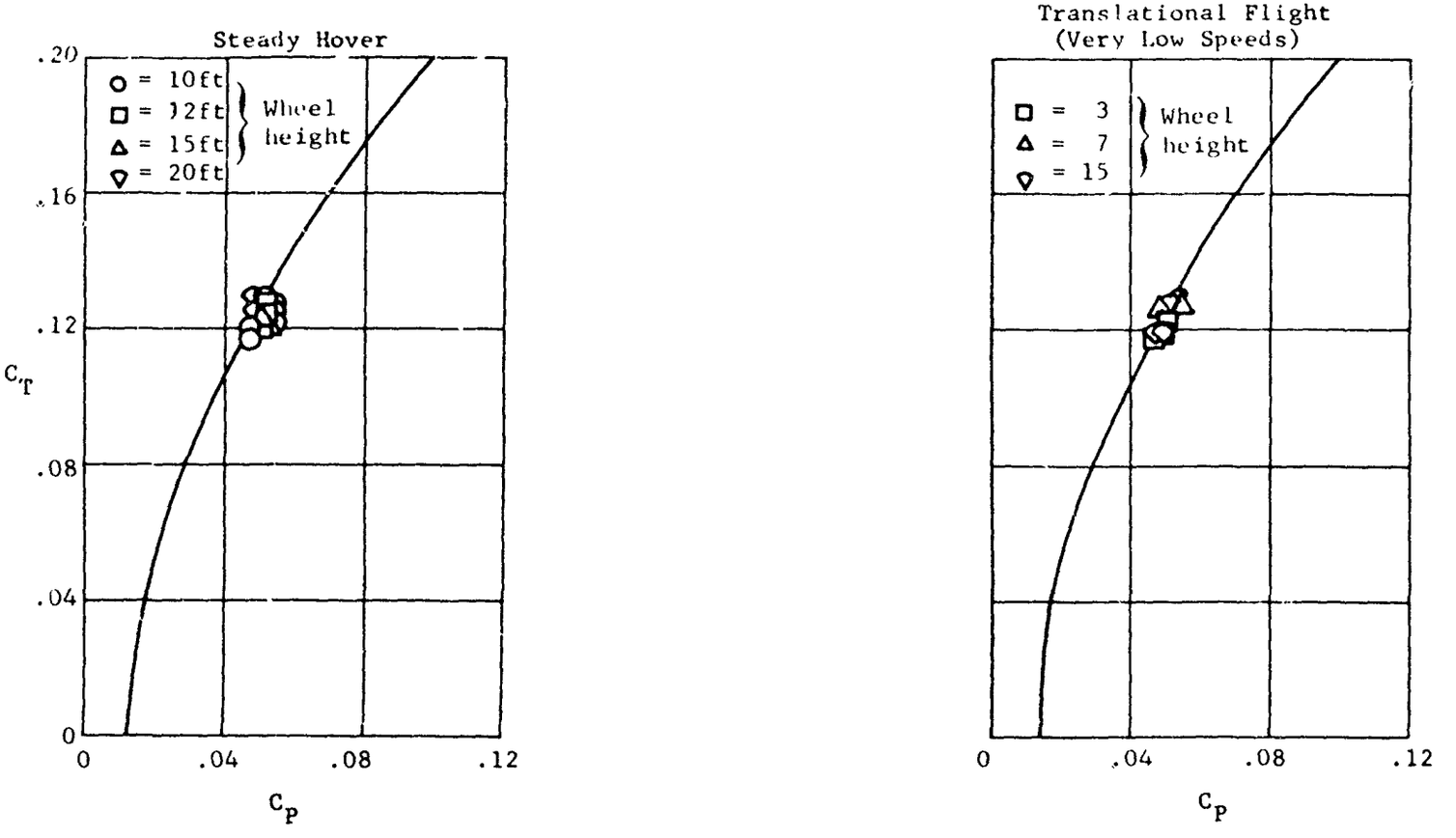

Figure 325. X-19, flight numbers 8 through 22, thrust coefficient vs power coefficient for steady hover and translational flight.

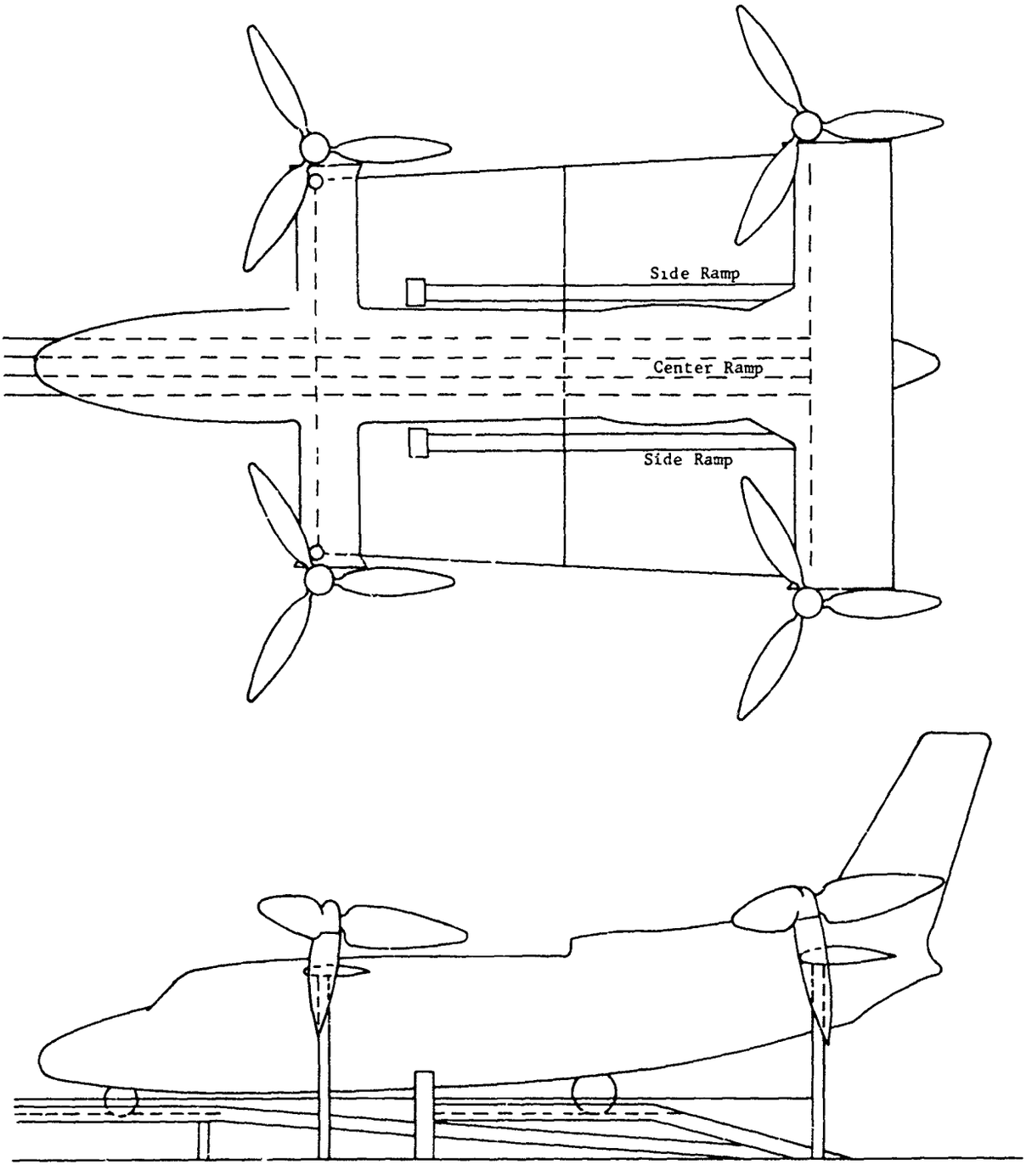

Figure 326. X-19, test installation for ground effect tuft study.

a general flow towards the rear was observed. As power was increased, the tufts located on the center transverse shifted position from one of pointing in an aft horizontal direction to pointing vertically upwards. Thus, the washes were now combining under the aircraft and giving rise to an upwash (fountain effect).

g. System Thrust Response to Power Excursions

One of the factors involved in the determination of the hover "avoid" regions is the system thrust decay and response characteristics following a single engine failure.

Ground Run No. 97 simulated an engine failure condition by chopping the throttle of one engine while operating at hover power. The other engine was either left unchanged or simultaneously accelerated to maximum power. Figure 327 shows the thrust transients obtained with the above procedure.

Working with the thrust transients of Figure 327 the vertical motion of the aircraft in an actual situation may be estimated. Figure 328 shows the vertical velocity vs. time that would result if the pilot reacted to the engine failure (maximum power on remaining engine), and if the pilot did not react (no change in throttle setting of remaining engine). Figure 329 is the altitude the aircraft would lose as a function of time. Figure 330 eliminates the time element and shows the vertical contact velocity as a function of the altitude at which the engine failure is assumed to have taken place.

The case most representative of an actual situation is that where the pilot responds to the failure and applies power on the remaining engine. Reference to Figure 330 shows that if the failure occurred at an altitude of 10 feet the aircraft would contact the ground with a velocity of 10 feet/second. This confirms the lower boundary of the hover avoid region which limited the aircraft to 10 feet of altitude.

h. Fuel Consumption

Engine fuel flow has not been monitored in flight testing to date.

An attempt was made to estimate fuel consumption by reading the fuel quantity gauges before and after a flight. The resulting calculated values of fuel consumption differed so widely as to be unusable and were disregarded.

Tests subsequent to Flight No. 22 have incorporated provisions for measuring fuel flow directly.

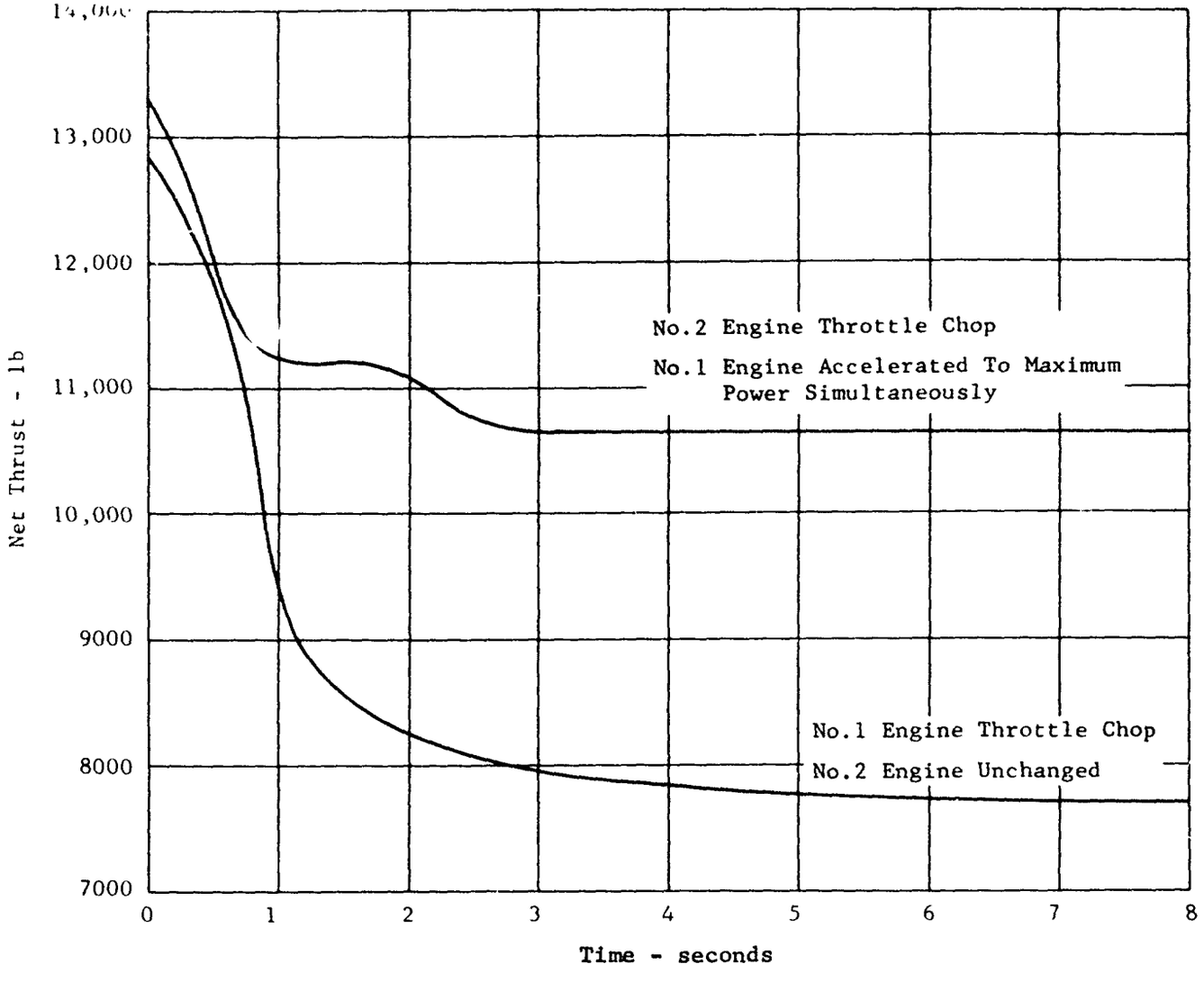

Figure 327. X-19, ground run number 97, thrust transient following throttle chop.

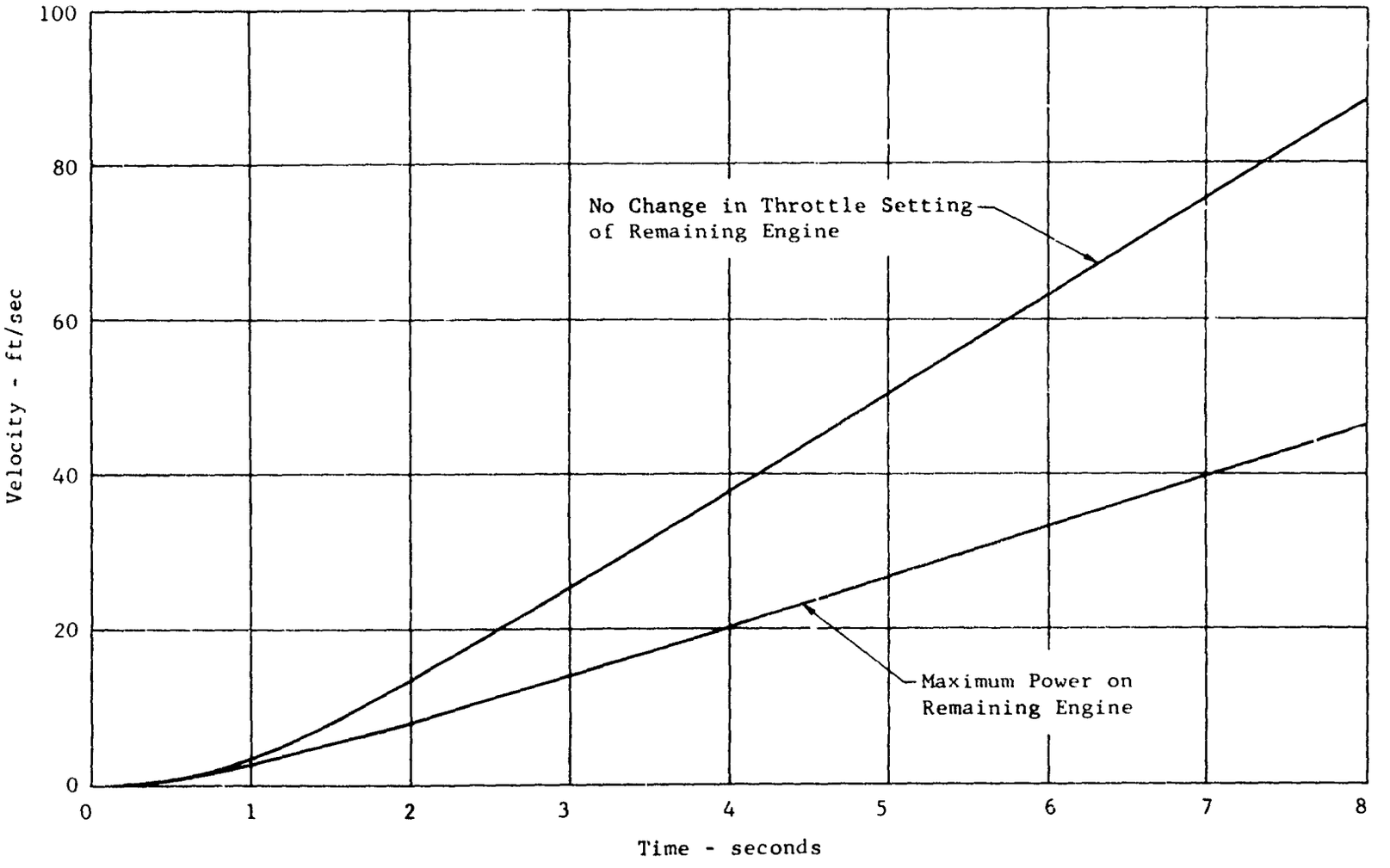

Figure 328. Estimated descent velocity vs time following a single engine failure in hover (based on X-19 ground run number 97).

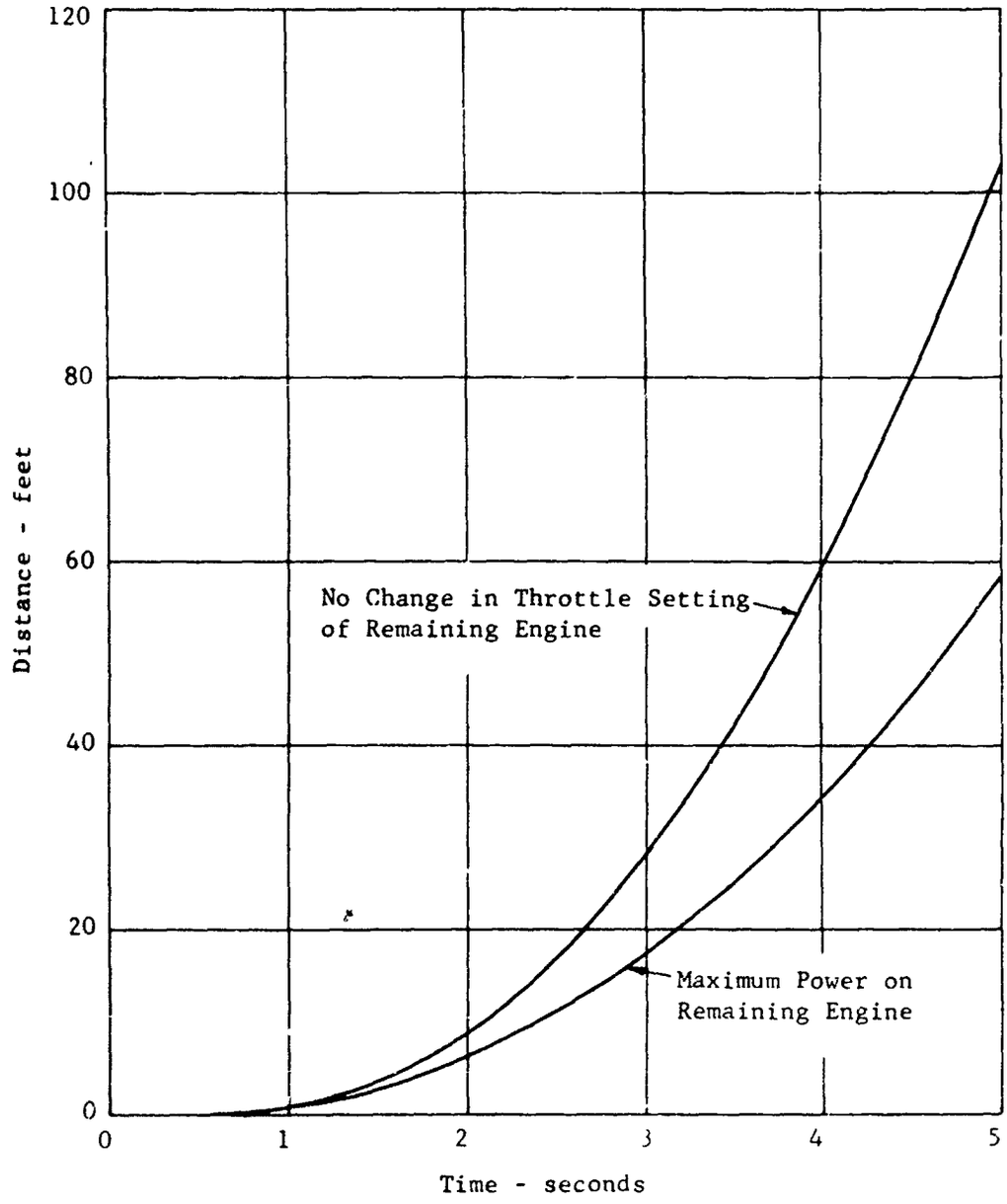

Figure 329. Estimated altitude lost vs time following a single engine failure in hover (based on X-19 ground run number 97).

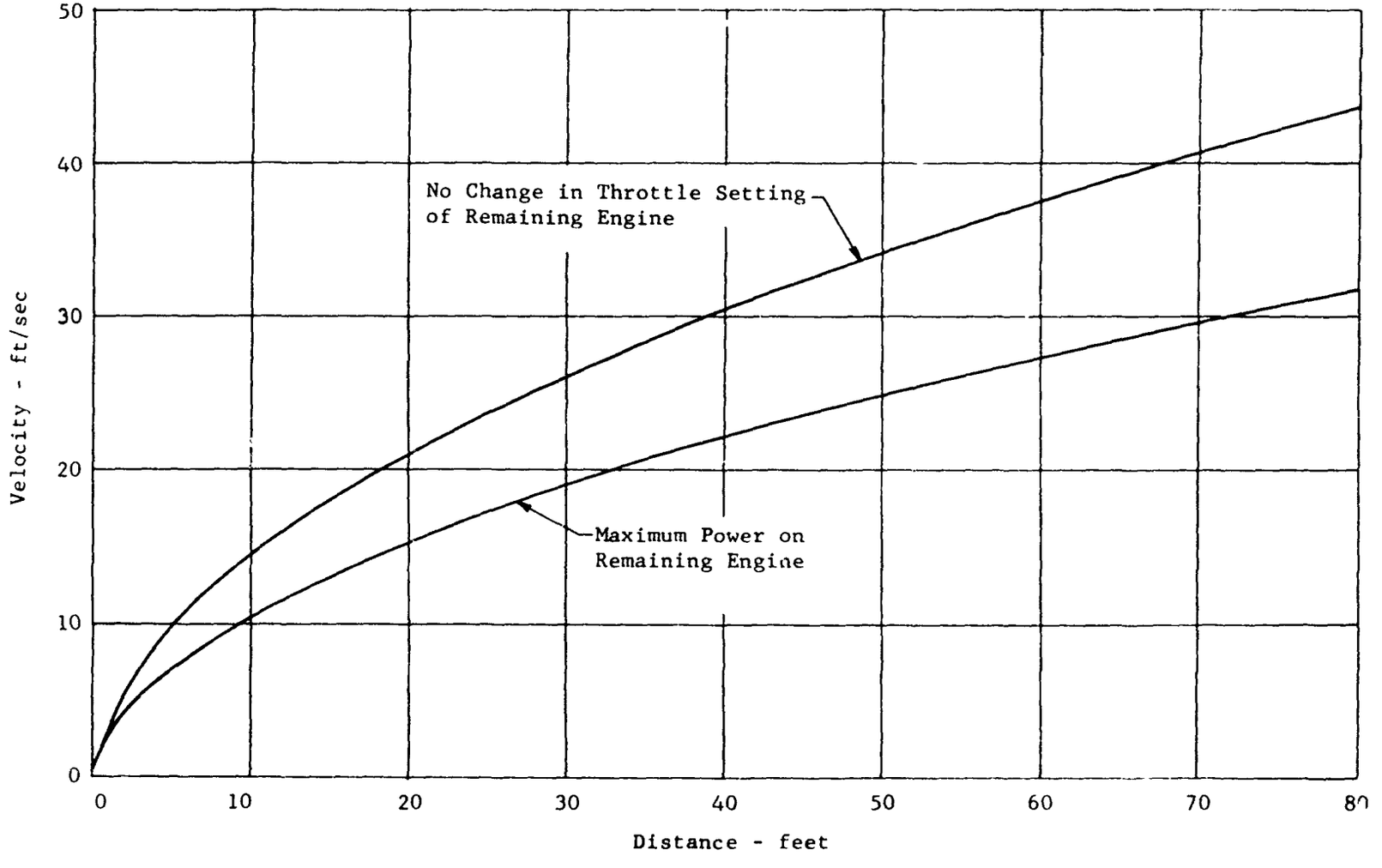

Figure 330. Estimated descent velocity vs altitude lost following a single engine failure in hover (based on X-19 ground run number 97).

5. AIRCRAFT STABILITY AND CONTROL

The flight test conducted with the X-19 airplane covered the speed range from hover to approximately 100 knots. In the lower speed range more data is available than at speeds above 70 knots as only four flights were made at speeds above 70 knots. Generally, the overall stability and control of the airplane was very nearly that predicted on the basis of the experience gained with the X-100 airplane, helicopters, and fixed base simulator tests.

a. Initial Hover Stability and Control Results

During the early hover tests, flights 1 to 22, no formal pilot opinion ratings were recorded. However in reviewing the pilot reports and records, it was apparent that considerable difficulty was experienced by the pilot in controlling the aircraft in hover. A large part of the problem was due to flying the machine without the SAS operating and therefore the necessary artificial damping. Initial tests were made close to the ground where the aircraft experiences mild and unpleasant upsetting moments which caused the pilot to lose confidence and produce large pilot induced oscillations which further complicated his problems. Due to this situation the initial flights were almost simultaneous takeoffs and landings without gaining much real knowledge on the behavior of the aircraft.

When the pilot gained enough confidence in the aircraft to fly at an altitude above five feet, satisfactory flights were accomplished. At this time it was determined that adequate control was available to fly the aircraft in hover without the necessity of the use of SAS. Control and flight characteristics were found to be adequate so that a good summary flight could be accomplished illustrating standard hovering maneuvers.

b. Pilot Opinion Rating

Starting with flight 23 formal pilot opinions were obtained using the Cooper rating system. This system is based on a numerical rating scale from 1 to 10. A rating of 1 is the optimum where 10 is catastrophic. The Cooper scale is given in Table XXII. In using the scale it was found that ratings within one half a point would be obtained which indicates that the system is repeatable and gives useful data. Therefore, the remainder of the stability and control and handling characteristics will be discussed in terms of Cooper ratings.

c. Flight Tests With S.A.S. Inoperative

With the S.A.S. inoperative the lack of rate damping inherent in the X-19 design made hovering a demanding pilot function, with Cooper Ratings of between 4 and $4\frac{1}{2}$.

High control activity introduced in opposition to aircraft motion resulted in oscillations in which adequate pilot control lead was difficult to establish. As a result pilot induced oscillations in pitch and roll were experienced until the pilot learned to minimize control activity.

Figure 331 illustrates the scope of Category 1 flight testing accomplished with the X-19. Results are for unaugmented stability. It can be noted that airborne conversion/reconversion flying has progressed to 42.5 knots, and taxi testing to 47 knots. In general, steady test conditions were established during taxi with a main landing gear reaction load of approximately 1000 lb. or less. This is significant in that runway surface undulations must have provided external disturbances about all three axes. During taxi the nose wheel was closely maintained at a height of six inches above the runway.

Figures 332 and 333 present pilot ratings (Copper Scale) about the longitudinal and lateral axes, respectively. It can be noted that a steady improvement in flying qualities is reported. The rating at hover was based on many tests. All other speeds have had at least two pilot ratings.

Extensive fixed-base flight simulation in the 0 to 85 knot speed band was conducted. These results are also plotted in Figures 332 and 333. For comparison, only the ratings of pilot J. V. Ryan are plotted in order to get a direct comparison with his flight test ratings. It can be noted that although the rate of improvement of handling qualities with speed is nearly the same from both sources, the fixed-base simulator ratings are poorer by about 4 Cooper points. This difference is obviously due to the simulator display (visual cues) and lack of motion cues. A hover rating of 4.0 was obtained on the NORAIR moving-base simulator; a substantiation of the aforementioned thesis for rating differences. Thus, the fixed-base simulator results should logically be adjusted to lower Cooper Scale levels, Table , as is done in Figure 332.

Of significance is the simulator rating at 49 knots As was stated earlier, wind tunnel test results formed the basis for simulation input data. Throughout the history of X-19 tunnel testing in transition configurations, unstable moment curves have been found at the 82.5 degree tilt angle, corresponding to a scheduled speed of 49 knots. For simulation purposes this stability derivative was employed. These derivatives stem almost exclusively from propeller forces and moments. In view of the satisfactory pilot ratings offered in actual flight for this configuation, at nearly the schedule speed, it appears that the simulator rating at 49 knots can be discarded, at least with the S.A.S. operating.

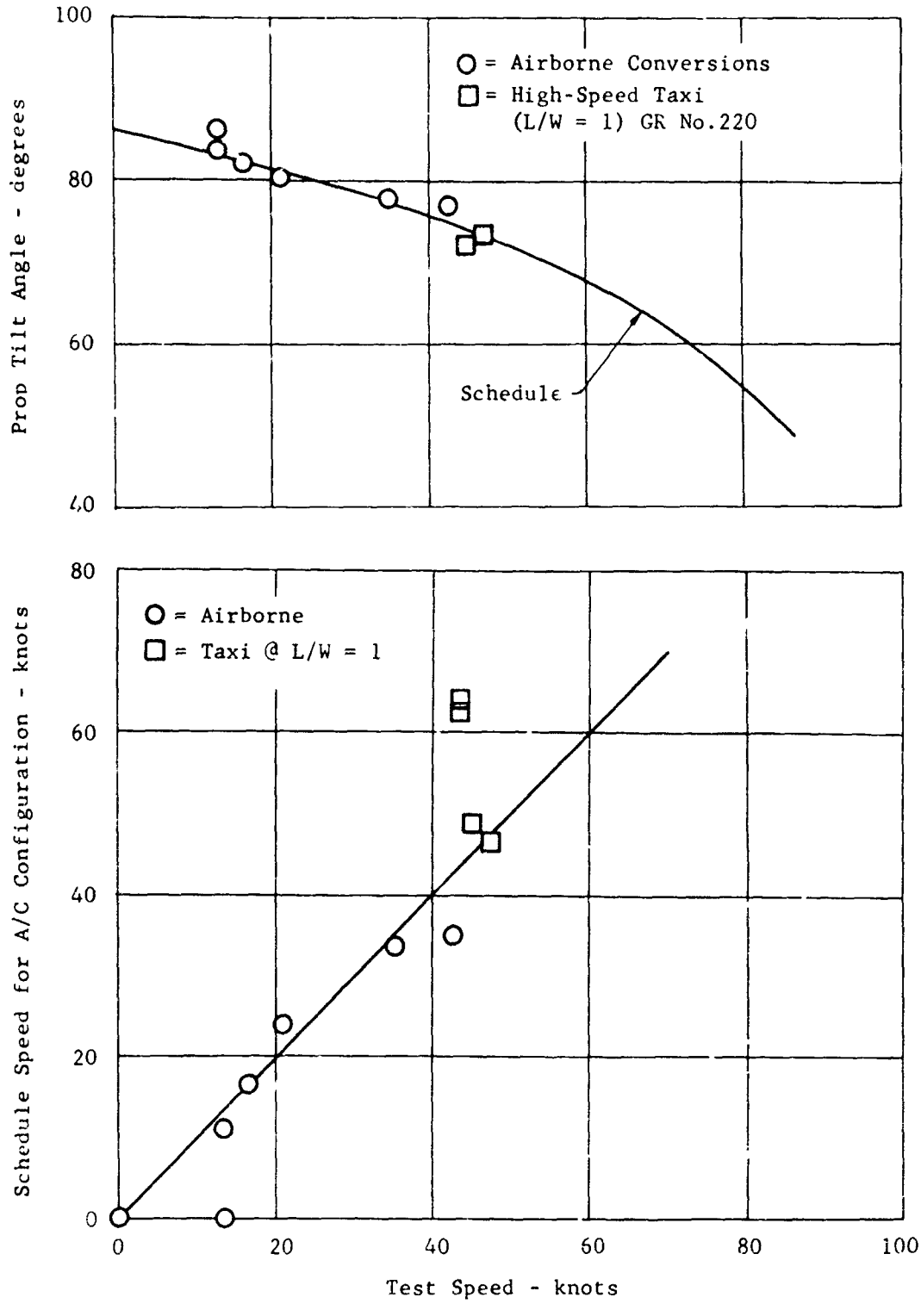

Figure 331. X-19, category I flight test program, scope of configuration testing through January 1965.

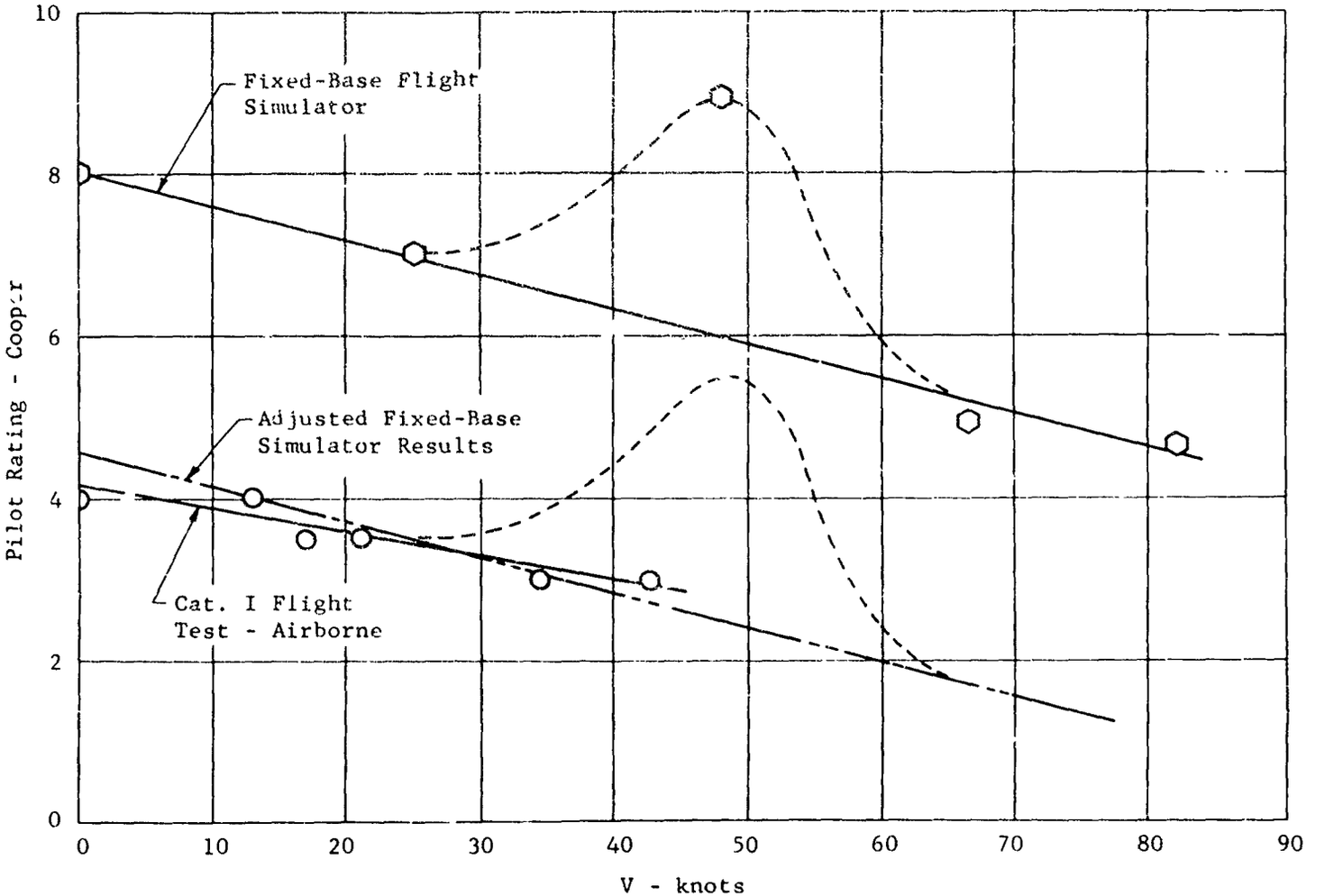

Figure 332. X-19, low speed longitudinal handling qualities, with S.A.S. "off" in both axes (Pilot: J.V. Ryan).

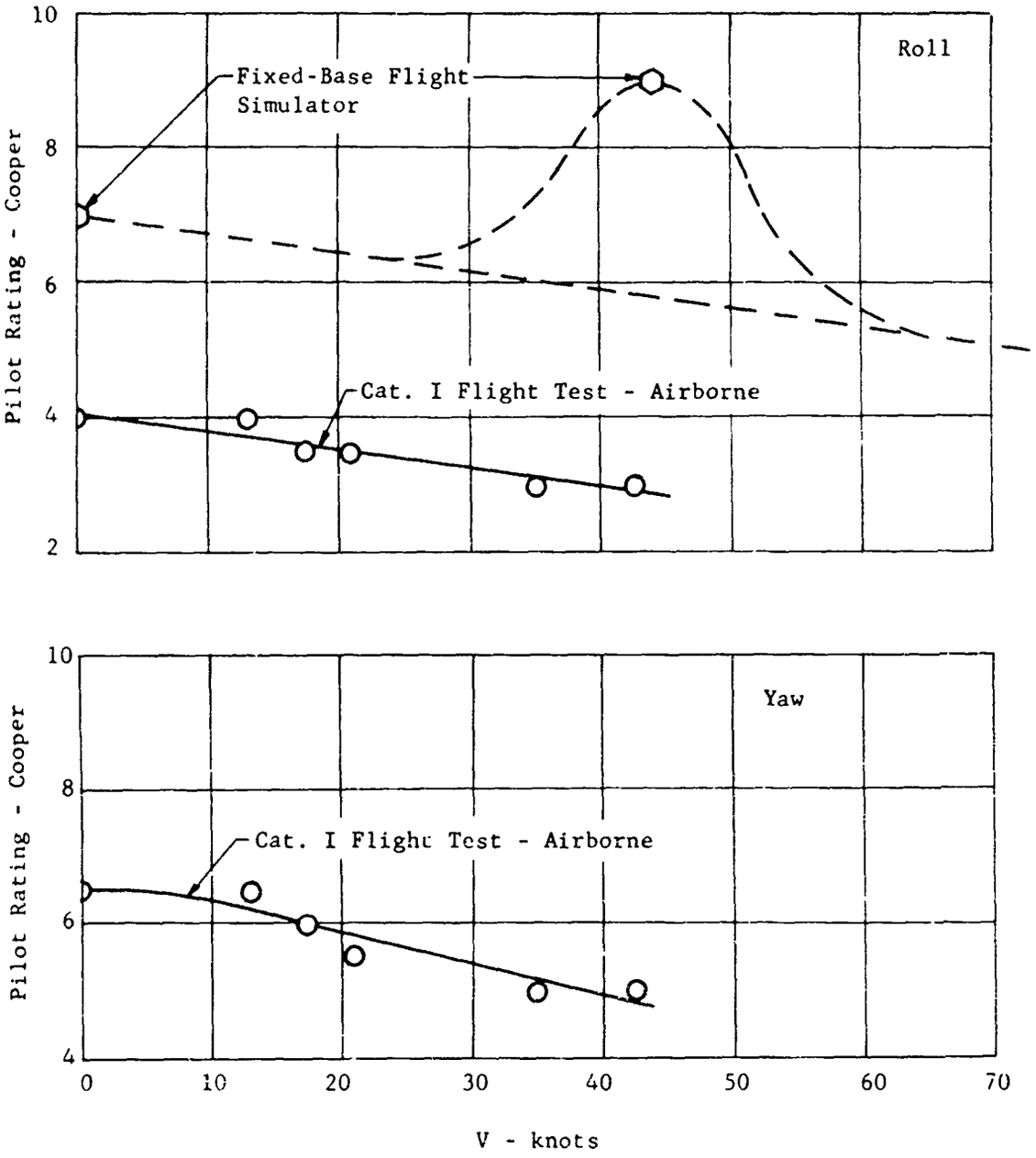

Figure 333. X-19, low speed lateral handling qualities with S.A.S. "off" in both axes (Pilot: J.V. Ryan).

TABLE XXI. - COOPER PILOT OPINION RATING SYSTEM

Operating Conditions	Adjective rating	Numerical rating	Description	Primary mission accomplished	Can be landed
Normal operation	Satisfactory	1	Excellent, includes optimum	Yes	Yes
		2	Good, pleasant to fly	Yes	Yes
		3	Satisfactory, but with some mildly unpleasant characteristics	Yes	Yes
		4	Acceptable, but with unpleasant characteristics	Yes	Yes
Emergency operation	Unsatisfactory	5	Unacceptable for normal operation	Doubtful	Yes
		6	Acceptable for[1] emergency condition only	Doubtful	Yes
		7	Unacceptable even for[1] emergency condition	No	Doubtful
No operation	Unacceptable	8	Unacceptable - dangerous	No	No
		9	Unacceptable - uncontrollable	No	No
	Catastrophic	10	Motions possibly violent enough to prevent pilot escape	No	No

[1]Failure of a stability augmenter.

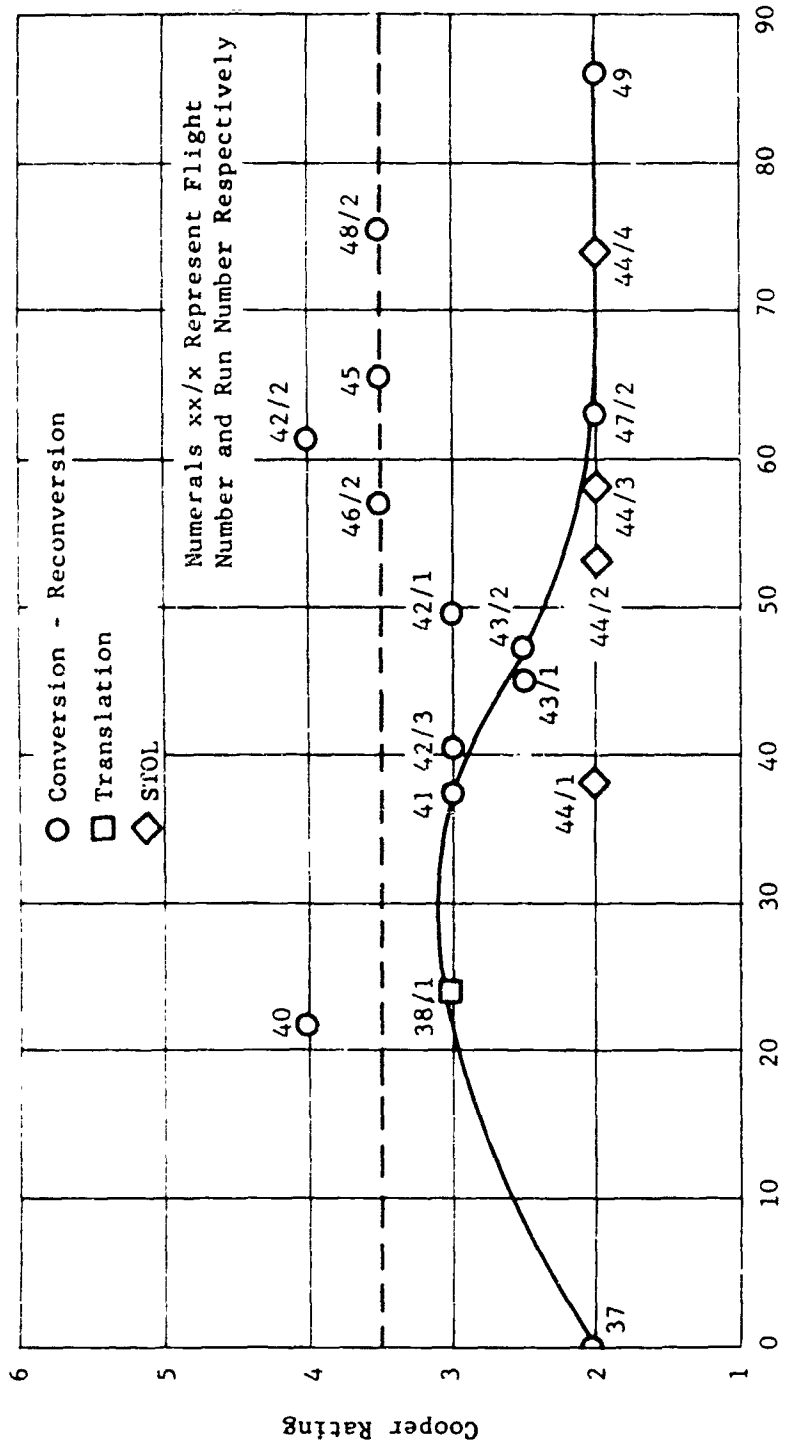

Figure 334. X-19, pilot opinion rating as a function of airspeed, pitch axis. Electronic pitch SAS on.

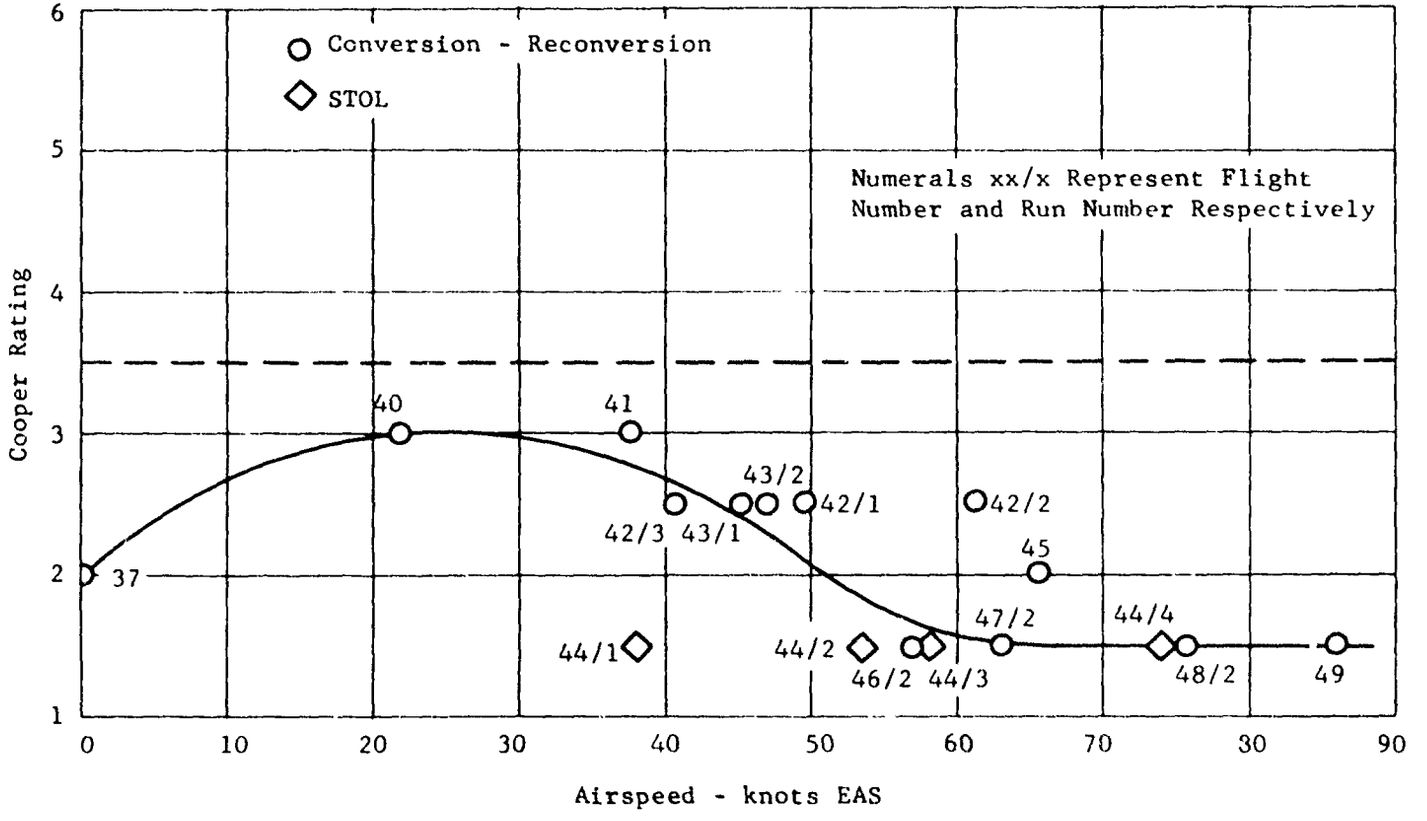

Figure 335. X-19, pilot opinion rating as a function of airspeed, roll axis. Electronic roll SAS on.

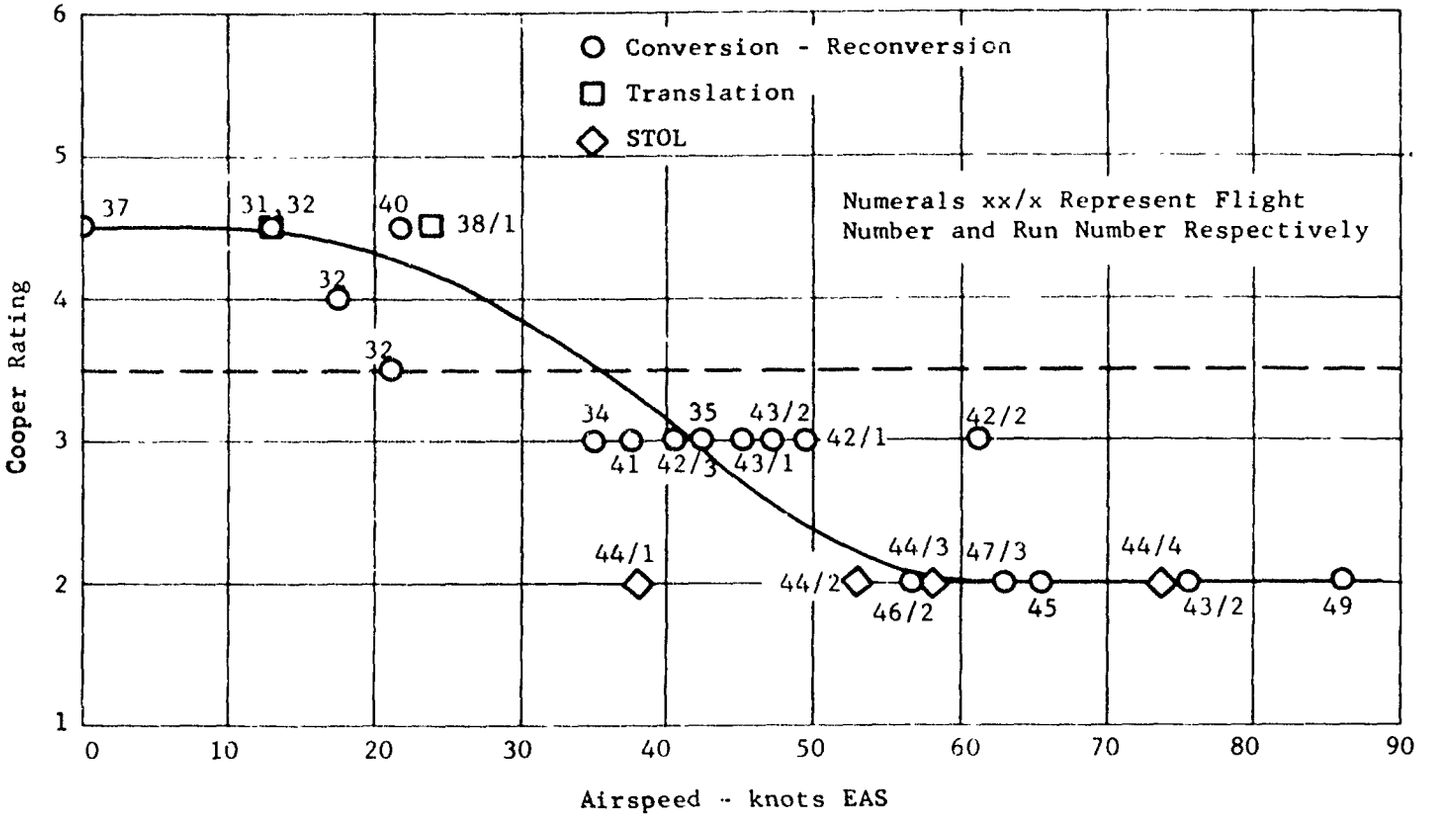

Figure 336. X-19, pilot opinion rating as a function of airspeed, yaw axis. No stability augmentation.

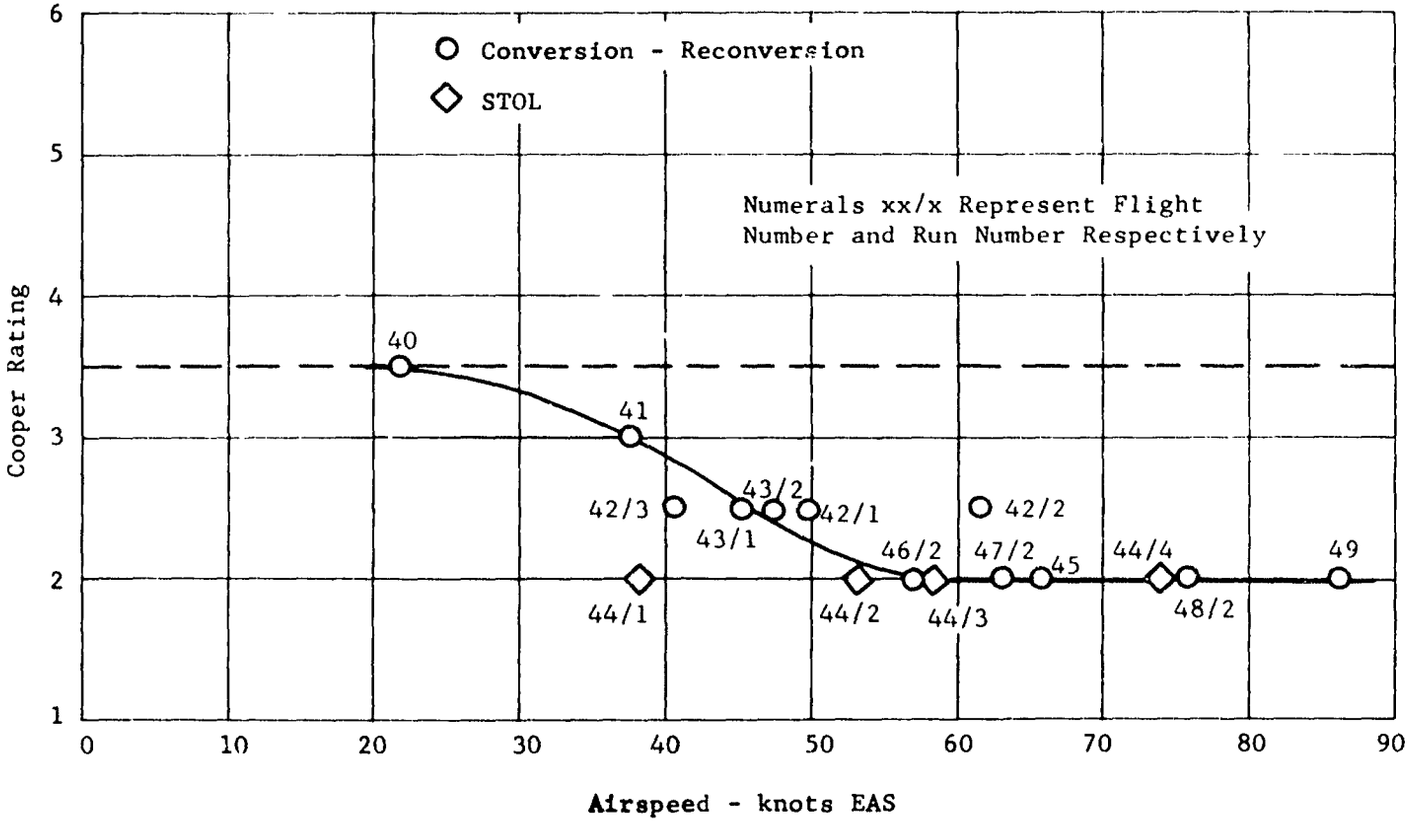

Figure 337. X-19, pilot opinion rating as a function of airspeed, height control. Height control system on.

d. STOL Operations

Flight test experience in STOL operations was limited. However, all indications were that STOL take-offs and landings between 20 and 70 kts. airspeed were straight-forward. The STOL take-off tests showed that the power required decreased with speed indicating good overload capability as was predicted. No test were made to demonstrate minimum field length in either take-off or landing, so distances are not available. The STOL test were done easily and the aircraft indicate satisfactory handling qualities at these conditions.

REFERENCES

94. Contract AF33(657)-13017

95. E. M. Allen, H. V. Borst, V. P. Meyer, Technical Analysis of X-19 Crash, Curtiss-Wright Report No. 014-681, dated 20 September 1965, Revised 11 October 1965

96. Curtiss-Wright Corp., VTOL Systems Division, X-19 S/N 62-12197, Flight No. 50 Crash Area Component Layout Photograph (FAA National Aviation Facilities Experimental Center, Atlantic City, New Jersey, Photo File No. 3950-25)

97. Curtiss-Wright Corp., VTOL Systems Division, X-19 S/N 62-12197, Flight No. 50 Flight Path Superimposed on FAA National Aviation Facilities Experimental Center, Atlantic City, New Jersey, Drawing No. XC-501 Titled "NAFEC 1000 N.J. Grid" (Original given to X-19 Accident Review Board).

98. L. K. Linn, A. V. Coles, X-19 Flight Test Final Summary Report against Contract No. AF33(657-13017), Item 2., Curtiss-Wright Report No. 014-835, dated 3 January 1966

99. E. Hassel "Aerodynamic Performance Summary" Curtiss-Wright Report No. 014-251, dated February 13, 1964.

SECTION XIII

ASSESSMENT OF RESULTS AND CONCLUSIONS

SECTION XIII

ASSESSMENT OF RESULTS AND CONCLUSIONS

1. INTRODUCTION

This section is devoted to thoughts, ideas and commentaries. For the most part the content extends the Statement of Work, by presenting the thoughts of various contributors to the X-19 program. In some instances, untested and unproven ideas are presented. In others, experience has guided the individual to his specific conclusions.

2. OVERALL X-19 CONCEPT AND ITS DERIVATION

a. Radial Lift Propellers

The flight tests of the X-100 airplane proved that the tilt propeller VTOL airplane could be flown over a wide range of flight conditions from hover to cruise without encountering adverse effects of trim changes, wing stall, buffet, etc. Further, the tests indicated that the propellers do generate large radial force which can be used in place of wing area required for the transition flight conditions. It should be noted the X-100 had a wing loading in excess of 170 psf; consequently propeller radial lift was an important part of the overall lift required during the transition flight mode.

The concept of the use of propeller radial lift had been questioned by many investigators. It was stated that although lift is generated by the propeller radial force, that the drag associated with that force is large and also the loss of thrust due to the shaft operating at an angle of attack is very large. With the final result of the equivalent drag ratio, it is unacceptably low. For this reason the critics of the principle stated that the idea had no merit, and it was better to use the wing to generate lift. In actual fact, the propeller radial force has a lift drag ratio approximately equal to the cotangent of the shaft angle of attack, so that for a propeller shaft angle of attack of 2° the lift drag ratio is approximately equal to 28.6, which is good even for a wing. If one considers the loss of thrust due to the propeller operating at the shaft angle of attack, it is observed that the loss is approximately equal to the cosine of the angle of attack which for 2° is .9994, hardly a significant loss. At the shaft angle of attack of 2°, the blade section angle of attack will vary by no more than $\pm$ 2°, which does not increase the mean drag coefficient of the blade section significantly. Even if the blade section is operating at the most unacceptable condition where the change in angle of attack would cause a rise in the mean drag, the effect on overall propeller efficiency is small. When the propeller is operating at the cruise condition and near high design levels of efficiency, a change of drag would influence the overall efficiency by a very small amount, less than 1%. When this loss is considered, the propeller is still capable of generating a lift drag ratio equal to the overall aircraft lift drag ratio and

provides significant levels of lift. At the design cruise condition, analysis indicated that the propeller would generate at least 20% of the lift required while maintaining high levels of lift drag ratio equivalent to the wing alone.

Part of the argument for the use of propeller radial lift to supplement the wing lift was the possibility of reducing wing weight by eliminating the requirement for wing area. The claimed advantage is significant as long as the reduction in wing weight can be proportional to the area. Unfortunately, this is not quite true. As with the small wings encountered on such an aircraft, significant increases in weight per unit area are required to provide the stiffness of structural characteristics necessary for this type of aircraft.

To see the overall importance of radial lift, the entire aircraft configuration must be reviewed for operation on a given mission. When this is done the following factors will be observed:

(1) Increased levels of thrust to horsepower ratio can be generated with propellers installed on fixed wing aircraft as the disk loading can be lower than in the case of the tilt wing aircraft. This is possible as the slipstream generated by the propeller is not needed to prevent wing stall during transition.

(2) The wing can be designed for optimum performance at the cruise flight condition, as the propellers can be used to provide the lift necessary during conversion.

(3) Propeller designed to provide increased radial lift can be made to operate at lower tilt angles during conversion than normally designed propellers. Because the blade width is added inboard with high radial force propellers, higher values of absolute blade thickness can be used and still maintain low drag inboard blade sections. With properly designed fiberglass blades with low thickness ratio the blade weight will be below the weight of conventional metal blades.

b. Tilt Propeller, Fixed Wing Configuration

The use of propellers for providing lift in hover, transition and cruise plus thrust at all forward speed flight conditions is considered to be technically sound, so long as the maximum design cruising Mach number is less than 0.75 to 0.8. The propeller of course must tilt approximately 90° to fulfill these lift and thrust design requirements. For any disk loading, high levels of Figure of Merit can be obtained at hover, and good efficiency is possible at the cruise condition. The tendency is for the propeller to be underloaded in cruise; this can lead to some losses in efficiency, unless the hover and cruise flight condition are properly matched. A reduction of turbine speed between hover and cruise is helpful in this respect. However, it is not the entire answer. The best procedure to obtain peak performance is the proper matching of

propeller disk power and wing loadings to the condition. By proper design and matching, the hover performance of the propellers can attain a Figure of Merit of 78 to 80% while the cruise efficiency can be on the level of 80 to 85%. This cruise level of performance is very close to that obtained with conventional aircraft.

With a fixed wing design the static slipstream produced by the propeller creates a blowdown loss on the wings and nacelle which reduces the hover lift. This loss is the main disadvantage of the fixed wing tilt propeller configuration. The effects of this loss can be minimized through a small increase in propeller disk area, as this increases the available thrust to horsepower. Deflection of the wing flaps and the addition of flow controlling vanes also reduces the download loss. Additional research and testing should prove to be fruitful in overcoming this difficulty. This was indicated by the limited program accomplished by this contractor.

Flight tests have shown that the blowdown loss on the wing becomes zero at very low flight speeds. Depending somewhat on the configuration, this occurs at speeds from 25 to 35 knots. It appears that flow is rapidly displaced aft, thereby generating an increased circulation about the wing. This characteristic, along with good translational propeller lift characteristics, makes possible a rapid reduction of power with increased flight speed; see Section XII. As a result, the tilt propeller fixed wing aircraft does have good overload capacity when using conventional and STOL take-off operating techniques. The X-19 and X-100 airplanes were often criticized for having no overload STOL flight capability; flight tests with both airplanes have proved this to be untrue.

The advantage of the fixed-wing tilt-propeller configuration is realized also in the area of improved flight characteristics in transition. Since the wing is fixed to the fuselage, the aircraft is handled like a conventional airplane; it is not necessary to worry about wing stall within the normal aircraft angle of attack range. Also, the propeller does not exhibit a sharp stall characteristic. Therefore during the conversion maneuver little danger of stall or buffet will be observed. In addition, the airplane will have a wide tilt-angle speed band because of the favorable characteristics of the tilt-propeller fixed-wing combination. This makes possible a simpler conversion/reconversion maneuver, so important to the VTOL airplane.

c. Tandem Wing Configuration

(1) General

The tandem wing propeller configuration has many advantages in the hover and low speed flight operating regimes. Satisfactory hover control powers are obtained about all axes, and cross coupling of controls can be eliminated. The airplane can be built in larger sizes without exceeding present day propeller diameter experience.

Although many advantages can be found for the tandem wing configuration, experience gained from the design and development of the X-19 indicate that serious faults are inherent in this type of aircraft. For example, to have a practical and light transmission, the propeller on the tandem wing airplane will be located at the ends of the wings with the center of tilt at approximately the one-third chord point. With equal diameter propellers designed for peak efficiency at the hover condition, it is desirable to have the take-off center of gravity located midway between the fore and aft propellers. For this c.g. location, the propellers will lift equally and the power split will also be equal fore and aft. Unfortunately, when the propellers are tilted down to the cruise condition, a c.g. near the 50% location results in an unstable configuration, unless a large rear wing and a large vertical tail are used. Such a combination becomes heavy and inefficient. By moving the c.g. forward so that the propellers lift unequally at take-off, the area requirement for obtaining longitudinal stability at the rear wing is reduced. When the c.g. is moved forward the propellers operate off peak efficiency and thus require more total power, which tends to reduce the take-off gross weight. The weight of the transmission increases as the steady power on the front propellers increases. On the X-19, the maximum hover aft c.g. was located at approximately the 43% station; the rear wing had double the area of the front wing.

This c.g. location resulted in loss of hover lift of approximately 3% compared with the 50% c.g. location. In addition the download loss was greater on the rear propellers due to the increased wing area. These losses must be charged to the basic configuration. The total hover lift loss is at least 6%.

A vertical take-off and landing airplane should have a light efficient structure to obtain an airplane that is competitive with present vehicles. The tandem wing aircraft appears to be inherently heavier than competitive types. One reason for this is the torsion and bending loads induced in the fuselage by the wings and propellers. This, coupled with the heavy wings and tail is another problem encountered with the tandem configuration. The chore of coupling the propellers to the tandem wing machine is also considered a major problem. This is further complicated by the problem of finding a proper location for the engines and leads to a heavy transmission system.

(2) Stability and Control

From a stability and control standpoint the tandem wing, tandem propeller configuration is an extremely complex engineering design. Estimation of stability and control derivatives is possible, within the current state-of-the-art, to an acceptable degree. However, much is yet to be learned regarding the characteristics of such an aircraft. Following are the major advantages and disadvantages of the X-19 concept from a stability and control point of view.

(a) Advantages:

(aa) Pitch and Roll Control in Hover

The "four poster" configuration provides excellent pitch and roll control by means of the hover lift devices, minimizes power expenditure for control, and eliminates the need for any auxiliary control device. Zero control cross-coupling through transition is easily accomplished.

(bb) High Radial Force Propellers (Damping Effect)

The high propeller damping in cruise configuration allows very small static margins in order to yield wholly acceptable dynamics.

(b) Disadvantages:

(aa) Short Moment Arms

Of necessity the center of gravity falls approximately midway between the fore and aft wings, and the required wing area is provided by two small wings rather than one large one. These inherent characteristics leave the vertical tail, the elevators and the ailerons with comparitively short moment arms which result in severe penalties, namely:

(i) Vertical Tail

In order to provide sufficient directional stability the vertical tail area is large. Its center of pressure is located a substantial vertical distance above the center of gravity and thus the tail makes a significant contribution to dihedral effect (C_{l_β}). The large value of this derivative was the cause of most of the X-19's lateral-directional stability and control deficiencies.

(ii) Aileron Power

Although this was not considered a serious deficiency, control power is clearly limited by the small wing span. Initially the ailerons were located on the front wing until it was realized that their effectiveness was drastically reduced by the change in downwash at the rear wing. For example, right aileron down produces an increase in front right wing lift but also an increase in downwash angle at the right rear wing. This causes a decrease in effective angle of attack of the right rear wing and hence a decrease in lift.

(iii) Elevator Power

Large elevator angle per "g" and elevator angles to trim were required at low speed (due also to the non-linear C_m vs α characteristic) resulting in high trim drag.

(bb) High Wings

The shoulder mounting of the wings provided the major contribution to rolling moment derivative C_{l_β} . It is of course recognized that this wing position is the only logical one for a number of other important reasons, including transmission cross-shafting, propeller ground clearance, minimum transmission complexity (for the given engine location), etc. Negative dihedral may provide a solution but would create problems involving the transmission system shafting.

(cc) High Radial Force Propellers

A direct effect on the side force derivative C_{y_β} of the aircraft.

(i) C_{y_β} - Yawing moment derivative

Propeller radial force provides about 50% of the total contributions to C_{y_β} . The resulting value of C_{y_β} is high and adversely affects the airplane's ride quality when flying in lateral turbulence.

(ii) Hinge Moments

With the propellers providing a substantial portion of lift in the cruise configuration, the wing area required decreases. The X-19's wings were extremely small in area but aerodynamically thick, the latter to provide structural integrity and fairings over the transmission shafting. Hinge moment variation with surface deflection of control surfaces on thick wings is normally quite non-linear, making both the estimation of hinge moment C_{h_δ} and the design of a manual system difficult tasks. In the case of the X-19, it was necessary to install power boost on both elevator and aileron systems to overcome the high hinge moments at large control surface deflections, and to provide linear stick force gradients.

Power boost of course adds to the cost, weight and complexity. It would be unreasonable to judge such an obtuse effect as a basic design deficiency, but it is an interesting by-product of a new design philosophy.

(dd) Hover Yaw Control

Hover yaw control deficiencies are discussed in some detail in Section VI, paragraph 9.b.; suffice it to state here that the X-19's hover yaw control would be unacceptable in an operational aircraft.

d. Control Power

In cruise the X-19 deviated from MIL-F-8785 (ASG) control requirements in two areas, namely, by not meeting the stated pb/2v minimums or the steady sideslip requirement. Regarding the pb/2v requirement, it was felt that these specifications, evolving from service experience with single wing aircraft, were not directly applicable to the tandem wing X-19 type which has a much smaller wing span than conventional aircraft. This is influencing as the specification was derived based on the helical speed of the wing tip. As a result, a minimum design value for maximum steady roll rate of 40 deg/sec was selected, a value which was considered adequate for a transport type VTOL airplane. To increase the roll rate above the selected minimum would have necessitated larger capacity power boost or the installation of an elevon or spoiler system.

Steady sideslip capability was "apparently" limited by the available lateral control power, in that full aileron was required for trim at considerably less than specified sideslip angles (refer to Section VII, Paragraph 1.b.(5)(e)).

This however is not so much a reflection of aileron power as it is upon the derivative C_{l_β} . The unusually high value of C_{l_β} is discussed in Section XIII, Paragraph 4.c. and Section VII, Paragraph 5.b.(2)(b). It is directly responsible for generating large rolling moments during sideslip maneuvers and hence creates the need for inordinately high aileron power.

Longitudinal control (elevators) conformed to MIL-F-8785 (ASG) for cruising flight.

Hover control powers deviated from MIL-H-8501A. This deviation was intentional and resulted from analysis of the various hover and low-speed handling qualities studies available at the time, together with C-W's own simulator and X-100 flight test experience. The following maximum angular accelerations were specified, and used, for the X-19:

Pitch:	0.682 rad/sec^2
Roll:	1.75 rad/sec^2
Yaw:	0.121 rad/sec^2

The very low yaw acceleration was partially justified on the basis of a predicted N_v of essentially zero, and zero control cross-coupling. Yaw control is discussed in some detail in Section VI, Paragraph 9.b.

For transition, flight control was effected by both the propellers and conventional aerodynamic surfaces. Propeller control was phased out mechanically with decreasing propeller tilt angle in such a manner that available control moments were held constant or allowed to increase slightly to about 80 knots. Beyond this, control moments were allowed to vary smoothly until the propellers were fully tilted down. Propeller pitch and roll control were phased out completely at 160 knots, and directional control at 100 knots.

For transition, the propeller contributions to control were designed for zero coupling about any of the axes while normal lateral-directional coupling resulted from the rudder and ailerons (i.e., the aerodynamic contributions to control). This philosophy of control led to good ratings of handling qualities during Category I flying as reported in Section VI, Paragraph 4.

e. Transmission Design Philosophy

Design philosophy of the X-19 transmission system has been the subject of many heated discussions. Questions, which have not been completely resolved include: time histograms versus infinite life, addition of control and throttle loads, weight growth, air density and center of gravity effects. Comments concerning these parameters will be made.

First, however, the evolved design philosophy will be described. To start with, the transmission was initially designed for an aircraft weighing 10,000 pounds. The center of gravity was realistically defined and generous torque increments were allowed for control deflections. No allowance for excessive throttle-imposed torques was allowed. From this basic concept, an external

physical envelope was defined. With the inevitable weight growth that accompanies new aircraft, the transmission torque requirements grew.
Correspondingly, the moments of inertia were growing, which in turn required higher control moments. Both of these factors contributed to the obsolescence of the original transmission. The designers were hard put to uprate the transmission within the physical envelope. It was inevitable that a hover time-torque histogram evolved. This histogram was pertinent to combined pitch-roll maneuvers. Yaw inputs would be added into the histogram on a separate time basis. The governor system was designed to preclude a throttle input in excess of 20 percent. One of the major questions to be answered was how to allot the total time to the histogram. Obviously, a hover mission consumes life faste than a cruise mission.

By contrast, helicopters are designed to accept full throttle torque at infinite life. Control deflections (pitch, roll) have but small influence on the torque. It is understood the present tilt wing designs (single wing) adhere to this philosophy. Unquestionably, this philosophy is costly in weight. However, there appears to be no movement to depart from this point of view.

Undoubtedly, the X-19 transmission can be designed to an infinite life philosophy including: Full throttle and control deflection; most forward center of gravity and low air density. The weight penalty however would be prohibitive. This philosophy is unrealistic for an X-19 type of aircraft. It is believed that a realistic design can be evolved which yields infinite life without adding all inputs algebraically. It is further believed, that had the aircraft attained additional flight experience, the answer would have been obtained.

Experience has demonstrated one point in a dramatic fashion. A minimum requirement would be to design for maximum throttle-imposed torque, or limits established by a throttle stop. The designer must accept the application of full throttle as an instinctive pilot reaction in certain maneuvers and that excess torque must be passed safely through the system.

It is likely that experience would have demonstrated a maximum additive control deflection, had the test program continued. In the case of the X-19, this would have been a harsher nacelle-design condition than full throttle. Without the benefit of experience, it is belived the nacelle system should be designed to infinite life for this condition. Furthermore, this design point should reflect the most forward center of gravity and lowest air density anticipated.

Since the VTOL concept is in early development compared with the fixed wing airplane, a lesson can be learned from fixed wing philosophy. Many companies, in establishing basic airframe loads, recognize the weight growth problem. They anticipate this by designing to a somewhat higher weight than the initial target value. The weight penalty is not too harsh and the aircraft then has general growth potential. Therefore VTOL designers should reflect growth in their transmission designs. One such reflection would be to anticipate a physical envelope somewhat larger than required for the target weight. Then if necessary, the transmission could be uprated with lesser efforts in the future. It has been difficult, in the past, to convince people to design a VTOL transmission to a higher than target weight. Yet, experience has repeatedly shown that this is not conservative. The weight will grow.

f. Gust Sensitivity

The susceptibility of the X-19 longitudinal dynamics to gusts and other atmospheric turbulence was predicted to be equal to, or less than, current subsonic jet transports. The lateral modes, however, were predicted to respond to a very wide range of gust frequency.

The broad band width of the lateral response was due mainly to the fact that in addition to the normal Dutch Roll mode the X-19 possessed a spiral-roll (sometimes called "lateral phugoid") mode, rather than the customary aperiodic roll and spiral modes. This additional oscillatory mode, combined with large values of C_{y_β} and C_{l_β} presented what was thought to be a less than desirable situation regarding lateral gusts. It meant that lateral disturbance corrections to the aircraft would be frequent and would require significant levels of control moment.

g. Propeller Control Problems

In a VTOL airplane such as the X-19, the propeller control system should be emphasized as a major design area. It is felt this was not sufficiently recognized in the early design stages. Consequently, an all mechanical design evolved which was required to do the following: (1) pass all pilot control motions into the coordinator; (2) have the coordinator unscramble the signals and generate four separate output signals; (3) pass the coordinator outputs through four independent mechanical linkages connecting the coordinator to each of four nacelle gain changers; (4) magnify the nacelle input signal as a function of tilt angle (one for each propeller); and (5) pass the magnified signal from the nacelle gain changer to a propeller hydraulic servo system which generates the propeller blade angle.

Experience in rigging the control system showed that the coordinator, nacelle gain changer, and propeller servo system required further rigging development. The problem encountered resembles a chair with four extensible legs, each of which extends a different amount than desired. The result is a wobbly chair. In the case of the X-19 control system, the assymmetry results in control deflection in the transition regime, or torque imbalance in cruise.

The nacelle gain changers were originally installed in the system to provide greater resolution power to the coordinator, and to provide a varying propeller low-pitch stop with tilt variation. Although these aims were adequately met, the inevitable occurred. Each of the nacelle gain changers were slightly different due to manufacturing tolerances. Therefore they required a greater than desired rigging and calibration effort. This effort was in fact made; and toward the end of the program the system was considered adequate for the X-19 flight operation anticipated. The Number 2 airplane, in the meanwhile was being modified to provide a more precise rigging procedure. No doubt the control system would have functioned as required.

From the problems encountered with the control system, it is quite obvious the nacelle gain changers should never have been installed. Furthermore, all of the gain should have been built into the coordinator or its counterpart. The rigging and linkages should have been devised in such a manner that manufacturing tolerances would be lost in the linkage motion. Subsequent designs originating within the company did in fact accomplish these ends.

A subtlety encountered within the control system should be mentioned here. Let us assume the resolution of the control system is defined and a tolerance error is transmitted to the propeller. The greater the Activity Factor of the propeller, the larger will be the deviation in thrust or torque generated at the propeller. In other words, the greater the propeller sensitivity to blade angle change, the more restrictive will be the tolerances within the control system. The high normal force propeller tends toward the high blade angle sensitivity. Hence some of the resolution problems encountered in the X-19 are attributable to the propeller. This is a typical example of the control system tolerances mitigating the attributes of high normal force.

3. OPERATIONAL FLIGHT CONSIDERATIONS

a. Engine-out Safety

One of the major problems encountered with the design of VTOL aircraft is that of engine-out safety. Unless rotors operating at low disk loadings are used, it will not be possible to make safe landings by autorotating. For this reason it is necessary to provide for engine-out safety in other ways.

Most fixed wing aircraft are in serious trouble when a complete power failure is encountered. The airplane must be flying in an area where an emergency landing is possible, to have any chance of survival when all the engines are "lost". As a cruising VTOL aircraft is considered to be more nearly like a fixed wing aircraft than a helicopter, it is considered unrealistic to expect 100% safety when a complete power failure is encountered. For this reason it is believed that the VTOL airplane should be protected in the same manner as a conventional fixed wing airplane, only for the case when one engine becomes inoperable.

Protection against a failure of one engine should also be similar to that provided in conventional aircraft. That is, below a certain speed and altitude an engine failure would result in an aborted flight, whereas above this critical speed and altitude the flight could continue after an engine failure. Such failure conditions would be quite restrictive, especially with a two-engine aircraft such as the X-19, where the critical speed-altitude point is 45 knots and 20 feet. This failure criteria would result in a requirement for a considerable take-off and landing area and thus tends to defeat the original VTOL idea. It would appear that the main task would be to reduce this critical speed and increase the altitude, so that true VTOL flight characteristics would be obtained. By increasing the number of engines and improving the capacity of the landing gear it is believed that the desired level of engine-out safety can be obtained along with true VTOL operation.

b. Cruise Stall Characteristics

The X-19 configuration is quite unusual. The wings are of high wing loading ($W/S \simeq 80$ psf) and medium aspect ratio between ($4.7 > AR > 6.8$). Without the propellers mounted the front wing stalls at approximately $\alpha_{fus} = 14$ degrees. The rear wing, because of the downwash, stalls at about $\alpha_{fus} = 19$ degrees. Both wings are thick, so that the stall is very gentle. With no propellers, the airplane stalls at about $\alpha_{fus} = 14$ degrees, but does not experience a lift falloff. The lift above stall is fairly constant. The pitching moment becomes heavily stable as the front wing goes through stall and continues negative beyond the capability of the elevator (a safe characteristic). When the rear wing stalls the moment curve flattens out and for several degrees of α_{fus} continues beyond the capability of the elevator.

When the propellers are mounted on the model, one sees a change in the pattern of the front wing stall. Apparently the propeller wake energizes the boundary layer and the wing does not stall until perhaps α_{fus} = 19 degrees. The rear wing pattern does not change strongly due to the propeller influence. The airplane's lift curve changes radically with the propellers mounted. The propeller normal force increases the lift slope about 35 percent and delays the stall. In one wind tunnel test, the fuselage attitude was brought to α_{fus} = 29 degrees. The $C_{L_{max}}$ = 1.85 (untrimmed) was approached in a gentle curvature. (Note that flaps were neutral). The lift curve resembled that of a low aspect ratio wing. The pitching moment is slightly less stable due to the propellers. However at the higher attitudes the pilot will run out of control power. Although the pitching moment curve does become more positive in the stall region, it always remains negative. Therefore the possibility of a locked-in stall does not exist.

A question which frequently arose was, can the aircraft be pitched to the capability of the elevator? The reason for this is the possibility of a buffet problem. There was no known indication in the wind tunnel of model buffeting near the stall. Yet one wonders whether any vortices shed from the front wing would intercept the rear wing and generate a buffet condition. It is not known whether other tandem wing designs of the past have encountered this problem. It is believed that had this condition existed, aerodynamic fairing could have been a solution. The flight tests that were performed never even hinted at this possibility.

Handling and Flying Qualities

In general, the aim with regard to flying qualities was to comply with MIL-H-8501A in hover and MIL-F-8785 (ASG) in cruise. During transition, the object was to comply with MIL-H-8501A when the primary response to longitudinal stick was attitude and to MIL-F-8785 when the response was by aerodynamic forces of conventional lifting surfaces. Many conflicting situations arose, of course, and were usually resolved by means of simple fixed-base flight simulation.

The aforementioned aim was accomplished for the most part. The only notable exceptions were the cruise configuration roll rates and steady sideslips of MIL-F-8785 (ASG) and the hover control power and response of MIL-H-8501A.

The design philosophy which evolved resulted in satisfactory pilot opinion ratings with SAS on throughout the Category I testing (up to 90 knots). Pilot opinion ratings of 2, in hover operation were obtained about the pitch and roll axes. Above 50 knots pilot opinion ratings of 2 were obtained about all three control axes as well as the height control system.

Development of a good stability augmentation system was demonstrated to be well within the state-of-the-art with the electronic pitch and roll rate plus position SAS.

Based on analysis and the limited quantity of flight test data available the airplane was predicted to possess a wide transition corridor in terms of speed range at a fixed propeller tilt angle.

Cruise flying qualities were predicted to be satisfactory, with the possible exception of a roll-yaw control problem. Although good lateral stability was predicted, rudimentary fixed-base simulation indicated a control coordination problem traceable to the large dihedral effect (C_{l_β}). One of the problems associated with the tandem layout is that the c.g., of necessity, lies approximately mid-way between front and rear wings with the result that vertical tail moment arm is relatively short. This situation led to the very large X-19 tail necessary for static directional stability. It contributed significantly to the already high C_{l_β} derivative (due to the shoulder wing position) and the high C_{y_β} derivative (due largely to high propeller radial force). The overall result was that in cruise the X-19's lateral-directional handling qualities left much to be desired. Lateral acceleration due to a lateral disturbance was high (due to high C_{y_β}) coupled with large roll angle excursions (due to high C_{l_β}).

If any further details on the aerodynamic design, performance, stability and load analysis characteristics of the X-19 are required, the summary reports Curtiss Wright numbers 014-251, 014-252 and 014-253 should be consulted.

Unclassified
Security Classification

DOCUMENT CONTROL DATA - R&D

(Security classification of title, body of abstract and indexing annotation must be entered when the overall report is classified)

1 ORIGINATING ACTIVITY (Corporate author) Curtiss-Wright Corporation VTOL Systems Division Caldwell, New Jersey	2a REPORT SECURITY CLASSIFICATION Unclassified 2b GROUP --------

3 REPORT TITLE

THE X-19 V/STOL TECHNOLOGY - A CRITICAL REVIEW

4 DESCRIPTIVE NOTES (Type of report and inclusive dates)

Final Report

5 AUTHOR(S) (Last name, first name, initial)

Fluk, Harold

6 REPORT DATE	7a TOTAL NO OF PAGES	7b NO OF REFS
May 1967	619	98

8a CONTRACT OR GRANT NO	9a ORIGINATOR'S REPORT NUMBER(S)
AF 33(615)-3940 b PROJECT NO	AFFDL-TR-66-195
c d	9b OTHER REPORT NO(S) (Any other numbers that may be assigned this report) WAD R864 F

10 AVAILABILITY/LIMITATION NOTICES Each transmittal of this document outside the agencies of the U.S. Government must have prior approval of the Air Force Flight Dynamics Laboratory, V/STOL Technology Division (FDV).

11 SUPPLEMENTARY NOTES	12 SPONSORING MILITARY ACTIVITY
--------	AF Flight Dynamics Laboratory (RTD) Attn: FDV Wright-Patterson AFB, Ohio

13 ABSTRACT This report contains a condensed description of the X-19 V/STOL Technology. The broad categories discussed include in Section I a review of the developments leading up to the X-19 program. Sections II through VI are devoted entirely to the propellers and the considerations involved in design. The radial force principle is postulated in Section II. Interference effects on the wings due to the propellers are discussed in Section III. The propeller aerodynamic design in hover and cruise is presented in Section IV. Section V is devoted to the structure and control mechanisms of the propeller. Section VI relates to the use of propellers as in airplane control device. The tandem wing principle is discussed in Section VII, covering stability, control, and drag. Section VIII is devoted solely to ground effects. The wind tunnel research activity leading up to the X-19 is presented in Section IX. The structural loads in hover, transition and cruise are discussed in Section X. Section XI presents information pertinent to landing procedures in hover or cruise in the event of power failure. A summary of the flight test program is given in Section XII, including aircraft and hardware performance characteristics. Finally, Section XIII is devoted to a general discussion and assessment of the aircraft's unorthodox features.

DD FORM 1 JAN 64 1473

Unclassified
Security Classification

Security Classification

14 KEY WORDS	LINK A		LINK B		LINK C	
	ROLE	WT	ROLE	WT	ROLE	WT
X-19 V/STOL Technology Radial Force Propeller Propeller - Airplane Control Tandem Wing Concept Tilting Propellers Flight Test Results of X-19 Wing - Propeller Interference Effects Wind Tunnel Experiments of X-19 Power Transmission System Utility Transport						

INSTRUCTIONS

1. ORIGINATING ACTIVITY: Enter the name and address of the contractor, subcontractor, grantee, Department of Defense activity or other organization *(corporate author)* issuing the report.

2a. REPORT SECURITY CLASSIFICATION: Enter the overall security classification of the report. Indicate whether "Restricted Data" is included. Marking is to be in accordance with appropriate security regulations.

2b. GROUP: Automatic downgrading is specified in DoD Directive 5200.10 and Armed Forces Industrial Manual. Enter the group number. Also, when applicable, show that optional markings have been used for Group 3 and Group 4 as authorized.

3. REPORT TITLE: Enter the complete report title in all capital letters. Titles in all cases should be unclassified. If a meaningful title cannot be selected without classification, show title classification in all capitals in parenthesis immediately following the title.

4. DESCRIPTIVE NOTES: If appropriate, enter the type of report, e.g., interim, progress, summary, annual, or final. Give the inclusive dates when a specific reporting period is covered.

5. AUTHOR(S): Enter the name(s) of author(s) as shown on or in the report. Enter last name, first name, middle initial. If military, show rank and branch of service. The name of the principal author is an absolute minimum requirement.

6. REPORT DATE: Enter the date of the report as day, month, year, or month, year. If more than one date appears on the report, use date of publication.

7a. TOTAL NUMBER OF PAGES: The total page count should follow normal pagination procedures, i.e., enter the number of pages containing information.

7b. NUMBER OF REFERENCES: Enter the total number of references cited in the report.

8a. CONTRACT OR GRANT NUMBER: If appropriate, enter the applicable number of the contract or grant under which the report was written.

8b, 8c, & 8d. PROJECT NUMBER: Enter the appropriate military department identification, such as project number, subproject number, system numbers, task number, etc.

9a. ORIGINATOR'S REPORT NUMBER(S): Enter the official report number by which the document will be identified and controlled by the originating activity. This number must be unique to this report.

9b. OTHER REPORT NUMBER(S): If the report has been assigned any other report numbers *(either by the originator or by the sponsor)*, also enter this number(s).

10. AVAILABILITY/LIMITATION NOTICES: Enter any limitations on further dissemination of the report, other than those imposed by security classification, using standard statements such as:

(1) "Qualified requesters may obtain copies of this report from DDC."

(2) "Foreign announcement and dissemination of this report by DDC is not authorized."

(3) "U. S. Government agencies may obtain copies of this report directly from DDC. Other qualified DDC users shall request through

_____."

(4) "U. S. military agencies may obtain copies of this report directly from DDC. Other qualified users shall request through

_____."

(5) "All distribution of this report is controlled. Qualified DDC users shall request through

_____."

If the report has been furnished to the Office of Technical Services, Department of Commerce, for sale to the public, indicate this fact and enter the price, if known.

11. SUPPLEMENTARY NOTES: Use for additional explanatory notes.

12. SPONSORING MILITARY ACTIVITY: Enter the name of the departmental project office or laboratory sponsoring *(paying for)* the research and development. Include address.

13 ABSTRACT: Enter an abstract giving a brief and factual summary of the document indicative of the report, even though it may also appear elsewhere in the body of the technical report. If additional space is required, a continuation sheet shall be attached.

It is highly desirable that the abstract of classified reports be unclassified. Each paragraph of the abstract shall end with an indication of the military security classification of the information in the paragraph, represented as *(TS)*. *(S)*. *(C)*. or *(U)*

There is no limitation on the length of the abstract. However, the suggested length is from 150 to 225 words.

14 KEY WORDS: Key words are technically meaningful terms or short phrases that characterize a report and may be used as index entries for cataloging the report Key words must be selected so that no security classification is required. Identifiers, such as equipment model designation, trade name, military project code name, geographic location, may be used as key words but will be followed by an indication of technical context. The assignment of links, rules, and weights is optional.

Unclassified
Security Classification